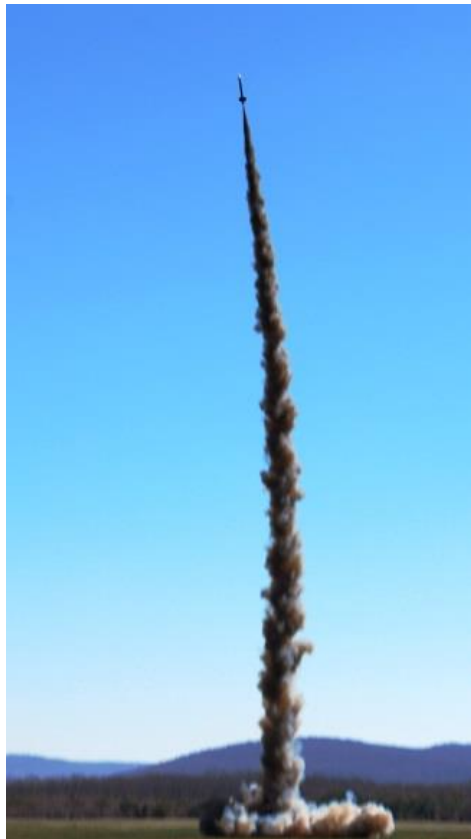


Vanderbilt University

2014-2015 NASA Student Launch

Flight Readiness Review



March 16, 2015

Dexter Watkins – *President, Rocket Project Coordinator, Website Manager*

Fred Folz – *Vice President, Design Engineer*

Connor Caldwell – *Treasurer, Safety Officer, Design Engineer*

Jacob Moore – *Secretary, Design Engineer*

Chris Lyne – *CFD, Design Engineer*

Alex Goodman – *Design Engineer*

Cameron Ridgewell – *Design Engineer*

William Emfinger – *AGSE Project Coordinator*

Pranav Kumar – *AGSE Project Coordinator*

Andrew Voss, Mitchell Masia, Myles Lacy – *Field Engineers*

Ben Gasser – *Robotics Mentor*

Dr. Brian Lawson – *Robotics Mentor*

Robin Midgett – *Safety and Rocketry Mentor*

Dr. Amrutur Anilkumar – *Project Advisor*

Table of Contents

1	General Information	19
1.1	Faculty Advisors	19
1.1.1	Project Advisor	19
1.1.2	Outreach Advisor	19
1.2	Mentors.....	19
1.2.1	Safety and Rocketry Mentor	19
1.2.2	Robotics Mentors	19
1.3	Team Members.....	20
1.3.1	Project Coordinators	20
1.3.2	Senior Design Team.....	20
1.3.3	Field Engineers	21
1.4	NAR Association.....	21
1.5	Vanderbilt Aerospace Club Constitution	22
2	Summary of Project.....	23
2.1	Team Summary	23
2.2	Launch Vehicle Summary.....	23
2.3	AGSE/Payload Summary.....	23
3	Changes Made Since CDR	25
3.1	Changes Made to Vehicle Criteria	25
3.2	Changes Made to Payload/AGSE Criteria	25
3.3	Changes Made to Project Plan	26
3.4	CDR Feedback Response	26
4	Vehicle Criteria.....	30
4.1	Design and Construction of Launch Vehicle	30
4.1.1	Systematic Launch Vehicle Design Review	31
4.1.2	Flight Reliability and Confidence	41
4.1.3	Launch System and Platform	43
4.1.4	Launch Vehicle Systems Requirements and Verification	44
4.1.5	Workmanship and Mission Success.....	49
4.1.6	Safety and Failure Analysis	50
4.2	Full-Scale Flight Results	52
4.2.1	March 15, 2015 Launch	52

4.2.2	Comparison with Predictions	55
4.3	Subscale Flights Results.....	60
4.3.1	November 2014.....	60
4.3.2	December 2014	62
4.4	Comparison of Subscale to Full-Scale Launch Vehicle.....	65
4.4.1	Comparison Overview	65
4.4.2	Vehicle Design Comparison	66
4.4.3	Mass Statement	67
4.5	Recovery Subsystem	68
4.5.1	Recovery System Overview.....	68
4.5.2	Rocket Separation	69
4.5.3	Rocket Parachute Recovery	71
4.5.4	Payload Parachute Recovery.....	72
4.5.5	Avionics and Avionics Bays	73
4.5.6	Deployment Charge and Altimeter Layout.....	76
4.5.7	Recovery System Testing	78
4.5.8	Avionics Bay Structure	84
4.5.9	Recovery Telemetry Electronics.....	85
4.5.10	Safety and Failure Analysis	86
4.6	Mission Performance Predictions.....	86
4.6.1	Mission Performance Criteria	86
4.6.2	Vehicle Design Comparison	87
4.6.3	Dimensional Drawings of Launch Vehicle.....	88
4.6.4	Simulations and Predictions.....	88
4.6.5	Kinetic Energy Calculations	101
4.7	Vehicle Verification	103
4.7.1	NASA Statement of Work Verification.....	103
4.8	Vehicle Safety and Environment.....	111
4.8.1	Safety Officer and Responsibilities	111
4.8.2	Failure Modes Analysis and Mitigation.....	112
4.8.3	Personnel Hazards and Concerns.....	112
4.8.4	Environmental Hazards and Concerns.....	115
4.9	Payload Bay Design	115

4.9.1	Subscale Design Overview	115
4.9.2	Changes after Subscale Launches	116
4.9.3	Final Design Overview	117
4.9.4	Integration of Payload Bay with Rocket.....	124
4.9.5	Payload Bay Testing and Verification	125
5	AGSE Criteria.....	130
5.1	AGSE Experimental Concept.....	130
5.1.1	Creativity and Originality	130
5.1.2	Uniqueness and Significance	131
5.1.3	Challenge of Design.....	132
5.2	AGSE Science Value	133
5.2.1	Objectives	133
5.2.2	Literature Review.....	134
5.2.3	Success Criteria.....	135
5.2.4	Experimental Logic, Approach, and Method of Investigation	136
5.2.5	Test and Measurement, Variables, and Controls	138
5.2.6	Expected Data and Accuracy/Error Analysis	140
5.2.7	Preliminary Experiment Process Procedures	142
5.3	AGSE Development Strategy.....	144
5.3.1	ROS Component Model, Modeling Language, Toolsuite, and Code Generators	145
5.3.2	AGSE Prototype Control Software	152
5.3.3	AGSE Prototype Control Circuitry	152
5.3.4	Final AGSE Image Processing and Object Detection Software	154
5.3.5	Final AGSE Control Circuitry	175
5.3.6	Iterative Development Progress Outline	183
5.4	Initial AGSE System Design.....	187
5.4.1	System Summary	187
5.4.2	Subsystems Overview	190
5.4.3	Prototype AGSE Fabrication and Verification	198
5.4.4	Lessons Learned from AGSE Prototype.....	200
5.5	Final AGSE Design	200
5.5.1	System Summary	200
5.5.2	Subsystems Overview	204

5.5.3	User Interface Panel.....	220
5.5.4	AGSE Fabrication and Verification.....	223
5.5.5	Workmanship and Mission Success.....	242
5.5.6	Testing and Verification	242
5.5.7	Integration Plan.....	244
5.5.8	Precision of Instrumentation and Repeatability of Measurement	244
5.5.9	Test and Measurement, Variables, and Controls	246
5.5.10	Expected Data and Accuracy/Error Analysis	247
5.5.11	Electronics Systems and Safety Switches.....	247
5.6	NASA Statement of Work Verification	247
5.7	Safety and Mission Assurance Analysis	253
5.7.1	AGSE Carrying Case and Transport.....	253
5.7.2	Preliminary Failure Modes Analysis	254
5.7.3	Personnel Hazards and Concerns.....	254
5.7.4	Environmental Hazards and Concerns.....	255
6	Failure Modes and Risk Assessment	256
6.1	Launch Vehicle	256
6.1.1	Vehicle Development Table	256
6.1.2	Vehicle Preliminary Failure Mode Analysis.....	260
6.1.3	Personnel Hazard Risk Assessment	268
6.1.4	Vehicle Environmental Hazards and Concerns	269
6.2	AGSE	272
6.2.1	AGSE Preliminary Failure Modes	272
6.2.2	AGSE Environmental Hazards and Concerns	276
7	Launch Operations Procedures.....	278
7.1.1	Launch Procedure Flowchart	278
7.1.2	Launch Checklists.....	279
7.1.3	Launch Abort Conditions.....	288
7.1.4	Post-Flight Inspection	289
7.2	Safety and Quality Assurance	289
7.2.1	Recovery Preparation.....	290
7.2.2	Motor Preparation	290
7.2.3	Igniter Installation.....	290

7.2.4	Launch Procedures.....	290
7.2.5	Troubleshooting	291
7.2.6	Post-flight Inspection	291
7.2.7	Additional Risks.....	291
8	Activity Plan	292
8.1	Budget Plan	292
8.1.1	Funding Plan	292
8.1.2	Itemized Budget	292
8.2	Timeline	303
8.2.1	Major Milestone Schedule	304
8.2.2	Critical Project Path	305
8.3	Educational Engagement Plan and Status	306
8.3.1	Educational Plan	306
8.3.2	Educational Lesson Plan Summary	306
8.3.3	Educational Lesson Plan Details.....	307
8.3.4	Educational Engagement Status.....	307
9	Conclusion.....	313
10	Appendix.....	314
10.1	Safety and Regulations Documents.....	314
10.2	Electrical Drawings	315
10.2.1	AGSE Statechart	315
10.2.2	Payload Bay Statechart	316
10.2.3	Payload Bay Control Electronics	317
10.2.4	AGSE Control Electronics.....	318
10.3	Project Timeline	320
10.3.1	Gantt Chart.....	320
10.4	Sources	324
10.5	AGSE Machining Plan	326
10.6	Machine Drawings	328

List of Figures

<i>Figure 1: Full CAD Rendering of Final Rocket Design</i>	30
--	----

Figure 2: Photo of Rocket Lying Horizontally in Acrylic Rocket Stands	30
Figure 3: Photo of Rocket Standing on its Tail Cone	31
Figure 4: Concept of Flight Operations	32
Figure 5: Tail section schematic demonstrating centering ring placement.....	33
Figure 6: Construction of Motor Mount	34
Figure 7: Block diagram of force transmission.....	34
Figure 8: Fin alignment jig	36
Figure 9: Dimensioned fin drawing	37
Figure 10: Method of Applying Carbon Fiber to Tailcone Section.....	38
Figure 11: Photo of Newly-Improved Tailcone Section.....	38
Figure 12: AGSE Table and Launch Rail Support	44
Figure 13: Vanderbilt Materials Science Hydraulic Press with Buckled Blue Tube Specimen ...	47
Figure 14: Results from Compression Test of Blue Tube in LABView Interface	47
Figure 15: Rocket Construction Flowchart.....	49
Figure 16: Risk Assessment Matrix.....	51
Figure 17: Pictures clockwise: (a) payload bay check out before launch, (b) launch pad checkout and rocket mounting, (c) perfect rocket flight, (d) complete recovery, (e) payload bay check out after launch.....	53
Figure 18: Avionics Bay Altimeter Data: (i) Altitude reached (3008 ft.); (ii) landing speed under rocket parachute ~ 40 fps., (iii) landing speed following payload jettison ~ 28.4 fps.....	54
Figure 19: Payload compartment altimeter data: (i) landing speed under rocket parachute 40 fps. (ii) landing speed under payload parachute 23.9 fps.	54
Figure 20: Comparison between simulated and actual flight data showing good parity between the two.....	56
Figure 21: Full-scale rocket design logic based on subscale flight and results	58
Figure 22: Evolution of the full-scale rocket from proposed to actual design following subscale flight studies.....	59

Figure 23: Flight 1 (a) take off at lower than anticipated speed, (b) motor burning through, (c) independent landing of payload and tail sections, (d) burnt-through tail section.....	61
Figure 24: (a) Altitude reached (1100ft) as opposed to a predicted altitude of 1990 ft.....	61
Figure 25: Flight takeoff and recovery in side winds, ideal trajectory and landing	63
Figure 26: (a) Altitude reached (1840ft) as opposed to a predicted altitude of 1850 ft.....	63
Figure 27: Payload bay motor-based activation and manual payload placement.....	65
Figure 28: Comparison of Key Criteria between Full-Scale and Subscale Flight Vehicles.....	65
Figure 29: Recovery System Flowchart.....	69
Figure 30: Recovery System Schematic	69
Figure 31: Recovery System Flowchart.....	71
Figure 32: Side View of Avionics Bay, blast caps visible.....	73
Figure 33: Arming Switches Mounted Inside Avionics Bay (Armable from Outside of Rocket in Launch Configuration).....	75
Figure 34: Bottom of Avionics Bay (Shock Cord U-Bolt Attachment can be clearly seen)	75
Figure 35: Altimeters mounted on tray, batteries mounted on back (Not Shown)	76
<i>Figure 36: Avionics mounting nuts embedded directly into central avionics bulkhead</i>	76
Figure 37: Diagram of Altimeters' Circuits	77
Figure 38: Ground-Based Deployment Testing	78
Figure 39: The Vanderbilt Shocktube acts as a convenient vacuum chamber for altimeter testing	79
Figure 40: Placement of avionics bay in the Vanderbilt Shocktube	80
Figure 41: Comparison of main and backup altimeter performance in vacuum chamber testing	81
Figure 42: Experimental Data from Shock Cord Yield Testing	83
Figure 43: Side View of Avionics Bay (Notice smaller compartment for mass ballast).....	84
Figure 44: Big Red Bee RF Transmitter	85
Figure 45: Kenwood D7 Radio	86

Figure 46: Payload bay RF transmitter mount.....	86
Figure 47: Location of Centers of Gravity and Pressure of Competition Rocket.....	88
Figure 48: The variation of landing drift and apogee with flight stability margin (there is a landing drift advantage, apart from additional stability, to flying at SSM of 1.85).....	89
Figure 49: Flight Acceleration vs. Time (maximum acceleration is +6g)	90
Figure 50: Flight Vertical Velocity vs. Time (maximum velocity at motor burnout is 450 fps). .	90
Figure 51: Flight Static Stability Margin vs. Time (stability margin quickly increase to 2.6 within seconds of flight).....	91
Figure 52: Cesaroni J380 Thrust Curve	92
Figure 53: Rocket Apogee vs. Wind Speed (11 mph ground winds are typical in April; -5 deg launch angle is most typical with S-N winds at the site)	92
Figure 54: Rocket Landing Drift vs. Wind speed (the landing drift is <2500 ft. for all possible flight conditions; typical would be 11 mph winds, -5 deg launch).....	93
Figure 55: Variation of apogee with flight coefficient of drag; apogee varies with flight CD, which will depend on the prevailing side wind conditions and the pitching of the rocket.	93
Figure 56: Wireframe Geometry of Fluid Domain (left) and Rocket (right).....	95
Figure 57: Mesh of Fluid Domain (left) and Rocket (right)	95
Figure 58: Close-Up of Tailcone Mesh (left) and Nosecone Mesh (right).....	96
Figure 59: Pressure Distribution over Surface of Rocket	96
Figure 60: Streamline Surrounding Rocket (left) and Vortices Forming behind Tailcone (right)	97
Figure 61: Streamlines around Rocket with Flow Perpendicular to Rocket Axis	98
Figure 62: Vortex Formation around Fins (left) and Nosecone (right)	98
Figure 63: Illustration of MATLAB simulation force balance and geometry	100
Figure 64: Comparison of drift predictions between Rocksim and own MATLAB code	101
Figure 65: Comparison of apogee predictions between Rocksim and own MATLAB code	101
Figure 66: CAD Rendering of First Payload Bay Design.....	115
Figure 67: Flowchart of Force Transmission in Payload Bay	116

Figure 68: CAD of Final Payload Design.....	117
Figure 69: Machined Internals of Payload Bay; 1 – Sabot, 2 – Payload, 3 – Payload Tray, 4 – Electronics Tray	118
Figure 70: Motor Mount and Forward Bulkhead.....	118
Figure 71: Payload Bay Motor with Wiring	119
Figure 72: Flowchart of Force Transmission in Final Payload Bay Design	119
Figure 73: Electronics Tray with Mounted Boards and Battery	120
Figure 74: Payload Bay Statechart.....	121
Figure 75: Female Bulkhead, Sample Tray, and Retention	123
Figure 76: Top: Payload Bay inserted into Rocket Body, Bottom: Breakaway connection.....	123
Figure 77: Disassembled Payload Bay	124
Figure 78: Rocket With Payload Bay Open.....	125
Figure 79: Payload bay altimeter and port holes	127
Figure 80: Payload bay vacuum chamber.....	128
Figure 81: Payload bay altimeter verification through comparison with avionics altimeters	129
Figure 82: Flowchart of AGSE Construction Phases	142
Figure 83: AGSE ROSML model snippets.....	146
Figure 84: AGSE Development GUI.....	147
Figure 85: Component-based software model of the AGSE. The main design of the components is that motor control components have timers (e.g. servoTimer) which run the control loops to ensure the current state reaches the goal state. These goal states can be set by clients (e.g. armRotation_client) which send a goal to the server and receive the current state of the motor (position or orientation) in the response from the server. The arm_controller component implements the high-level state control of the system and therefore has client objects which it can use in its timer operation to query the state of the system and update the goals for each of the subsystems of the AGSE. All components of the system subscribe to the controlInputs message, which is published by the user_input_controller component. This component is responsible for reading the state of the user input switches and sending that state throughout the system. In this way, all components can respond immediately to any commands, e.g. the pause command, and ensure proper state is maintained at all times.	150

Figure 86: Integration of Component-based software development with the AGSE electronics. Here, the Image Processing, path planning and high-level operation is handled by the NVIDIA Jetson TK1; The image acquisition and motor feedback and control is performed by a BeagleBone Black (BBB) that is located at the top of the AGSE (closer to the camera and the gripper). Lastly, another BBB handles the user control and operation.....	151
Figure 87: Statemachine implemented by the arm_controller component of the system. This is the high-level communications and control of the AGSE which relies on the lower-level motor control and feedback provided by other software components in the system.	152
Figure 88: Prototype motor control circuitry wired together on a breadboard. The BeagleBone Black (BBB) at the top of the image handles the GPIO control of the linear actuators' H-Bridges, the UART serial control of the 3 servo motors (which are daisychained), the prototype linear actuator analog position feedback, and the final AGSE linear actuator digital quadrature pulse encoded position feedback (shown unconnected).....	154
Figure 89: Object Tracking with OpenCV.....	156
Figure 90: Tracking a Blue Listerine Oral Mist.....	157
Figure 91: Tracking a Green Cupcake Box	157
Figure 92: Tracking in Low Light Conditions.....	158
Figure 93: Tracking Target Sample	159
Figure 94: Orientation Changes	159
Figure 95: AGSE Sample Detection Performed on typical “Lab” level lighting. Notice the bounding box and the additional levels of grayscale-based filtering in the center images. A bitwise-AND operation is performed on the HSV-based filter and the grayscale-based filtering schemes to obtain a more thoroughly filtered image in the bottom left.	160
Figure 96: AGSE Sample Detection in over-exposed environments. This is one of the tests that show the usefulness of a secondary processing technique (grayscale-based filtering) helps. The top right filtered image is the result of HSV-based filtering. The center-right image is the grayscale-based filtering image. Here, it is clear that the grayscale image has failed to help due to over exposure. However, by applying a bitwise AND-ing procedure, the filtered image resulting from a combination of the HSV and Grayscale-based filtered images is the best of both methods. Bottom Left, notice the improved filtered image that reduces the clutter and makes the sample stand out more clearly. From here, it is a simple algorithm to extract a candidate sample, based on its dimensions.....	161
Figure 97: AGSE Sample on a wooden plate.	162
Figure 98: AGSE Sample on a red cloth.....	163

Figure 99: AGSE Sample on a computer desk. Notice the bright light next to the sample that is completely filtered out by the processing	163
Figure 100: AGSE Sample on a brown carpet.....	164
Figure 101: AGSE Sample on a typical computer desk with other similarly colored objects....	164
Figure 102: AGSE Sample sitting on the shadow of a table.....	165
Figure 103: AGSE Sample under focused light.....	165
Figure 104: Another low light test with the camera closer to the sample.....	166
Figure 105: Multiple-Sample Detection at runtime.....	167
Figure 106: AGSE Sample Detection – MBA Outreach	168
Figure 107: Online processed image, shown to the audience	168
Figure 108: AGSE Sample Detection – Images acquired from Jetson TK1	169
Figure 109: Payload Bay Marker.....	170
Figure 110: This image is a good summary of our image processing. It shows both payload bay marker detection and sample detection with the camera mounted to the gripper. Notice in many of the filtered images, the gripper phalanges can be seen by the camera but are filtered out by image processing.....	171
Figure 111: Detection Markers attached to the Rocket Payload Bay Area. Notice in the bottom left, the filtered image shows that the marker on the left is affected by the tape used to hold it. The tape affects the white and black markings that are used for detection. This is the reason why in the detected image on the bottom right, only the right marker is detected. This indicates to us that the reflective nature of the tape affects payload bay detection and should therefore be avoided.....	172
Figure 112: Multiple Marker Detection with nearby payload. Each payload bay marker has an ID assigned at calibration time. Using the IDs of the detected markers, the camera position from the payload bay can be easily derived.	173
Figure 113: Camera detecting the payload bay and also a part of the sample. Notice that even though the sample is not completely visible, the image processing accurately detects a candidate. Secondly, notice the lighting around the gripper and a better taping technique – No part of the marker itself is affected by the taping as the tapes do not touch any of the black markings. This is a good representation of the robustness of our image processing algorithm.	174
Figure 114: Payload Bay Detection at an alternate angle with the payload bay not aligned with the plane of the gripper.	174

Figure 115: AGSE Motor Control Board Schematic.....	176
Figure 116: Board layout design and fabricated board for the AGSE BBB Motor Control cape (top). On the right side of the board, we have the 12V input for the power and motor circuits, as well as the 12V motor outputs for both the radial linear actuator and the vertical linear actuator (R Axis and Z Axis, respectively.). Also on the right side is the 12V servo motor connector which connects to all of the servo motors in the AGSE. The left side of the board connects to the two 5V quadrature encoders which provide feedback to the AGSE about the position of the two linear actuators. All components for the board will be mounted on the top of the board.....	177
Figure 117: Bottom of the AGSE Motor Control Board. Here you can see the underside traces for the board. Also included are relevant pictures the team wanted to have on the board reflecting our love of aerospace engineering and space exploration.....	178
Figure 118: Fabricated AGSE Motor Control BBB Cape.	179
Figure 119: Completed AGSE Motor Control BBB Cape mounted as a cape on the BBB.	179
Figure 120: BBB Cape with MOSFETs Shown	180
Figure 121: Connectors attached to BBB Cape	181
Figure 122: 7" Touchscreen Cape attached to BBB	181
Figure 123: Underside of Screen Attached to BBB	182
Figure 124: Team P.R.I.S.M. Automated Ground Support Equipment (CAD and Physical Prototype).....	188
Figure 125: AGSE Maximum and Minimum Reach	188
Figure 126: Sample to be retrieved by AGSE	189
Figure 127: Visual representation of the operational workspace of the AGSE	189
Figure 128: Integrated Dynamixel turntable with integrated DC motor.....	190
Figure 129: Turntable Base Attached to Plywood Base. The donut (bottom acrylic piece) attaches to the thin turntable disc. The acrylic baseplate bolts to the donut. The vertical guide rods are fit through both acrylic pieces and attached with shaft collars.	191
Figure 130: Another view of the AGSE base. The bolts connecting the acrylic baseplate and donut can be seen.....	191
Figure 131: Vertical stage, supported by thrust bearings on four steel guide rails.....	192
Figure 132: View of vertical linear actuator mounted on AGSE base	193

Figure 133: Top plate attached after vertical carriage is installed	193
Figure 134: Gripper Arm Supporting Gripper	194
Figure 135: CAD Model of Modified Gripper Design	195
Figure 136: Prototype AGSE Gripper.....	196
Figure 137a-b: Original Gripper in Open and Closed Configurations	196
Figure 138: Flowchart of AGSE Prep Work.....	199
Figure 139: Flowchart of Overall AGSE Construction	199
Figure 140: Flowchart of AGSE Base and Tower Construction	199
Figure 141: Flowchart of Vertical Carriage Construction	199
Figure 142: Flowchart of Gripper Construction	199
Figure 143: Flowchart of AGSE Arm Construction	199
Figure 144: Full AGSE CAD Render	202
Figure 145: Maximum reach of the AGSE is 25 ½ inches above the ground and 19 ½ inches from the central rotation axis.....	203
Figure 146: Minimum reach of the AGSE allows it to reach the ground and its own table, approximately 3 inches from its center axis.	203
Figure 147: Faulhaber 2237S012CXR Motor.....	207
Figure 148: Motor with Gearhead Attached	208
Figure 149: Speed vs. Torque for 2237S0xxCXR series Motor with our Motors' Operating Conditions.....	209
Figure 150: CAD Rendering of AGSE base featuring acrylic servo mount (left) and adjustable length legs	210
Figure 151: AGSE Render of profile view of AGSE table. Servo connects to pulley and timing belt, rotating the bottom pulley to spin the main AGSE tower.....	211
Figure 152: AGSE Table Underside, featuring pulleys and timing belt to drive main rotation .	211
Figure 153: CAD Render of the AGSE Tower encoder and motor mount.....	212
Figure 154: CAD Render of the AGSE vertical carriage.	213

Figure 155: CAD Render of the horizontal plates, separated by acrylic plates	214
Figure 156: CAD Render of camera mounted on AGSE wrist dropdown from horizontal carriage	215
Figure 157: CAD Render of underside view of AGSE gripper and horizontal carriage. Camera is mounted above the gripper on the acrylic-mounting wrist.	216
Figure 158: CAD Render of open (left) and closed (right) gripper configurations.	217
Figure 159: Foam Lined Gripper Phalange	217
Figure 160: Top-Down View of UIP.....	221
Figure 161: Different Views of UIP CAD with Dimensions.....	221
Figure 162: Screen attached to BBB showing Payload Bay and Sample Detection	222
Figure 163: Flowchart of Overall AGSE Construction	223
Figure 164: Flowchart of AGSE Prep Work.....	223
Figure 165: Exploded View of Rotational Table Elements.....	224
Figure 166: AGSE Table CAD	224
Figure 167: Top (left) and Bottom (right) view of Servo Sled CAD.....	225
Figure 168: Servo Spindle CAD	225
Figure 169: Servo Shaft CAD	226
Figure 170: Bearing Cup CAD	226
Figure 171: Baseplate CAD	227
Figure 172: Vertical Carriage Plate CAD	227
Figure 173: Side Plate CAD	228
Figure 174: Horizontal Carriage Plate CAD.....	228
Figure 175: Horizontal Motor Mount CAD.....	229
Figure 176: Vertical Motor Mount CAD	229
Figure 177: Flowchart of AGSE Base Construction.....	230

Figure 178: Flowchart of Vertical and Horizontal Carriages Construction.....	231
Figure 179: Flowchart of Tower Assembly	234
Figure 180: Flowchart of Gripper and Arm Construction	236
Figure 181: AGSE Legs fit through the bottom of the mock carrying case	253
Figure 182: Prototype AGSE Secured in Mock Carrying Case.....	254
Figure 183: Flowchart of Launch Day Procedures	278
Figure 184: Pie Chart of Incurred Costs	293
Figure 185: Pie Chart of Projected Costs.....	293
Figure 186: Critical Project Path.....	305
Figure 187: Pre- and Post-Outreach Statistics for Rural Schools	309
Figure 188: Test Results Before and After Outreach.....	309
Figure 189: Results of Hunters Bend Outreach Evaluation.....	310
Figure 190: 7 th grade students at Winfree Bryant Middle School learn more about the shape and purpose of fins on a rocket.....	311
Figure 191: AGSE Statechart.....	315
Figure 192: AGSE Statechart with Payload Bay Interaction.....	315
Figure 193: Payload Bay Statechart.....	316
Figure 194: Payload Bay Control Electronics	317
Figure 195: AGSE Buffer Circuit Diagram	318
Figure 196: AGSE Motor Control Diagram for Linear Actuators.....	319
Figure 197: Gantt Chart for Rocket Portion of Project.....	320
Figure 198: Gantt Chart for Payload Bay Portion of Project.....	321
Figure 199: Gantt Chart for AGSE Portion of Project.....	322
Figure 200:Gantt Chart for NASA Timeline	323
Figure 201: Machining Plan Developed by Team for AGSE	326

Figure 202: Sample Detail Table of AGSE Machined Part for Back Side Plate within Vertical Carriage.....	327
---	-----

List of Tables

Table 1: Comparison of Flight Predictions with Results	55
Table 2: Details of the first flight showing that the landing energy criteria and the payload ejection and landing criteria were successfully met.....	62
Table 3: Details of the second flight showing that the landing energy criteria and the payload ejection and landing criteria were successfully met.	64
Table 4: Comparison of Key Parameters for Full-Scale Launch vs. Subscale Launch	66
Table 5: Full-Scale Vehicle Mass	67
Table 6: Subscale Vehicle Mass Limits	68
Table 7: Vacuum Chamber Test Results for Altimeters	82
Table 8: Results from Shock Cord Yield Testing	83
Table 9: Final Launch Vehicle Parameters	87
Table 10: NASA Statement of Work Verification Plan.....	103
Table 11: Chemicals and Material Safety Hazards	113
Table 12: Payload Bay Testing and Verification.....	125
Table 13: Vertical Motor Selection Spreadsheet.....	206
Table 14: Horizontal Motor Selection Spreadsheet	207
Table 15: Verification and Testing of AGSE Table	231
Table 16: Vertical and Horizontal Carriage Verification and Testing	233
Table 17: Tower Verification and Testing	235
Table 18: Gripper and Arm Verification and Testing	237
Table 19: Overall Systems Verification.....	238
Table 20: Integrated Systems Verification	241
Vanderbilt University – Flight Readiness Review	17

Table 21: Verification Status	243
Table 22: Project Management Risk and Mitigation	256
Table 23: Vehicle Failure Modes and Risk Assessment.....	260
Table 24: Propulsion Failure Modes and Risk Assessment.....	263
Table 25: Recovery System Failure Modes and Risk Assessment	264
Table 26: Personnel Hazard Risk Assessment.....	268
Table 27: Environmental Impact on Rocket	269
Table 28: Rocket Impact on Environment	271
Table 29: AGSE Structural Failure Modes	272
Table 30: AGSE Electrical Failure Modes	273
Table 31: AGSE Software Failure Modes and Development Risks	274
Table 32: Environmental Impact on AGSE	276
Table 33: AGSE Impact on Environment.....	277
Table 34: Itemized Budget and Projected Costs	294
Table 35: Parts List As Flown.....	298
Table 36: Costs as Flown	303
Table 37: Machine Drawings Parts Tree	328

1 General Information

1.1 Faculty Advisors

1.1.1 Project Advisor

Dr. Amrutar Anilkumar
Professor of the Practice
Department of Mechanical Engineering
Amrutar.V.Anilkumar@Vanderbilt.edu

1.1.2 Outreach Advisor

Dr. Heather Johnson
Assistant Professor of the Practice of Science Education
Department of Teaching and Learning
Heather.J.Johnson@Vanderbilt.edu

1.2 Mentors

1.2.1 Safety and Rocketry Mentor

Robin Midgett
Safety and Rocketry Mentor
Senior Electronics Technician
NAR Level II Certified
Department of Mechanical Engineering
Robin.Midgett@Vanderbilt.edu

1.2.2 Robotics Mentors

Ben Gasser
Graduate Student, Mechanical Engineering
Benjamin.W.Gasser@Vanderbilt.edu

Brian Lawson, PhD
Post-Doctoral Researcher, Mechanical Engineering
Brian.E.Lawson@Vanderbilt.edu

1.3 Team Members

1.3.1 Project Coordinators

Dexter
President, Rocket Project Coordinator
Graduate Student, Mechanical Engineering
Dexter.A.Watkins@Vanderbilt.edu

William
AGSE Project Coordinator
Graduate Student, Electrical Engineering
Emfinger@isis.Vanderbilt.edu

Pranav
AGSE Project Coordinator
Graduate Student, Electrical Engineering
PKumar@isis.Vanderbilt.edu

Toshia
Outreach Coordinator
Graduate Student, Chemistry
Toshia.L.Wrenn@Vanderbilt.edu

Anna
Outreach Assistant
Graduate Student, Materials Science
Anna.E.Sandberg@vanderbilt.edu

1.3.2 Senior Design Team

Fred
Vice President, Design Engineer
Senior, Mechanical Engineering
Frederick.R.Folz@Vanderbilt.edu

Connor
Safety Officer, Treasurer, Design Engineer
Senior, Mechanical Engineering
Connor.R.Caldwell@Vanderbilt.edu

Jacob
Secretary, Design Engineer
Senior, Mechanical Engineering
Jacob.D.Moore@Vanderbilt.edu

Chris
CFD, Design Engineer
Senior, Mechanical Engineering
Christopher.T.Lyne@Vanderbilt.edu

Cameron
Design Engineer
Senior, Mechanical Engineering
Cameron.P.Ridgewell@Vanderbilt.edu

Alex
Design Engineer
Senior, Mechanical Engineering
Alexander.J.Goodman@Vanderbilt.edu

1.3.3 Field Engineers

Mitchell
Junior, Computer Engineering
Mitchell.J.Masia@Vanderbilt.edu

Andrew
Junior, Mechanical Engineering
Andrew.D.Voss@Vanderbilt.edu

Myles
Junior, Mechanical Engineering
Myles.A.Lacy@Vanderbilt.edu

1.4 NAR Association

Music City Missile Club, NAR #589
Officers: Brian Godfrey, *President*
 Chris Dondanville, *Vice-President*
 Robin Midgett, *Treasurer*, treasurer@mc2rocketry.com
 Fred Kepner, *Secretary*
 Russ Bruner, *Advisor*

1.5 Vanderbilt Aerospace Club Constitution

Preamble:

The Vanderbilt Aerospace Club is a volunteer student organization that has two primary purposes: it competes in the NASA SL (Student Launch) Rocket Competition and conducts aerospace related educational outreach to middle schools and high schools in Middle Tennessee. The Aerospace Club activities apply directly to Engineering students and their practice, as well as to students from schools of Arts and Science, educating those who may be interested in school science teaching.

Constitutional Articles:

- a.** The Aerospace Club must have a mechanical engineering professor who serves as the faculty advisor. In addition, the club must also have a financial advisor pursuant to Vanderbilt policy.
- b.** All students are welcome to participate in the aerospace club with caveat that the largest membership that can compete and be active in the SL competition is 15 members; however, preference is given to upperclassmen (seniors and juniors).
- c.** Students who want to join the club and compete in the SL competition must demonstrate qualities that will contribute to the club's mission and success at the competition. Such qualities may include prior rocketry experience, interest in aerospace engineering or science teaching as a career, a good academic standing, and a strong work ethic in a field that is of use to the team (particularly educational outreach or engineering).
- d.** The club meets every Thursday from 12:15-1:00 in the Mechanical Engineering Hall in Olin School of Engineering.
- e.** The NASA SL Competition serves as the senior design project for the Mechanical Engineering Curriculum.
- f.** Members of the Aerospace Club who participate in the SL Competition must be actively involved in the club and dedicate several hours per week to working on competition related items.
- g.** The members of the Aerospace Club must actively seek to promote Aerospace and STEM education and outreach in Middle Tennessee.
- h.** The President, Vice President, Secretary, and Treasurer of the Aerospace team that participates in the SL Competition must be recommended by the Aerospace Club faculty advisor.
- i.** Any amendments to this Constitution can be made by a vote of the members and approved by the faculty advisor.

Member's Rights and Expectations

- j.** Any member of the Vanderbilt Aerospace Club cannot be discriminated based on sexual orientation, gender, race, ethnicity, or socio-economic class.
- k.** Members of the Vanderbilt Aerospace Club must show an enthusiastic and professional involvement in the club.
- l.** Any member who is a part of the SL competition must represent Vanderbilt University with all due decorum and professionalism.

2 Summary of Project

2.1 Team Summary

The Vanderbilt University Aerospace Club is a student organization located in Nashville, Tennessee. The Project Faculty Advisor is Dr. Amrutur Anilkumar, Professor of Mechanical Engineering, and the Safety and Rocketry Mentor is Robin Midgett (NAR Level II Certified, NAR #589). The club's Outreach Advisor is Dr. Heather Johnson, Assistant Professor of the Practice of Science Education in the Department of Teaching & Learning. The mailing address of the club is as follows:

Amrutur Anilkumar
Department of Mechanical Engineering
VU Station B #351592
2301 Vanderbilt Place
Nashville, TN 37235-1592

2.2 Launch Vehicle Summary

Vanderbilt's full scale rocket will have a body diameter of 4", an overall length of 58.4", and an overall weight of 14.5 lb. (11.65 lb. w/o motor). The selected motor is a Cesaroni J 380, which is an off-the-shelf reloadable 54 mm motor. This specific motor has been chosen for its short burn time of 2.7sec allowing for higher initial vehicle velocity as the rocket departs the launch rail causing straighter flight while remaining subsonic throughout ascent. The predicted and targeted altitude of the rocket is 3065ft AGL. The recovery system for this rocket is a simple deployment system comprised of a rocket parachute deployed at apogee and a nose cone section deployed at 1000ft AGL for a separate recovery of the payload. The recovery system is controlled by a redundant pair of barometric pressure based altimeters. The payload will be housed in the nose cone of the rocket and will contain its own parachute and altimeter in order to ensure safe return to the launch area after jettisoning from the rocket body.

Vanderbilt's subscale model has a body diameter of 4", an overall length of 64" and an overall weight of 13.8 lb. (12.25 lb. w/o motor) including payload. The selected motor for the subscale launch vehicle was a Cesaroni J 330, which again was chosen for its short burn time of 2.3sec as well as a similar propulsive profile to ensure similar G-levels at takeoff and similar rail exit velocities between the subscale and full scale models. This model had a predicted and targeted altitude of 1850ft AGL. The recovery system for the subscale rocket was a simple deployment system, comprised of one rocket parachute deployed at apogee. The payload section was deployed at 800ft and had a dedicated parachute to ensure safe landing.

2.3 AGSE/Payload Summary

The task of safely and autonomously lodging the payload in the rocket payload bay requires a degree of precision that is relatively unobtainable by most vehicular robotics. As a result,

Vanderbilt will be constructing a robotic arm with 4 degrees of freedom and a textured gripper to securely transport the payload from the ground to the payload bay. This system will allow for the verifiable retrieval and storage of the payload once it is placed near the base of the rocket. The Payload Retrieval and Internal Storage Module (P.R.I.S.M.) system is designed primarily around creating a robust and secure design that will be able to locate and deposit the payload in a secure compartment that will restrain it for flight. Ultimately, this design is built to complete the task objectives quickly and reliably.

The four degree-of-freedom AGSE design integrates a combination of two revolute joints for orientation purposes and full rotation about the center axis with a series of two prismatic joints. These two prismatically actuating joints, from which the name P.R.I.S.M. is derived, allow the robot to translate vertically as well as radially from the revolute center axis. This allows the robot to operate within a set of predictable cylindrical coordinates, eliminating revolute joint-based singularities in the robot's vertical and horizontal trajectories. Though the design does put limits on the vertical and horizontal ranges of the AGSE, it will allow for easy access of both the payload and the payload bay without interfering with the rocket body.

3 Changes Made Since CDR

3.1 Changes Made to Vehicle Criteria

Both the rocket and payload parachutes have been reduced to 30" elliptical parachutes. This modification allows for lower drift while still satisfying the maximum landing energy requirement.

Other than this change to the recovery system, the rocket is the same as the one shown in CDR.

3.2 Changes Made to Payload/AGSE Criteria

The payload bay now includes a breakaway connector that provides a method for communication between the AGSE and payload bay in addition to the Hall Effect sensor. Upon the team's raising of the rocket, the magnetic breakaway connect disconnects easily and automatically as the rocket is readied for launch. Additionally, the design of this magnetic breakaway connector is such that it passively rejects connection attempts which would lead to incorrect circuit connections.

The AGSE system has evolved significantly since CDR. Rather than using off-the-shelf linear actuators, the team has decided to use motor and lead screw systems, a design used in the payload bay. The team has used lessons learned from the fabrication and assembly of the payload bay to design the new AGSE system. In addition to this modified method of actuation, a table for the AGSE has been designed that allows the rocket to be laid horizontally on it during competition. This table also includes a new rotational system for the AGSE tower that reduces wobble during movement as compared to the old turntable design. The table has adjustable legs much like the rocket launch pad.

The AGSE electronics hardware has evolved through a few different iterative testing phases as well. Having developed the initial prototype AGSE, which met NASA's requirements for sample retrieval and insertion as outlined in the RFP, and which was demoed for CDR, we took the lessons we learned about the electronics, control systems, and motors and developed a more reliable, simpler, and more capable design for our final AGSE. Having ironed out the issues of controlling many different types of motors simultaneously (e.g. DC linear actuators, PWM-based servos, 12V servos, and 7V servos), we homogenized the electronics of the AGSE where we could to improve the reliability of each of the systems by decreasing both hardware and software complexity. As such, our AGSE is now designed around 12VDC motors for linear actuation and 12VDC servo motors for controlling all of the rotary degrees of freedom of the AGSE. Furthermore, we iterated through lessons learned from the hardware/software interface, such as overcoming the lack of available and usable inputs to our main processing board (the Nvidia Jetson TK1). We found that the Jetson did not provide either the required general-purpose input/output (GPIO) or the required special purpose I/O such as analog-to-digital conversion (ADC) or quadrature pulse decoding, both of which are useful for linear actuator positioning feedback.

Additionally, the software for the AGSE has seen dramatic improvements since CDR. While the main AGSE software (which is written in C++ and utilized the Robot Operating System middleware, ROS) was being developed, the prototype control code (written in python) was also developed. We developed these two code-bases in parallel to meet our own deadline of a functional prototype AGSE by CDR. However, since CDR, the team has finished the development of the final AGSE software, written in C++ and using ROS. The final AGSE software consists of (1) a software component-based modeling language which allows us to specify high-level system properties and requirements, (2) code generators which allow us to generate executable code from the models that is verified to conform to the models and which performs the desired task of each specific component of the AGSE, and (3) the implementation code for each software component which allows us to perform the mission specific tasks such as motor control, sample detection, and payload-bay detection. Using these tools we developed, we were able to increase the reliability of the AGSE system and decrease the development and testing time required for performance verification.

3.3 Changes Made to Project Plan

Because of inclement weather and FAA permit issues in February, the full-scale launch was moved to March 15, 2015.

All other changes about the actual implementation of the project design can be found in the appendix, section *10.3: Project Timeline*.

3.4 CDR Feedback Response

1. The plots from the altimeter data show outlier points at the drogue and main chute deployment events. Can the team explain the origin of these points and the possible impact they can have on recovery?

The altitude data is based on pressure readings in the avionics bay, which is open to the outside through small holes. Most of the time, this means that the pressure in the bay is equal to atmospheric pressure, but during deployment events, some of the pressure from the black powder explosion in the adjoining chamber leaks into the bay causing a spike in pressure which is read as a massive drop in altitude. In theory, this could trip additional charges by simulating a rapid descent. In our case, this would mean “tricking” the altimeters into deploying the payload bay at apogee rather than 1000 ft.

This is a known problem in rocketry, which has been solved by the manufacturers of the altimeters. There is a small delay period where the altimeter waits to ensure that an increase in pressure is sustained before responding. The separation event and openings in the avionics bay drain the additional pressure back to atmospheric long before the altimeters register the change as “real.”

Although this alone would be sufficient to solve the problem, the team also takes steps to mitigate the effect as much as possible. Sealant is used around the edges of the bay and all holes (typically for wires or mounting). Because the altimeters are designed to handle this, the more

pressing concern is actually the physical effect of the pressure wave on the electronics within the bay. If too much is allowed to pass through, wires could be disconnected, or boards damaged. Our current sealant has been successfully used to avoid this problem for many years now, so the team is satisfied that it will not be a problem.

Another concern is the main and the back-up charges going off at the same time at apogee. The intensity of the blasting process could generate forces large enough to deploy the payload section at apogee, especially if the payload shifts in the payload compartment or if the payload section is not properly harnessed by an adequate number of shear pins. The solution to this potential problem is to deploy the back-up charge after a suitable delay so that an intense blast wave is not generated with two charges going off simultaneously.

2. Can the team elaborate on the weather cocking the sub-scale rocket experienced during launch?

The rocket was subjected to unsteady side winds early in flight causing light cocking beyond typical equilibrium for the mean wind conditions. The stabilizing response from the fins (characterized by the static stability margin and rail exit velocity) was sufficient to right the course of the rocket without any oscillatory over-correction (which results from “over-stable” design such as stability margins greater than about 1.8), so the vehicle returned to the expected trajectory. The 16 ft launch rail (double the typical length) allows our rocket to reach higher speeds before being subjected to moments from the wind, this has been shown through several launches to be the most effective setup, as it allows us to remain dynamically stable in unsteady winds with a lower stability margin and thus gives us a less extreme loss of apogee altitude under higher steady wind speeds.

In the first subscale flight, wind cocking was exacerbated by a ‘failing thrust scenario,’ as the motor burnt through the casing and the rocket flight was underpowered. In the subsequent flight (subscale flight 2), wind cocking was not a problem, despite the rocket taking off in high winds (>11 mph). The stability mechanism in the rocket worked well. Here, with a higher thrust motor, wind cocking could have been lower. For the NASA SL, the rocket motor chosen is a J380, which will meet the slightly higher thrust requirement, while keeping the overall launch mass the same. Regardless, since the motors chosen are commercial solid propellant motors, one has to arrive at a selection compromise keeping the structural, dynamical, and apogee issues in mind.

3. Does the boat tail serve as motor retention, or is just for aerodynamic purposes? If it is not for retention, what form of motor retention is the team using?

The boat tail is solely an aerodynamic component, reducing flow separation and thus decreasing the axial drag coefficient. It provides no motor retention or support. Our motor is retained using the AeroPack motor retainer which we purchased from Apogee Rockets. This motor retainer is a two piece system, one male and one female threaded piece. The male piece is epoxied onto the motor tube before insertion of the motor. Once the motor has been placed within the motor tube, the female piece is threaded onto the male piece, securing the motor in place. There is a lip at the nozzle of the motor that rests on a similarly sized lip in the motor retainer that transfers the thrust

of the motor into the motor tube and subsequently to the body of the rocket through the retaining bulkheads. The female piece also helps to hold the motor inside the rocket after burnout.

4. How is the payload compartment locked in place?

The motor turns the leadscrew until the male aluminum bulkhead is compressed against the female bulkhead. The leadscrew system is non-backdrivable, so no axial force can actuate it. The Hall Effect sensor that is used to actuate it functions through a state system in which the payload bay is locked either open or closed until it receives a signal to actuate. In order for the Hall Effect sensor to give a positive signal, a strong magnet must be held against it for a constant 3 seconds. This time delay guarantees that there will be no false positive signals that may accidentally open or close the payload bay unless it is supposed to. Please refer to the state charts included in the Appendix for more information on the actuation of the payload bay.

5. During the presentation, the reviewers heard that the rocket emits an EM field. Is this correct? If so, what kind of impact will this have on electronics?

The rocket does not emit an EM field. The previous design used a Hall Effect sensor to look for a magnet on the gripper of the AGSE, but this is orders of magnitude too far away to affect the avionics. Furthermore, that system of communication has since been replaced with a pull-away connection that will allow the AGSE to pass the pause command to the payload bay. Either way, the rocket's electronic systems are in no danger of being affected by EM fields from any of the rocket or AGSE subsystems.

6. Where will the team acquire its meteorological data from?

Ultimately, the targeting accuracy (apogee) of the rocket will depend on the prevailing winds. And hence, despite the most accurate modelling, there is an element of chance. While the pad weight cannot be changed prior to NASA SL, nevertheless, it would be necessary to stay on top of the wind data.

We have on hand a Kestrel hand held anemometer to provide wind speeds at ground level (~5ft). However, wind speeds at 30ft would be more appropriate. These will be gathered through these weather monitoring stations nearby to the launch field:

- i. KALTONEY14 (Toney Alabama)
- ii. KMDQ Weather, nearest airport to Toney Alabama.

For the Manchester launching grounds, it would be (i) KTNMANCH10, and (ii) Tullahoma Regional Airport.

7. The team mentioned during the presentation that it plans to control drift through operation and not design. Operation is not something that can be controlled easily. It is much easier to control something's design than its operation.

Design is the key to this process, unless, it turns out that there is a possibility that the rocket can be launched into the winds and the wind direction is suitably oriented away from the crowds.

A history of prevailing winds in April in Toney, AL, does lend credence to this scenario; but, clearly it is too specific to the geographics and makes launch a chancy process. From a design standpoint, there are two aspects to drift that need to be noted. (1a) If the rocket is way over stable ($SSM > 2$), it will curve into the winds and show a larger drift at apogee, and thereby, will land closer to the launch pad when returning back to ground. The penalty paid here would be a lower apogee. (1b) If the rocket's stability is just right (~ 1.5), then it will drift less at apogee but land farther from the launch site with the same side winds. (2) Drift from the launch pad can be better controlled through the selection of the landing parachutes, where the landing speeds can be kept higher and the landing time reduced (provided the landing energy requirements are met).

With these considerations in mind, the team has changed the rocket parachutes from a 4ft simple bell parachute to an elliptical 3ft one.

4 Vehicle Criteria

4.1 Design and Construction of Launch Vehicle

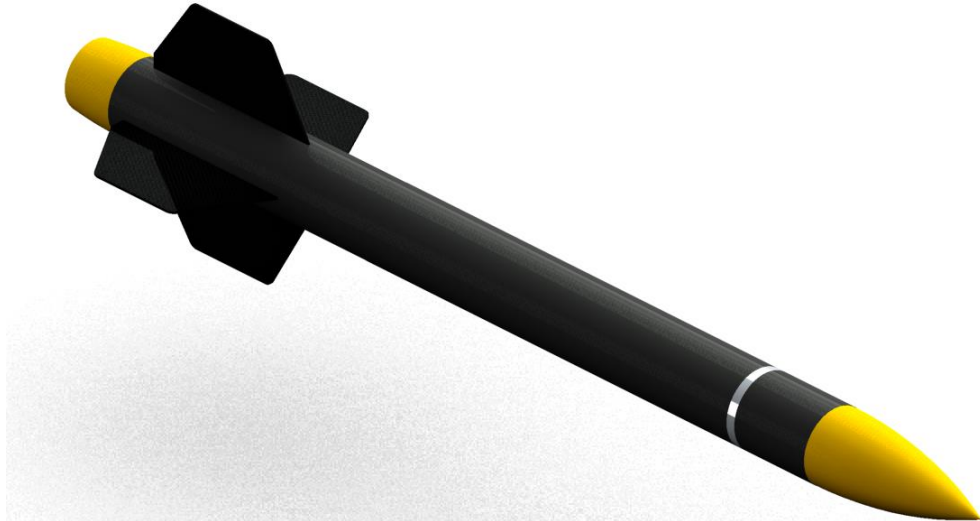


Figure 1: Full CAD Rendering of Final Rocket Design



Figure 2: Photo of Rocket Lying Horizontally in Acrylic Rocket Stands



Figure 3: Photo of Rocket Standing on its Tail Cone

4.1.1 Systematic Launch Vehicle Design Review

The Vanderbilt Aerospace Club's Student Launch vehicle has been designed to receive the sample from the AGSE and then take it to the prescribed apogee of 3000ft AGL and jettison it at 1000ft AGL. In addition, it is designed to be successfully recovered such that it can be reused if desired. Our launch vehicle has a body diameter of 4", with a length of 58.4", and has an assembled pad weight of 14.45 lb. This requires smaller, separable sections to facilitate transportation and assembly. The concept of flight operations is illustrated below, in *Figure 4*.

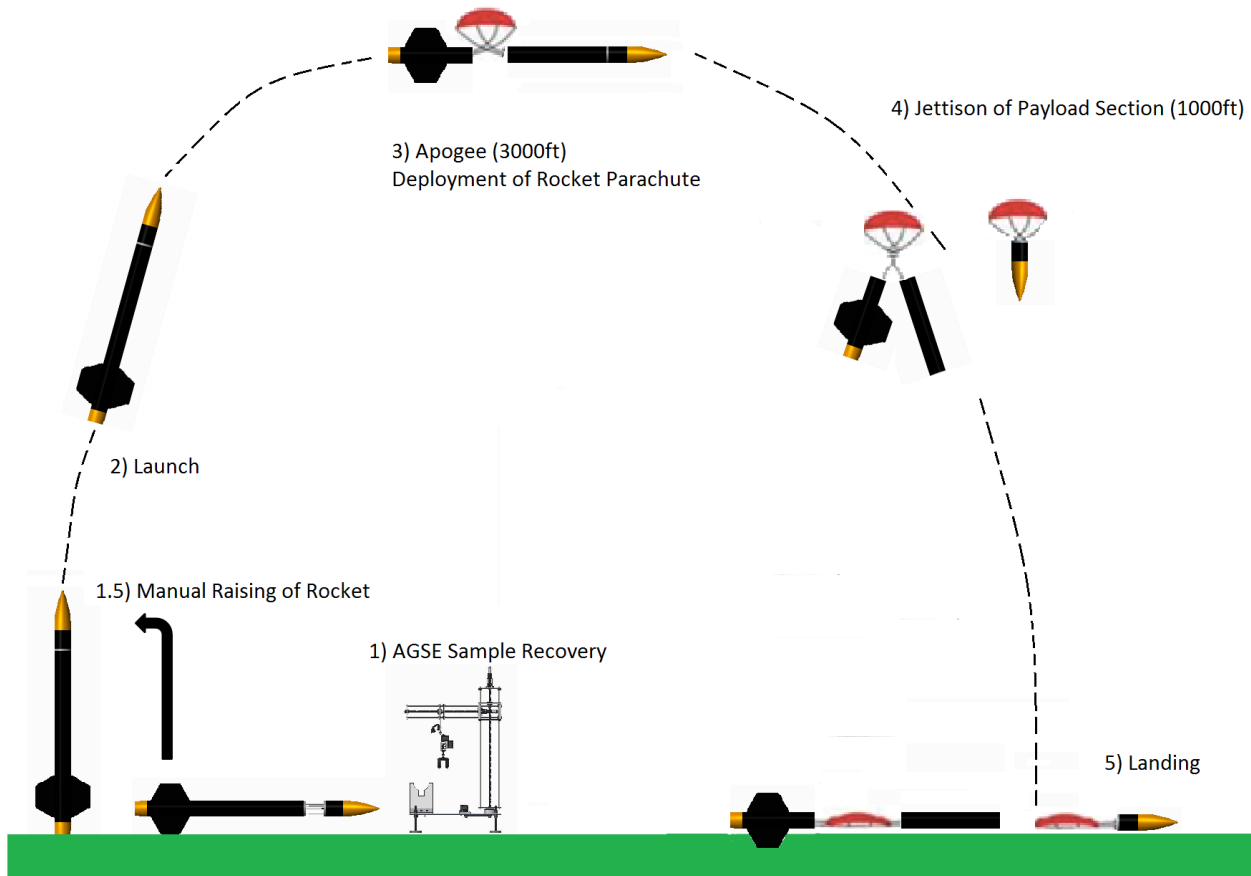


Figure 4: Concept of Flight Operations

The vehicle systems will be described in detail along with their functional requirements and performance characteristics. The systems are as follows:

1. Propulsion
2. Stability
3. Structures
4. Aerodynamics
5. Recovery
6. Electronics

4.1.1.1 Propulsion

The function of the Propulsion System is to launch the rocket from the ground into flight with the proper amount of thrust. The Motor, Motor Retention, and Launch-Rail Interface are the subsystems of the Propulsion System. The propulsion subsystems are described below.

4.1.1.1.1 Motor Selection

Motor selection is a critical first step in rocket design that directly impacts all subsequent design decisions. For this rocket, the chosen motor is a Cesaroni P54-3G J380 Smoky Sam. This 54mm

motor will give us a more constant thrust curve as well as a high exit velocity in order to ensure straight flight with a minimal static stability margin. With a 2.7sec burn time, the maximum generated thrust is 434.6N and the average generated thrust is 386.3N. The total weight of the motor is 2.85lb and the final weight of the motor after burnout is 1.16lb. Thrust curve data for this particular motor can be obtained and was used in our rocket simulations. This is discussed more completely in section 4.6.4: *Simulations and Predictions*.

4.1.1.2 Motor Retention

The substantial force of the rocket motor on the rocket body (resultant from a peak of ~ 10 g's acceleration at launch) necessitates a very robust motor retention system. This system not only has to withstand tremendous amounts of force but also must resist off-axis vibration to ensure straight flight. This motor retention system, working in coordination with the fin centering rings, is shown below, in *Figure 5*. A picture of the subscale rocket's motor sleeve section with retention rings exposed is shown in *Figure 6*.

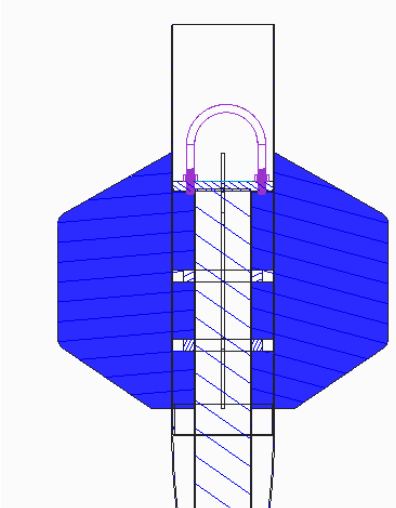


Figure 5: Tail section schematic demonstrating centering ring placement



Figure 6: Construction of Motor Mount

The motor tube is a 54mm blue tube sleeve made to fit around the motor casing of the 54mm motor we will be using. There is a solid bulkhead made of 3/8" thick plywood at the front section of the motor mount with a slight indentation to allow the motor mount tube to center on the bulkhead. There are then three more centering rings evenly spaced along the motor mount to distribute the forces of launch evenly. Each centering ring is epoxied to the motor mount tube with smooth 2-ton epoxy fillets. The centering rings are also epoxied to the four fins in a similar manner. The fins are then epoxied to the outer tube of the body to complete the force transmission to the rocket body (more detail in section 4.1.1.2: *Stability System*).

The following block diagram shows how the force of the motor is transmitted to the rocket body:

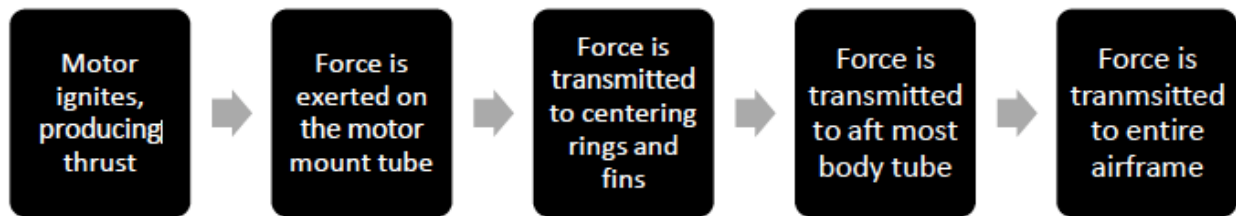


Figure 7: Block diagram of force transmission

4.1.1.1.3 Launch-Rail Interface

We will be utilizing button-style screw launch lugs as rail guides for our launch vehicle. The base of the rail guide that interfaces with the rocket body tube will be held in place by carefully inserting a wood screw through its central cavity into the middle centering ring of the motor mount. The first lug will be placed precisely halfway between two of the fins on the tail section to ensure no interference between the fins and the rail during launch. Then, a string is tied to the first launch lug and pulled taut to the tip of the rocket nosecone. This gives a perfect axial line

down the rocket along which the second launch lug is installed. It is installed just below the avionics bay in the forward section so that it is as close to the CG as possible without interfering with avionics bay insertion.

4.1.1.2 Stability System

The Stability System ensures that our rocket will fly as high as desired and as straight as possible. The two subsystems that affect Stability are Rocket Fins and Mass Adjustments. The stability subsystems are described below.

4.1.1.2.1 Fins

Symmetry is essential in the design of the fins because an asymmetric design would generate a moment about the center of mass of the rocket. This symmetric design is possible with three fins, but much more feasible with four fins. Thus, we decided to build the four fin design using a jig to ensure that the fins are mounted at perfect right angles to each other.

The strength of these fins and this “through-the-wall” design, along with the suitability of the material, has been verified through previous years’ experiences and tests as well as test launches earlier this year. This year’s team will also test this design during a full-scale launch before competition. The fin stability system has been considered successful based on the following criteria: (i) there is no visible damage to the fins upon recovery (cracks, breaks, chips, etc.), and (ii) the trajectory of the rocket is largely straight and vertical.

The design of the fin assembly is dictated by the necessary strength and robustness the fins must have in order to achieve a stable and safe flight. To address the issue of strength, the fins are constructed out of Dragon Plate 1/8” quasi-isotropic carbon fiber sheet. This material is selected for its strength, resistance to vibration, rigidity, and precision when forming. The advantage of using the carbon fiber material is that it provides an unparalleled strength to weight ratio. Since carbon fiber is supplied in plies, a water jet cutter is used to cut the shape specified by our CAD drawings out of a sheet of carbon fiber.

Once the fins are cut, they will be permanently joined to the rocket motor tube using the rocket fin assembly jig fixture (*Figure 8*) that was built with laser cut components and is displayed below. This fixture is essential in order to be sure that the fins are mounted properly, in the exact desired location.

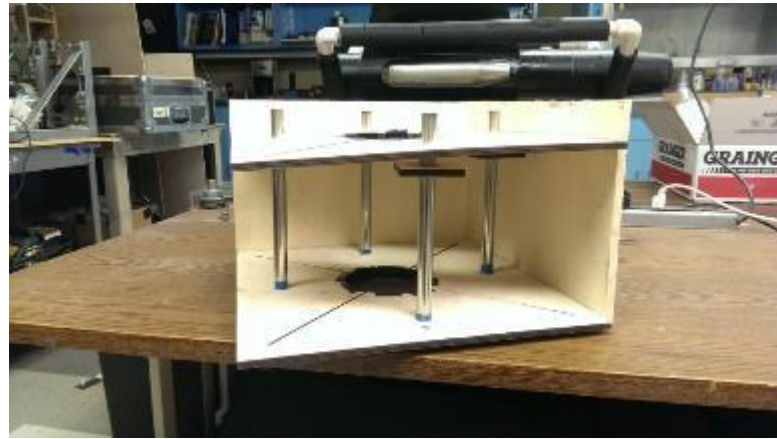


Figure 8: Fin alignment jig

The fins will be located perpendicular to one another so that the rocket will not spin. The fins will be sanded down to fit flush against each rocket motor centering ring, the pylon mounting, and the rocket motor tube. A bead of 5-minute epoxy will be placed on the inside of the fins and held in place with the assembly fixture and pressure applied from the fin-alignment jig. After the epoxy has cured for each fin, an epoxy fillet will be added to each fin corner to increase the epoxy attachment surface area, thus increasing tensile and compressive strength of the epoxy bond between the fins and the rocket motor tube. The fins and rocket motor tube will eventually be mated and epoxied into the tail-fin section rocket body tube. The “through-the-wall” design implemented here ensures that there are many points of attachment to the aft-most section of the rocket body.

An additional consideration in designing the fins is an “indent” at each fin’s top-most section to limit the amount of intrusion into aft section space caused by the through-the-wall design. The fin drawing is shown below in *Figure 9*. A fillet on the inner corner of the indented portion is incorporated to avoid a stress concentration failure. To further increase strength and reduce fluttering, the epoxy joints, as well as a significant portion of the fins, are coated with an additional layer of carbon fiber and epoxy. The epoxy used to create the joints is Devcon 2-Ton Epoxy. This epoxy is chosen because it possesses both high-strength (supports up to 2,500 psi) and is non-flammable and waterproof. Epoxy is also excellent for binding wood with composite components and other diverse materials.

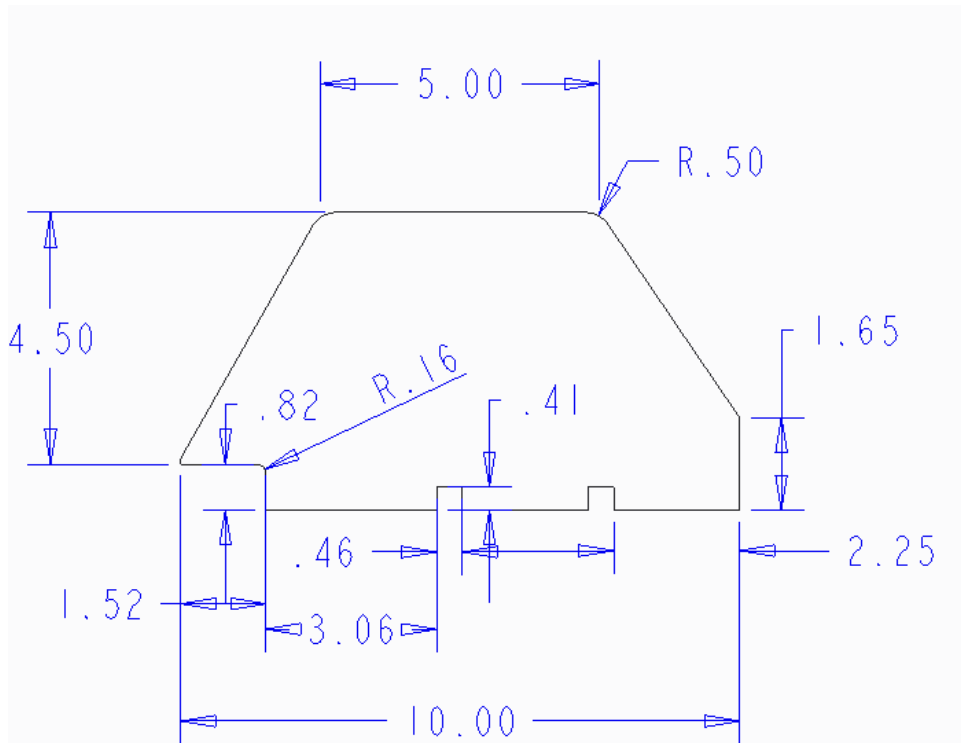


Figure 9: Dimensioned fin drawing

The main issue regarding the carbon fiber of the previous rocket prototype was a general "bumpiness" in the final product that was the result of air bubbles within the epoxy and carbon fiber while it was setting. The most significant negative effect of these resulting irregularities was an increase to the drag coefficient, while also detracting from the aesthetics of the rocket. To improve upon this process, we not only changed our method, but the materials as well. While using the same carbon fiber as the previous prototype, we opted for a higher strength, longer cure time, and less viscous epoxy mixture that improved the quality of the final carbon fiber layer in several ways. First, the stronger epoxy allowed for a more rigid final state, that if done correctly, would be more resistant to damage and wear. Second, the longer cure time allowed us to adjust the carbon fiber as necessary for up to 16 hours, before it was fully set after 24 hours. Finally, the reduction in viscosity allowed us to, as described next, removed air bubbles more easily during the process.

The primary goal in changing the process by which we laid and set the carbon fiber strips was to eliminate the problem of an uneven carbon fiber layer. To accomplish this, we sought to apply significant and even pressure to the carbon fiber and epoxy layers for the duration of its setting period. Before this could be done, however, the carbon fiber had to be smoothed out thoroughly to ensure a bubble free environment. This was done by putting down a primary coat of epoxy on the body of the rocket (Blue Tube), then laying down the manually pre-cut carbon fiber strips that would create fillets running from 1.25" up one fin, across the body tube, then up the adjacent fin another 1.25". Once the strips were laid, we applied fingertip pressure perpendicular to the surface of the rocket. A layer of plastic wrap, coated with more epoxy was then laid down on top of the carbon fiber and more perpendicular pressure applied.

This plastic layer created a non-stick buffer between the epoxy soaked carbon fiber and strips of Blue Tube placed on top of the plastic, allowing constant, even pressure to be applied to the curing strips of carbon fiber without fear that the extra blue tube would become stuck to the carbon fiber layer:

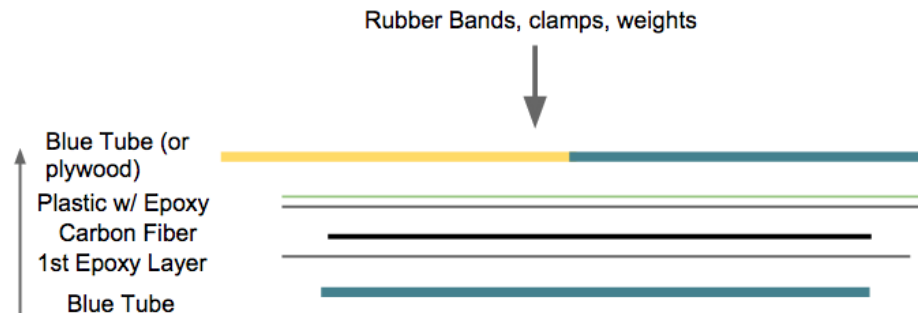


Figure 10: Method of Applying Carbon Fiber to Tailcone Section

Before the blue tube was laid down, however, putty spreaders were used to push air bubbles and extra epoxy from the body of the rocket into the fillets and then up along the fins onto pre-laid painters tape. Along the fins, plywood was used, rather than curved strips of Blue Tube, in order to apply constant, even pressure along the flat face of the fins.

Pressure was then applied to the topmost Blue Tube and plywood by a hose clamps and spring clamps respectively, ensuring maximal surface smoothness and preventing air bubbles from returning to the epoxy soaked carbon fiber. After 24 hours, the carbon fiber was sanded down and excess epoxy sanded off the blue tube and fins, resulting in a very smooth, strong, and elegant final product:



Figure 11: Photo of Newly-Improved Tailcone Section

4.1.1.2.2 Mass Adjustment

The final mass of each section of the full-scale launch vehicle came out very close to our predicted 11.65 lbs. A detailed listing of the mass of each section can be found in section 4.4.3: *Mass Statement*. Originally, we had designed the rocket to include a ballast bay that is located at the fore section of the avionics bay. This would have allowed us to add up to an additional 10 oz. of weight in case our final rocket came under our predicted weight. However, after some mass adjustments, we were able to get our rocket weight almost exactly to our prediction and thus the ballast bay will fly empty.

Another important part of the masses of the rocket is the location of the CG of the launch vehicle. More information on the CG and Stability Margin can be found in section 4.6.4: *Simulations and Predictions*.

4.1.1.3 Structural Systems

The structural systems of our rocket allow the rocket to maintain its shape and structural integrity throughout the launch and recovery. The primary structural subsystems include the rocket body tube, tube coupling, and payload bay. The structural subsystems are described below.

4.1.1.3.1 Rocket Body Tube

The rocket body tube provides a structural airframe that supports all other rocket subsystems. As such, the requirements for this component are sufficient strength and workability. The material chosen for the rocket body tubes is 4.0" Blue Tube ($t = 0.057"$) from *Apogee Rockets*. The Blue Tube is made from cellulosic fiber and are rated for strengths comparable to fully cured phenolic tubes, but with much greater impact resistance. In the event that a given rocket section lands with a greater kinetic energy than expected, the impact resistant blue tube may mitigate damage to the rocket subsystems. Verification for this design choice has come from results from previous years, which have demonstrated that blue tube is a workable, robust material that can withstand the forces experienced during each stage of the rocket launch. For our full scale rocket, the longest unsupported section of blue tube used in the rocket body is 11". Compression testing on a 16" length of blue tube was carried out this year to ensure that the smaller tube will not yield during launch. A more detailed explanation of this test can be found in Section 4.1.4.3.1: *Rocket Body Tube Verification*. The blue tube is sensitive to moisture, so the entire interior and exterior of the rocket tube will be treated with a water repellent polyurethane coating, to protect it from the elements during flight and after landing.

4.1.1.3.2 Tube Coupling

Since the rocket design calls for three individual sections that must separate during the recovery phase, there must be an adequate system for keeping the different sections together during ascent. This is done by coupling the separate tube sections using nylon 4-40 bolts, or shear pins. The coupling tube, affixed to the aft end of the payload and forward sections, has an outer diameter equal to the inner diameter of the body tube, and is fixed to the section just aft of it with epoxy. The sections are then mated, and holes drilled through both the outer and coupling tubes of the other mated section to allow for the shear pins to be inserted. Three shear pins will be inserted 120 degrees apart to ensure equal spacing of the shear load during flight. The calculation

for the amount of blast charge required to separate these shear pins will be explained further in *Section 4.5.2: Rocket Separation*.

4.1.1.3.3 Payload Bay

The payload bay also houses structural components of the rocket in its attachment to the nosecone. Refer to section *4.9: Payload Bay Design* for a detailed description and analysis of the payload integration.

4.1.1.4 Aerodynamics Systems

The aerodynamic subsystems include the rocket's nose cone and tail cone. These subsystems give the rocket an aerodynamic advantage and are described below.

4.1.1.4.1 Nose Cone

The purpose of the nosecone is to add an aerodynamic shape to the forward end of the rocket, reducing the axial coefficient of drag and thus total drag in that direction. The nosecone is attached to the rocket with epoxy, firmly connecting it to the payload section. The nosecone is an ogive-shaped plastic nosecone from Apogee Rockets. The 9.5" nosecone has been extended to a 18.4" payload section using Blue Tube to house the payload containment chamber and electronics. The 8.9" addition consists of 4.9" of added length to the total height of the rocket and 4" of coupler tube that both houses the electronics and mates it to the forward section. This selection for material and shape have been tested and verified by previous years' experiences, and has been proven to work in our full-scale launch.

4.1.1.4.2 Tail Cone

Basic fluid dynamics establishes that any drastic cross section change along the rocket will increase the drag profile of the body. In order to reduce this effect on the base of the rocket a tail cone was added with a diminishing cross sectional area contours so that the rocket body tube is more streamlined. The end of the tail cone extends 3" past the end of the tail-section's Blue Tube and is slightly regressed from the motor exit nozzle. There is a 1" section of blue tube separating the aft edge of the fins from the beginning to the tail cone. In the subscale flight vehicle the boat-tail was made of rapid prototyped ABS plastic, but we decided to go with a different design for the full-scale model.

This time, the boat-tail was constructed from carbon fiber using a similar process as the one used to stabilize the fins. The main difference was that it needed to be formed around a mold, as the only part of the rocket to its interior are the motor and motor tube. To do this, a spare nosecone was placed into a cylinder of plaster to create the proper cavity, which was then filled with more plaster to create a viable mold around which carbon fiber could be laid. The mold was wrapped in the same plastic used on the fins and then wrapped with carbon fiber and coated with more epoxy. The plaster cavity was then coated with releasing agent and the carbon fiber and mold were inserted into the cavity. Once the carbon fiber had been allowed to cure for 24 hours, it was removed and then cut and sanded down to size and epoxied to the end of the rocket using a 1" section of coupler tube.

4.1.1.5 Recovery System

As mentioned earlier, the launch vehicle employs a simple deployment recovery system, consisting of a single rocket parachute. The nosecone itself is fitted with a dedicated parachute to ensure safe deployment and recovery of the sample. The 30" diameter elliptical rocket parachute will deploy at apogee, approximately 3085ft AGL. Next, while under the influence of the rocket parachute, the payload section will be jettisoned at 1000ft AGL. Upon its ejection, the payload section will fall separately from the remainder of the rocket under the effects of a separate 30" diameter elliptical parachute. More detail on the design of the recovery system can be found in section *4.5: Recovery Subsystem*.

4.1.1.6 Electrical Systems

The two electrical systems of the rocket are the recovery and payload bay systems. Recovery system electronics include altimeters and batteries. This system composes the avionics system and is housed in the avionics bay. More information on the avionics and avionics bay can be found in section *4.5.5 Avionics and Avionics Bays*. An electronics system is also used to control the actuation of the payload bay and is housed in the payload bay electronics bay. More information on this system and its casing can be found in section *Error! Reference source not found.: Error! Reference source not found..*

4.1.2 Flight Reliability and Confidence

4.1.2.1 Mission Statement

Our mission is to acquire and transport a sample, under conditions laid out by the NASA Student Launch Mini-MAV competition. This requires the use of a fully autonomous ground system, AGSE, capable of visually identifying both the sample and the payload bay section of the rocket, picking up the sample, and moving it from its initial location to the containment tray in the payload bay. The Payload Bay is a self-actuating containment tray housed within the nosecone of the rocket, which is designed to open and close upon receiving a command from the AGSE and to protect the sample during flight. Finally, a launch vehicle will be required to transport the sample, contained within the payload bay, to an apogee of 3000ft and then jettison the entire payload bay portion at 1000ft. This system will require a recovery system which deploys a single rocket parachute at apogee and a payload parachute at 1000ft.

4.1.2.2 Requirements

First and foremost, for the mission to be a success, it must be conducted in accordance with all NASA imposed requirements and regulations, from planning to construction to final execution. An outline of the team's verification of satisfying NASA's baseline requirements can be found in section *4.7.1: NASA Statement of Work Verification*. Beyond this however, the Vanderbilt Aerospace Club has derived a list of additional requirements and mission success criteria.

4.1.2.2.1 Launch Vehicle Requirements

1. The rocket must be designed and built with all safety considerations, risk mitigation procedures, and environmental concerns in mind.

2. The launch vehicle shall be capable of being transported in sections and assembled at the launch site.
3. The rocket body must have a factor of safety of at least 4.
4. All payload components must be supported by internal structures anchored at bulkheads rather than directly to the rocket body.
5. No internal cavities in the launch vehicle shall be isolated from the atmospheric pressure (and thus create an inadvertent pressure vessel).
6. Cavities containing black powder charges must be isolated from all other components (excluding corresponding chute when applicable).
7. The launch vehicle must minimize unused space and mass.
8. The aft section must be capable of withstanding high temperatures (200+°F) in order to withstand the recirculation of hot air during initial launch phase.

4.1.2.2.2 Recovery System Requirements

1. The launch vehicle shall incorporate redundant deployment charges and corresponding altimeter settings for each parachute to increase vehicle reliability
2. The launch vehicle shall cover all parachutes with a fire retardant blanket so as to mitigate fire exposure during deployment events.
3. The launch vehicle shall incorporate an anti-zipper design so as to avert a potential "zipper" effect that can result in damage to the rocket body. The rocket parachute and payload bay parachute shroud lines can deploy with sufficient force to tear through the launch vehicle body tube. Such an event could cause severe damage to the launch vehicle, and thus, the launch vehicle could become non-reusable.
4. The altimeter arming switches must reside within the avionics bay and not within the chute compartments to prevent the switches or wires from being sheared off during chute deployments.

4.1.2.3 Mission Success Criteria

4.1.2.3.1 Launch Vehicle Mission Success Criteria

1. The launch vehicle must attain an altitude of 3000ft AGL ±300ft.
2. The rocket parachute must deploy within 2.0sec after apogee is reached.

4.1.2.3.2 Payload Bay Mission Success Criteria

1. The Payload Bay must open to receive sample when activated.
2. The Payload Bay must remain open until sample is securely inside and then fully close without dislodging the sample.
3. The sample must remain stationary and undamaged throughout flight.
4. The Payload Bay must withstand all forces of launch and deployment, maintaining structural integrity and aerodynamic advantage.

5. The Payload Bay avionics must jettison sample at 1000ft AGL \pm 200ft, and payload parachute must fully unfurl.
6. The Payload Bay electronics must remain capable of opening after landing, so the sample can be retrieved, but must do so without allowing the sensors to open the bay during flight.

4.1.2.3.3 AGSE Mission Success Criteria

Mission Success Criteria for the AGSE System can be found in section 5.2.3: *Success Criteria*. Our primary concern while designing the robotic arm was to consider a design where the arm itself was not part of the rocket that eventually takes flight. This immediately removes several weight and power-related limitations of designs where the retrieving system is entirely within the confines of the rocket. Our secondary goal was to identify a stable and robust design that had sufficient degrees of freedom to reach a target within a defined radius while not being over-specified or over-built. This enabled us to build an arm that is similar in construction to the SCARA robotic arm designs [19], [20], [21] but using lead-screw guide-rails as used in other domains such as remote surgery techniques [22]. This removes part collision concerns and greatly simplifies the actuation along the coordinate axes and therefore the kinematics.

4.1.3 Launch System and Platform

4.1.3.1 Launch Pad

The launch pad from previous years has been modified to align more closely with the design goals of this year's team. As it existed before, it was a solid 3'x3' square plate of 1/4" thick plate steel. Each corner had an angled leg mount, which allowed for the attachment of four adjustable feet which are threaded through holes in the leg mount attachments. On top of the platform is a hinged and lockable rail erector, to which we attach a 3-mast aluminum tower. This tower's sole purpose is to support the launch rail before, during, and after launch. The launch rail is attached by sliding it over two buttons which have been mounted to one of the masts of the tower.

Our changes to the previous design were centered on a simple goal of reducing the distance of the launch platform to the ground, and thereby making sample collection easier. In order to accomplish this, we have eliminated the current leg design. Instead of bolting in leg attachments and then attaching feet, we have drilled holes for the feet directly into the plate steel. Then, using threaded legs and nuts welded to the underside of the launch pad, we are still able to adjust the platform to a level surface but are now able to do so approximately 6" closer to the ground. This change decreases the required height of the AGSE, allowing for a lighter and more stable design.

In addition, we have constructed another platform that serves the dual roles of supporting the rocket/launch rail in its horizontal position and supporting the AGSE. This platform is balanced on the same threaded leveling feet as the improved launch pad. The plate is 1ft by 2ft with the longer dimension perpendicular to the launch rail. On one side of the platform is an acrylic stand that bolts into the platform and is shaped to vertically support and horizontally stabilize the launch rail and the rocket on it. This prevents the moment of the rocket and 16ft launch rail from tipping the launch pad and protects the rocket from rocking on the rail and damaging the

alignment lugs. It also prevents the rocket from shifting out from under the AGSE during insertion. On the opposite side of this platform is the base of AGSE. Using this platform to support both the rail and the AGSE ensures that the Payload bay is always in the workspace of the AGSE. See the image below for visual representation of this new support.

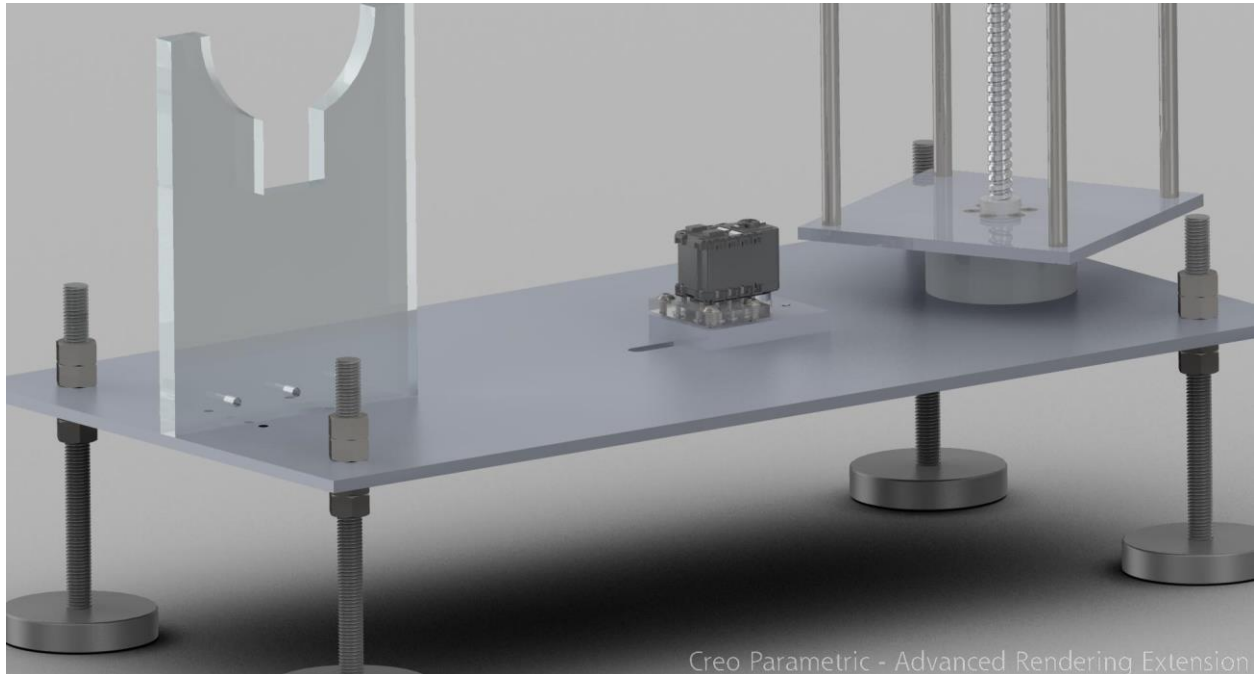


Figure 12: AGSE Table and Launch Rail Support

4.1.3.2 Launch Ignition System

The launch ignition system consists of a 12V battery connected to 500ft leads. The leads go through a safety switch system to the motor igniter. The safety switch ensures that no voltage differential is delivered to the electric match igniter until a key is inserted into the safety switch and a button is pressed. Before pressing the button to fire the igniter, our Safety Mentor, Robin Midgett, loudly announces to the field a 5 second countdown to launch. We also ensure that all members are at least 300 yards from the launch pad at the time of launch for safety precautions.

4.1.4 Launch Vehicle Systems Requirements and Verification

4.1.4.1 Propulsion Verification

4.1.4.1.1 Motor Retention Verification

The motor retention system experiences its most violent forces at launch and thus is vital to the success of the rocket. We have taken much care in the design and construction of the retention system to ensure that it will be able to withstand these forces. We are employing an AeroPack 54mm-L motor retainer to serve this purpose. The female piece was epoxied in place after attaching the boat-tail to the tail section. On launch day, the loaded motor casing will be inserted into the motor tube and the male piece will be threaded over the female piece, securing the motor

in place. The threads do not undergo significant force, as their only purpose is to fight gravity to hold the motor inside the motor tube when it is not burning.

Once the motor is ignited, the force is transmitted from the nozzle of the motor to the female piece of the AeroPack motor retaining ring and into the motor tube. As described earlier it is then transferred through the centering rings and fins into the body of the rocket. Through 4 different field launches, we have verified that the current design is more than strong enough. In fact, even when our motor failed on the first launch, our motor retention system held up under the extremely high impact forces when the tail section collided with the ground after falling 1000 feet unhindered by a parachute. After these results, we are confident that the motor retention system is of adequate strength.

4.1.4.1.2 Launch-Rail Interface Integration

The most important aspect of the launch rail interface is that the alignment be perfect. Any error on the alignment of the launch lugs will cause the initial flight of the rocket to not be vertical. In order to ensure proper alignment, we placed the first launch lug directly between two fins and screwed it into the middle centering ring in the tail section. Next, we tied a string around the launch lug and pulled it taut while aligning it with the tip of the nosecone to determine the central axis of the launch vehicle. We then mounted the second launch lug in the forward section just aft of the avionics bay along this line to guarantee correct orientation. This ensured that the take-off was as straight as possible.

The second most important aspect of the launch rail is that we limit friction at take-off as much as possible. This is achieved using petroleum Vaseline. Prior to mounting the rocket on the launch rail, both the launch lugs and the rail itself are coated with Vaseline to reduce friction to a negligible level.

The last important aspect of the launch rail interface is verifying that the launch pad is aligned perpendicular to gravity. We understand that the ground at the launch site may not be perfectly flat, and have thus included adjustable legs so that the launch pad can be adjusted to the surface upon which it is resting. These have been adjusted since our previous launches to better accommodate our AGSE. Using a drill press, we drilled holes into the existing launch pad and welded 1/2" nuts onto the underside of the launch rail. We then purchased 1/2" threaded leveling feet from McMaster-Carr and milled a flat on it near the foot so that we can use a standard wrench to adjust the height and level of the legs when resting on the ground. This reduced the overall height of our launch pad while also ensuring a level and sturdy launch surface. In addition, the launch pad was coated with rust-preventing paint so that it will be able to be used in future years.

4.1.4.2 System Stability Verification

4.1.4.2.1 Fin Assembly Verification

There is successful heritage on previous Vanderbilt Student Launch teams on this type of fin assembly. In addition, all four of our launches have proven that the fin design we are using is successful. In fact, even after the tail section of our first launch crash landed, the fin remained undamaged, proving that it is more than robust enough to survive the parameters of the

flight. However, when it came time to construct our full-scale launch vehicle, we employed even more care in making sure its construction was correct. As was detailed above in *Section 4.1.1.2.1: Fins*, the procedure for the carbon fiber layup was carefully and methodically done to ensure perfect flight. After using the same fin jig again for the full-scale rocket, visual inspection revealed the fins were aligned properly and measurements ensure they were in the proper locations as specified by the CAD and used in our simulations. At the full-scale launch, the flight pattern successfully demonstrated that the fins properly stabilize the rockets flight, without causing spin, and can easily withstand a ground impact at the reported descent velocity.

4.1.4.2.2 Mass Adjustments Verification

The vertical location of the center of gravity was determined with the tip of the nose cone as the origin and by measuring each individual section's & large component's mass and distance from this point. From this, the center of gravity with respect to the vertical orientation of the rocket was calculated. In addition, we measured the empirical CG of the rocket to verify its location.

On the first construction of our full scale rocket, we came out approximately 1 lb over our estimated mass and thus needed to cut weight in order to reach our target height with the motor we had designed it for. In order to do this, we analyzed all of the interchangeable parts of the rocket and located several areas where we could save weight. First we looked at interchanging all steel structural parts (such as U-bolts and nuts) with aluminum, then we looked at eliminating the ballast bay, as well as reducing our nylon shock cord thickness from $\frac{1}{2}$ " to $\frac{1}{4}$ ". After testing the $\frac{1}{4}$ " 1500lb shock cord, we determined that it was more than strong enough to serve our purposes and cut weight enough to bring us back within our estimated range. Results from the test can be found in *Section 4.5.7: Recovery System Testing*. Therefore, we were able to retain our ballast system though we do not expect to fly any ballast once the paint has been applied.

4.1.4.3 Structural Verification

4.1.4.3.1 Rocket Body Tube Verification

Since the rocket body tube will experience its largest compressive forces during motor burn, with the weight of the rocket pulling it down and the thrust of the motor pushing up, the compressive strength of the Blue Tube material must be considered. These specifications for the 4" diameter Blue Tube can be easily found online, but to completely make sure of its load carrying ability the rocket body tube sections have been placed in a load cell and tested for their ultimate compressive strengths. The load cell used for testing is located in the Material Science Laboratory on campus. The longest length of Blue Tube that will solely support a compressive load is the top 11" of the forward section. Thus, a 16" section has been compression tested in the Vanderbilt Materials Science hydraulic press. The compression tests have revealed that the tube can withstand 3600lbf, and the team's Blue Tube is only expected to see a maximum force of around 75lbf. This gives a factor of safety of over 40. A visual representation of the compression test is located below in *Figure 13: Vanderbilt Materials Science Hydraulic Press with Buckled Blue Tube Specimen*.



Figure 13: Vanderbilt Materials Science Hydraulic Press with Buckled Blue Tube Specimen



Figure 14: Results from Compression Test of Blue Tube in LABView Interface

4.1.4.3.2 Tube Coupling Verification

In order to couple the main body sections of Blue Tube, we are using the specified coupler sizes of Blue Tube. These have been carefully manufactured so that the outer diameter of the coupler tube is just smaller than the inner diameter of the main body tube. One side of the coupler tube is held in place with Devcon 5-minute epoxy, anchoring it to one of the coupled sections. The remaining coupler tube is then inserted into the mating piece of body tube and holes are drilled through both the outer tube and the coupler to allow placement of a shear pin. The shear pin holds the two sections together under all of the forces of launch but is sheared when the deployment charges are blown.

The coupling of the three sections has been tested by 3 subscale launches as well as 3 deployment tests and the full-scale test launch. The deployment test has proven the reliability of the shear pins to hold until the blast charges are blown while there is little to no risk of harming the launch vehicle or any of the team members. Having seen successful tube separation in all three of our subscale launches, we are confident that the design for tube coupling will function correctly.

4.1.4.3.3 Payload Integration Verification

The payload bay integration was tested comprehensively to ensure proper functionality during all the stages of the rocket launch. At first and second subscale launches, a dummy payload bay was jettisoned at 800ft. to verify proper separation of the nose cone section and deployment of the nose cone recovery system. The third subscale launch included a prototype payload bay. This prototype demonstrated full open/close functionality and structural similarity to the full scale payload bay. This flight and payload section separation verified the structural integrity of the linkages that actuate the payload section, as well as the normal operation of the electronic components throughout the flight. More information on the test flights of the payload bay can be found in section 4.3: *Subscale Flights Results*.

In addition to the subscale launches, there will be one full scale launch before the competition in April. This full scale launch will comprehensively test each subsystem of the rocket, as well as the successful integration of these subsystems to accomplish the overall mission objective.

4.1.4.4 Recovery System Verification

For verification simulations of the recovery systems, see section 4.6.4: *Simulations and Predictions*. In addition to calculations, ground based testing on the recovery system is performed before each launch, testing the altimeters' accuracy and the amount of deployment charge used. Details on these tests can be found in section 4.5.7: *Recovery System Testing*.

4.1.4.5 Electrical Systems Verification

Verification of the electrical systems includes testing of the recovery electronics and payload bay electronics. More information on these two systems can be found in sections 6.1.2.3: *Recovery System Failure Modes and Risk Assessment* and **Error! Reference source not found.: Error! Reference source not found.**

4.1.5 Workmanship and Mission Success

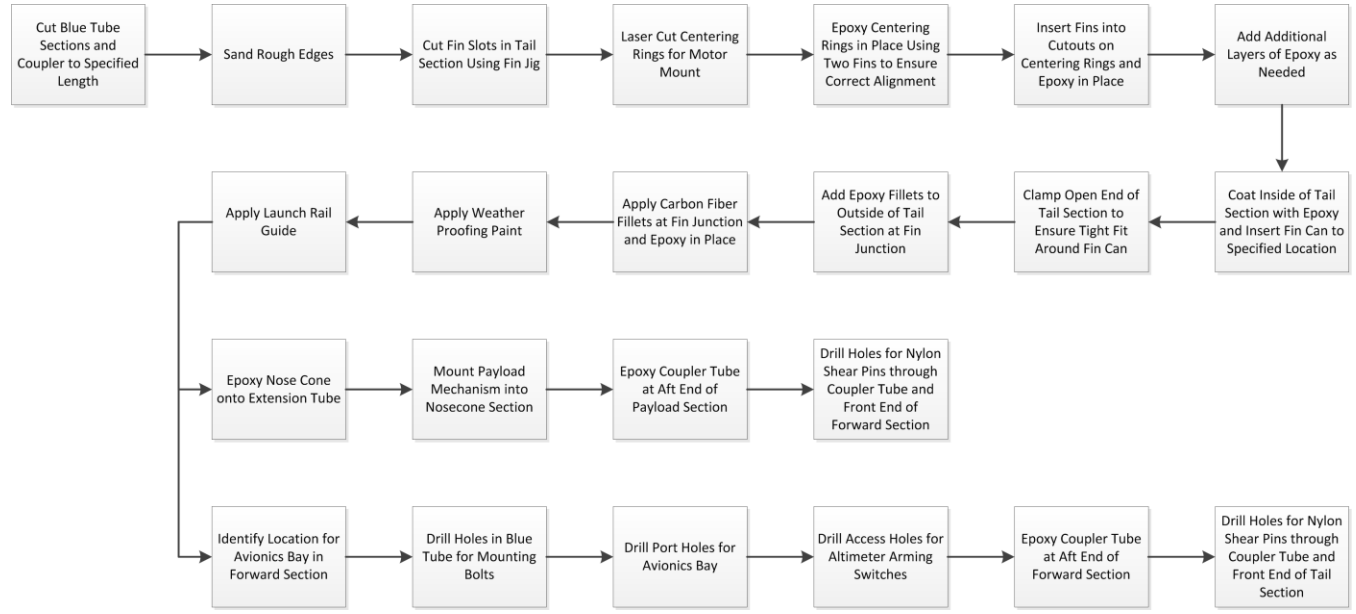


Figure 15: Rocket Construction Flowchart

The Vanderbilt Aerospace Club strives to accomplish risk mitigation proactively, rather than retroactively. Former club launch vehicle design faults and other SL team launch vehicle failures are used as examples to anticipate potential failures with construction of the launch vehicle. One such example of this is the fireball anti-zipper that is used on the launch vehicle to keep the shock cord from ripping through the fuselage (a problem that plagued former Vanderbilt teams and other SL teams).

Additionally, workmanship and fabrication of the launch vehicle, payload bay, and AGSE are overseen by the engineering faculty advisor Professor Anilkumar, faculty safety advisor Robin Midgett, and student safety officer Connor Caldwell, as well as Robotics Mentor Ben Gasser. To ensure exceptional workmanship of the launch vehicle, payload bay, and AGSE, all assembly tasks are first identified and analyzed before actual fabrication begins. This attribute of the team can be seen in the design of the payload section retention rings.

The payload bay system was very carefully modeled in CAD before being manufactured using precision instruments (lathes, mills, etc.). Additionally, the weight of the payload system is carefully offset around the axis of symmetry of the launch vehicle. This foresight ended up proving very advantageous when the full launch vehicle was assembled and flown. Finally, the Vanderbilt Aerospace Club believes in the motto “test like you fly.” As such, the recovery system has been extensively tested (altimeter tests, deployment tests, and multiple full scale launches), and payload section to AGSE interfacing and functionality will be thoroughly tested during multiple ground tests. Testing all functional launch vehicle, payload bay, and AGSE components helps to reduce the possibility of unforeseen failures or problems that may arise on competition day.

It is the team's belief that extreme care and attention to detail must be taken in each step of the design process, manufacturing process, and testing process in order to achieve mission success. Furthermore, if a team member has a question, an answer is sought from the safety advisor and mentor, or faculty advisor, or from other reliable sources before proceeding with their activities.

4.1.6 Safety and Failure Analysis

4.1.6.1 Risk Assessment Matrix

In order to fully assess the risks associated with the launch, we have developed a risk assessment matrix (*Figure 16*) that categorizes and ranks all risks according to their likelihood of occurrence and severity of consequence. Likelihood of occurrence is given a rating from 1 – 5 with 1 being the least likely and 5 the most. The corresponding designations for each in order from 1 – 5 are **rare, unlikely, moderate, probable, and very likely**. The consequence is given a rating from A – E with A being the least consequence and E being the greatest. The designations for each in order from A – E are trivial, minor, moderate, high, and critical. When each scale is set up in a matrix, a combination of the two values can be very enlightening as to the relevance of the risk. Interpreting the risk designation is also quite intuitive since low alphanumeric combinations correspond to the least worrisome risks while high alphanumeric combinations represent larger risks.

Color-coding has also been added to the matrix to designate which risks require mitigation of some sort. Risks highlighted in green are considered low risk and either require no mitigation or have no reasonable means of mitigation. These either have a very low probability of occurrence or the consequence of occurrence is so small that serious consideration to mitigate the risk is not necessary. Risks highlighted in yellow are considered moderate risks and should be mitigated, but the overall risk posed to the mission and safety of those involved has been deemed acceptable. Risks highlighted in red are more serious than those in green and can have serious consequences on the success of the mission or the safety of those involved, but the combination of their occurrence and consequence ratings places them in the middle of the matrix. This means that the risk to mission success or injury is either fairly low/unlikely or that the risk has been mitigated in some way to bring it down from the most serious category. The most critical category is highlighted in red, signifying that these are the most hazardous risks to either mission success/personal safety or have the greatest likelihood of occurrence. These risks are deemed unacceptable and must be mitigated in some way for the rocket/payload to be safe to launch. In the tables outlining risks for the various sections/payloads of the rocket, no risk can be classified with a red rating post-mitigation.

	Consequence					
Likelihood		Trivial	Minor	Moderate	High	Critical
	Rare	A1	B1	C1	D1	E1
	Unlikely	A2	B2	C2	D2	E2
	Moderate	A3	B3	C3	D3	E3
	Probable	A4	B4	C4	D4	E4
	Very Likely	A5	B5	C5	D5	E5

Figure 16: Risk Assessment Matrix

The explicit meanings of each likelihood and consequence rating are outlined as follows:

Likelihood

- Rare (1) – Chances of occurrence are almost non-existent. Mitigation need only exist for the most critical risks.
- Unlikely (2) – Chances of occurrence are very low but do exist. Mitigation should exist for high-risk consequences.
- Moderate (3) – Chances of occurrence are moderate. Mitigation should exist for all risks resulting in greater than minor consequence.
- Probable (4) – Occurrence is more likely than not. Mitigation should occur for all but the most trivial risks.
- Very Likely (5) – Occurrence is to be expected. Mitigation is required for all but the most trivial risks.

Consequence

- Trivial (A) – Occurrence of risk results in no effect on rocket/payload performance or safety of all persons involved. No mitigation is needed.
- Minor (B) – Occurrence of risk results in minor damage that is either easily repairable or has no effect on rocket/payload performance. No risk for injury to persons involved. Mitigation should exist for the most likely risks.
- Moderate (C) – Occurrence of risks results in some damage to rocket/payload that could negatively affect performance and/or result in minor injury to persons involved. Mitigation should exist for most risks.
- High (D) – Occurrence of risk results in major damage to rocket/payload that will negatively affect performance and/or result in serious injury to persons involved. Mitigation should exist for all but the rarest risks.
- Critical (E) – Occurrence of risk results in catastrophic damage to rocket/payload that will eliminate performance capability and/or result in serious injury/death to persons involved or bystanders. Mitigation must exist where possible.

Combined Rating

- Low (Green) – Risk falls within an acceptable range of probability and consequence. Mitigation strategies should be implemented if possible but are not mission critical.
- Moderate (Yellow) – Risk should be evaluated for potential mitigation strategies.
- Critical (Red) – Risk has an unacceptable level of likelihood and consequence. Mission should not proceed until viable mitigation strategies are created and implemented.

All risks recognized by members of the team have been recorded and evaluated by the safety officer. Each risk has been given a risk assessment rating prior to any mitigation as well as post-mitigation in order to quantify the steps taken by the team in designing and fabricating the rocket/payloads to make it as safe and reliable as possible. In all following risk assessment tables, each risk has been outlined along with possible causes, overall effect to the rocket/payload, mitigation strategy, verification of implemented verification strategies, and two risk assessment values for pre- and post-mitigation that have been color-coded for easy comparison.

All risk tables using this risk assessment matrix are documented in section 6: *Failure Modes and Risk Assessment*.

4.1.6.2 Vehicle Development Risk Table

The risks and the plans for risk mitigation in the context of how each risk factor will affect the project with regard to successful and timely completion of fabricating the launch vehicle are outlined in a risk assessment table in section 6.1.1: *Vehicle Development Table*.

4.2 Full-Scale Flight Results

4.2.1 March 15, 2015 Launch

The flight rocket had a height of 58.4" and a pad mass of 14.55 lb. The separation between CG and CP was measured at 7.125" resulting in a flight stability margin of 1.78. The payload compartment carried the flight payload and all the flight control and instrumentation systems. The open-close functionality of the payload compartment was tested before rocket assembly. The rocket flew on a J380SS motor with a positive acceleration of 5 g and a rail exit velocity of 70 fps.

Two independent wind measurements, from the nearby Tullahoma airport, and from the handheld Kestrel anemometer established a steady ground wind speed of 6 mph, with occasional gusts up to 10 mph. The winds were blowing from the Northeast to the Southwest. Accordingly, the launch rail was tilted 5 degrees into the incoming northeast wind direction. The skies were clear during launch and the entire rocket trajectory could be visualized. The smoky nature of the rocket exhaust made the identification process doubly easy.

The launch pad modifications to accommodate the AGSE for the NASA SL required careful field assessment, after which, the rocket was loaded on the 16ft rail. The rocket motor ignited as expected and the rocket cleared the 16ft rail successfully. With no wind gusts at launch, the rocket did not weathercock, instead it slowly turned into the wind as seen from the rocket plume

signature. The rocket reached an altitude of 3008 ft. The 30" rocket parachute opened at apogee and the payload section was ejected at 1000 ft. and landed on its own 30" parachute. The payload section and the rest of the rocket were recovered within 550ft of the launch pad. The full scale rocket flight was a complete success.



Figure 17: Pictures clockwise: (a) payload bay check out before launch, (b) launch pad checkout and rocket mounting, (c) perfect rocket flight, (d) complete recovery, (e) payload bay check out after launch

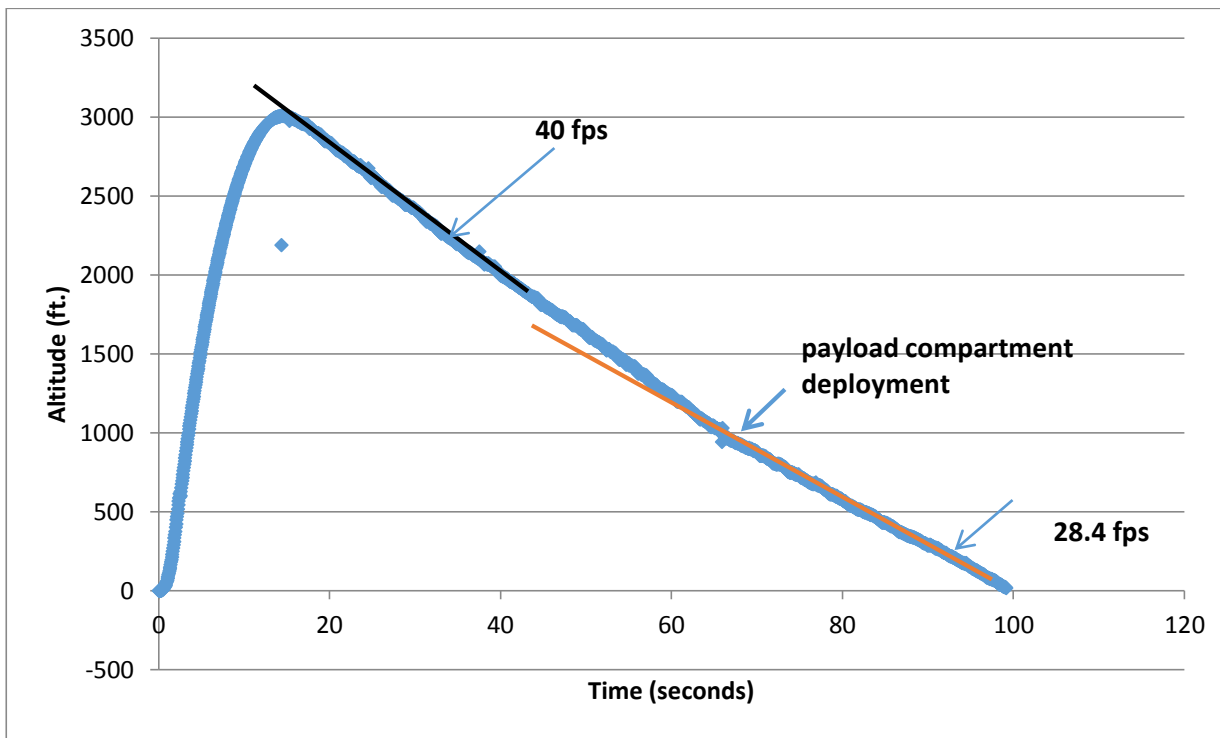


Figure 18: Avionics Bay Altimeter Data: (i) Altitude reached (3008 ft.); (ii) landing speed under rocket parachute ~ 40 fps., (iii) landing speed following payload jettison ~ 28.4 fps.

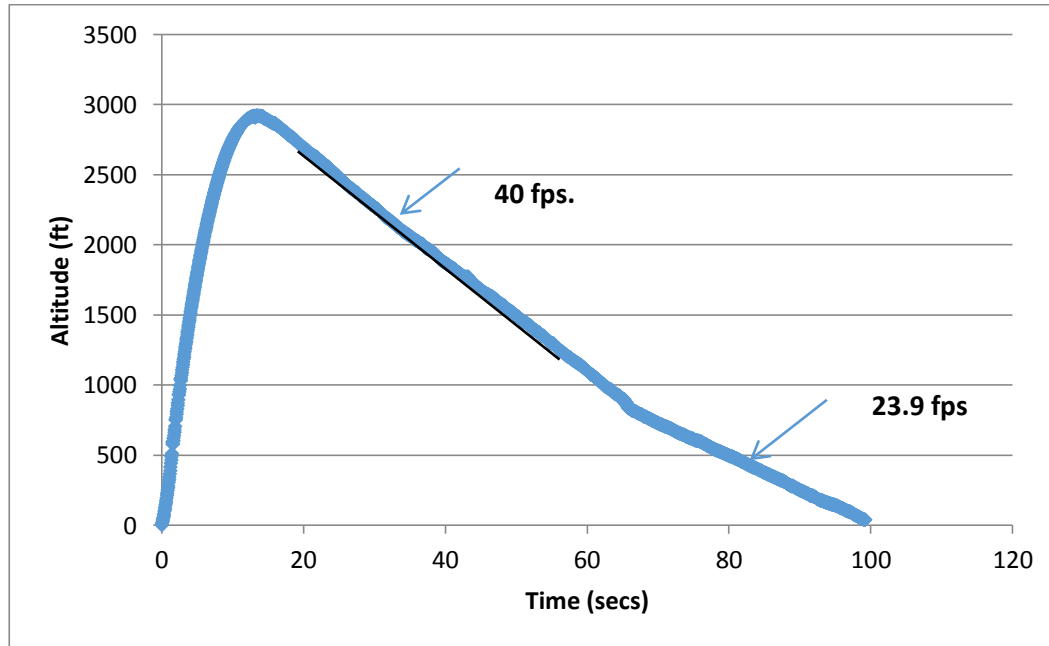


Figure 19: Payload compartment altimeter data: (i) landing speed under rocket parachute 40 fps. (ii) landing speed under payload parachute 23.9 fps.

4.2.2 Comparison with Predictions

The following table provides a detailed comparison between the simulation-predicted and the actual flight data for the various criteria outlined.

Table 1: Comparison of Flight Predictions with Results

Criterion	Rocket w/motor	Payload section	Forward section	Tail section
Take-off mass (lb.)	14.55	4.85	3.85	5.85
Landing mass (lb.)	12.85	4.85	3.85	4.15
Predicted Apogee (ft.)	3100			
Actual Apogee (ft.)	3008			
Parachute size		30" elliptical	30" elliptical	30" elliptical
Deployment charge (gm.)		2.0 (2.0)	3.0 (3.2)	
Speed under rocket parachute (fps.)		40 fps	40 fps	40 fps
Estimated speed under rocket parachute (fps.)		42.3	42.3	42.3
Measured Landing Speed (fps.)		23.9	28.4	28.4
Estimated Landing speed (fps.)		24.8	31	31
Landing energy of the heaviest part (lbf-ft.)		43	48.2	52.0
Estimated Landing Energy (lbf-ft.)		46.3	56.7	61.1
Landing drift (ft.)		600	550	550
Estimated Landing Drift (ft.)		450	450	450

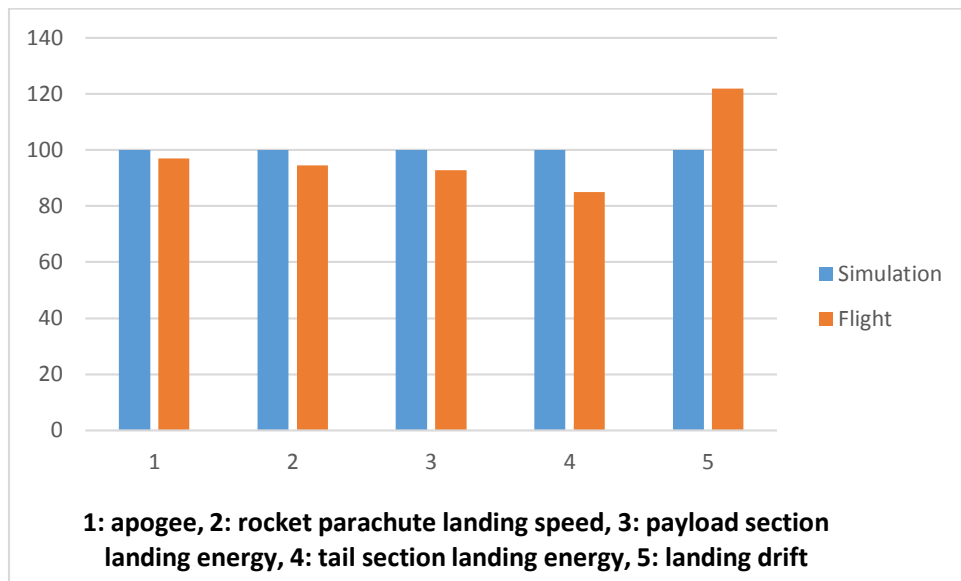


Figure 20: Comparison between simulated and actual flight data showing good parity between the two.

4.2.2.1 Analysis

The rocket flight was an unqualified success and validated the design criteria of not adding any additional ballast mass to reach 3000ft. apogee. The two noticeable factors are (i) the apogee is about 100ft lower than expected, and (ii) the landing drift is about 100ft. higher than expected. The lowered apogee while definitely acceptable, as it achieves the target altitude of 3000 ft., can be explained by probably the presence of stronger winds at altitude, curving the trajectory. The higher landing drift can be explained by the observation that the landing speed of the tail section is lower than predicted. This can be attributed to (i) some amount of lofting that is noticed in the presence of side winds, (ii) additional drag due to the forward and the tail sections on long shock cords, the drag of which is unaccounted for in the simulations.

Based on the full-scale flight, the Vanderbilt team is comfortable that their designed rocket can reach an apogee of 3000 ft (with an uncertainty of about 150 ft), and that the rocket parts can be recovered within the launch field of 2500ft. radius for a variety of allowed wind conditions. The final full scale design has been arrived at carefully scaling up the subscale flight data to arrive at the optimal design.

4.2.2.2 Simulations

See section 4.6.4: *Simulations and Predictions* for a detailed listing of all simulations and predictions used in designing the full scale launch vehicle.

4.2.2.3 Impact of Subscale Flight Data on Full Scale Rocket Design

The impact of the three subscale launches and NASA evaluations can be summarized as follows:

- (i) Full scale rocket can have three sections.

- (ii) Full scale rocket can deploy a suitable payload parachute at apogee and there is no need for additional parachute deployments for the main rocket section.
- (iii) Full scale rocket of 4" diameter can accommodate the payload bay actuation and size requirements.
- (iv) A 30" elliptical parachute on the payload section and a 30" elliptical parachute in the main/drogue section can meet the landing energy criteria of all the parts.
- (v) A J 380SS motor can meet the altitude ceiling as required.
- (vi) The parachute chambers can be smaller for better utilization of space and thereby, full-scale rocket can come out shorter.
- (vii) The full-scale rocket can be designed for 12.65 lb. mass w/o motor and thereby, there can be substantial impulse savings on the flight motor.
- (viii) Stability margin of 1.5 or above is good for flight.

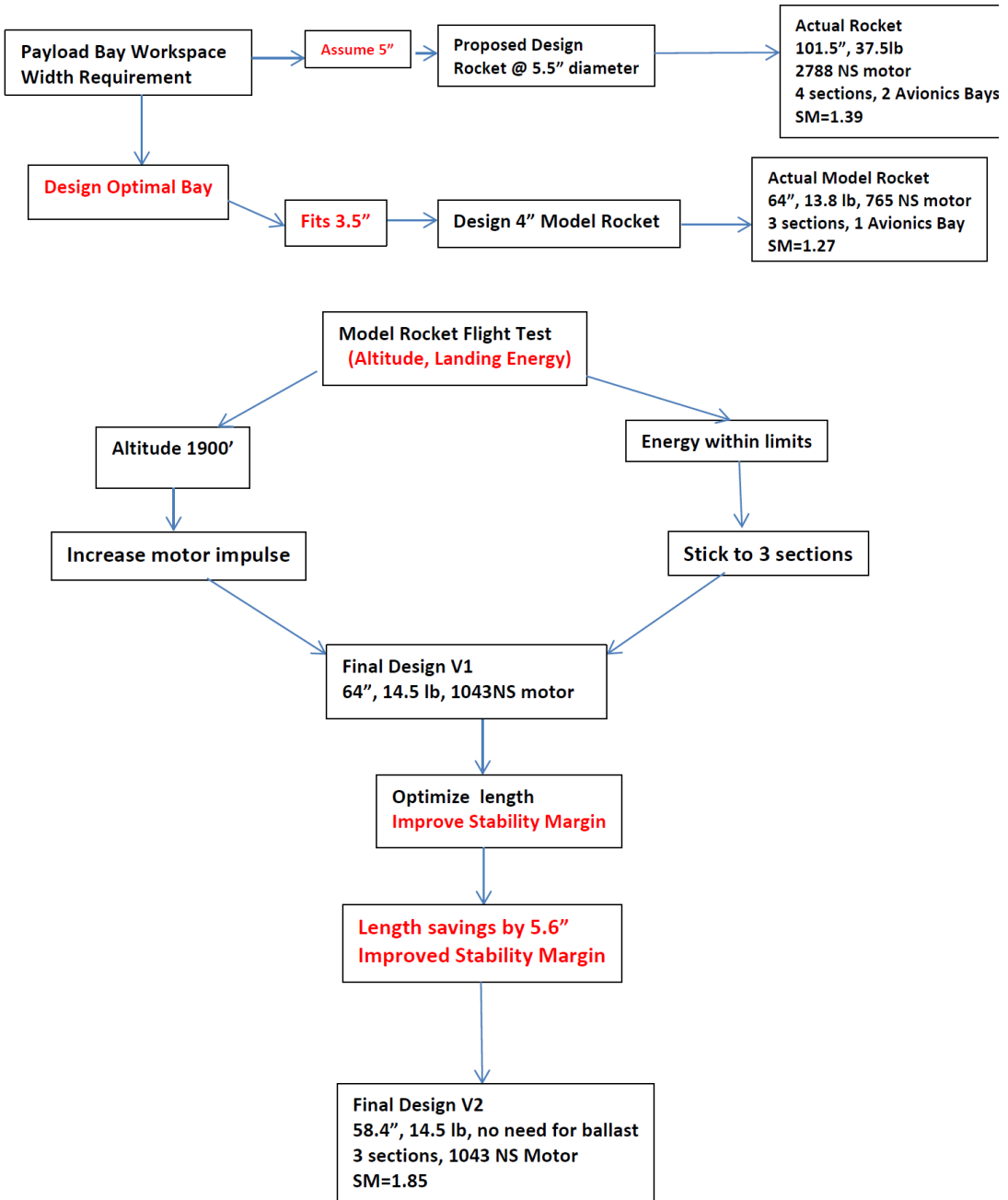


Figure 21: Full-scale rocket design logic based on subscale flight and results

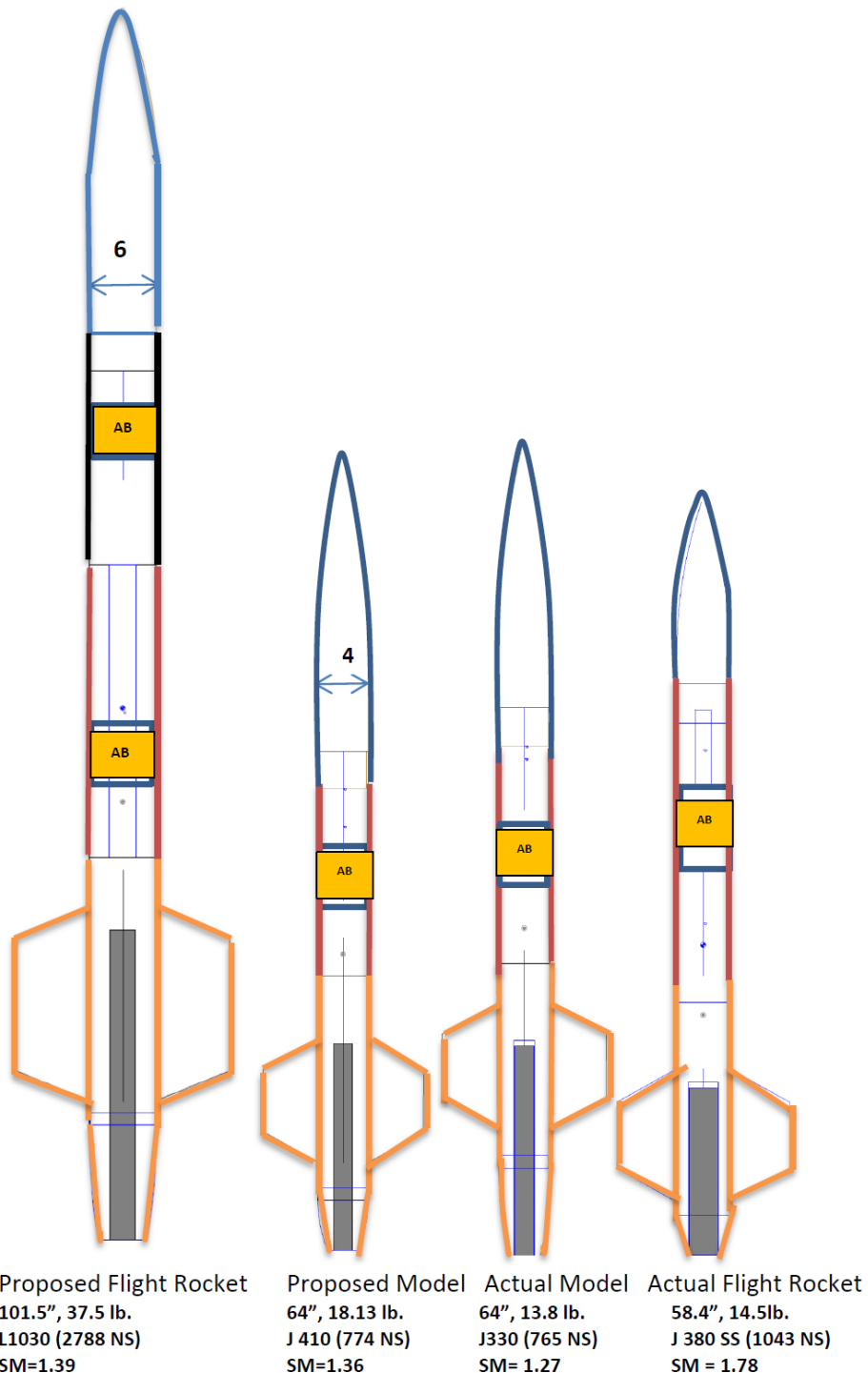


Figure 22: Evolution of the full-scale rocket from proposed to actual design following subscale flight studies.

4.3 Subscale Flights Results

4.3.1 November 2014

4.3.1.1 Flight 1

The PDR proposed model rocket had a height of 64" and a mass of 18.13 lb., with a stability margin of 1.36. As we constructed the rocket, the actual mass of the rocket came out lower due to lower payload section mass requirements and selection of lighter materials. The first rocket on the launch pad was a 64" long, with a mass of 13.9 lb. and a stability margin of 1.27. The payload compartment carried a 3.5 lb. dummy mass. The rocket flew on a Cesaroni J410 motor with a positive acceleration of 6.3g and a rail exit velocity of 84 fps. The projected altitude for this lighter rocket was 1990ft.

At launch, the rocket motor ignited as expected, however, the flight vehicle did not achieve the anticipated rail exit velocity. The rocket could be seen severely windcocking and pretty soon it became clear that the rocket motor was burning through the tail section with accelerated burn. While the rocket landed as anticipated and the payload section ejected as anticipated at 800 ft., the flight was deemed a failure. Pictures and descriptions from the flight accompanied by a picture of the burnt-through tail section are shown in *Figure 23*, while the data from the flight is compared to the predicted flight in *Figure 24*.



Figure 23: Flight 1 (a) take off at lower than anticipated speed, (b) motor burning through, (c) independent landing of payload and tail sections, (d) burnt-through tail section.

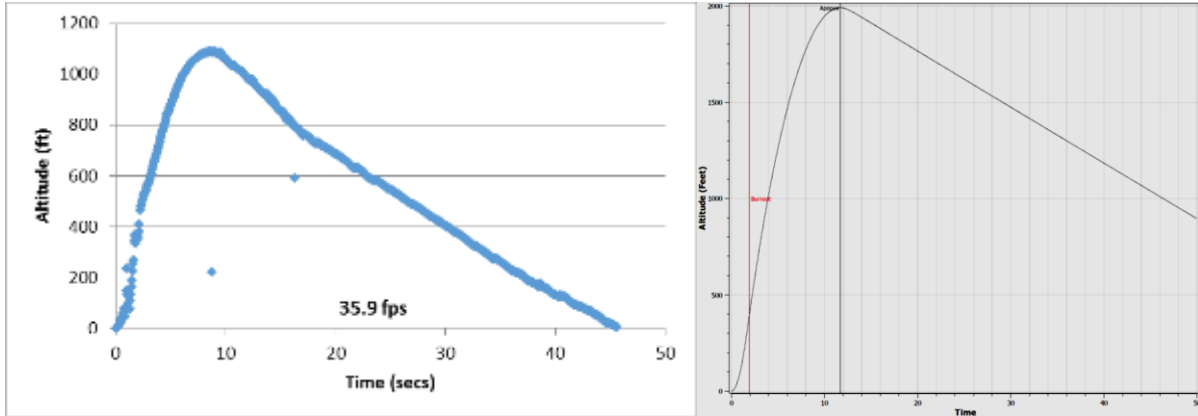


Figure 24: (a) Altitude reached (1100ft) as opposed to a predicted altitude of 1990 ft.

4.3.1.2 Flight 1 Analysis

Based on flight observations, and follow up studies, it became clear that the propellant grains had a faster burn rate than the exhaust nozzle could handle. This led to a pressure rise and eventual explosion of the rocket canister. Since the motor was a fast burn motor, a substantial amount of propulsive thrust was still generated to sustain flight, and the safety of the flight and personnel was ensured by the rocket trajectory. Since the rocket reached an altitude of 1100ft and the rocket parachute deployed as expected, the payload section could be ejected at 800ft. and it landed on its own parachute; all the rocket components landed within 300 ft. of the launch pad.

A careful analysis of the launch protocol revealed that the loaded rocket motor could have sustained cracks due to it being dropped during transport. Common modes of failure in solid rocket motors include fracture of the grain, failure of case bonding, and air pockets in the grain. All of these produce an instantaneous increase in burn surface area and a corresponding increase in exhaust gas and pressure, which may rupture the casing. With additional surface area, the motor burn rate was much faster, and the chamber pressure much higher than designed for leading to a catastrophic failure.

As a consequence to this flight, it was decided to abandon the faster-burning J410 motor, and switch to a slower burning J330 motor that the team had prior experience and success with. The rocket tail section was put through a redesign. The motor switch also ensured that the take-off acceleration was at 5.5g as opposed to a higher 6.3g that resulted from lowered mass. Also, it was decided to switch the parachutes and have the 3ft parachute on the payload and the 4ft parachute on the main rocket body to balance out the landing energies and still keep them within the 75lbf-ft energy requirements. Data from the flight is shown in **Table 2**.

Table 2: Details of the first flight showing that the landing energy criteria and the payload ejection and landing criteria were successfully met.

Criterion	Rocket w/ motor	Nose Cone	Mid Section	Aft Section
Mass	13.8 lb	5.2 lb	2.9 lb	4.4 lb
Predicted Apogee	1990 ft			
Parachute Size		4 ft	3 ft	3 ft
Deployment Charge		2 gm	3.5 gm	
Speed under 3ft Rocket Chute after apogee		36 fps	36 fps	36 fps
Speed under parachute after 800ft		18 fps on 4' chute	27.4 fps	27.4 fps
Landing Energy		26.3 lbf-ft	34 lbbf-ft	51.3 lbf-ft

References on Solid Propellant Motor Failure:

- i. Akpan, U.O., Dunbar, T.E., and Wong, F. C., ‘*Probabilistic Risk Assessment of Solid-Propellant Rocket Motors*’, Journal of Spacecraft’s & Rockets Vol. 40 No. 3, 2003.
- ii. NASA Website: <http://ti.arc.nasa.gov/tech/dash/pcoe/solid-rocket-motor-failure-prediction/introduction/>
- iii. Godai, T. ‘Flame Propagation into the Crack of a Solid Propellant Grain’, AIAA Journal, Vol.8, No. 7, 1970
- iv. Sutton & Biblarz, ‘Rocket Propulsion Elements’, Wiley (8th edition), pp. 537-593, 2010

4.3.2 December 2014

4.3.2.1 Flight 2

The rocket on the launch pad was a 64” rocket, with a mass of 13.8 lb. and a stability margin of 1.27. The payload compartment carried a 3 lb. dummy mass. The rocket flew on a J330 motor with a positive acceleration of 5.5 g and a rail exit velocity of 80 fps. The projected altitude for this lighter rocket was 1859 ft. in 11 mph winds

The rocket motor ignited as expected and the rocket cleared the 16ft rail successfully. The rocket recovered from the effects of the side winds rapidly, and reached an altitude of 1840 ft. The 4ft rocket parachute opened at apogee and the payload section was ejected at 800 ft. and landed on its own 3 ft. parachute. The payload section and the rest of the rocket were recovered within 1000ft of the launch pad. The rocket flight was a complete success with the apogee prediction close to 99%, shown in *Figure 25*. The data is compared to the prediction for altitude in *Figure 26*.

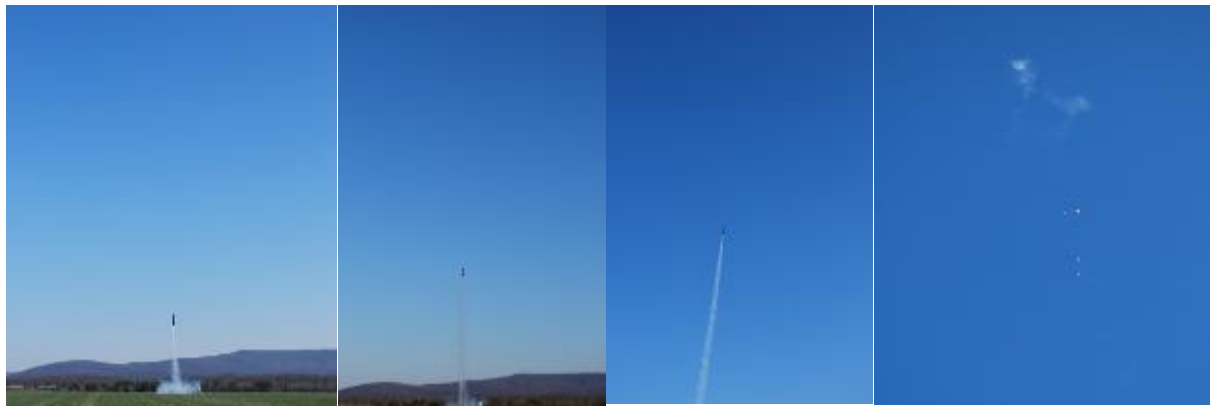


Figure 25: Flight takeoff and recovery in side winds, ideal trajectory and landing

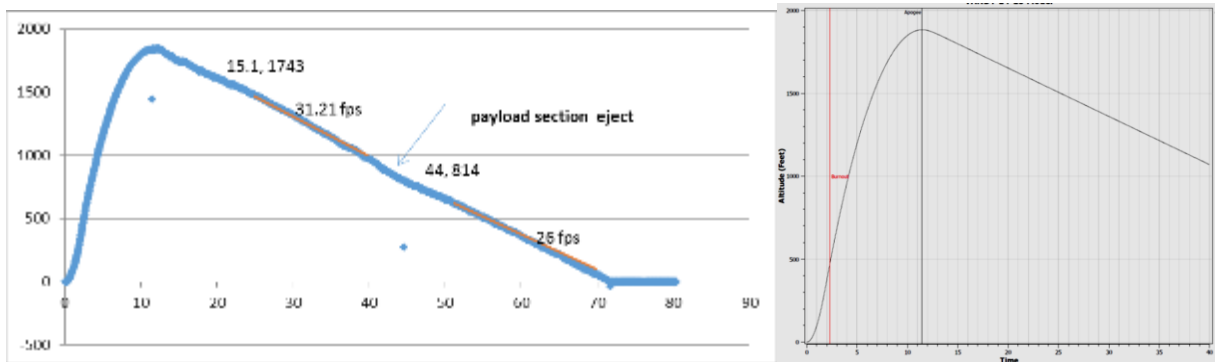


Figure 26: (a) Altitude reached (1840ft) as opposed to a predicted altitude of 1850 ft.

4.3.2.2 Flight 2 Analysis

The flight and recovery of all rocket and payload parts were very successful. The landing energies are as indicated in the following table.

Table 3: Details of the second flight showing that the landing energy criteria and the payload ejection and landing criteria were successfully met.

Criterion	Rocket w/motor	Nose cone	Mid section	Aft section
Mass	13.8 lb	5.75 lb	3 lb	4.25 lb
Predicted Apogee	1990 ft			
Parachute size		3ft	4ft	4ft
Deployment charge		2 gm	3.5gm	
Speed under 4ft Main/Drogue after apogee		31.2 fps	31.2 fps	31.2 fps
Speed under parachute after 800 ft		24 fps on 3' parachute	26 fps	26 fps
Landing energy		51.4 lbf-ft	31.5 lbf-ft	44.6 lbf-ft

A careful analysis of the flight reveals that a 3ft parachute would be sufficient to land the payload section and a 4ft parachute would be sufficient to land the rest of the rocket body within the energy limits prescribed for the flight. However, using a higher drag 3ft parachute and a lower mass on the payload section would reduce its landing energy further. Most importantly, it has become clear that despite reaching an altitude of 2000ft., the rocket sections don't seem to drift much while landing.

4.3.2.3 Flight 3

An actual payload was flown this time. The mechanism of payload compartment actuation and the feasibility of manually placing the payload were checked out, shown in *Figure 27*. Additionally, the ability of the payload compartment to stay shut during flight and deployment was checked out. The nose cone section of the previous flight was switched out with an actuated payload compartment of almost identical mass (0.375 lb. lighter) such that the flight stability margin, rocket length and flight mass remained almost the same. The rocket again flew on a J330 motor, took off beautifully and reached an altitude of 1955 ft. against a predicted altitude of 1976 ft. in low winds. There was minimal windcocking and almost perfect flight. The nosecone and the tail sections were recovered perfectly within 800 ft. of the launch site.



Figure 27: Payload bay motor-based activation and manual payload placement

4.4 Comparison of Subscale to Full-Scale Launch Vehicle

4.4.1 Comparison Overview

In order to accurately represent our full-scale launch with a subscale launch we had to incorporate several factors. Of these factors, we decided that Static Stability Margin, Payload Compartment Mass Percentage of rocket mass, Landing Energy of the payload section and the tail section, Take-off G level, and Rail exit velocity as the most important. The design decisions that led to rocket sizing, motor sizing, and parachute sizing were the result of simulating these values as best as possible. The chart below is a visual representation of the comparison of these values for the full-scale and subscale models.

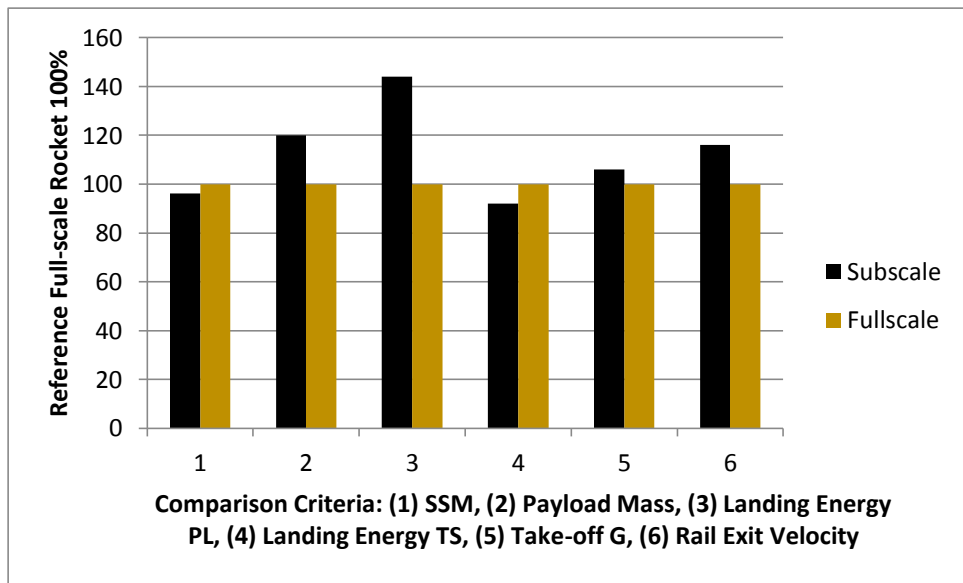


Figure 28: Comparison of Key Criteria between Full-Scale and Subscale Flight Vehicles

As can be seen in the chart above, we have achieved parity in Static Stability Margin, take-off acceleration, landing energy of the largest part of the tail section. We have improved landing

energy of the payload section (by lowering it), with lowered payload mass and higher drag parachute. We have a slightly lower takeoff speed, but the speed of 70 fps is much larger than the 45 fps minimum required to clear the launch pad.

4.4.2 Vehicle Design Comparison

Table 4: Comparison of Key Parameters for Full-Scale Launch vs. Subscale Launch

Dimension/Description	Full-Scale Model	Subscale Model
Total Height (in)	58.4	64
Diameter (in)	4	4
Loaded Weight (lb.)	14.55	13.8
Static Stability Margin	1.78	1.27
Rail Exit Velocity (fps)	70	80
Average Acceleration (+G)	5.0	5.4
Apogee Altitude (ft. AGL)	3085	1850
Payload Section		
Parachute Diameter (in)	30 (Elliptical)	36 (Simple Bell)
Parachute CD	1.5-1.6	1.2
Landing Mass (lb.)	5.64	5.75
Parachute Deployment Altitude (ft. AGL)	1000	800
Landing Speed (fps)	23.9	25.2
Max Landing Energy (lbf-ft)	43	56
Main Section		
Rocket Parachute Diameter (in)	30 (Elliptical)	48 (Simple Bell)
Rocket Parachute CD	1.5	1.2
Rocket Parachute Deployment Altitude (ft.)	3085	1850

AGL)		
Landing Mass (lb.)	8.0	7.4
Landing Speed (fps)	24.8	21.3
Max Landing Energy (lbf-ft)	39.63	31
Motor Details		
Motor Description	Cesaroni Pro-54 J380	Cesaroni Pro-38 J330
Diameter (mm)	54	38
Length (cm)	32	41.9
Total Weight (g)	1293	702
Average Thrust (N)	382	325.3
Max Thrust (N)	434.6	459.3
Total Impulse (Ns)	1043	765
Burn Time (s)	2.7	2.3

4.4.3 Mass Statement

The following table details the mass of the rocket components.

Table 5: Full-Scale Vehicle Mass

Section	Target Lower Mass Limit @ CDR(lb.)	Target Upper Mass Limit @ CDR (lb.)	Actual Launch Vehicle Mass @ FRR (lb.)	Optimized Final Launch Vehicle Mass @ FRR (lb.)
Payload section (including nosecone, payload bay, avionics bay)	4.5	4.75	4.96	4.65
Forward section (including payload and rocket parachutes, and avionics bay)	3.0	3.625	4.38	3.85

Tail Section (Including motor, fins, bulkheads)	3.25	3.50	3.29	2.95
Paint & Dressing	0.25	0.25	0.25	0.20
Total:	11.00	12.125	12.88	11.65

Table 6: Subscale Vehicle Mass Limits

Section	Predicted Mass (lb.)	Actual Mass (lb.)
Payload Section (Including nosecone, model payload, parachute)	5.5	5.5
Forward Section (Including avionics bay, rocket parachute)	6	3
Tail Section (Including motor, fins, bulkheads)	6	3.5
Paint & Dressing	0.6	0.25
Total:	18.1	12.25

At CDR, the projected mass of the yet-to-be-built competition rocket was predicted between 11.0 and 12.125 lbs. with a mean at 11.55 lb. Following the construction, in the first iteration, the mass came out as 12.88 lb, way above the targeted regime. The team systematically reduced the mass of the rocket by swapping out the $\frac{1}{2}$ " Kevlar shock chord with $\frac{1}{4}$ " Kevlar shock cords, and replacing the bulkhead steel U-bolts with aluminum and bigger steel quick-links with smaller quick-links, without compromising safety and reliability.

A case in point is the breaking strength of the $\frac{1}{4}$ " Kevlar cord. A 17" piece of the cord was tested in the load frame, using the same knot at each end we use in the field. The material broke at 4.8kN, nearly 1100 pounds; exceeding our needs. More information on this test can be found in *Section 4.5.7: Recovery System Testing*.

4.5 Recovery Subsystem

4.5.1 Recovery System Overview

Recovery of the launch vehicle will be accomplished by a rocket parachute deploying at apogee. The avionics bay will have two independent *PerfectFlite Stratologger CF* altimeters which will initiate all parachute deployment and will also collect altitude data. One altimeter will be considered the “main” while the second altimeter will be a redundant “backup” altimeter. Each altimeter will have its own 9V battery, arming switch, and black powder charges. There will be an additional altimeter in the payload section to independently establish the descent energy of the

payload section, when jettisoned off at 1000ft. A flowchart outlining the general path of logic in the recovery system is shown next, in *Figure 29*.

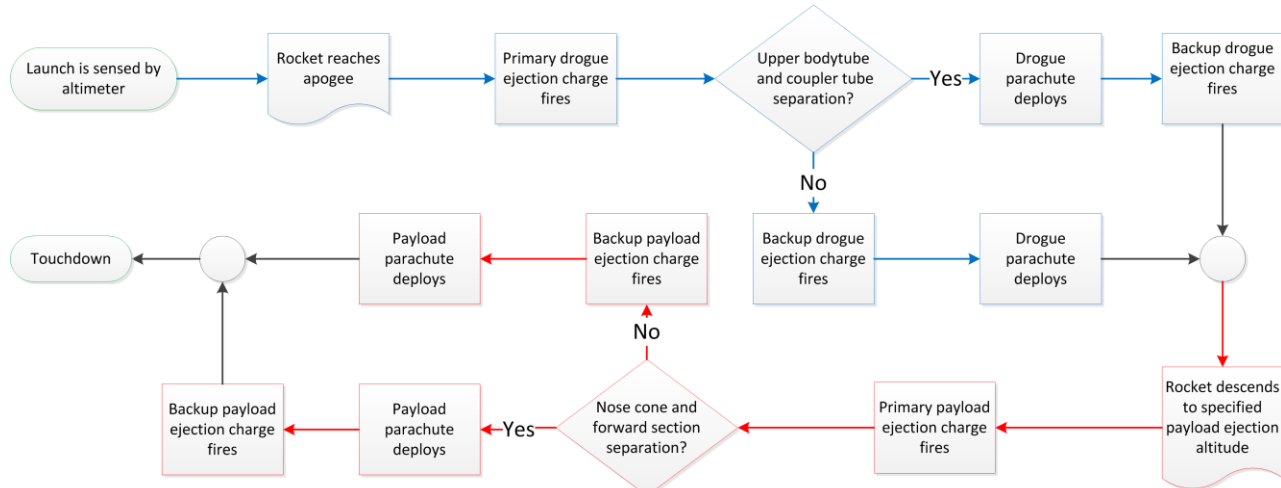


Figure 29: Recovery System Flowchart

4.5.2 Rocket Separation

Rocket separation will occur in two events: the rocket parachute deployment and the payload jettison. The two separation events will occur (1) at the joint between the forward section and the aft section, (2) at the joint between the payload section and forward section. The payload and forward sections will house the payload parachute, while the forward section will house the avionics bay. The forward section will additionally house the rocket parachute. This process is sketched in *Figure 30*.

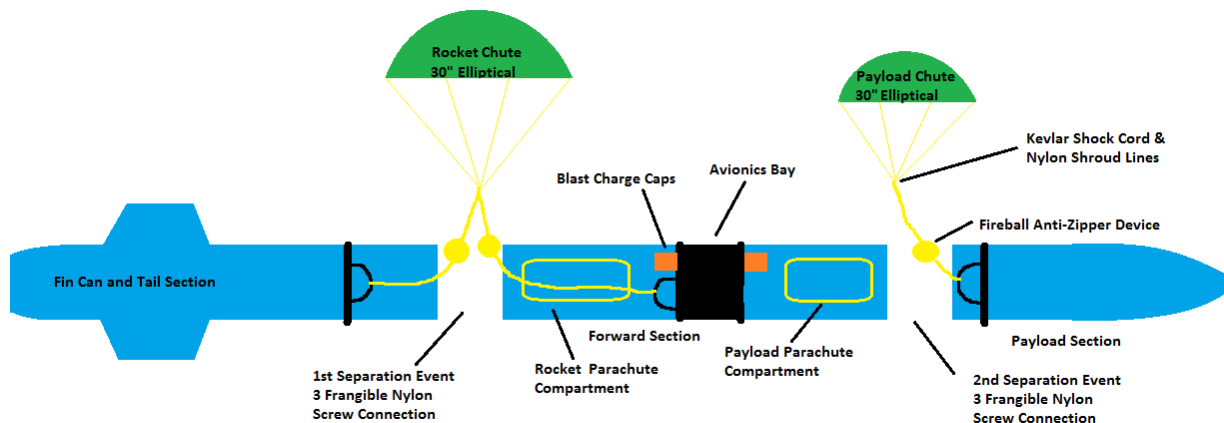


Figure 30: Recovery System Schematic

Physical separation will be achieved via controlled detonation of pyrotechnic charges located on bulkheads separating the rocket sections to create positive pressure inside the parachute bays. The pyrotechnic charges selected for both deployment events are 4F black powder charges specifically sized to create at least 210lb of separation force per charge. For each deployment

event both a primary and a backup charge, each capable of independently forcing separation and controlled by their own altimeters, will be detonated to ensure rocket separation.

The 210lb of separation force generated by each charge will be large enough to shear three #4-40 nylon screws that will secure the nosecone and upper body tube together in their places not including friction. The maximum rated shear strength for the #4-40 screws is 70lb per screw.

$$F = \sigma A = 10,000 \frac{lb}{in^2} * \frac{\pi}{4} * (0.095in)^2 = 70 lb$$

Consideration of the rocket geometry and application of the ideal gas law provided:

Ideal gas equation:

$$PV = nRT$$

Where for 4F Black Powder combustion:

$$R = 266 \frac{lb_f \cdot in}{lb_m \cdot R^\circ}$$

$$T = 3300R^\circ$$

$$P = \frac{210lbs}{12.6} in^2 = 16.7 psi$$

$$L = bay\ length$$

$$V = 12.6 \cdot L (in)$$

$$m = 453 * \frac{PV}{RT} \text{ in grams}$$

The length of the compartment between the bottom of the nosecone avionics bay and the dividing bulkhead in the forward section is 7.5". Solving the ideal gas equation for "m" with L = 7.5" shows that at least 0.81 grams of powder will be needed for successful separation and release of the payload parachute. Similarly, the length of upper side of the aft avionics bay to the dividing bulkhead in the forward section is 10.5". Solving the ideal gas equation for "n" with L = 10.5" shows that at least 1.15 grams of powder will be needed for successful separation and release of the rocket parachute. Using previous experience and to ensure separation, a factor of safety of 2.5 will be used. This leads to 3.0, 2.0 gm of powder being used for the rocket parachute, and the payload parachute. The backup charges will be 3.2 and 2.0 gm. respectively; these charges will be set to go off 1" after the rocket parachute at apogee, and at 900 ft. for the payload section.

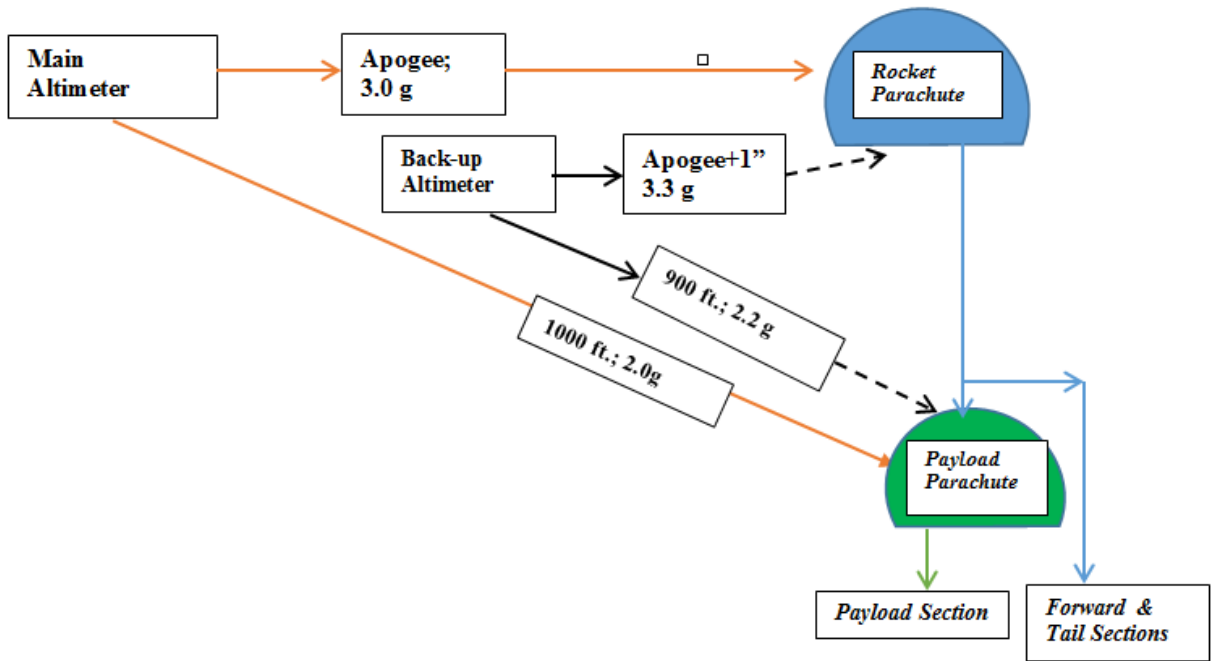


Figure 31: Recovery System Flowchart

For the subscale model, a similar approach was taken. The rocket separation occurred at two stages: 1) the joint between the forward section and the payload section, and 2) at the joint between the forward section and the tail section. The same shear pin structure was used, but the amounts of powder required for the blast were slightly different because of different lengths of tube. The distance from the bottom of the bulkhead in the nosecone to the top of the avionics bay in the forward section was 8". Using L=8", we found that we needed at least 0.87g of powder. For the other separation event, the length between the bottom of the avionics bay and the bulkhead at the top of the motor was 15", requiring 1.6g of powder. Using the same factor of safety as above, we needed 2g and 3.5g respectively for each separation event.

4.5.3 Rocket Parachute Recovery

The first separation event occurs immediately after the rocket reaches apogee and starts dropping down. This will use a 30" diameter *fruity-chute* elliptical parachute. It will provide a stabilized descent at approximately 42.3 ft. /sec for a rocket of weight 12.8lb. A Nomex/Kevlar parachute protection pad will surround the parachute to prevent it from being burned by hot ejection gasses. For moderate to high wind conditions a 30" chute is ideally suited to forestall excessive wind drift. The drogue parachute will attach to a 30ft. Kevlar 1/4" shock cord via quick link. The shock cord connects to a short 1/2" wide Kevlar harness near the ejection charges where fireproof material is needed. The shock cord, rated minimally at 1500lb (test verified @ 1100 lb.), will tether the drogue parachute to the aft end of the avionics bay and the forward end of the tail section, again using quick links. Furthermore, nine 43" nylon shroud lines (86" continuous) will attach the parachute to the shock cord. A cross stitch seam type using #400 flat line threads will connect the nylon parachute sections. These parachute materials are lightweight but also strong enough to safely return the rocket to the ground. Using quick links, the shock cord will tether the

parachute to the tail section and the forward section (rigidly bolted to the body tube) via two $\frac{1}{4}$ " steel U bolts. These U bolts will be bolted to bulkheads within the rocket. The same attachment method will be used for the payload chute shock cord on the payload section side.

Landing speed with a 30" drogue from 3010ft to 1000ft is calculated as follows:

$$V_{ld} = \sqrt{\frac{mg}{0.5\rho C_D A}} = \sqrt{\frac{56.8N}{0.5 * 1 \frac{kg}{m^3} * 1.5 * 0.456m^2}} = 12.9 \frac{m}{s} = 42.3 \text{ fps}$$

At 1000 ft., once the nose cone is jettisoned, the landing speed drops to 31 fps and the landing energy of the heaviest section of the fin can and payload bay.

$$KE_{largest\ part} = \frac{\left(\frac{W}{g}\right) \cdot V^2}{2} = \frac{(4.1) \cdot 31 \text{ fps}^2}{2 \times 32.2} = 61.1 \text{ lbf-ft} < 75 \text{ lbf-ft}$$

Experience shows that there will be some lofting from the side winds and the landing energy will be slightly lower than estimated.

4.5.4 Payload Parachute Recovery

The second separation event occurs at 1000ft. and initiates the payload recovery process. Payload recovery will use a 30" diameter *elliptical* type parachute. This will provide a stabilized descent at approximately 24.8 fps for a payload of weight 4.85 lb. A Nomex/Kevlar parachute protection pad will surround the parachute to prevent it from being burned by hot ejection gasses. Depending on wind conditions, the drogue chute size may change to forestall excessive wind drift.

Landing speed with a 30" elliptical parachute from 1000ft is calculated as follows:

$$V_{ld} = \sqrt{\frac{mg}{0.5\rho C_D A}} = \sqrt{\frac{21.5N}{0.5 * 1.1 \frac{kg}{m^3} * 1.5 * 0.456m^2}} = 7.6 \frac{m}{s} = 24.8 \text{ fps}$$

Landing energy of the payload section: $4.85 \text{ lb} * \frac{24.8^2}{2 \times 32.2} = 46.3 \text{ lbf-ft} < 75 \text{ lbf-ft}$

The landing energy assumes absolutely no ground wind; however, our experience has been that the ground wind speed contributes to lofting and the actual landing speeds with the main are substantially lower.

The payload parachute will be connected with a quick link to a 15 ft., 1/4" wide Kevlar shock cord rated minimally at 1500lb (tested @ 1100 lb.). The shock cord connects to a short 1/2" wide Kevlar harness near the ejection charges where fireproof material is needed.

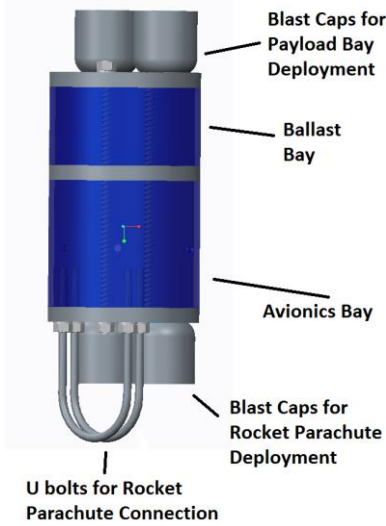


Figure 32: Side View of Avionics Bay, blast caps visible

4.5.5 Avionics and Avionics Bays

The avionics bay is designed to house all of the electronics required for activation of the recovery system. In addition, there will be a separate compartment on the fore side of the avionics bay to allow for ballast to be added if the assembled weight falls short of our predicted weight as it has in our other iterations. It will protect these electronics from many things including but not limited to: the explosive forces experienced during black powder ejection charge ignition, the vibrations during rocket flight, and radio-frequency interference. The avionics bay will also allow exposure to the atmosphere for the altimeters to sense the pressure outside of the rocket so that they may accurately record altitude and trigger the recovery system at the appropriate altitudes. Furthermore, the avionics bay will allow for altimeter activation on the launch pad once the rocket is fully assembled.

The location and size of the static pressure ports are important. The ports will be located on the altimeter bay and situated in such a way as to minimize air turbulence caused by obstructions forward of the ports. To calculate the size of the static pressure ports, we use a formula from “Modern High-Power Rocketry 2”, written by Mark Canepa.

Single Static Pressure Port Sizing:

$$D_p = \frac{V_b}{400}$$

where D_p is the diameter of the port, and V_b is the volume of the avionics bay. This equation is valid for altimeter bay volumes of up to 100 cubic inches.

For multiple static pressure ports, we have the following formula:

Multiple Static Pressure Port Sizing

$$\widehat{D_p} = 2D_p/N$$

where N is the desired number of static pressure ports.

Applying these formulas to our avionics bay, we have:

$$D_p = \frac{4\text{in} * \pi * 2.6\text{in}^2}{400} = 0.212 \text{ in}$$

Should we desire three static port holes, the diameter of each port should be:

$$\widehat{D_p} = \frac{2D_p}{N} = \frac{2 * 0.212\text{in}}{3} = 0.141 \text{ in}$$

The avionics bay will therefore use three 3/16" static pressure port holes, equally spaced radially around the bay. Using 3/16" holes will give us an increased margin and ensure the altimeter are sensing the correct atmospheric pressure.

Verification of the port sizes will come from inspection of the rocket velocity data, which will confirm that parachutes were ejected at the appropriate altitudes. Additionally, proper parachute deployment will also verify the ports are appropriately sized.

In order to prevent premature arming of the ejection charges by the altimeters while the rocket is being assembled or carried to the launch pad, the avionics bay is designed such that the altimeters can be easily armed from the exterior of the rocket body while the rocket is on the pad and ready to launch. To accomplish this, two arming screw switches accessible from outside the rocket will be mounted to inside avionics bay, and wired such that the altimeters cannot be powered until the switches close the connection. The screw switches are chosen because once they are armed, they will not accidentally change to the off position due to vibrations and the stresses of a high-g takeoff. The screw switch system has been validated by previous years' experience, and will be tested again during our three full scale launches. The altimeter arming switches in last year's rocket were mounted directly on the rocket body (outer blue tube) and not physically inside the altimeter bay. Thus, the back ends of the switches were in the same space as the rocket chute and shock cords. *This year the switches will be mounted inside the avionics bay but will still be switchable from outside the rocket.* This will prevent the possibility of the rocket chute shearing the switches off during deployment thus causing power loss to the altimeters. In addition to increasing ease of assembly, mounting the switches inside the altimeter bay will also increase the reliability of the recovery system. A photo showing the arming switches mounted to the upper avionics bulkhead is shown next.



Figure 33: Arming Switches Mounted Inside Avionics Bay (Armable from Outside of Rocket in Launch Configuration)

The photo above also shows the batteries resting on the bottom bulkhead of the avionics bay.

CAD images of the avionics bay, where the altimeters and batteries will be housed, are shown below. These images show both ends of the bay, the static pressure ports, the igniter electrical terminals, and also show the $\frac{1}{4}$ "-20 U-bolts and threaded rods which are the main structural components. Furthermore, the rocket parachute blast caps can also be seen on the bottom side of the avionics bay. Images of the built avionics bay are shown as well (*Figure 35*, *Figure 36*).



Figure 34: Bottom of Avionics Bay (Shock Cord U-Bolt Attachment can be clearly seen)

The pictures below more clearly show how the altimeters fit inside the avionics bay. This year, the altimeters will be mounted on opposite sides of a $3/8$ " x 1.25 " x 4.75 " plywood board. This allows the overall length of the avionics bay to be reduced when compared to last year's avionics bay in which the altimeters were mounted on the same side of the board. Photos of the altimeters mounted to the board are shown below. Note that the batteries are secured to the bottom avionics

bulkhead where they will be less likely to move since they can “rest” on the bottom bulkhead while at the same time being secured via other means.

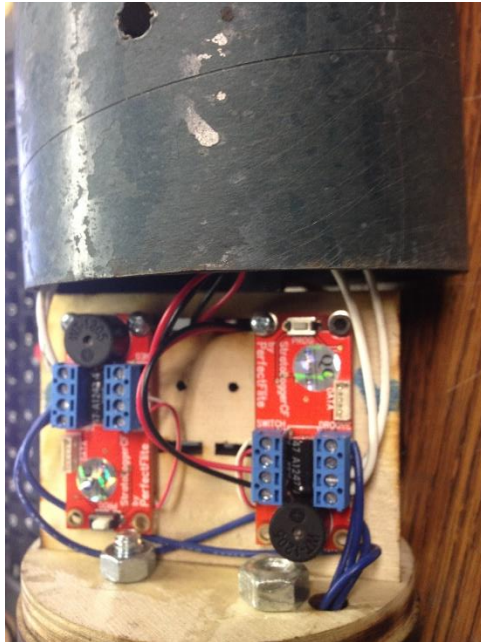


Figure 35: Altimeters mounted on tray, batteries mounted on back (Not Shown)



Figure 36: Avionics mounting nuts embedded directly into central avionics bulkhead

4.5.6 Deployment Charge and Altimeter Layout

The deployment charges are located on the top and bottom sides of the avionics bay. These charges are for the payload parachute and the rocket parachute respectively. For each set of charges, there is a main charge and a backup charge to ensure rocket separation. The main

altimeter is responsible for firing the main deployment charges for both the payload and the rocket parachutes, and the backup altimeter fires the backup charges for each.

The altimeters are located side by side and mounted onto the birch plywood platform that is epoxied to the middle bulkhead. The batteries will be located on the other side of the plywood platform. Each altimeter will be connected to its own dedicated power source (9V battery), its own dedicated arming switch, and its own igniters and black powder charges. As previously stated, the charges for the payload, rocket parachutes will be 2.0, 3.0 grams respectively, with backup charges being 2.0 and 3.2 g respectively.

The following figure shows how the Stratologger Altimeters will be connected with the deployment charges for the parachutes.

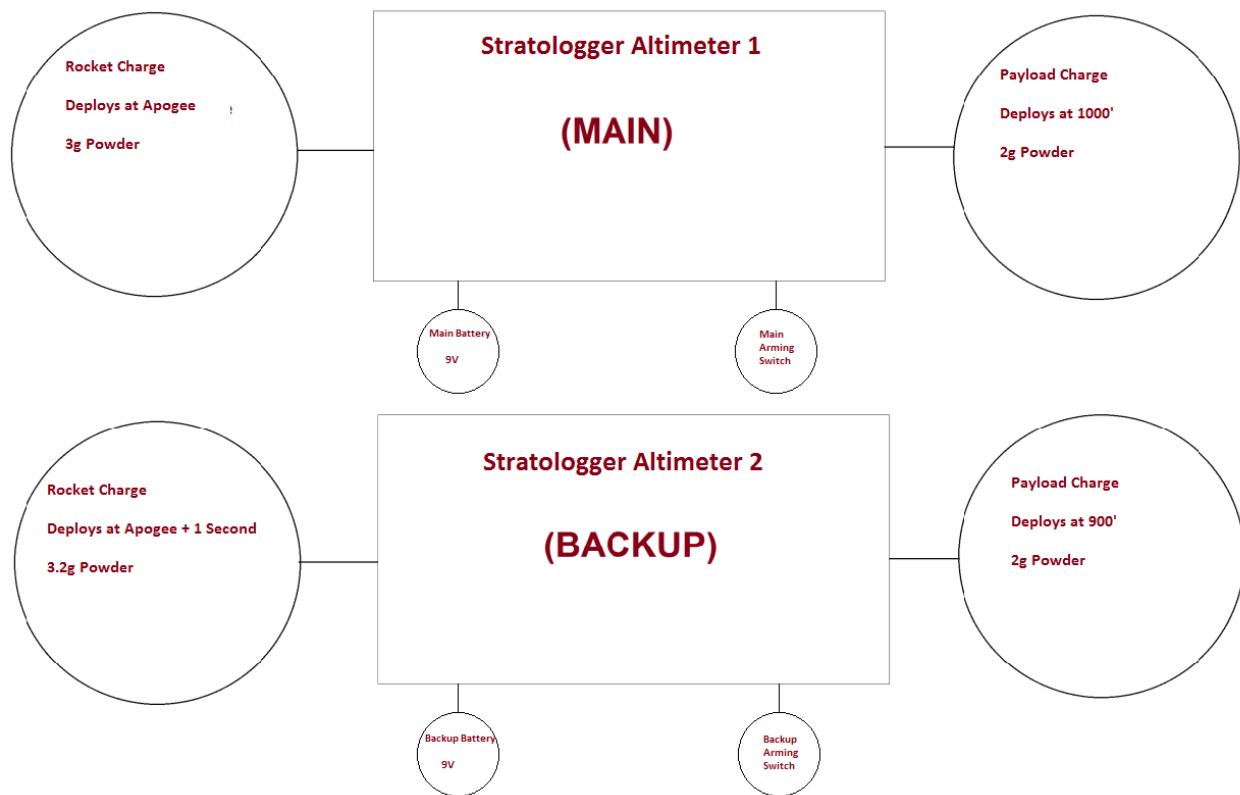


Figure 37: Diagram of Altimeters' Circuits

As can be clearly seen, all aspects of the recovery system have a second, *independent* copy of each component. This means that the entire rocket recovery system is redundant. See sections 4.5.7: *Recovery System Testing* and 6.1.2.3: *Recovery System Failure Modes and Risk Assessment* for proof of recovery system testing ensuring that both the main and backup systems are in optimal working order.

4.5.7 Recovery System Testing

A complete test of the deployment system on the rocket is carried out before each launch (a picture of this is shown in *Figure 38*). The test consists of two different aspects: testing the deployment charges / rocket separation, and testing the altimeters.

To test the rocket separation, the rocket is fully assembled with the parachutes properly packed and installed and all appropriate amounts of black powder in their respective locations. Igniters are connected to a custom control box allowing them to be manually ignited. The rocket is placed in a safe outdoor location with no objects or people near it. The entire protocol is monitored and managed by safety mentor Robin Midgett and student safety officer Connor Caldwell. The payload charges are then ignited. After verifying proper separation, the payload section is moved to the side to avoid collisions, and the rocket chute charge is fired. This completes the test of the rocket separation, and verifies the proper amount of black powder, proper shear screw usage, and to a certain extent proper parachute packing.



Figure 38: Ground-Based Deployment Testing

The altimeters are tested by first placing them in a sealed metal canister in which a vacuum can be developed. The Vanderbilt shock tube was used for this purpose, being designed to generate negative pressures well beyond the scope of altimeter testing.

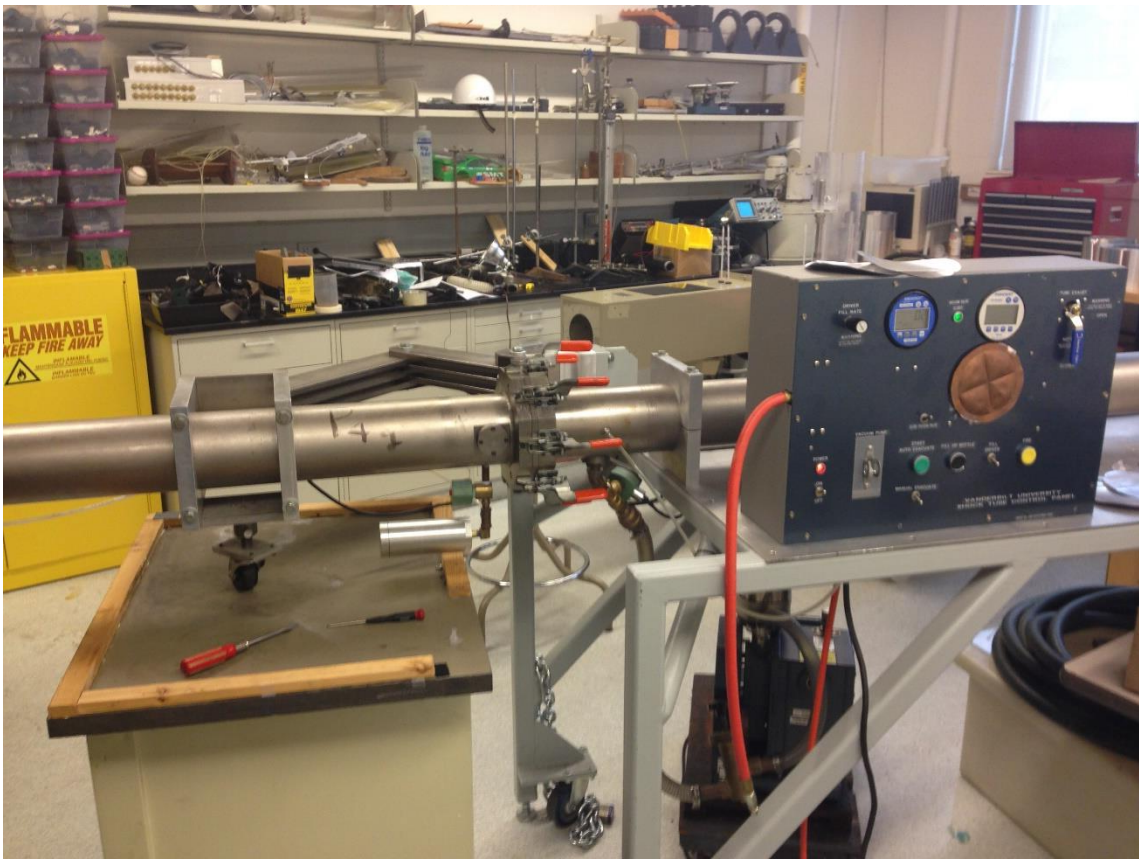


Figure 39: The Vanderbilt Shocktube acts as a convenient vacuum chamber for altimeter testing

At this point, the altimeters are already powered on and have igniters (no black powder) connected to the respective main and drogue parachute electrical leads. A vacuum of 1.5 psi about is developed in the chamber simulating a rocket ascent to an apogee of approximately 3000ft. Once that vacuum pressure is reached, air is slowly returned to the chamber until the pressure equalizes with the surroundings simulating rocket descent. The altimeters and igniters are inspected to verify each igniter was lit. Furthermore, data from the atmospheric simulation is acquired from the altimeters. This data will be analyzed to ensure that the igniters lit at the proper altitudes.

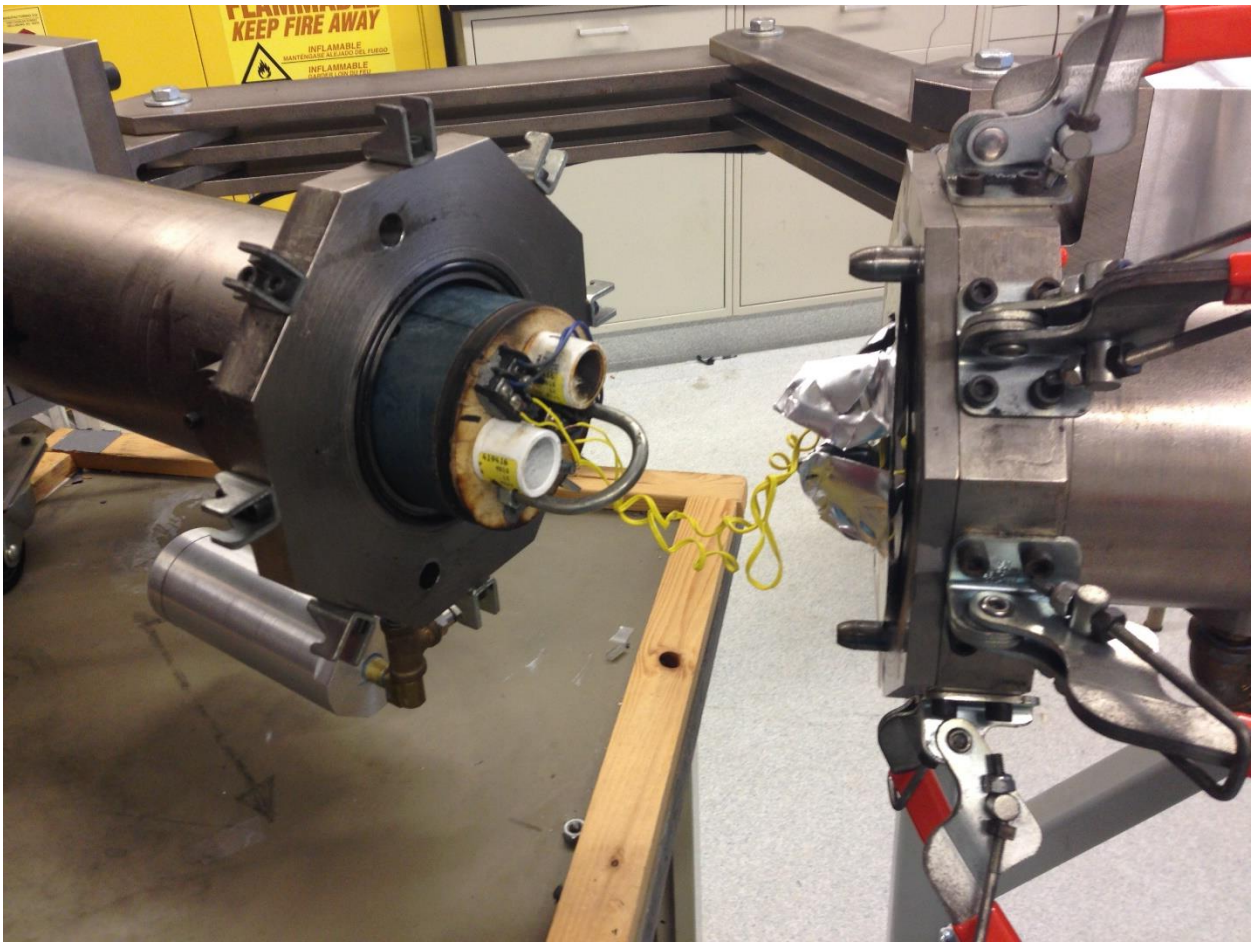


Figure 40: Placement of avionics bay in the Vanderbilt Shocktube

The deployment and vacuum tube altimeter tests will verify that the recovery system works as expected and can safely and bring the rocket to the ground.

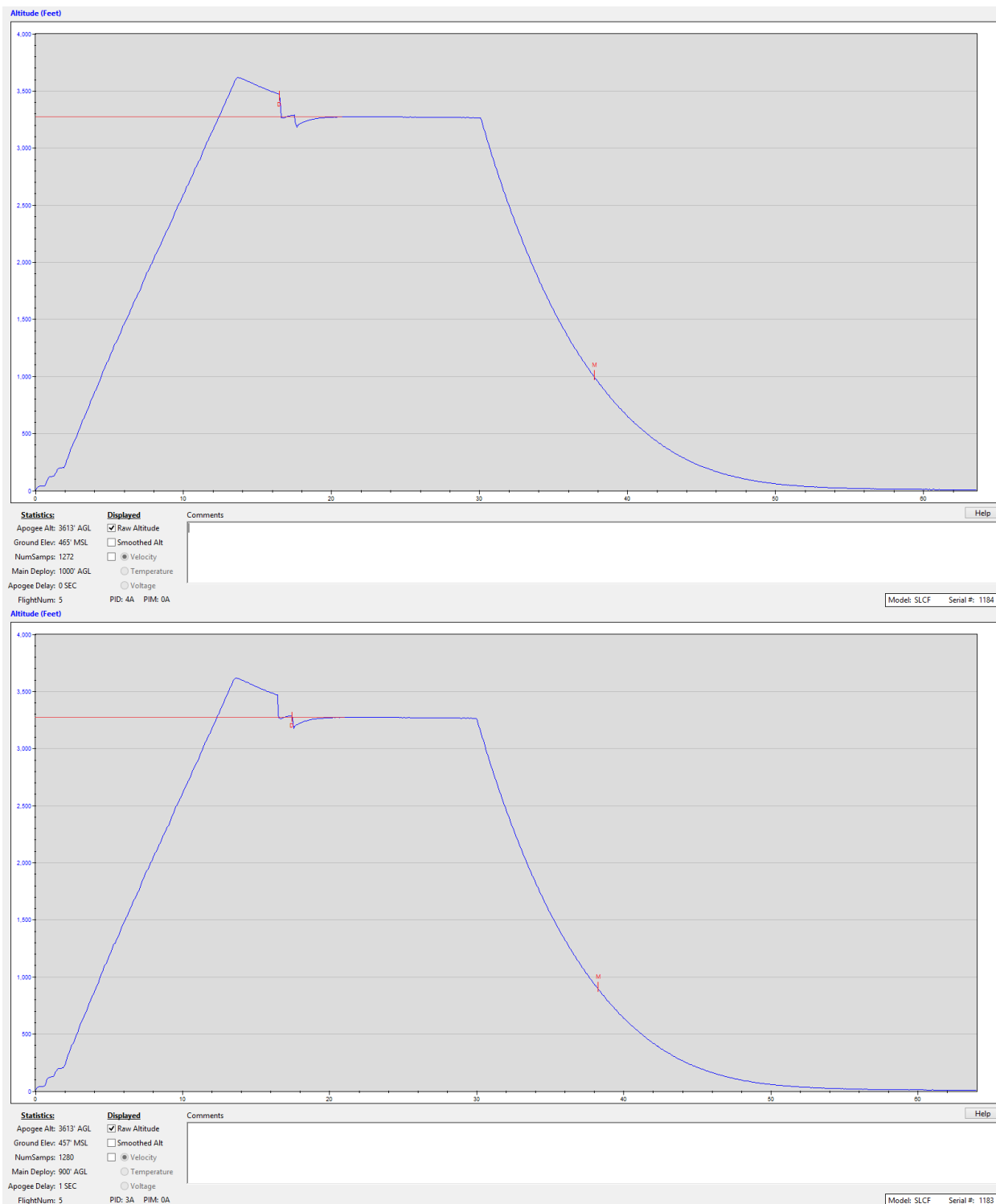


Figure 41: Comparison of main and backup altimeter performance in vacuum chamber testing

As can be seen in the above figure, both the main and backup altimeters behaved exactly as expected. Both saw an increase in elevation proportional to the decrease in pressure inside the vacuum chamber. Both altimeters logged apogee, and the electric matches (sans deployment

charges) can clearly be seen to have blown due to the two sudden dips in altitude that correspond to the deployment event stated by the altimeter circuitry. The reason that these dips are seen for both apogee deployment events but neither of the main events is simply due to electric match placement. The apogee event matches were placed near the avionics bay port holes on the opposite side of the avionics bay on display in *Figure 40*, while the main event electric matches, as depicted in *Figure 40*, were placed significantly farther away to avoid being prematurely ignited by sparks from the drogue matches.

The table below summarizes the data recorded during the vacuum chamber test from both the main and backup altimeters and proves that both of the systems independently measure and log the same information (within some small amount of error) and therefore are completely functional.

Table 7: Vacuum Chamber Test Results for Altimeters

	Main Altimeter	Backup Altimeter
Apogee (ft. AGL)	3613'	3613'
Ground Elevation (ft. MSL)	465'	457'
Total Number of Samples	1272	1280
Steady State Altitude (after apogee and before total repressurization)	3284'	3282'

In addition, we performed a comprehensive ultimate yield test on the $\frac{1}{4}$ " Kevlar shock cord to verify that the lighter weight shock cord could be employed without fear of a recover system failure. We loaded a 17" section of the shock cord into the loading frame and measured about a 1100 lb ultimate tensile strength with our field-tied knots. The shock cord is rated at 1500 lb using the manufactured knots, and that is the version that was used in our full-scale launch. Data from the yield test can be seen below in *Figure 42* and *Table 8*.

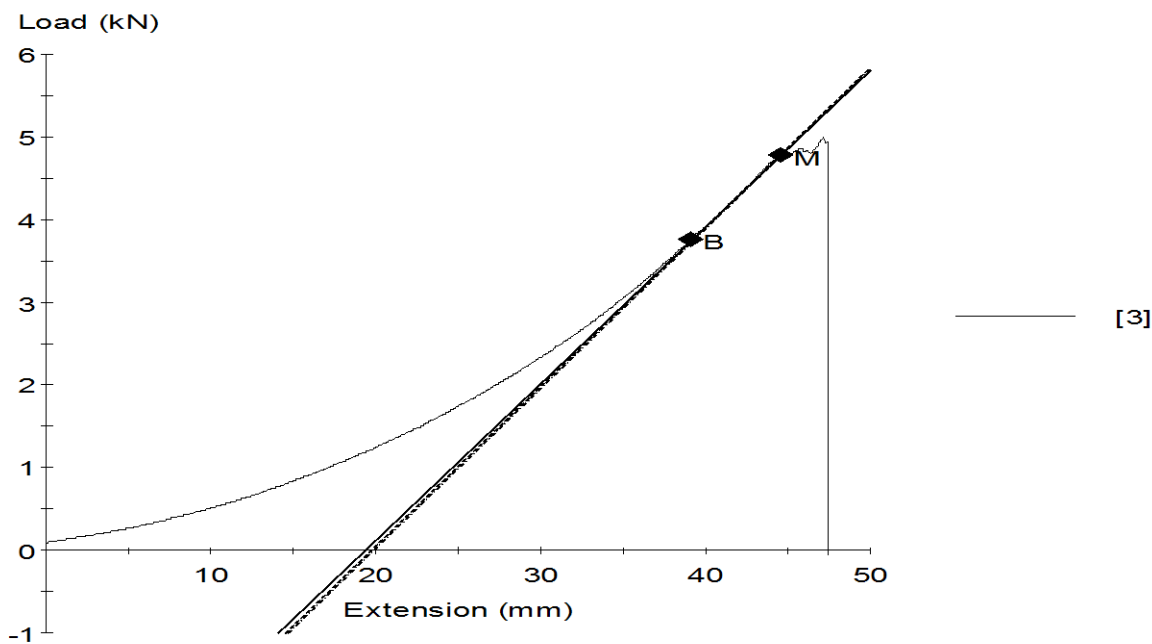


Figure 42: Experimental Data from Shock Cord Yield Testing

Table 8: Results from Shock Cord Yield Testing

Name	Value	Units
Diameter	6.000	mm
Specimen Comment		
Peak Load	5001.107	N
Peak Stress	176.9	MPa
Strain At Break	0.934	mm/mm
Modulus	347.004	MPa
Break Load	4874.875	N
Break Stress	172.413	MPa
Elongation At Break	47.463	mm
Load At Offset Yield	4760.205	N

4.5.8 Avionics Bay Structure

The rocket avionics bay (shown in *Figure 43*), which is mounted inside the forward section of the rocket (between the rocket and payload parachutes) will consist of a small section of coupling blue tube, two bulk heads, threaded aluminum rods, and two U-bolts. The avionics bay will also be split into two sections, one containing the avionics electronics and the other leaving empty space for additional ballast if necessary. The 4" coupling tube will be used so that the electronics bay can slide into the larger diameter rocket tube of the forward section and be bolted in place. This tube will also allow the avionics bay to be easily sealed from the blast pressure. An additional 2" section of coupler tube will house the additional ballast mass. Two $\frac{1}{4}$ "-20, 5 1/2" long 6061-T6 aluminum threaded rods will be cut to hold the avionics bay and ballast bay together. The three bulkheads will be laser cut and consist of two separate 3/8" birch plywood pieces glued together. One will have an outer diameter equal to the outer diameter of the coupling tube and the other will have an outer diameter equal to the inner diameter of the coupling tube, so it can slide in and be held in place. The bulkheads will have holes for the two threaded rods in addition to two 5/16" U-bolts where the parachute shock cords can be attached. The electronics will be mounted to a 3/8" thick 1.25" by 3" birch plywood board that will be epoxied into a slot on the middle bulkhead. The coupling tube will be inserted into the forward section of the rocket at the desired location where the center of the coupling tube is 10" from the bottom of the section. Then three 1/4" holes will be drilled 120° apart through both the rocket body tube and coupling tube to ensure proper alignment. Three $\frac{1}{4}$ "-20 aluminum nuts will be secured into the inside of these holes on the coupling tube to serve as an anchor for the low profile $\frac{1}{4}$ "-20 aluminum bolts that will hold the electronics bay and forward section tube together. Four nuts total, one on each end of each threaded rod will hold the electronics bay together by "clamping" the bulk heads to the coupling tube section (with electronics board inside, sitting on the threaded rods). Once assembled, the avionics bay will be slid into the forward section and bolted into place.

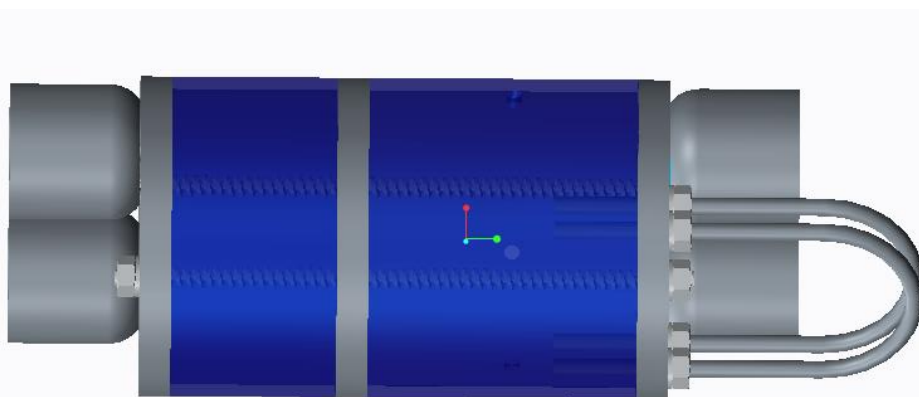


Figure 43: Side View of Avionics Bay (Notice smaller compartment for mass ballast)

The 6061-T6 threaded aluminum rods have a tensile strength of 42,000 psi. Thus, for a minor diameter of 0.188", each rod can withstand 1166 lb of force before yielding.

$$F = \sigma A = 42000 \frac{lb}{in^2} * 0.02776 in^2 = 1165 lb$$

With two rods, the total force that can be transferred through the avionics bay is 2332 lb. Thus for a 12 lb rocket there is a safety factor of almost 200. This will also allow for the increased impulse loading the rods will experience as the parachutes open and the rocket decelerates. The same logic also holds for the U-bolts, which are the same size and material as the threaded rods. There are two U-bolts on each end of the avionics bay to add redundancy for the shock cord attachment.

4.5.9 Recovery Telemetry Electronics

Two launch vehicle precision location devices, one installed in the payload bay and one in the rocket body, are incorporated into the launch vehicle on competition day in order to make the recovery efforts as efficient as possible. If line of sight with the launch vehicle is broke at any time, the telemetry electronics will aid in a rapid recovery of the launch vehicle. As stated, each independent section of the rocket (payload, rocket body) will have its own transmitter for easy recovery. The device used will be the Big Red Bee Transmitter.

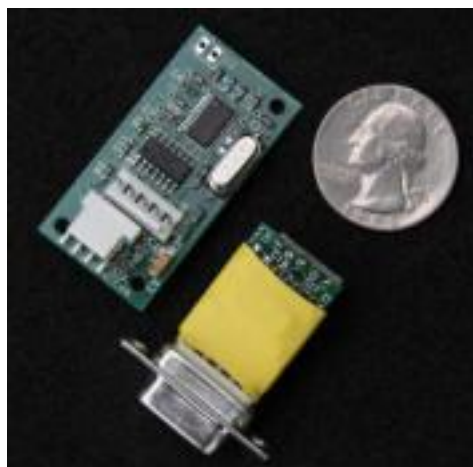


Figure 44: Big Red Bee RF Transmitter

The BeeLine TX is a small radio device that sends an RF signal to a handheld radio. The user can then use a directional antenna to detect the general direction of the launch vehicle and commence recovery operations. This device weighs 1 ounce. The handheld radio to be used is a Kenwood D7 radio. This radio is a commercially available radio and features an LCD screen for integrated in rocket recovery



Figure 45: Kenwood D7 Radio

As in previous years, the transmitter will be mounted to a portion of the rocket parachute's shock cord. The transmitter's small size and low weight means that it has no impact on the performance of the rocket's recovery system, as proven by multiple years of successful rocket recovery while mounting the transmitter in this fashion.

Due to limited space in the payload section, the transmitter will instead be mounted inside the nosecone, opposite the sample recovery tray. This provides an ample amount of free space for the transmitter's antenna to properly straighten and emit a high quality signal.

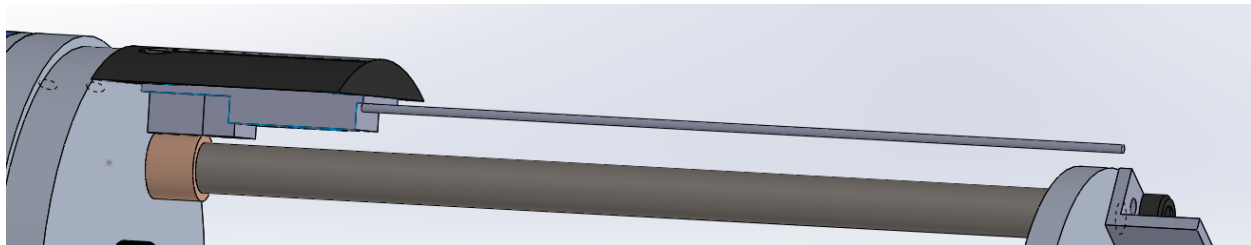


Figure 46: Payload bay RF transmitter mount

4.5.10 Safety and Failure Analysis

The safety and failure analysis for the recovery system is discussed in section 6.1.2.3: *Recovery System Failure Modes and Risk Assessment*.

4.6 Mission Performance Predictions

4.6.1 Mission Performance Criteria

1. The rocket should take-off perfectly following ignition and have a substantial speed (~70 fps) leaving the launch rail.
2. Rocket flight shall be stable (SSM between 1.5 & 2.0), and be able to negotiate side winds and wind shear.
3. The launch vehicle must attain an altitude of 3000ft AGL $\pm 150\text{ft}$.
4. The rocket parachute must deploy within 2.0 sec after apogee is reached.

5. The landing speed of the rocket from apogee shall be around 42.5 fps to minimize drift.
6. The payload compartment shall be deployed at 1000ft \pm 100 ft.
7. There shall be only three sections to the rocket to minimize complexity.
8. The landing drift of all rocket parts shall be less than 2500ft. under all launch conditions.
9. The rocket parts shall not sustain any damage while landing.
10. The rocket parts shall not be affected by humidity conditions during flight, and ambient wet conditions at landing; that it be specifically protected against moisture damage.

4.6.2 Vehicle Design Comparison

Table 9: Final Launch Vehicle Parameters

Total Height (in)	58.4	Rocket Parachute Diameter (in)	30
Diameter (in)	4	Rocket Parachute CD	1.5-1.6
Loaded Weight (lb.)	14.5	Rocket Parachute Deployment Altitude (ft. AGL)	3065
Static Stability Margin	1.85	Charge usage for Rocket Parachute ejection (gm.)	3.0 (3.2)
Rail Exit Velocity (fps)	70	Shear Pins (4-40)	3
Average Acceleration (+G)	5.0	Final Landing Mass (lb.)	7.75
Apogee Altitude (ft. AGL)	3065 AGL	Final Landing Speed (fps) of forward & tail section	31
Parachute Diameter (in)	30" (elliptical)	Max Landing Energy of forward and tail sections (lbf-ft)	61
Parachute CD	1.5-1.6	Motor	Cesaroni J380
Payload Compartment Landing Mass (lb.)	4.85	Motor Diameter (mm)	54
Payload Parachute Deployment Altitude (ft. AGL)	1000	Motor Length (cm)	32
Payload section Landing Speed (fps)	24.8	Motor Total Weight (g)	1293

Payload section Max Landing Energy (lbf-ft)	46.3	Motor Average Thrust (N)	380
Charge usage for Payload compartment ejection (gm.)	2.0 (2.0)	Motor Max Thrust (N)	434.6
Payload chamber shear pins	3	Motor Total Impulse (Ns)	1043
		Motor Burn Time (s)	2.7

4.6.3 Dimensional Drawings of Launch Vehicle

Dimensional drawings of the launch vehicle are shown in the appendix, section *10.6: Machine Drawings*. The machine drawings are much the same as those shown in Vanderbilt's CDR, but any changes since then are shown in FRR's appendix.

4.6.4 Simulations and Predictions

Mission performance was predicted through the use of *Rocksim v9.0*. The input parameters are shown in *Figure 47***Error! Reference source not found.**. Rocksim was also used to model the rocket, and was run to determine the aerodynamic profile associated with the rocket. The performance predictions made use of the rocket mass of 11.65 lb. and the launch ready mass of 14.5 lb. No additional mass will be added to the rocket.

Competition Rocket

Length: 58.4000 In. , Diameter: 4.0000 In. , Span diameter: 13.0000 In.
 Mass 232.0198 Oz. , Selected stage mass 232.0198 Oz. (User specified)
 CG: 32.5418 In., CP: 39.9555 In., Margin: 1.85
 Engines: [J380-SS-None,]

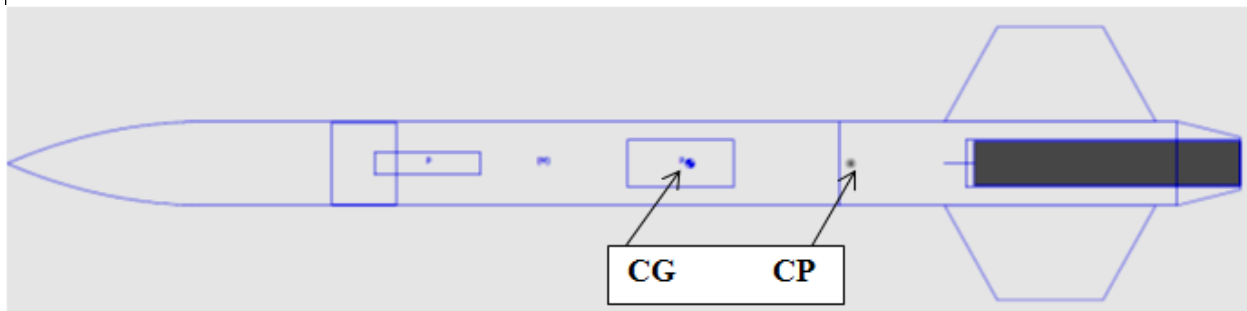


Figure 47: Location of Centers of Gravity and Pressure of Competition Rocket

4.6.4.1 Flight Stability Margin

When the launch rocket was completed, it stood at 58.4" with the payload section measuring 15.4", the forward section 24", and the tail section 19". The forward section has two compartments for the payload parachute and the rocket parachute, each measuring 7.5" and 10.5" respectively. These were chosen in the original design to accommodate the respective parachutes

and the shock cords. However, as the design evolved, we switched to a 30" elliptical parachute for both the deployments to minimize landing drift, and switched to $\frac{1}{4}$ " Kevlar shock cords to lower launch mass. The end result is that the payload parachute compartment is bigger than necessary, and the upward shifted CG leads to a more than expected stability margin of 1.85 as against a planned 1.4.

The team evaluated the dynamical flight scenarios for the rocket against shorter rocket versions (55.4", and 56.4"), which would result in stability margins of 1.5 and 1.62 respectively. Detailed simulations in *Rocksim* for very strong winds of 25mph reveal that the additional stability margin does help in reducing landing drift. The team has decided to go with the higher stability margin of 1.85, instead of further optimizing the flight rocket by reducing its length by 3", as they see landing drift being affected favorably. Reducing the length of the rocket by 3" of blue tube material has very little effect on the launch mass.

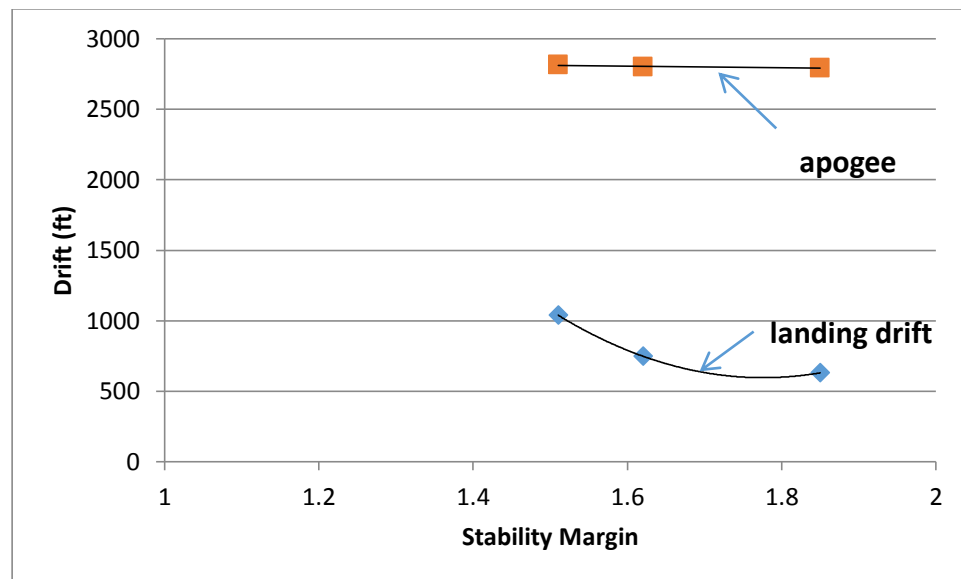


Figure 48: The variation of landing drift and apogee with flight stability margin (there is a landing drift advantage, apart from additional stability, to flying at SSM of 1.85)

The additional *Rocksim* simulation results are shown below:

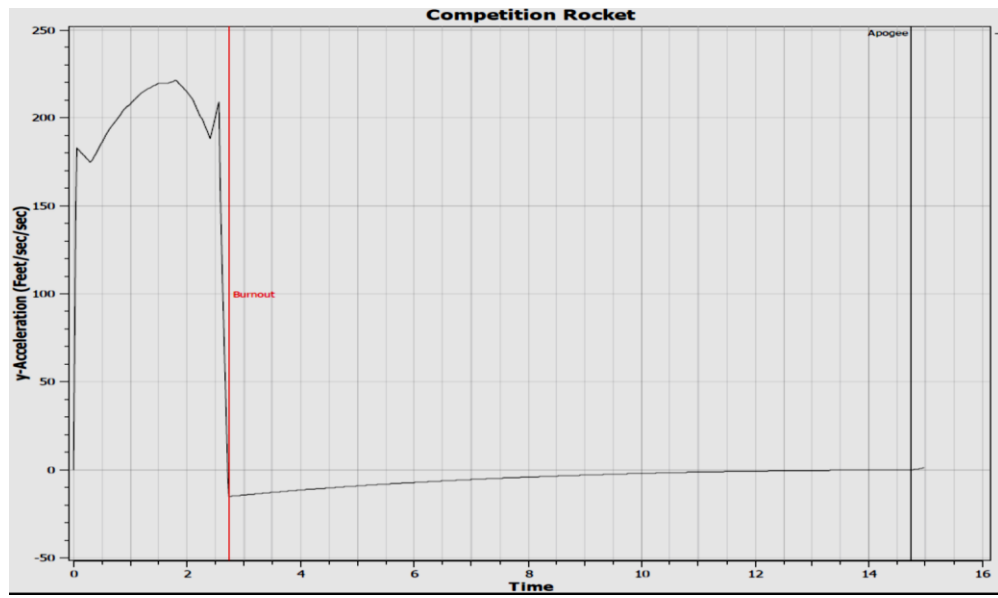


Figure 49: Flight Acceleration vs. Time (maximum acceleration is +6g)

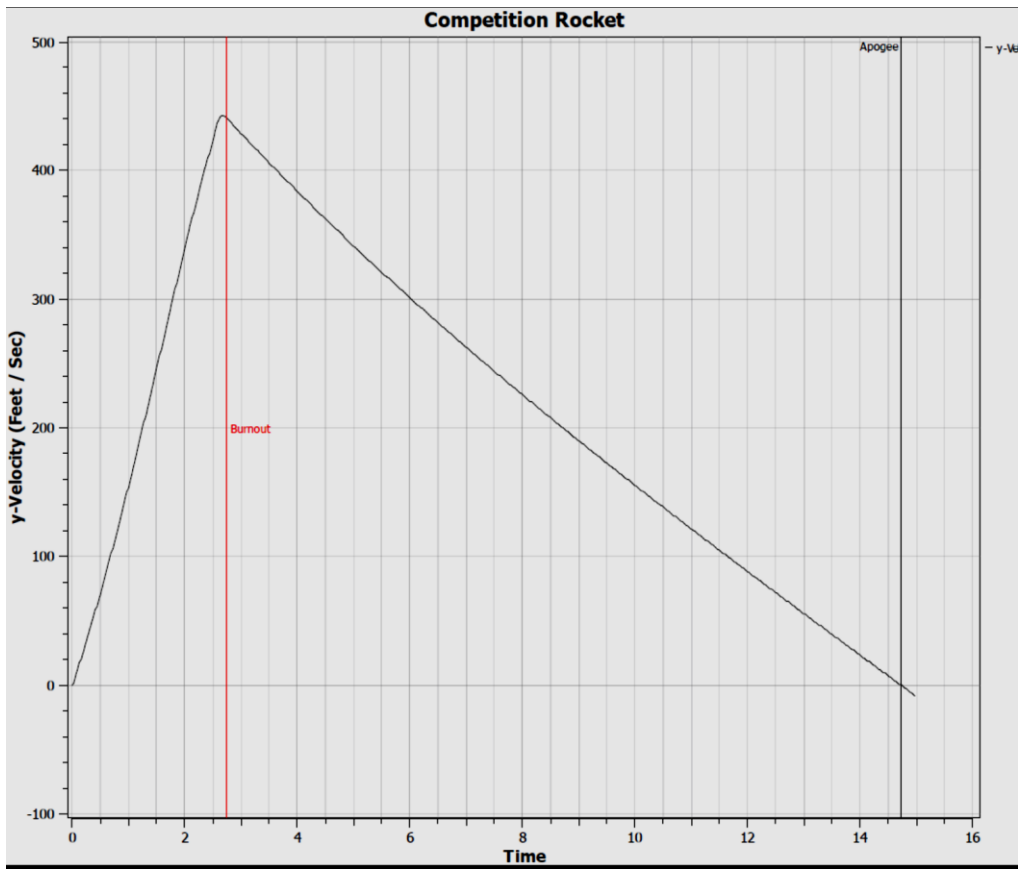


Figure 50: Flight Vertical Velocity vs. Time (maximum velocity at motor burnout is 450 fps)

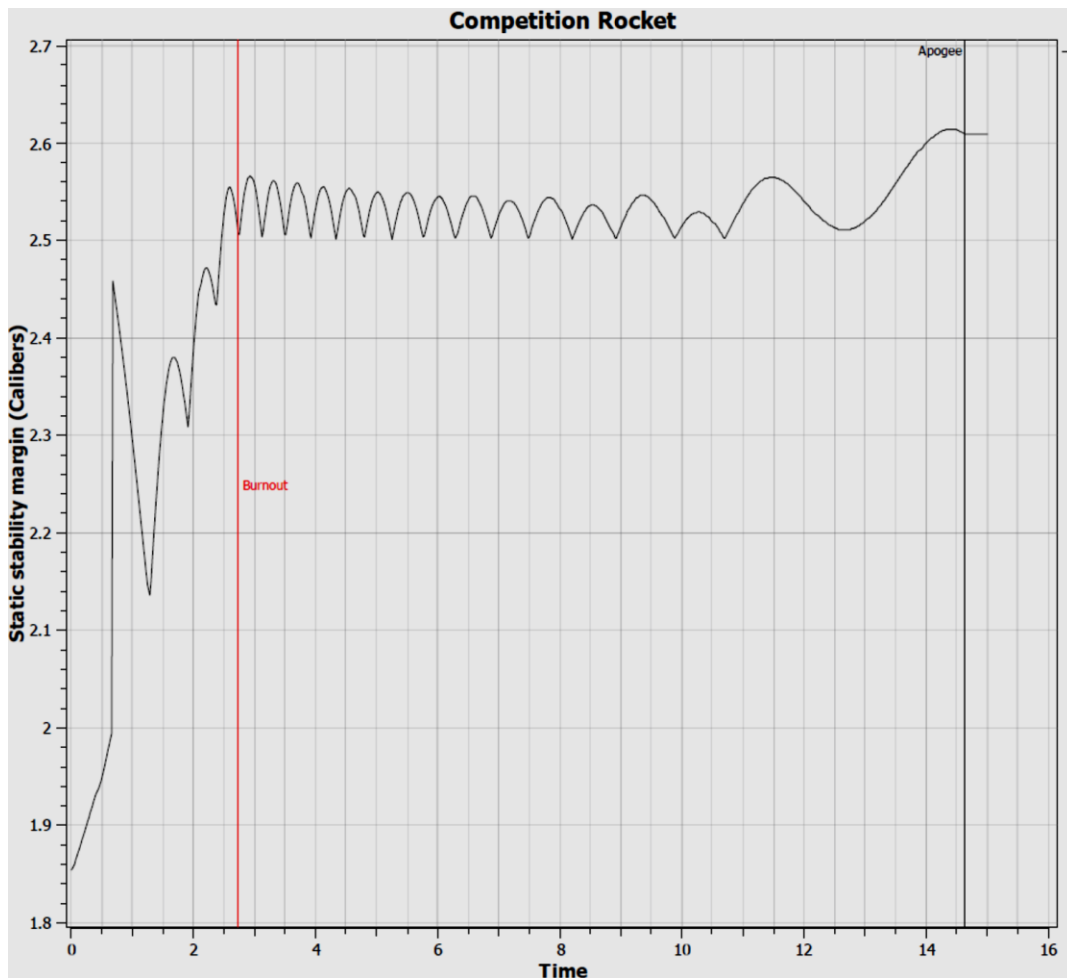


Figure 51: Flight Static Stability Margin vs. Time (stability margin quickly increase to 2.6 within seconds of flight)

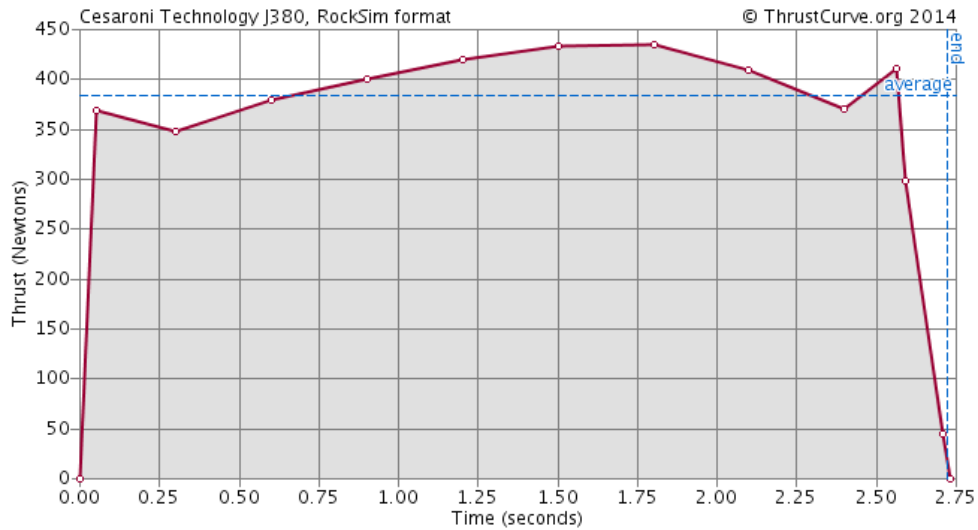


Figure 52: Cesaroni J380 Thrust Curve

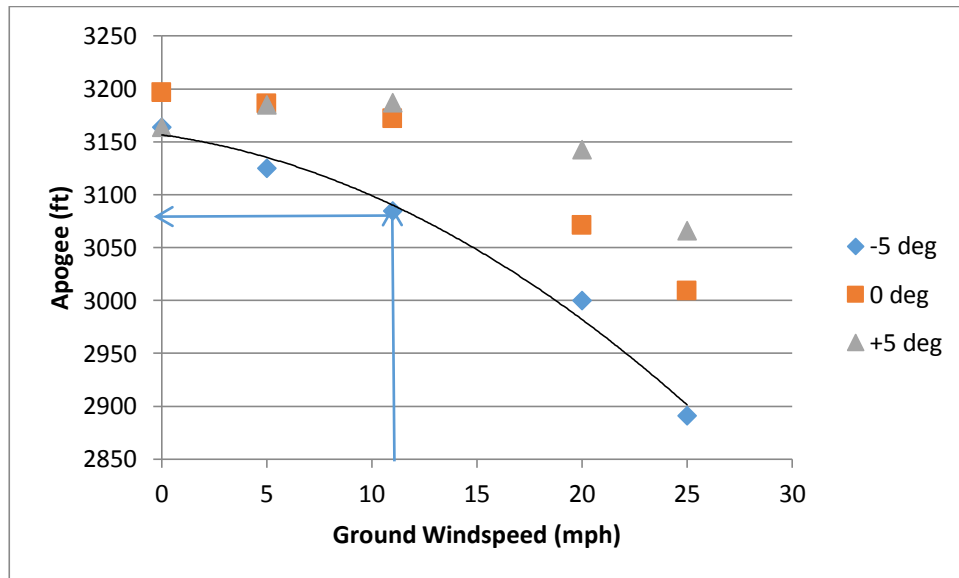


Figure 53: Rocket Apogee vs. Wind Speed (11 mph ground winds are typical in April; -5 deg launch angle is most typical with S-N winds at the site)

The *RockSim* simulations provided the following results of landing drift with ground wind speed. The simulations have been run for both $+5^\circ$ (with wind) and -5° (into wind) launch scenarios. The simulations basically take a constant lateral wind speed in the estimations. As winds greater than 20 mph constitute a launch abort condition, drift greater than 2500ft is not anticipated under acceptable flight conditions.

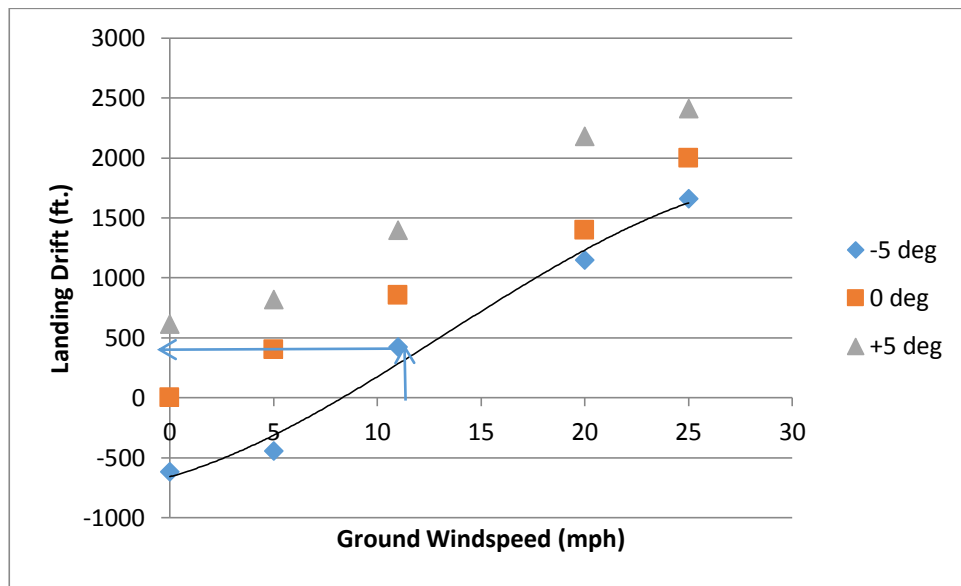


Figure 54: Rocket Landing Drift vs. Wind speed (the landing drift is <2500 ft. for all possible flight conditions; typical would be 11 mph winds, -5 deg launch)

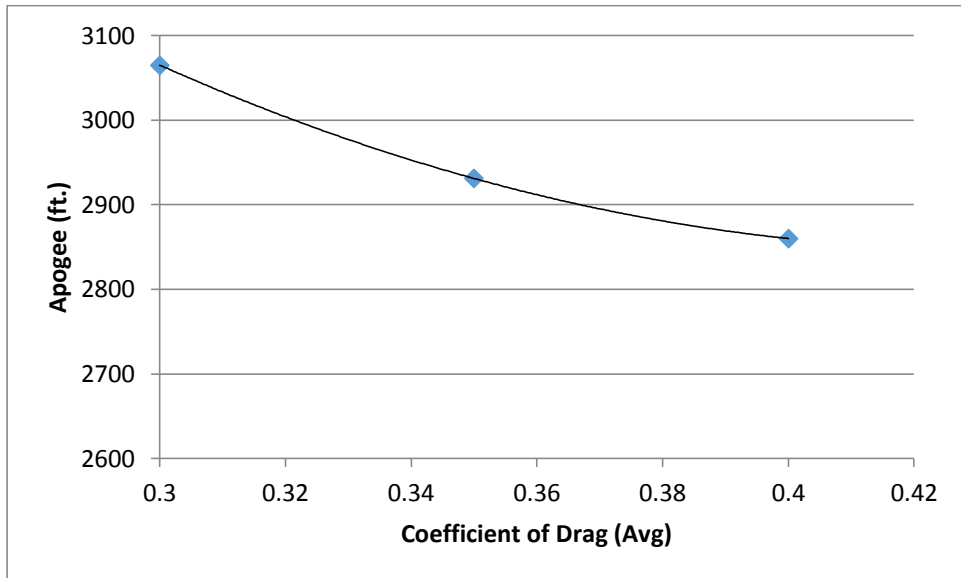


Figure 55: Variation of apogee with flight coefficient of drag; apogee varies with flight CD, which will depend on the prevailing side wind conditions and the pitching of the rocket.

The salient features of the simulations are as follows:

- (i) The maximum positive acceleration during take-off is ~ 6 g (5 g avg.)
- (ii) The maximum flight speed at motor burnout is ~ 450 fps.
- (iii) The velocity at launch rail departure is a robust 70 fps.

- (iv) The stability margin of ~ 1.85 at launch pad, and quickly rises to 2.6 just at motor burnout. Rocket flight will be stable and can handle robust side winds.
- (v) There is minimal apogee variation with wind speed as simulated up to 25 mph.
- (vi) The Vanderbilt flight will meet an apogee window of 3000 ft. ± 150 ft., without need for additional mass.
- (vii) Landing drift is within 2500ft of the launch pad for winds up to 25 mph (fig. 11).
Note: the drift is highest when launched +5 deg with the wind and lowest when launched -5 deg into wind.

4.6.4.2 Computational Fluid Dynamics Study of Rocket

4.6.4.2.1 Introduction

Rocket trajectory analysis is one of the most complex problems that aerospace engineers routinely encounter. Temporal and spatial variation in wind conditions, geometric irregularities, and other minor unknowns can have a drastic effect on rocket trajectory and landing site. Furthermore, if the rocket deviates significantly from its design trajectory, whether due to wind or any of a number of factors, apogee will decrease significantly. There are commercial packages, such as *RockSim* by Apogee Components that predict rocket trajectory based on a number of input parameters with regards to rocket design. In order to better understand the factors that influence such a trajectory, we seek to build a numerical model that can effectively predict our rocket trajectory. This model will be compared against simulation results from *RockSim*, as well as flight data from the next launch in order to verify its accuracy.

Our numerical model operates in the X-Z plane, representing only a 2D trajectory in order to simplify analysis. In order to resolve forces on the rocket body, forces are separated into components both tangential and normal to the flight axis. This enables the use of two separate coefficients of drag, in order to capture the effects of side wind on the rocket. In order to use this approach, the coefficient of drag for the rocket body must be established for both axial and parallel flow. To find these values, a computational fluid dynamics model was created in ANSYS and evaluated against known drag characteristics. These results will be fully integrated into our numerical model, and compared against flight data in our FRR report to NASA. Below, the creation and results of this simulation are detailed.

4.6.4.2.2 Physics

In order to simulate fluid dynamics interactions, the ANSYS CFX module was used. The CFX module allows users to simulate compressible fluid interactions and supports a wide variety of boundary conditions. Among these is the ability to assess slip conditions at the wall, a characteristic that affects boundary layer characteristics and therefore skin friction drag. The CFX module also supports transient modeling, hence the model could be expanded upon to solve for the transient conditions involved in rocket flight. For these reasons, ANSYS was chosen to conduct the simulation in order to provide a professional analysis of the 3-D flow field surrounding the rocket in flight.

4.6.4.2.3 Geometry

Firstly, the model geometry was created in Creo 2.0 using standard CAD procedures. In order to simulate the fluid interactions surrounding the rocket, the fluid domain itself had to be created as the geometry. This means that the rocket shape was essentially hollowed out of the domain in order to indicate the absence of fluid elements in that region. Wireframe pictures of the domain and the rocket geometry are below.

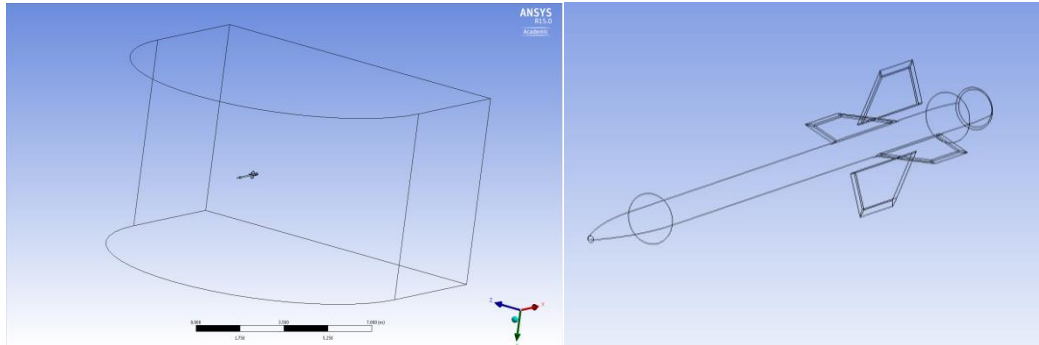


Figure 56: Wireframe Geometry of Fluid Domain (left) and Rocket (right)

4.6.4.2.4 Mesh

Using the imported CAD geometry, a mesh was generated using the workbench meshing tool, which was set to optimize the mesh for CFX. By using this optimization scheme, the convergence characteristics of the model were improved, leading to a more stable model and faster solution times.

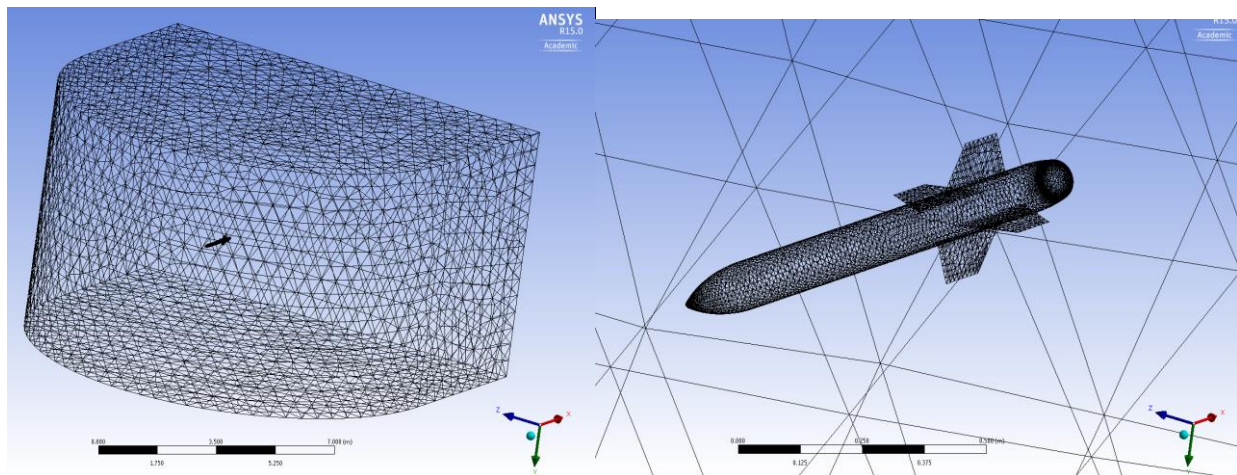


Figure 57: Mesh of Fluid Domain (left) and Rocket (right)

In addition to the use of the automatic meshing tool, the mesh was refined in several key regions in order to better capture the complex flow conditions surrounding these regions. Among these is the fin can section, which can generate considerable vortices in the rocket wake. This effect alone can modify the rocket's flight path in unpredictable ways, potentially putting a rotational force on the rocket and causing it to rotate about the flight axis. Below are detailed pictures of the mesh refinements at the fin section and nosecone.

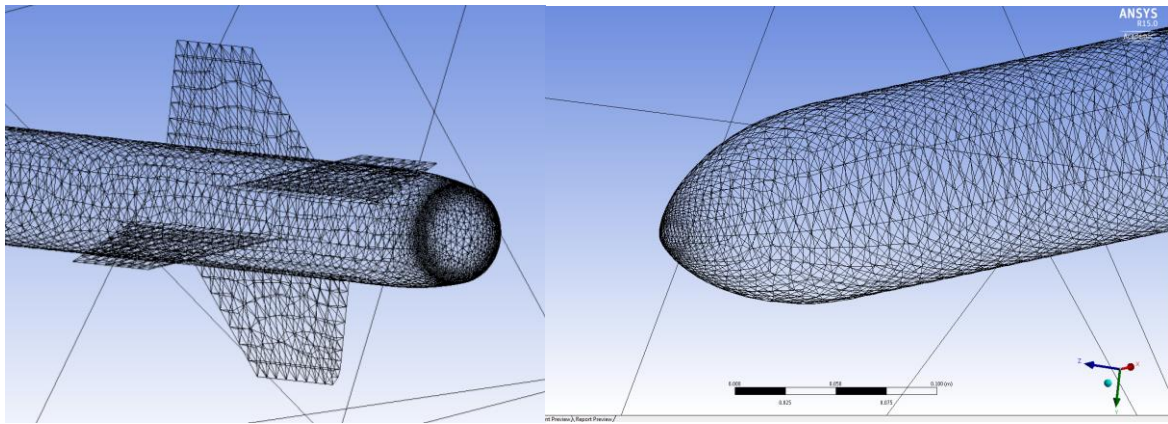


Figure 58: Close-Up of Tailcone Mesh (left) and Nosecone Mesh (right)

4.6.4.2.5 Axial Flow

For our first simulation, we were interested in modeling the drag characteristics of the rocket along the flight axis at a flight speed of 100 m/s. This case is more easily modeled than other flight angles because the vorticity in the flow is much less than at any other angle. At this flight angle, there is no net force across the fins causing the rocket to turn. The pressure distribution resulting from these flow conditions are shown in the figure below. Note that there is minimal variation in pressure along the axis of the rocket away from the nosecone section. This agrees with the expected pressure distribution from consideration of a long cylinder in axial flow. Despite the uniformity of pressure along much of the rocket, there are small areas of flow stagnation (maximum pressure) at the nose cone tip and front of the fins. The drag resulting from stagnation against both of these regions is greatly mitigated by the aerodynamic shaping of the sections.

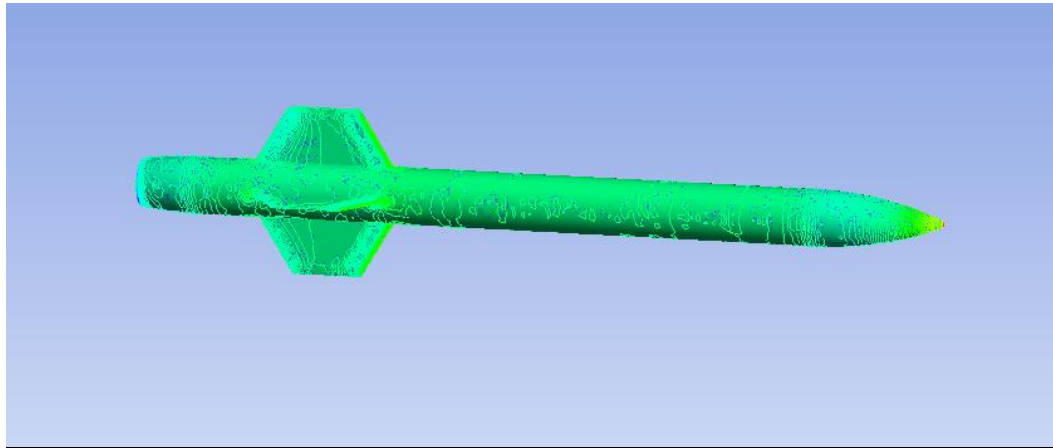


Figure 59: Pressure Distribution over Surface of Rocket

In addition to looking at the resulting pressure distribution, we would like to visually inspect the flow field around the rocket to ensure it matches the expected flow field. General characteristics should include a lack of significant vortex formation, rough axial symmetry, and a low pressure region behind the tail end of the rocket. The figures below show this flow field, indicated by

streamlines that are colored according to flow velocity. This region can be seen below (right), accompanied by the formation of a small vortex. On the left is an overview of the streamlines surrounding the rocket.

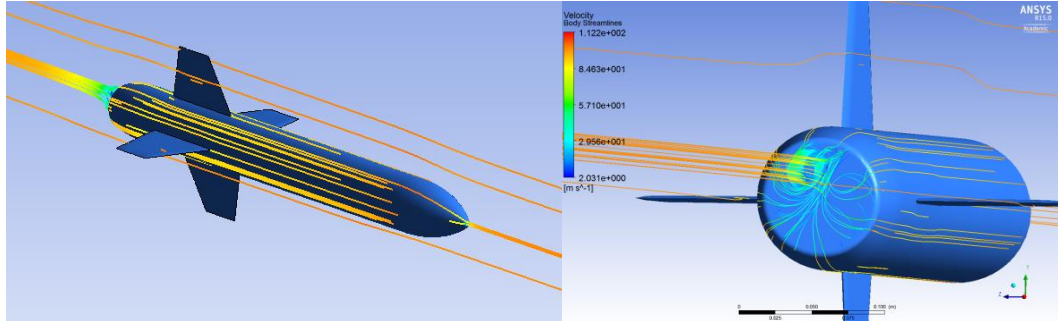


Figure 60: Streamline Surrounding Rocket (left) and Vortices Forming behind Tailcone (right)

Evaluating the pressure distribution at the surface of the rocket, we can find the drag characteristics of the rocket body to be 15.72 N. We can then consider the data non-dimensionally, by calculating an axial coefficient of drag for the rocket. That calculation was conducted as follows.

$$F_{Drag} = \frac{1}{2} \rho V^2 * A * C_D \text{ thus } C_D = \frac{F_{Drag}}{\frac{1}{2} \rho V^2 * A} = \frac{15.72 N}{\frac{1}{2} * 1.2 \frac{kg}{m^3} * (100 \frac{m}{s})^2 * 0.0077 m^2} = 0.34$$

Where C_d is the coefficient of drag, rho is the air density, and A is the representative area (frontal area of rocket).

This establishes the axial coefficient of drag to be $C_{D,Axial} = 0.34$. This value agrees well with simulation results from past rockets, which utilized a geometrically similar design.

4.6.4.2.6 Side Wind Flow

In order to obtain the rocket coefficient of drag perpendicular to the flight path, we simulate the rocket in a cross wind and calculate drag. This simulation case is considerably more complex than the axial case because of the lack of axisymmetry. Because of the shape profile of the fins, vortices form behind them and result in a swirling flow pattern. The presence of such vortices goes hand in hand with an increase in drag. This is because vortices represent disorder in a flow which tends to make viscous effects more prevalent. In this way, vortices are similar other entropy generating phenomena, in that the process reflects an irreversible loss in the system.

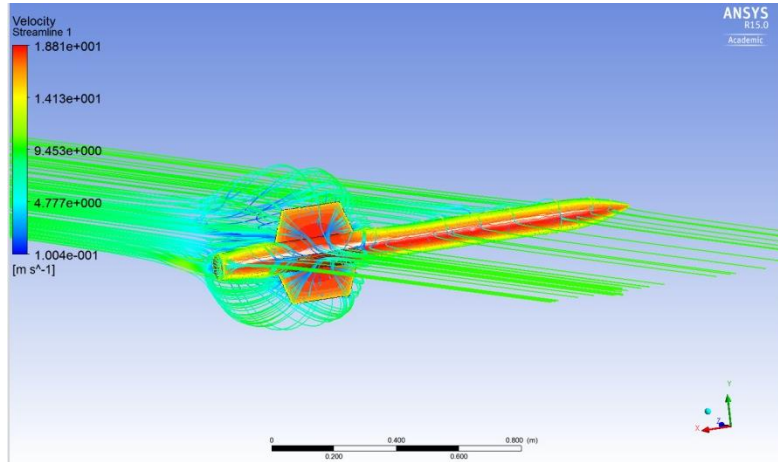


Figure 61: Streamlines around Rocket with Flow Perpendicular to Rocket Axis

Below are detailed views of the vortex formation around the fin can region as seen from the back (left) and front (right) ends of the rocket. These flow patterns include complex 3-D interactions that cannot be solved for in an analytical manner.

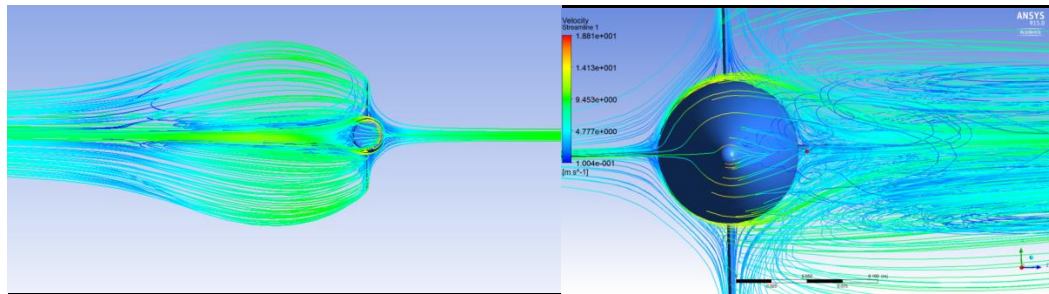


Figure 62: Vortex Formation around Fins (left) and Nosecone (right)

To establish a coefficient of drag for side winds, we use the same methodology as in the axial flow case. Despite this similarity in calculation, the representative area used in the calculation is the projected area of a cylinder the diameter and length of the rocket, not including the fins. The reason this representative area was chosen is that it allows for comparison of the simulated coefficient of drag to an established analytical value for a cylinder, which is 1.2 within this Reynolds number regime.

The coefficient of drag can be calculated as follows, using a side wind speed of 10 m/s and a simulated drag force of 9.553 N:

$$C_D = \frac{F_{Drag}}{\frac{1}{2} \rho V^2 * A} = \frac{9.553N}{\frac{1}{2} * 1.2 \frac{kg}{m^3} * (10 \frac{m}{s})^2 * 0.1434m^2} = 1.11$$

Somewhat surprisingly, the coefficient of drag for the rocket in a cross flow is lower than that of the corresponding cylinder ($C_d = 1.2$). There are several possible explanations for this phenomena. This is most likely due to the fact that the rocket's nosecone and boat tail (tail cone)

reduce the representative area of the cylinder, a statement that is expressed mathematically below.

$$A < 0.1434 \text{ m}^2$$

Due to this reduction in area, it is likely that the coefficient of drag would be higher than 1.2 if the projected area accounted for the nosecone and boat tail geometries. Regardless, the choice of representative area has no bearing on the dynamics of the rocket itself and our drag force will be unaffected by our choice of conventions.

4.6.4.2.7 Conclusions

The results of our simulation are summarized by the calculated coefficient of drag for flow tangential and normal to the flow, denoted as axial and normal, respectively.

$$C_{D,Axial} = 0.34$$

$$C_{D,Normal} = 1.11$$

These coefficients allow for the calculation of drag force at any given point in the rocket's trajectory, which provides the necessary structure of a numerical model to predict rocket trajectory. Since drag force has the greatest effect at high speeds, the coefficient of drag will not vary substantially with Reynolds number. This is a characteristic of an inertially dominated flow that is insensitive to changes in flow velocity. This assertion was validated by running preliminary simulations at different flow velocities.

With the ground work laid for the calculation of aerodynamic drag, we can set out to develop a numerical model that will predict important parameters about our rocket flight. These parameters include predicted apogee, max velocity, acceleration, drift, and several other key parameters. By developing a numerical model and establishing parity with RockSim and test flight data, we hope to gain a better understanding of the dynamics of rocket flight in order to refine and defend our design from an academic standpoint.

4.6.4.3 MATLAB Rocket Simulation

In order to more thoroughly validate the simulations results from *Rocksim*, the team has created our own rocket flight simulation using MATLAB. This simulation takes into account the thrust and mass curves of the motor, launch angle, axial drag, and the effects of steady side winds as it tracks altitude, drift, and orientation throughout the flight. Using the parameters established in Section 4.6.4.2, the MATLAB simulation uses force and moment balance to calculate linear acceleration in the axial (v) and radial (u) directions as well as angular acceleration for a given time step. From these values it can calculate axial and radial velocities using a finite difference scheme. Finally, it uses the same scheme to update the altitude and drift, which are transformations from u-v according to the orientation, θ , of the rocket, and calculates α , the discrete change in θ over this time step.

$$m \frac{dv}{dt} = T - \frac{1}{2} \rho V^2 C_{D,Axial} A - \frac{1}{2} \rho W^2 C_{D,Radial} A_{Fins} \sin(\theta) - mg * \cos(\theta) \quad (1)$$

$$m \frac{dv}{dt} = mg * \sin(\theta) - \frac{1}{2} \rho u^2 C_{D,Radial} A_{Side} - \frac{1}{2} \rho W^2 C_{D,Radial} A_{Fins} \cos(\theta) \quad (2)$$

$$I \frac{d^2\alpha}{dt^2} = \frac{1}{2} \rho W^2 C_{D,Radial} A_{Fins} \cos(\theta) * l - \frac{1}{2} \rho V^2 C_L A_{Fins} \alpha * l \quad (3)$$

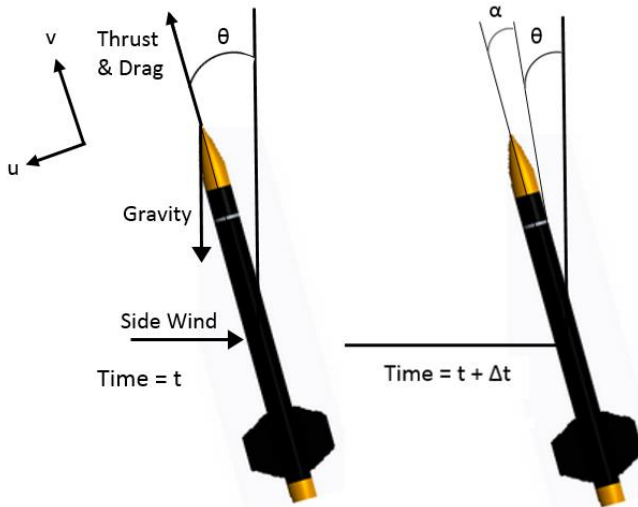


Figure 63: Illustration of MATLAB simulation force balance and geometry

Once the rocket has reached apogee, denoted by an angle of 90° , the simulation reports the drift and altitude at that time. From there, it calculates the amount of time it will take to reach the ground given the parachute area and C_d and the section mass. The drift under the parachute is predicted as the time of descent multiplied by the wind speed. This value is added to the drift at apogee for a final drift prediction.

The results of this simulation are exactly as desired. Although this is not a professional product like *Rocksim*, the way it is written in conjunction with the meticulously calculated aerodynamic properties give it credibility in that it is highly customized to best represent this one rocket. This means that it is important that the simulated results match up both with the full scale test launch data, and the *Rocksim* results.

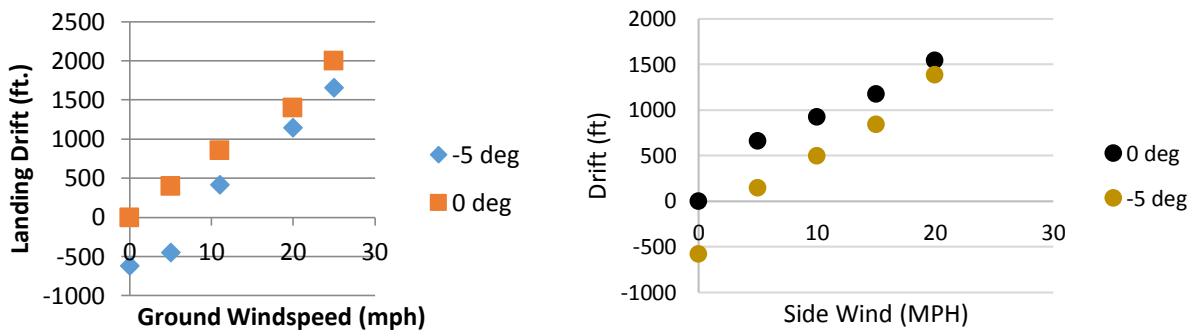


Figure 64: Comparison of drift predictions between Rocksim and own MATLAB code

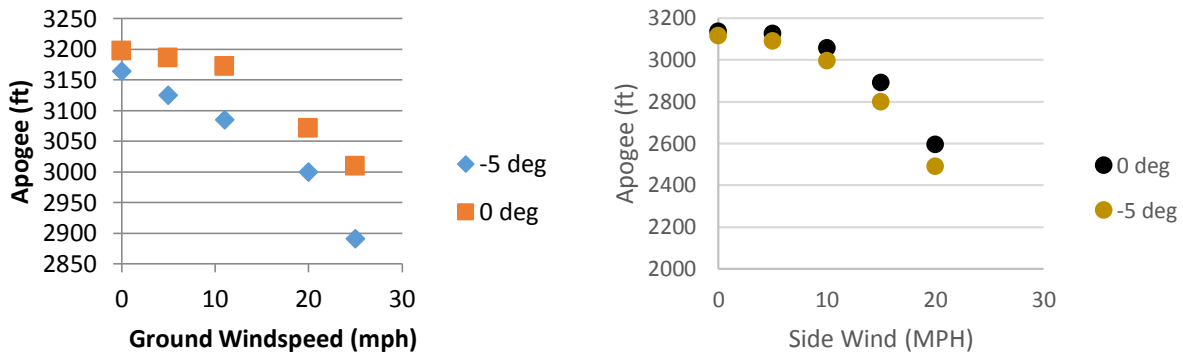


Figure 65: Comparison of apogee predictions between Rocksim and own MATLAB code

The results drift predictions are extremely close. The MATLAB simulation shows a slightly larger jump from 0 to 5 mph winds, but after that, no point differs by more than about 100 ft, and most are far closer than that. Given differences in numerical methods and equation setup, this is in very good. Trends are also clearly the same. In the apogee, there is a little more difference, but not much. Up to about 15 mph, the two agree very closely. Beyond that point, the shape of the curve is obviously the same, but the two simulations disagree slightly about the degree to which the wind will bring down the apogee. This may have to do with differences in calculating rocket orientation. Many simulations calculate theta as the arctan of the velocities in the x and z directions. Regardless, the difference only shows up at very high wind speeds. Both systems predicted the full scale test launch to reasonable accuracy. For a 14.55 lbs. rocket (including motor) launching at a -5° angle in 6 mph winds, the MATLAB code predicts an apogee of 3061 ft, compared to an actual apogee under those conditions of 3008 ft.

4.6.5 Kinetic Energy Calculations

It is important to ensure that the landing energy of each independent section of the rocket (payload section and main rocket section) is below the maximum limit of $75 \text{ lb}_f \cdot \text{ft}$ set by NASA. Landing energy is dependent on each section's landing velocity (Terminal Velocity, TV). The equations for both landing velocity and energy are as follows:

$$TV = \sqrt{\frac{2mg}{C\rho A}}$$

$$KE = \frac{\left(\frac{W}{g}\right) \cdot V^2}{2}$$

Landing speed with a 30" rocket parachute from 3010ft to 1000ft is calculated as follows:

$$V_{ld} = \sqrt{\frac{mg}{0.5\rho C_D A}} = \sqrt{\frac{56.8N}{0.5 * 1.1 \frac{kg}{m^3} * 1.5 * 0.456m^2}} = 12.9 \frac{m}{s} = 42.3 \text{ fps}$$

At 1000 ft., once the nose cone is jettisoned, the landing speed drops to 31 fps and the landing energy of the heaviest section of the fin can and payload bay.

$$KE_{largest\ part} = \frac{\left(\frac{W}{g}\right) \cdot V^2}{2} = \frac{(4.1) \cdot 31 \text{ fps}^2}{2 \times 32.2} = 61.1 \text{ lbf-ft} < 75 \text{ lbf-ft}$$

Experience shows that there will be some lofting from the side winds and the landing energy will be slightly lower than estimated.

The second separation event occurs at 1000ft. and initiates the payload recovery process. Payload recovery will use a 30" diameter elliptical type parachute. This will provide a stabilized descent at approximately 24.8 fps for a payload of weight 4.85 lb. A Nomex/Kevlar parachute protection pad will surround the parachute to prevent it from being burned by hot ejection gasses. Depending on wind conditions, the drogue chute size may change to forestall excessive wind drift.

Landing speed with a 30" elliptical parachute from 1000ft is calculated as follows:

$$V_{ld} = \sqrt{\frac{mg}{0.5\rho C_D A}} = \sqrt{\frac{21.5N}{0.5 * 1.1 \frac{kg}{m^3} * 1.5 * 0.456m^2}} = 7.6 \frac{m}{s} = 24.8 \text{ fps}$$

Landing energy of the payload section: $4.85 \text{ lb} * \frac{24.8^2}{2 \times 32.2} = 46.3 \text{ lbf-ft} < 75 \text{ lbf-ft}$

The landing energy assumes absolutely no ground wind; however, our experience has been that the ground wind speed contributes to lofting and the actual landing speeds with the main are substantially lower.

These same calculations will be run for the subscale model as well. For the payload/nosecone section, with a mass of 5.5lb (2.5kg), a 3.5ft (1.067m) diameter parachute, a parachute C_d of 1.2 (given by manufacturer), we find that the landing velocity and energy are:

$$TV = \sqrt{\frac{2mg}{C\rho A}} = \sqrt{\frac{2 \cdot 2.5\text{kg} \cdot 9.8 \frac{m}{s^2}}{1.2 \cdot \frac{1.1\text{ kg}}{m^3} \cdot \left(\frac{\pi}{4}\right) (1.067\text{m})^2}} = 6.44 \frac{m}{s} = 21.14 \text{fps}$$

$$KE = \frac{\left(\frac{W}{g}\right) \cdot V^2}{2} = \frac{\left(\frac{5.5 \text{ lb}}{32.2 \frac{\text{ft}}{\text{s}^2}}\right) \cdot (21.14 \text{fps})^2}{2} = 38.2 \text{ lb}_f \cdot \text{ft}$$

For the main section of the rocket, with a mass of 17.2lb (7.818 kg), a 6ft (1.829m) diameter parachute, a parachute C_d of 2.2 (given my manufacturer), we find that the landing velocity and energy (of the largest section) are:

$$TV (\text{combined section}) = \sqrt{\frac{2mg}{C\rho A}} = \sqrt{\frac{2 \cdot 7.818\text{kg} \cdot 9.8 \frac{m}{s^2}}{2.2 \cdot \frac{1.1\text{ kg}}{m^3} \cdot \left(\frac{\pi}{4}\right) (1.829 \text{ m})^2}} = 4.909 \frac{m}{s} = 16.11 \text{fps}$$

$$KE (\text{largest part}) = \frac{\left(\frac{W}{g}\right) \cdot V^2}{2} = \frac{\left(\frac{6.67\text{lb}_f}{32.2 \text{fps}^2}\right) \cdot (16.11 \text{fps})^2}{2} = 26.9 \text{lb}_f \cdot \text{ft}$$

4.7 Vehicle Verification

4.7.1 NASA Statement of Work Verification

Shown below is a table outlining NASA's requirements described in the Request for Proposal. The requirement given by NASA is compared with any additional team-derived requirements. The verification status of these requirements is shown. Green text indicates completion of verification, while red indicates incomplete verification.

Table 10: NASA Statement of Work Verification Plan

NASA Requirement	Team-Derived Requirement (if applicable)	Verification Status
The vehicle shall deliver the payload to, but not exceeding, an apogee altitude of 3,000 feet above ground level	Computer simulation along with flight testing will verify that the design meets this	Computer simulation has given a weight estimate that our rocket must approach for the motor that we have

(AGL).	altitude requirement.	selected.
The vehicle shall carry one commercially available, barometric altimeter for recording the official altitude used in the competition scoring.	Perfect Flight <i>Stratologger</i> altimeters will be purchased and one will be designated as responsible for recording the official competition altitude.	Altimeters have been purchased and used in all three flights.
The launch vehicle shall be designed to be recoverable and reusable. Reusable is defined as being able to launch again on the same day without repairs or modifications.	We will perform ground testing of recovery system as well as test launches to ensure safe recovery. We will also design the rocket to be modular so that each piece can be easily reassembled following recovery.	Ground testing has been performed before each of the launches to ensure recovery functionality.
The launch vehicle shall have a maximum of four (4) independent sections. An independent section is defined as a section that is either tethered to the main vehicle or is recovered separately from the main vehicle using its own parachute.	The design of the launch vehicle shall minimize the number of sections for the sake of mass and space efficiency.	The rocket has three sections: tail, forward, and payload.
The launch vehicle shall be limited to a single stage.		The vehicle's only method of propulsion is the Cesaroni P54-3G J380 Smoky Sam; therefore, the rocket is single stage.
The launch vehicle shall be capable of being prepared for flight at the launch site within 2 hours, from the time the Federal Aviation Administration flight waiver opens.		From experience launching the subscale and full-scale rockets, the rocket can be prepared in fewer than 2 hours.
The launch vehicle shall be capable of remaining in launch-ready configuration at the pad for a minimum of 1	The altimeters and payload bay will use fresh 9V batteries on launch day.	Based on the current draw of the Stratologger altimeters, they should be able to be powered on the launch pad for

<p>hour without losing the functionality of any critical on-board component.</p>		<p>over 10 hours, given a large factor of safety.</p> <p>The battery in the payload bay is only used to actuate the sliding nosecone. The battery has enough charge to perform several open/closes.</p>
<p>The launch vehicle shall be capable of being launched by a standard 12 volt direct current firing system. The firing system will be provided by the NASA-designated Range Services Provider.</p>		<p>The launch ignition system consists of a 12V battery connected to 500ft leads. The leads go through a safety switch system to the motor igniter. The safety switch ensures that no voltage differential is delivered to the electric match igniter until a key is inserted into the safety switch and a button is pressed.</p>
<p>The launch vehicle shall use a commercially available solid motor propulsion system using ammonium perchlorate composite propellant (APCP) which is approved and certified by the National Association of Rocketry (NAR), Tripoli Rocketry Association (TRA), and/or the Canadian Association of Rocketry (CAR).</p>		<p>The full-scale rocket uses a Cesaroni J380 motor.</p>
<p>The total impulse provided by a launch vehicle shall not exceed 5,120 Newton-seconds (L-class).</p>		<p>The Cesaroni J380 uses 1043 N-s of total impulse.</p>
<p>Pressure vessels on the vehicle shall be approved by the RSO and shall meet the following criteria...</p>		<p>The rocket does not use any pressure vessels.</p>

<p>All teams shall successfully launch and recover a subscale model of their full-scale rocket prior to CDR. The subscale model should resemble and perform as similarly as possible to the full-scale model, however, the full-scale shall not be used as the subscale model.</p>	<p>Results from the subscale flights will be used to influence the design of the full-scale rocket. The subscale model will use a smaller motor and therefore have a lower target apogee than the full-scale.</p>	<p>The subscale model was flown three times prior to the design of the full-scale model. The full-scale model draws on the volume and mass efficiency of the subscale.</p>
<p>All teams shall successfully launch and recover their full-scale rocket prior to FRR in its final flight configuration. The rocket flown at FRR must be the same rocket to be flown on launch day. The purpose of the full-scale demonstration flight is to demonstrate the launch vehicle's stability, structural integrity, recovery systems, and the team's ability to prepare the launch vehicle for flight. A successful flight is defined as a launch in which all hardware is functioning properly (i.e. drogue chute at apogee, main chute at a lower altitude, functioning tracking devices, etc.). The following criteria must be met during the full scale demonstration flight:</p> <ul style="list-style-type: none"> • The vehicle and recovery system shall have functioned as designed. • The vehicle shall be flown in its fully ballasted configuration during the full-scale test flight. Fully ballasted refers to the same amount of ballast that will be flown during the competition flight. 		<p>The rocket as flown in the full-scale launch will be identical to the rocket flown on competition day.</p>

<p>Each team will have a maximum budget they may spend on the rocket and the Autonomous Ground Support Equipment (AGSE). Teams participating in Mini-MAV are limited to \$5,000. The cost is for the competition rocket and AGSE as it sits on the pad, including all purchased components. The fair market value of all donated items or materials shall be included in the cost analysis. The following items may be omitted from the total cost of the vehicle: shipping costs, team labor costs.</p>	<p>The treasurer of the club will keep a bill of materials detailing all of the parts used in the competition rocket, payload bay, and AGSE system that prove the equipment falls under the \$5,000 limit.</p>	<p>As seen in section 8.1.2: <i>Itemized Budget</i>, the cost of launch and sample recovery equipment falls under \$5,000.</p>
<ul style="list-style-type: none"> • The launch vehicle shall not utilize forward canards. • The launch vehicle shall not utilize forward firing motors. • The launch vehicle shall not utilize motors that expel titanium sponges (Sparky, Skidmark, MetalStorm, etc.). • The launch vehicle shall not utilize hybrid motors. • The launch vehicle shall not utilize a cluster of motors. 		<p>The rocket uses none of these.</p>
<p>The launch vehicle shall stage the deployment of its recovery devices, where a drogue parachute is deployed at apogee and a main parachute is deployed at a much lower altitude.</p>	<p>This will be controlled by the altimeters and black powder charges. These will be ground tested prior to launch, and confirmed through full-scale flight testing.</p> <p>With only three sections, the rocket shall only have two</p>	<p>The rocket parachute acts as a drogue parachute at apogee until descent to 1000ft at which point it acts as the main parachute.</p> <p>This scheme was proven to work in the subscale and full-scale flights.</p>

	parachutes, the rocket parachute and the payload parachute.	
Teams must perform a successful ground ejection test for both the drogue and main parachutes. This must be done prior to the initial subscale and full scale launches.		Deployment tests were performed before every launch.
At landing, each independent section of the launch vehicle shall have a maximum kinetic energy of 75 ft-lbf.	This will be demonstrated through computer simulations and verified with full-scale test flight.	Computer simulations have been run and completed showing each section falls under the KE requirement. The full-scale flight confirmed this.
The recovery system electrical circuits shall be completely independent of any payload electrical circuits.	The recovery system electronics and payload electronics are housed in different sections within the rocket body.	A prototype payload bay was flown with its own electronics separate from the recovery system in subscale flight. The full-scale payload compartment is completely separate from the avionics bay.
The recovery system shall contain redundant, commercially available altimeters. The term “altimeters” includes both simple altimeters and more sophisticated flight computers. One of these altimeters may be chosen as the competition altimeter.	There will be two sets of redundant altimeters, each pair controlling separate black powder charges.	Construction of avionics bay is complete. The bay has been flown and successfully achieved recovery.
A dedicated arming switch shall arm each altimeter, which is accessible from the exterior of the rocket airframe when the rocket is in the launch configuration on the		For each launch, the altimeters have been accessible by a screwdriver from the outside of the rocket body.

launch pad.		
Each altimeter shall have a dedicated power supply.	There will be a 9V battery controlling each altimeter (4 of them). These will be wired such that the circuit is completed when the arming switch is engaged.	Avionics bay constructed accordingly.
Each arming switch shall be capable of being locked in the “ON” position for launch.	This requirement of the arming switches has been tested by previous years, and will be tested by this year's team during the full-scale launch.	Avionics bay constructed accordingly.
Removable shear pins shall be used for both the drogue and main parachute compartments.	The number and size of shear pins to be used will be determined through mathematical analysis and then confirmed with ground testing, and eventually full-scale flight testing.	Ground-based deployment testing before each launch confirms our shear pin size.
An electronic tracking device shall be installed in the launch vehicle and shall transmit the position of the tethered vehicle or any independent section to a ground receiver.	There will be a RF transmitter that will be tested on the ground to ensure functionality. It will also be tested with the full-scale test launch in both the main rocket section and the payload section.	The devices used are a BigRedBee 70 cm BeeLine GPS and a Beeline Transmitter, and these were tested during full-scale launch.
Any rocket section, or payload component, which lands untethered to the launch vehicle shall also carry an active electronic tracking device. The electronic tracking device shall be fully functional during the official flight at the competition launch site.		The RF transmitter can communicate with the tracking devices located in the rocket section and in the payload section. The team will use these during the competition launch.
The recovery system electronics shall not be	This will be ground tested to ensure that the electronics	Ground testing has been performed, and recovery

<p>adversely affected by any other on-board electronic devices during flight (from launch until landing).</p>	<p>experience no interference from transmitting devices and do not prematurely set off black powder charges or have disrupted pressure readings.</p> <p>The AGSE system shall not use electromagnetic fields for communication as this may cause malfunction in these devices.</p>	<p>electronics are reusable after each flight we've performed.</p> <p>The AGSE communicates with the rocket payload bay using a breakaway connector and a permanent magnet mounted on the gripper.</p>
<p>The recovery system altimeters shall be physically located in a separate compartment within the vehicle from any other radio frequency transmitting device and/or magnetic wave producing device.</p>		<p>The recovery system electronics are all housed in the avionics bay, separate from all other transmitting devices.</p>
<p>The recovery system electronics shall be shielded from</p> <ul style="list-style-type: none"> • All onboard transmitting devices, to avoid inadvertent excitation of the recovery system electronics. • All onboard devices which may generate magnetic waves (such as generators, solenoid valves, and Tesla coils) to avoid inadvertent excitation of the recovery system. • Any other onboard devices which may adversely affect the proper operation of the recovery system electronics. 		<p>The recovery system electronics are all housed in the avionics bay, separate from all other transmitting devices.</p>

4.8 Vehicle Safety and Environment

4.8.1 Safety Officer and Responsibilities

Robin Midgett will act as safety mentor for the Vanderbilt University 2014-2015 NASA SL team with Connor Caldwell serving as the student safety advisor. Robin has held this position for several years, providing extensive qualification and experience, and he is Level 2 certified. His office is located down the hall from the SL laboratory, and he is commissioned for multiple consultations daily. Robin will oversee all operations which impose at least a moderate safety concern as well as all launches. Further measures will be taken to ensure that all team members are briefed on all possible safety concerns throughout the project and properly instructed on appropriate safety measures.

When Robin is not available when the team is working, as in the evenings or weekends, Connor will serve as the Safety Officer for the team. He was chosen as the Student Safety Officer because of his experience with safe operation and teaching in the use of machine shop tools and equipment as he has been serving as a teaching assistant for the Vanderbilt University Machining Class for two semesters. He has shadowed Robin in his Safety Officer duties during launches and been instructed in the proper safety practices for activities such as loading rocket motors and detonation charges, the safe use, storage, and transportation of chemicals and energetic materials, and everyday safety procedures for the SL lab.

The responsibilities for the Safety Officer and Safety Mentor will be the same: to ensure the safety of all members of the Vanderbilt Aerospace Club, any bystanders, and the environment during the design, creation, test, and launch of their rocket. As mentioned above, the only difference in responsibility is that the Student Safety Officer will be in charge of safety practices while Robin is not available. The specific responsibilities of any safety officer include:

- Proper use and storage of chemicals/energetic materials
- Identify safety risks and propose sufficient mitigation practices
- Ensure compliance with all NAR rules and regulations
- Bringing fire extinguisher and first aid equipment to every launch and relevant test
- Ensuring proper charging and handling of high pressure air vessels
- Overseeing all relevant vehicle and payload tests
- Creating and updating pre-launch checklists and procedures
- Ensuring safe and secure transportation of hazardous/essential materials (like motor, black powder, igniters)
- Packing the motor a few days before launch
- Cleaning the motor case after each launch

4.8.2 Failure Modes Analysis and Mitigation

See section 6.1.2: *Vehicle Preliminary Failure Mode Analysis* for tables explaining various risks the team may face during a launch in relation to the overall rocket vehicle, the consequences each risk has, and our plan to mitigate these risks.

4.8.3 Personnel Hazards and Concerns

A thorough evaluation of the possible hazards associated with the vehicle has been made with respect to the user as well as the environment. This evaluation has led to the Vanderbilt Aerospace club adopting its own set of safety practices and rules that must always be followed when performing operations that could potentially be hazardous. This includes using heavy machinery or equipment, hand tools, chemicals, energetic materials, electronics, high-pressure vessels and lines, combustible or flammable materials, and any other potentially harmful substance or tool. The use of tools, machinery, and chemicals or energetic materials must be accompanied by the wearing of safety glasses and any other relevant safety equipment as well as proper lighting and ventilation. All parts must be properly supported before machining with any tool and all loose clothing, hair, or jewelry must be tied back or removed.

The most important rule is always to use common sense and ensure you have the proper training and experience before performing an operation. This involves asking questions to more experienced members and working in teams as often as possible. When a team member is working on any portion of the rocket that could be hazardous, at least one other member of the team with knowledge of the operation must be present. Working in teams also ensures that a team members with compromised decision-making faculties (for example, due to a personal issue or lack of sleep) will not bring harm to themselves or the project. Team members keep each other in check and hold one another accountable.

The hazards associated with the vehicle involve the storage of combustible substances such as motors and black powder as well as the igniters and adhesives. The material safety data sheets pertaining to any aspect of the vehicle and its operation have been obtained and thoroughly studied in preparation for the fabrication and future use of the materials necessary. Precautionary measures are being taken to ensure that no harmful or explosive substances can be misplaced or misused. Any explosive materials such as the black powder, motors, and motor replacements are kept locked in a type-4 MAGloc U.S. Explosives box, the key to which is held solely by the safety and rocketry mentor Robin Midgett. The adhesives are kept on low, sturdy shelves to prevent spilling; and aprons, latex gloves, and particle masks are mandatory during any fabrication process. Composite materials such as fiberglass and carbon fiber are also kept on designated shelves and are each wrapped in a layer of plastic followed by a subsequent layer of thick brown paper in order to minimize the amount of fibers released throughout the lab. With respect to the environment, no toxic substances are poured down the drain but rather are sealed in plastic containers and properly disposed.

Serving as the student safety officer, Connor Caldwell oversees and signs off on all activities after carefully evaluating protocols, procedures, exposures, etc. He retains the right to assign multiples of students on a project and establishes the best operating condition for each hands-on activity. Connor is also in charge of ensuring that all members of the team, particularly those

involved in the fabrication and machining of rocket/payload components, are properly trained and use safe practices when using machinery, tools, chemicals, and any other potentially hazardous fabrication methods. As stated in section 4.8.1: *Safety Officer*, Connor is well qualified to ensure these safe practices; but the rest of the team is also well-versed in safe use of equipment. All team members who use the machine shop have either taken Vanderbilt's machining course or have other education and extensive experience in the use of the equipment.

All relevant safety documents and information are posted on the Vanderbilt Aerospace Club website. These include Federal Aviation Regulations, High Power Rocket Safety Code, Shop Safety Guidelines, Design Studio Rules and Bylaws, and MSDS Information. After consulting the MSDS sheets for the hazardous materials that the team could possibly come in contact with or use, the following summarizing table has been developed for quick referencing:

Table 11: Chemicals and Material Safety Hazards

Chemicals and Material Safety Hazards		
Material	Risk to Health	Risk Mitigations
Loctite Fast Cure Epoxy	Eye, skin, and respiratory irritation	Use in a ventilated area, with chemical resistant gloves and eye protection.
Two Part Polyurethane Pour Foam-Part A	Eye, skin, and respiratory irritation	Use in a ventilated area, with chemical resistant gloves and eye protection
Two Part Polyurethane Pour Foam-Part B	Eye, skin, and respiratory irritation	Use in a ventilated area, with chemical resistant gloves and eye protection
West Systems Epoxy Resin	Eye, skin, and respiratory irritation	Use in a ventilated area, with chemical resistant gloves and eye protection
West Systems Epoxy Hardener	Eye, skin, and respiratory irritation	Use in a ventilated area, with chemical resistant gloves and eye protection
Soller Composites Carbon Fiber and Fiberglass	Eye, skin, and respiratory irritation	Use in a ventilated area, with heavy-duty gloves and eye protection.
Cesaroni Pro54 Profire Igniter	Combustion, burn risk	Use outside, with face and body protection. Have fire-fighting method on hand. Keep away from heat.
Cesaroni Pro54 Rocket Motor	Combustion, burn and explosion	Use outside, with face and body protection. Have fire-fighting

Reload Kit	risk	method on hand. Keep away from heat.
Black Powder	Combustion, burn and explosion risk. Respiratory irritation	Use in a ventilated area/outside. Use body/face protection. Have fire-fighting method on hand. Keep away from heat.
JB Weld Epoxy Steel Resin	Eye, skin, and respiratory irritation	Use in a ventilated area, with chemical resistant gloves and eye protection
JB Weld Epoxy Steel Hardener	Eye, skin, and respiratory irritation	Use in a ventilated area, with chemical resistant gloves and eye protection
Acetone	Eye, skin, and respiratory irritation	Use in a ventilated area, with chemical resistant gloves and eye protection
Isopropyl Alcohol	Eye, skin, and respiratory irritation	Use in a ventilated area, with chemical resistant gloves and eye protection
Ethyl Cyanoacrylate	Eye, skin, and respiratory irritation	Use in a ventilated area, with chemical resistant gloves and eye protection
Polyurethane Spray Coat	Eye, skin, and respiratory irritation	Use in a ventilated area, with chemical resistant gloves and eye protection
Spray Paint	Eye, skin, and respiratory irritation	Use in a ventilated area, with chemical resistant gloves and eye protection
Acrylic Cement	Eye, skin, and respiratory irritation	Use in a ventilated area, with chemical resistant gloves and eye protection

Along with the chemical and material safety hazards outlined in **Table 11** above, team members will encounter hazards in the machining and fabrication operations involved with building and testing the rocket and AGSE. See section *6.1.1: Vehicle Development Table* for a table outlining these potential hazards.

4.8.4 Environmental Hazards and Concerns

An important consideration when designing a rocket is the nature of the environment in which it will be launched. The launch environment undoubtedly has the potential to impose certain risks onto the performance of our mission. We have identified the main risks, along with mitigation strategies, associated with launching into a non-ideal environment.

In addition to mitigating the environment's effects on the rocket, the Vanderbilt Aerospace Team has a commitment to minimizing its impact on the environment. We've identified some of the hazards we might encounter on the launch site that will have a negative impact on the environment. We have also outlined our plan of action to mitigate and reduce those hazards. In addition to the procedures outlined in the table, we make decisions when designing and building our rocket that will minimize our environmental impact. For example, we try to minimize the amount of consumable rocket mass. The vast majority of the rocket, excluding propellant, is reusable. Additionally, we take care to avoid hazardous chemicals when possible and always use a fume hood when dealing with toxic liquids with a high vapor pressure.

Tables concerning the risks imposed by the environment on the rocket and vice versa may be found in section 6.1.4: *Vehicle Environmental Hazards and Concerns*.

4.9 Payload Bay Design

The primary requirement for the payload bay is to facilitate the placement, capture, and secure restraint of the payload for flight. In order to develop a robust design, the payload bay has gone through several stages of design development. In the following sections we will review the evolution of our payload bay culminating with our final payload bay design, testing procedures, and integration into the flight vehicle.

4.9.1 Subscale Design Overview

Since payload recovery is a mission critical task, the subscale payload bay design focused on secure containment of the payload, robust interaction with the AGSE, and ease of fabrication. For this reason, a sliding nosecone design was developed which utilized a number of rapid prototyped parts including the payload tray, electronics bay, and several other functional pieces.



Figure 66: CAD Rendering of First Payload Bay Design

The subscale payload bay was put through comprehensive testing procedures before eventually flying in the subscale launch on December 11th. After this subscale launch the payload bay in

flight performance was evaluated and subsequent modifications were made to the competition payload bay design.

4.9.1.1 Design Evaluation

The subscale payload bay served as a platform for testing the linear drivetrain design. While the carriage and guide rod assemblies proved to be effective in supporting the nosecone, actuating components proved complex and difficult to troubleshoot. This characteristic made a thorough analysis of the system's structure tenuous. The figure below shows how force propagates through the subscale payload bay drivetrain.

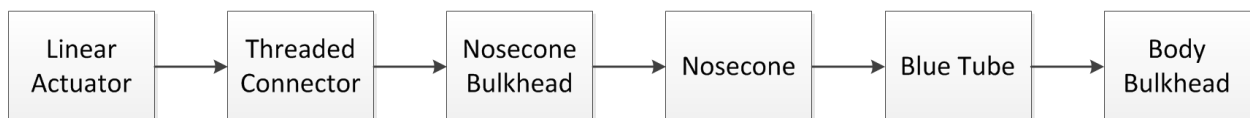


Figure 67: Flowchart of Force Transmission in Payload Bay

The electronics systems of the payload bay maintained functionality throughout all testing procedures and supported payload bay operation effectively. The subscale electronics system was therefore used as a basic platform upon which additional functionality was added. This added functionality is detailed in section 4.9.3.3: *Electronics*.

4.9.1.2 Integration and Compatibility with AGSE

The physical separation of the AGSE and payload bay microcontrollers requires that the systems be able to communicate wirelessly. Thus need for a wireless communication protocol gave rise to a number of different electronics communication options of various degrees of complexity. For the subscale payload bay, a Hall Effect sensor based system was developed and flight tested. Since this protocol has been thoroughly tested and has proven a reliable means of communication, it has been incorporated into the final electronics system as a redundant communication protocol.

For a discussion of the primary communications protocol for the updated payload bay, refer to section 4.9.3.6: *Integration and Compatibility with AGSE*.

4.9.2 Changes after Subscale Launches

After the successful completion of our subscale launch and a thorough evaluation of the in-flight performance of all rocket systems, several important design changes were made to the payload bay in order to improve its functional characteristics and ensure reliability. These changes are discussed in the following sections contained within 4.9.3: *Final Design Overview*.

Several major changes to the structural and drivetrain components were made, driven both by the need for functional improvements and a larger factor of safety for component strength. In addition to changes to the payload bay drivetrain, material choice was reevaluated throughout the design. A detailed discussion of the material choices for the final design can be found in section 4.9.3.5: *Justification of Materials*.

The electronics system has also undergone significant changes from our prototype design. Among these improvements is the addition of several redundant systems. These redundancies serve to increase the reliability of our overall system while adding minimal cost and complexity. Modifications to the electronics system are detailed in section 4.9.3.3: *Electronics*.

The fabrication techniques used to make the final payload bay also differed significantly from the prototype design. This change was dictated by the new material choices and the need for additional precision in the drivetrain components. The processes used to fabricate the final payload bay were detailed extensively in the payload bay section of the CDR.

4.9.3 Final Design Overview

The final payload bay design to be integrated into the flight vehicle features a robust design that has been tested comprehensively to inform progressive design refinements. This approach has allowed us to arrive at an optimized design, which provides rugged functionality alongside a lightweight, compact footprint. The following sections outline the final design choices as they apply to the payload bay section.



Figure 68: CAD of Final Payload Design

4.9.3.1 Structural Assemblies

The main structural assemblies of the payload bay have remained much the same as in the prototype design. All major components are connected via the steel guide rods, which provide rigid structural support as well as functional support of the drivetrain. The design also includes several bulkheads, an electronics bay, and a payload containment tray as was featured in the prototype design.



Figure 69: Machined Internals of Payload Bay; 1 – Sabot, 2 – Payload, 3 – Payload Tray, 4 – Electronics Tray

A carbon fiber payload containment tray has been fabricated to hold the payload sample. After the bay is fully opened, the sample can be inserted anywhere in the tray. Angled edges have been added to the tray sides in order to provide guidance to the sample as it is inserted. By providing this tapered edge, the sample can be successfully placed in a much larger area by the AGSE, which greatly reduces the precision demands on the AGSE system.

In conjunction with this payload tray, a retention sabot slides into place and constrains the sample tightly within the tray. This sabot closely matches the sample geometry, and includes foam pieces which sandwich the payload during flight, further preventing movement of the sample.

4.9.3.2 Drivetrain

One of the key differences between the payload bay prototype and the final design is the means of actuation. While the prototype utilized an off the shelf linear actuator, the final design implements a custom lead screw driven mechanism. The lead screw is situated between two mated bulkheads. The first bulkhead is constrained to the rocket body while the other is attached to the nosecone. By turning the lead screw, the second bulkhead translates as a means of opening and closing the payload bay. Below are pictures of the motor assembly and lead screw prior to integration into the flight vehicle.



Figure 70: Motor Mount and Forward Bulkhead

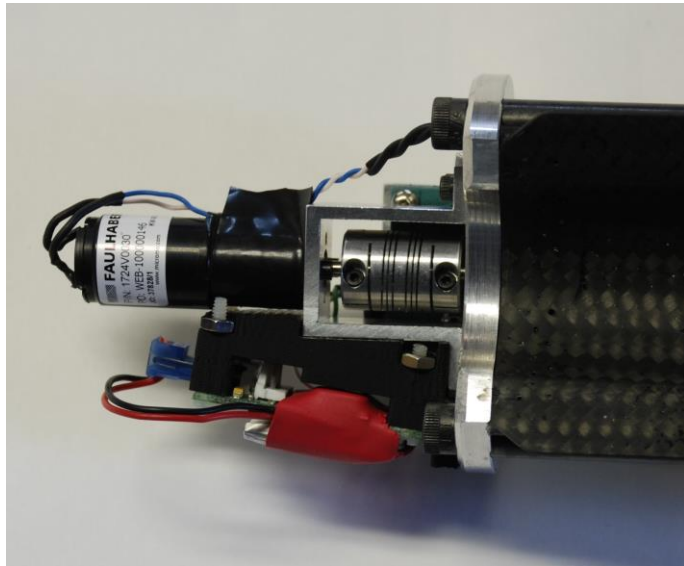


Figure 71: Payload Bay Motor with Wiring

The primary consideration that led to the choice of a lead screw method of actuation is the need to maintain a high “clamping” force between the male and female bulkheads when the payload bay is closed. This clamping force will prevent the payload bay from opening during rocket flight, when it will experience variety transient and steady forces. A lead screw assembly is an ideal candidate to provide such a clamping force due to its non-backdriveability. Once the lead screwed is turned to a given position, an axial force applied on the threads will not cause the screw to turn. That is, the frictional forces caused by an axial load on the lead threads are greater than the torque produced by that load. This characteristic allows the drivetrain motor to be de-energized when not opening or closing, saving a significant amount of electrical energy and increasing the overall reliability of the system.

A chart detailing the path of force transmission through the updated drivetrain design is shown below.

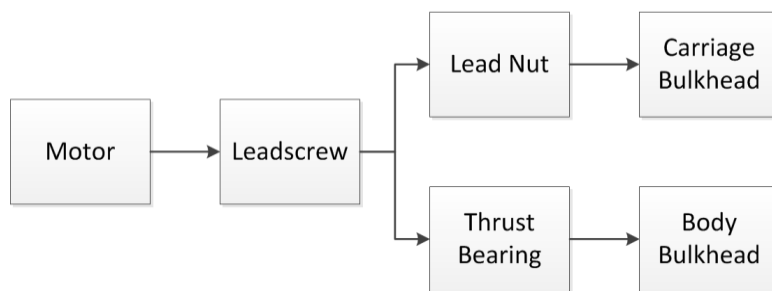


Figure 72: Flowchart of Force Transmission in Final Payload Bay Design

The force path has been significantly simplified from the prototype design, and force is only transferred along drivetrain components rated to support the expected load. This methodology has a significant advantage over our previous force transmission path in that it greatly increases the reliability of our system. Further justification for our redesigned drivetrain is reflected in

section 4.9.3.5: *Justification of Materials*, in that all rapid prototyped pieces have been removed from the path of force transmission.

4.9.3.3 Electronics

While the payload bay still utilizes the same microprocessor, additional features were added to the electronics system in order to increase redundancy and overall system reliability.

Firstly, the motor controller electronics were updated to accommodate the electrical demands of the lead screw motor. This included the addition of limit switches at the extents of the nose cone travel that provide the ability to sense the position of the nose cone and prevent over extension of the drivetrain. When the nosecone is closed, the corresponding limit switch will detect the proper mating of the bulkheads. At this point, the onboard microcontroller will increase the power sent to the lead screw's motor for a brief period of time, squeezing the nosecone shut with a substantial force. Due to the non-backdriveability of the lead screw, this high closing force will serve to keep the nosecone tightly secured for flight even when power to the motor is no longer applied. This feature greatly decreases the overall electrical energy required for payload bay operation, and ensures that the nosecone will not open in the event of power loss.

Additionally, the communication interface between the AGSE and Payload Bay has been changed substantially to implement a wired USB connection, and is discussed extensively in section 4.9.3.6: *Integration and Compatibility with AGSE*.

To satisfy the requirement for an on board tracking device, as set forth by NASA, a radio frequency transmitter has been added to the payload electronics system. The corresponding antenna is mounted inside the payload bay section, and facilitates long distance tracking by our portable radio frequency receiver. For more information regarding this locator, refer to section 4.5.9: *Recovery Telemetry Electronics*.

Finally, the electronics systems were mounted onto a dedicated electronics sled, which provides a sturdy mount and impact dampening to the systems within the electronics bay.

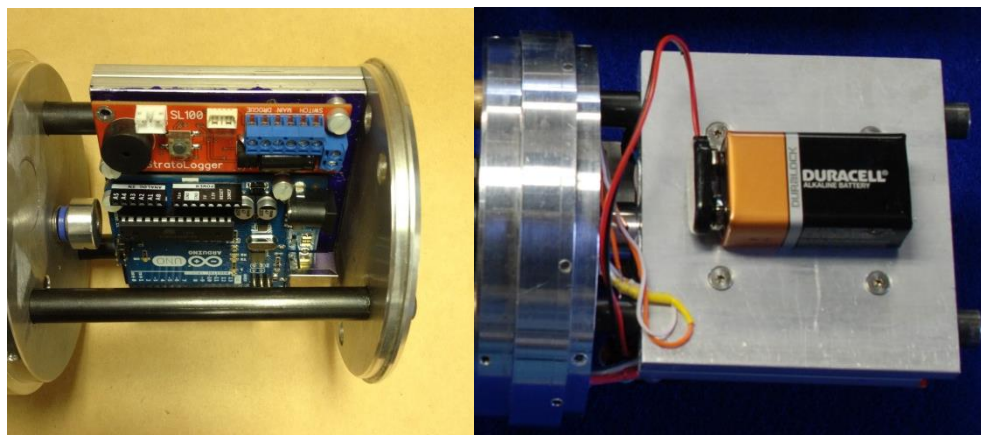


Figure 73: Electronics Tray with Mounted Boards and Battery

4.9.3.4 Software

The final payload bay electronics system utilizes software that has co-developed with the hardware it supports. As such, the payload bay control logic has remained largely the same since the subscale launch. Modifications since the subscale launch include the addition of a redundant communication protocol to interface with the AGSE, which is detailed in [4.9.3.6: Integration and Compatibility with AGSE](#).

The Payload Bay control logic has been designed with reliability and fault mitigation as the primary focus. In addition to the checks and balances within the software logic, the payload bay can also communicate its state to the AGSE to inform decisions made by the AGSE software.

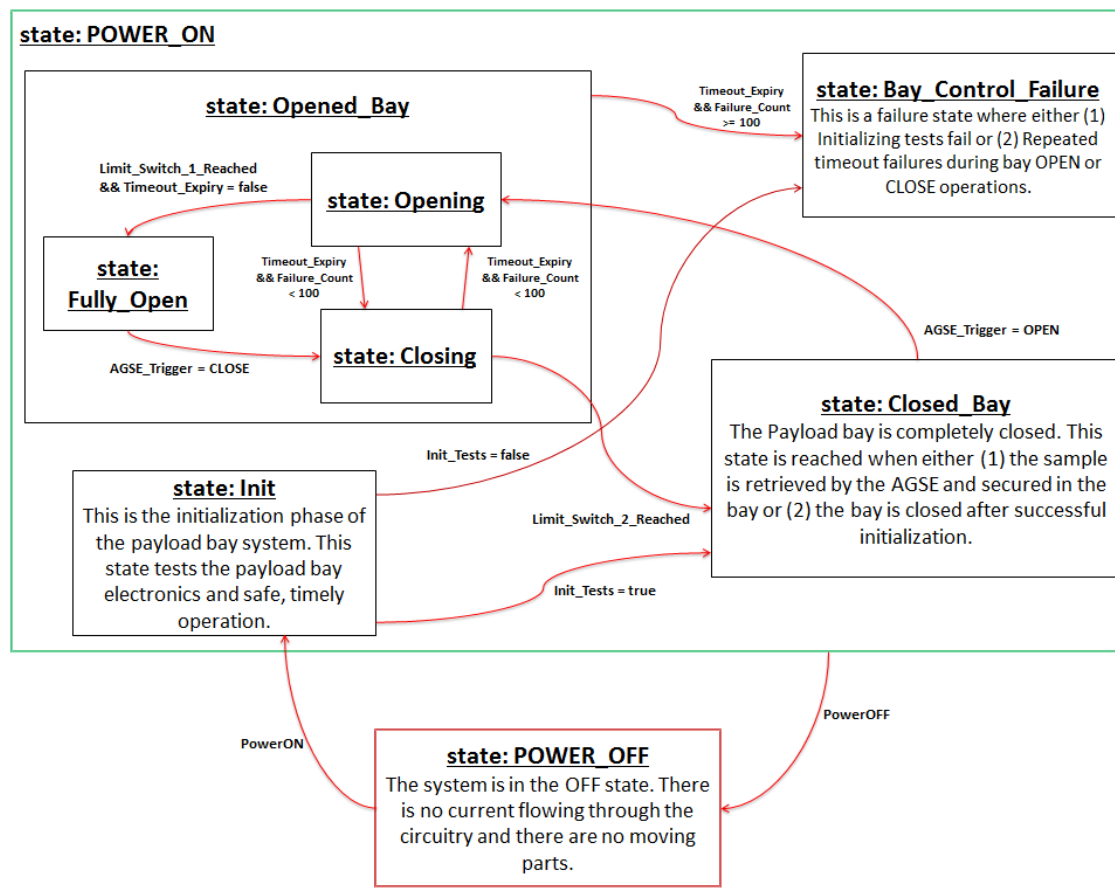


Figure 74: Payload Bay Statechart

As can be seen above, the progression of the payload bay software includes several checks to ensure proper function. The system begins in the Power Off State until it is powered on, where it enters the Initialization state. In this initialization phase, it tests itself to determine if the electronics are functioning properly. If it fails these tests, it enters a Failure state, where a debugging procedure can be initiated. However, if the initial tests are passed, it enters the Closed Bay state, where the payload bay is completely closed and awaiting instruction to open. When the AGSE triggers it to open, the payload bay enters the opening state, where the bay slowly opens until it either reaches a limit switch or a timeout limit. If it reaches the limit switch first, it enters the Fully Open state where it will await signal from the AGSE to close. However, if the timeout count occurs before the limit switch is reached, it will immediately begin closing because there is an issue in the opening procedure. This failsafe ensures that the payload bay will be securely closed for launch even if there is an issue opening it. A signal from the AGSE can also trigger the system to enter the Closing state from the Fully Open state as well. While in the Closing state, the payload bay will continue to close until it reaches the second limit switch and reenters the Fully Closed state. Again, the payload bay will remain in this state until a Power Off signal is given or the AGSE triggers it to open again.

4.9.3.5 Justification of Materials

When considering material choice for our final design, several factors including overall strength, reliability of structural integrity, and impact resistance were considered in the context of our rocket flight and landing procedures.

Although the rapid prototyped pieces used in the payload bay prototype provided the necessary surface area for epoxy, they contributed to structural unreliability elsewhere in the system. This is because 3D printed parts are prone to manufacturing defects that can greatly impact the structural integrity of the part. These defects are often in the internal structure of the part, making them nearly impossible to detect prior to failure. Additionally, since the parts are printed in layers, the composite part is inherently anisotropic and is susceptible to delamination between subsequent layers. For these reasons, only non-structural parts of the final payload bay were rapid prototyped and all structural members were made of either aluminum or steel, as is detailed below.

For the non-load bearing Aft and Forward bulkheads, 6061 aluminum was chosen because it is cheap, easy to machine, and is readily available. For the Male and Female bulkheads, 7075 aluminum was procured. 7075 aluminum was chosen due to its very high strength and great machinability. For the guide rails, low carbon steel rod was chosen to minimize deflection of the rods during operation. Carbon fiber was chosen for the sample tray since it is not a load bearing component and can therefore be as light as possible. The complex geometry of the sample retention sabot lead to it being 3D printed from ABS plastic.

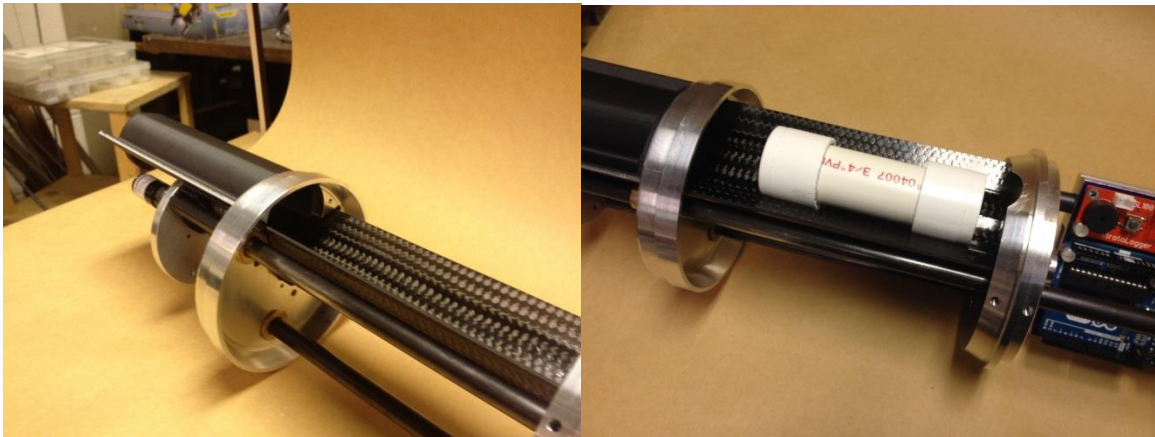


Figure 75: Female Bulkhead, Sample Tray, and Retention

4.9.3.6 Integration and Compatibility with AGSE

The primary means of communication between the AGSE and the payload bay is through a USB break away connector that facilitates wired serial communication and power transmission between the two electronic systems. This communication interface allows the AGSE to directly issue commands to the payload bay microprocessor. This communication bus attaches via a commercially available magnetic break away connector, pictured below.

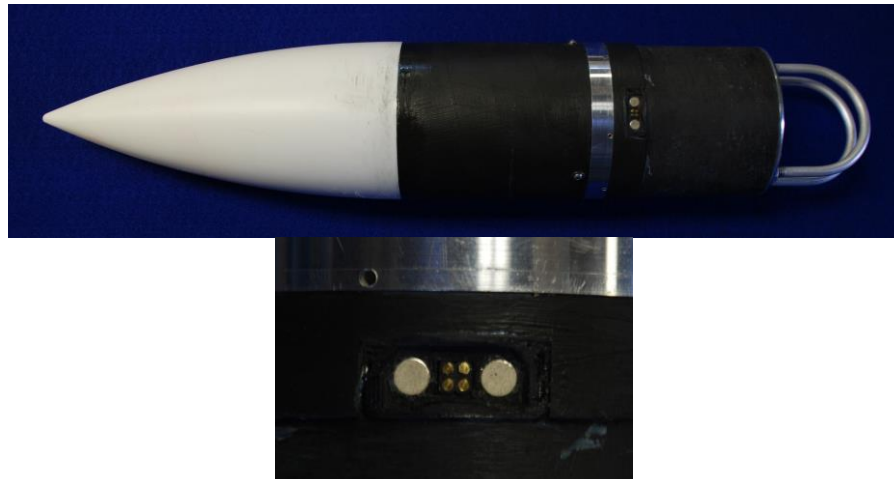


Figure 76: Top: Payload Bay inserted into Rocket Body, Bottom: Breakaway connection

Because the breakaway connector is inherently prone to disconnection, the Hall Effect sensor based protocol that was used in the subscale prototype acts as a backup system in case the wired communication is severed prematurely. This protocol, which has been proven effective in the subscale launch and several subsequent tests, acts as a safeguard against potential disruption of communications.

In addition to serial communication capabilities, the USB connector is also configured to support power transfer between the AGSE and payload bay. Although the system is not currently configured to source power to the payload bay motor through this connector, the current implementation provides power to the microprocessor and altimeter in the payload bay. The

connector has the capability to source the motor power as well, in order to add a redundant power source for payload bay actuation.

4.9.3.6.1 Simplicity of Integration Procedure

Through the development of redundant communication systems, we have greatly mitigated the chances of electronics communication failure. Such a malfunction would result in mission failure, and has been fully addressed our design development.

As such, the payload bay has undergone iterative design changes in order to reduce the complexity of system development. By taking this adaptive approach to development, we have arrived at a fully integrated, optimized system while maintaining simplicity of operation.

4.9.4 Integration of Payload Bay with Rocket

In addition to its functional requirements, the payload bay must satisfy the practical needs of integration with the flight vehicle. Therefore, the interface between the two was well defined in the early stages of design. The payload bay has been developed as a modular section of the flight vehicle, capable of ejecting and recovering under an independent parachute.

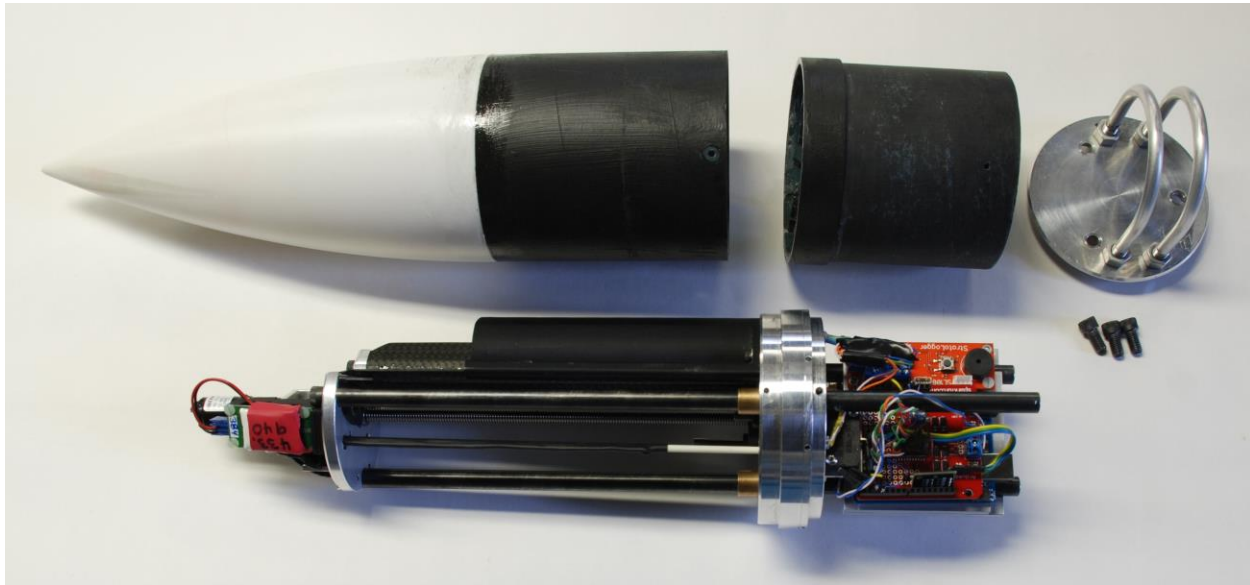


Figure 77: Disassembled Payload Bay

After being fully assembled, the payload bay was inserted into the forward section of the rocket, and shear pins were placed through the rocket body and payload coupler tube to connect the sections. At the time of payload section separation, the shear pins between the sections are broken via a separation charge and the payload section.

The picture below shows the payload bay section integrated into the launch vehicle. Note the location of the aluminum bulkheads, and the seamless integration of the section into the launch vehicle as a whole.



Figure 78: Rocket With Payload Bay Open

4.9.5 Payload Bay Testing and Verification

The fully developed payload bay system underwent extensive testing after its completion. These tests were designed to provide a total evaluation of all structural, mechatronic, and electrical systems within the payload bay. Reliability is considered a paramount concern and was therefore evaluated in nearly all testing procedures.

Table 12: Payload Bay Testing and Verification

Part/Functionality Tested	Method of Test	Results
Does the payload bay drivetrain successfully provide open/close functionality in a timely and reliable manner?	The payload bay was actuated a number of times to verify normal operation. Motor current draw was recorded, and actuation time was measured. These testing procedures were repeated with a low battery and actuation characteristics were noted.	The payload bay drivetrain was shown to repeatedly actuate in response to commands. Motor current draw remained well below the maximum intermittent current draw specified by the motor manufacturer. The drivetrain was also shown to function on a low battery, although actuation time increased markedly
Does the payload bay drivetrain correct itself from a jam scenario?	The payload bay was repeatedly actuated and exposed to moment applied to the nosecone in order to initiate a frictional bind. The moment was then removed and the natural response of the drivetrain was observed and its characteristics noted	The drivetrain was shown to self-correct from a jamming scenario in all tested scenarios. This demonstrates that the corrective moment associated with a jam is great enough to overcome friction and allow the carriage to freely slide.
Does altimeter properly track changes in altitude? Are the venting port holes adequately sized for flight conditions?	The payload bay was fully assembled with the altimeter armed. The section was then placed into a vacuum chamber along with the main avionics bay and a vacuum was drawn to simulate change in altitude. This	The data collected by the payload bay altimeter matched that recorded by the avionics bay almost exactly. The testing procedure is further detailed in section 4.9.5.1: <i>Avionics System Testing</i> .

	simulated change in altitude was matched to flight conditions and data from the altimeters was recorded for analysis.	
Does the payload bay primary communications system, facilitated by a USB connection, demonstrate reliable behavior?	The connection between the payload bay and AGSE was initiated, and commands were repeatedly sent to the payload bay in order to verify successful data transmission.	The USB connection provided unwavering data transmission capabilities in all tested scenarios.
Does the payload bay backup communications system, facilitated by a Hall Effect sensor, provide reliable backup functionality?	The payload bay was initiated in the closed state and commands were repeatedly issued by the AGSE using the prescribed communications protocol. Actuation functionality and characteristics were noted.	The Hall Effect sensor based communication protocol demonstrated reliable detection of AGSE commands in all tested scenarios. Thus showing the utility of this system for fault mitigation.

4.9.5.1 Avionics System Testing

In order to record the descent trajectory of the payload section under its own parachute, a Stratologger altimeter was installed in the payload electronics bay. This altimeter detonated no charges, and its only purpose was to ensure the payload bay was below the maximum landing energy.

In order to verify the proper functionality of the altimeter, a vacuum chamber test was conducted and results were compared to the main avionics bay results. This test also served to verify adequate venting to the altimeter, as described in the following section.

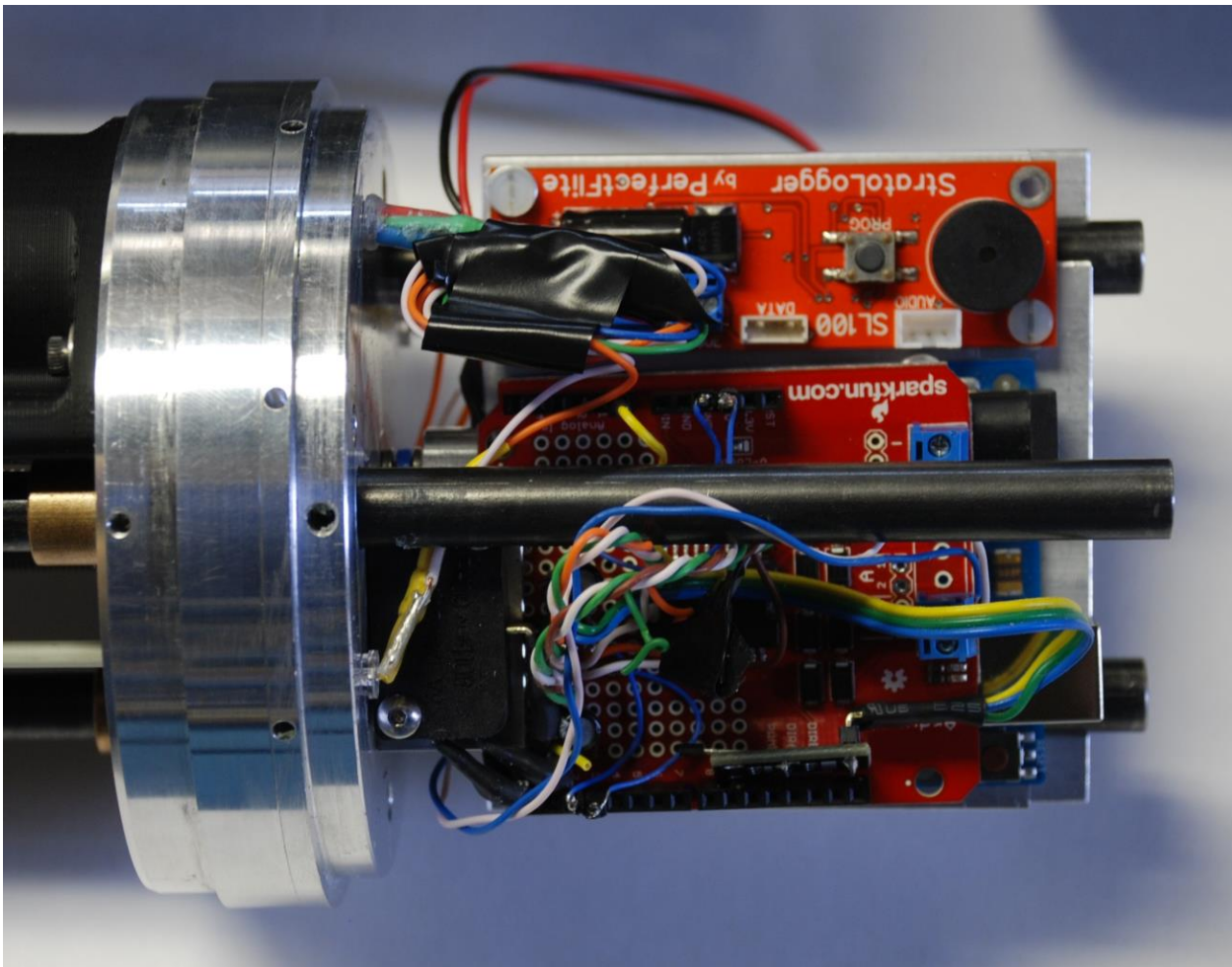


Figure 79: Payload bay altimeter and port holes

In order to provide proper venting to the altimeter, 4 equally spaced port holes were machined in the payload bay's male bulkhead, as can be seen in *Figure 79*. These holes are necessary to ensure the altimeter is properly exposed to the ambient pressure during descent.

The accuracy of this altimeter was verified by comparing it with the recovery system altimeters. Due to the large diameter of the payload bay, 4" compared to the avionics bay's 3.9", the payload bay was too big to insert in the Vanderbilt Shocktube for vacuum chamber testing as has been done in the past. To solve this problem a small vacuum chamber was improvised using a sealed 5-gallon bucket and the in-house vacuum lines provided to multiple labs on campus. The entire payload bay was assembled and armed, and then placed within the new vacuum chamber (*Figure 80*) along with the fully assembled and prepped avionics bay. The hose was then connected to an in-house vacuum line and the entire system depressurized.



Figure 80: Payload bay vacuum chamber

As can be seen in the following figure, the payload bay properly vented and responded to pressure change. It is important to note that the most important piece of information is not the steady-state altitude displayed, but instead the rate of change, the slope, of altitude as the chamber was initially pressurized, since this is what would be affected if the port holes were undersized. This is shown by the red line on the graph, and can be seen to match nearly perfectly with the main avionics bay.



Figure 81: Payload bay altimeter verification through comparison with avionics altimeters

5 AGSE Criteria

5.1 AGSE Experimental Concept

5.1.1 Creativity and Originality

The baseline requirement for the AGSE is that it autonomously retrieves the sample and places it into the launch vehicle's secure bay. The adaptability of this task is the most defining variable, as the requirements could be accomplished by simply placing the sample at a precise position and orientation, inputting the given coordinates into the AGSE, and letting it operate from based on a preprogrammed set of location-based steps. However, in a Mars mission, sample coordinates would not necessarily be known, nor would the location of the rocket be a precisely pre-measured value. When sample acquisition is so paramount to the mission success, the acquisition system needs to be robust enough to adapt to unknown variables. This is why we have chosen to use image processing and object detection to find the sample and to plan the path of our robotic arm. By knowing the position and orientation of the AGSE linkages both with respect to the sample and to the payload bay, the linear transformation, and thus the optimal path, from the sample to the payload bay can be calculated. Though the feat of image processing and object detection exceeds the baseline requirements that NASA has laid out for the AGSE, we believe it to be a critical feature in any design of an AGSE, giving it more autonomy than it would have if its "start" and "end" coordinates were its commands.

The novelty of this solution is in the application. The Vanderbilt Aerospace Team draws influence from a number of fields in which its members have previous experience. While image processing, and the particular algorithms we employ, have been created and used in the past, they have been limited to specific application, almost exclusively in environments where precision and repeatability dramatically supersede weight and resilience to environmental conditions. Operating rooms and manufacturing environments are controlled, making dust, wind and inconsistent placement of objects nonfactors. Similarly, machining tools and other such equipment used in mass production have large, heavy frames to prevent bending. Addressing these concerns is at the heart of the design process when preexisting systems are reconfigured to sole new problems in different fields.

In addition, we have designed our AGSE to be modular in nature, allowing seamless transition between different types of actuators and end effectors. The modularity of the robotic arm design could prove useful in a Mars mission as the robot manipulator's use could be interchanged by another mechatronic system that alters the functional purpose. For example, a drilling attachment could be placed at the end of the arm in order to dig for a sample; and then the drilling attachment could be easily removed and replaced with the gripper to pick up a subterranean sample. This modularity thus not only facilitates in the ease of design and construction of the robot, but also expands the functionality of the entire AGSE system.

Furthermore, the modularity of the AGSE not only includes the hardware systems but also the software systems and their design. Because some of our team members have research and

development backgrounds in software modeling, analysis, and code-generation, we have created a modular, extendable, and powerful software modeling and code generation toolsuite. The software modeling allows us to describe at a high-level the different parts of the software subsystems (the software components) and how they interact with each other to produce the overall AGSE mission functionality. Using this modeling paradigm, we can develop more precise descriptions of the software systems, we can ensure the correctness of their interaction patterns, and because we generate most of the code (4700 lines of code generated out of 7777 lines of code written; 60% generated) we can ensure the correctness of the code. Additionally using the component-based generated code, we break the requirements of the AGSE software down into indivisible software components and can write the code for each component separately from the other components. This modular software design approach allows us to produce more reliable software faster and enables us to extend the capabilities of our software system relatively easily.

5.1.2 Uniqueness and Significance

There are countless ways to design for the autonomous retrieval of a sample near the rocket launch pad. As a part of the design process, the Vanderbilt Aerospace Team explored options ranging from rovers and quadcopters to all manner of robotic arms and even the possibility of a launch pad that moves to the sample. While several of these designs have merit, each competing design was eventually rejected for possessing some flaw or excessively complex element. Our crane design, by contrast, meets all of the criteria while remaining simple enough to be light and modular.

When one thinks of previous Mars missions involving terrain exploration, rovers are the first engineering solution to come to mind. While the rover design allows great range in sample retrieval, it is difficult to design for reliability, as it has many failure modes, including loss of control communication, drivetrain failures, and the possibility of rough terrain to navigate. Additionally, the rover would still have to be able to operate robotics, and all of the challenges that come with a robotic arm solution. Doing this on top of a wheel base adds additional complexity, sources of error, and modes of failure. Such added complexity can create a system which is difficult to orient without also translating. Our design errs instead on the side of reliability and robustness. With a stationary robotic arm, there are significantly fewer failure modes, and, if failure does occur, it can be communicated across the system more effectively and thus more easily mitigated.

Another design with great range is the quadcopter. With the low weight of the sample, creating a design that can precisely navigate the terrain and bring the sample back quickly would be very doable. The ability to go higher while searching would be a big advantage when searching as well. Unfortunately, this design has three major issues. First, there would be significant problems with time of operation because of the high power consumption associated with sustained flight. A quadcopter with enough battery life to search for a significant period of time would have to devote a significant portion of its total weight to batteries. Second is the application to the real SLS mission. The atmosphere on Mars has a low density, and thus a quadcopter would have extreme difficulty operating under these conditions. Finally, the positioning precision of the quadcopter would be affected by a number of factors unknown to the

designer, particularly the wind speed and direction. These factors, among a number of other potential conditions, would place significant restrictions on the operating environment in which a quadcopter could reliably retrieve the sample.

Even narrowing down the design choice to a robotic arm left us many options from which to choose. There are many types of arm designs, from SCARA to the Stanford Manipulator, which use different combinations of prismatic and revolute joints to achieve similar workspace areas. While complexity varies, these designs, despite their upsides in manipulability, tend to have a lessened reliability with the increased number of joint variables. In fact, in terms of robotic arm design, reliability tends to decrease with an increase in complexity—at least, in a project timeline as short as the SL competition. For this reason, we have chosen for our robotic arm design that has only the joints needed to perform the precise task. This means a more reliable system, without sacrificing relevant functionality. It also means power consumption, and thus energy storage requirements, are lower. While there are no competition requirements in weight and total energy, a system designed for extra-terrestrial applications would need to consider these factors in depth.

By using only four degrees of freedom, we use the minimum amount of movements necessary to enable the AGSE to orient along and pick up the sample and place it in the rocket. The robotic arm can travel in Cartesian space in x-, y-, and z-coordinates using the prismatic joints and base rotation, allowing the arm to reach the object. With a revolute joint at the gripper, the fourth degree of freedom, the robot is able to account for different orientations of the object. While this operational space is limited by height and reach, it is a more predictable and reliable system than most of its more traditionally revolute joint-based counterparts.

In accordance with this design philosophy, we have chosen to use prismatic joints rather than revolute ones. This design will allow the horizontal arm motor to be placed close to the main base structure of the arm, reducing load on the arm's structural members. Both of the prismatic joints are controlled from the base structure, leaving only the servomotors controlling the gripper and its orientation outside of the base structure. In terms of workspace, the prismatic design offers the same range as a revolute design would offer. A fully revolute system may be more simply equipped to reach around to its backside, but we accommodate this movement in our prismatic design by using a rotating turntable base.

In the simplicity of our design is a type of elegance that cannot be achieved with a more complex design. Our design uses the exact number of motors and actuators needed to accomplish the task, no more and no less. This improves reliability and the robustness of the system by minimizing the number of functional parts without having to sacrifice the mission functionality of the entire arm. In a Mars sample recovery mission, it is most important to reach the goal of actually retrieving the sample and placing it in the ascent vehicle. If a simple design can achieve this end, then it will be the optimal choice to implement for such a mission.

5.1.3 Challenge of Design

The 2014-2015 SL competition incorporates aspects of mechanical engineering that are not usually considered in the design of rockets, most notably robotics, mechatronics, and system

dynamics. Along with the fluid mechanics, heat transfer, thermodynamics, controls, instrumentation, and materials science utilized in the design of a rocket, the team must incorporate these other fields in creative ways in order to fulfill the sample retrieval requirements of the AGSE. The payload bay design and AGSE also incorporate elements of machine design as well, giving this project a wide breadth of applications in mechanical engineering. The challenge is in consolidating these different fields of study into the design, fabrication, and testing of a robust AGSE and its constituent subsystems.

5.2 AGSE Science Value

5.2.1 Objectives

The responsibility of the AGSE is to identify the sample placed within its workspace, secure it, move it to the location within the payload bay for storage, release it, and finally move away so that other systems can perform their appointed tasks. In handling this problem, the Vanderbilt Aerospace Club looks to draw solutions from a variety of other fields. Image processing and its use in guiding robotics is not a novel concept, but it is one that has been primarily limited to a few fields. In particular, medical robotics use imaging to aid remote control, and automated control is a subject of research. The field of manufacturing uses image processing to identify objects for manipulator interfacing in various ways. Circuit board fabrication uses fiducial alignment markers, much like those used on our payload bay, to orient manipulators relative to the boards.

These solutions have much broader application than they are currently used for. Creatively applying these principals to our Mars-based sample recovery problem serves to demonstrate that this technology can be successfully adapted to new fields. This will open the door to further research and advancement in application of these systems, for which the design must be successfully altered to meet the requirements specific to this field.

In the case of our application, mass and power restrictions add new challenges, and a lack of environmental control must also be addressed. Factories and operating rooms rarely have dust or high wind speeds, and can set temperature and humidity levels to ideal, constant values. Adding these factors causes issues with precision and reliability. Designing the system to prevent or handle these challenges is a big part of the innovation inherent in our design. Furthermore, ample power is available to these systems in their “native” environments, and they don’t have to be transported over long distances. It is far easier to avoid precision and tolerance problems when the arms can be as thick and dense as needed to avoid bending and limit vibrations. Finally, when a medical or manufacturing robot breaks down, it can be repaired or replaced. On the surface of Mars, that isn’t possible. This means that the robustness of the system is of greater importance even without taking into account the environmental effects. The team is confident that in solving these challenges, we can demonstrate that image processing as an input for fully autonomous controls can be extended to many other fields of engineering.

5.2.2 Literature Review

This section briefly describes aspects from existing scientific literature that inspired our system composition, elaborating on the implications of design choices in the various sub-systems such as image processing, grippers, manipulators and arm construction. The highest-priority system goal from the perspective of the AGSE sub-system is to design, implement and deploy a safety and mission-critical sample retrieval device. This device (1) surveys its surroundings to identify an object of interest, (2) paths to this object, (3) collects the object using a retrieval mechanism and (4) secures this object in a destination. The automation of the above sequence of steps along with the nature of the Martian environment add layers of complexity to the design, including complex computer vision techniques, programmed intelligence and fault tolerance. We have surveyed the literature of robotics engineering to identify necessary considerations when designing and building our retrieval system. The following 3 sections walk through the considerations and influential previous work for the AGSE. References can be found in the appendix, section *10.4: Sources*.

5.2.2.1 Computer Vision

One of the key motivations for using Computer Vision [1] techniques to identify and retrieve a foreign sample is the run-time automation that can be realized. It is often the case that obtaining significant remote access to deployed sub-systems on planets such as Mars is difficult and nondeterministic. For such systems, the level of automation directly influences the effective usefulness of the deployment. Computer Vision techniques have been applied to a heterogeneous range of systems such as Medical Robotics [2], Mobile emergency assistance [3], Industrial robotics [4] where the applications are as diverse as the processing algorithms. In Medical Robotics, imaging systems have been used for several image-guided invasive and non-invasive medical procedures [5], [6], [7] and [8]. The confidence required for the wide-scale use of such techniques stems from the robustness and repeatable applicability of the processing algorithms. Many of these techniques are not completely automated in order to meet safety requirements but are certainly guided by processed images obtained from controlled sensors. Path planning [9], [10] techniques that follow modular and theoretical image processing principles can be easily applied to domain-specific problems such as controlled sample retrieval. At its core, the retrieval problem can be broken down into (1) Sample Reachability and (2) Sample Manipulation. Sample Reachability is handled by the image processing outputs that feedback and control the actuating motors. This also avoids the need for collision avoidance techniques such as proximity sensing [18]. Furthermore, the modularity of the processing techniques and the wide-scale availability of off-the-shelf image manipulation algorithms [11], [12] that interface with embedded system cameras provide the necessary foundations for a reliable and robust vision-based arm control sub-system for the sample retrieval problem. One of the main performance measures of interest here is the accuracy of the image guidance. This depends on not only the precision obtained from image processing but also the degrees of freedom that are available for actuation. Though mission-critical concerns such as cumulative failure probabilities and power-to-weight ratios have limited the extent to which our robotic arm is capable of moving, the precision obtained from image processing and perceived depth [13] will allow efficient path planning and guidance to the arm.

5.2.2.2 Gripper Design

The design of the AGSE gripper is influenced by a number of factors. Due to the remote nature of the device and the size of the target sample, we decided on a simple claw-based gripper similar to [14], [15]. Some of the design choices such as number of claws are determined based on the maximum allowable weight, power requirements and modularity of development as we can hot-swap gripper designs without changing much of the control software. We have also identified some interesting design principles that enable high versatility to the gripping such as nonholonomic gripping [16], grasping with slippage and handling objects with variances in mass, size and texture [17]. However, we have limited our design to be optimal for carrying the target sample (as defined for this project) to simplify the design and to improve predictable movement and path planning towards the center of the sample. Since the image processing software works in a closed loop with this gripper design, the size and shape of the gripper affects the points in space where the camera can be mounted on the arm (and therefore the viewing angles) and also the accuracy of the path planning. All of these reasons inspired our gripper choice and arm designs.

5.2.2.3 Robotic Arm

Our primary concern while designing the robotic arm was to consider a design where the arm itself was not part of the rocket that eventually takes flight. This immediately removes several weight and power-related limitations of designs where the retrieving system is entirely within the confines of the rocket. Our secondary goal was to identify a stable and robust design that had sufficient degrees of freedom to reach a target within a defined radius while not being over-specified or over-built. This enabled us to build an arm that is similar in construction to the SCARA robotic arm designs [19], [20], [21] but using lead-screw guide-rails as used in other domains such as remote surgery techniques [22]. This removes part collision concerns and greatly simplifies the actuation along the coordinate axes and therefore the kinematics.

5.2.3 Success Criteria

The team has identified 7 Mission Success Criteria specific to the AGSE:

1. The AGSE must distinguish the sample from the environment including other cylindrical objects within its operating space.
2. The AGSE must grab and move the sample without damaging it in any way, including dropping it.
3. The AGSE must identify and avoid any obstacles within its operating space.
4. The AGSE must identify and precisely locate the rocket Payload Bay compartment.
5. The AGSE must place the sample completely within the containment area of the payload bay so as not to interfere with the closing process.
6. The AGSE must respond appropriately to the PAUSE command whenever given, without losing the ability to continue its assigned task once freed.

- Once finished, the AGSE must assume a position such that it will not interfere with the launch of the rocket or sustain any damage as a result of its proximity to the launching rocket.

5.2.4 Experimental Logic, Approach, and Method of Investigation

The primary objectives of the AGSE are to autonomously locate, retrieve, and deposit the payload in the rocket bay without interfering with or damaging either the rocket or the payload. Using the hazard and failure criteria for the AGSE (*6.2.1: AGSE Preliminary Failure Modes*) we may qualitatively evaluate any hazards to the rocket body, the payload, or the AGSE itself during the retrieval process. These qualitative tests should ensure that no part of the process damages any of the operational components.

The major experimental challenge addressed by the AGSE is the ability to autonomously detect, retrieve, and deposit the payload in the rocket. Since there will be no human interaction with the AGSE during the retrieval process, the collection of the payload will rely entirely on the ability of the image-processing software to detect the location of the payload, its orientation, and the corresponding location and orientation of the rocket payload bay. Since the payload is of a known shape and coloring, this software can be optimized specifically to detect objects with the same visual qualities as the payload.

Investigation into the ability of the AGSE to accomplish the designated requirements relies on the accomplishing of several steps, the same steps of the retrieval process. Each process can be tested on a systematic level to ensure that the AGSE subsystems will successfully interact to complete the overall objectives. It should be noted that although some final integration is still in the process of being tested and improved, **all of the subsystems and individual components of the AGSE have been tested**. The iterative process that will be used will demonstrate subsystem functionality will begin at the most basic functional levels, and progress towards fully complex system operation. This approach is outlined as follows:

User Control capabilities:

- Start the AGSE and issue the pause command using the user-input panel's pause switch. Verify that the light correctly displays the proper pattern and that the AGSE stops. This verifies the functionality of the pausing system. **COMPLETE**
- From the paused AGSE state, unpause the system using the user-input panel's pause switch. Verify that the light correctly displays the proper pattern and the AGSE resumes operation from the state previous to the pause state. This verifies the unpause functionality of the AGSE system. **COMPLETE**
- Thoroughly test the pause and unpause functionality described above for every state and every state transition in the system to ensure that all states and state transitions can be paused and unpased. **FINAL INTEGRATION TESTS IN PROGRESS**

Ensuring full operational ability within predicted workspace:

- Manual control of the AGSE actuators to move and orient throughout its operational workspace; this verifies the ability of the AGSE to have the necessary capacities to perform the other aspects of the payload capture process. **COMPLETE**
- Simulated automatic control of the AGSE actuating joints before AGSE programming; this ensures that the trajectory generation and operation of the AGSE can be operated without reaching singularities or violating operational boundaries, which could damage the AGSE or create a hazard to operators. **COMPLETE**
- Planned control of the AGSE actuators to move and orient throughout its operational workspace; this verifies that the software being run on the AGSE will be able to control the required tasks to accomplish its goals. **COMPLETE**
- Autonomously generated behavior by the AGSE to safely detect, retrieve, and transport the payload and no other objects from the starting location to the payload bay; this verifies that the AGSE is capable of the operation requirements in a reliable fashion. **FINAL INTEGRATION IN PROGRESS**

Image processing search protocol and payload recognition:

- Image capture from the gripper mounted USB camera; this verifies the basic functionality of the camera and its interface to both the electronics of the system as well as the operating system kernel of the system **COMPLETE**
- Write an image to the onboard storage; this verifies the data collection system.
- Capture images in a sequence rate ≥ 10 images/second; this verifies the speed of data acquisition. **COMPLETE**
- Write images in sequence (rate ≥ 10 images/second) to the onboard storage; this verifies the speed of data collection. **COMPLETE**
- Process a single image to detect continuous edges and shapes in the image; this creates the infrastructure for payload detection. **COMPLETE**
- Process a single image for the location of the payload relative to the camera location; this verifies that the AGSE will be able to move toward the payload. **COMPLETE**
- Process a single image for the orientation of the payload relative to the camera orientation; this verifies that the AGSE will be able to align the gripper phalanges with the axis of the payload. **COMPLETE**
- Process images of the sample in different orientations, lighting conditions, and environments. This ensures the capability of the camera and detection software to accurately detect the sample's position and orientation under various conditions. **COMPLETE**
- Process images of the payload bay in different orientations, lighting conditions, and environments. This ensures the capability of the camera and detection software to accurately detect the payload bay's position and orientation under various lighting conditions. **COMPLETE**

- Process images received at a rate \geq the rate of image collection; this ensures that there will be no deadlock between the image acquisition and robot motion. **COMPLETE**
- Develop a search protocol for the AGSE to sweep its operational area for the payload; this verifies that, even if the payload is not directly in the view of the camera from the start, the AGSE will still be able to either locate it or determine that it is not available. **COMPLETE**

Payload retrieval from detected location:

- With an identified target, servo the AGSE using cylindrical coordinates to the location of the payload; this verifies that, having identified the payload, the gripper may be moved to the correct position. **COMPLETE**
- With the gripper in position, detect and reorient the AGSE gripper to retrieve the payload; this ensures that, with a detected payload, that payload can be picked up accurately and consistently. **COMPLETE**
- Use the autonomous software to detect a successfully retrieved payload and move the AGSE gripper (containing the payload) toward the payload bay; this will ensure that the AGSE can move and orient to the payload bay using a safe velocity. **COMPLETE**
- Use AGSE object detection to find the payload bay-mounted fiducial markers; this ensures that the payload bay can be discovered and its orientation detected. **COMPLETE**
- Create and execute payload bay open and close protocol; this will verify that the payload bay can be opened and closed. **COMPLETE**
- Create and execute payload pick-up and put-down protocol; this verifies that the AGSE will be able to move the payload to the payload bay and place it successfully. **COMPLETE**
- Use the developed communication protocol and send messages from the AGSE to the payload bay telling it to open and close. This verifies the communications channel and subsystems between the AGSE and the payload bay work to provide the required mission functionality for autonomous opening and closing of the payload bay. **COMPLETE**

Enhancing design functionality (additional, optional features):

- Provide instrumentation to detect that the payload is being gripped; this provides verification that the payload has been retrieved and deposited without being dropped. **TESTING IN PROGRESS**
- Create obstacle avoidance parameters in AGSE movement protocol to avoid rocket collisions (as the rocket will be within the workspace of the AGSE). **TESTING IN PROGRESS**

5.2.5 Test and Measurement, Variables, and Controls

There are several parameters that must be measured and controlled in the development and testing of the AGSE. The AGSE system has many mechatronic components to control, making for a challenging implementation of the design, having to use code, electronics, and hardware all

in conjunction with each other. The most important measurements, variables, and controls to consider in the design and testing of the AGSE are outlined as follows:

- Each motor's current and voltage requirements must be considered while also taking into account the overall power usage of the system. These factors influence the requirements for the battery used to power the AGSE. *A result of this consideration is the homogenization of the AGSE system motors to all run off of 12 VDC. Additionally, it was determined that the current draw of the prototype linear actuators (4A max load) was excessive, as was their output power so the motors for the final version were scaled down. This saves weight and power requirements dramatically.*
- The speed of the gripper, linear actuators, and turntable base must all be taken into account. The AGSE system should be able to complete its task in a reasonable amount of time. *The speed of movement has been measured, along with the operating ranges for each of the motors. We determined (and calculated) that the linear actuators could allow us full range of motion in less than a minute. The servo motors can be parametrically set based on torque and speed requirements and we found that the default settings allow for subsecond gripper actuation, subsecond gripper rotation, and safe arm rotation in less than 10 seconds.*
- The position of the servomotor controlling the rotation of the gripper must be calibrated to the amount of current it is given. This will ensure accurate control of the rotation of the gripper by the microcontroller. *This requirement has been handled by changing the servo motor controlling the gripper.*
- The control of the linear actuators and servos must be implemented. The linear actuators do not include position feedback, for which we add quadrature encoded pulse modules which provide accurate position feedback and integrate directly with our BeagleBone Black hardware. The BeagleBone Black includes built-in quadrature encoded pulse decoding hardware. The control of these elements must be measured against the actual position of the actuators at a given position in order to ensure accurate knowledge of position of each actuator within the AGSE. *We have verified that our motor control algorithms give us accurate positioning control.*
- The weight of the sample must be taken into account. Although the given sample is will be relatively low, it is important to consider the maximum limitations of the AGSE. If a sample is too heavy, it might cause the entire robot to tip over; or the gripper might not be able to grasp the object correctly. *The sample has been verified to not cause any detectable change in orientation or position of the AGSE, even at maximum extension.*
- The robot must be able to move from its start position to the object and from the object to the payload bay. The path planning of the AGSE will be able to combine the mechanical aspects of the actuators, electronics needed to power them, and the coding needed to calculate the required movement of each and provide the correct set of commands to the AGSE in order to go to the sample, retrieve it, and deliver it to the payload bay. *We have successfully demoed*

the high-level control of the AGSE as it detects and picks up a sample, finds the payload bay, and properly inserts it into the payload bay.

- In order to determine the position of the object relative to the AGSE, image processing will be used. First of all, the power requirements of the camera and processor used to locate the object must be taken into account. Second, angle of the camera allowing the best view of the space around it should be determined, as this will make finding the object less difficult. *We have determined that the current draw of the Jetson is less than 1A@12V at max load. We have determined that using the wide field-of-view HD camera we have chosen oriented facing the ground provides ample detection space.*
- It is useful for the codes controlling the payload bay and each aspect of the AGSE to be written in the same language. This improves the robustness of the programming behind the control of the actuators. *We have developed c++ code generators which generate most of the code used by the AGSE. The rest of the code for the AGSE deals specifically with the mission functionalities and was written by hand into the generated code.*

5.2.6 Expected Data and Accuracy/Error Analysis

A fully functional AGSE needs to be analyzed to derive useful metrics that can help refine the design parameters. This section briefly describes the performance metrics of interest on each sub-system. For each performance metric, there are factors that could result in error in the measurable values we are interested in that should be taken into account during the development of the AGSE system.

- Camera Feed Sampling Rate: We will identify a stable, minimum sampling rate at which the sensing camera feed is received and processed. This is the number of image frames per second that is inputted to the Image Processing sub-system. At each frame, a global detect-plan-move loop is executed until a globally relevant point in space is reached. Once the arm is moved to a desired location, a new frame (or set of frames) is analyzed and processed. In order to not damage the gripper or any physical object that is in close proximity to the gripper, the image processing unit that is responsible for actuation must receive camera input at a minimum rate relative to a unit of arm movement. *We have verified that the camera can provide an image feed to the Jetson TK1 at a rate higher than 30 frames per second.*
- Sample Detection Time: The Image Processing software combines many image processing algorithms to identify the desired sample in a frame of camera input. Once detected, the control system triggers the actuation of the arm in order to move towards the sample. The interesting metric here is identifying the average-case time taken for an initialized AGSE to identify a sample on the ground and mark it as "detected". This elapsed time is dependent on the relative position of the sample from the AGSE and is a measure of the efficiency of the image processing and arm control. *We have verified that the image detection algorithm used to detect the payload bay can be run in tandem with the sample detection image processing software at greater than 20 frames per second on the Jetson TK1. We are in the process of*

measuring the average time it takes our search algorithm to move the AGSE and find the sample in the available workspace.

- Payload Bay Detection Time: Similar to sample detection time, this is a measure of the average-case time taken for the AGSE to accurately identify the relative position of the payload bay. This is important to make sure that a retrieved sample is securely placed in the bay. *We have verified that the image detection algorithm used to detect the payload bay can be run in tandem with the sample detection image processing software at greater than 20 frames per second on the Jetson TK1. We are in the process of measuring the average time it takes our search algorithm to move the AGSE and find the payload bay in the available workspace.*
- Gripper Offset from Sample Center: The efficiency and accuracy of the arm control can be measured by identifying the maximum distance from the center of the sample to the center of the gripper base. The closer the gripper is to the center of the sample, the smaller will be this offset. The accuracy of sample gripping is important to secure the sample and not unintentionally drop it. *We have been verifying the accuracy of our sample detection algorithm in camera space. We have rigidly mounted the camera and the gripper so that we have a known translation and rotation projection matrix for transforming image space positions to workspace positions. We have been testing the control algorithms for the motors to determine the accuracy of positioning.*
- Electric Power: Power requirements for a fully functional AGSE system is a metric that shows the efficiency of the system design. The minimum power required by the AGSE should be enough to sufficiently power all sub-system components but never more than a specifiable upper bound. Necessary precautionary measures are taken at power junctions to prevent damaging effects of unexpected power draws. *We have determined that the current draw of the AGSE under full load will not exceed 6A@12V. Furthermore, we expect that the system will never draw full load except in an error condition (e.g. jamming). We have ensured that the power supply has over-current protections to protect the AGSE.*
- Environmental Tolerance: Tolerance to environmental changes such as lighting shows the robustness and repeatability of the AGSE system. Changes in lighting should not affect the sample or payload detection time. *We have tested the robustness of the payload bay and sample detection algorithms under various lighting and environmental condition and found that the algorithms' performance exceeded our expectations. Descriptions of those test results are given in Section 5.3.4.*
- Incorrect Detection: This is an average-case count of the number of times the AGSE incorrectly identifies an unknown object as the desired sample. Comparisons are made against objects that have a similar shape but not the desired size or vice versa. Tested calibrations on the image processing should enable low probabilities for such failures leading to robust design. *We have tested and iteratively refined our image processing software to*

minimize the number of false positives and false negatives. The robustness of our image processing software is described in Section 5.3.4.

- **Repeatability:** This is a measure of the number of times the AGSE can perform the sample retrieval operations on a specific scenario. This is observed for a set of scenarios to identify the repeatability and robustness of the run-time system. *We have been testing the AGSE under various scenarios to validate that the AGSE can indeed perform the sample acquisition repeatedly.*

5.2.7 Preliminary Experiment Process Procedures

The design of the AGSE was an iterative process. By using linear actuators in the first design, the AGSE prototype was able to be built quickly and tested during the construction of a more sophisticated lead screw design. The second design is near completion, but because of the old model and the nature of the software developed, this has not inhibited progress on the control and electronics side of the AGSE. With this iterative process, steps were taken one by one that worked toward full functionality of the AGSE system, integrating them along the way, adding more features. **We are currently transitioning into Phase 4 of the AGSE development.**

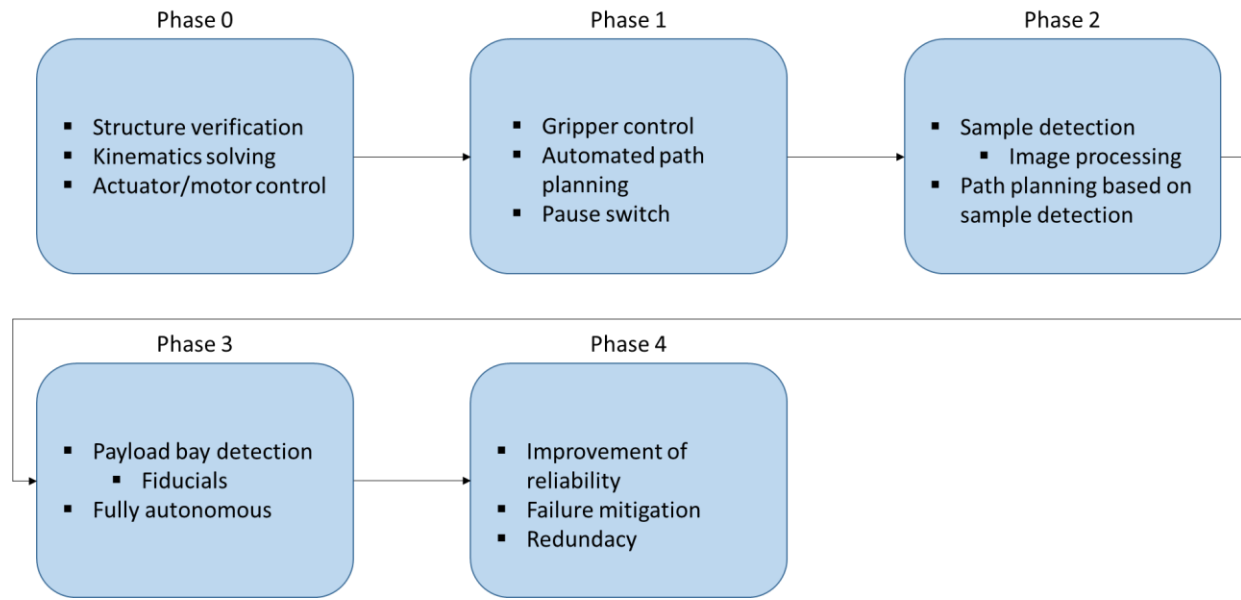


Figure 82: Flowchart of AGSE Construction Phases

5.2.7.1 Phase 0: Structure, Simple Kinematics, and Actuator Control

The first step, title “Phase 0,” focused on understanding the robotic system at a basic level. Before any of its movement could be modeled, its joint and structural integrity had to be analyzed. The joints must allow the desired movement without obstructing another joint’s movement, and the structure must be able to stand both in static and dynamic conditions. Both of these factors were tested after constructing the robot by allowing it to stand on its own and then testing whether it can still stand while moving different actuators and while being subjected to different loads.

The entire robot has also been studied in order to determine the kinematics of the system, taking into account the effect of each actuator on the others. This has been simulated by software, and then tested with manual control of the robot, inputting different signals to different actuators and observing the results.

The actuator control uses the knowledge of the kinematics of our AGSE system and integrates them with the sensor feedback at key locations to provide an up-to-date precise model of the current state of the AGSE system. Using this state knowledge and the kinematics equations, we have developed the software to precisely position and orient the gripper of our AGSE. This functionality allows the AGSE system to take as input the relative positions and orientations of both the sample and the payload bay.

5.2.7.2 Phase 1: Gripper Control and Path Planning

Phase 1 is the first stage of the AGSE design that is considered fully deliverable in terms of the NASA SL competition. Phase 1 improved upon Phase 0 by adding control of the gripper and automated path planning.

Control of the gripper is achieved using a built-in servomotor. Once again, its “open” and “closed” positions had to be calibrated for control. Another consideration is the amount of force the gripper exerts on the object. If the gripper closes too hard, it may damage the sample or possibly itself, stripping the gearing mechanisms that drive it. For this reason, the correct amount of position will be determined that allows reliable gripping of the object yet does not damage either the sample or the gripper.

Automated path planning allows the system to be able to move from one given position to another. Using the kinematics of the robot system with the input of the object and payload bay positions, the system is able to determine how to move its different actuators in order to go from the first position to the next. With the position of the object and of the rocket both known and inputted into the system, thus it satisfies the baseline requirement that the AGSE autonomously retrieve the sample. This can be tested using different known positions of the sample and payload bay and confirming that the AGSE move from one to another correctly.

In addition to these improvements, a master pause switch is added to the AGSE as per the rules of the competition. This switch stops movement of the entire robot once triggered for safety purposes.

5.2.7.3 Phase 2: Simple Sample Detection

The sample detection uses the edge detection and line detection algorithms described in the image processing design section, and will be based on off-the-shelf software designed to run on our hardware. This subsystem will provide the AGSE with the functionality required to autonomously detect the location and orientation of the sample, removing the requirement of sample position and orientation as input to the system. In order to test the image processing system, the object can be placed in different orientations and different lightings in order to ensure that the camera can detect the sample in a wide variety of conditions.

5.2.7.4 Phase 3: Simple Payload Bay Detection

Payload bay detection will use image-based fiducial detection that will provide the AGSE the ability to detect the position and orientation of the payload bay. With this subsystem's functionality, the AGSE will no longer need input about the position and orientation of the payload bay, removing all of its required inputs and allowing it to fulfill its mission goals completely autonomously within its operational range. Different positions of the payload bay can be tested to confirm that the camera can determine exactly where the sample needs to be deposited based on the fiducials.

5.2.7.5 Phase 4: Improvement of Reliability

Phase 4 focuses on reducing the frequency and effects of failures in the AGSE system. Throughout Phases 0-3, the most common failures of the system will be recorded; and it is these that we will try to eliminate in this phase. Some ways to improve the reliability of the design are to introduce redundancies into the system, mitigate the negative effects of faults, and include state space preservation, allowing the position of the system to be known even during failure. More specific improvements will be devised as the building of the AGSE progresses.

5.3 AGSE Development Strategy

For the development of the hardware and software components of the AGSE sample capture system, we followed a model-driven iterative design and development. This process ensured that at every step of the development, we had complete models of the system we were building (with respect to both hardware and software) as well as evaluations regarding the performance of the system and its effectiveness at meeting our design criteria. Furthermore, by developing the system in a component-based fashion, we were able to iteratively address design concerns and improve subsystems of the AGSE without having to completely rebuild the entire AGSE.

Following this process, we developed the following subsystems of the AGSE for its first prototype (demoed in a video for CDR):

- vertical linear actuator and carriage
- horizontal / radial linear actuator and carriage
- base servo motor for AGSE rotation with turntable and mounting plate
- gripper phalanges
- gripper wrist servo motor for gripper rotation
- gripper actuation servo motor for gripper opening and closing
- image processing and object detection software component for sample detection
- linear actuator software control
- base servo software control
- gripper wrist software control
- gripper actuation software control

Having already progressed further in the development cycle for the payload bay, we had developed a custom complete hardware solution for a linear actuator that provided us with a

more robust and efficient solution than using an off-the-shelf linear actuator. From the development of that system, we had determined not only that the custom linear actuator and drivetrain would be better for the AGSE with respect to weight, power, and size requirements, but also that we were capable of developing such a system in a relatively quick time-frame.

However, the AGSE system is more complex than the payload bay since it requires one entire linear actuator and carriage plate / guide rod system to be mounted to another linear actuator and carriage plate / guide rod system to provide the horizontal and vertical axes translation. Additionally, the system composed of these two linear actuators must be mounted to the top of a rotating base to provide us with the cylindrical workspace we determined would be best for the AGSE system. All of these design complications led us to the conclusion that we should first build a prototype AGSE system using off the shelf linear actuators and grippers, so that we could ensure that the integration of these systems would work before spending the time and money on the development of the custom system.

Because we knew this system to be the prototype, and not necessarily the final electrical components that we would be using in the final system, we split our software and electrical development into several parallel efforts, which were relatively independent of each other.

5.3.1 ROS Component Model, Modeling Language, Toolsuite, and Code Generators

We developed a complete component model and implementation (in C++) for the *Robot Operating System* (ROS) middleware. Our component model removes the need for synchronization primitives such as mutexes, semaphores, message queues, and condition variables in our multi-thread, multi-process, and multi-node component-based code. Such synchronization primitives are normally required when writing multi-threaded or multi-process code to ensure data integrity, but the design of the component model removes that requirement from the application developer while still providing the safety and integrity required. This component model allows us to specify timers which invoke certain operations which are enqueued into the component's operation queue. All services provided by this component or data subscriptions this component has must go through this operation queue. What this means is that any client's request of a service provided by this component or any data published on a topic to which the component subscribes is enqueued as an operation in the operation queue. Using this queue, we ensure that (1) all components may only be executing one operation at a time and (2) no component's operation can be interrupted by another operation of the same component.

We also developed a modeling language (written using ANTLR) and tool suite (written in python) which allows us to specify the software components of the system, their interactions, the data types they use, and their mapping to nodes in the system. This modeling language allows us to ensure (1) the correctness of the software configuration, (2) the correctness of the component interactions, and (3) the reliability of the generated software. The reliability of the software is ensured though the use of our custom code-generators which generate the infrastructural code to facilitate the component creation, scheduling, and middleware interfacing which is directly specified in the model or can be determined from the model. For this reason, we chose to use the ROS middleware since it was lightweight (both size and effect on performance) and since it was relatively easy to develop a component model and code generators for. The tool suite we

developed allows us (the developers) to create the software models in a visual fashion (rather than using text editors) and in this way to inspect the models visually to get a more comprehensive understanding of the components in the system and their interactions. This visualization has the added benefit of providing an easy communications mechanism between members of the team, since it is easy for them to understand how the software of the system is designed based on this model representation.

5.3.1.1 Modeling Language and Code Generators

The *plumbing* for this AGSE software is a carefully controlled *grammar*. The grammar is our *modeling language* that enables strict descriptions of the system. The above ROSML model of the AGSE is represented as an *.rml* file in the file system. This model is parsed to generate all of the infrastructural code that is required by the AGSE.

Snapshots of the ROSML model of the AGSE can be seen below. Notice the structured and precise specification of the component building blocks. Each *agse_package* consists of important messages and services that are globally used by the components. These follow rules laid out by ROS and are either published or subscribed by other components. The *processes* that execute the AGSE functionality are called *ROS nodes* and contain instances of the relevant components. For example, *an engine node consists of a certain number of cylinder components that together enable its functionality*.

```
// ROS Package - agse_package
package agse_package
{
    // Set of ROS Messages
    messages
    {
        // ROS msg - sampleState
        msg sampleState
        {
            agse_package/samplePosition pos;
            agse_package/sampleOrientation orientation;
        }
        // ROS msg - samplePosition
        msg samplePosition
        {
            float32 r;
            float32 theta;
            float32 z;
        }
        // ROS msg - sampleOrientation
        msg sampleOrientation
        {
            float32 theta;
            float32 phi;
        }
        // ROS msg - controlInputs
        msg controlInputs
        {
            bool paused;
            bool start;
            bool stop;
        }
    }

    // Set of ROS Nodes in this package
    nodes
    {
        node arm
        {
            // Instantiating components in ROS node
            component<arm_controller> arm_controller_i;
        }
        node positioning
        {
            // Instantiating components in ROS node
            component<radial_actuator_controller> radial_controller_i;
            component<vertical_actuator_controller> vertical_controller_i;
            component<servo_controller> servo_controller_i;
        }
        node user_input
        {
            // Instantiating components in ROS node
            component<user_input_controller> user_input_controller_i;
        }
        node imager
        {
            // Instantiating components in ROS node
            component<image_sensor> image_sensor_i;
        }
        node detector
        {
            // Instantiating components in ROS node
            component<image_processor> image_processor_i;
        }
    }
}
```

Figure 83: AGSE ROSML model snippets

5.3.1.2 Development Environment & Graphical User Interface

One of the key ideas we have been pushing for from the beginning of the AGSE system design is *Iterative Development*. We have always wanted to be able to provide a simple mechanism by which (1) designs can be quickly prototyped, (2) switched around, (3) conveniently modified for

quick and robust software development. To this end, we have developed a Graphical User Interface (GUI) called *ROSMOD Editor*. This editor works in conjunction with our modeling language and simplifies the user interface and development experience.

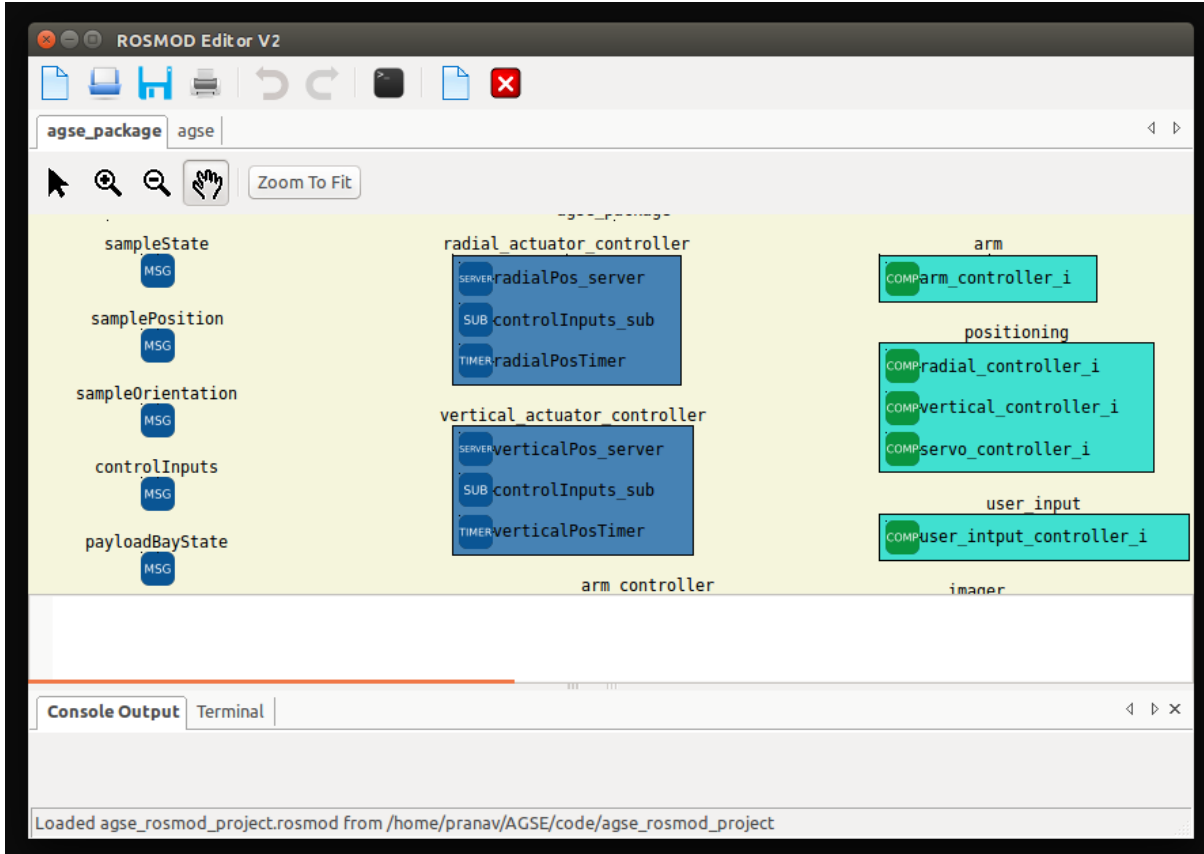


Figure 84: AGSE Development GUI

The editor also provides a means to easily express design ideas, component-based interactions and robust code generation requirements. Features such as bash terminal emulation, hardware specification, distributed deployment engine and rapid prototyping and analysis provide a means to fault resilient iterative software design.

Because the code generators (written in python using cheetah templates) generate most of the code which runs our system, we are able to not only cut down on the time it took to develop the code, but also ensure the correctness of the generated code since much of the generated code is similar or duplicated code between software components. The generated code handles the following functions:

- Sets up the application's processes and each process' components
- For each component it configures:
 - Any data types (topics) on which the component publishes (sends) to other components

- Any data types (topics) on which the component subscribes (receives) from other components
- Any methods (functions) which the component provides as a service (server) to other components
- Any methods (functions) which the component requires as a service (client) from other components
- The initialization routine of the component
- Any timers required for the component

Registering the publishers/subscribers and clients/servers with the ROS discovery and connection infrastructure, ROSCORE With all of this generated code, all that we had to write for the AGSE system (after writing the generators and modeling tools of course) was the actual business logic for any of the callbacks we needed. Such callbacks include what happens when each component receives the pause command, or what happens when the goal position is updated for the horizontal/radial actuator controller component. By only having this kind of purely mission goal-oriented code to write and modularizing it in such a way so as to keep it separated from the rest of the infrastructure code, we keep the mission goal code simpler, easier to read, easier to write, and easier to debug.

The design of the software components, how they communicate with each other, and how state is maintained was accomplished using our modeling and code generation tools, shown in Figure 85. The modeling, generation, and deployment software we wrote allows us to specify models visually, as shown in the figure, and then generate software components which use the ROS communications middleware and are executable on the AGSE computing hardware. For reference, the model consists of the following types of software objects:

- **Messages** (MSG in the model): these define data types (c++ objects) which can be published on or subscribed to by components in the system
- **Services** (SRV in the model): these define data types (c++ objects) which consist of request and response objects that define an interface that is either provided by a server or invoked by a client
- **Component Definitions** (middle column): components are single-threaded units of functionality of a program. A component can have any number of ports (publish, subscribe, client, server) or timers and processes requests from those ports or timers in first-in-first-out (FIFO) order through the component operation queue. A component may have only one operation active at a time.
- **Publishers / Subscribers** (PUB/SUB in the model): asynchronously send or receive data according to the message type specified to or from all other components which have publishers/subscribers on that message type.
- **Clients / Servers** (CLIENT/SERVER in the model): synchronously send and receive data for the specific interface defined by the service provided or required.

- **Timers** (TIMER in the model): periodically call a subroutine for the component. This allows the component to periodically fetch sensor data or acts as the backbone for the control loops of the system.
- **Nodes** (Far right column): a POSIX process which may have one or more component instances. Nodes may be run on any hardware host in the system.
- **Component Instances** (COMP in the model): a POSIX thread inside a Node which uses the component definition reference's implementation.

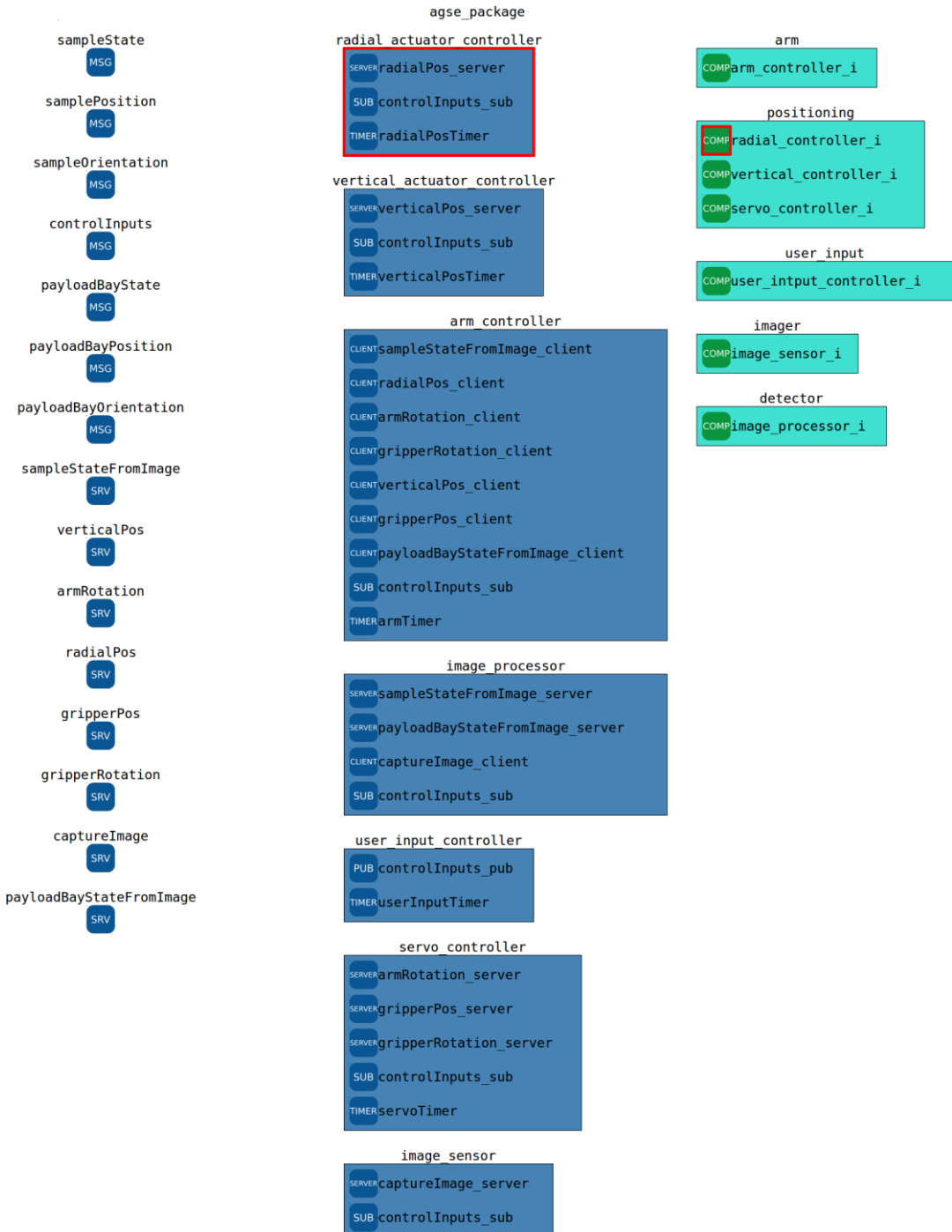


Figure 85: Component-based software model of the AGSE. The main design of the components is that motor control components have timers (e.g. servoTimer) which run the control loops to ensure the current state reaches the goal state. These goal states can be set by clients (e.g. armRotation_client) which send a goal to the server and receive the current state of the motor (position or orientation) in the response from the server. The arm_controller component implements the high-level state control of the system and therefore has client objects which it can use in its timer operation to query the state of the system and update the goals for each of the

subsystems of the AGSE. All components of the system subscribe to the controlInputs message, which is published by the user_input_controller component. This component is responsible for reading the state of the user input switches and sending that state throughout the system. In this way, all components can respond immediately to any commands, e.g. the pause command, and ensure proper state is maintained at all times.

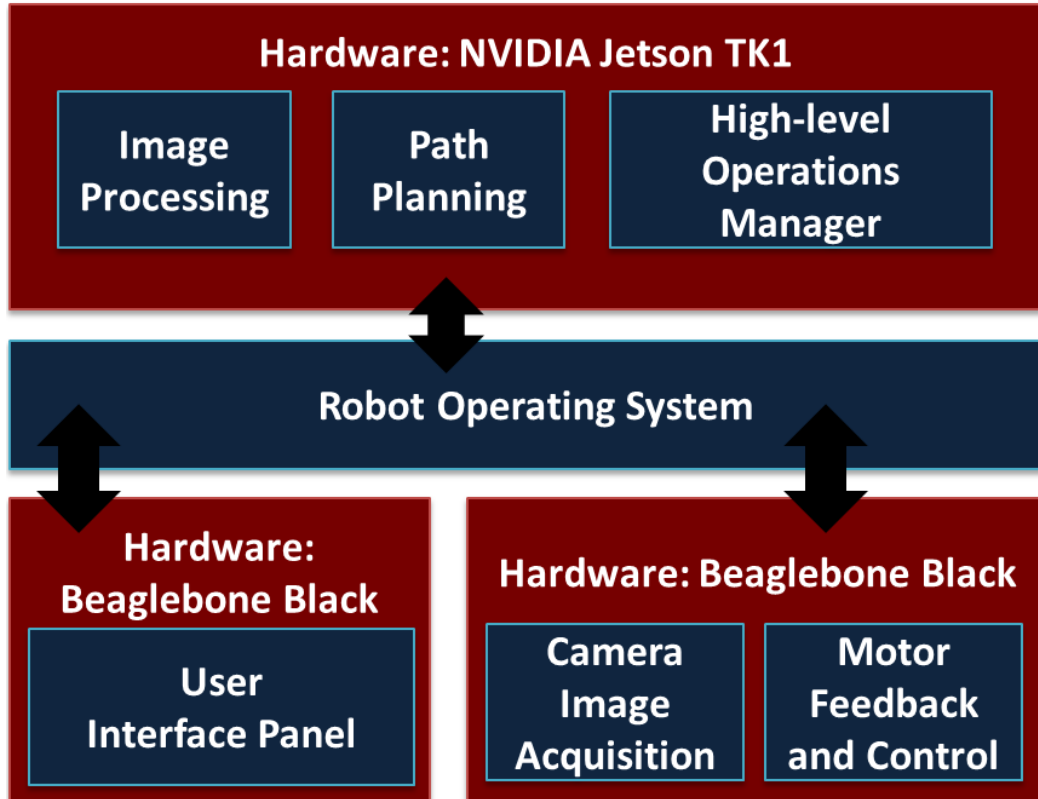


Figure 86: Integration of Component-based software development with the AGSE electronics. Here, the Image Processing, path planning and high-level operation is handled by the NVIDIA Jetson TK1; The image acquisition and motor feedback and control is performed by a BeagleBone Black (BBB) that is located at the top of the AGSE (closer to the camera and the gripper). Lastly, another BBB handles the user control and operation.

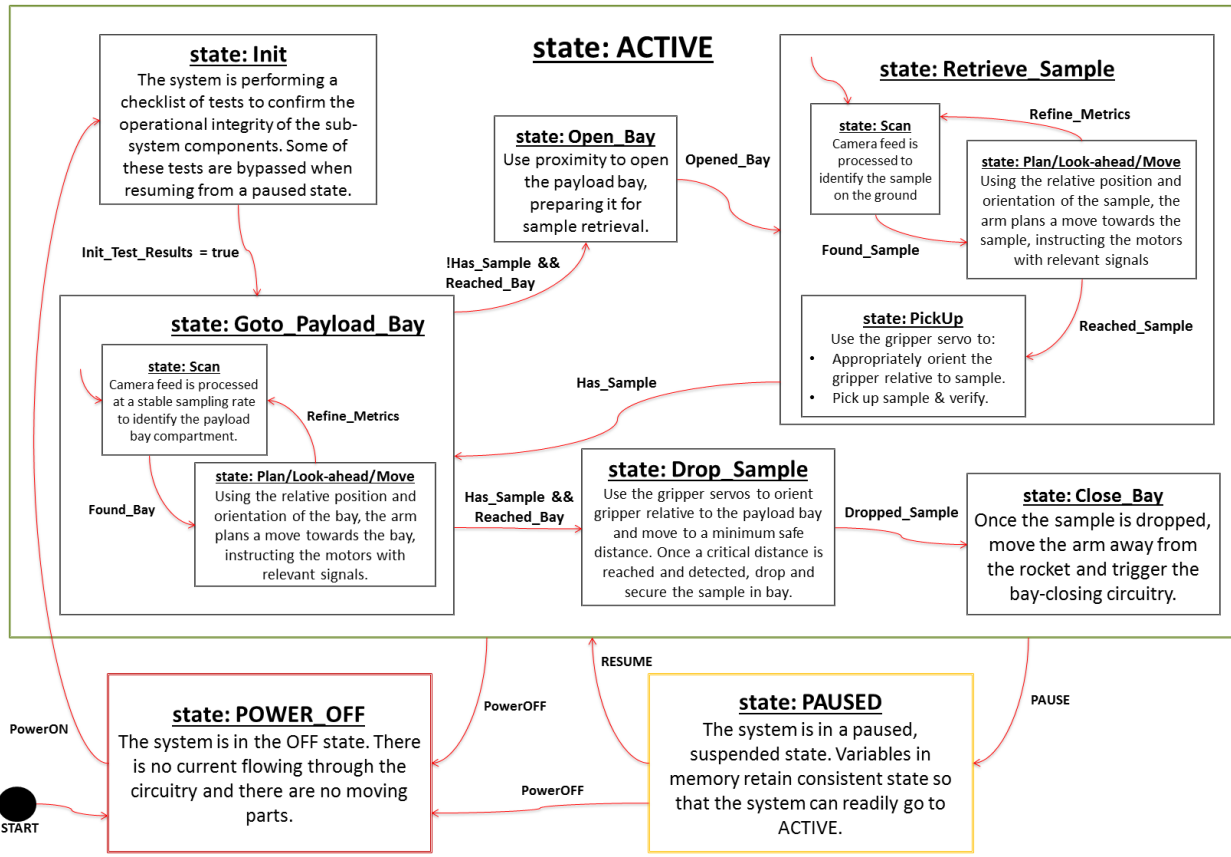


Figure 87: Statemachine implemented by the arm_controller component of the system. This is the high-level communications and control of the AGSE which relies on the lower-level motor control and feedback provided by other software components in the system.

5.3.2 AGSE Prototype Control Software

The AGSE prototype control software had to serve the following functions:

- control the dynamixel xl320 servo for the gripper phalanges actuation
- control the gripper wrist rotation servo (PWM based control)
- control the LAC-12 horizontal linear actuator
- control the LAC-12 vertical linear actuator
- control the dynamixel MX-28T base rotation / turntable servo

5.3.3 AGSE Prototype Control Circuitry

The AGSE prototype control circuitry functioned to facilitate communication and control of all the AGSE hardware. To perform this functionality, we required the following sub-circuits (Shown in Figure 88, below):

- An H-Bridge which could handle 3-5A @ 12V for the vertical linear actuator. This H-Bridge, shown in its relevant schematic, consists of 2 PFETs and 2 NFETs, (FQP27P06 and FQP30N60L, respectively), which form the 12V H-Bridge for the motor, as well as 2

NPN transistors (2N2222) which allow the Jetson to control the motor's power and direction.

- An H-Bridge which could handle 3-5A @ 12V for the horizontal linear actuator, using the same circuit design as described above for the vertical linear actuator.
- A buffer circuit to allow serial communication between the full-duplex UART on the Jetson TK1, running at 1.8V, and the half-duplex UART on the dynamixel xl320 servo, running at 5V. This circuit, which is shown in its relevant circuit schematic, consists of 2 NPN transistors (2N3904) connected in a buffer configuration, running off a VDD of 7.2V (the xl320's power supply). The input to the buffer is the Jetson's UART TX pin, and the output of the circuit is connected to both the servo's combined TX/RX pin, as well as to the Jetson's UART RX pin, through a resistor divider to bring the voltage from the 5V of the motor to the 1.8V of the Jetson. An incremental update to the prototype design and circuit to test functionality related to the final AGSE design was moving the servo motor control to the BeagleBone Black (BBB). Since the BBB controls the linear actuators and their feedback (analog in the prototype, digital quadrature pulses in the final version), moving the servo motor control to the BBB allowed for better wire routing and a consolidation of circuitry.

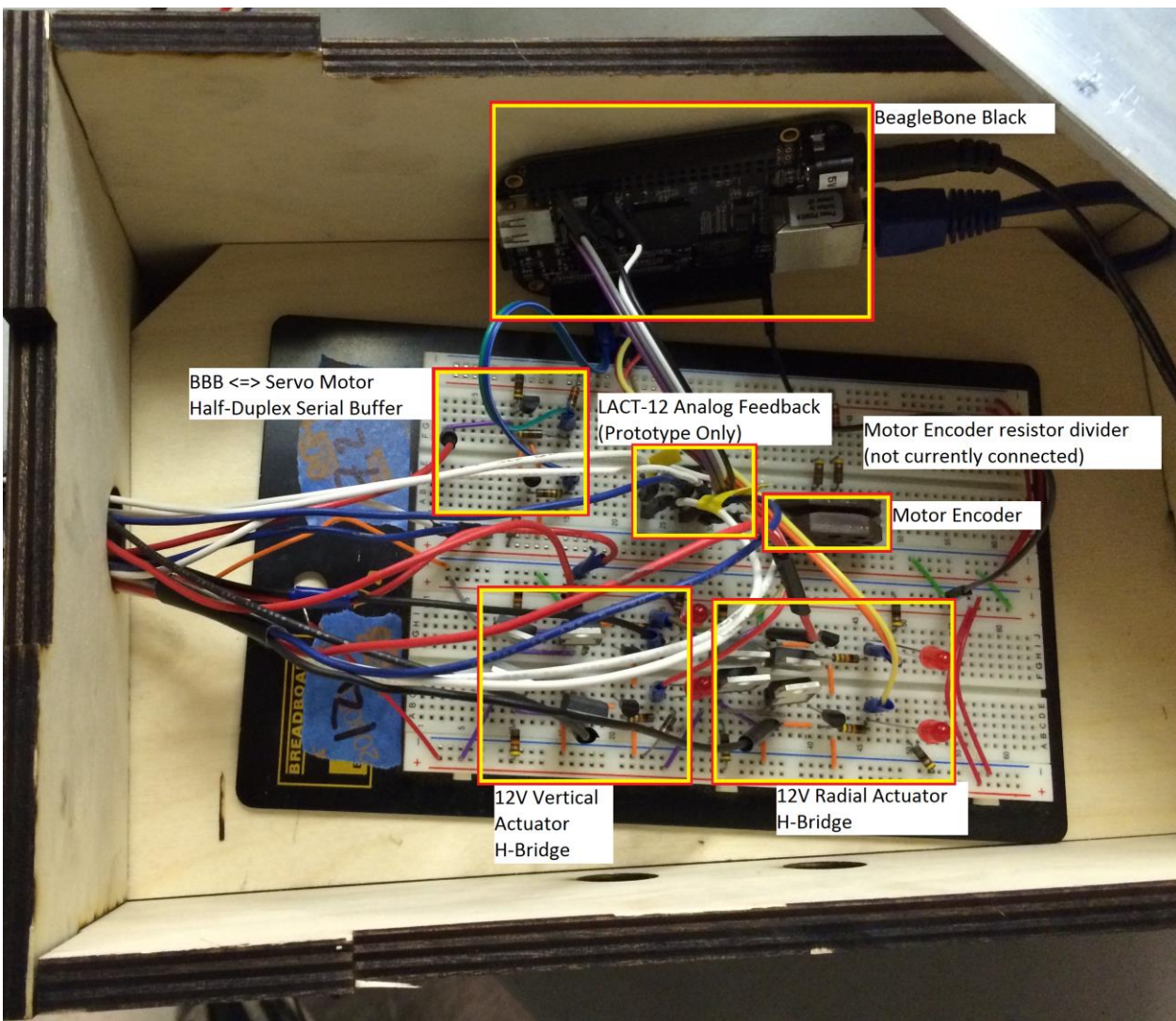


Figure 88: Prototype motor control circuitry wired together on a breadboard. The BeagleBone Black (BBB) at the top of the image handles the GPIO control of the linear actuators' H-Bridges, the UART serial control of the 3 servo motors (which are daisychained), the prototype linear actuator analog position feedback, and the final AGSE linear actuator digital quadrature pulse encoded position feedback (shown unconnected).

5.3.4 Final AGSE Image Processing and Object Detection Software

5.3.4.1 OpenCV Library

OpenCV is an open source Image Processing library created by Intel that enables rapid prototyping experimental tools for computer vision. The library consists of over 500 functions, several dozen examples and application programming interfaces for languages such as C, C++ and Python. The library is also compatible in several operating system platforms including Windows, Linux, Android and iPhone. The library is released under a BSD license for academic and commercial use and there are several pages with interactive examples that demonstrate its power. Its wide spread use in the industry as a prototyping base lead to our confident choice.

The tools that are shipped with OpenCV enable image processing tasks such as color mapping, grey scale conversions, histogram equalization, object profiling, detection and tracking.

5.3.4.2 Real-time Object Tracking

In order to correctly identify an important scientific sample, the AGSE must understand the dimensions, physical structure and appearance of this sample. The appearance of the sample is an important specification to ensure that a “*look-alike*” is not mistakenly chosen by the AGSE gripper for retrieval. Accurately describing the sample appearance in visible light provides a certain level of uniqueness that physical dimensions cannot provide. This enables a higher chance of successful retrieval as the probability of uniqueness of sample is high when one of the considered parameters is the visual confirmation of the target object. Therefore, our goal with sample detection is to use a sufficiently powerful camera with self-adaptive focal lengths and high resolution to capture its field of view, process its feed, filter out noise and identify the target sample.

Real-time Object Tracking using OpenCV is a method of identifying and tracking an object in 3 dimensional space by translating its visual appearance to 2 dimensions, removing surrounding noise and filtering out image pixels of interest. This process is two-fold. Firstly, the image processing consists of *extracting* out colors of interest. This is primarily done by translating a camera image encoded as a matrix of RGB (Red-Green-Blue) colors to a HSV (Hue-Saturation-Value) image space. These dimensions represent the Hue, Saturation and Color Intensity of the image. By choosing a high saturation and intensity, colors closer to black can be quickly filtered out. Once the pre-processing filters out background colors and presents a HSV image, noise removal schemes such as *erosion* and *dilation* filters are used to remove noisy blotches of pixels, all of which visually collide with the target sample. For instance, a white target sample such as a car has similar color specifications to a white golf ball near it. However, when attempting to detect and track the white car, the white golf ball, though white, is treated as noise and filtered out. This is important to remove objects (or any random collection of pixels) that distract the image processing from successfully identifying our target object.

Once irrelevant noise is removed from the processed image, it is then the requirement of image processing to identify the unique object that remains in the filtered image, draw a contour around the detected object and mark its (1) *center*, (2) *bounded radius*, and (3) corners. Once marked, this object is then tracked in real-time for providing periodic feedback to the Arm Controller about the relative position of the detected object from the camera lens.

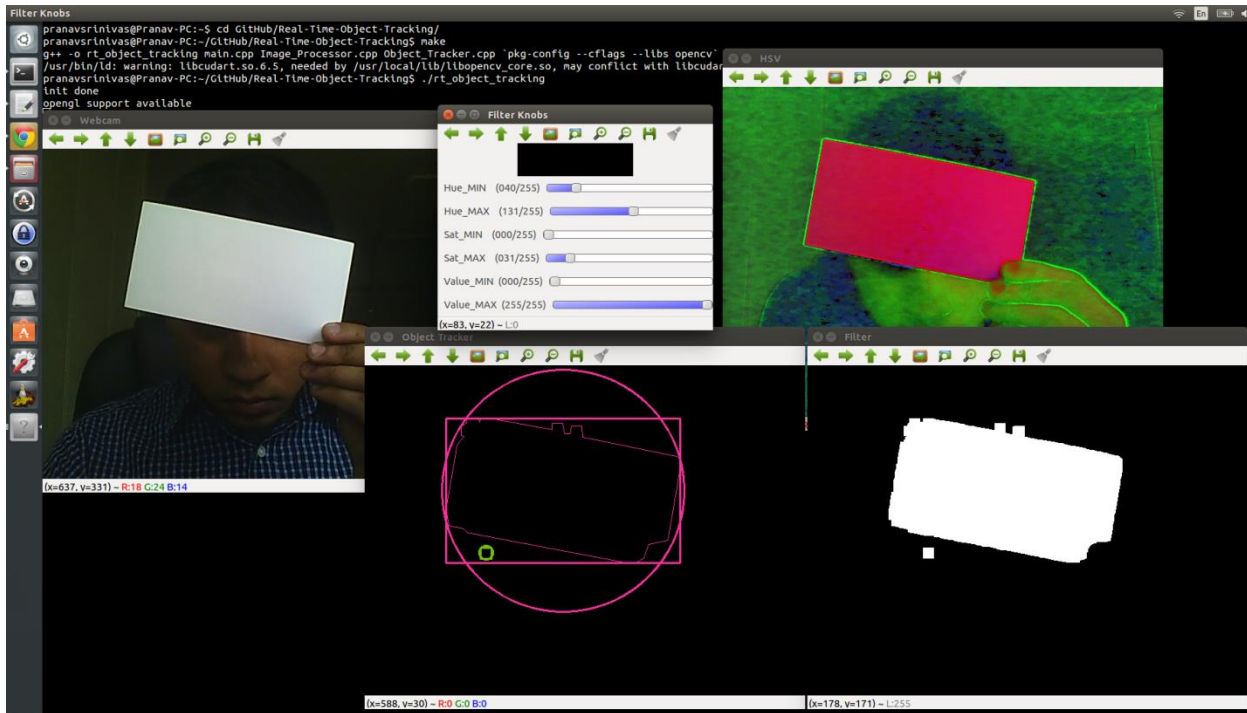


Figure 89: Object Tracking with OpenCV

This process can be used to detect a heterogeneous variety of objects, each with unique physical profiles and perceived colors. Consider Figure 1, showing the object tracking process for a white sheet of paper. The windows on this image are titled to represent semantics. The *Webcam* feed is the raw feed provided by the camera. This is the starting point of image processing. The *Image* on the *HSV* window shows the translated HSV image space. This is an automatic pre-processing step. Now, using the filter knobs in the application, a desired hue, saturation and value threshold is chosen. This includes lower and upper bounds on accepted values. These values dictate (1) the colors of interest, and (2) the colors to be filtered out. The window *Filter* shows the filtered image. This window represents the filtered version of the camera feed, only keeping pixels of interest. Once filtered, the final step of the process is to automatically parse and identify the corners of the presented object. In this case, the window *Object Tracker* shows the polygonal contour identified around the white sheet of paper. A rectangle approximates the orientation of the sample in relation to the camera and the outer circle bounds the maximum surface area of the sample. This figure is also a representation of the accuracy of the image processing and the degree to which background noise can be robustly filtered out. Further examples and applications of this method can be seen in the following screenshots.

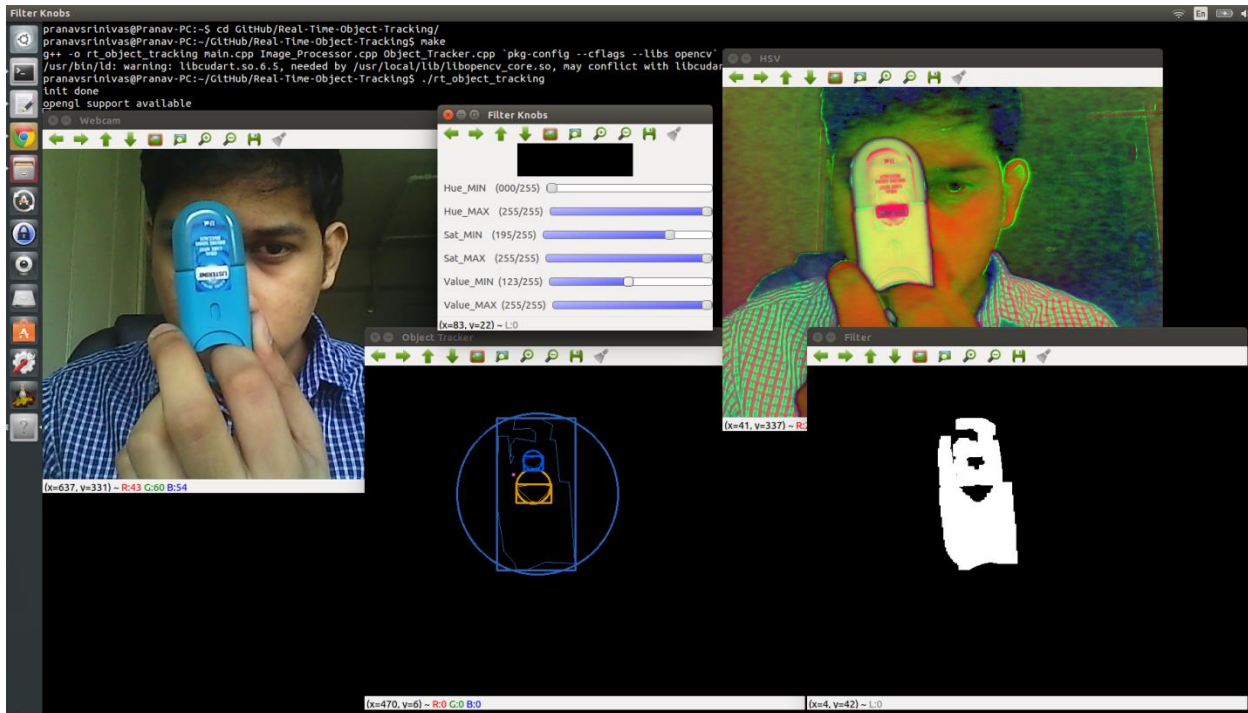


Figure 90: Tracking a Blue Listerine Oral Mist

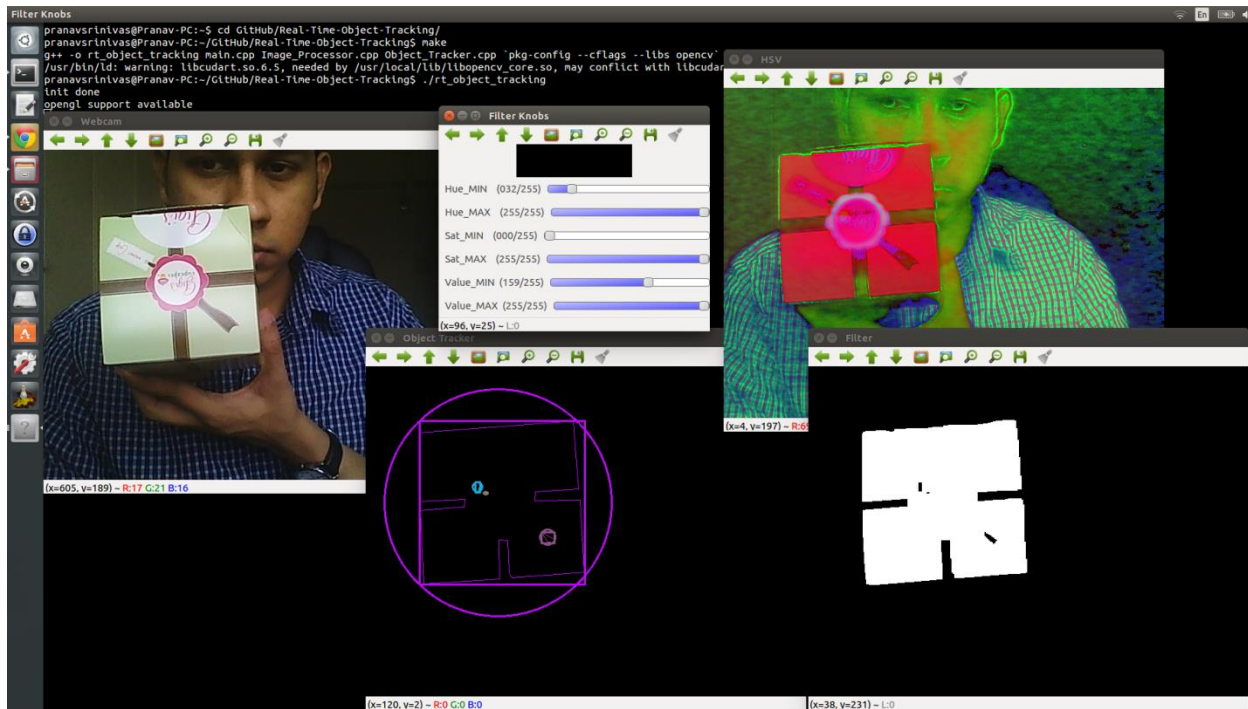


Figure 91: Tracking a Green Cupcake Box

The robustness of the approach has also been tested in low-light conditions. Although the desired HSV values need to be appropriately set, once they are profiled, the object is successfully tracked in real-time.

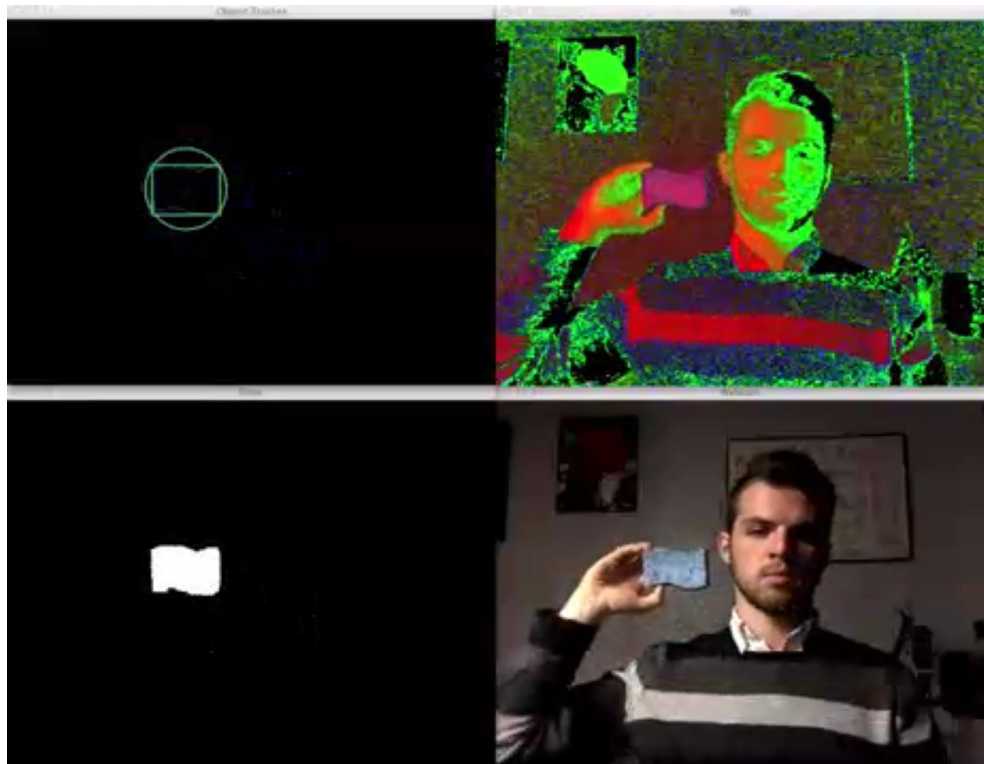


Figure 92: Tracking in Low Light Conditions

5.3.4.3 Testing Sample Detection Scheme

The Object Tracking technique described above has been successfully applied to our target sample. The sample has been placed in several lighting conditions against a variety of backgrounds to test our object tracking mechanisms. Some of the lessons learnt here include the need for additional parameters such as (1) minimum and maximum target object size, (2) minimum number of positive detection samples, and (3) maximum number of contagious pixels to qualify as a single object. The following screenshots show our algorithm tracking a target sample with orientation changes at real-time.

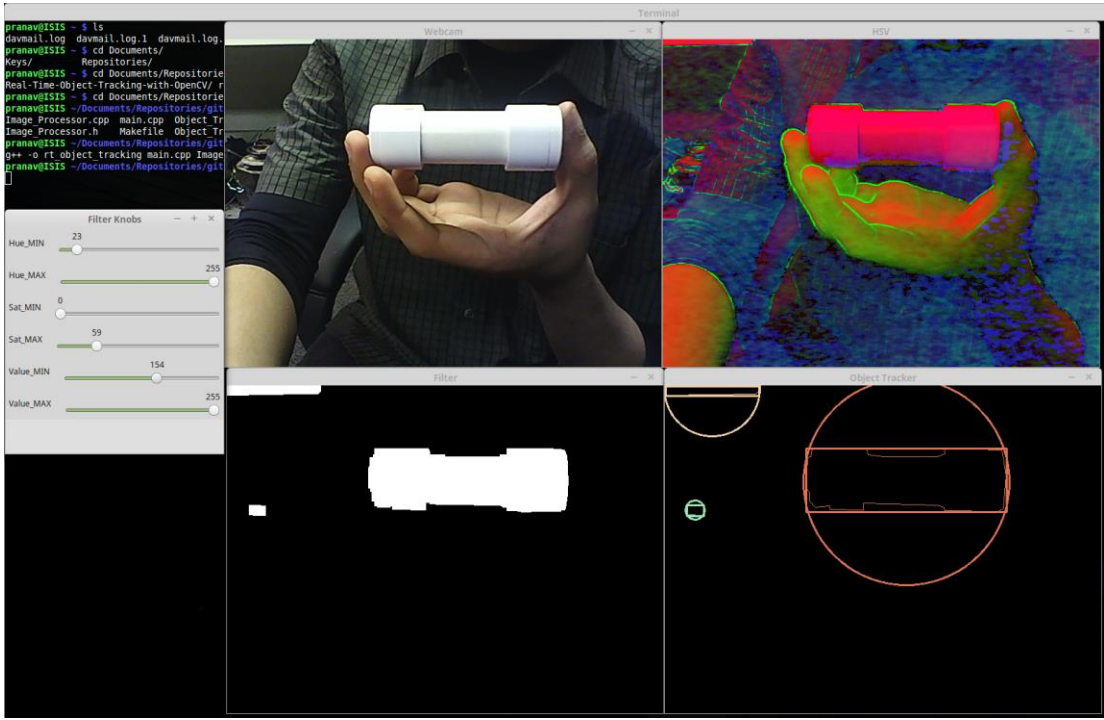


Figure 93: Tracking Target Sample

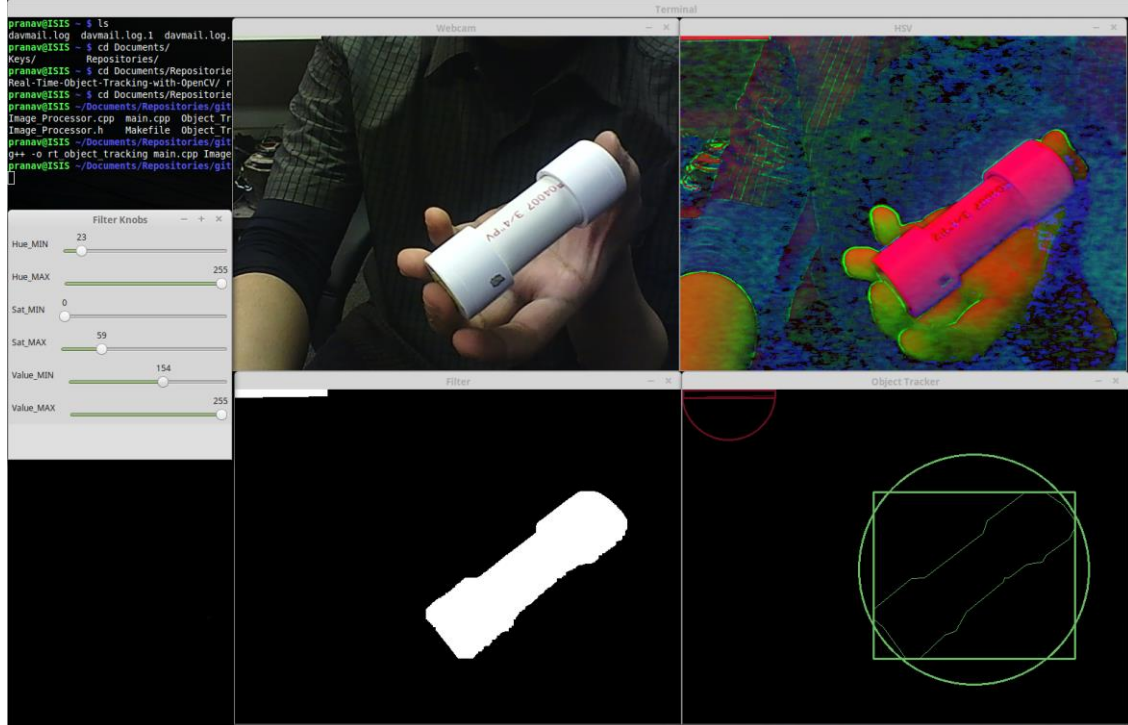


Figure 94: Orientation Changes

Furthermore, using the NVIDIA Jetson TK1 has provided a greatly improved frame rate of up to 20 frames per second of continuous real-time processing. This may reduce to a lower rate to synchronize with the frequency of arm control but has been tested to ensure that the frequency of

image processing always stays above the required minimum rate. The following subsections show test results of image processing for our target sample using ROS and integrated grayscale and YCrCb image processing and threshold assignments. Notice the bounding boxes drawn around the sample that detects the sample area, angle, orientation, length, width and finally its relative position from the camera's feed.

5.3.4.4 Preliminary Testing

First level of sample detection tests used the HSV-based filtering scheme we have described above.

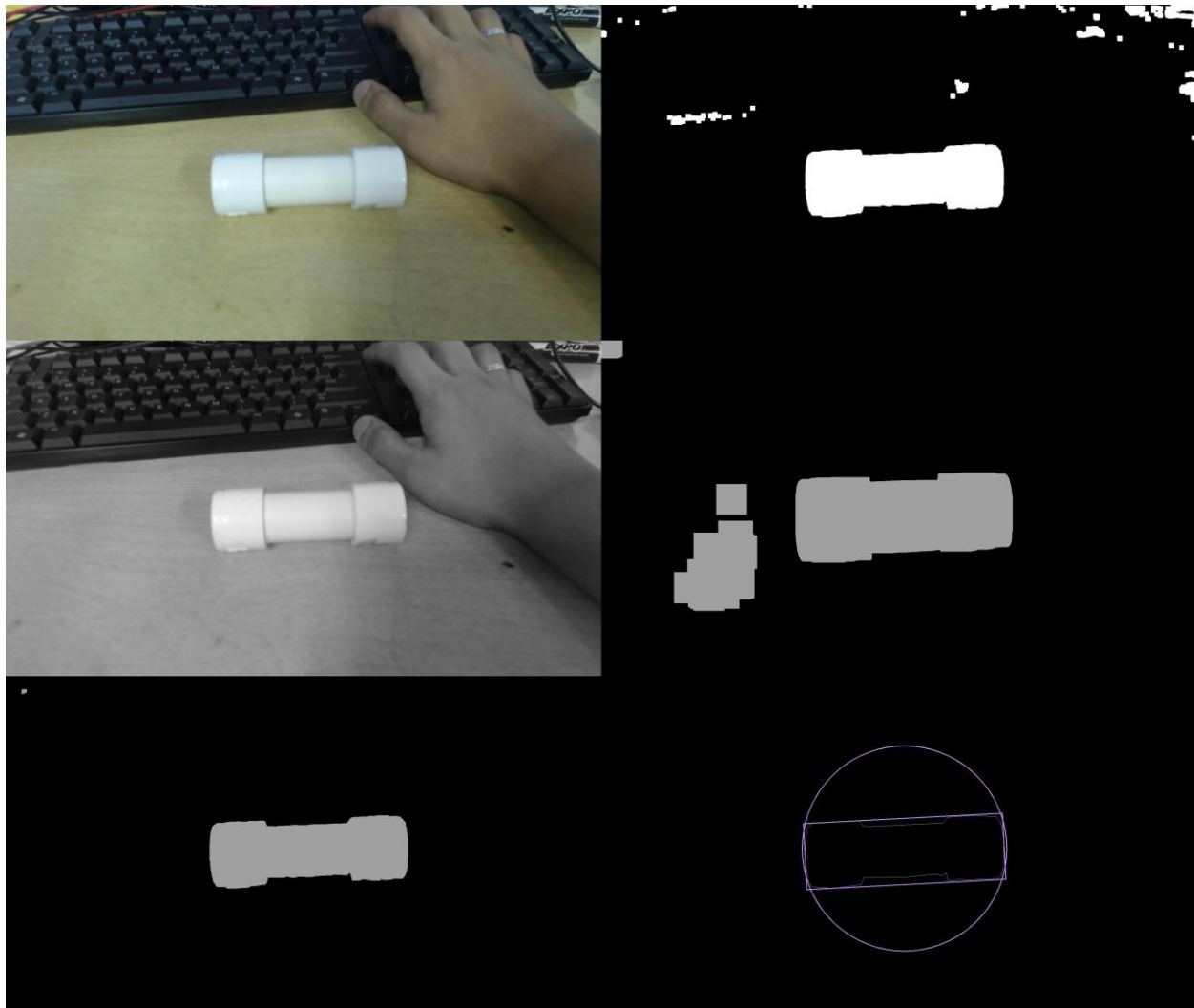


Figure 95: AGSE Sample Detection Performed on typical “Lab” level lighting. Notice the bounding box and the additional levels of grayscale-based filtering in the center images. A bitwise-AND operation is performed on the HSV-based filter and the grayscale-based filtering schemes to obtain a more thoroughly filtered image in the bottom left.

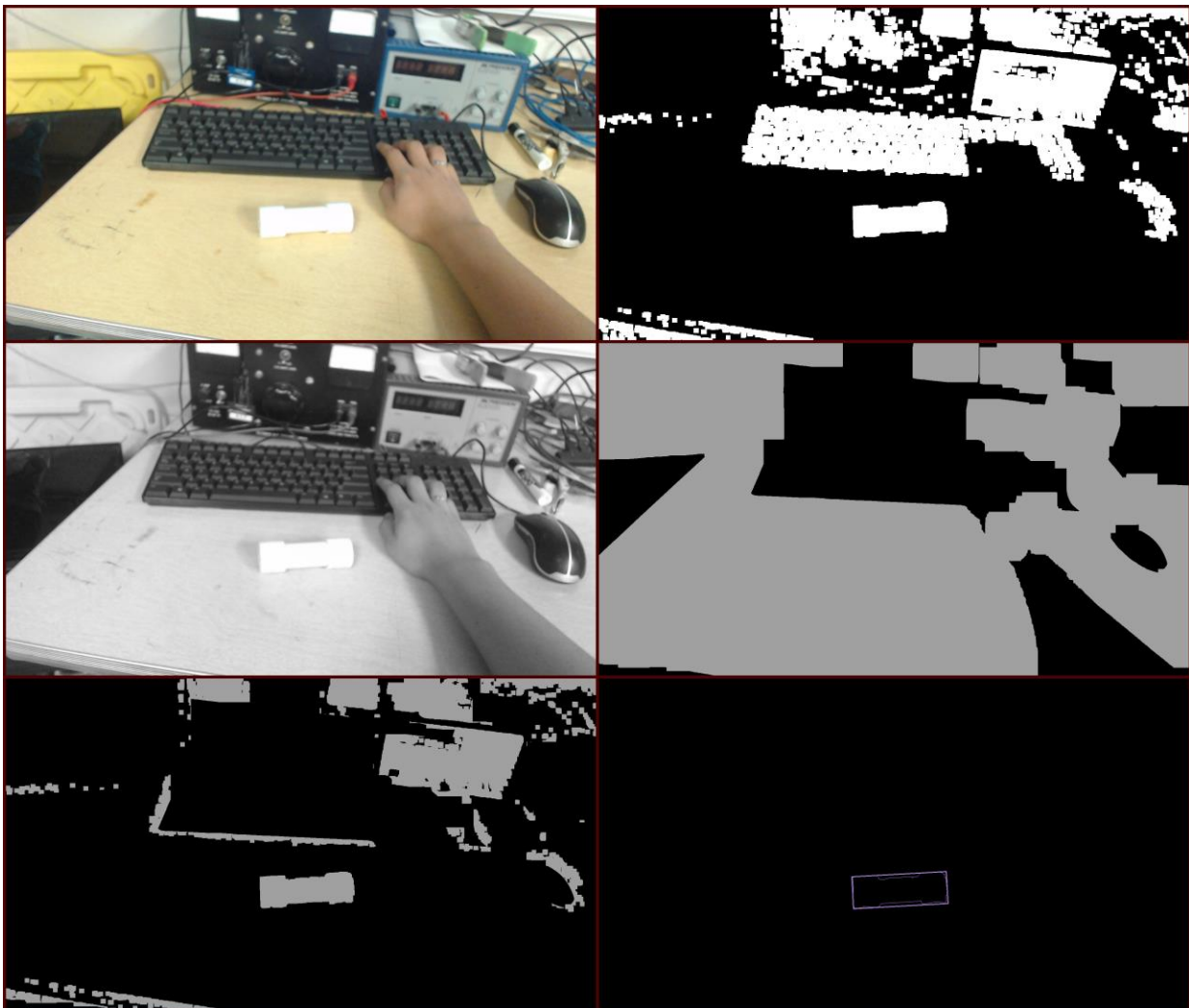


Figure 96: AGSE Sample Detection in over-exposed environments. This is one of the tests that show the usefulness of a secondary processing technique (grayscale-based filtering) helps. The top right filtered image is the result of HSV-based filtering. The center-right image is the grayscale-based filtering image. Here, it is clear that the grayscale image has failed to help due to over exposure. However, by applying a bitwise AND-ing procedure, the filtered image resulting from a combination of the HSV and Grayscale-based filtered images is the best of both methods. Bottom Left, notice the improved filtered image that reduces the clutter and makes the sample stand out more clearly. From here, it is a simple algorithm to extract a candidate sample, based on its dimensions.

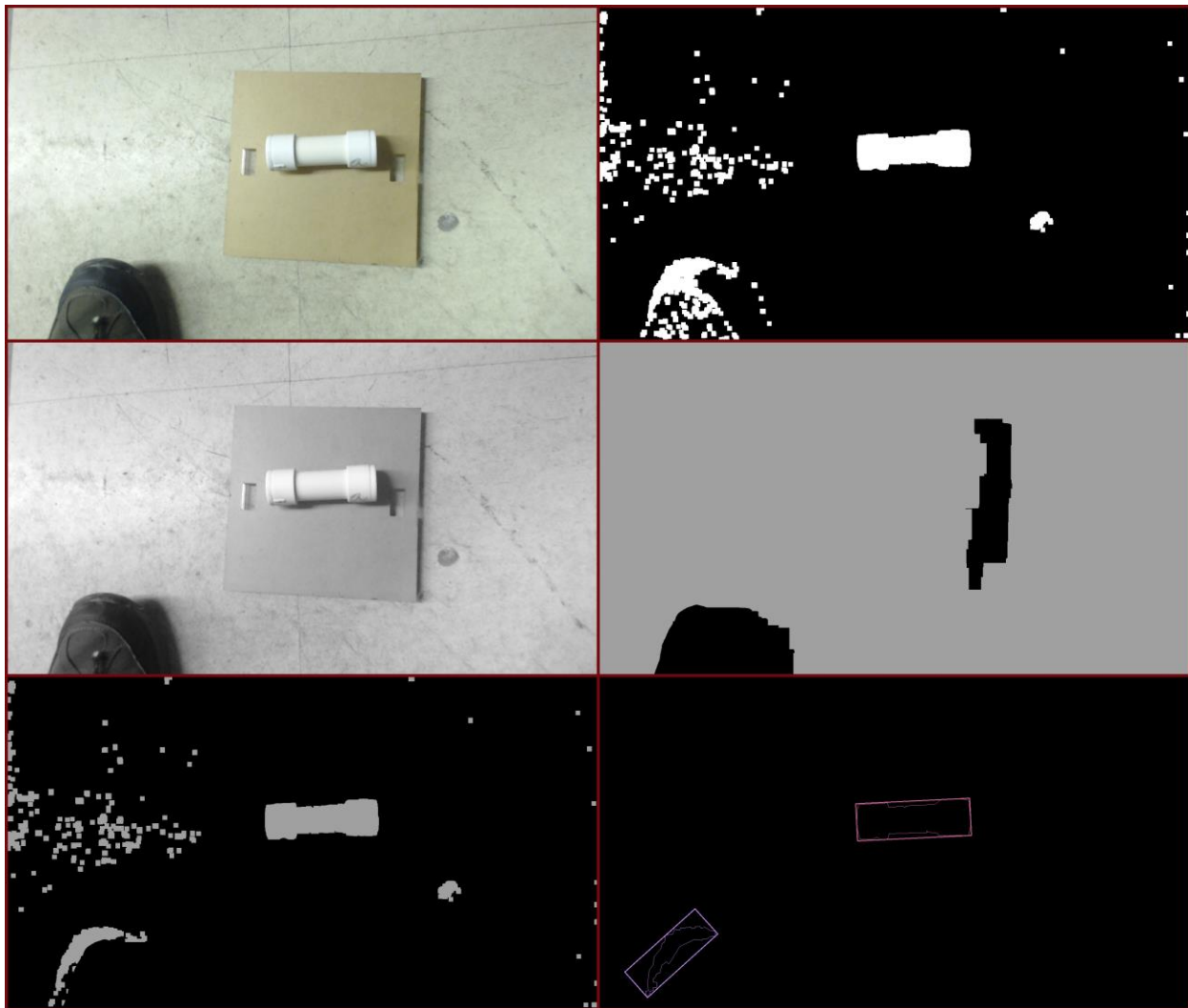


Figure 97: AGSE Sample on a wooden plate.

Notice in the above image that part of the shoe in the raw image is identified by the image processing as a valid sample. This required to be fixed. We improved on this work by adding bounds on the area, sample height, sample width, height to width ratio, area of sample to area of contour ratio and the position of the detected sample in the processed image. Our secondary layers of testing and processing improvements are shown below.

5.3.4.5 Area-based Filtering and Testing



Figure 98: AGSE Sample on a red cloth



Figure 99: AGSE Sample on a computer desk. Notice the bright light next to the sample that is completely filtered out by the processing



Figure 100: AGSE Sample on a brown carpet



Figure 101: AGSE Sample on a typical computer desk with other similarly colored objects

5.3.4.6 Low-light Testing



Figure 102: AGSE Sample sitting on the shadow of a table.



Figure 103: AGSE Sample under focused light



Figure 104: Another low light test with the camera closer to the sample.

5.3.4.7 Multiple-Sample Detection

Detecting multiple samples and analyzing the optimum detection and path planning schemes is important as it improves the functional quality of the AGSE and makes the resulting device also more reliable.

In the following figure, 2 samples are placed on sand. The AGSE searches for the samples and reaches the plate holding the samples. It notices the objects on the plate and detects two separate and unique samples, instead of a single blob of a white, large “object”. This is an important test as it ensures the correctness of the image processing algorithm. It ensures that the sample is accurately detected even when multiple similarly looking objects are placed beside it.

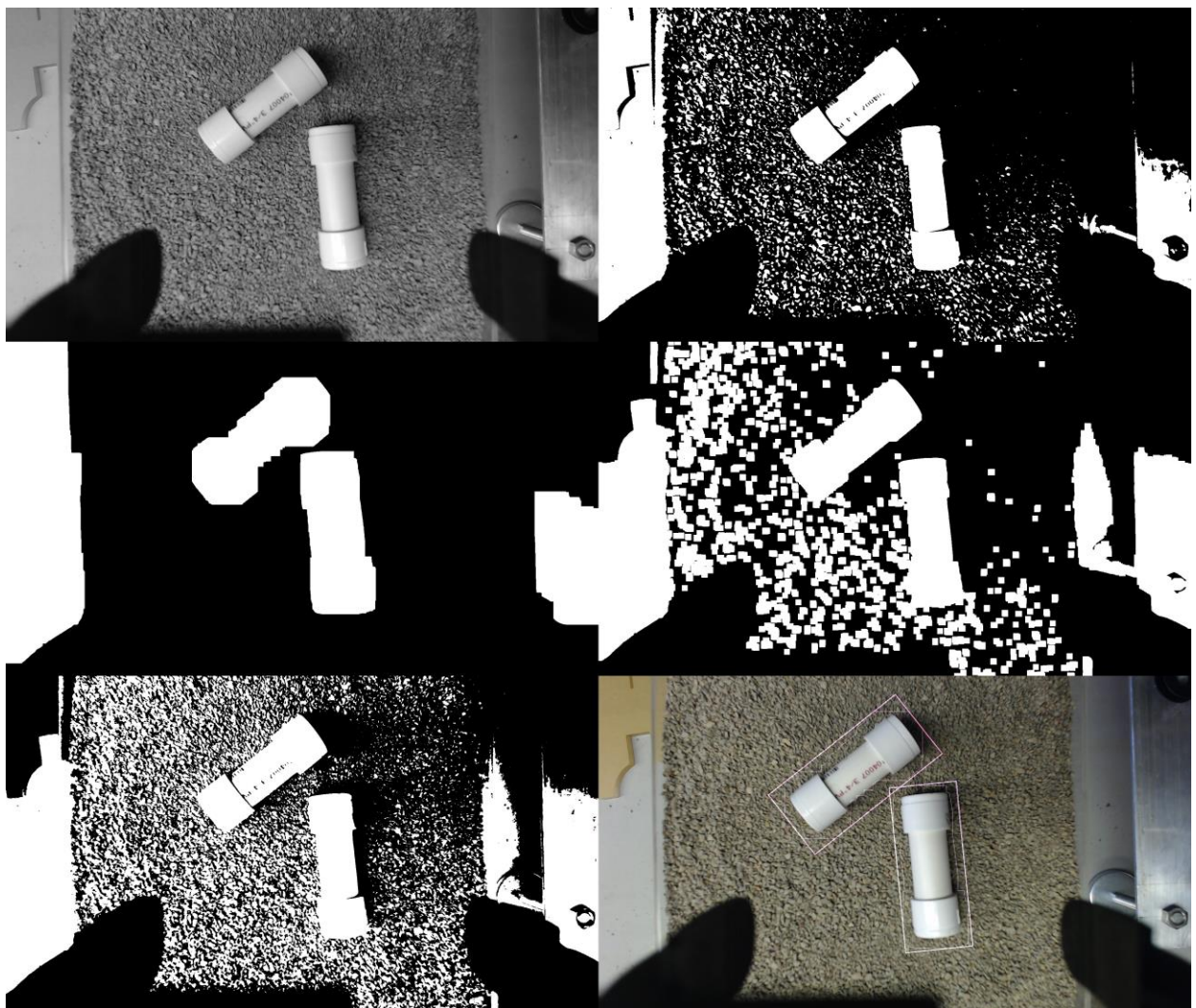


Figure 105: Multiple-Sample Detection at runtime.

5.3.4.8 Sample Detection at the MBA Outreach Demonstration

The following is the sample detection result from the MBA outreach demonstration. The sample is detected as always by image processing on the Logitech camera feed, with the camera mounted securely on the gripper.

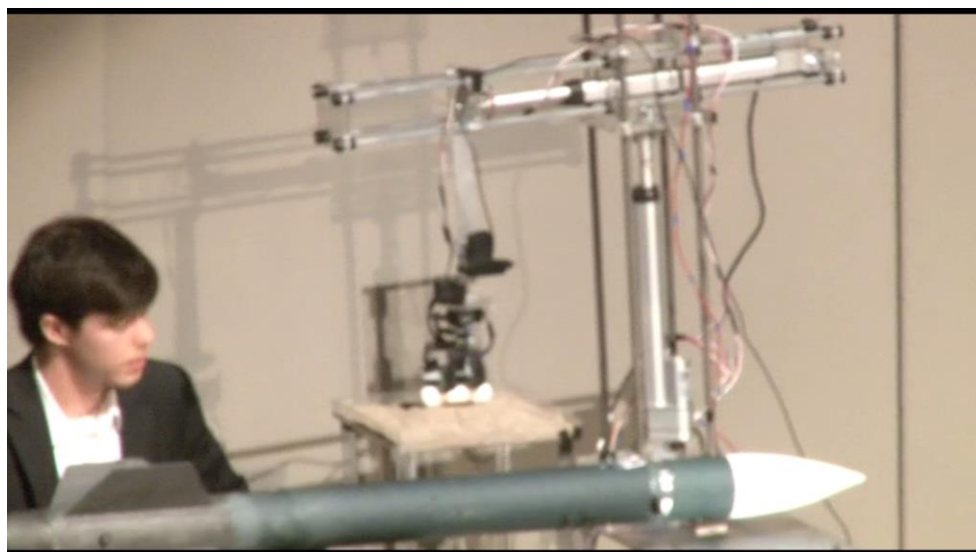


Figure 106: AGSE Sample Detection – MBA Outreach

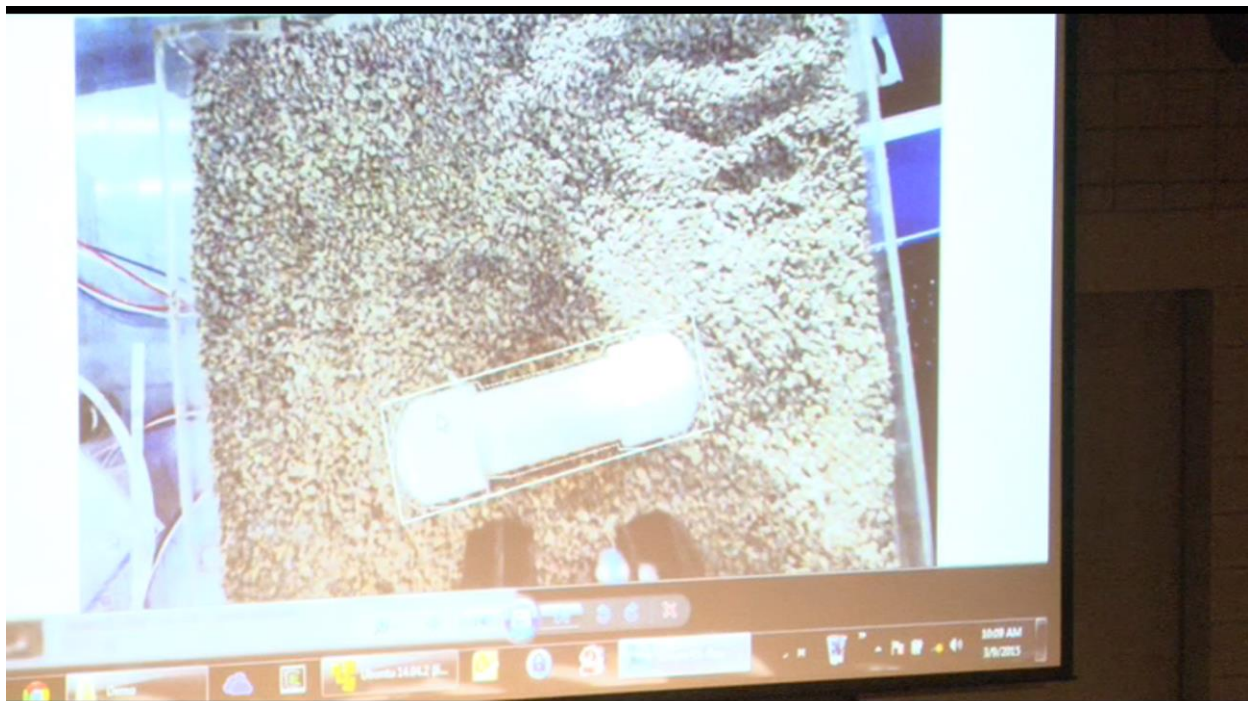


Figure 107: Online processed image, shown to the audience

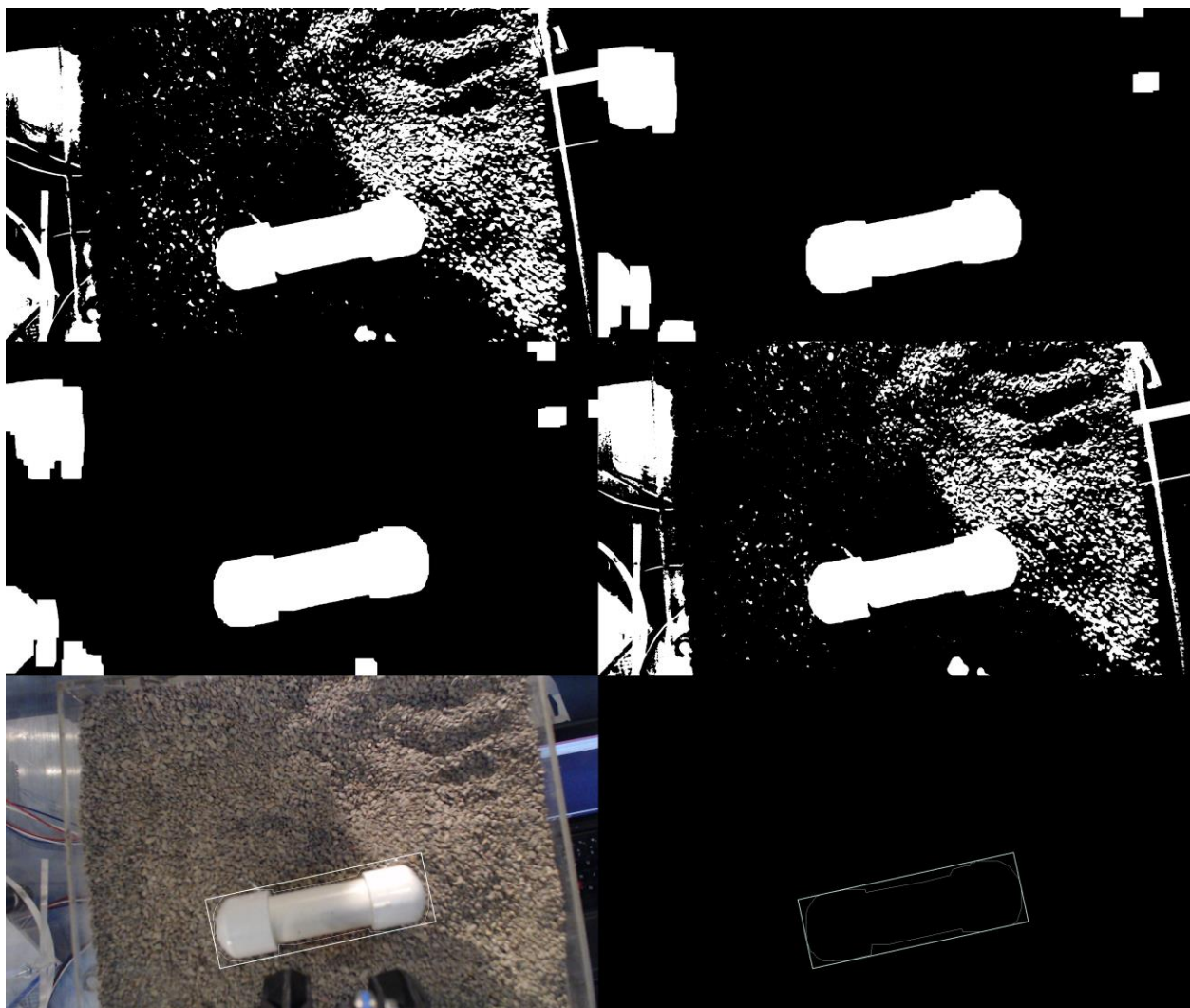


Figure 108: AGSE Sample Detection – Images acquired from Jetson TK1

5.3.4.9 Payload Bay Detection – Finding the Rocket

Our first order requirement for the AGSE to acquire a sample is to find the payload bay of the rocket. This is necessary because the payload bay has to be automatically opened so that the sample can be placed in it. Similar to sample detection, we have incorporated an image processing scheme that accurately locates the payload bay. This scheme is as follows.

We have a “marker” that is assigned to an area around the payload bay. This marker is a sheet of paper that consists of a “code”, similar to a QR code. The goal of image processing is to filter this marker from its surroundings and detect its ID, identify the location of the camera from the marker and finally calculate the location of the payload bay from the gripper. The following figure shows the small marker image, detected by image processing. The marker, as seen in the figure, is a unique combination of black and white lines that coexist and stand out.

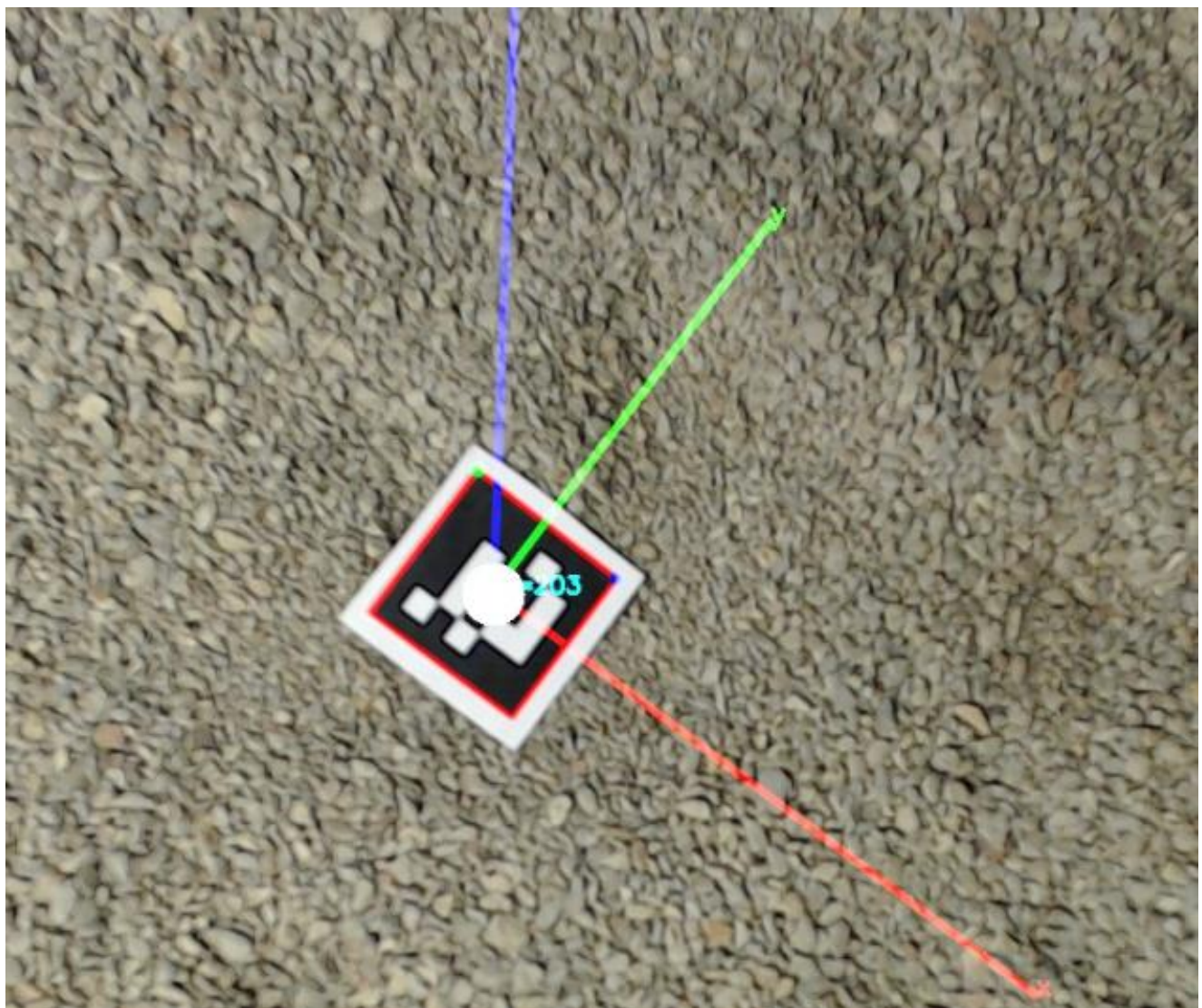


Figure 109: Payload Bay Marker.

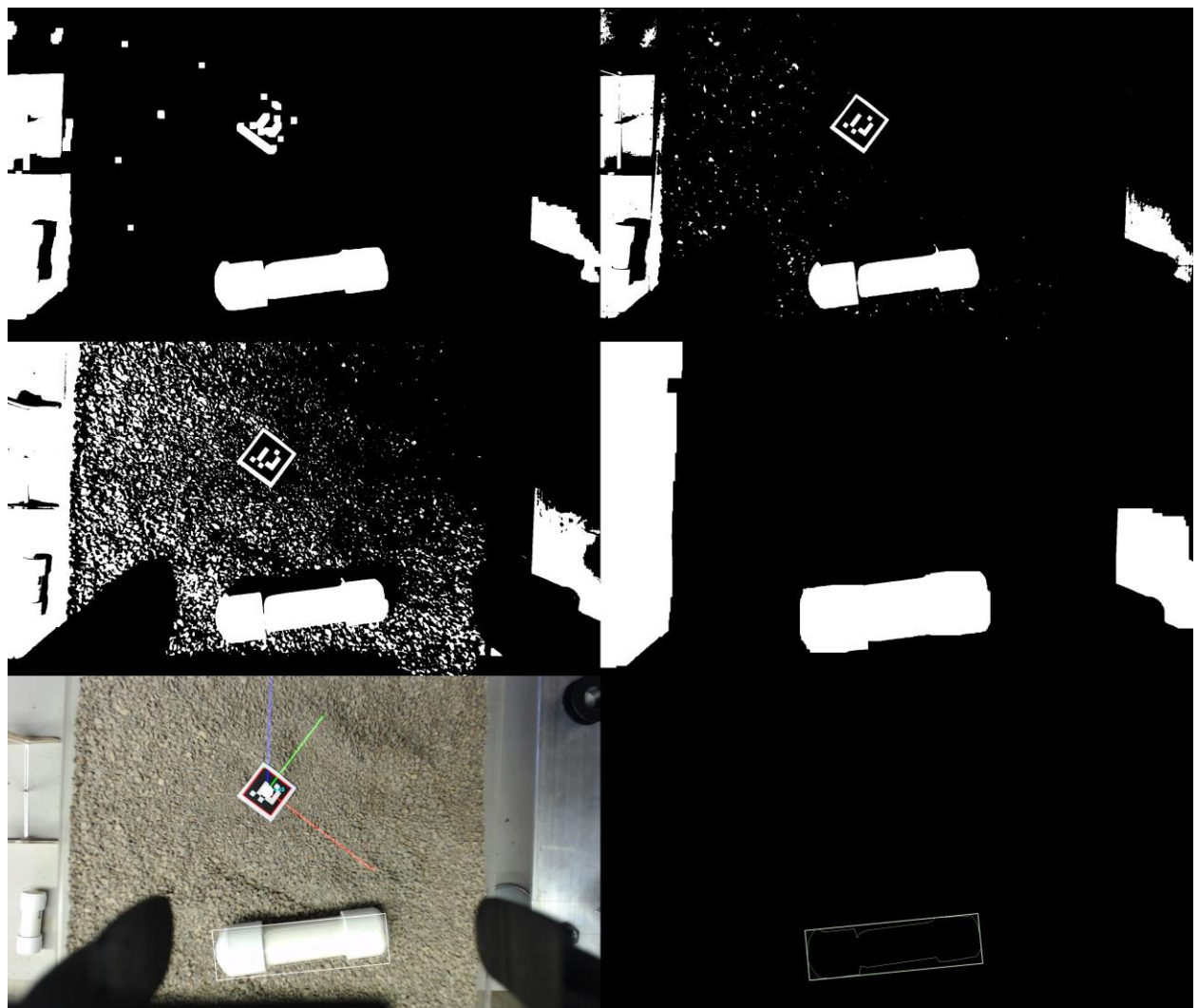


Figure 110: This image is a good summary of our image processing. It shows both payload bay marker detection and sample detection with the camera mounted to the gripper. Notice in many of the filtered images, the gripper phalanges can be seen by the camera but are filtered out by image processing.

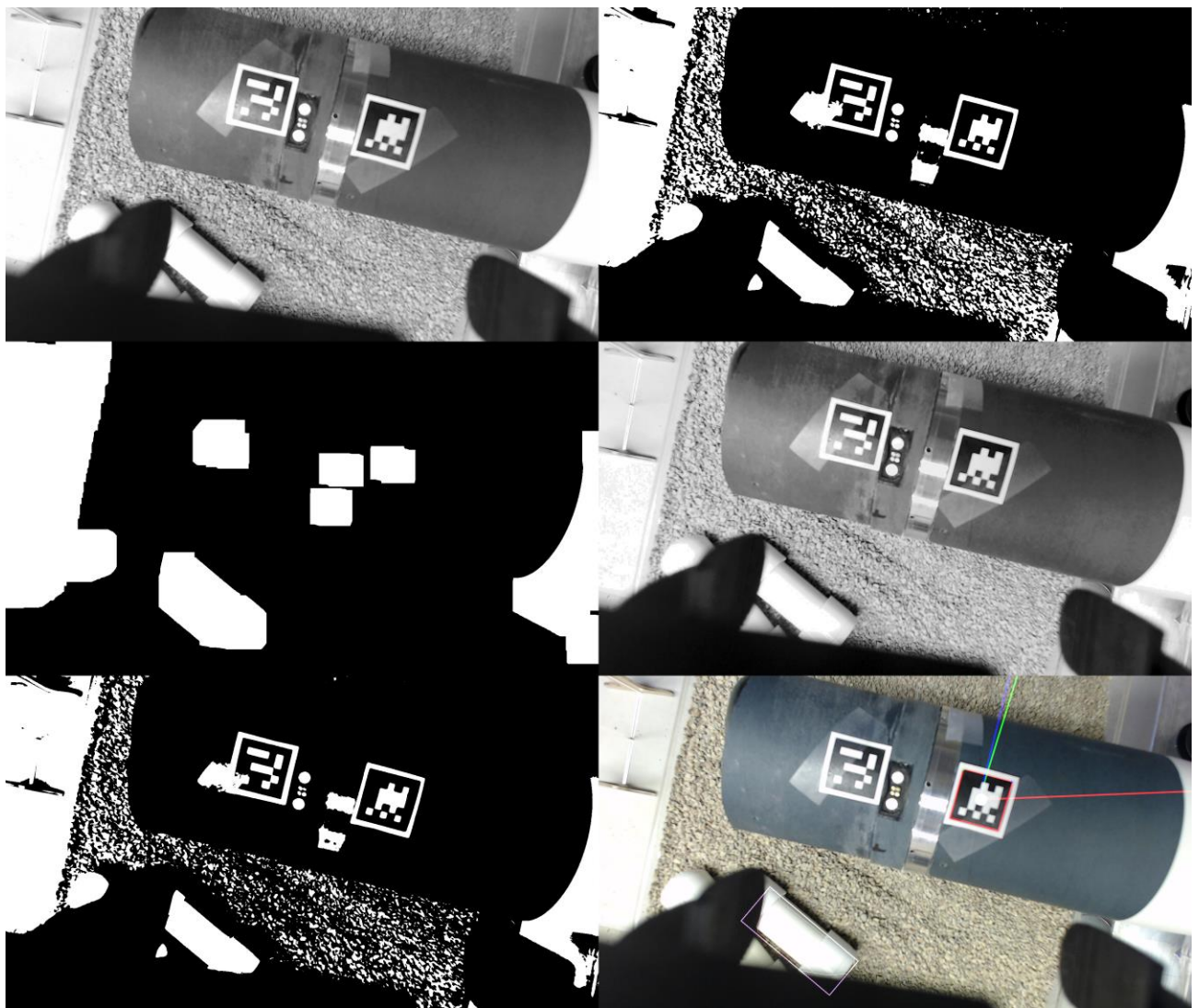


Figure 111: Detection Markers attached to the Rocket Payload Bay Area. Notice in the bottom left, the filtered image shows that the marker on the left is affected by the tape used to hold it. The tape affects the white and black markings that are used for detection. This is the reason why in the detected image on the bottom right, only the right marker is detected. This indicates to us that the reflective nature of the tape affects payload bay detection and should therefore be avoided.

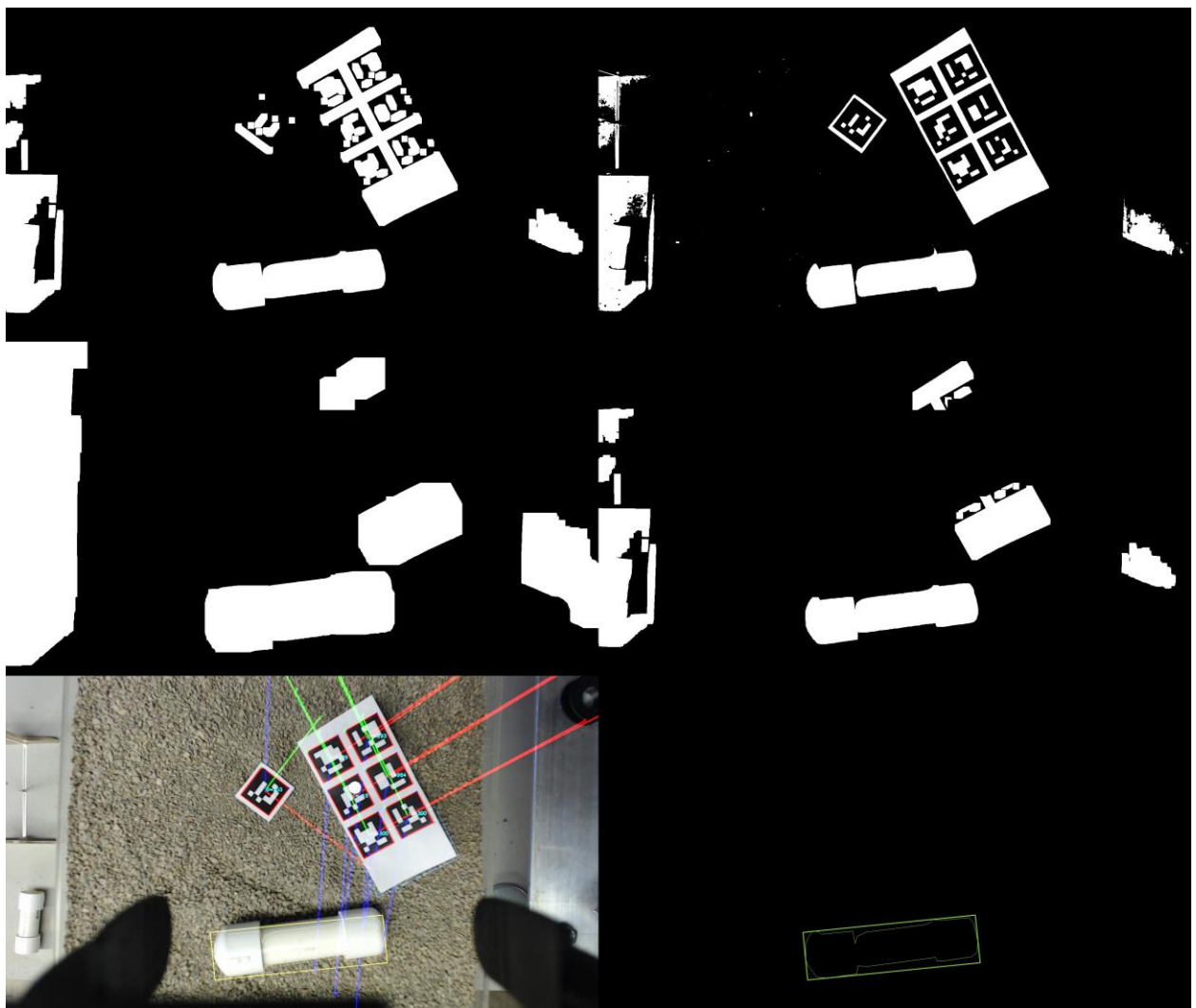


Figure 112: Multiple Marker Detection with nearby payload. Each payload bay marker has an ID assigned at calibration time. Using the IDs of the detected markers, the camera position from the payload bay can be easily derived.

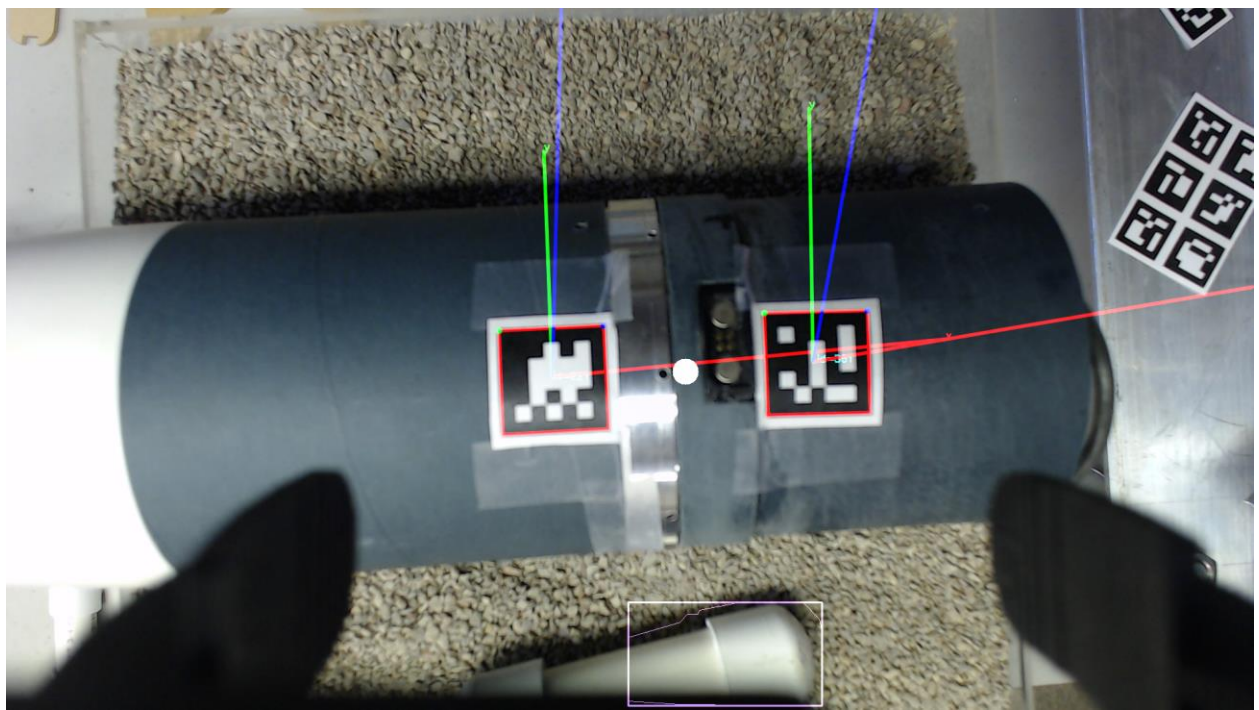


Figure 113: Camera detecting the payload bay and also a part of the sample. Notice that even though the sample is not completely visible, the image processing accurately detects a candidate. Secondly, notice the lighting around the gripper and a better taping technique – No part of the marker itself is affected by the taping as the tapes do not touch any of the black markings. This is a good representation of the robustness of our image processing algorithm.

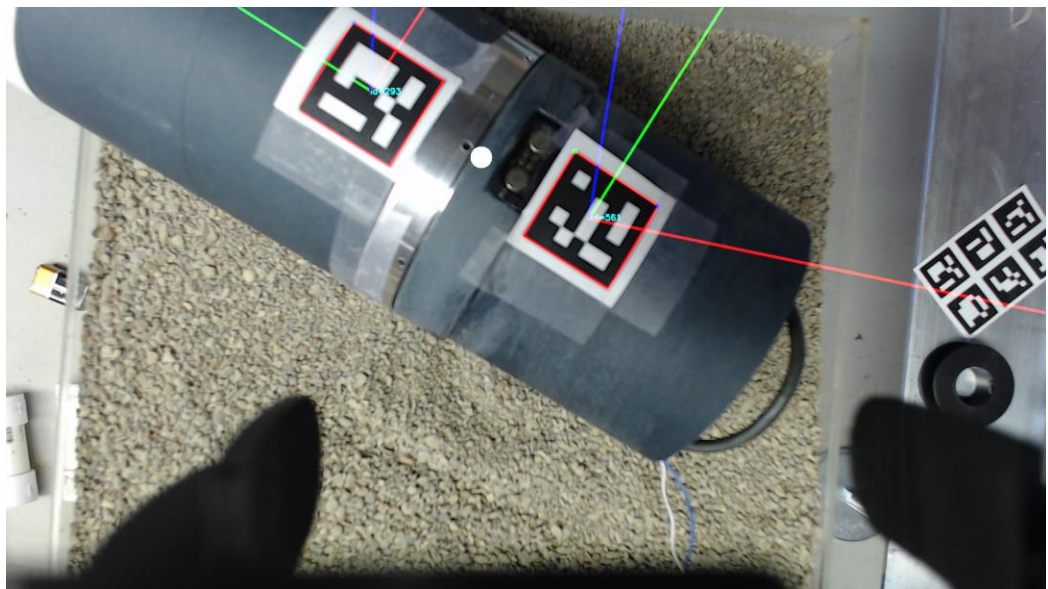


Figure 114: Payload Bay Detection at an alternate angle with the payload bay not aligned with the plane of the gripper.

5.3.5 Final AGSE Control Circuitry

Having determined that the H-Bridges we developed were sufficient for the prototype's off-the-shelf motors, which require more power than the final AGSE motors (but are the same voltage), we decided to use the same H-Bridge circuits for the final AGSE. Similarly, we use the same serial buffer circuit in the final AGSE as we used in the prototype AGSE, however we bias it to the voltage of the new servo motors (the dynamixel AX-12A) which run at 12 V. Finally, we used an off-the shelf switched mode power supply (SMPS) DC/DC converter and isolation circuit to step the battery voltage down to the main 12V power required for most of the systems components. This 12V supply powers the Jetson, the Linear Actuators, and all the servo motors. The linear actuator encoders and the BeagleBone Blacks all run off of 5V, for which use a DC/DC LDO on the BBB to step the 12V down to 5V. The motor control board which connects as a cape to the BBB is shown as a schematic in *Figure 88* and laid out as a board in *Figure 115* and *Figure 116*.

This board mounts as a cape onto the BBB which handles the motor control for the AGSE. It contains the 12V linear actuator H-bridges, a 12V to 5V dc/dc converter (LDO) which provides the BBB with power from the main AGSE power connector and which powers the linear actuators' position encoders. It also contains the resistor dividers to allow the 5V quadrature encoded pulses (QEP) to be safely connected to the 3.3V eQEP hardware of the BBB. Finally, it also contains the serial buffer to allow the full-duplex 3.3V UART transmission and receive (TX/RX) pins to connect to the servo motors' 5V half-duplex UART combined tx/rx pin. Each of these subsystems is broken out to their relevant connectors for their cables.

Vanderbilt Aerospace Club : AGSE Motor Control Board

This schematic encompasses the electrical design of the AGSE motor control board. These circuits meet the following goals:

1. Vertical DC linear actuator motor control
2. Radial DC linear actuator motor control
3. Encoder Feedback for vertical motor encoder
4. Encoder Feedback for radial motor encoder
5. 12 V to 5 V power regulation for BeagleBone Black
6. Serial Buffer for controlling daisychained servos:
 - * Main gripper servo motor
 - * Gripper wrist rotation servo motor
 - * AGSE arm base rotation servo motor

This board mounts as a cape on the BeagleBone Black, providing it power and handling the associated connections for motor feedback and control.

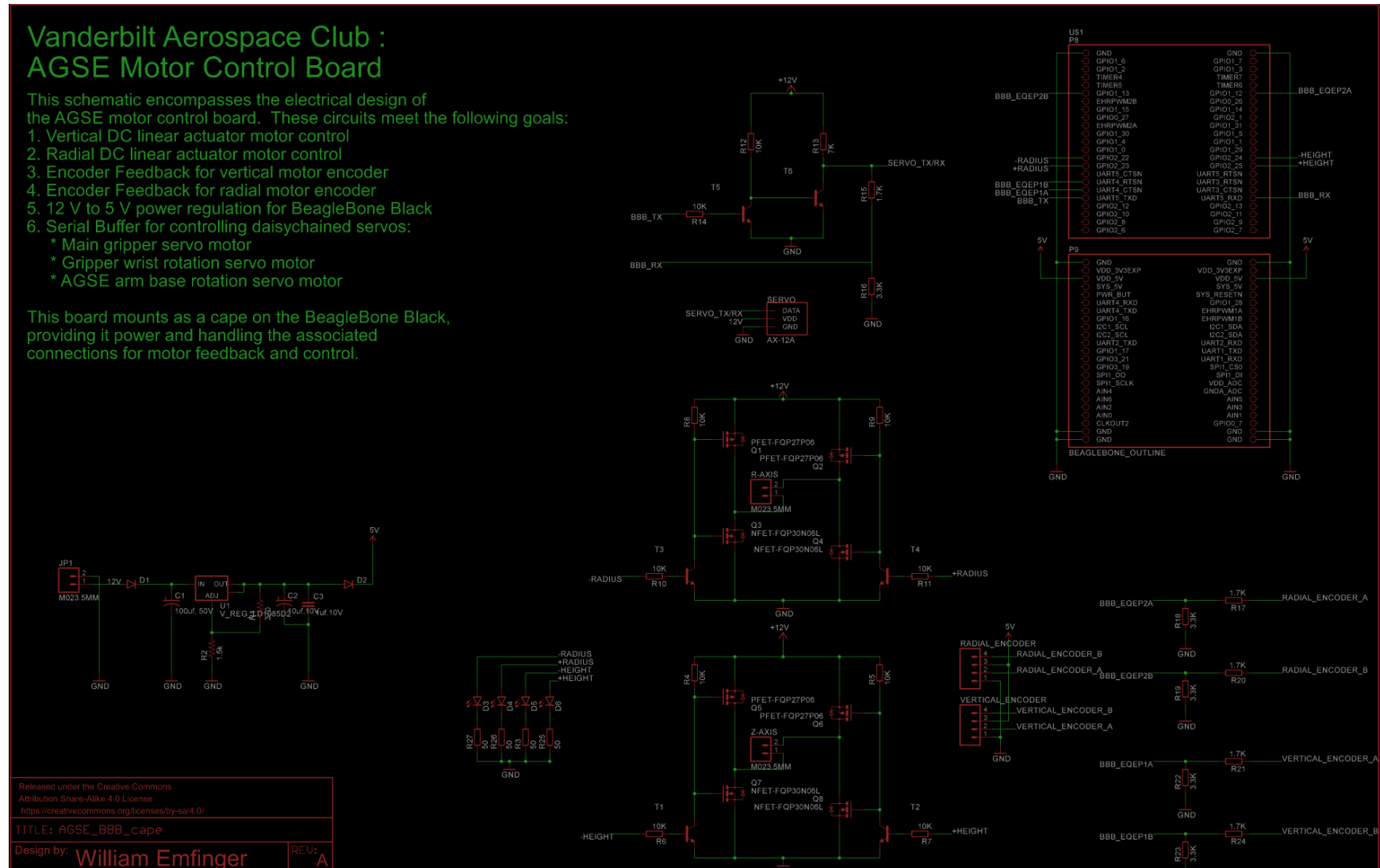


Figure 115: AGSE Motor Control Board Schematic.

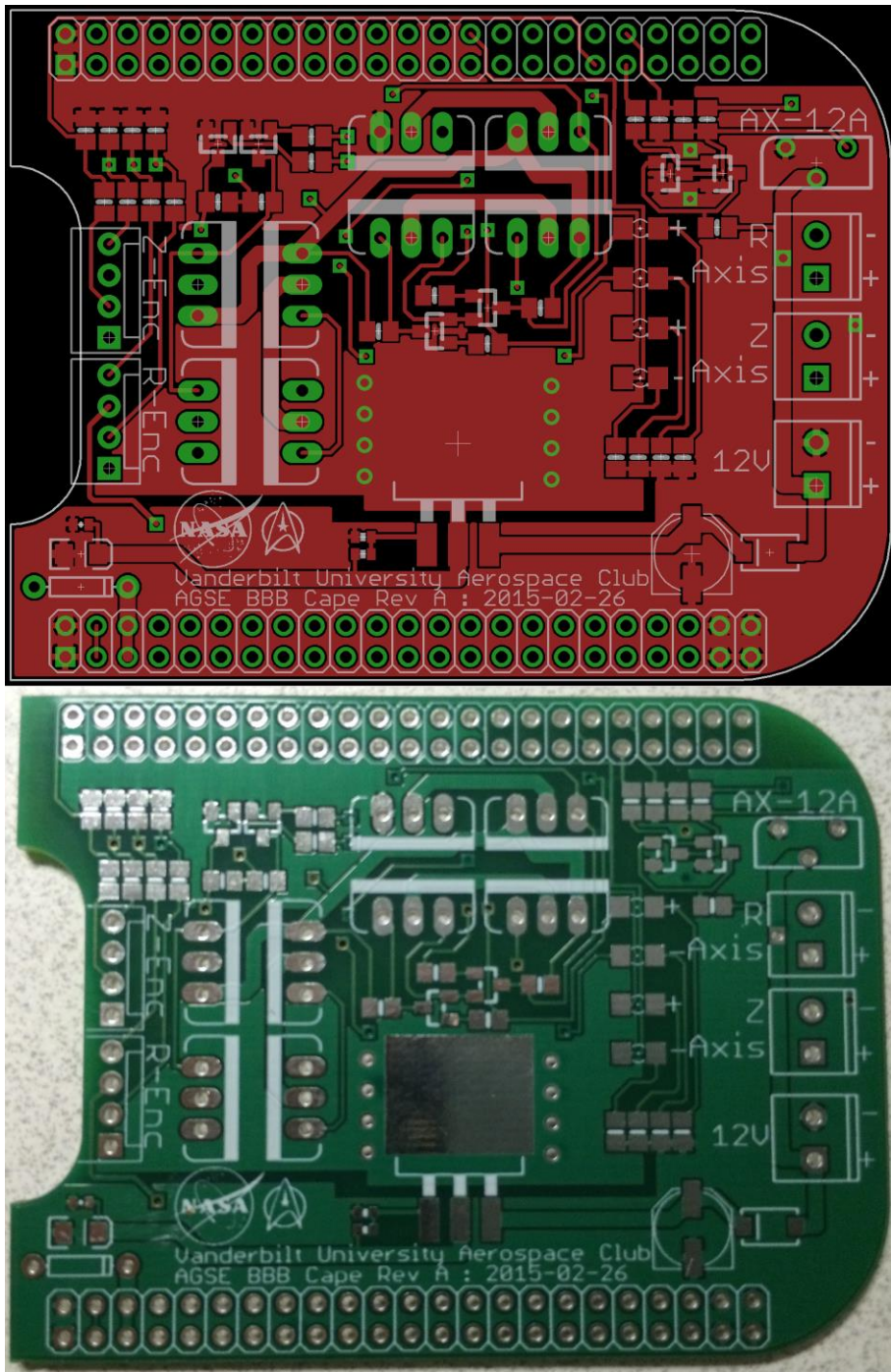


Figure 116: Board layout design and fabricated board for the AGSE BBB Motor Control cape (top). On the right side of the board, we have the 12V input for the power and motor circuits, as well as the 12V motor outputs for both the radial linear actuator and the vertical linear actuator (R Axis and Z Axis, respectively.). Also on the right side is the 12V servo motor connector which connects to all of the servo motors in the AGSE. The left side of the board connects to the two 5V quadrature encoders which provide feedback to the AGSE about the position of the two linear actuators. All components for the board will be mounted on the top of the board.

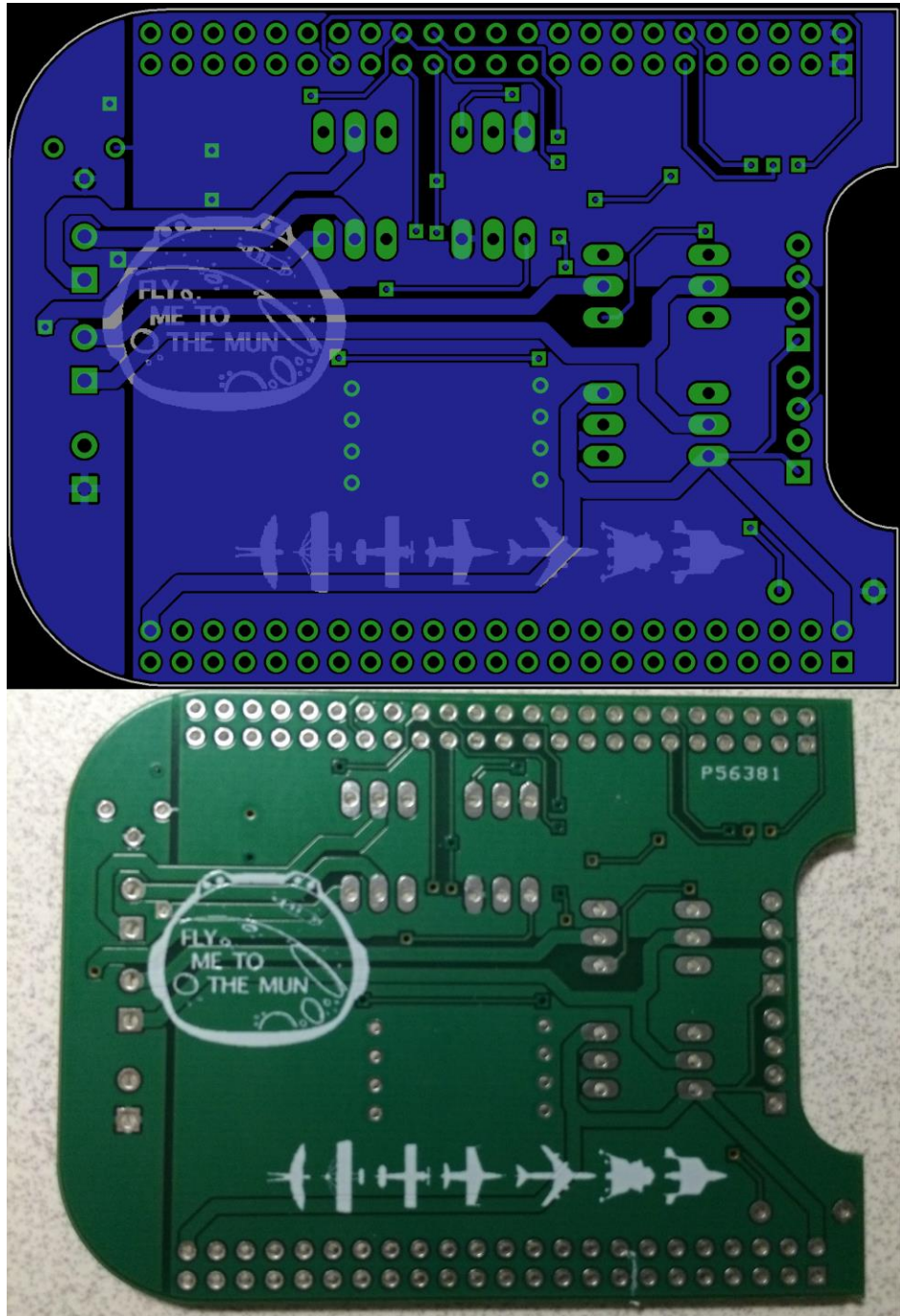


Figure 117: Bottom of the AGSE Motor Control Board. Here you can see the underside traces for the board. Also included are relevant pictures the team wanted to have on the board reflecting our love of aerospace engineering and space exploration.

We have completed the fabrication of this board, as shown in Figure 118 and Figure 119. After the fabrication testing was completed (ensuring that there were no shorts in the circuits and each component was properly connected), we performed a few functional tests to ensure the correctness of the board.

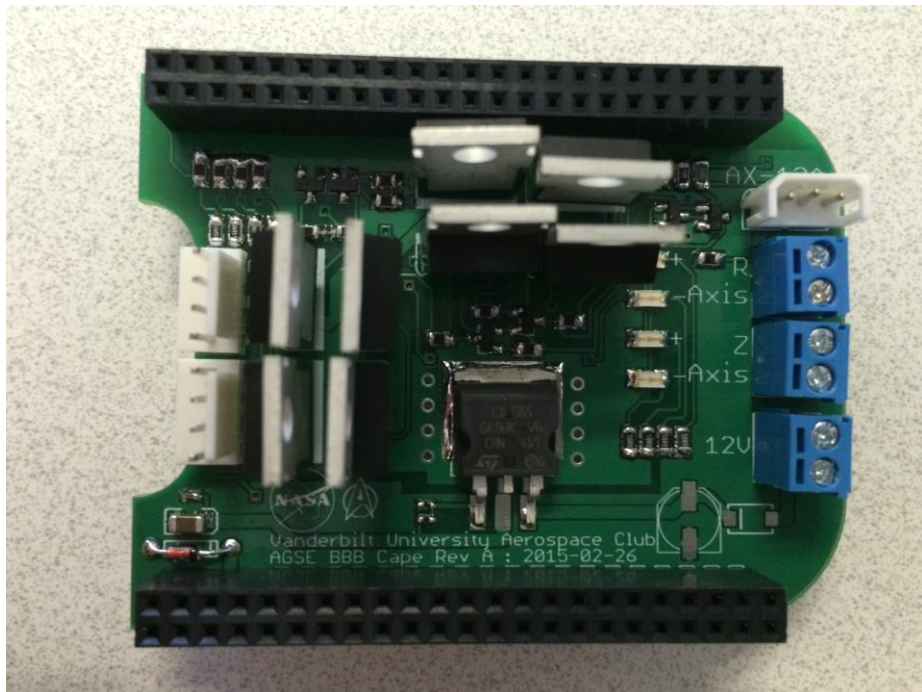


Figure 118: Fabricated AGSE Motor Control BBB Cape.

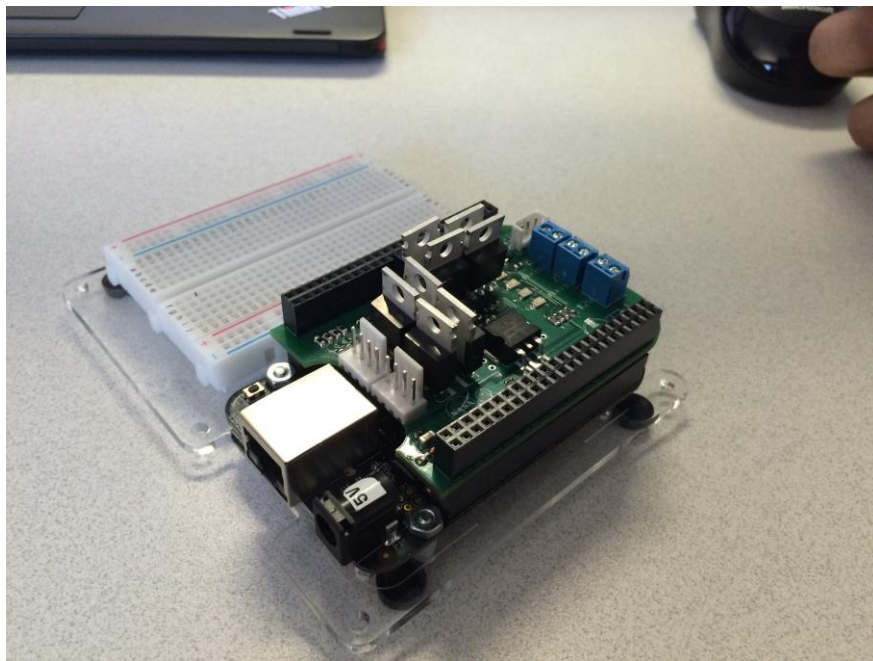


Figure 119: Completed AGSE Motor Control BBB Cape mounted as a cape on the BBB.

- **Test 1: Power test:** We applied 12V and Ground input power lines to the just the Motor control board at the 12V power supply screw terminals. This power was provided by a stable bench-top power supply. The application of this power tested that no components were incorrectly wired, and measurement of the voltages at various parts of the circuits

(esp. the output of the DC/DC LDO regulator) verified that the power subsystems of the board were indeed performing their required functions.



Figure 120: BBB Cape with MOSFETs Shown

- **Test 2: Boot test:** We powered down the motor control board, mounted the board on top of the BeagleBone Black, and then applied power to the board. The mounting of the cape and subsequent power and boot test verified that the board connections are correct for the BBB and that the LDO can properly power the BBB. The other result of this test was the current draw at the source which was measured as 0.2A@12V.
- **Test 3: Connections test:** We kept the motor control board and the BBB connected, powered them down, and then connected the servos to the servo connector and an encoder to the encoder connector before applying power. This test verified the correctness of the connector and showed that the board can supply enough power for the board and its connections. The other result of this test was another current draw measurement at the source which was measured as 0.25A @ 12V.

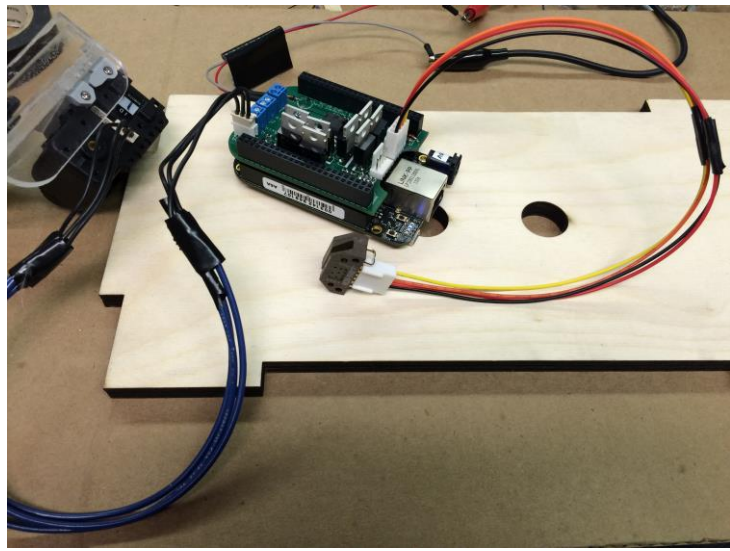


Figure 121: Connectors attached to BBB Cape

- **Test 4: Screen test:** We powered off the BBB, took the cape off of the BBB, and applied the 7" touchscreen cape to the BBB, which will be used with the user-interface panel. We then connected our cape to the expansion slot and powered up the system through our cape's power port. This test verified that the cape that we made can be used as a power converter for the screen/BBB combination in the user-interface panel. The other result of this test was a measured current draw at the source of 0.65A@12V.

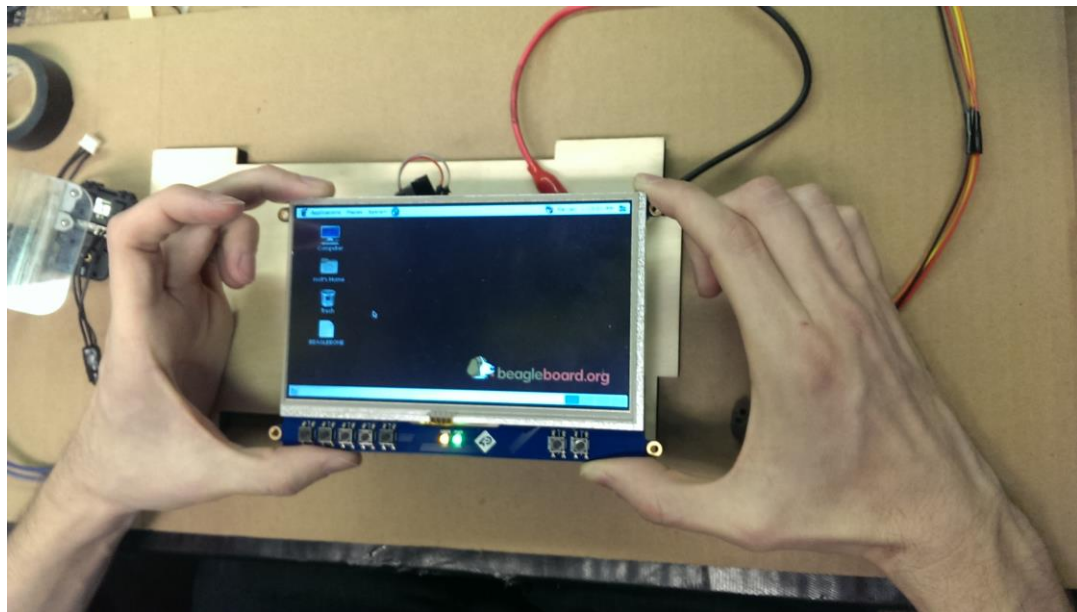


Figure 122: 7" Touchscreen Cape attached to BBB

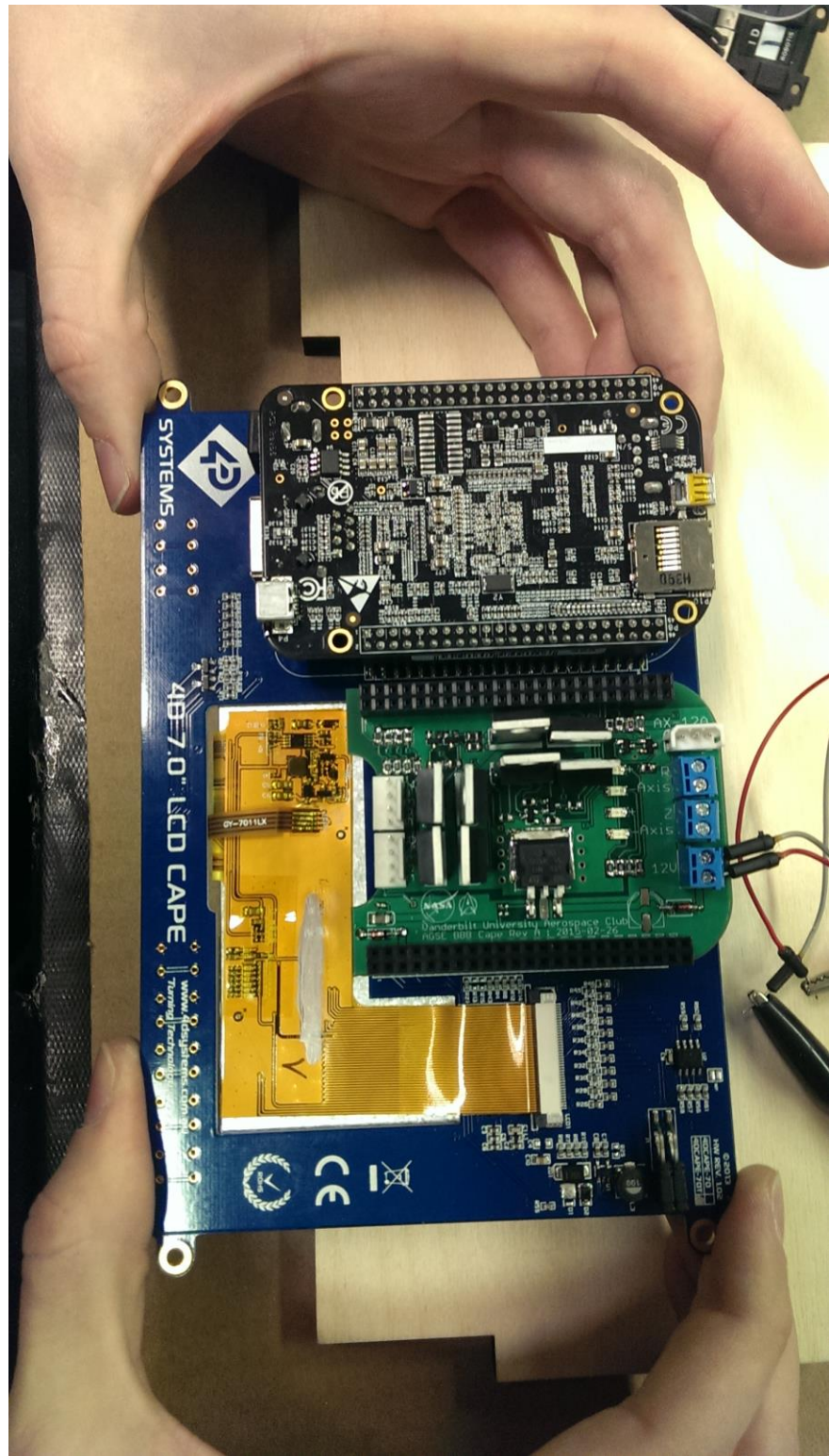


Figure 123: Underside of Screen Attached to BBB

5.3.6 Iterative Development Progress Outline

- Started with prototype (AGSE v1):
 - AGSE system (shown in CDR)
 - Hardware
 - Base:
 - Unstable off the shelf turntable: caused a lot of wobble and uncertainty in the positioning of the arm during rotation
 - Bad servo control : serial protocol used did not play nicely with the other servos' protocols
 - Horrible power consumption (~300 mA @ 12 V while doing nothing, not even holding position)
 - Linear Actuators:
 - Misaligned mounting led to some jamming of horizontal actuator
 - Waste space and weight (w.r.t. required power and throw)
 - Gripper:
 - Flimsy modification of off the shelf gripper; not enough force could be applied and error in positioning was too high
 - two different servos
 - Analog (PWM) servo had issues with noise picked up by long cable from control board; meant we should shorten the cable and go to a fully digital control servo motor
 - Small servo couldn't be daisychained with larger (base rotation) servo
 - Small servo is not as well documented and not as well supported
 - Breadboard circuits for H-Bridges and serial buffers
 - A few iterations of these circuits were developed as the design was refined
 - Off the shelf h-bridges we had on hand were not powerful enough
 - many different voltage levels required (5V, 12V, 1.8V, 7.2V)
 - Issues with the servos
 - couldn't be daisychained: didn't have the same communications protocol and didn't run on the same voltage levels.
 - Datasheets provided by vendors were wrong and contradictory
 - libraries provided by vendors were quite buggy (took a while to figure out)
 - Off the shelf linear actuators:
 - analog feedback was an issue for our board and is more susceptible to noise
 - Current draw was higher than we would have liked (spiked to 3A per motor)
 - Mounting was difficult
 - Sourcing actuators with the throw we wanted was difficult
 - Jetson
 - Could run the software to control the motors, the image processing, etc.
 - Certain kernel versions had driver issues with the camera (had to modify the kernel to ensure a working camera)

- Kernel modules for communicating with the BBB (using FTDI/RNDIS) were buggy and incorrectly configured; we had to connect the two boards using ethernet and a network switch.
- Couldn't interface with all of the hardware
 - not enough free GPIO for user input switches
 - no analog input for motor potentiometer feedback (only required for prototype)
 - no encoder input for motor encoders (if we wanted)
- Overall:
 - Showed that we could get the system up and running
 - didn't have full camera integration
 - didn't have good feedback from the motors
 - met the requirements set out in NASA's RFP
 - picked up object in known orientation/position and placed it in payload bay of known orientation/position
 - had issues with jamming, noise, and power consumption
 - Code wasn't very maintainable and could not be distributed among nodes
 - Control code was split between Arduino and Jetson without clear delineation of responsibilities
- Software
 - Prototyped in python
 - Grabbed sample from known (pre-programmed) position and orientation
 - Not very maintainable; software was not cleanly split to delineate the responsibilities of the different subsystems and interfaces were not clearly defined or even adhered to
 - Camera & object detection code was not integrated; c++ detection of sample worked but was not integrated into the python prototype motor control code
 - Code was split among jetson and Arduino without a means of maintaining the two codebases and ensuring they could interface properly with each other as the code evolved
 - Serial communications issues (servo & Arduino) and noise issues (servo pwm)
- Modeling Language / Code Generators
 - Component model and ROS concepts modeled (msg/srv/timer/pub/sub/client/server, component, nodes)
 - Code generated for build system, component model, and workspace
 - No concepts of hardware or deployment
 - No code preservation -> made iterative development more difficult
 - Useful for designing the system and describing the interactions of the system components
- Editor

- Could describe system software and use the generator to create the code
- Used for testing out the modeling of the AGSE system and generating code
- No code deployment or hardware description/assignment

- Second Phase (AGSE v2):

- New version of AGSE:
 - Hardware
 - Base:
 - Custom-built turn-table / rotation control
 - Stable base with very small positioning error
 - Unification of system servos
 - same protocol
 - same voltage
 - good current draw vs. holding power
 - daisychaining for wire management
 - mounted well to sturdy platform
 - Linear Actuators:
 - Custom built
 - Reusing design principles and lessons from payload bay
 - Using encoders for positioning feedback
 - Same voltage level as servos
 - Lower power
 - No wasted space (i.e. volume and mass go down, work area goes up)
 - Gripper:
 - Same servos as base (voltage / protocol)
 - Higher torque for better gripping
 - Better design for phalanges (w.r.t. consistently grabbing sample)
 - Integration of camera
 - Circuitry:
 - H-Bridges for two linear actuators
 - Serial buffer for full-duplex uart @ 3.3V to half-duplex uart @ 5V
 - Resistor dividers for 5V QEP to 3.3V eQEP hardware
 - Power filtering and step-down from 12V (Motors / Jetson) to 5V (BBB & encoders)
 - Separate power conversion and isolation board for batteries (48V) to main system power (12V)
 - Jetson:
 - Runs the image processing / object detection
 - Captures images using video4linux (v4l) library from the webcam
 - Runs the overall high-level system planning
 - Runs ROSCORE discovery mechanism and ROS backbone
 - connects using Ethernet to motor control BBB and user input panel BBB
 - Motor Control BeagleBoneBlack (BBB):
 - Many GPIO pins for motor control (to two H-bridges)
 - Servo control through serial buffer

- eQEP (enhanced Quadrature Encoded Pulse) hardware integrated into processor for motor position feedback
 - connected to jetson using TCP
- User Input Panel and its BeagleBone Black (BBB):
 - Directly connected to main switches (keyed switch for power, missile switch for pause)
 - Extra user-input switches for more interesting feedback
 - Designed with inspiration from the Apollo DSKY
 - Connected to the network switch for direct communications with the rest of the AGSE
 - 7" touchscreen to provide interesting feedback (webcam feed, detected positions/orientations, and current position/orientation, etc.)
 - Backlit acrylic plates with text to provide clear visual feedback about current AGSE state
 - Auditory feedback through speaker
- Overall:
 - More space efficient
 - More power efficient
 - Better materials and better construction
 - unification and simplification of system hardware and software components
 - integration of image processing and camera for autonomous sample detection and retrieval from anywhere within the workspace of the AGSE
 - Software
 - ROS based
 - provides communications middleware between processes on the same node or on different nodes
 - Abstraction above TCP & socket level transfers
- Component Based Software (Our component model and implementation for ROS, ROSMOD)
 - threading model
 - interaction pattern model
 - separation of concerns between different subsystems
 - Scheduling model (timer and event based scheduling)
- Downgraded Linux kernel version to support simple device tree overlay for switching GPIO mode and enabling subsystems of the processor
 - useful for the configuration of the hardware based quadrature encoder decoding (eQEP)
- Integrated all main subsystem code into generated C++ ROS / ROSMOD code
 - supports reading linear actuator position through eQEP kernel driver
 - supports controlling linear actuators through GPIO
 - supports reading system switch states for propagation to rest of system
 - supports reading and writing to servo motors for control of the base rotation, gripper rotation, and gripper position
 - supports image processing code and camera image gathering

- supports communications between system components to achieve overall system goals
- Modeling Language / Code Generators
 - support for describing the hardware configuration of the system
 - host names
 - host IP addresses
 - host architecture
 - host login information
 - host hardware configuration scripting
 - support for describing deployment configuration for a specific hardware and software configuration
 - ROS Node (process) to Host (hardware) mapping with process identifier (name)
 - Code generators preserve business logic
 - developer generates baseline code from model -> adds some business logic code to function stubs -> changes model -> regenerates base code; business logic from before is preserved
 - shortens iterative development time
 - increases utility and decreases user or system errors
- Editor with deployment
 - specify system software model (component based)
 - specify hardware configuration and hosts' attributes
 - specify software to hardware mapping
 - Deploy the software onto the system
 - monitor status of deployed software

5.4 Initial AGSE System Design

5.4.1 System Summary

Our initial Automated Ground Support Equipment design (*Figure 124*) involves the fabrication and operation of a four degree of freedom robotic arm with an additional end effector to retrieve the payload (*Figure 126*) and safely deposit it in the payload bay. This design is comprised of a revolute base joint with prismatic actuation of vertical and horizontal axes and an additional revolute joint above the end effector to provide support for multiple payload-to-robot placement orientations. With these joints the robot operates freely in a cylindrical workspace (*Figure 127*) situated about its center.



Figure 124: Team P.R.I.S.M. Automated Ground Support Equipment (CAD and Physical Prototype)



Figure 125: AGSE Maximum and Minimum Reach

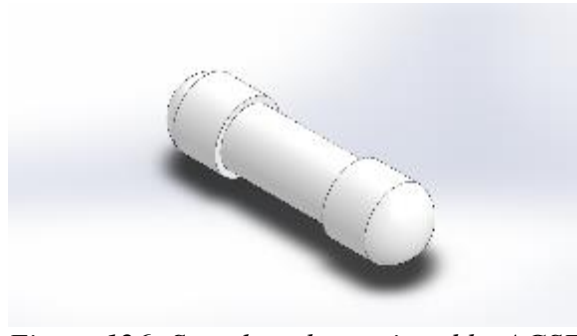


Figure 126: Sample to be retrieved by AGSE

The robot sits 37.5" tall and almost 35" wide along the radial axis. It has a maximum reach of approximately 20" and a minimum reach of 8" (*Figure 125*) about its central axis, giving it adequate manipulability to perform the tasks of retrieving and depositing the payload. While in the prototyping stage, these dimensions were sufficient to successfully complete the required task of picking up the sample and delivering it to the rocket; however, because the design is limited in its vertical reach, this design will be improved by modification of the linear actuator. The AGSE design was carefully deliberated so that modification is straightforward enough to take singular replacements in a modular way without affecting the entire structure. The individual actuators may be replaced with only minor changes to the original frame and design because of its modularity. In this way, this design is adaptable to the requirements of the challenge without getting entrapped in unnecessarily complex functional detail. (*Section 0*)

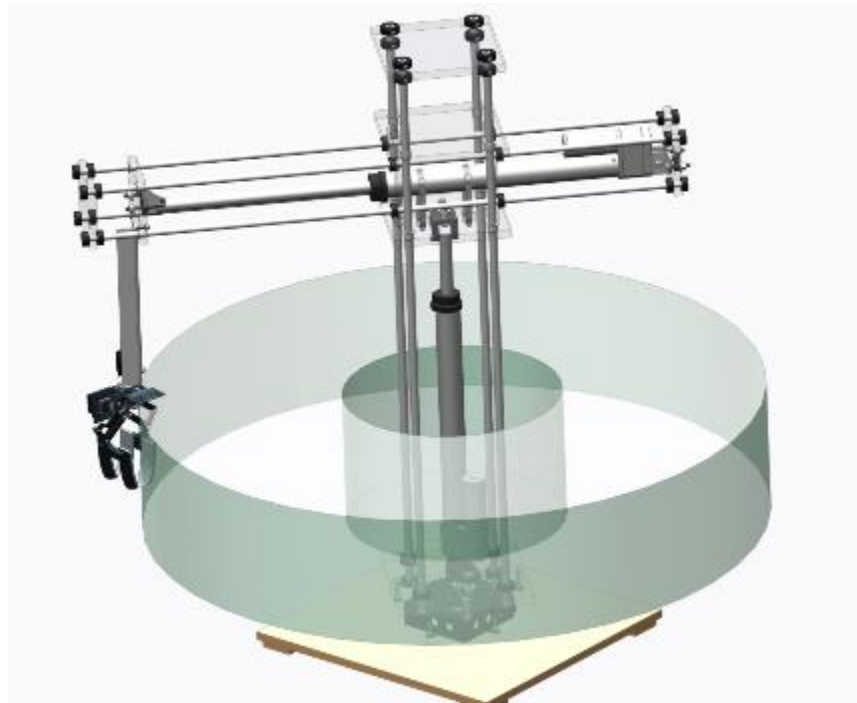


Figure 127: Visual representation of the operational workspace of the AGSE

5.4.2 Subsystems Overview

5.4.2.1 Actuators

The robot is attached to a platform base that is wide enough to prevent tipping moments. The base currently on the AGSE has a footprint of 16" by 16", and is constructed from $\frac{1}{2}$ " thick birch plywood. Four 1/2" thick plywood legs are screwed below this base at its four corners to allow room for the bolts connecting the turntable to the base platform. Our final design integrates the AGSE base with a stand used to support the launch rail in its horizontal position. This version features adjustable legs that will ensure the AGSE base is parallel to the launch pad, rather than the ground.

Our AGSE design features centrally located actuators and structural members, and thereby can keep the center of gravity for the composite system within the base dimensions with a significant factor of safety. By designing the system such that the center of gravity stays well within the base dimensions, the possibility that the AGSE tips over due to environmental loading (wind, etc.) are to be greatly mitigated.

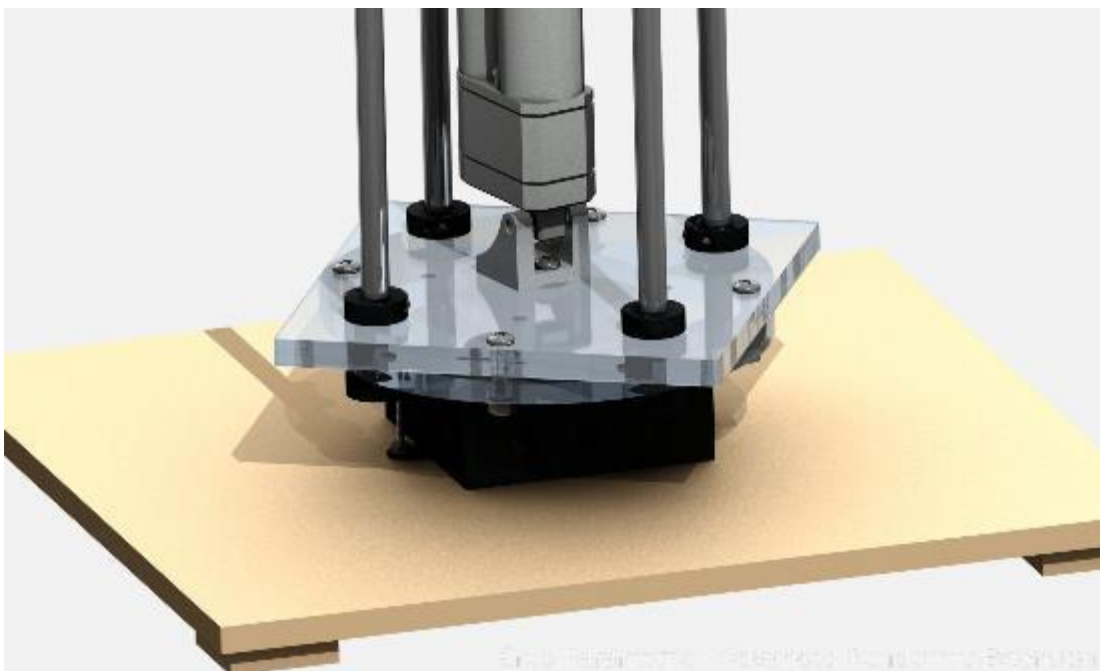


Figure 128: Integrated Dynamixel turntable with integrated DC motor

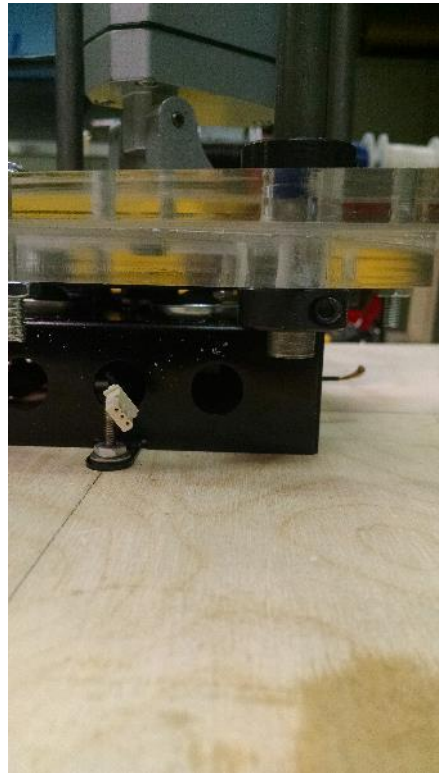


Figure 129: Turntable Base Attached to Plywood Base. The donut (bottom acrylic piece) attaches to the thin turntable disc. The acrylic baseplate bolts to the donut. The vertical guide rods are fit through both acrylic pieces and attached with shaft collars.



Figure 130: Another view of the AGSE base. The bolts connecting the acrylic baseplate and donut can be seen.

The driving rotation of the robot is generated by a Dynamixel MX-28T DC motor turntable (*Figure 128*) with integrated driver and reduction gearbox. This turntable provides a 193:1 gear ratio providing appropriate torque up to 22in-lbf to rotate the entire robotic arm. Additionally, the

wide base of the turntable provides enough support and contact surface area to dampen vibrations caused by this base rotation. This turntable is attached to an 8" acrylic circular ring, nicknamed the "donut," that allows the rotating disc platform of the turntable to attach to another acrylic plate of size 8"x8" that acts as the support for the rotating tower of the AGSE. Thus the donut is placed between the turntable base and acrylic platform at the bottom of the AGSE tower. The acrylic base is bolted to the donut, and the vertical $\frac{1}{2}$ " guide rods are fed through both. Steel shaft collars secure the guide rods to the acrylic base. The vertical linear actuator is mounted to the acrylic base using a bracket and a bolt connected through the acrylic base within the donut hole.

Linear actuation for the vertical and horizontal platforms is provided by commercially available linear actuators. These actuators are designed to provide axial force in response to a position command issued by the corresponding motor controller. Since these actuators are designed only for axial loading, a guide rail structure has been designed to prevent any moments from being applied to the actuators. To ensure moment is taken only by the guide rails, both actuators are supported at each end by a pin connection. These pins are oriented perpendicularly, effectively giving the actuators a passive spherical degree of freedom at each end. This connection design ensures that only axial force can be applied to the actuators, and that moments applied to the actuators or platforms cannot be supported by the actuators themselves. To further lessen stresses associated with applied moment, nylon sleeve bearings are used to promote smooth linear motion along the guide rods.

Vertical movement is driven via a Trossen Robotics lead screw driven linear actuator having a 12" throw with integrated position feedback. This linear actuator can handle axial forces up to 107 lb_f, providing a comfortable margin of safety to lift all translating components of the AGSE, as well as overcome frictional forces in the drivetrain. The weight of this actuator is a substantial portion of the total system weight, causing the composite center of gravity to remain close to the geometric center of the AGSE. This promotes a stable base on which the AGSE can operate.

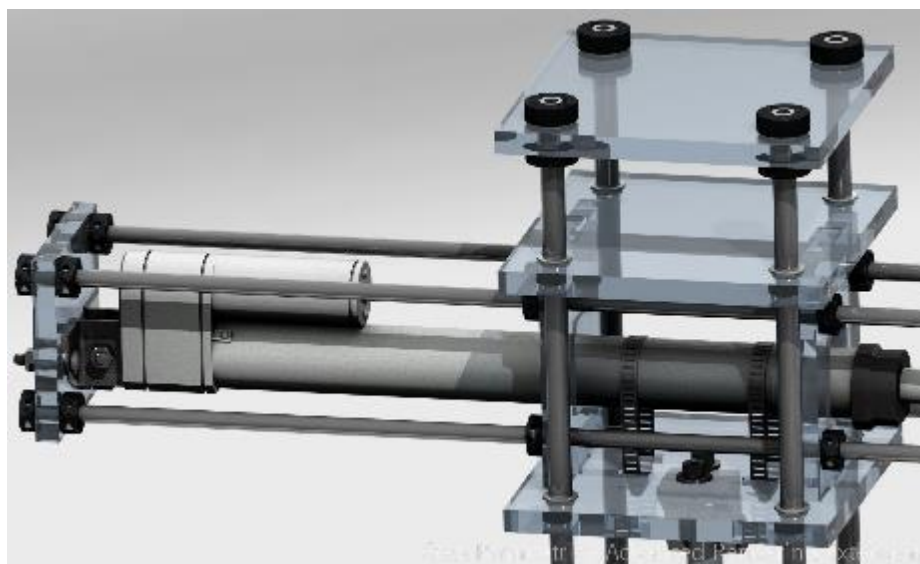


Figure 131: Vertical stage, supported by thrust bearings on four steel guide rails



Figure 132: View of vertical linear actuator mounted on AGSE base



Figure 133: Top plate attached after vertical carriage is installed

This vertically driven stage (*Figure 131*) supports a second Trossen Robotics linear actuator, which will provide the horizontal motion for the robotic arm. This motion is supported by 4

guide rails, which are connected to more acrylic plates to provide structural integrity to the system. This design also employs nylon sleeve bearings for low friction translation.

From the horizontal carriage on the guide rods hangs an aluminum L-bracket that acts as the “arm” of the end effector. This bracket is bolted to the horizontal carriage and moves along with it. Another much shorter bracket is bolted to the arm bracket in order to mount the gripper. Rotation of the end effector is provided by a Hitec servomotor mounted on top of the gripper and attached to the smaller L-bracket (see *Figure 134* for more detail). This motor provides orientation control and feedback for the gripper below it.



Figure 134: Gripper Arm Supporting Gripper

Because of the robot’s high-powered joint system, it should be able to reach between its two furthest points under maximum load in less than the 10sec it takes to extend both linear actuators. Each joint of the robot is encoded to ensure maximum control over both position and speed. This will allow avoidance of any kind of dangerous malfunctions because we can know the position of each link of the robot based entirely on the output numbers from the enclosed electronics, and this in turn will avoid approximation-based malfunctions.

5.4.2.2 Manipulator

The current manipulator design is based on a coupled gear design that can retract and expand its foam-padded phalanges to accommodate the cylindrical payload.

The gripper is driven by a Dynamixel XL-320 servomotor. This modified gripper has several features that improve upon the initial CrustCrawler model. For one, using the Dynamixel servomotor allows us to utilize its force feedback feature, giving us the ability not only to detect whether the object has been properly gripped or not but also to ensure that neither the payload nor the phalanges themselves will be damaged by closing the gripper too tightly. Additionally, it allows detection of a serious error such as a dropped payload. Another added feature is utilizing a 3D-printed pair of 2-pronged phalanges instead of using the stock 1-pronged phalanges. This ensures a more reliable grip on the sample payload, giving it more surface area for gripping. Another improvement is that we've attached foam to the pads of the 4 phalanges, allowing for even more surface area for grip. The foam also allows the phalanges to squeeze the payload more for a better grip without any risk of damaging either component. Compare *Figure 137* and *Figure 135* for a visual explanation of the changes made to the gripper design.

A plate mounted at the top of the gripper allows room for our camera to be mounted. If the plate proves to be insufficient in terms of space for the camera to be installed, another plate can be either rapid prototyped or machined to accomplish this requirement.



Figure 135: CAD Model of Modified Gripper Design



Figure 136: Prototype AGSE Gripper

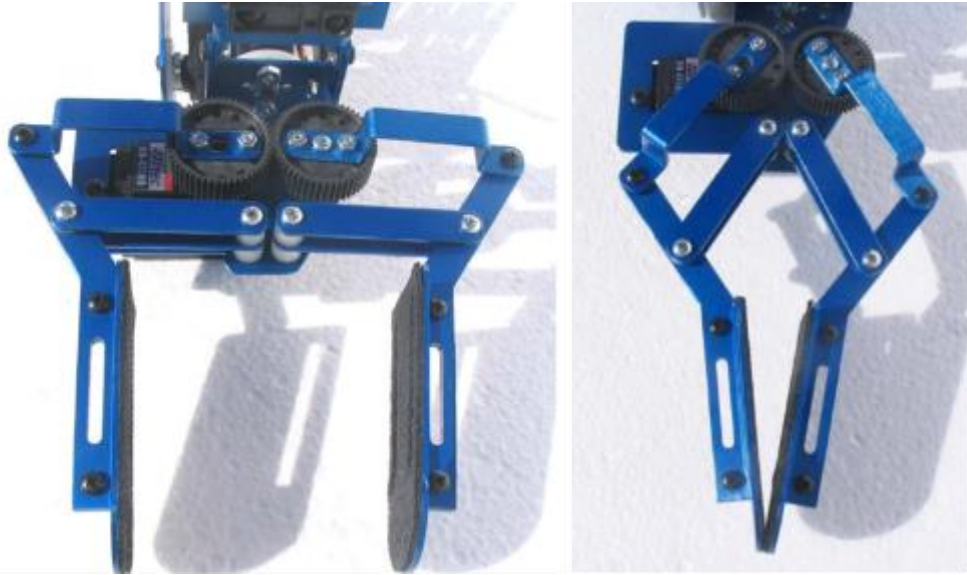


Figure 137a-b: Original Gripper in Open and Closed Configurations

This design will provide the needed manipulability of the payload while still being compact enough to avoid imposing further design restrictions on the payload bay, which must be able to accommodate the phalanges of the gripper. This design criterion was chosen so that the payload can be placed into the payload bay without dropping the payload. This method of placement

mitigates the risks associated with improper insertion into the payload bay, a condition that could prevent the bay from sealing for flight and jeopardize the mission.

In order to interact with the payload bay, the manipulator will have a magnet fixed to the end of one of its phalanges. This magnet will be detected by a Hall Effect sensor located at the inside wall of the payload bay. This method of interaction between the AGSE and payload bay should provide a simple interface that is unaffected by wireless communications and makes very few assumptions about the operating environment.

5.4.2.3 Electronics and Software

The differences in the electronics and software side from the first to second AGSE design was not as distinct as the mechanical components, evolving according to the outline in section 5.3.6: *Iterative Development Progress Outline*.

More detail on the electronics and software can be found in the corresponding section in the final AGSE design, section 5.5.2.7: *Electronics and Software*.

The electromechanical systems are outlined below. The electronics and software side of the AGSE is at the heart of allowing the robot to work as a functioning system. As of now, we have developed working prototypes of all mechanical systems, electrical systems, and software.

- Mechanical:
 - horizontal, vertical carriages for the arm
 - gripper
 - gripper linkage
 - horizontal movement of the arm
 - vertical movement of the arm
 - angular movement of the arm
 - angular movement of the wrist
 - actuation of the gripping mechanism
- Electrical:
 - communication circuitry for:
 - Jetson to XL-320 Servo
 - Jetson to MX-28T Servo
 - Jetson to Arduino
 - Driver circuitry for the high-power horizontal and vertical linear actuators
- Software:
 - image-based object detection; GPU accelerated
 - controls for:
 - linear actuators (height, radial)
 - wrist, gripper, and base servo motors
- Performed unit tests of all mechanical, electrical, and software subsystems.

- Performed integration tests for the AGSE system

More information on the setup of the circuits controlling the AGSE actuation can be found in the appendix, section *10.2.4: AGSE Control Electronics*.

5.4.2.4 Power Requirements

In terms of powering the actuators in the AGSE, there are three elements that must be powered: the gripper servos, the turntable base, and the linear actuators. A 7V circuit powers each of the gripper servo while 12V is needed to power the turntable and the linear actuators. For our initial testing of the AGSE, we have been using a tabletop power source but will soon transition to using batteries to power the actuators. These batteries will likely be mounted on the base of the AGSE.

One aspect we have considered while designing the AGSE is the practicality of being able to power such a device on Mars, such as in the SLS Mission. Solar power on Mars [23] is a function of the incident solar radiation, the thickness of the Martian atmosphere, and the makeup of the Martian atmosphere. The thinness of the Martian atmosphere helps to compensate for the increased perihelion of Mars with respect to the surface-usable solar radiation. Example data from the Viking Lander 1 site, indicated that during the middle of a midsummer solar day on mars, over 500W/m^2 were available to solar collectors on the surface of Mars. From 0800-1600 solar time, the irradiance exceeded 200W/m^2 . Conservatively, with a 10% efficient collector with an area of 1m^2 , the system would have at its disposal, 20W for the 8 hours between 0800 and 1600 solar time.

Further, given that the system will not require maximum power throughout the duration of the day, the excess energy harvested can be used to charge the system's batteries. In this way, the system can remain functional despite inclement solar or atmospheric conditions.

These data were used to determine power goals for the AGSE system. Given that the AGSE should operate remotely on the Martian surface, we consider design decisions which would enable such functionality. Therefore we impose upon our design a constraint that the AGSE should consume no more than 20W, for both battery and solar power design considerations. We will continue to refine our design to meet these criteria.

5.4.3 Prototype AGSE Fabrication and Verification

A prototype AGSE was constructed in order to validate our design and its key functionalities, such as object detection and automated path planning based on image processing. Before starting this prototype, prep work including laser cutting of the plates, carriages, and platforms used in the AGSE and assembly of the gripper and turntable was carried out. This initial work along with a general outline of the different sections of AGSE assembly is detailed in the following flowcharts.

Prep Work

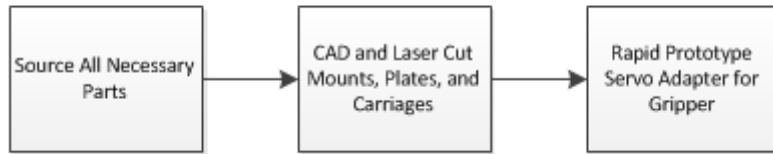


Figure 138: Flowchart of AGSE Prep Work



Figure 139: Flowchart of Overall AGSE Construction

Base and Tower

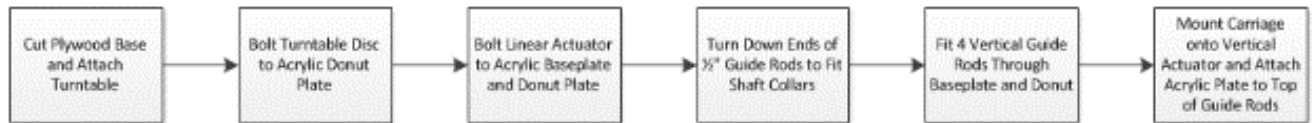


Figure 140: Flowchart of AGSE Base and Tower Construction

Vertical Carriage

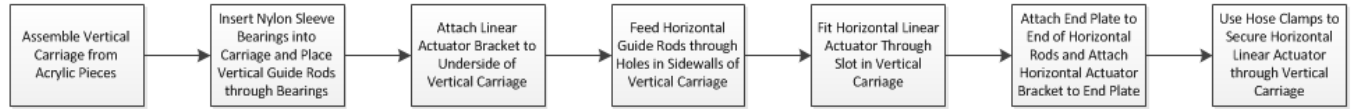


Figure 141: Flowchart of Vertical Carriage Construction

Gripper

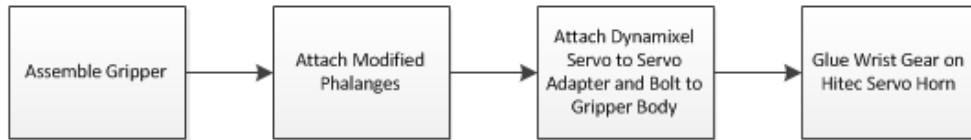


Figure 142: Flowchart of Gripper Construction

AGSE Arm



Figure 143: Flowchart of AGSE Arm Construction

5.4.3.1 Power

Our tests of the AGSE utilized a tabletop power-source. By monitoring the current draw of each motor as it operates and knowing the nominal voltages for each one, we can size batteries that will be able to provide power to all subsystems. Careful consideration has been made in the design process such that the system does not draw an excessive amount of power, as it mirrors a design that would have to operate on Mars where efficient power use is of utmost importance.

5.4.4 Lessons Learned from AGSE Prototype

This prototype design process yielded beneficial information which was able to incorporate into the final AGSE design:

- The servo motor datasheets, design documents, and sample code (from manufacturer) were incorrect
- The Dynamixel servo motors could not be daisychained as we had hoped, as they ran on different voltage levels (and used different communications protocols)
- The servo motor controlling the base rotation (turntable) consumed too much current during standby (300 mA at 12V)
- The servo motor controlling the gripper rotation, since it was controlled simply by using PWM, was susceptible to electrical noise. this caused jittering and some hysteresis in the gripper orientation
- The linear actuators chosen for off the shelf consumed a lot of current, wasted space (i.e. unextended they took up more space than we wanted to use), did not have a long enough throw, and provided only analog feedback about position
- The linear actuator's analog feedback could not be used by our main processor board (the Jetson TK1) since it had no on-board analog to digital converters (ADC).
- We were able to simultaneously develop the image processing and sample detection code for the final AGSE
- We were able to simultaneously develop the hardware/software modeling language, development toolsuite, code generators, and code for the final system, since many of these lessons (especially with respect to the servo and linear actuator complications) were encountered early in the prototype's development

5.5 Final AGSE Design

5.5.1 System Summary

The final AGSE design includes the many of the same conceptual elements while eliminating weaknesses and structural issues. The AGSE still uses linear actuation about a centrally located rotary joint in order to operate within a cylindrical workspace. A second prismatic joint moves a horizontal carriage in the cylindrical coordinate r direction. A final degree of freedom is achieved through the addition of an orienting servo mounted above the AGSE's end actuator. These elements have been carried over, from the previous version, but much of the materials selection and structural elements have been changed in order that the AGSE be a more developed and robust system for retrieving and depositing the payload. The AGSE stands approximately 42

inches tall, though its adjustable legs make it possible to lower this height below 40 inches. The horizontal arm is 25 inches in length from the back of the vertical carriage to the end of the horizontal guide rod plate.

Because some of our team members have research and development backgrounds in software modeling, analysis, and code-generation, we have created a modular, extendable, and powerful software modeling and code generation toolsuite. The software modeling allows us to describe at a high-level the different parts of the software subsystems (the software components) and how they interact with each other to produce the overall AGSE mission functionality. Using this modeling paradigm, we can develop more precise descriptions of the software systems, we can ensure the correctness of their interaction patterns, and because we generate most of the code (4700 lines of code generated out of 7777 lines of code written; 60% generated) we can ensure the correctness of the code. Additionally using the component-based generated code, we break the requirements of the AGSE software down into indivisible software components and can write the code for each component separately from the other components. This modular software design approach allows us to produce more reliable software faster and enables us to extend the capabilities of our software system relatively easily.

Uniqueness and Significance goes into greater detail about the advantage our design, particularly with respect to other solutions.



Figure 144: Full AGSE CAD Render

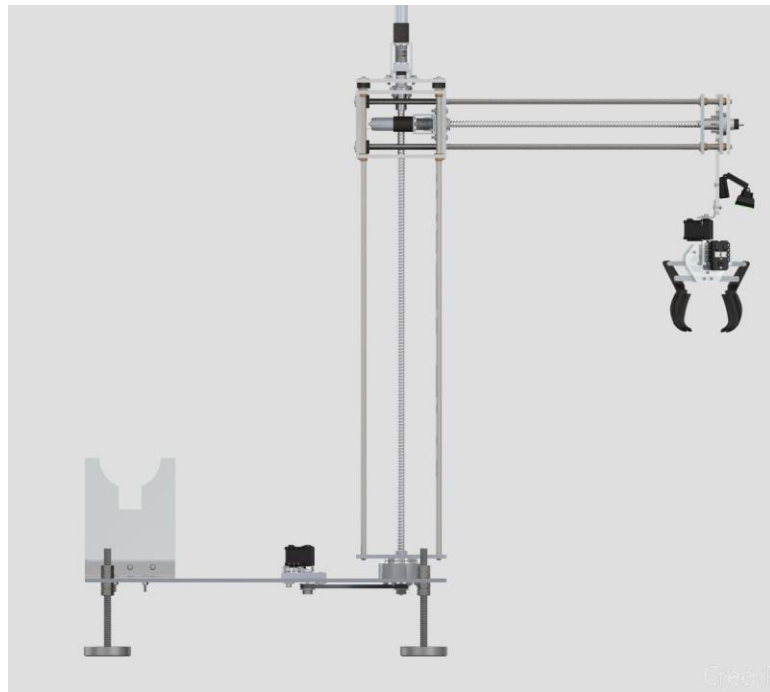


Figure 145: Maximum reach of the AGSE is 25 $\frac{1}{2}$ inches above the ground and 19 $\frac{1}{2}$ inches from the central rotation axis.

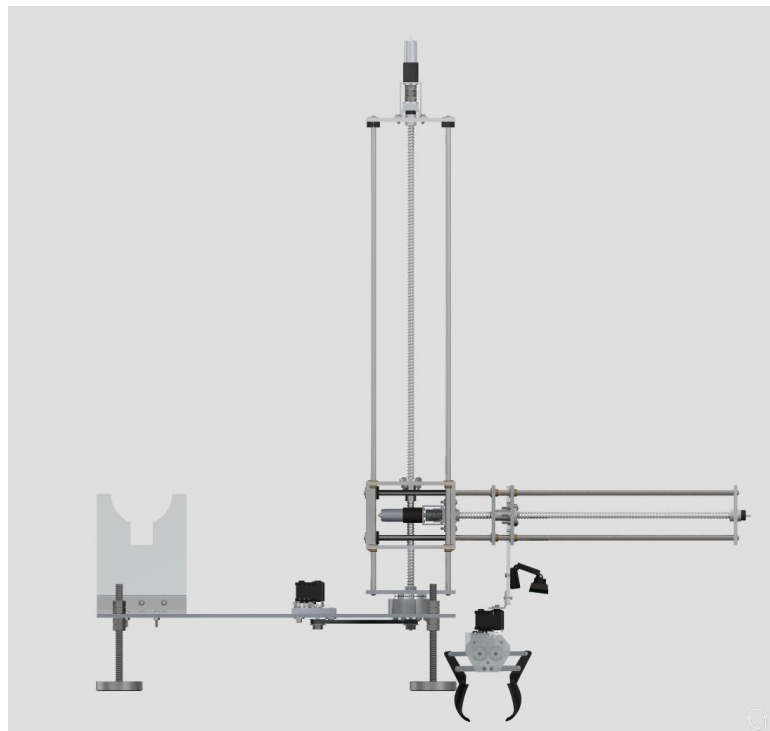


Figure 146: Minimum reach of the AGSE allows it to reach the ground and its own table, approximately 3 inches from its center axis.

5.5.2 Subsystems Overview

5.5.2.1 Actuators

5.5.2.1.1 Motor Sizing

The motors driving the lead screws were sized with considerations of force needed to push against the weight of their respective carriages with a factor of safety of 1.5, required speed for our ten minute retrieval requirement, and voltage matching the battery choice.

As a sample calculation, the vertical motor sizing process is shown next.

$$\sum M = M_{gripper\ assembly} + M_{guide\ rods} + M_{end\ plates} + M_{hor.\ carriage\ plates} + M_{lead\ screw} \\ + M_{fasteners} + M_{hor.\ motor} + M_{counterweight} + M_{vert.\ carriage}$$

$$\sum M = 1kg + 1.72kg + 0.36kg + 0.63kg + 0.4kg + 0.5kg + 0.25kg + 8.625kg + 1.23\ kg \\ = 14.715\ kg$$

Most of these numbers were estimates, so the resulting mass is rounded along with a factor of safety and then rounded once more.

$$M_{rounded} * FS = Rounded\ Mass\ Allowance$$

$$15kg * 1.5 = 22.5kg \rightarrow 20kg$$

$$20kg * 9.81 \frac{m}{s^2} = 196.2\ N\ of\ force\ required$$

Using this required force along with properties of the lead screw and lead nut drivetrain, the required torque was then calculated.

W = weight, Dm = mean thread diameter, f = friction estimate, L = lead, α = pitch

$$Torque\ Required = \frac{W * Dm}{2} * \frac{f * \pi * Dm + L * \cos(\alpha)}{\pi * Dm + L * \cos(\alpha) - f * L} * \frac{1000mNm}{1Nm}$$

$$Torque\ Required \\ = \frac{196.2N * 0.01016m}{2} * \frac{0.1\pi * 0.01016m + 0.00254m * \cos(0.253)}{\pi * 0.01016m * \cos(0.253) - 0.1 * 0.00254m} \\ * \frac{1000mNm}{1Nm} = \boxed{183.774\ mNm}$$

Using the known full distance of travel of the lead screw (0.762m) and our target travel time of 1 minute, the motor speed was then determined.

$$Motor RPM = \frac{\frac{Distance}{Time}}{distance per revolution} = \frac{\frac{0.762m}{1 minute}}{0.00254 \frac{m}{rev}} = [300RPM]$$

With the required speed and torque known, the motor power was then determined.

$$P = \tau\omega$$

$$P = 183.774 \text{ mNm} \frac{1 \text{ Nm}}{1000 \text{ mNm}} * 300 \frac{\text{rev}}{\text{minute}} * \left(\frac{2\pi}{\text{rev}}\right) \left(\frac{1 \text{ minute}}{60s}\right) = [5.8W]$$

The calculation was performed similarly for the horizontal motor. The spreadsheets detailing the calculations are shown next.

Table 13: Vertical Motor Selection Spreadsheet

Torque Requirement Calculations			
	Mass Each (kg)	Quantity in Assembly	Extended Mass
Gripper Mass			
structure, servos, wiring, etc.	1		1 1
Horizontal Section Mass			
Guide rods - 3/8" Steel, 30" Length	0.43		4 1.72
End Plates - Aluminum, 1/4" thick, 4"x4" rectangle	0.18		2 0.36
Translating Platform- Aluminum	0.63		1 0.63
Lead Screw	0.4		1 0.4
bolts, screws, wires, etc.	0.5		1 0.5
Motor, Motor bracket, Flex Coupler	0.25		1 0.25
Counter Weight (mass centered at 6" from center)			8.625
Vertical Platform Mass			
Translating Platform 6x6	1.23		1 1.23
		Total Platform Mass moved by Vertical Screw	15
		Factor of Safety	1.5
		Mass Allowance	20
		W (Total Newtons of Force)	196.2
		L - Lead (meters)	0.00254
		dm - Mean Thread diameter (meters)	0.01016
		alpha_n (rad)	0.253072742
		friction (estimated)	0.1
		Torque Required for Vertical Stage (mNm)	183.774
Speed Requirement Calculations			
		Full distance translation of platform (meters)	0.762
		Time allowed for full translation in one direction (minutes)	1
		Linear distance moved due to one rev of screw (m/rev)	0.00254
		Required leadscrew RPM	300
		Motor Power (Watts)	5.8

Table 14: Horizontal Motor Selection Spreadsheet

Torque Requirement Calculations	
	Force (Newtons)
Horizontal Forces	
Friction, jamming, etc.	44.48
Other	22.24
Total Expected forces on Screw	67
	15.06295
Factor of Safety	1.5
W (Total Newtons of Force)	101
	22.70683
L - Lead (meters)	0.00254
dm - Mean Thread diameter (meters)	0.01016
alpha_n (rad)	0.253072742
friction (estimated)	0.1
Torque Required for Horizontal Stage (mNm)	95
Speed Requirement Calculations	
Full distance translation of platform (meters)	0.6096
Time allowed for full translation in one direction (minutes)	0.75
Linear distance moved due to one rev of screw (m/rev)	0.00254
Required leadscrew RPM	320
Motor Power (Watts)	3.17

Using these required speed, torque, and power requirements and keeping in mind that the AGSE batteries are 12V, the motors were chosen.

The Faulhaber 2237S012CXR with 26A 16:1 gear head was chosen and is shown below.



Figure 147: Faulhaber 2237S012CXR Motor



Figure 148: Motor with Gearhead Attached

The motor with the gearhead has the following properties.

$$\tau_{continuous} = 12 \text{ mNm}; P = 8.1 \text{ W}; \omega_{continuous} = 4450 \text{ rpm}$$

With the 16:1 gearhead, the torque is increased at the expense of the continuous speed.

$$16 * \tau_{continuous} = 16 * 12 \text{ mNm} = 192 \text{ mNm} = \tau_{gearhead}$$

$$\frac{\omega_{continuous}}{16} = \frac{4450 \text{ rpm}}{16} = 278.125 \text{ rpm}$$

However, at the very worst case, only a max of 183.8 mNm of torque can be required at any time, so the lowest continuous speed can be assumed to be slightly higher, yielding sufficient RPM to make the travel time low enough for the team-designed requirement.

With a torque requirement of 183.8 mNm and a speed requirement of 300 rpm, it can be shown that the current draw is less than the max-rated current draw of the motor.

$$P = \tau\omega$$

$$P = 183.774 \text{ mNm} * 300 \text{ RPM}$$

$$P = 183.774 \text{ mNm} \left(\frac{1 \text{ Nm}}{1000 \text{ mNm}} \right) * 300 \text{ RPM} \left(\frac{2\pi \text{ rad}}{1 \text{ rev}} \right) \left(\frac{1 \text{ min}}{60 \text{ s}} \right)$$

$$P = 5.77 \text{ W} = IV$$

$$5.77W = I * 12V$$

$$I = 0.481 \text{ A} < I_{continuous} = 0.9A$$

Similarly for the horizontal stage, the motor provides more than double the torque required for the horizontal stage (95 mNm). With this allowance in torque, the speed at which we run the motor can likely be increased, to be determined through testing.

$$P = \tau\omega$$

$$P = 95 \text{ mNm} * \left(\frac{1 \text{ Nm}}{1000 \text{ mNm}} \right) * 320 \text{ RPM} \left(\frac{2\pi \text{ rad}}{1 \text{ rev}} \right) \left(\frac{1 \text{ min}}{60 \text{ s}} \right)$$

$$P = 3.18 \text{ W} = IV$$

$$3.18W = I * 12V$$

$$I = 0.265A < I_{continuous} = 0.9A$$

Thus, under the worst case operating conditions for both the horizontal and vertical stages, the current draw is significantly less than the rated current from the thermal limit for continuous use, meaning we have no risk of burning out our motors during testing. In addition to these calculations, the normal operating conditions of each stage is shown to be within the continuous operating range of the motor based on the motor curves (without the gearbox). This is shown next.

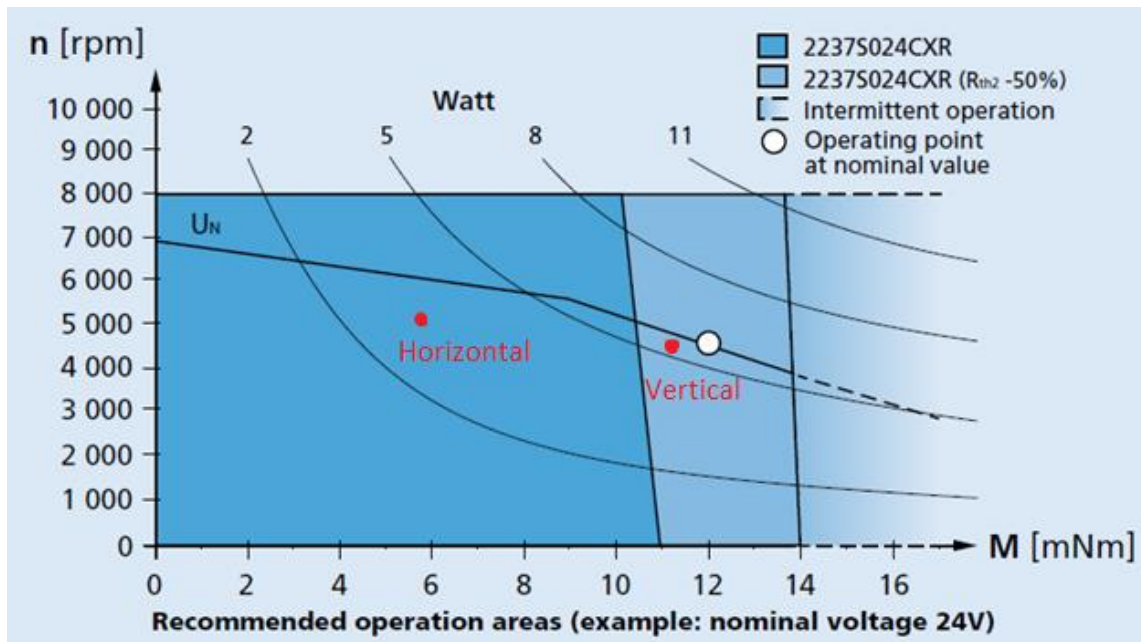


Figure 149: Speed vs. Torque for 2237S0xxCXR series Motor with our Motors' Operating Conditions

5.5.2.2 AGSE Table

The AGSE rests on a 24 x 12 inch aluminum table designed specifically to accommodate the rocket launch rail and the AGSE's main rotational actuation. The table is supported by four

adjustable 5/8-inch thick steel legs. Each leg has a foot at the base with movable plastic underside to accommodate discrepancies between the operational plane of the rocket's payload bay and the ground.

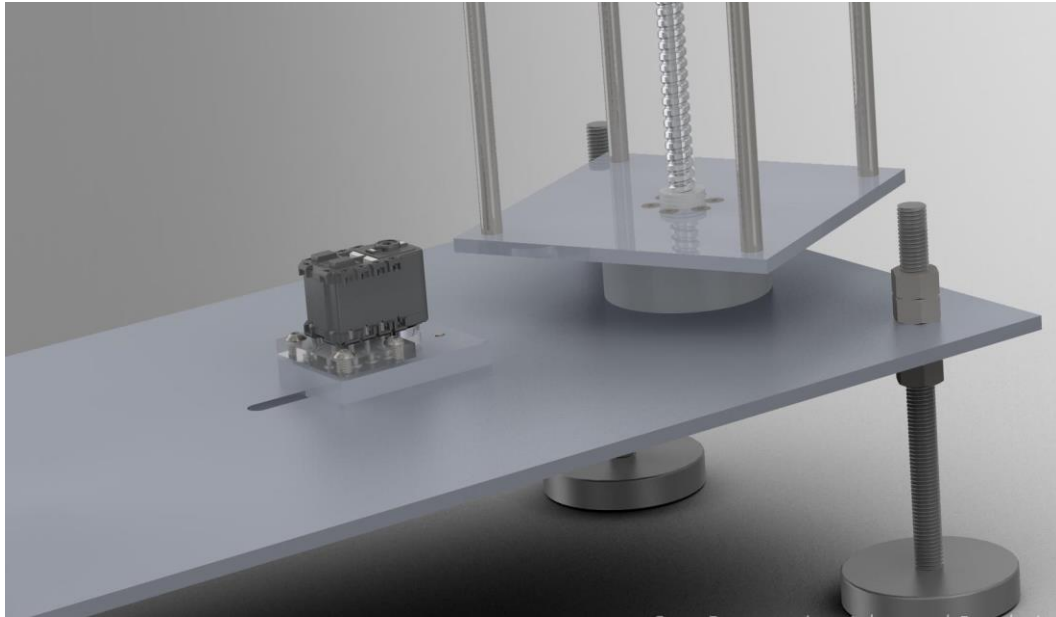


Figure 150: CAD Rendering of AGSE base featuring acrylic servo mount (left) and adjustable length legs

These two support features provide the support for the AGSE. The functional elements of the table begin with the Dynamixel AX-12A servo mounted off center of the table's surface. The servo is connected to an adjustable sled that allows us to create tension in an under-mounted timing belt-pulley system that drives the main rotation of the AGSE tower

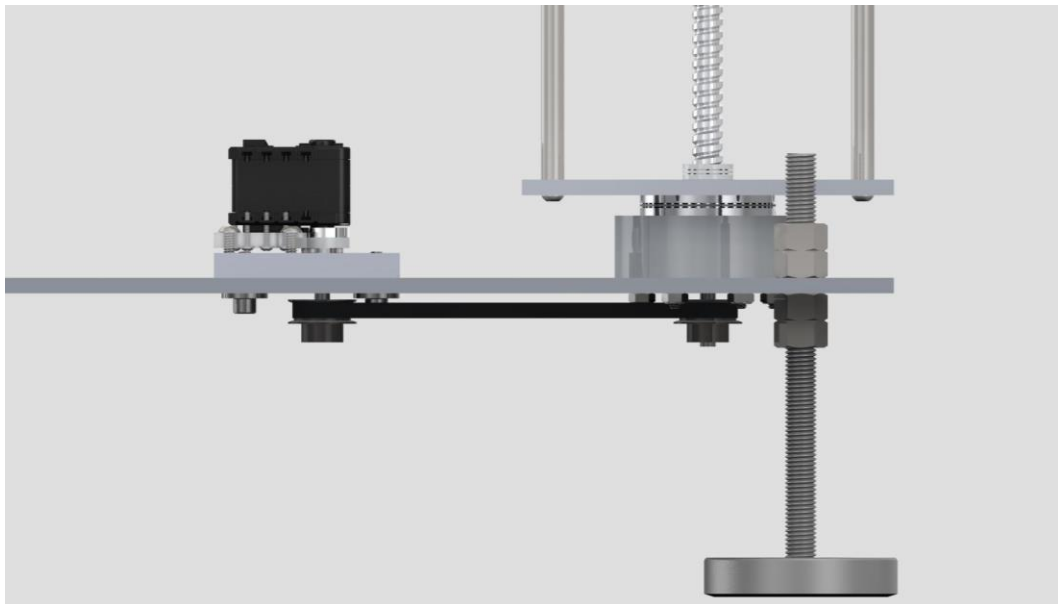


Figure 151: AGSE Render of profile view of AGSE table. Servo connects to pulley and timing belt, rotating the bottom pulley to spin the main AGSE tower.



Figure 152: AGSE Table Underside, featuring pulleys and timing belt to drive main rotation

The pulleys are supported by multiple rotary and thrust bearings in order to provide smooth rotation with limited stress on the system. This system spins the AGSE's base plate, providing full rotation about the AGSE's center axis. This system is a substantial change from the previous iteration, with most structural elements made of aluminum, eliminating the potential risks of having many acrylic elements as structural members. Additionally, the pulley system allows the AGSE base to be supported by roller bearings, spaced out to prevent substantial moments. The original AGSE design, which featured a CrustCrawler turntable base, proved too shaky to

provide reliable position feedback of the end effector, and was replaced by this more reliable system. Construction of elements of this system is outlined in section 5.5.4.1.1 *AGSE Table*.

5.5.2.3 AGSE Tower

The AGSE vertical tower is approximately 32 ½ inches tall, featuring the same four-guide-rod, center actuation featured in the previous iteration. However, the Trossen Robotics linear actuators have been replaced with a lead screw design similar to that of the payload. The driving motor is located with a rotary encoder on top of the tower, offering feedback to the motion of the AGSE. For more information regarding the sizing of this motor, see Section 5.5.2.1 *Actuators*. For the construction process specifications see 5.5.4.4 *Tower Assembly*.

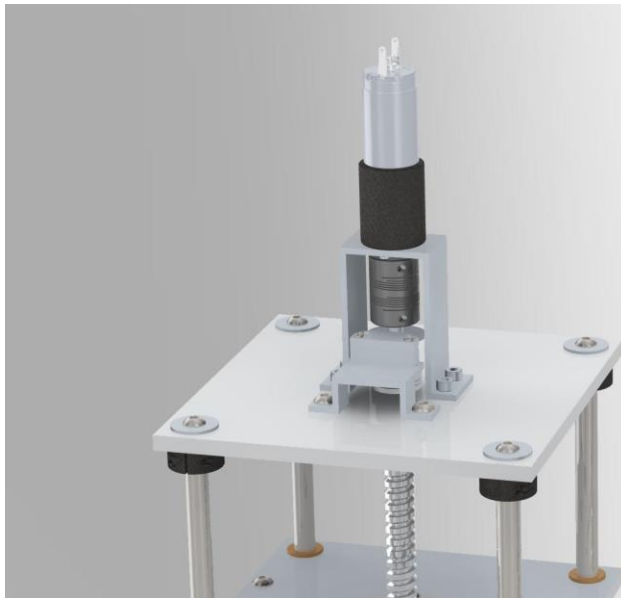


Figure 153: CAD Render of the AGSE Tower encoder and motor mount

The AGSE tower consists of both the assembly of the vertical section and the horizontal lead screw system that allows the AGSE to actuate both of its two carriages. The AGSE has a set of four steel guide rods to support the movement of both of its actuating lead screws. These guide rods are bolted to plates at either end to maintain accurate spacing and prevent drifting of the guide rods position. Lead screws are both shortened and turned down sections of commercially available ½ inch 303 stainless steel lead screws. They are coupled at the motor facing ends (top of the vertical tower and interior of the vertical carriage) to motors that are able to rotate them within press-fit roller bearings at either end. By rotating the lead screw assembly we are able to move the corresponding lead nuts, which are attached to the vertical and horizontal carriages of the AGSE.

At either end of both lead screw sections (the horizontal and vertical sections) limit switches may be placed to locate the AGSE immediately. To locate either carriage of the AGSE, the carriage may be actuated until it reaches its limit switch. Using this known location the feedback provided by the end-mounted rotary encoders provide more precise location information.

5.5.2.4 AGSE Vertical Carriage

The vertical carriage is moved by a lead nut that pushes the two parallel aluminum plates that make up its top and bottom. These $\frac{1}{4}$ inch aluminum plates support the horizontal actuation of the AGSE and house its driving motor. The horizontal guide rods are affixed to the vertical carriage that holds the main cantilever moment of the horizontal system. These rods are threaded through the carriage and affixed to the back plate of the carriage, alleviating much of the moment created by the AGSE gripper assembly.

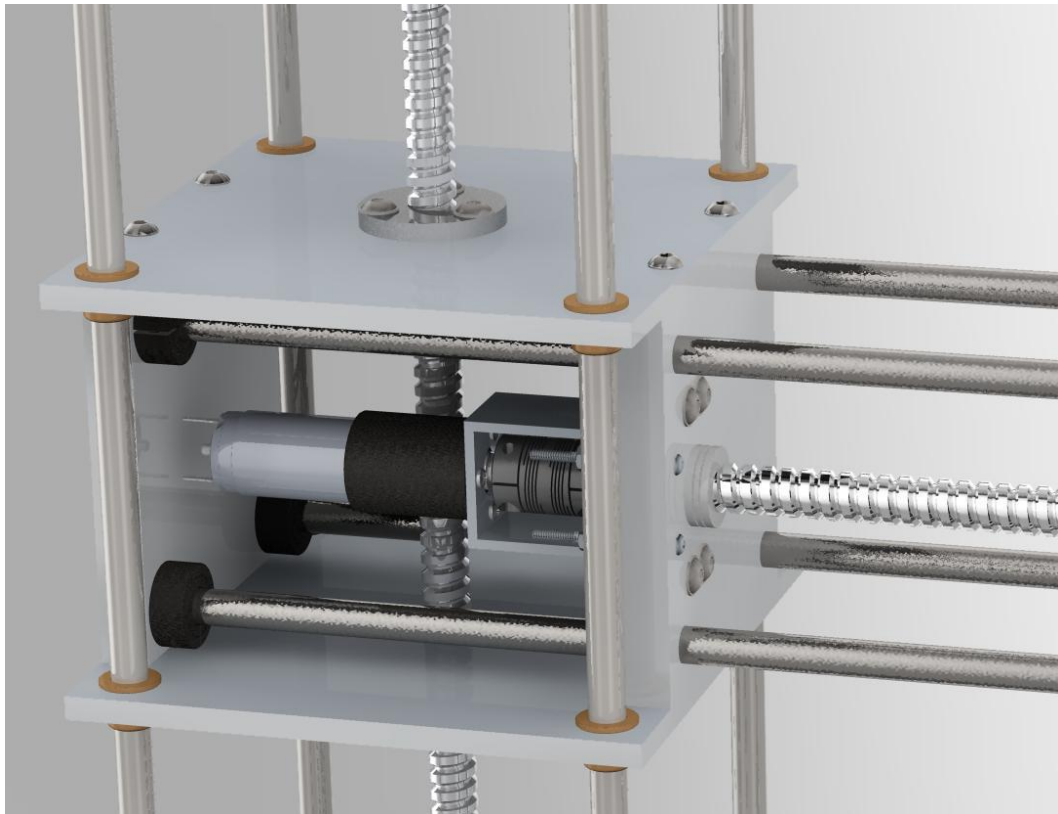


Figure 154: CAD Render of the AGSE vertical carriage.

The aluminum plates are supported on the guide rods by brass bushings that assist in smooth motion along the steel guide rods. The bushings are reamed and fit to the guide rod width via a press fit into the aluminum plates. With the supporting lead nut's movement, the vertical carriage has approximately 24 inches of throw, substantially more than the 12 of the previous iteration. This has been accomplished while cutting the weight of the Trossen Robotics linear actuators. The motor and gear head system used to drive the vertical carriage is located atop the AGSE tower.

5.5.2.5 AGSE Horizontal Carriage

The horizontal carriage consists of two aluminum plates with press fit bushings to promote movement along the horizontal steel guide rods. These rods are set 3 x 3 inches apart, and allow approximately 16.4 inches of throw for the 2 inch thick horizontal carriage. The carriage itself

supports several acrylic plates that space the aluminum pieces apart, decreasing any concentrated shear on any particular location along the guide rods. A lead nut placed off center of the horizontal plate's center allows the horizontal motor and gear head, mounted inside the vertical carriage. This nut may be pushed along the horizontal lead screw to drive the primary radial motion of the AGSE (Figure 155)

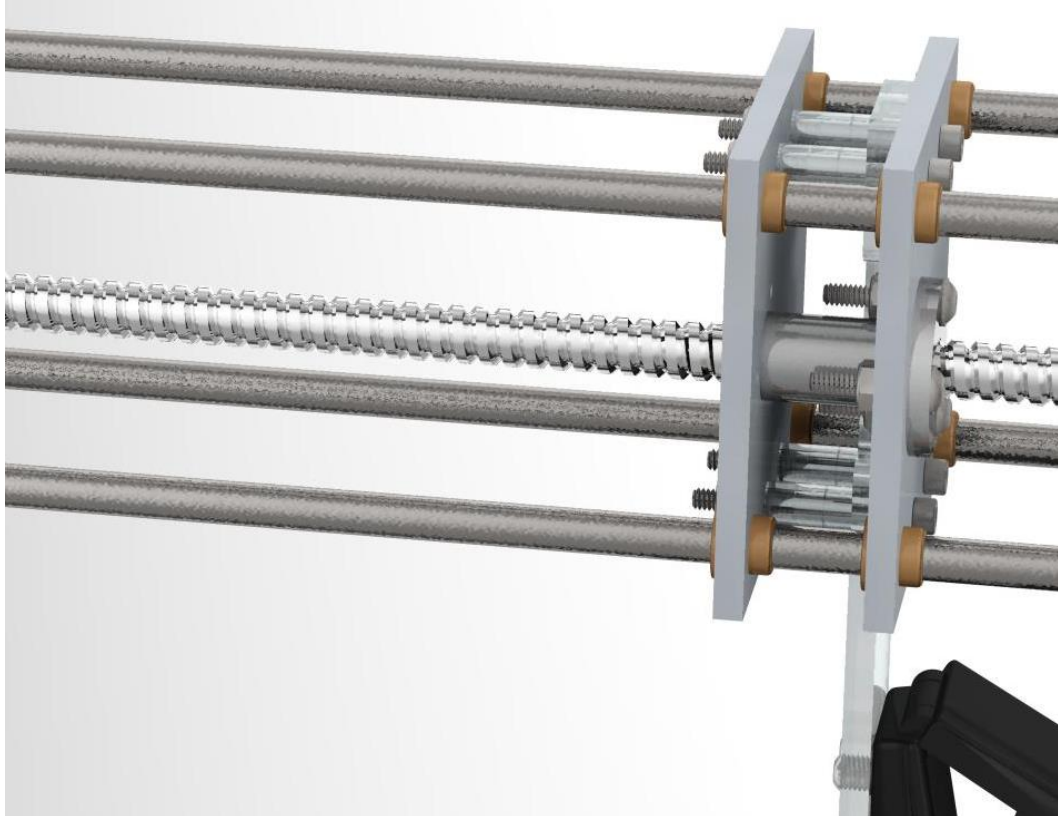


Figure 155: CAD Render of the horizontal plates, separated by acrylic plates

These acrylic plates drop down as a wrist to the AGSE manipulator. On the acrylic wrist, a Logitech C920 webcam is mounted, facing down at the gripper to serve as the optical sensor for the AGSE (Figure 156). The wrist terminates in a custom bracket attached to one of the AGSE's three Dynamixel AX-12A servo motors. This servo allows for the orientation of the AGSE's end effector, providing support for a dynamic set of payload orientations on the ground. For construction methods of the horizontal carriage, see Section 5.5.4.3.1 Horizontal and Vertical Carriage Assembly.

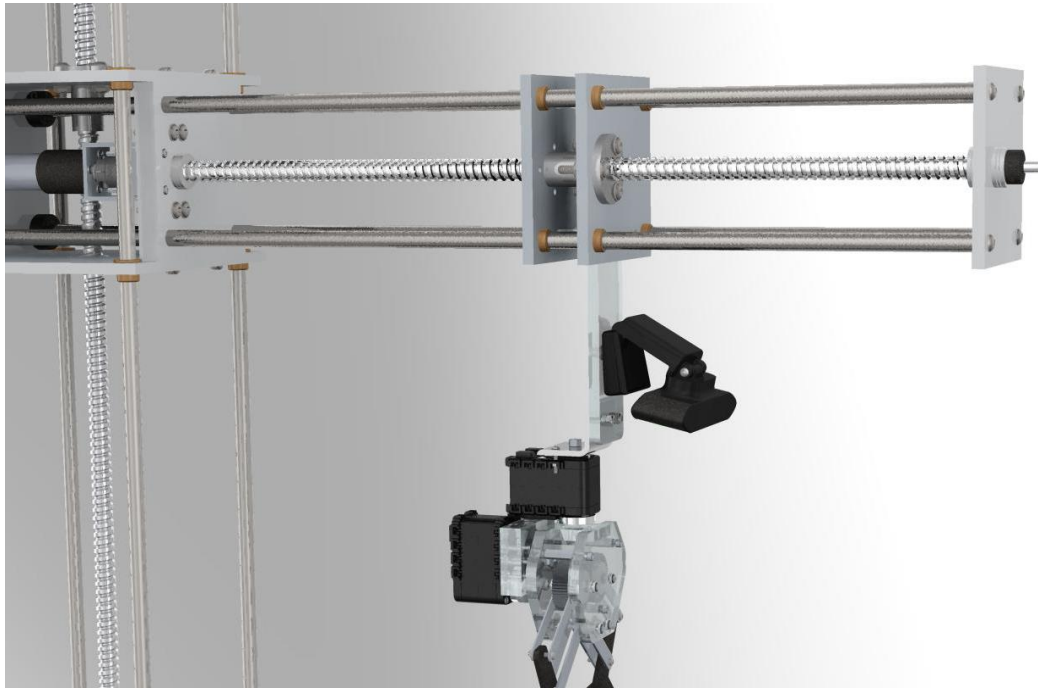


Figure 156: CAD Render of camera mounted on AGSE wrist dropdown from horizontal carriage

5.5.2.6 Manipulator

The original design of the AGSE used a commercially available CrustCrawler actuator, modified to include a four-phalange design for increased reliability. Though this design was heavily modified during the development process, the team has opted to remove it entirely, developing our own functionally similar but more structurally sound version. To decrease gear slippage, we have added acrylic support structures and locking nuts to the rotary gear connections. The Hitec servo provided with the order was replaced with a Dynamixel AX-12A servo that has significantly more power and daisy-chains well with the other servo motors in our system.

The body of the gripper consists of the gear set from the CrustCrawler gripper mounted onto two acrylic plates, cut to protect the gear assembly from the outside while providing two structural points to hold gear elements in place, thus limiting the changes of gear slippage. The driving gear is secured to the output shaft of the AX-12A servo motor via a locknut and screw combination set into both acrylic plates. The casing itself connects to the wrist-mounted AX-12A through a series of four crossed holes that provide a strong connection to the rest of the AGSE body.

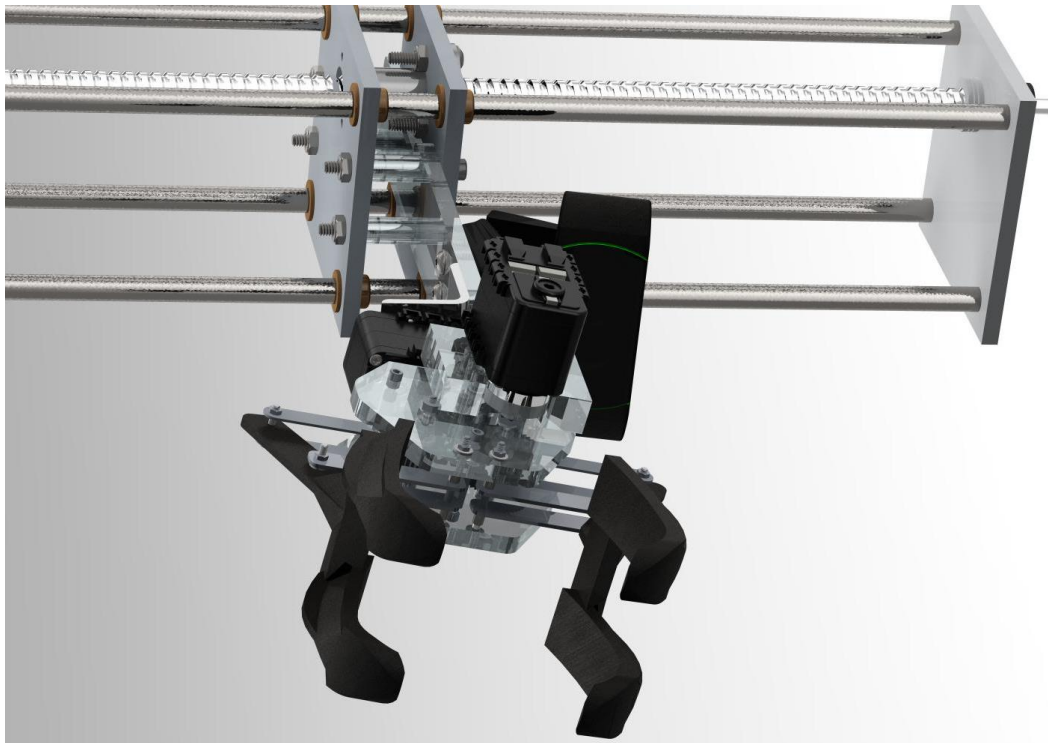


Figure 157: CAD Render of underside view of AGSE gripper and horizontal carriage. Camera is mounted above the gripper on the acrylic-mounting wrist.

Additionally, we have redesigned the phalanges of our gripper to better secure the payload. Our gripper uses a four-prong design that is able to hold the payload just short of both ends to prevent tipping. The prongs are made of rapid-prototyped ABS plastic and are curved at the end to scoop the payload up off the ground during gripper closure. Our testing protocols have allowed us to rapid prototype and test a number of phalange designs, allowing us to select a gripper that is able to gently scoop the payload while still securely holding it for transport. Additionally, to provide added security to the gripping ability of the AGSE, each phalange is lined with $\frac{1}{4}$ inch of foam, allowing the AGSE to maintain a semi-light grip on the payload without risking slippage.

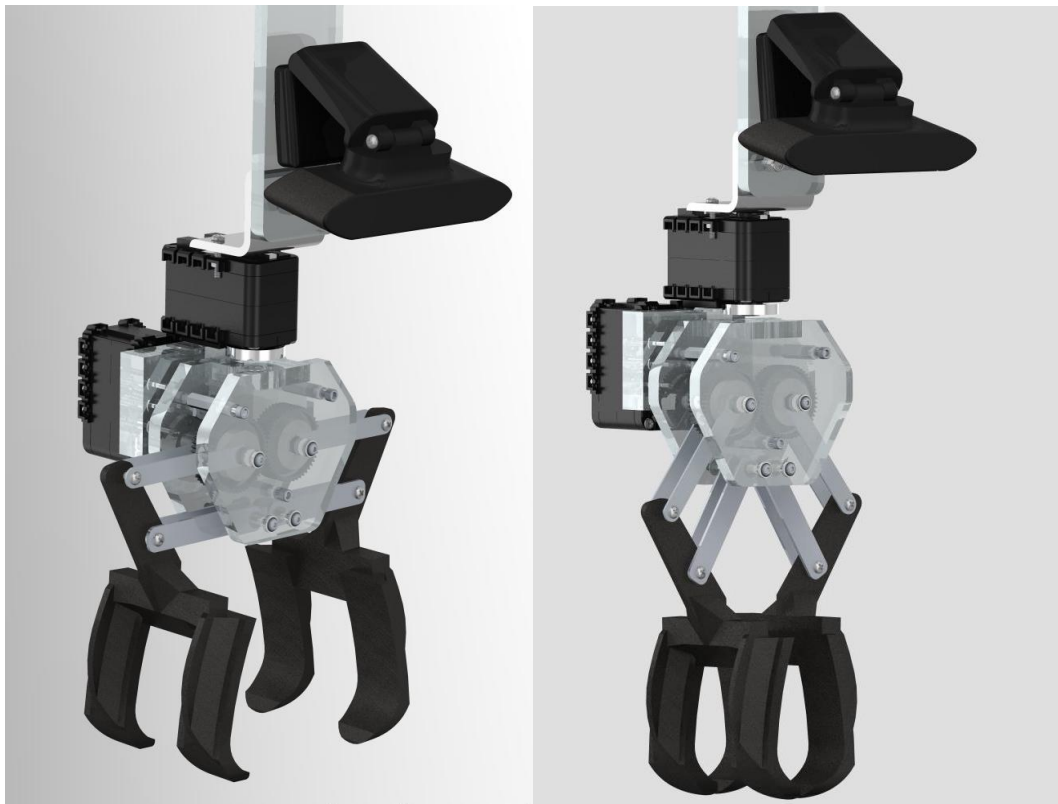


Figure 158: CAD Render of open (left) and closed (right) gripper configurations.



Figure 159: Foam Lined Gripper Phalange

5.5.2.7 Electronics and Software

5.5.2.7.1 Overall Goals of AGSE System Software

The AGSE system software's operation goals are outlined below:

- Verify Subsystem Functionality
- Detect the sample from an image
 - Object position
 - Object relative orientation
- Detect the payload bay from an image
 - Payload bay position
 - Payload bay relative orientation
- Navigate to sample
- Navigate to payload bay
- Open payload bay
- Verify sample acquisition
- Verify sample insertion
- Close payload bay
- Minimize sample hold time

5.5.2.7.2 Motivation for Image Processing

Given (1) the prevalence of cameras and imaging hardware, which has (2) further increased the availability of high-performance image processing hardware and software, and (3) the versatility provided by imaging-based sensing, we have chosen to use a camera combined with image processing hardware and software as the base of the sample detection subsystem of the AGSE. This camera integrates directly with our main processing board, the NVIDIA Jetson TK1. Furthermore the Jetson, designed to add high fidelity image processing to robotics applications, contains 192 parallel GPU cores, which support both OpenGL and CUDA parallel programming and image processing applications. Parallel image processing, segmentation, and object detection algorithms have been heavily researched and developed using both CUDA and OpenGL, and provide us with a large base of users and application code.

5.5.2.7.3 Sample Description

The sample will be of an overall cylindrical shape. When viewed from all unoccluded non-coaxial angles, the sample will have as part of its defining shape outline two straight lines. These lines' relative angle, theta, will converge to 0 (parallel) as ϕ , the angle between the view vector and the sample axial vector, approaches $\frac{\pi}{2}$. At all other angles the lines' infinite extrusions will intersect and produce θ . The θ in image space provides the system with enough information to create the inverse perspective transform, which produces from theta the camera-space ϕ , providing the angle between the camera and the sample's axial vector. Furthermore, we can optionally improve the sample detection by making one of two assumptions about the color of the sample. Either we can assume the sample to be of uniform diffuse color, or we can assume the sample to have some defined pattern to the color of its surface.

5.5.2.7.4 Relevant Object Detection Methods

The main classes of image-based object detection and segmentation we have available utilize as their base functions one or more of the following: (1) color segmentation, (2) depth segmentation, (3) edge segmentation, (4) line segmentation. Color segmentation in its basic form assumes that an object has a uniform diffuse color, which is distinct from the background of the image. Depth segmentation, in its basic form, assumes that an object has a uniform perceived depth or perceived depth profile which is distinct from the background depth or depth profile of the image. Edge segmentation in its basic form segments the image using a combination of color and contrast, producing edges between each segment of the image. Line segmentation can be an extension of edge segmentation, which filters out all segment edges whose straight lengths fall below some threshold.

5.5.2.7.5 Chosen Object Detection Algorithms

Given the image-space sample description provided above, we have chosen to use line segmentation as the base of the sample detection software subsystem of the AGSE. Additionally, given the two possible assumptions that can be made about the sample's diffuse color, we can integrate color based object detection based on a color profile for the sample. This technique can be utilized to check that the screen-space area between two detected lines conforms to the sample's color profile (which may be a pattern or solid color), and therefore provide a higher degree of confidence for sample detection.

5.5.2.7.6 Algorithm I/O

The edge detection and color segmentation algorithms both take as input the raw camera image sample. The output of the edge detection algorithm is a binary image where any non-zero value marks an edge between two different segments of the image. The output of the color segmentation is a segmented image in which all pixels of a detected object (of a certain color or color profile) are replaced with the color or color profile of the object. The output of the edge detection algorithm is used as the input of the line detection algorithm. The line detection algorithm outputs the same type of binary image, except any non-straight edges falling below a certain straightness threshold will have been filtered out.

5.5.2.7.7 Modifications to OTS Algorithms

Because there may be occluding objects in the sample detection space, such as rocks, grass, or possibly man-made objects, we may, for improved sample detection capability and more versatility with respect to sample location, modify the chosen sample detection algorithms described above. Such a modification may include changing how the results from the different (orthogonal) sample detection algorithms are weighed in the calculation of detection confidence. Alternatively, the modification may adapt the off-the-shelf (OTS) algorithms to adjust their internal parameters for line/object segmentation. Such modifications may be required in the case of large numbers of partially occluding objects or in the case of large changes in contrast or light in the captured images. Finally, these modifications can be autonomously integrated into a state-machine that reconfigures these parameters to provide the highest sample detection confidence.

5.5.2.7.8 Trajectory Planning

By correctly modeling the linkages and operational limits of the AGSE arm using the inherent encoding of the selected servo motors, control of the robot can be accomplished using the inverse kinematics and base reference frame transformation using the visual feedback provided by the camera. Once recognition of the object's position relative to the base of the robot arm is found, visual servoing will provide the basis of autonomous movement from the current position to the required position to enclose the center of the payload cylinder. Similarly, with a recognized trajectory between the base of the AGSE and the rocket payload, the AGSE will be able to deposit the payload in the bay and retract its manipulator. The points on this path will be established via the computer vision provided by the USB cameras. Travel between these points should be relatively simple, minimizing the unnecessary fluctuations in velocity or acceleration. With preprogrammed recognition of the payload deposit procedure, the robot will be programmed to avoid any sort of collision with the rocket by altering the kinematic null space of its operational workspace. By adding this precaution, the robot should be able to pick up, move, and deliver the payload without damaging or colliding with the rocket in any way.

5.5.2.8 Power

We have chosen 2 12V sealed lead-acid batteries which will be configured in series to power the AGSE. We are using an off the shelf DC/DC switched mode power supply (SMPS) to provide high efficiency conversion from the combined battery voltage to the 12V regulated supply which powers all of the AGSE systems. The batteries and power supply will be protected and mounted on the base plate of the AGSE, and the weight of the batteries (8 lb each) will help ensure stability of the AGSE during all of its operations. These batteries have enough stored energy (12Ah each) to power the AGSE at full load for multiple hours. The dc/dc converter has protection circuitry to protect the AGSE from short circuits, overloads, overvoltages, and incorrect input polarity. Since the AGSE has been determined to not require more than 6A under maximum load, the 8.4A continuous supply capability will provide ample power to the system. The 12V output of this power supply is routed to all of the main AGSE systems: (1) the Jetson, (2) the network switch, (3) the user interface panel, and (4) the motor control board. The motor control board's H-bridges use this 12V power to provide power to the 12V servo motors and the 12V linear actuators.

5.5.3 User Interface Panel

The User Interface Panel (UIP) acts as the main monitoring, safety, and—if needed—control device for the AGSE. It includes features required by NASA such as the pause switch and the master “on” switch while also including extra, team-designed features, such as a live feed of the camera-vision of the AGSE and auditory feedback. The UIP is hardwired to the control board of the AGSE, satisfying the NASA requirement.

The renderings of the CAD design of the UIP are shown next. The UIP was modeled after the Apollo DSKY, using missile switches and various state lights.



Figure 160: Top-Down View of UIP

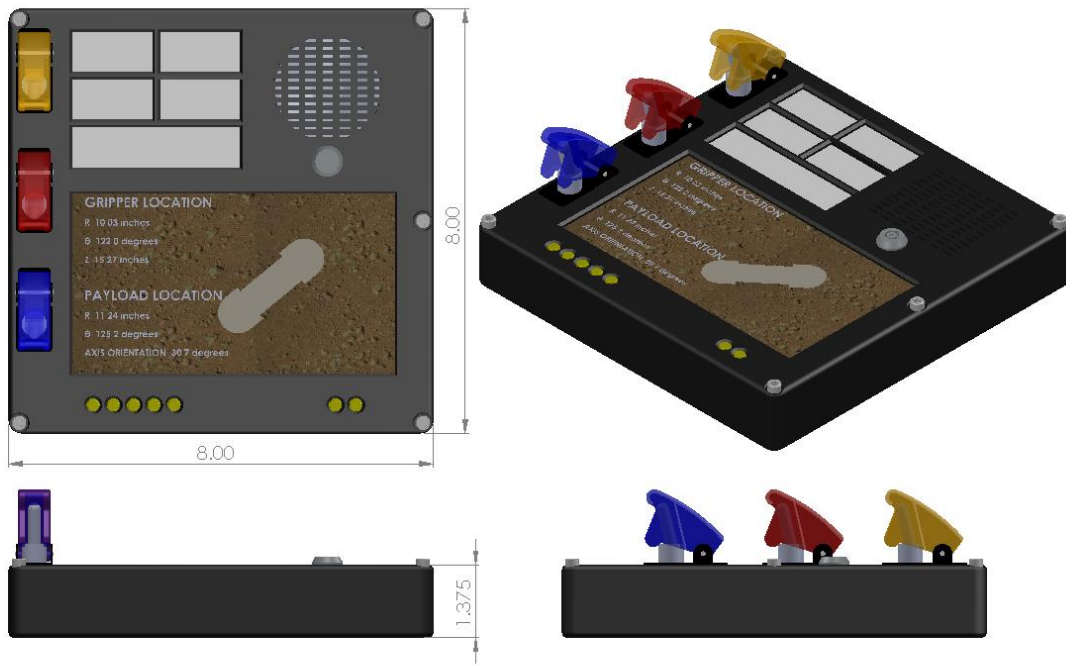


Figure 161: Different Views of UIP CAD with Dimensions

The AGSE system monitors at all times a pause switch located on the UIP (the missile switch with the yellow shield). The activation of this pause switch, read by the main AGSE control

board will send the entire system into a PAUSED state. During this state, feedback will be provided to the user in the form of a solid amber LED. When the AGSE is unpause, the LED blinks at 1 Hz. The panel houses the master switch as well (the keyed switch), which powers on and off the entire AGSE. There are also two additional user input switches that provide a means of adding new feedback, which will be implemented as testing progresses.

The code has been designed to respond immediately to the activation of the pause switch, and engineered to save its current state for the resuming of correct operation upon exiting the PAUSED state. By minimizing the latency for communication between the subsystems of the AGSE we can provide proper propagation of the PAUSED state transition to all parts of the system to maximize safety.

Finally, an additional feature that was added is a live feed of the AGSE gripper camera. This is shown using a 7" LCD touchscreen mounted onto a BeagleBone Black. This screen can show more information about the AGSE's operation, such as the detected object and its orientation, the AGSE's current position and orientation, and what step of the retrieval process the AGSE is on.

Finally, there will be backlit acrylic plates with text that will provide clear visual feedback about current AGSE state along with auditory feedback through a speaker.

Shown below is an example of a screen that could be shown on the user interface. It shows the camera's detection of the payload bay and the sample as well. This screen is attached to the BeagleBone Black that controls the UIP.



Figure 162: Screen attached to BBB showing Payload Bay and Sample Detection

5.5.4 AGSE Fabrication and Verification

The final AGSE was constructed with the construction plan of the prototype AGSE in mind. The final design takes the functionalities of the prototype AGSE and improves upon them, including a large workspace, more efficient power usage, and more reliable movement. Before starting this model, prep work including sizing and cutting of aluminum plates, carriages, and platforms used in the AGSE, modification of the gripper, and improvement of the turntable was carried out. The construction process for the second AGSE design is outlined as a whole below and then in more detail in the following sections. Testing and verification of each of the subsystems of the AGSE has been completed, and final improvements on the total integration are being made on a daily basis.



Figure 163: Flowchart of Overall AGSE Construction

5.5.4.1 Prep Work

Prep work for the construction of the AGSE took the most time due to the required precision in machining all of the parts out of aluminum. This required extensive use of lathes and milling machines along with vertical and horizontal bandsaws, arbor presses, and various hand tools.

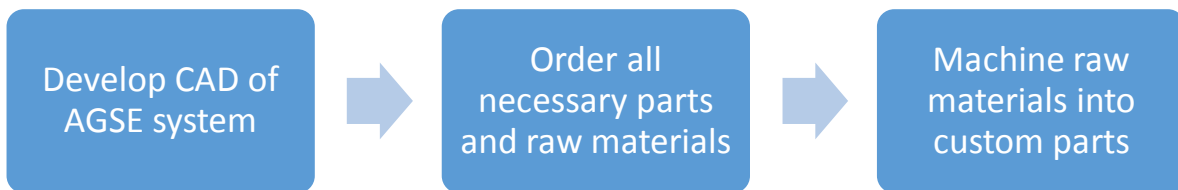


Figure 164: Flowchart of AGSE Prep Work

As seen in section 5.5.2: *Subsystems Overview*, CAD of the model was the first thing to be developed. Designing the structure in CAD before construction allowed us to know about and eliminate possible interferences or other impossibilities in the design of the AGSE. Using the dimensions of the various plates and shafts, machine drawings were then developed by the team in order to aid with the machining process. These can be found in section 10.6: *Machine Drawings*. In addition to the machine drawings themselves, a spreadsheet organizing the labor according to each team member's skills in the machine shop and schedule was created, outlining tasks and giving more detail on the tools necessary to complete each part. This spreadsheet also ranked the difficulty of making each part and assigned rankings of necessary precision needed when making one. Parts of the spreadsheet can be found in the appendix, section 10.5: *AGSE Machining Plan*.

Many parts were machined in the process. They are outlined in the next subsections.

5.5.4.1.1 AGSE Table

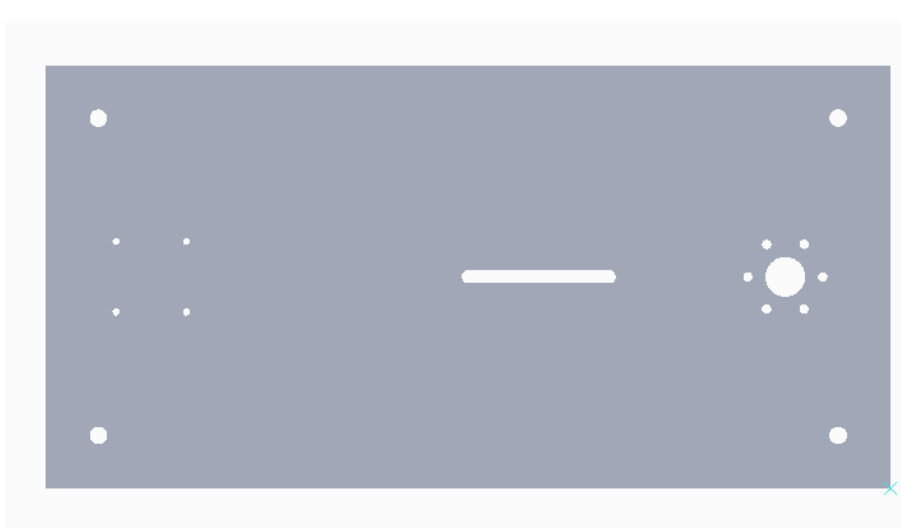
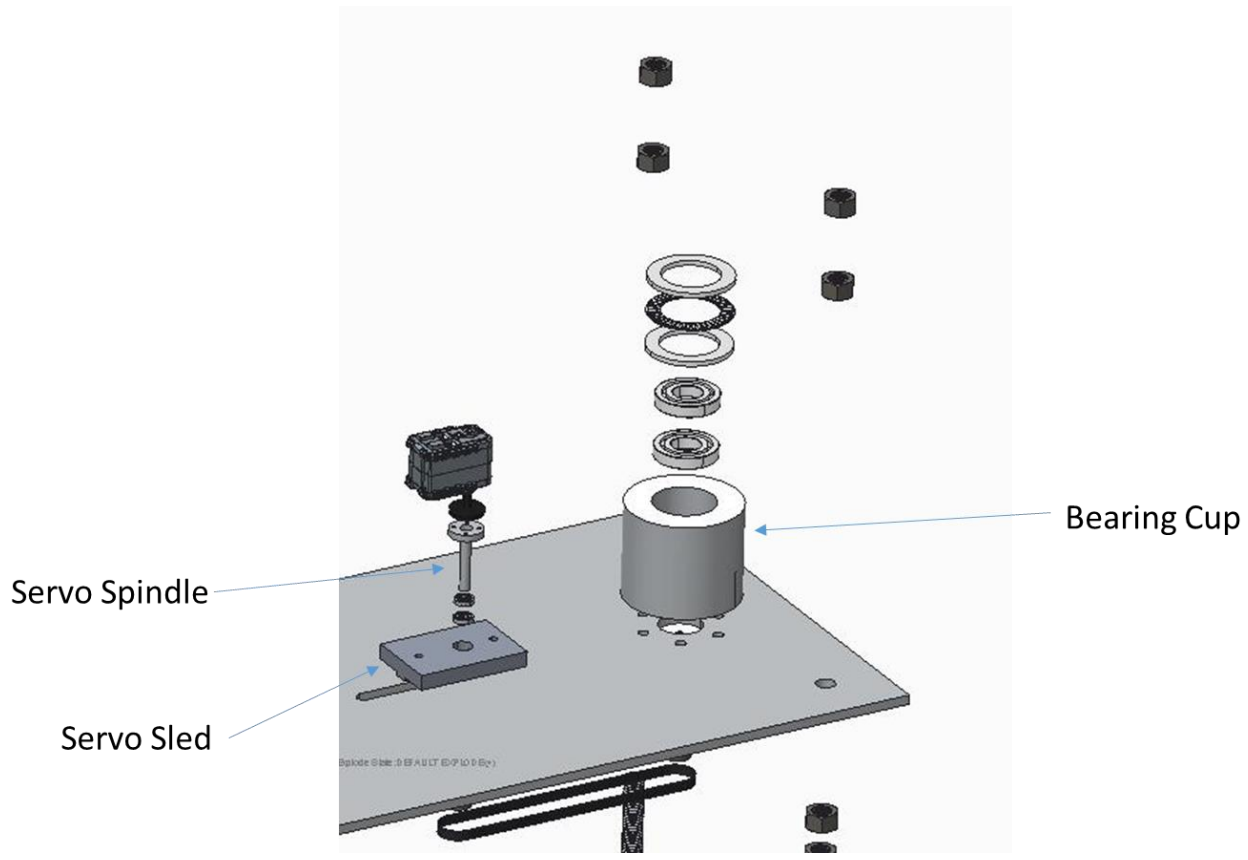


Figure 166: AGSE Table CAD

The AGSE table was machined using a mill out of a $\frac{1}{4}$ " thick aluminum 24" x 36" plate. There are four threaded holes in the four corners through which the AGSE legs are screwed through along with holes on the left side for the brackets supporting the rocket stand. The slot in the

middle acts as a hole through which the base rotation motor can be adjusted to properly tension the timing belt connecting it to the main shaft of the AGSE base. On the right is the hole through which the main AGSE shaft is fed through along with surrounding bolt holes for the bearing cup to be attached to the table.

5.5.4.1.2 Servo Sled

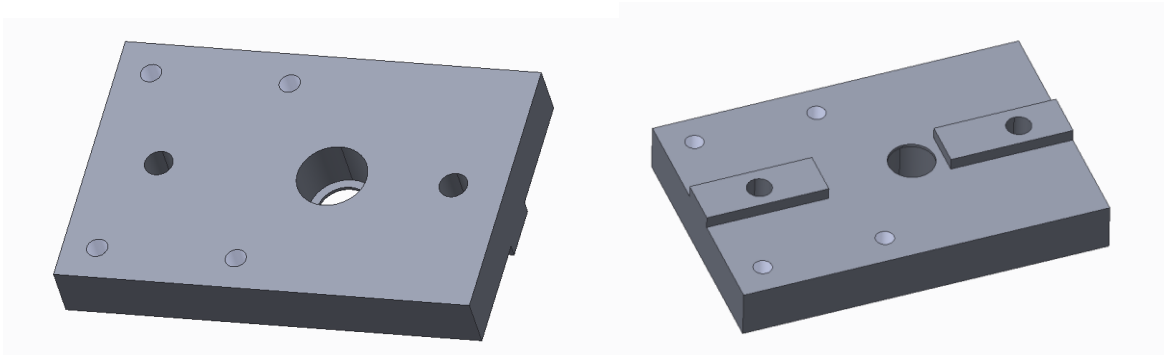


Figure 167: Top (left) and Bottom (right) view of Servo Sled CAD

Made with a mill, the servo sled is made of $\frac{1}{2}$ " aluminum and attaches to the base rotation servo on its top side using a laser cut acrylic adapter plate. It has a recessed through hole on which radial ball bearings are placed and through which the servo spindle is fed. On the bottom side, two ridges are used to locate it in its slot on the AGSE table. The two other larger through holes are used to fit clamping fasteners that hold the servo sled in place and tension the timing belt.

5.5.4.1.3 Servo Spindle

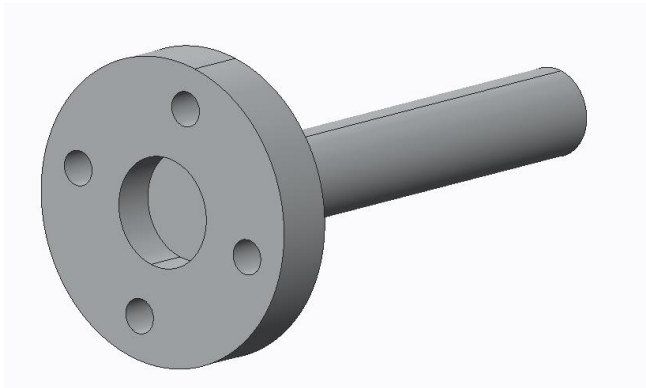


Figure 168: Servo Spindle CAD

The servo spindle was made on a lathe out of brass. The thinner part of this piece has a pulley mounted on it using a set screw. The wider part mounts onto the horn of the base rotation servo using the four through holes and four bolts. The recessed hole in the thicker part serves as a cavity for the screw attaching the servo horn to the servo shaft to sit in without interfering with the connection.

5.5.4.1.4 Servo Shaft

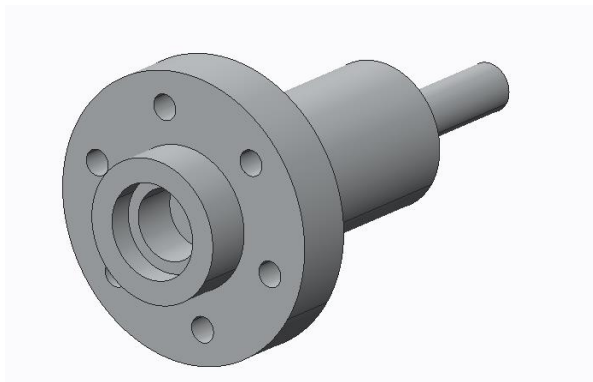


Figure 169: Servo Shaft CAD

The servo shaft acts as the main shaft for the rotation of the AGSE. It was machined out of aluminum on a lathe. The smallest end attaches to a pulley connected to the pulley on the servo spindle by a timing belt. Thus, rotation of the base rotation servo rotates the servo shaft and therefore the whole AGSE. The middle thicker part is press fit into radial ball bearings in order to minimize wobble of the AGSE tower. The six holes in the widest part attach the servo shaft to the AGSE baseplate. The recessed hole at the end of the shaft holds a radial ball bearing that keeps the vertical lead screw from deflecting angularly.

5.5.4.1.5 Bearing Cup

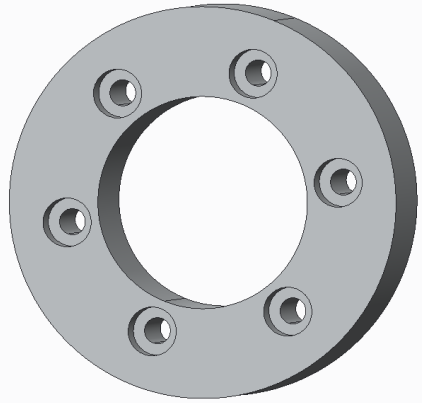


Figure 170: Bearing Cup CAD

The bearing cup surrounds the servo shaft and bolts to the AGSE table. It transmits any radial loads to the AGSE table and supports the weight of the AGSE tower under a thrust bearing. It was machined out of aluminum using a lathe, and the middle was drilled out using a drill bit on the lathe.

5.5.4.1.6 Plates

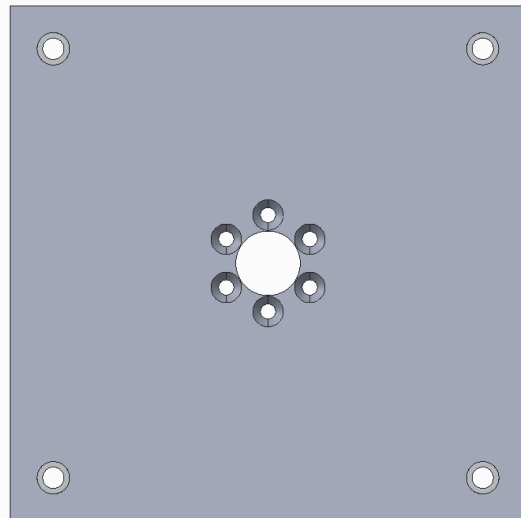


Figure 171: Baseplate CAD

The baseplate was machined out of $\frac{1}{4}$ " aluminum on a mill. The six holes surrounding the center lead screw hole are countersunk. The four holes at the corners are recessed for the vertical guide rods to fit into. The top plate is virtually identical except with holes for encoder and motor mounts and minus the six holes surrounding the middle hole.

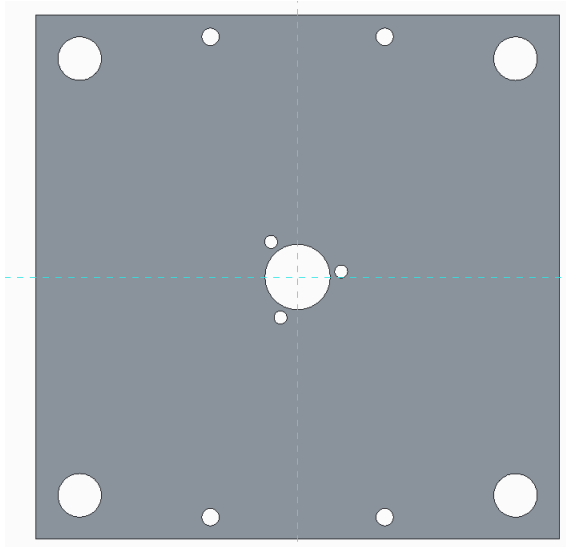


Figure 172: Vertical Carriage Plate CAD

The vertical carriage plate was machined out of $\frac{1}{4}$ " aluminum and contains four holes at the corners for bronze bushings to be press fit into for translation along the guide rods. The four holes at the top and bottom at the center of the plate allow the top and bottom carriage plates to be bolted into the carriage side walls. The middle hole and three holes surrounding it serve as the mount for the lead nut. These were made on the mill.

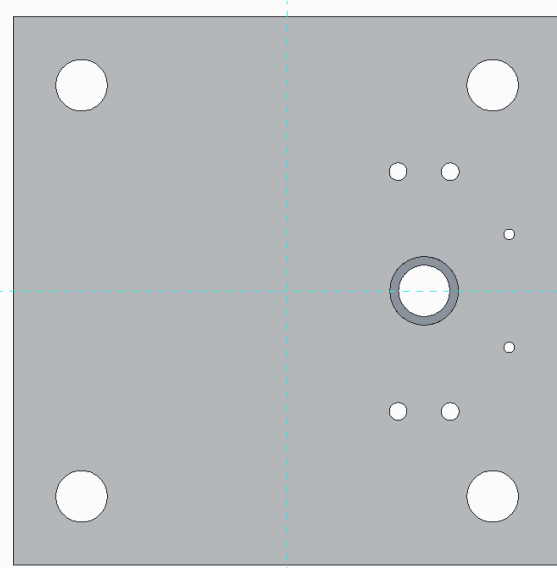


Figure 173: Side Plate CAD

The side plates were made of $\frac{1}{2}$ " aluminum (in order to be bolted into on its sides) on the mill. It contains holes for bushings for the horizontal guide rods, a hole for the horizontal lead screw with a recess for a radial bearing, and holes for the horizontal motor mount. The other side plate only includes the four corner holes. On the $\frac{1}{2}$ " sides of the plates, threaded holes were tapped so that the vertical carriage plates could attach to these side plates.

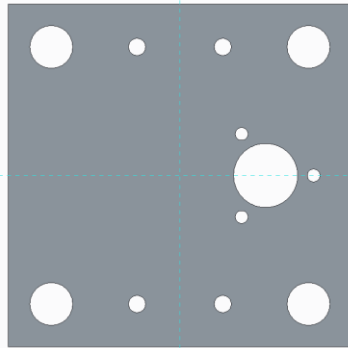


Figure 174: Horizontal Carriage Plate CAD

The horizontal carriage plates ($\frac{1}{4}$ " aluminum) are much like the vertical carriage plates. They include holes for the bronze bushings and mounting holes for the lead nut. It also includes four holes for a space piece which separates the plates, decreasing the moment applied by the off-center lead screw. The horizontal end plate is much the same except it only has the four corner holes and a hole for the end of the lead screw and for a radial bearing.

5.5.4.1.7 Lead Screws and Guide Rods

The lead screws and guide rods were all machined to size on the lathe. The guide rods' ends were tapped using a hand tap after being drilled into on the lathe. The lead screws' ends needed

to be turned down to standard diameters in order for bearings, encoder wheels, and shaft couplings to the motors to be attached.

5.5.4.1.8 Motor Mounts

Motor mounts were made for both the vertical and horizontal motors driving the lead screws in order to fit couplings, encoder wheels, and thrust bearings. The CAD of each is shown below.

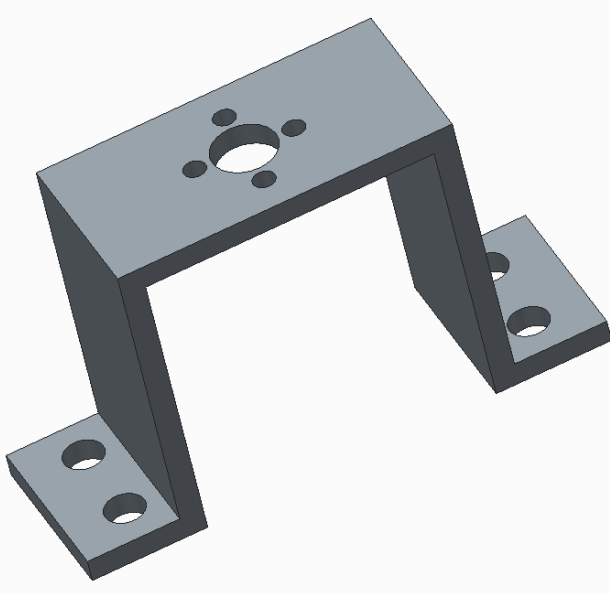


Figure 175: Horizontal Motor Mount CAD

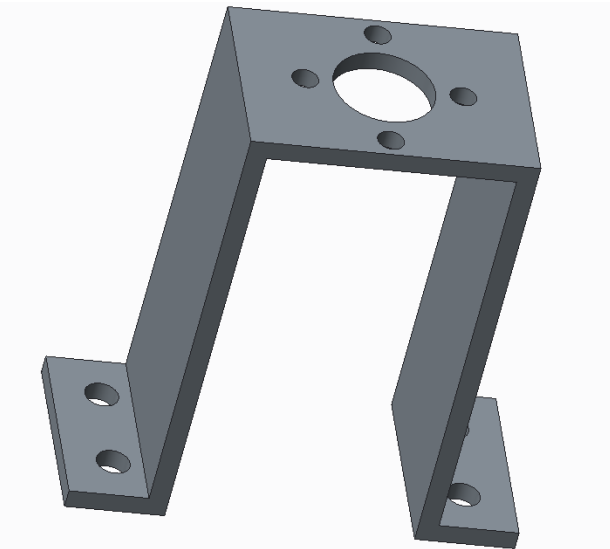


Figure 176: Vertical Motor Mount CAD

5.5.4.2 Table

5.5.4.2.1 Table Assembly

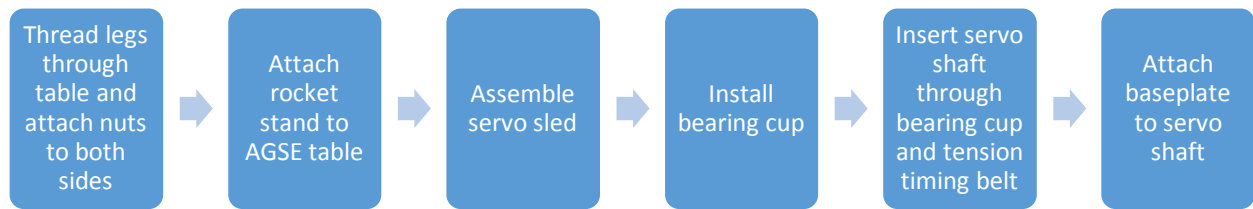


Figure 177: Flowchart of AGSE Base Construction

1. Screw the AGSE legs through the threaded holes in the corners of the AGSE table
2. Tighten nuts on both sides of plate on legs
3. Attach rocket stand to AGSE table using two aluminum L-brackets as support
4. Attach servo spindle to base rotation servo
5. Bolt base rotation servo to servo adapter
6. Fit radial ball bearings into servo sled
7. Bolt servo adapter to servo sled
8. Place servo sled in the slot in the AGSE table so that the spindle goes down through the table
9. Attach pulley to servo spindle using set screw
10. Bolt bearing cup to AGSE table
11. Fit two radial ball bearings into bearing cup, using a cut section of PVC in between them as a spacer
12. Fit the servo shaft through the radial bearings
13. Attach the other pulley to the bottom of the servo shaft at the same height as the first pulley
14. Fit ball bearing into top of servo shaft (where lead screw will fit eventually)
15. Place thrust bearing on top of bearing cup
16. Bolt AGSE baseplate to servo shaft
17. Place timing belt on the two pulleys and tension it using the bolts and wing nuts attached to the servo sled

5.5.4.2.2 Table Verification

Verification of the AGSE table and rotation system was performed by attaching the first AGSE prototype and to the new AGSE baseplate. The base rotation servo proved sufficient in rotating the tower, and rotational control was established. During the testing of the AGSE table with the first AGSE prototype, the full-scale rocket was placed on a launch rail identical to the launch rail used in our launch pad in order to verify the placement of the payload bay section relative to the AGSE. The old AGSE was able to retrieve a sample from a stand and place it into the rocket's payload bay. With the greater workspace of the new AGSE, this test confirmed the arrangement of the rocket relative to the AGSE tower.

Table 15: Verification and Testing of AGSE Table

Part/Functionality Tested	Method of Test	Results
Is the AX-12A servo sufficient for rotation of the AGSE base?	During the development of the other parts of the new AGSE, the first prototype of the AGSE was mounted onto the new AGSE table. Using the servo and the pulley system, base rotation was tested.	The AX-12A provided enough torque to be able to rotate the AGSE.
Can the table be easily leveled?	Using two levels at a corner of the AGSE table, the height of each leg of the AGSE table was adjusted until both levels indicated the table was leveled.	The table was able to be leveled.
Can the rocket on the launch rail rest on the rocket stand on the AGSE table?	The rocket was slid onto the launch rail and was laid onto the rocket stand on the AGSE table. The other end was supported by another stand.	The rocket and launch rail fit into the rocket stand on the AGSE.
Is the rocket within the workspace of the AGSE when placed on the table?	The rocket was placed on the AGSE rocket stand as stated above. Using the prototype AGSE (which has less of a reach than the new AGSE), a mock sample recovery was performed.	The prototype AGSE was able to reach the payload bay when mounted to the new AGSE base. With the new AGSE's reach being greater than the old one's, we confirmed the arrangement of the base with respect to the stand before even building the tower of the AGSE.

5.5.4.3 Vertical and Horizontal Carriages

5.5.4.3.1 Vertical and Horizontal Carriages Assembly



Figure 178: Flowchart of Vertical and Horizontal Carriages Construction

1. Bolt the horizontal motor onto the horizontal motor mount
2. Attach the shaft coupling to the motor shaft
3. Fit radial ball bearing into side plate
4. On outside of side plate, place a thrust bearing for the lead screw to be fed through
5. Feed lead screw through ball bearing and thrust bearing through side plate
6. Attach encoder wheel to lead screw shaft
7. Bolt horizontal motor mount onto side plate, attaching the shaft coupling to the lead screw shaft
8. Place sleeve bearings in freezer and then press fit them into the vertical and horizontal carriages (16 bearings)
9. Bolt side plates to vertical carriage plates on top and bottom
10. Attach lead nut to top vertical carriage plate
11. Feed horizontal guide rods through side plates
12. Slide horizontal carriage plates onto horizontal guide rods
13. Attach lead nut to the carriage plate farthest from the center of the AGSE
14. Place thrust bearing around end of lead screw
15. Plate horizontal end plate over thrust bearing and around the guide rods
16. Place another thrust bearing around the exposed end of the lead screw shaft fit through the end plate
17. Clamp these thrust bearings down using a shaft collar
18. Bolt down the guide rods to the plate using the tapped holes at the end of the guide rods
19. Mount the encoder onto the side plate the motor is attached to
20. Adjust the height and position of the encoder and encoder wheel so that the encoder wheel can freely spin within the encoder
21. Place shaft collars on the other end of the guide rods
22. Bolt through the other side plate into the tapped holes at the other end of the guide rods
23. Adjust the shaft collars to mitigate off-axis movement

5.5.4.3.2 Vertical and Horizontal Carriages Verification

The verification of this section of the AGSE focuses on smooth translation of the carriages along the guide rails. Tests under different loads are being performed—loads that cause moments on the guide rails and carriages which could possibly cause jamming. In addition, the off-axis placement of the horizontal lead screw is of high interest. This inherently causes momentary loading, so it is imperative the two horizontal carriages be placed at a distance from one another so that this moment is mitigated. Motor power must also be tested. Because the payload bay motor (a Faulhaber 1724A006SR motor with a 28:1 gearhead) performed better than expected in the payload bay, it was tested for potential use as the servo motor for the sake of saving room in the budget for other improvements.

Table 16: Vertical and Horizontal Carriage Verification and Testing

Part/Functionality Tested	Method of Test	Results
Do the horizontal carriages slide easily along the guide rods?	The horizontal guide rods were installed into the vertical carriage. The two horizontal carriages were then slid onto the guide rods and moved back and forth.	The carriages exhibited a significant amount of resistance when slid back and forth. As a result, the bushings were reamed out to 3/8" ID to minimize variability in the parts and remove any sharp edges in the bushings themselves.
Can the lead screw move the carriage when rotated by hand?	After press fitting the bushings into the horizontal carriage plates, the lead screw was installed. The lead screw, screwed into the lead nut, was then turned by hand.	The lead screw could be turned easily by hand, meaning that the bushings fit more nicely onto the guide rods after reaming.
Does the lead screw's off-center placement on the horizontal carriage assembly jam it?	A moment is applied to the horizontal carriage assembly by the off-center loading provided by the lead screw. A second horizontal carriage plate was added to minimize this and actuation was tested by hand.	Adding a second horizontal carriage plate greatly reduced the adverse effects of having the lead screw mounted off-center from the plates. The farther the plates are spaced apart, the lesser the moment (at the cost of losing horizontal reach). As a result, a 1" space is used between the two carriage plates, a distance found to be sufficient in minimizing jamming due to moments.
Is the horizontal motor sufficiently powered to turn the horizontal lead screw?	Because the payload bay motor performed well in the payload bay assembly, an extra one was tested as the method for horizontal AGSE actuation.	Though the payload bay motor could actuate the horizontal movement of the AGSE, it performed close to its power limits and would have a full-travel time greater than our target travel time. From this test, we determined it would be wiser to use the same motor vertical actuation uses because we know it is sufficiently

		powered and it reduces the number of unique parts in the assembly.
Can the horizontal carriage recover from a temporary jam?	A moment is applied to the horizontal carriage until it jams. The moment is then removed and the horizontal carriage is set to actuate under normal conditions.	This added feature has not yet been tested, but based on the payload bay's ability to "unjam" and the similar design of the horizontal carriage assembly, we expect it to be able to recover from a jam.

5.5.4.4 Tower

5.5.4.4.1 Tower Assembly

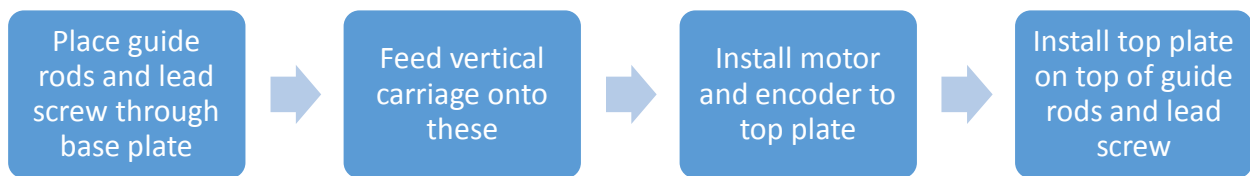


Figure 179: Flowchart of Tower Assembly

1. Place vertical guide rods on AGSE baseplate and bolt through the plate into the tapped ends of the guide rods
2. Place thrust bearing over center hole in baseplate and fit lead screw through the thrust bearing into radial ball bearing in servo shaft
3. Fit vertical carriage assembly onto guide rods and lead screw, turning the lead screw to fit the vertical lead nut onto the drivetrain
4. Place shaft collars onto the top of the guide rods. These allow for adjustability in the case of minor differences in length of the guide rods
5. Place thrust bearing onto top of lead screw
6. Fit radial ball bearing into top plate
7. Fit top plate onto top of guide rods and lead screw
8. Place thrust bearing on top of top plate around the lead screw
9. Attach a shaft collar to the turned down lead screw shaft on top of the thrust bearing
10. Install the encoder wheel onto the shaft on top of the shaft collar
11. Attach the vertical shaft coupling after the encoder
12. Bolt the vertical motor to the vertical motor mount
13. Fit the vertical motor shaft into the other end of the shaft coupling and bolt the vertical motor mount to the top plate

14. Bolt the encoder onto the encoder mount
15. Bolt the encoder mount to the top plate
16. Adjust the height and position of the encoder and encoder wheel so that the encoder wheel can freely spin within the encoder
17. Bolt through the top plate into the top of the guide rods, placing washers in between the plate and the heads of the bolts
18. Adjust the shaft collars on the bottom of the top plate so that the top plate is level

5.5.4.4.2 Tower Verification

Verification includes moment tests on the vertical actuation of the AGSE. The design of the horizontal stage minimizes deflection by using steel guide rods (as opposed to the aluminum ones used in the first prototype). As a result, the horizontal stage is much heavier and causes a greater moment on the tower of the AGSE. This could cause three problems: jamming of the vertical stage on the guide rods, overall tower deflection, or even tipping of the entire AGSE. These potential issues will be examined during testing of the AGSE, and if they prove to be problems, a counterweight will be added opposite the horizontal stage.

Aside from these, the speed of the actuation will be tested in order not to run the risk of running the motor under too much power and damaging it. The current draw under different speeds will be studied therefore in order to mitigate the risk of burning out the motor.

Table 17: Tower Verification and Testing

Part/Functionality Tested	Method of Test	Results
Does the vertical carriage slide easily along the vertical guide rods?	The vertical guide rods were installed into the AGSE table base. The vertical carriage (with the horizontal assembly included) was then slid onto the guide rods and moved back and forth after attaching the top plate too.	The carriages exhibited a significant amount of resistance when slid back and forth, especially due to the moment the horizontal arm imposed on the tower. As a result, the bushings were reamed out to 3/8" ID to minimize variability in the parts and remove any sharp edges in the bushings themselves.
Can the lead screw move the carriage when rotated by hand?	After press fitting the bushings into the vertical carriage plates, the lead screw was installed. The lead screw, screwed into the lead nut, was then turned by hand.	The lead screw could be turned easily by hand, meaning that the bushings fit more nicely onto the guide rods after reaming.

Is the vertical motor sufficiently powered to turn the vertical lead screw?	The vertical motor was attached to the lead screw using a shaft coupling and controlled to turn so that the vertical carriage translated both up and down.	The vertical motor successfully caused the vertical carriage to translate, but because of concerns of jamming caused by a moment applied to the guide rails by the horizontal assembly, a counterweight will likely be added.
Can the vertical carriage recover from a temporary jam?	A moment is applied to the vertical carriage until it jams. The moment is then removed and the vertical carriage is set to actuate under normal conditions.	This added feature has not yet been tested, but based on the payload bay's ability to "unjam" and the similar design of the vertical carriage assembly, we expect it to be able to recover from a jam.

5.5.4.5 Gripper and Arm

5.5.4.5.1 Gripper and Arm Assembly

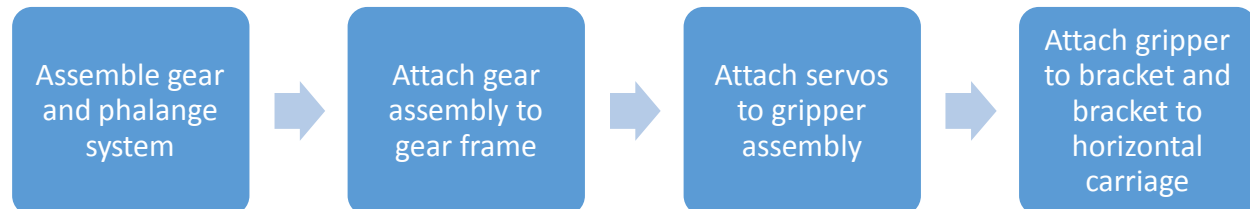


Figure 180: Flowchart of Gripper and Arm Construction

1. Prepare workspace: Lay out all major gripper components and associated hardware. Verify that all components and hardware are present and in working condition.
2. Attach gear axles and associated hardware to both gears
3. Attach gear linkages to gears via locknuts on gear axles; Verify secure attachment
4. Feed gear axles through corresponding holes in gear frame. Attach nuts on backside to secure axles to gear frame bottom plate
5. Mount standoffs on gear frame bottom plate via 10-24 bolts
6. Bolt gear frame top plate via 10-24 bolts into top side of standoffs
7. Thread nuts onto tops of both gear axles; Tighten to snug
8. Attach wrist rotation servo to associated bolt holes in gear frame via M2 machine screws
9. Bolt servo mounting plate onto gear frame bottom plate
10. Thread servo spindle onto gear drive axle; Tighten against locknut on drive axle
11. Bolt servo to mounting plate via M2 machine screws

12. Bolt servo output shaft to servo spindle via M2 machine screws
13. Attach wrist rotation servo to corresponding bracket on AGSE arm via 10-24 bolts
14. Connect servo wiring via daisy chain to main AGSE electronics

5.5.4.5.2 Gripper and Arm Verification

The component testing performed on the gripper subsystem included a wide range of functional and structural tests. These tests were designed to ensure proper functionality of the gripper in all operational scenarios, and to verify that individual components performed as expected.

These tests successfully validated our gripper design in all but one scenario, in which the gripper phalange failed structurally when gripping an object. This result led to a thorough redesign of the phalange to address structural weaknesses. Once complete, this redesigned phalange was tested using the same protocol as its predecessor and performed well in all testing scenarios.

Table 18: Gripper and Arm Verification and Testing

Part/Functionality Tested	Method of Test	Results
Do the gripper gears transmit torque from gear axles to gears?	The gripper gears were mounted via the associated hardware to their gear axles. The gears axles were then fixed to a vice to constrain them, and a known torque was placed on the gears. The magnitude and direction of torque was varied within the operational range of the gear box.	The gears showed the necessary torque transmission characteristics in all test cases and showed considerable resistance to loosening when exposed to cyclical loading.
Does the wrist rotation servo provide adequate range of motion and positional precision?	The wrist rotation servo was connected to the associated electronics and physical components. It was then commanded to operate to the extents of its range of motion repeatedly.	The servo demonstrated precise operation well outside of the required range of motion of 180 degrees. We noted that the PID settings of the servo give rise to “jerky” motions, and that servo movements could likely be smoothed out by manipulation of these settings
Is the gripper phalange shape	For each set of phalanges, the	Several of our phalange

well suited to capturing the sample?	gripper was assembled and used to grasp the payload in a variety of positions. Multiple trials were conducted and data was recorded regarding the success rate of each phalange design. Data was then compared across designs to evaluate the effectiveness of each.	designs had difficulty grasping the sample from all orientations, particularly as the misalignment between the gripper and sample positions grow large. Our final phalange design showed excellent grasping characteristics, including scooping from uneven ground and correcting for gripper misalignment.
Is the gripper phalange well suited to the structural requirements of capturing the payload?	Gripper was assembled and attached to AGSE arm. The gripper was then taken through steps of normal operation. This included gripping objects of varying size and gripping with the maximum force that can be applied by the gripper motor	The gripper system performed well with the notable exception of gripping a wide object with maximum grip force. In this scenario, the phalange structurally failed under the grip force. This led to a redesign of the phalange, in which the point of failure was strengthened greatly and the test was conducted again. This new design passed all test requirements and performed well

5.5.4.6 Evaluation and Verification Metrics for System Components

Table 19: Overall Systems Verification

Subsystem	Functional Requirements and Performance Characteristics	Evaluation and Verification Metrics	Status
Gripper	Allow the AGSE to grasp and manipulate the payload sample	Demonstration of successful payload capture and secure	Gripper has shown ability to pick up sample from ground

	reliably	grasping of payload from relevant points within the AGSE workspace	consistently.
Gripper	Allow the AGSE to set the payload into the Payload Bay.	Demonstration of the AGSE's ability to release the sample in such a way that it consistently ends up in the Payload Bay's containment tray and avoids dropping the sample from a distance that might cause harm to it or the tray.	Payload can be consistently placed within the tray, without dropping it from an excessive height.
Carriage Platforms	Facilitates low friction linear motion under all operating conditions	Demonstration of ability to accurately actuate in vertical direction under centered load.	Load of 4 kg (over 35% of the AGSE's total weight) has no negative effect on actuation or accuracy.
Carriage Platforms	Facilitates low friction linear motion under all operating conditions	Demonstration of ability to accurately actuate in vertical direction under off-axis load.	Vertical testing complete, motor able to drive lead screw despite off-axis load of horizontal carriage assembly.
Guide Rail Assemblies	Provide structural support for carriage platforms. Designed to take all moments associated with expected operation conditions without noticeable deflection	Demonstration of ability to accurately actuate in radial direction when gripper load exceeds expected conditions by factor of safety of no less than 2.	Horizontal motion accomplished under opposing loads
Base Structure	Provide stable attachment point for	Testing of AGSE tipping conditions to	AGSE is stable at all

	other components. Designed to prevent tipping of AGSE	ensure adequate factor of safety for base dimensions.	positions
Base Structure	Provide rotational degree of freedom	Evaluation of rotational precision and repeatability to ensure overall positional precision is adequate	Base rotation control established using AGSE prototype
Control Electronics	Provide computational power for instrumentation data processing and trajectory planning. Outputs motor control signals accordingly	Modular testing of software to verify reliability in image processing and path planning. Demonstration of repeatable, precise motor control under maximum load conditions	In progress: visual servoing has been developed and tested for individual components but not for whole system
Instrumentation and Data Acquisition	Provide visual data regarding the location and orientation of the payload sample and payload bay. Provide positional feedback to be used for closed loop motor control.	Demonstration of repeatable identification of payload and rocket position and orientation	Object and payload detection have been tested and confirmed under various lightings and object positions and orientations

5.5.4.6.1 Software Verification

The software for the AGSE can be broken down into the following subsystems: (1) kinematics and actuator control, (2) sample detection, (3) and Payload Bay detection. We will break the verification plan of the AGSE into smaller verification plans for each of those subsystems.

Kinematics and Actuator Control:

To verify the functionality of the kinematics and actuator control subsystem, we must ensure that it meets the following criteria: (1) the actuator control must, given, as input, a desired state, properly format the commands for the actuator to arrive at that state, and (2) the feedback must provide the capability to request the current state of each actuator's sensor and convert it to the current state of the system, and (3) the kinematics solver must, given a current AGSE state and a desired AGSE state, produce the sequence of actuator control inputs to transition between the two states. Using these criteria, we can write unit tests which automatically verify each function

according to the dependency tree. For instance, the unit test for actuator control can be run independently of the unit test for feedback. These two tests together however, provide not only the capability to run the unit tests for the kinematics solver but also can provide information about the state of each actuator. If all of the unit tests for both the feedback and the actuator control fail, we can safely assume that there is an electronics error or other software error in the system. However, combinations of failing and working unit tests in either category show that the electronics and communications systems work between the processing board and the actuators, and that there is a bug in the system with failing unit tests.

Sample Detection:

To verify the functionality of the sample detection subsystem, we must ensure that it meets the following criteria: (1) for each image processing algorithm, an input sample image (read from disk) must always produce the corresponding output sample image (also read from disk), (2) for the composite sample detection algorithm, a sample input image (read from disk) must always produce the sample output image (also read from disk), and finally (3) the sample detection algorithm should properly locate the sample in a laboratory test environment. For the algorithm unit tests, the lack of a generated output image or a discrepancy between the sample output image and the generated output mage indicates test failure. If all unit tests for (1) pass, the unit tests for (2) can be executed; similarly, if all unit tests for (2) pass, the unit tests for (3) can be executed.

Payload Bay Detection:

To verify the functionality of the payload bay detection software, the same criteria and unit tests can be used that were used by the sample detection verification. All that is required to be changed is the functions that are called by the unit tests and the sample dataset used as sample inputs and sample outputs.

For more information on the testing of the software, see section 5.3.4: *Final AGSE Image Processing and Object Detection Software*.

5.5.4.7 Evaluation and Verification Metrics for Integrated System

Table 20: Integrated Systems Verification

System Component	Functional Requirements and Performance Characteristics	Evaluation and Verification Metrics	Status
Drivetrain	Provide repeatable manipulator positioning and control regardless of loading condition	Demonstration of repeatable grasper positioning and orientation for sample	Complete

		capture	
Data Acquisition and Processing	Provide reliable data acquisition from visual systems as well as position feedback from actuators	Verification of consistent identification of sample position and orientation.	Complete
Data Acquisition and Processing	Provide reliable data acquisition from visual systems as well as position feedback from actuators	Characterization of positional resolution as a function of applied load	Complete
Electrical Power System	Provide adequate power to actuator motors, isolate control electronics from electrical fluctuations	Comprehensive characterization of electrical system when subjected to peak loads	Complete
Electrical Control System	Implement path planning to output motor controls according to sample position data. Interface with payload bay control system to open and close payload bay to capture sample.	Demonstration of optimized path planning based on known sample position and orientation. Verification of reliable interaction with payload bay electronics.	Compete

5.5.5 Workmanship and Mission Success

Section 4.1.5: *Workmanship and Mission Success* contains a thorough explanation of the team's design and construction policies ensuring product quality and mission success. The AGSE has been designed in this manner, with extensive CAD and hand calculations preceding construction. Components made in house use precision tools such as the lathe, mill, and laser cutter. Similarly, mentors have been present for design presentations by team members and have overseen construction efforts.

5.5.6 Testing and Verification

The verification plan is centered on the AGSE's ability to achieve each of its mission success criteria.

Table 21: Verification Status

Mission Success Criterion	Verification Method	Status
The AGSE must distinguish the sample from the environment including other cylindrical objects within its operating space.	Apply edge-detection and line-detection to static environment with just sample	Software has successfully identified the payload and tracked it as it moved through an otherwise static environment.
	Static environment with multiple objects	Software has successfully separated the payload from other objects in field of view and from noisy background.
The AGSE must grab and move the sample without damaging it in any way, including dropping it.	Use manual control of AGSE to grab and move sample.	Payload picked up from initial r, θ, z and moved manually to new position.
	Integrate automated control scheme and pick up and move sample.	Complete
The AGSE must identify and avoid any obstacles within its operating space.	Instruct AGSE to autonomously move sample from one side of rocket (on launch pad) to other.	Complete
The AGSE must identify and precisely locate the rocket Payload Bay compartment.	Place Payload Bay in camera's field of view and have it give coordinates for each fiducial.	Complete
The AGSE must place the sample completely within the containment area of the payload bay so as not to interfere with the closing process.	Manually place sample in payload bay and test ability to close and open without jamming.	Successful open and close with payload inside. This test will be continually performed as incremental improvements are made to the payload bay.
The AGSE must respond appropriately to the PAUSE command whenever given, without losing the ability to continue its assigned task	Pause system during each phase of AGSE task:	Complete

once freed.		
	Search	Complete
	Pickup	Complete
	Transport	Complete
	Placing Sample	Complete
	Moving away from rocket	Complete

5.5.7 Integration Plan

In order to ensure the proper functionality of the AGSE, each of its constituent subsystems will be extensively tested as individual components. Once the functionality of each subsystem has been successfully demonstrated and documented, the subsystems will be integrated according to the plan outlined in section 5.2.7: *Preliminary Experiment Process Procedures*.

The interaction between the AGSE and Payload Bay will be accomplished through the use of serial communication through a breakaway connector. This connector attaches magnetically to the outside of the payload bay in the nose section and automatically breaks away when the rocket is manually raised. Alternatively, if communication fails between them or if the connection is accidentally severed, a Hall Effect sensor is used as a backup, triggered by a permanent magnet mounted on the gripper.

The computationally intensive tasks associated with this interaction will be accomplished by the AGSE microcontroller rather than the Payload Bay microcontroller. This decision was made so the payload bay electronics systems can be minimized, reducing complexity and mass for flight.

5.5.8 Precision of Instrumentation and Repeatability of Measurement

More detail on the precision of instrumentation can be found in sections 5.2.4: *Experimental Logic, Approach, and Method of Investigation*; 5.2.5: *Test and Measurement, Variables, and Controls*; and 5.2.6: *Expected Data and Accuracy/Error Analysis*. The primary objectives of the AGSE are to autonomously locate, retrieve, and deposit the payload in the rocket bay without interfering with or damaging the either the rocket or the payload. Using the hazard and failure criteria for the AGSE (See section 6.2.1: *AGSE Preliminary Failure Modes*) we may qualitatively evaluate any hazards to the rocket body, the payload, or the AGSE itself during the retrieval process. These qualitative tests should ensure that no part of the process damages any of the operational components.

The major experimental challenge addressed by the AGSE is the ability to autonomously detect, retrieve, and deposit the payload in the rocket. Since there will be no human interaction with the AGSE during the retrieval process, the collection of the payload will rely entirely on the ability of the image-processing software to detect the location of the payload, its placed orientation, and

the corresponding location and orientation of the rocket payload bay. Since the payload is of a known shape and coloring, this software can be optimized specifically to detect objects with the same visual qualities as the payload.

Investigation into the ability of the AGSE to accomplish the designated requirements relies on the accomplishing of several steps, the same steps of the retrieval process. Each process can be tested on a systematic level to ensure that the AGSE subsystems will successfully interact to complete the overall objectives. The iterative process that will be used will demonstrate subsystem functionality will begin at the most basic functional levels, and progress towards fully complex system operation. This approach is outlined as follows:

Ensuring full operational ability within predicted workspace:

- Manual control of the AGSE actuators to move and orient throughout its operational workspace; this verifies the ability of the AGSE to have the necessary capacities to perform the other aspects of the payload capture process.
- Solve for the forward and inverse kinematics of the AGSE links; this allows the construction of a trajectory generating program for modeling and simulation.
- Simulated automatic control of the AGSE actuating joints before AGSE programming; this ensures that the trajectory generation and operation of the AGSE can be operated without reaching singularities or violating operational boundaries, which could damage the AGSE or create a hazard to operators.
- Planned trajectory-based control of the AGSE actuators to move and orient throughout its operational workspace; this verifies that the software being run on the AGSE will be able to control the required tasks to accomplish its goals.
- Image processing search protocol and payload recognition:
 - Image capture from the gripper mounted USB camera; this verifies the basic functionality of the camera.
 - Write an image to the onboard storage; this verifies the data collection system.
 - Capture images in a sequence rate ≥ 10 images/second; this verifies the speed of data acquisition.
 - Write images in sequence (rate ≥ 10 images/second) to the onboard storage; this verifies the speed of data collection.
 - Process a single image to detect continuous edges and shapes in the image; this creates the infrastructure for payload detection.
 - Process a single image for the location of the payload relative to the camera location; this verifies that the AGSE will be able to move toward the payload.
 - Process a single image for the orientation of the payload relative to the camera orientation; this verifies that the AGSE will be able to align the gripper phalanges with the axis of the payload.

- Process images received at a rate \geq the rate of image collection; this ensures that there will be no deadlock between the image acquisition and robot motion.
- Develop a search protocol for the AGSE to sweep its operational area for the payload; this verifies that, even if the payload is not directly in the view of the camera from the start, the AGSE will still be able to either locate it or determine that it is not available.
- Payload retrieval from detected location:
 - Use resolved rates trajectory generation and visual servoing to move the AGSE gripper toward the payload; this will ensure that the AGSE can move and orient to the payload using a safe velocity.
 - Use resolved rates trajectory generation and visual servoing to move the AGSE gripper toward the payload bay; this will ensure that the AGSE can move and orient to the payload bay using a safe velocity.
 - Create and execute payload bay open and close protocol; this will verify that the payload bay can be opened and closed.
 - Create and execute payload pick-up and put-down protocol; this verifies that the AGSE will be able to move the payload to the payload bay and place it successfully.
- Enhancing design functionality:
 - Provide instrumentation to detect that the payload is being gripped; this provides verification that the payload has been retrieved and deposited without being dropped.
 - Create obstacle avoidance parameters in the AGSE trajectory generation; this will ensure that the AGSE cannot collide with either the rocket body or any other potential obstacles.

5.5.9 Test and Measurement, Variables, and Controls

There are several parameters that must be measured and controlled in the development and testing of the AGSE. The AGSE system has many mechatronic components to control, making for a challenging implementation of the design, having to use code, electronics, and hardware all in conjunction with each other. The most important measurements, variables, and controls to consider in the design and testing of the AGSE are outlined as follows:

- Each motor's current and voltage requirements must be considered while also taking into account the overall power usage of the system. These factors influence the requirements for the battery used to power the AGSE.
- The speed of the gripper, linear actuators, and turntable base must all be taken into account. The AGSE system should be able to complete its task in a reasonable amount of time.
- The position of the servomotor controlling the rotation of the gripper must be calibrated to the amount of current it is given. This will ensure accurate control of the rotation of the gripper by the microcontroller.
- The control of the linear actuators and turntable must be implemented in addition to the servos. The linear actuators include integrated position feedback, which can be measured

and controlled using the controllers built for them. The turntable base comes with its own controller as well, providing position feedback. The control of these elements must be measured against the actual position of the actuators at a given position in order to ensure accurate knowledge of position of each actuator within the AGSE.

- The weight of the sample must be taken into account. Although the given sample is will be relatively low, it is important to consider the maximum limitations of the AGSE. If a sample is too heavy, it might cause the entire robot to tip over; or the gripper might not be able to grasp the object correctly.
- The robot must be able to move from its start position to the object and from the object to the payload bay. The path planning of the AGSE will be able to combine the mechanical aspects of the actuators, electronics needed to power them, and the coding needed to calculate the required movement of each and provide the correct set of commands to the AGSE in order to go to the sample, retrieve it, and deliver it to the payload bay.
- In order to determine the position of the object relative to the AGSE, image processing will be used. First of all, the power requirements of the camera and processor used to locate the object must be taken into account. Second, angle of the camera allowing the best view of the space around it should be determined, as this will make finding the object less difficult.
- It is useful for the codes controlling the payload bay and each aspect of the AGSE to be written in the same language. This improves the robustness of the programming behind the control of the actuators.

5.5.10 Expected Data and Accuracy/Error Analysis

The AGSE offers great repeatability of measurement as it is not flown in the rocket and risks much less damage. In addition, with such a robust design, the AGSE will be able to operate countless times in tests, limited only by the lifetime of its batteries.

5.5.11 Electronics Systems and Safety Switches

See the appendix, section 10.2: *Electrical Drawings*, for electrical schematics of the payload bay, which the AGSE interacts with, and all the possible states the AGSE software can be in.

5.6 NASA Statement of Work Verification

Shown below is a table outlining NASA's requirements described in the Request for Proposal. The requirement given by NASA is compared with any additional team-derived requirements. The verification status of these requirements is shown. Green text indicates completion of verification, while red indicates incomplete verification.

NASA Requirement	Team-Derived Requirement (if applicable)	Verification Status
Teams will be required to	Camera-based vision will be	Manual capture of the

capture and contain a payload, launch it, and eject it during the launch vehicle's descent.	<p>used by the AGSE to increase autonomy.</p> <p>Capture and containment of the payload will take no more than 10 minutes</p>	<p>payload, placement into the payload bay, and automatic closing of the payload bay have been accomplished.</p> <p>Camera vision has proven it can detect payload among other similarly-shaped <i>or</i> similarly-colored objects. The algorithms are in place</p> <p>Manual control of the AGSE in this test took significantly less than 10 minutes.</p>
Teams will position their launch vehicle horizontally or vertically on the launch pad.	The AGSE base table will include a stand for the rocket to rest on in the horizontal position.	The AGSE base table has been built according to this design and has adjustable legs to match the height of the launch rail.
A master switch will be activated to power on all autonomous procedures and subroutines.	The master switch will be part of the user interface panel of the AGSE.	This is accomplished using the UIP, which is being built in its final version.
After the master switch is turned on and all systems are booted, a pause switch will be activated, temporarily halting all AGSE procedure and subroutines. This will allow the other teams at the pads to set up, and do the same.	The pause switch will also be part of the user interface panel.	This is accomplished using the UIP, which is being built in its final version.
After setup, one judge, one launch services official, and the team will remain at the pad. During autonomous procedures, the team is not permitted to interact with their AGSE.	At this point, the user interface panel will not be used to control any part of the AGSE (display only). Separate features such as camera view and position can be seen on the panel though.	Autonomous control of the AGSE has been established, meeting NASA's requirement.
After all nonessential personnel have evacuated, the pause switch will be		This is accomplished using the UIP, which is being built

deactivated.		in its final version.
Once the pause switch is deactivated, the AGSE will capture and contain the payload within the launch vehicle. If the launch vehicle is in a horizontal position, the launch platform will then be manually erected by the team to an angle of 5 degrees off vertical, pointed away from the spectators. The launch services official may re-enable the pause switch at any time at his/her discretion for safety concerns.	The physical connection between the AGSE and payload bay will not have to be manually disconnected, allowing more autonomy.	Autonomous control of the AGSE has been established, meeting NASA's requirement.
After the erection of the launch vehicle, a team member will arm recovery electronics.	At this point, the same team member will listen to the altimeters' beeping to confirm their settings are correct.	This method has been proven to work during all team launches.
The igniter is manually installed and the area is evacuated.		This is the standard launch procedure for the team.
Once the launch services official has inspected the launch vehicle and declares that the system is eligible for launch, he/she will activate a master arming switch to enable ignition procedures.		This is the standard launch procedure for the team.
The Launch Control Officer (LCO) will activate a hard switch, and then provide a 5-second countdown.		This is the standard launch procedure for the team.
At the end of the countdown, the LCO will push the final launch button, initiating launch.		This is the standard launch procedure for the team.

The rocket will launch as designed and jettison the payload at 1,000 feet AGL during descent.		This has been proven through the subscale and full-scale launches.
For the purpose of this challenge, ASGE is defined as all mechanical and electrical components not part of the launch vehicle, and is provided by the teams. Components may include the payload containment device, computers, batteries, etc.		The AGSE system design is fully autonomous along with the payload bay. Autonomy was tested on the first and second AGSE designs.
The payload containment system shall be fully autonomous with no human intervention.	The payload bay will include a backup autonomous trigger to actuate based on a signal from the ground based AGSE.	The payload bay includes a hard-wire, breakaway connector with which it communicates with the AGSE. As a backup, a Hall Effect sensor can be activated by a magnet mounted on the AGSE gripper. These have both been tested.
Any pressure vessel used in the AGSE will follow all regulations set by requirement 1.12 in the Vehicle Requirements section.		No pressure vessel is used in the AGSE.
As one of the goals of this competition is to develop equipment, processes, and technologies that could be implemented in a Martian environment, the AGSE and any related technology cannot employ processes that would not work in such environments. Therefore, prohibited technologies include: <ul style="list-style-type: none">• Sensors that rely on		None of these are used in the AGSE.

<p>Earth's magnetic field</p> <ul style="list-style-type: none"> • Ultrasonic or other sound-based sensors • Earth-based or Earth orbit-based radio aids (e.g. GPS, VOR, cell phone). • Open circuit pneumatics • Air breathing systems 		
<p>Each launch vehicle must have the space to contain a cylindrical payload approximately 3/4 inch in diameter and 4.75 inches in length. The payload will be made of $\frac{3}{4}$ x 3 inch PVC tubing filled with sand and weighing approximately 4 oz., and capped with domed PVC end caps. Each launch vehicle must be able to seal the payload containment area autonomously prior to launch.</p>	<p>A cover will be used to seal the payload within the payload bay.</p>	<p>A payload built to NASA's specs has been fit into the payload bay.</p>
<p>Teams may construct their own payload according to the above specifications, however, each team will be required to use a regulation payload provided to them on launch day.</p>	<p>The payload bay will be able to accommodate for slight differences in dimensions in expected payload.</p>	<p>The payload bay tray design has enough clearance to contain a sample of similar but not exact size and shape.</p>
<p>The payload will not contain any hooks or other means to grab it. A diagram of the payload and a sample payload will be provided to each team at time of acceptance into the competition.</p>		<p>The gripper does not rely on a hook to grasp the payload. It can pick it up directly from the ground.</p>
<p>The payload may be placed anywhere in the launch area for insertion, as long as it is outside the mold line of the</p>		<p>The payload will be placed within the workspace of the AGSE but not in the mold line of the rocket in all tests</p>

launch vehicle when placed in the horizontal or vertical position on the AGSE.		and on competition day.
The payload container must utilize a parachute for recovery and contain a GPS or radio locator.		The payload section uses a 30" elliptical parachute and contains an RF transmitter used in conjunction with the RF tracker on ground.
Each team must provide the following switches and indicators for their AGSE to be used by the LCO/RSO. <ul style="list-style-type: none"> • A master switch to power all parts of the AGSE. The switch must be easily accessible and hardwired to the AGSE. • A pause switch to temporarily terminate all actions performed by AGSE. The switch must be easily accessible and hardwired to the AGSE. • A safety light that indicates that the AGSE power is turned on. The light must be amber/orange in color. It will flash at a frequency of 1 Hz when the AGSE is powered on, and will be solid in color when the AGSE is paused while power is still supplied. 	The user interface panel, which is hard-wired to the AGSE, will have a master switch, pause switch, and safety light.	This was accomplished in the first AGSE. These features were accomplished in the new one using the UIP, which is being built in its final version.

5.7 Safety and Mission Assurance Analysis

5.7.1 AGSE Carrying Case and Transport

With an electromechanical system as large as the AGSE, it is important to be able to transport the system without damaging it, especially because the team must travel a far distance for the NASA SL Competition Launch Day. Fortunately, the team had a chance at a dry run of transporting the prototype AGSE to Montgomery Bell Academy for an outreach event. Using a wooden crate normally used to carry supplies during launch days, four holes were drilled through the bottom using a paddle drill. These holes were spaced according to the location of the AGSE table legs so that the legs could fit up through the bottom of the box into the AGSE table itself, anchoring down the AGSE to the bottom of the box. The legs going up through the table and the AGSE being secured to the bottom are shown below.



Figure 181: AGSE Legs fit through the bottom of the mock carrying case



Figure 182: Prototype AGSE Secured in Mock Carrying Case

In order to prevent wobble in the tower and arm of the AGSE, the main AGSE frame was tied rigidly using bungee cords wrapped around the box. The gripper and gripper arm were detached and transported separately in order to mitigate risk of damage.

Although the mock carrying case is not the most sophisticated design, it was sufficient in protecting the AGSE's electrical and mechanical systems from being damaged during transport to the outreach event. This inspired a more robust carrying case design in which the base will attach through the bottom of the box just as in the mock case. However, instead of bungee cords to secure the AGSE structure, clips and fasteners attached to the wall of the box will be used, and a lid will be included. The gripper and gripper arm will still be transported separately.

5.7.2 Preliminary Failure Modes Analysis

Tables outlining a preliminary estimation of the primary failure modes the AGSE system may experience may be found in section 6.2.1: *AGSE Preliminary Failure Modes*. Each of these failure modes is accompanied by a likely effect and proposed mitigation strategy.

5.7.3 Personnel Hazards and Concerns

General personnel hazards and concerns are addressed in section 6.1.3: *Personnel Hazard Risk Assessment* relating to the general flight of the rocket as well as operation of the AGSE.

5.7.4 Environmental Hazards and Concerns

Just as with the vehicle, an important consideration when designing the AGSE is the nature of the environment in which it will be launched. Because the AGSE simulates an operation within a MAV mission, it is especially important to consider environmental factors in light of Mars's harsh environment. Even on Earth though, the launch environment undoubtedly has the potential to impose certain risks onto the performance of our mission. We have identified the main risks along with mitigation strategies associated with operating the AGSE in a non-ideal environment, and tables containing these may be found in section 6.2.2: *AGSE Environmental Hazards and Concerns*.

6 Failure Modes and Risk Assessment

For the sake of convenience, all tables analyzing failure modes and risks using *Figure 16: Risk Assessment Matrix* are aggregated in this section.

6.1 Launch Vehicle

6.1.1 Vehicle Development Table

This section will define the risks and the plans for risk mitigation in the context of how each risk factor will affect the project with regard to successful and timely completion of fabricating the launch vehicle.

Table 22: Project Management Risk and Mitigation

Project Management Risk and Mitigation				
Risk	Overall Effect	Risk Rating	Mitigation Strategy	Post-Mitigation Risk Rating
Unavailability of parts or delays in parts delivery	Cause delays in construction of the rocket and payload attachment scheme. Could lead to rushing through work or settling with parts that are not compatible with an ideal design.	B3	Start the design process very early, and allow room in the design for the use of parts other than those initially selected: flexibility in design without the compromise of safety or science value.	A3

Vehicle Testing Failure	Vehicle parts are destroyed or damaged during ground testing or flight testing. Could lead to ordering new materials late in the year and running the risk of not completing the project on time.	E3	Design the vehicle components after extensive mathematical and physics analysis in order to ensure that a damaging failure will not occur. Only conduct tests with the potential to cause damage once a robust design has been developed and implemented. Set up an inventory of spare parts and components for building a second rocket within a week	E1
Weather Launch Delays	Inability to meet CDR and FRR timelines and obligations	D2	Have multiple possibilities for launch by working with launch clubs in the Tri-State area of TN, AL, and KY.	D1
Failure of AGSE Electronics	Inability to pick up and place payload into rocket	E3	Test, Test, and Re-test AGSE electronics. Set up minimum deliverables even if some sub systems fail	E1
Failure of flight altimeter	Inability to deploy drogue and/or main parachutes	D2	Test and certify altimeters in simulated altitude chambers Fly two altimeters for redundancy	D1

Failure of NASA marked altimeter	Inability to report flight altitude	C2	Test and certify altimeter Fly SL competition altimeter in Payload Electronics bay to minimize effect of blasts during drogue and main deployments	C1
Access to Machine Shops	Delays in fabrication of various parts or rushed work. Impact on timely completion of the project.	B2	Ensure that contact with the machine shop operators is constant, and that available times for access are established.	B1
Personnel Shortage	Student or faculty members could be unavailable, which can lead to higher workloads for others, or the lack of technical knowledge of some system aspect.	B2	Make sure that the knowledge of rocket construction and testing techniques is known by the entire team. Make sure that the schedule is known by everyone so that people are not voluntarily absent/unavailable at inopportune times.	B1
School Holidays	Slows down the project and threatens timely completion and available times for testing.	A2	Ensure that the schedule for work and testing is designed with school holidays in mind, such that the team does not expect to have full access to equipment or personnel during those times.	A1

Overrun of Budget	Could threaten the feasibility of the project, as well as a violation of the rules of the competition.	C2	Keep a detailed budget and projected budget to minimize the chance of overspending. Make sure that every purchase is justified.	C1
Equipment Breakdown	Machine shop or laboratory equipment breakdown could cause a slowdown in production and threaten the timely completion of the project.	C1	Ensure that the team has access to multiple machine shops in case equipment in one place fails. Also, ensure that equipment is used and stored properly to minimize the likelihood that such a failure will occur.	B1
Ambiguous Product Lead Time	If the amount of time it takes for parts to ship is ambiguous or unknown, there could be unexpected delays in project development.	C3	Ensure somebody is responsible for knowing the lead times on all parts, and trying to eliminate all the ambiguity.	C2
Delays in Critical Path	If a portion of the project that is necessary to complete the next portion takes longer to complete than expected, there could be delays in project development.	C3	Make sure that realistic expectations are set for completion of elements along the critical path.	C2

Communication breakdown between team members	Failure to meet deadlines; failure to show results	D2	Frequent meetings to improve team morale and stress the importance of timelines, and chain of command. Recalibration of deliverables based on progress.	D1
--	--	----	--	----

6.1.2 Vehicle Preliminary Failure Mode Analysis

The following tables explain various risks the team may face during a launch in relation to the overall rocket vehicle, the consequences each risk has and our plan to mitigate these risks. The risks are divided into three categories:

1. Vehicle Failure
2. Propulsion Failure
3. Recovery Failure

6.1.2.1 Vehicle Failure Modes and Risk Assessment

Table 23: Vehicle Failure Modes and Risk Assessment

Vehicle Failure Modes and Risk Assessment					
Risk	Cause	Overall Effect	Risk Rating	Mitigation Strategy	Post-Mitigation Risk Rating
CG is too far aft	Poor overall rocket and section design Unnecessary weight	Insufficient stability for reliable flight	C3	Proper simulation of rocket characteristics using <i>RockSim</i> . Add ballast to nose cone of rocket if needed, which has ample room for dead weight.	B2
CP is too far forward	Poor overall rocket and section design	Insufficient stability for reliable flight	C3	Proper simulation of rocket characteristics using <i>RockSim</i>	B2

	Fin area too small			Increase fin size to move CP further back.	
Nose cone damage	Damage in landing of previous launches or during travel Not properly sealed from environmental hazards	Unstable flight Unusable nose cone	C3	Strong nose cone selection Protective paint coating Evaluate structural integrity after and before each launch	B2
Payload bay does not open or close properly	Failure of motors, misalignment of nosecone and rest of rocket	Inability to proceed with launch	D2	Have team check that the payload bay closes properly before prepping rocket for launch	D1
Lead screws in payload bay fail to stop turning	Failure of limit-switches	Damage to rocket shell, motors	C2	Install fuse on motor	C1
Loss of Payload Bay Control	Bug in payload bay code power failure	Payload bay fails to open to AGSE command; thereby, payload is not delivered to the rocket	E2	Repeatedly test payload bay design features; incorporate backup. Operate with payload bay open. Establish two ways to close payload bay door	E1
Payload bay reopens after launch	False positive signal from Hall Effect sensor	Change of rocket aerodynamics and flight path. Damage to payload and rocket	E3	Include “lock setting” in software after payload has been deposited to keep payload bay shut	E1
Fin failure or weakness	Damage in landing of previous launches or during travel Not properly sealed from environmental hazards	Unstable flight	D3	Correct construction techniques Protective epoxy coating Evaluate structural integrity after and before each launch	D2

Rocket comes loose from launch pad	Rail Lugs not securely mounted to rocket Extreme wind Team error in aligning rocket while attaching to pad	Rocket breaks free during initial phase of launch Potential damage to rocket, bystanders, and property Potential loss of rocket and payload.	D4	Button type screw on lugs used on rocket for secure attachment Careful precision of alignment while guiding rocket on launch rail	C2
Buckling or shearing of airframe	Shear pins do not shear Bulkheads unable to withstand force from motor during launch Weak bulkheads; poor seal to rocket body and/or motor tube	Unstable flight Potential loss of rocket	E3	Selection of strong airframe materials Use of proper manufacturing techniques	E2
Premature rocket separation	Faulty separation charge wiring Shear pins too small Altimeter malfunction	Unstable flight Recovery failure Unable to reach target altitude Potential loss of rocket	E3	Proper shear pins selection Ground-based deployment and altimeter testing	E2
Center ring failure	Unable to withstand motor force during launch Weak ring; poor seal to body and motor tube	Reduced stability Damage to/loss of rocket	E3	Proper ring size and construction Sufficiently strong materials used	E2
Bulkhead failure	Unable to withstand motor force during launch	Damage to/loss of avionics, payload, or	E3	Proper construction	E2

	Weak ring Poor seal to body and motor tube	rocket Unstable flight		Test for stability	
--	---	-------------------------------	--	--------------------	--

6.1.2.2 Propulsion Failure Modes and Risk Assessment

Table 24: Propulsion Failure Modes and Risk Assessment

Propulsion Failure Modes and Risk Assessment					
Risk	Cause	Overall Effect	Risk Rating	Mitigation Strategy	Post-Mitigation Risk Rating
Motor igniter fails	Faulty/incorrect igniter	Rocket does not launch Need to replace	C2	Proper igniter selection setup Proper power source	C1
Propellant fails to ignite	Improper motor packing Faulty propellant grain Damage during transportation	Rocket does not launch Need to replace	D2	Proper ignition setup Safety advisor oversees motor packing by student safety officer	D1
Premature propellant burnout	Improper motor packing Faulty propellant grain	Altitude estimate not reached	D2	Proper motor assembly Static fire testing	D1
Propellant explodes	Improper motor packing Faulty propellant grain Damage during transportation	Destruction of motor casing Catastrophic failure of rocket Potential injury to team or bystanders	E2	Proper motor assembly Safety advisor oversees motor packing by student safety officer	E1
Propellant burns through casing	Improper motor packing	Loss of thrust	E2	Proper motor assembly	E1

	Faulty propellant grain or casing Damage during transportation	Loss of stability Catastrophic failure of rocket		Safety advisor oversees motor packing by student safety officer Verification testing	
Improper assembly of motor	Incorrect spacing between propellant grains Motor case improperly cleaned End caps improperly secured	Motor failure including Unstable flight Altitude estimate not reached Potential damage to/loss of rocket	E2	Ensure proper training and supervision by safety advisor for motor assembly by student safety officer	E1
Motor mount fails	Insufficient mount strength Damage during previous launch/transportation	Motor launches through rocket Damage to/loss of rocket Unstable flight	E3	Proper motor mount construction Load verification testing Test launches	E2
Transportation/handling damage	Improper protection during transportation/handling	Unusable motor Incapable of safe launch Potential damage to/loss of rocket if used	E3	Proper storage overseen by safety advisor and student safety officer Certified member handling	E2

6.1.2.3 Recovery System Failure Modes and Risk Assessment

Table 25: Recovery System Failure Modes and Risk Assessment

Recovery System Failure Modes and Risk Assessment					
Risk	Cause	Overall Effect	Risk Rating	Mitigation Strategy	Post-Mitigation Risk Rating
Descent rate too		Potential to land outside of	C3	Verification testing of recovery system	C2

slow	Parachute C_d too high Cross-sectional area too great	authorized zone			
Payload parachute fails to deploy	Not enough drag in the air to blow the parachute out	Destruction of the payload compartment Potential harm to spectators or environment	E3	Use shallow parachute chamber and secondary small chutes	D2
Payload Section fails to separate	Payload section charges fail to cause separation	Additional mass added to main falling section Failure to complete payload jettison objective	E3	Calculations have been made that show failure of payload section separation does not cause excessive landing energy increase (shown after this table). Backup charges installed.	B2
Onboard fire in parachute compartments	Combustible material near separation charges	Potential damage to or loss of rocket, avionics or payload bay	D2	Isolation of ejection charges from flammable material Ground-based deployment testing	D1
Parachute tear	Parachute snags upon separation Improper transportation/storage	Decreased parachute performance leading to potential damage to/loss of rocket	D3	Inspect material for defects Proper and consistent packing technique Removal of potential snags within parachute compartment	C2
Avionics bay not properly sealed	Holes in rocket body or avionics bay Gaps between sections	Premature detonation of charges Estimated altitude not reached Potential damage to/loss of rocket	D3	Putty used in required areas to seal holes and gaps	D2
Descent rate too fast	Parachute C_d too low Cross-sectional area too small	Potential damage to or loss of rocket or payload	D3	Verification testing of recovery system	D2
Parachute or shroud line	Improper transportation,	Decreased parachute performance leading to potential	D4	Proper packing of recovery system	C2

tangle	storage, or packing	damage to or loss of rocket		Proper and consistent method of folding and storing after each use	
Parachute melts	Improper separation of/insulation between charges and parachute	Decreased parachute performance leading to potential damage to/loss of rocket	D4	Proper shielding from ejection charges Ground-based testing	D2
	Improper storage				
Rocket ripped apart upon chute deployment	Zippering effect of parachute harness	Catastrophic failure of recovery system Damage to/loss of rocket and payload	E3	Use Fireball anti-zippering device to distribute load to body	E1
Low battery	Not properly replacing before launch	Failure to ignite charges to deploy parachute Deploy at incorrect altitude Potential damage to/loss of rocket	E3	Pre-launch checklist ensures battery switch if low power	E1
Parachute sections come apart	Inadequate parachute design Poor stitching between sections	Catastrophic failure of recovery system Damage to/loss of rocket and payload	E3	Use semi-flat felled seam between sections Verification testing of recovery system	E2
Shroud lines become unattached	Weak stitching or materials	Catastrophic failure of recovery system Damage to/loss of rocket and payload	E3	Sew reinforcement onto shroud lines	E2
Parachute breakaway	Harness failure; weak mounting of recovery system to rocket body	Loss of parachute Catastrophic damage to/loss of rocket/payload Potential damage/injury to property/persons on ground	E3	Design strong retention system with shock absorption Load testing; multiple body attachment points	E2

Parachute deployment failure	Charges fail to deploy	Potential damage/injury to property/persons on ground	E3	Additional drogue parachute attached to main parachute	E2
Separation failure	Overly strong shear pins Inadequate charge or failure to detonate Altimeter failure	Catastrophic damage to/loss of rocket on landing Potential damage/injury to property/persons on ground	E3	Deployment charge testing Proper shear pin sizing/ strength Altimeter testing Redundant charges and altimeters Slightly oversized ejection charges	E2
Altimeter failure	Wires become unconnected Loss of power Arming switches fail	Failure to ignite charges to deploy parachute Deploy at incorrect altitude Potential catastrophic damage to/loss of rocket	E3	Employ backup altimeter Dedicated power supply Test for altimeter function prior to launch	E2
Arming switch failure	Faulty component Short in circuit	Failure to ignite charges to deploy parachute Deploy at incorrect altitude Potential catastrophic damage to/loss of rocket	E3	Test switches prior to rocket assembly Ground-based deployment test	E2
Shock cord failure	Faulty shock cord Fatigue failure	Parachute disconnect from rocket Potential catastrophic damage to/loss of rocket	E3	Inspect shock cord before packing parachutes	E2
Shroud lines or shock cords tangle after deployment	Excess rocket rotation Shock cords too long	Potential for parachute to not fully deploy Potential catastrophic damage to/loss of rocket	E3	Flight testing of recovery system Minimize shock cord length to nose cone Maximize cord length to tail section to	E2

			reduce rotation	
--	--	--	-----------------	--

6.1.3 Personnel Hazard Risk Assessment

Table 26: Personnel Hazard Risk Assessment
Personnel Hazard Risk Assessment

Risk	Cause	Overall Effect	Risk Rating	Mitigation Strategy	Post-Mitigation Risk Rating
Irritation of skin	Exposure to chemicals Allergic reaction	Discomfort and/or injury	C2	Latex or vinyl gloves will be worn when handling chemicals or known allergens.	C1
Flying debris from machining operations	Improper tool use or fixing	Personal injury	C3	Closed-toed shoes and long pants will be worn at all times in the shop. All members present during cutting operations will wear eye protection.	B2
Irritation of lungs	Inhalation of chemical fumes	Discomfort and/or damage to lungs	D2	Volatile chemicals will only be handled in well-ventilated rooms and under a fume-hood when possible.	D1
Irritation of eyes	Eye contact with chemicals or particulates Exposure to arc from arc-weld	Discomfort and/or vision impairment	D3	Appropriate eye protection will be worn for all activities involving machinery, chemicals, and welding.	D1
Hearing damage	Prolonged operation of heavy machinery	Disorientation and/or hearing loss	D3	Hearing protection will be worn when operating heavy machinery.	D1
Lacerations or cuts from machines or tools	Improper use of machines or equipment Improper fixing	Injury potentially requiring medical attention	D3	All team members performing potentially hazardous operations will be properly trained At least two members must be present for hazardous operations	D2

Burns	Leaving soldering iron on Touching welded parts immediately after welding Chemical spills	Personal injury	D3	All heat-producing tools will be turned off when not in use Heat-resistant gloves will be worn when handling hot parts Chemicals will be stored and handled safely	D2
Black powder explosion/ ignition while handling	Accidental connection to voltage source Static discharge	Hearing damage Disorientation Personal injury	E3	Black powder handlers will only work with small amounts at a time and ground themselves prior.	D1
Electric shock	Static build-up on equipment handler	Destruction of electrical components Black powder explosion	E3	Handlers of sensitive equipment will ground themselves to discharge static build-up.	E1
Getting caught in a machine	Loose fitting clothing or jewelry Long hair not tied back	Potential for serious injury or death	E3	Those performing machining operations will never wear loose fitting clothing or jewelry All long hair must be tied back	E1

6.1.4 Vehicle Environmental Hazards and Concerns

6.1.4.1 Environmental Impact on Rocket

Table 27: Environmental Impact on Rocket
Environmental Impact on Rocket

Risk	Overall Effect	Risk Rating	Mitigation Strategy	Post-Mitigation Risk Rating
Rain, mud	Launch pad could sink unevenly into the ground, resulting in a non-vertical launch Electronics short circuit	C3	The team will bring a level and, in the event of rain, plywood boards to prevent the Launchpad legs from sinking into the ground. Electronics enclosures will be sealed to prevent water	B2

	Moisture can cause the Blue Tube to swell and/or unravel		from seeping inside. We will also adhere to a No-Fly Guideline in the event of heavy rain. The entire body of the rocket has been coated in a weather-proofing polyurethane/wood stain mixture to protect it from moisture	
Concentrated sunlight or high temperature	Overheating of components Warping of enclosure Component failure	C2	Prior to being placed on the launch pad, the rocket will be assembled in a tent-shaded area	C1
Animals getting in the way of or tampering with rocket	Potential damage to/loss of rocket/payload	D1	All switches and actuators are located either inside the rocket or at the launch viewing area.	C1
Humidity	Rocket body and internal components swell	D2	Rocket body and internal components are coated with polyurethane spray coat or protective paint layer to seal out moisture. Air flow around the camera lens will eliminate fogging.	B2
Wind	Untethered hardware blown away; Assembly of the final rocket made more difficult. Side wind could cause the rocket to cock and fly in an off-angle trajectory, making recovery more difficult. Parachute drags the rocket along the ground, putting all protuberances at risk.	D3	The amount of hardware used in assembly on launch day shall be minimized through modularization into subassemblies. The rocket shall have a high margin of stability that increases as the main engine burns out. We will also adhere to a No-Fly Guideline that will identify unsafe wind speeds. All protuberances shall be rigidly attached to the rocket body.	B2

Dryness	Rocket body may shrink Launch rail guide interface with rocket body may experience compromised integrity.	E2	Internal features toleranced such that an improbable degree of shrinkage would be necessary to create a disturbance. Button-style launch rail guides will be rigidly mounted to the rocket body through bulkheads.	D1
---------	--	----	---	----

6.1.4.2 Rocket Impact on Environment

Table 28: Rocket Impact on Environment

Rocket Impact on Environment					
Risk	Cause	Overall Environmental Effect	Risk Rating	Mitigation Strategy	Post-Mitigation Risk Rating
Negative impact from littering	Trash is left at the launch site or is improperly disposed of	Litter could have a negative impact on wildlife and vegetation	B4	We will keep trash bags at our tent and document all parts that we bring to the launch site to ensure that everything is taken back with us.	B2
Harming of animals/wildlife	Animals venturing onto launch pad Rocket dragging through wildlife on landing	Detriment to the livelihood of said wildlife	C1	A visual scan of the launch field shall be conducted both prior to setting up for launch and before launching.	B1
Electrical components leech toxic chemicals into water if water landing	Landing in water and not recovering the rocket	Detriment to wildlife and vegetation	D1	Electrical components in separate enclosure to give some protection from environment.	B1
Fire at launch pad	Dry vegetation surrounding the launch pad can ignite from the heat of the main engine.	Damage to vegetation and potential hazard to nearby team members	D2	The team will be prepared with a fire extinguisher and be aware when setting up the launch pad of any combustible materials nearby. The launch pad shall not be placed near any such materials.	D1
Mid-air explosion of rocket	Internal failure of main engine	Scattering of foreign materials in a natural environment (littering)	E1	Motor is sourced from a reliable, commercial supplier and carefully handled according to checklists.	C1
Unsuccessful parachute	Insufficient or excessive parachute deployment	The rocket will come down and likely break	E3	The recovery system shall be extensively ground-tested to validate deployment	E1

deployment/ Parachute failure	charges and/or shear pins	apart upon ground impact.		charge calculations, parachute wrapping technique, and deployment method.	
----------------------------------	---------------------------	------------------------------	--	--	--

6.2 AGSE

6.2.1 AGSE Preliminary Failure Modes

The following tables outline a preliminary estimation of the primary failure modes the AGSE system may experience. Each of these failure modes is accompanied by a likely effect and proposed mitigation strategy.

Failure modes were divided into two primary categories:

1. Structural Failure Modes
2. Electrical Failure Modes
3. Software Failure Modes and Development Risks

6.2.1.1 AGSE Structural Failure Modes

Table 29: AGSE Structural Failure Modes

AGSE Structural Failure Modes				
Risk	Overall Effect	Risk Rating	Mitigation Strategy	Post-Mitigation Risk Rating
Support structure deforms unacceptably under load	AGSE geometry is altered, possibly leading to catastrophic structural failure. Deformation will also almost certainly result in compromising the positional accuracy of the system	E3	The support structure will be tested in a load cell to validate its rigidity and load bearing capacity.	E1
Carriage platform jams under applied moment	AGSE is incapable of providing linear actuation of platforms	E2	Carriage assembly will be tested in a load cell to verify that frictional forces do not cause the carriage assembly to jam. Moving parts will be lubricated during assembly	E1
AGSE Tips over due to	AGSE is rendered incapable of completing	E2	Base plate dimensions have been	E1

base moment	mission and possibly suffers catastrophic structural damage		determined by projected center of gravity calculations. AGSE will be tested at above the maximum expected base moment to verify adequate stability	
Robot kinematics change after reassembly	Positional accuracy of end effector is compromised	D3	Connecting brackets will utilize tapped holes in individual components, ensuring proper alignment of during assembly	D1
Transportation/ handling damage	Damage to AGSE structure, actuator, manipulator, or electronics	D3	Proper storage overseen by safety advisor and student safety officer Certified member handling	C1

6.2.1.2 AGSE Electrical Failure Modes

Table 30: AGSE Electrical Failure Modes
AGSE Electrical Failure Modes

Risk	Overall Effect	Risk Rating	Mitigation Strategy	Post-Mitigation Risk Rating
Actuator position sensing accumulates error	Will cause inaccurate positioning of end effector	C3	Limit switches will be placed at the extents of the actuator range. These switches will be used to calibrate the AGSE position sensors, and to disengage the motors to prevent damage to the drivetrain.	C2
Software bug causes improper AGSE behavior	AGSE cannot properly make decisions regarding its operation, and likely cannot complete the payload capture	E3	Software systems will undergo an extensive, modular testing process to find and eliminate errors.	E1
Malfunction of electrical subsystems	Possible electrical ramifications for other subsystems; Short circuit of primary electrical system	D2	Electrical subsystems will be designed with an in-line fuse to prevent excessive current from flowing to any individual components	D1
Overload of primary electrical system	Potentially dangerous current draws from battery, possibility of catastrophic battery failure	D2	Software will be designed to prevent simultaneous activation of electrically demanding subsystems. A battery protection circuit will be utilized as a backup to limit overall power draw from battery.	D1
Low battery	AGSE suffers critical power failure	C2	Pre-launch checklist ensures battery switch if low power	C1

AGSE Experiences a temporary loss of power	Data acquisition, motor control, and current state of AGSE data is lost	C2	Mechatronic systems will run a calibration routine at startup to ensure position control error is within acceptable limits	C1
--	---	----	--	----

6.2.1.3 AGSE Software Failure Modes and Development Risks

Table 31: AGSE Software Failure Modes and Development Risks

AGSE Software Failure Modes and Development Risks				
Risk	Overall Effect	Risk Rating	Mitigation Strategy	Post-Mitigation Risk Rating
Development machine failure	Code loss Delay in project Unusable AGSE	D2	We will be using a multiply-backed up development repository hosting our AGSE design and code which will ensure that even if all of the team's personal computers crash and all our local copies of the code and design are lost, we will have multiple backups available to continue where development left off.	B2
Personal Health Issues or Time Issues	Delays in development	C4	We have multiple competent developers working on the AGSE system who are each aware of the design and implementation details so that if any one team member is unhealthy or occupied by other work, the development can continue through the other team members.	A4
Hardware Lock-In and Complex Development	Setbacks in development of software, integration Prevention of testing of AGSE	C4	The development of the system proceeds in a modular approach, with development platforms being swapped in and out as the code and design matures. This allows the design and implementation to start off simple, with individual components (that are simpler to develop for) being replaced or removed and their functionality being integrated into a more sophisticated component. For instance, we can develop the code to control the actuators and receive the sensor data on simpler devices (like an Arduino), and migrate that code into the larger code base on the main platform as both platforms' code matures.	B3
Integration Issues	Delay in project Prevention of testing of AGSE	C3	By utilizing a modular design and implementation approach (with respect to both hardware and software) we can independently develop smaller units of functionality and test their integration in a more well-defined manner to ensure that each component works and works together before proceeding further with integration. The use of unit tests for each component aids in this strategy.	B2

Missing deadlines	Penalty in competition Delay in project	E2	By building the system in a modular manner and adding in more advanced features only as the basic features are guaranteed to work, we can ensure that at each stage of development we have a working system. Should one stage not be able to be finished due to deadline issues, we can fall back to the previous working stage. Finally, we have developed an in-depth development and testing timeline which ensures that each team member has a task and that their task is related to their areas of expertise.	E1
Software Complexity and Developmental Bugs	Delays in development in code Inability to find bug in complex code	C2	Much of our code complexity will come from the image processing algorithms that we will be using. To minimize the number of developmental bugs and challenges will be starting our implementations using off-the-shelf algorithms as a base. These will be provided as CUDA libraries, which enjoys a large user-base and many avenues of debugging and developmental assistance.	C1
Sample Detection Failures	Failure to autonomously retrieve sample Failure to meet NASA requirement that sample be autonomously retrieved	D3	We plan on tackling inconsistencies in sample detection by running multiple off-the-shelf image processing algorithms (on every input image frame) that detect the target sample. The results obtained from either sequential or parallel multi-algorithm image processing provide a measure of confidence about the relative position and orientation of the target sample. An average position and orientation is chosen and the gripper is moved to this position.	D1
Inconsistent State of the Control System	Unreliable and unpredictable movement of AGSE system Failure to retrieve object and place it in rocket Failure to meet NASA requirements	D2	The software design for the AGSE follows a strictly deterministic state machine. From every state, the system transitions into a deterministic and consistent new state under precisely defined conditions. All state variables that dictate arm movement and image processing are stored in persistent memory. If the system reaches an inconsistent state where some system-level constraints are not satisfied, the control rolls back to the nearest stable state. Indefinite control loops caused by propagating software faults are also detected and broken.	D1
Component Failures	Failure of AGSE Failure to meet NASA requirements	D4	System components such as the camera, processing and actuation units are integral to correct operation of the AGSE. Failures at the component-level are tackled by using (1) redundant sub-system units and (2) failure-tolerant software. Hardware-level redundancies are constrained by the overall power and weight specifications.	B2

			Software-level redundancies provide a stable control system platform to handle memory corruptions and unexpected state inconsistencies.	
--	--	--	---	--

6.2.2 AGSE Environmental Hazards and Concerns

6.2.2.1 Environmental Impact on AGSE

Table 32: Environmental Impact on AGSE
Environmental Impact on AGSE

Risk	Overall Effect	Risk Rating	Mitigation Strategy	Post-Mitigation Risk Rating
Rain, mud	AGSE could sink unevenly into the ground, resulting in balancing issues Electronics short-circuit	C2	The team will bring a level and, in the event of mud, plywood boards to prevent the AGSE from sinking into the ground. Electronics enclosures will be sealed to prevent water from seeping inside.	B2
Concentrated sunlight or high temperature	Overheating of components Warping of parts Glare on camera	C2	AGSE will be kept in the shade of the tent before operation System will be tested at different temperatures to avoid interference issues, especially closely-toleranced parts Camera will be tested in the sun	B2
Animals getting in the way of or tampering with AGSE	Potential damage or tipping of AGSE	D1	All switches and actuators are located either inside the AGSE or at the launch viewing area.	C1
Humidity	Condensation on electronics Gripper camera lens could become fogged	D2	Electronics will be covered in casing that is sealed to be water-resistant Camera lens will be checked before operation and cleaned off	B2
Dust/dirt	Collection of dust or dirt in AGSE could damage moving parts or electronics	C3	Moving parts and electronics and will be shielded from foreign materials	D1

	Camera lens could become too dusty to operate			
Wind	High winds could tip AGSE over or affect position of end effectors	D3	AGSE system will be tested under various wind conditions to confirm integrity of base structure and position of end effectors	B2
Wireless interference	Ambient wireless interference or interference from other teams could affect start and stop of our AGSE operations	D3	Develop a very specific communication protocol between wireless start-and-stop devices and AGSE	D1

6.2.2.2 AGSE Impact on Environment

Table 33: AGSE Impact on Environment

AGSE Impact on Environment					
Risk	Cause	Overall Environmental Effect	Risk Rating	Mitigation Strategy	Post-Mitigation Risk Rating
Negative impact from littering	AGSE parts break off	Litter could have a negative impact on wildlife and vegetation	B2	We will keep trash bags at our tent and document all parts that we bring to the launch site to ensure that everything is taken back with us. Design will be robust enough to ensure complete structural integrity	B1
Harming of animals/wildlife	Animals venturing near AGSE	Detiment to the livelihood of said wildlife	C1	A visual scan of the launch field shall be conducted both prior to setting up for launch and before launching.	B1
Electrical fire in AGSE	Batteries if not used properly may combust	Possible spread of fire	E2	The team will be prepared with a fire extinguisher. Batteries will be tested thoroughly under a variety of conditions and will be protected in a fire-proof casing. Battery circuit will prevent overload	D1

7 Launch Operations Procedures

7.1.1 Launch Procedure Flowchart

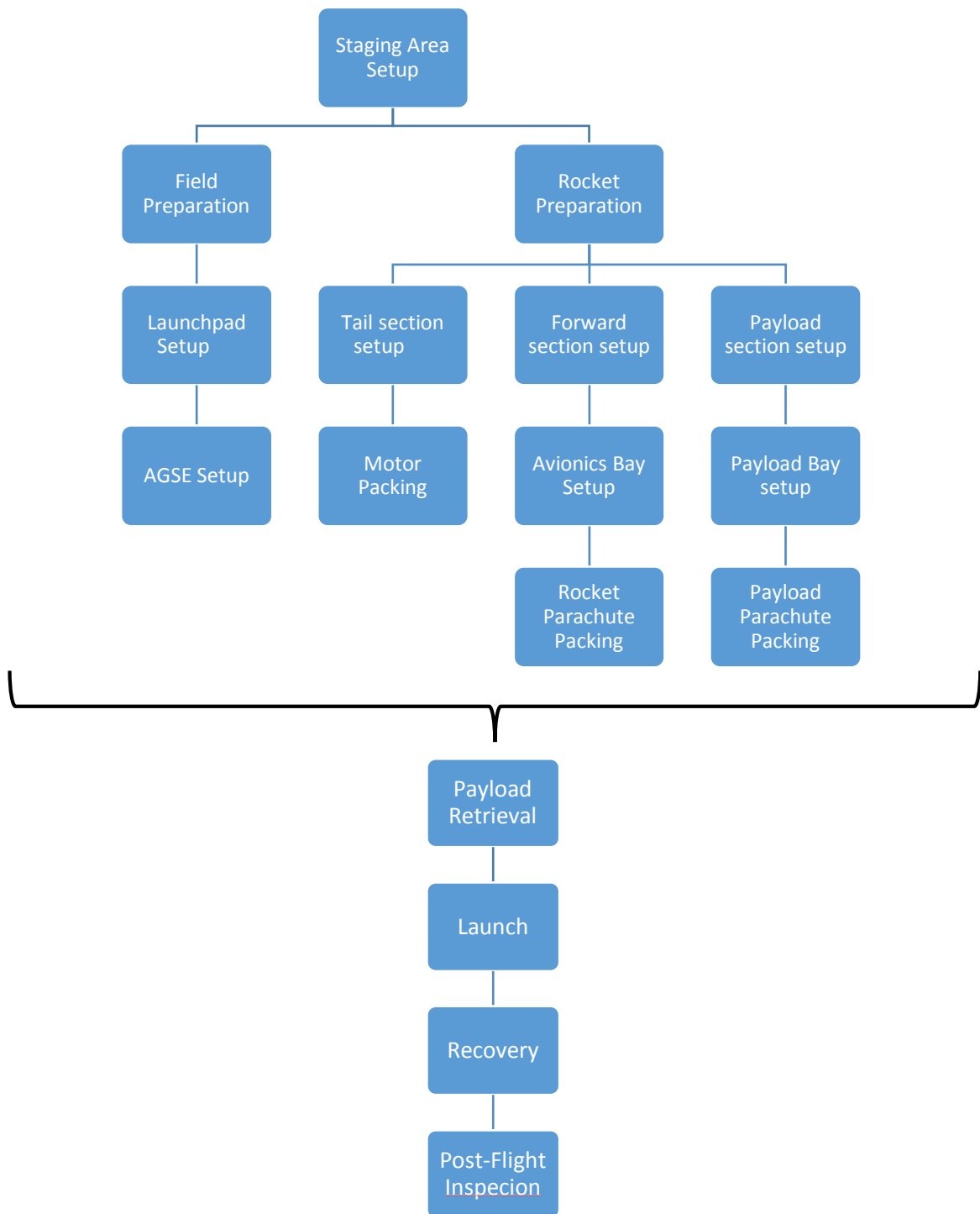


Figure 183: Flowchart of Launch Day Procedures

7.1.2 Launch Checklists

The team will review system preparation requirements well in advance of the launch. Safety oversight and launch procedures are managed by the launch leader. The safety officer, Connor, will oversee all operations where danger to people or rocket might exist. Team leaders will supervise the preparation of their respected areas. Formal integration of systems requires the launch leader's oversight. A member of NAR with appropriate certifications will oversee the assembly of the propulsion system. This is a quality control measure to ensure that mission essential systems are properly prepared for launch. All launch procedures are divided into systems along with the personnel required and are listed in the next section along with an inventory of tools, parts, and other supplies required for setup and launch.

7.1.2.1 Inventory Checklist

Launch Inventory Checklist

- Setup
 - Launchpad
 - Launch rail
 - Launchpad truss
 - Launchpad legs
 - Tables (x3)
 - Chairs
 - Tent and stakes
 - Tarp
 - Football
- Tools
 - Electric drill
 - Drill bits
 - Wire cutters
 - Wire strippers
 - Pliers
 - Set of Allen wrenches
 - Philips screwdrivers
 - Flathead screwdrivers
 - Set of small screwdrivers
 - Level
 - Mallet/hammer
 - Soldering iron and solder
 - Scissors and big shears
- Measuring Tools
 - Digital calipers
 - Tape measure
 - Multimeter
 - Handheld anemometer
- Adhesives

- 5-minute epoxy
- 2-ton epoxy
- Epoxy resin
- Electrical tape
- Gorilla tape
- Masking tape
- Batteries
 - 9V batteries
 - Extra drill battery
 - AGSE 12V batteries
- Avionics box
 - Putty
 - E-matches
 - Zip ties
 - StratoLogger* Altimeters
 - Avionics bay
 - Wire
 - RF transmitter
 - RF trackers
 - Laptop to setup altimeters
 - StratoLogger* manual
 - StratoLogger* USB adapter
- Rocket
 - Shear pins
 - Tail section
 - Payload section
 - Forward section
 - Rocket X-frames
 - Bungee cords
 - Carabiners
 - Motor
 - Rocket body (including payload bay)
 - Ignition supplies
 - 2 30" elliptical parachutes
 - Shock cords
 - Anti-zipper devices (Fireball)
 - Quick links
 - Black powder
 - Motor retention ring
- AGSE
 - AGSE vertical and horizontal stages
 - AGSE table
 - AGSE user interface panel
 - AGSE table legs
 - Extra wire

- Extra shaft collars
- PCBs and cases
- Payload Bay
 - 3/16", 3/32", 5/64", 1/16", 0.05", and 1.5mm Allen wrenches
 - 3/8" and 1/2" wrenches
 - Loctite
- Miscellaneous
 - Gold Sharpie
 - First aid kit
 - Latex gloves
 - Cooler
 - Rags
 - Baby powder

7.1.2.2 Setup and Assembly Checklists

Launch location Setup

- Unload equipment and materials from vehicles.
 - Setup tent and secure with stakes.
 - Assemble portable tables.
 - Place stands for each rocket section on tables.
 - Place rocket sections on stands.
 - Place avionics/electronics box on own table.
 - Ensure desired launch pad location will provide a sturdy base for rocket launch.
- ⚠ WARNING: If no such ground condition exists, abort launch.**
- Place launch pad components near desired launch location.

Launch Pad Setup

- Insert the four launch pad legs into the launchpad plate.
 - Minimize the height the launchpad is configured from the ground.
 - Bolt on the launch rail base to the main launch pad and face it away from any spectators.
 - Pivot the launch rail joint into a horizontal configuration.
 - Secure the top launch rail section to the base via the joining piece and secure with bolts ensuring a flush fit.
 - Reorient the launch rail to the vertical configuration and secure with bolts.
 - Use a level placed on the launch pad in a vertical configuration to verify that the launch pad is oriented perpendicular to the launch area. Adjust the leg heights by twisting the launch legs using a wrench to the necessary positions in order to ensure the launch rail is in the correct vertical alignment.
- ⚠ WARNING: This step is imperative for straight flight.**

- Undo the bolts that secure the launch rail in the vertical position and pivot the launch rail to be horizontal in order to integrate with the AGSE table.
 - If necessary, use ladder to support launch rail in horizontal position so that tipping does not occur.
 - Inspect fully assembled launch pad to ensure it provides a sturdy base for the rocket during launch.
- ⚠️ WARNING:** If any damage exists, abort launch.

AGSE Transport

- Unscrew legs from AGSE table.
- Detach gripper from gripper arm and store separately.
- Place AGSE into carrying case.
- Feed AGSE legs through the bottom of the carrying case into the threaded holes in the AGSE table in order to secure AGSE to bottom of the box.
- Reinforce this connection using the legs' nuts to clamp the table to the box from under the carrying case and from over the AGSE table.
- Attach clips in carrying case to parts of AGSE to mitigate wobbling during transport.
- When carrying the case, keep case upright at all times and avoid any bumps or disturbances.
- When the case is placed in a vehicle, strap it down with bungee cords.
- Reverse these steps during unpacking.

AGSE Setup

- Remove AGSE from carrying case.
- Place AGSE table so that the rocket, placed horizontally, is within the workspace of the AGSE.
- Set the height of the AGSE table to be coplanar with the launchpad.
- Level the AGSE
 - Set reference corner as the corner under which the ground elevation is highest.
 - Set up two levels perpendicularly from the reference corner to level the table.
- Lay the rocket launch rail onto the support on the AGSE table.
- Attach gripper to gripper arm and connect cables to wrist servo and camera.
- Mechanical systems check
 - Check that the base rotation motor is properly attached to the servo sled.
 - Check that the timing belt connecting it to the main AGSE rotation shaft is properly tensioned and that it rests correctly within the pulleys.
 - Ensure horizontal and vertical motors are properly attached to mounts and shaft couplings.
 - Ensure encoder wheels have not sustained damage in transport and that encoders are still attached in the correct places.

- Check the horizontal and vertical lead screws for any obstructions, damage, or debris.
- Check that the limit switches are properly mounted and can be triggered.
- Apply lubricant to guide rods if necessary.
- If possible, manually run vertical and horizontal motors to ensure movement in those directions.
- If possible, manually run AX-12A servos to ensure gripper movement, gripper rotation, and base rotation.
- Electrical systems check
 - Ensure that the batteries are not connected to the system and that no part of the AGSE is powered on.
 - Re-check that the system is not powered on. We must connect all cables of the system and verify their connection before applying power to the system.
 - Visually inspect all parts of the AGSE electronics (batteries, circuit boards, cables) for signs of damage.
 - Test connectivity of all cables using a multimeter. Ensure proper connectivity for all conductors of all cables and ensure no shorts between conductors.
 - Connect the usb camera to the Nvidia Jetson TK1's USB host port.
 - Connect an ethernet cable to the Jetson's ethernet port. Connect the other end of this cable to the network switch at the base of the AGSE.
 - Connect the Jetson power supply cable (split off from the main AGSE power supply cable) male plug connector into the Jetson's barrel jack power port.
 - Connect the Network Switch power supply cable (split off from the main AGSE power supply cable) male plug connector into the network switch's power port.
 - Connect the motor encoder connectors to the BBB Cape in their proper places. The connectors are locking and polarized to ensure no improper connections can occur. Make sure the radial actuator encoder is connected to the terminal marked on the PCB by "R-Enc" silkscreen and the vertical (z-axis) encoder is connected to the terminal marked on the PCB by "Z-Enc" silkscreen.
 - Connect the servo motor splitter cable (which goes to both the base rotation servo and the gripper rotation servo motors) male plug into the female connector marked AX-12A on the PCB. This connector is also a polarized locking connector to ensure no improper connections can be made.
 - Ensure that one of the servo motor splitter cable's connectors connects to the base rotation servo motor (which is a locking, polarized connector.)
 - Ensure that one of the servo motor splitter cable's connectors connects to the gripper rotation servo motor (also a locking, polarized connector).
 - Ensure that the short servo motor daisy-chain connector is connected to both the gripper rotation servo motor and the gripper positioning servo motor.

- Connect the positive and negative leads from the radial linear actuator motor to the screw-terminal on the BBB Cape marked "R Axis." The positive lead connects to the "+" terminal, and the negative lead connects to the "-" terminal.
- Connect the positive and negative leads from the vertical linear actuator motor to the screw-terminal on the BBB Cape marked "Z Axis." The positive lead connects to the "+" terminal, and the negative lead connects to the "-" terminal.
- Connect the positive and negative 12V power cable conductors (split off from the main AGSE power supply cable) to the "+" and "-" screw terminal connectors marked "12V" on the BBB Cape
- Connect the BBB Cape to the BeagleBone Black. This cape can only successfully mount in one orientation.
- Connect an Ethernet cable to the ethernet port of the BeagleBone Black. Connect the other end of this cable to the network switch at the base of the AGSE.
- Using a multimeter, measure the battery voltage for each of the two 12VDC Lead-Acid batteries. Use caution to not short the terminals of the battery! Ensure that the measured voltage is within the acceptable range of the batteries and the power supply (each battery should be within 11.5VDC-13.5VDC).
- Connect the batteries in series using the supplied battery connectors.

⚠ WARNING: Use caution not to short the terminals of the batteries
- Using a multimeter, measure the voltage over the two terminals coming from the batteries that are now connected in series. Ensure that the measured voltage is within the acceptable range for the input of the power supply (14-36VDC)

⚠ WARNING: Use caution not to short the two terminals
- Connect the negative battery connector to the negative power supply input on the DC/DC converter.
- Connect the positive battery connector to the positive power supply input on the DC/DC converter.
- Using a multimeter, measure the voltage across the output terminals of the DC/DC power supply. Use caution to not short the terminals of the power supply! Ensure that the measured voltage is within the acceptable range for the AGSE power (11.5-12.5VDC).
- Connect the main AGSE power cable to the DC/DC converter output terminals. Use caution to ensure proper polarity and no short circuits!
- Press the power-button on the Nvidia Jetson TK1
- Ensure the User Interface Panel powers on; screen should turn on and lights should turn on.

Tail Section Check and Assembly

- Insert the tail cone around the exposed rocket motor tube.

- Inspect the tail section for any damage from transportation and handling, specifically the structural integrity of the fins, body and motor tubes, and bulkheads.

Avionics Assembly and Integration

- Inventory all avionics equipment.
- Inspect all avionics equipment for safety and security.

⚠ WARNING: If any such components or equipment that cannot be readily repaired or replaced damage exists, abort mission.
- Ensure the StratoLogger altimeters are secure and set for apogee and 1000ft and that the connections are secure.
- Connect all charge ignition wires connecting altimeters to wire terminals outside the avionics bay. Seal interior holes on the bulkhead with putty.
- Connect arming switches to each altimeter.
- Place batteries in clip. Tape and zip tie. Check the 9V battery terminals.
- Check voltage on new 9V batteries.
- Connect 9V batteries to each altimeter and secure to lower avionics bay bulkhead using zip ties/tape.
- Verify correct wiring scheme for both altimeters.

⚠ WARNING: Failure to perform this step may result in incorrect deployment of recovery system in flight.
- Turn on RF transmitter in avionics bay.
- Install top avionics bay bulkhead thus enclosing avionics bay.
- Place parachute charges in blast caps and secure with blue painters tape.
- Inspect all separation ignition wires.
- Seal wire passage holes into avionics bay with removable putty.
- Place putty over all wire terminals in parachute sections to ensure screws do not loosen.

Payload Section

- Attach 9V battery to connectors.
- Test actuation of payload bay using Hall Effect sensor and magnet to trigger activation.
- Turn on RF transmitter in electronics bay.

Recovery System Assembly and Integration

- Take inventory of all recovery equipment.
- Inspect all Kevlar fiber shock cords, protective blankets, and anti-zipper devices for safety and security.
- NOTE:** Connect shock cords to bulkheads and bays before insertion when possible
- Forward section

- Mount avionics bay inside forward section, align and secure.
- Confirm that altimeter switches can be reached after installation inside forward section
- Seal avionics bulkheads with removable putty.
- Inspect static pressure ports for obstructions.
- Inspect rocket parachute for hardware defects and security
- Ensure all shock cord and parachute connections are in their proper locations.
- Visually inspect the deployment charges for secure connection (3.0g, 3.2g backup).
- Visually verify that deployment charges are secured in their respective blast caps.
- Fold and load payload parachute into nose cone followed by shock cord, folded using a z-fold.
- Join nose cone to forward section of rocket via three 4-40 nylon shear pins.
- ⚠️ WARNING: failure to use three shear pins may result in premature jettison of payload section in flight.**
- Payload section
 - Connect shock cord to top of payload section.
 - Connect opposite end of shock cord to parachute.
 - Connect bottom of avionics bay to its respective position on the shock cord.
 - Place payload parachute charges in blast caps in nose cone and secure with blue painters tape. (2.0g, 2.0g backup)
 - Inspect all separation ignition charges.
 - Connect parachute to nose cone bulkhead via a shock cord.
 - Inspect payload parachute for hardware defects and security.
 - Ensure all shock cord and parachute connections are in their proper locations.
 - Visually inspect the deployment charges for secure connection.
 - Visually verify that deployment charges are secured in their respective blast caps.
 - Load parachute and shock cord, folded using a z-fold, into forward section of rocket below avionics bay.
 - Join forward section of rocket to the aft section via three 4-40 nylon shear pins.
- Once rocket is loaded onto launch rail and ready for launch, arm each altimeter and listen for correct sequence of beeps before launching.

Rocket Motor Installation

- Motor should be stored in own container for transport and secured to avoid drops or impacts.
- ⚠️ WARNING: Failure to transport motor safely and securely may result in cracking of propellant grains and inflight motor failure.**
- Inspect the motor to ensure that no damage occurred during transportation or handling that could result in such failures.
- ⚠️ WARNING: If such damage has occurred, abort mission and safely dispose of faulty motor under the supervision of the safety officer.**

- Insert the Cesaroni P54-3G J380 motor into rocket motor tube and tighten the positive screw cap retention ring. Applying baby powder to the exterior of the motor can help facilitate installation.
- Verify that the positive screw cap retention ring is securely fastened to the rocket.

Launch Vehicle, Launch Rail, and AGSE Integration

- Carefully carry rocket assembly to the launch pad.
 - Line up the launch lugs that are attached with the rocket to the launch rail slots. Very slowly slide the launch lugs onto the rail guides making sure not to put a bending moment the rocket.
- ⚠ WARNING:** failure to slide launch lugs onto the rail guides slowly may result in detaching the launch lugs and flight failure
- Rest rail in horizontal position on rocket stand on AGSE table

7.1.2.3 Launch Checklist

- Start AGSE using User Interface Panel
 - AGSE autonomously collects sample and places it into payload section of rocket
- ⚠ WARNING:** if AGSE is showing any sort of dangerous or otherwise unpredictable behavior, hit pause switch
- Payload section closes and AGSE moves out of the way of the rocket
 - AGSE stopped using User Interface Panel
 - Once the launch vehicle is oriented so that the tail cone is placed one foot off the launch pad, slowly raise the launch rail back into a vertical configuration and bolt down the pad so that it will not pivot.
 - Altimeter-beeping sequence is all systems go.
 - Check for loose fittings in the fins, rocket sections, payload, and launch lugs.
 - Insert the Cesaroni Profire igniter into the rocket motor and attach the leads that connect the igniter to the ignition trigger.
 - Ensure the ignition system is wired to the power source.
 - Move to safe distance, at least 100yd from the launch pad.
 - Loudly announce that the “range is hot” and ensure everyone is a safe distance from the launch pad.
 - Insert the key and listen for high-pitch sound of continuity.
 - Ensure skies are clear of aircraft and birds.
 - Begin initial countdown to launch at T-minus 10 seconds.
 - At T-minus 1 second, depress button on ignition system to launch.
 - Immediately after launch, remove key from ignition system.
 - Disconnect ignition system leads from power source.

7.1.2.4 Post-Launch Checklist

- Visually track the rocket throughout the flight. Once the main parachute has opened, begin to predict the landing position. As soon as the launch vehicle lands during a full scale test flight begin heading towards the launch vehicle. Or on competition day, as soon as NASA gives the OK to go recover the launch vehicle begin to head towards the launch vehicle.
- Record apogee as measured by the altimeters by listening to the audible beeps produced by the StratoLogger altimeters.
- Carry the sections of the rocket back to the staging area.
- Mark and discard the 9V battery.
- Check for structural damage on the airframe.
- Check for rocket and payload parachute damage.
- Discard the spent engine casing.
- Check for fractures in the avionics section.
- Debrief the launch, including: motor used, rocket configuration, altitude achieved, avionics on-board, and rocket recovery.

7.1.3 Launch Abort Conditions

Along with the pre-launch checklists, a series of questions have been put together to ascertain whether the rocket is safe to launch. These questions must be answered by the safety officers prior to giving the go ahead to launch and serve to ensure there are no conditions with the rocket, payload, or environment that would prevent a safe launch. If any of the following questions are answered with a “**YES**”, the launch **must be aborted** unless the issue can easily and safely be solved.

- ⚠ Did damage occur to any of the following rocket/payload components during transport?
 - Motor
 - AGSE
 - Rocket or Payload Parachute
 - Avionics Board or *Stratologger* Altimeters
 - Rocket Vehicle Sections
 - Vehicle Fins, Nose Cone, or Tail Cone
 - Launch Pad
- ⚠ Are any untested or non-certified motors or other potentially unsafe materials being used in the flight?
- ⚠ Are motors being used that require certifications higher than those possessed by anyone present?
- ⚠ Is there any risk of the launch pad being unstable due to poor ground conditions?
- ⚠ Did any parts/connections become loose during transport?
- ⚠ Is there anyone within 300 feet of the launch pad?
- ⚠ Is there any equipment within 100 feet of the launch pad?
- ⚠ Is the launch pad within 1500 feet of any inhabited buildings or roadways?
- ⚠ Did the payload bay fail to close and seal properly?

- ⚠ Is the AGSE obstructing launch equipment in any way?
- ⚠ Do known wind speeds exceed 20mph?
- ⚠ Will weather conditions (precipitation, extreme heat, etc.) compromise the integrity of rocket materials, AGSE electronics, or payload bay electronics, or otherwise damage functionality of rocket components?
- ⚠ Are there any questions or concerns about the safety of the launch and those involved?
- ⚠ Have any items from the checklists or launch operational procedures been missed?
- ⚠ Is the actual rocket center of gravity location different from the simulated center of gravity location?

If any of the above questions are answered with a “**YES**,” **abort launch** unless the problem can be fixed without compromising the safety of the team, bystanders, or the rocket.

7.1.4 Post-Flight Inspection

After the launch, the payload system and remainder of the rocket must first be retrieved from their landing locations. Before handling any of the equipment, we first verify that there were no failures during flight that may cause injury if touched. Then, we first package up the parachute to avoid tearing the fabric and return to the launch site. Starting with the payload system, we first verify that the exterior and interior support systems are still intact. Then, we test the electronics by opening the payload bay and retrieving the payload from the launch vehicle. We then inspect the avionics bay and determine the height reached by the rocket and compare it to our simulations. After verifying that the avionics bay has been proven to have returned safely, we turn our attention to the tail section. The structural integrity of the fins is checked first, then the motor retainer is removed. The motor and motor casing are extracted from the tail section and the integrity of the motor mount tube is inspected. Last, the shock cords and parachutes are checked for any burns or tears. After inspecting the launch vehicle, the AGSE is inspected. Visual inspection of the structural supports of the AGSE is carried out to ensure that the launch did not affect the system. Then, actuation of each motor on the AGSE is performed to ensure that the electronics of the AGSE were not adversely affected by the launch. Once the inspection is completed, the launch vehicle, avionics bay, recovery system, payload system, and AGSE are packaged separately for the return trip.

7.2 Safety and Quality Assurance

The following sections describe the safety procedures for each of the following categories: recovery preparation, motor preparation, igniter installation, launch procedures, and post-flight inspection. The team’s rocketry and safety mentor Robin Midgett will be in charge of all launch procedures with the assistance of student safety officer Connor Caldwell, and students will not be put in charge of potentially dangerous activities. Every activity will have a safety protocol that will be loudly read out and monitored by a protocol officer on the team to help smooth and safe flow of activities.

7.2.1 Recovery Preparation

- Parachute can catch the wind when being prepared in the field, and this can be hazardous to personnel and the rocket. We will fold and prepare parachutes indoors.
- Handling of gunpowder charges for the recovery system:
 - The handling of gunpowder is by far the highest risk activity that will be done only by certified students under the close supervision of the safety officer.
 - Person responsible will wear proper safety gear
 - Will be assisted by safety officer and safety mentor in the process
 - Team will provide wind cover so gunpowder does not fly away
 - Exact measurements will be put in a small plastic pouch
 - Check that E-match is shorted to prevent premature explosion
 - Remove plastic sheathing around E-match
 - E-match will be introduced into the powder
 - Pouch sealed with a zip tie.
 - Risk of explosion prevented by only arming E-match at a safe time and making sure that none of the parties are in-line with the rocket.

7.2.2 Motor Preparation

- Will be mainly done by the Student Safety Officer Connor Caldwell and supervised by Safety and Rocketry Mentor Robin Midgett
- Safe activities will be handled by students as permitted by Safety Officer/Advisor
- Will be done on an isolated table free from ignition sources
- Igniter will be loaded only on the launch pad, as it is catastrophic to load it at any other time before.
- Gloves will be worn while handling grains.

7.2.3 Igniter Installation

- Only the Safety Mentor will undertake this task, after making sure that the igniter wire is shorted. He will do all these activities in close association with NASA range officers.

7.2.4 Launch Procedures

Launch Rail Safety:

- Launch rail to be horizontal in order to later integrate the launch vehicle and AGSE.
- Launch rail can fail if improperly fastened; launch rail will be properly supported by the field engineer team until all bolts are securely fastened and certified.

- A separate 8ft ladder will be taken to the launch site, so team members will not end up standing on the launch platform while reaching for anything on the rocket, such as altimeter arming switches.

Payload/AGSE Safety:

- The AGSE User Interface Panel is the main safety device when the AGSE operates. The UIP contains a pause switch that will pause the AGSE if it is observed to be doing any sort of dangerous or otherwise unpredictable action.
- Because of the autonomy of the Payload-AGSE system, there is little to no human interaction with them, mitigating risks to members of the team or any observers. People will be instructed to stand back though during the operation of the AGSE and payload bay.

7.2.5 Troubleshooting

- Only minor troubleshooting of rocket systems and components will happen on launch day.
- The only troubleshooting to be performed on site will be minor fixes that either take very little time and effort to accomplish or are only peripherally related to the success of the mission and safety of everyone involved.
- Any troubleshooting requiring extensive time or materials, whether it is a repair of a damaged or unsafe component or a malfunctioning system, will result in aborting the proposed launch to ensure the safety of everyone involved and critical mission success.

7.2.6 Post-flight Inspection

- Upon reaching the launch vehicle, immediately pull the main parachute down and fold it so that the launch vehicle will not be dragged off.
- Misfired motors and motor shells will be neutralized in water. All trash will be bagged and not disposed at the site. Field site will be left clean.

7.2.7 Additional Risks

See sections 6.1: Launch Vehicle and 6.2: AGSE for all risk assessments, including categorized risk ratings along with proposed and completed mitigation strategies for all rocket vehicle sections and components, payloads, launch operations, and environmental concerns. These sections include comprehensive tables listing all risk assessment information such as risk, cause, overall effect, mitigation strategy, pre- and post-mitigation risk rating, and verifications of mitigation strategies.

8 Activity Plan

8.1 Budget Plan

8.1.1 Funding Plan

The expenditures for previous years have been studied thoroughly and have provided a sound benchmark for estimating the expenses for this year's project. Funding is currently from the Vanderbilt University School of Engineering Dean's Office with the possibility of being reimbursed by the Tennessee Space Grant Consortium contingent on budget changes for the 2014-2015 school year. The total available budget for the design project and rocket construction is \$15,000.

8.1.2 Itemized Budget

The Vanderbilt Aerospace team has been working with a smaller budget this year than in the past and thus has had to keep a much tighter control on its expenditures throughout the year. The team treasurer, Connor Caldwell, has been responsible both for logging all purchases and incurred costs as well as updating the Vanderbilt Mechanical Engineering Department on our spending. Below is a detailed documentation of the team's budget as of FRR. As can be seen in *Table 34: Itemized Budget and Projected Costs*, after construction of the final rocket, payload bay, and AGSE, the team has approximately \$7,000 remaining in the budget. This may seem to be excessive, but looking at past years' expenses at final launch, we want to make sure to stay under budget. As shown at the bottom of the table, we have projected just under \$5,000 in travel costs for the final launch. Even though this figure is probably inflated, we still have nearly \$2,000 of cushion for last minute purchases or other incurred costs. Also included below are Pie Charts detailing our current and projected expenses, as well as a table detailing the cost "as flown" for both subscale launches as well as our final deliverables for the competition.

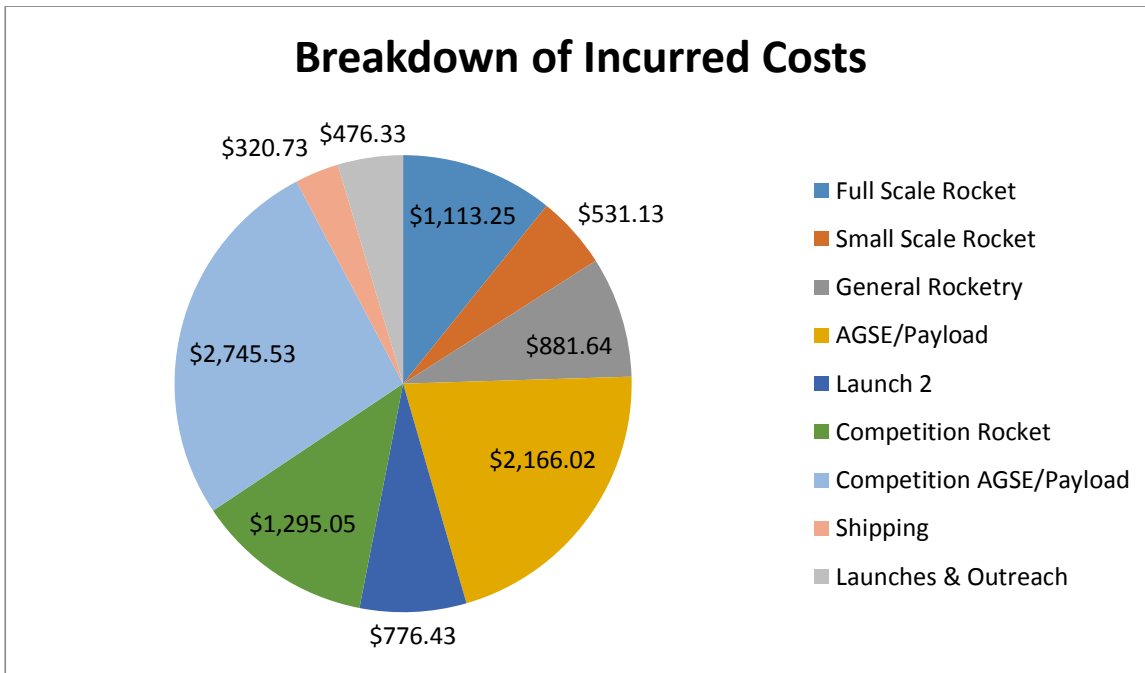


Figure 184: Pie Chart of Incurred Costs

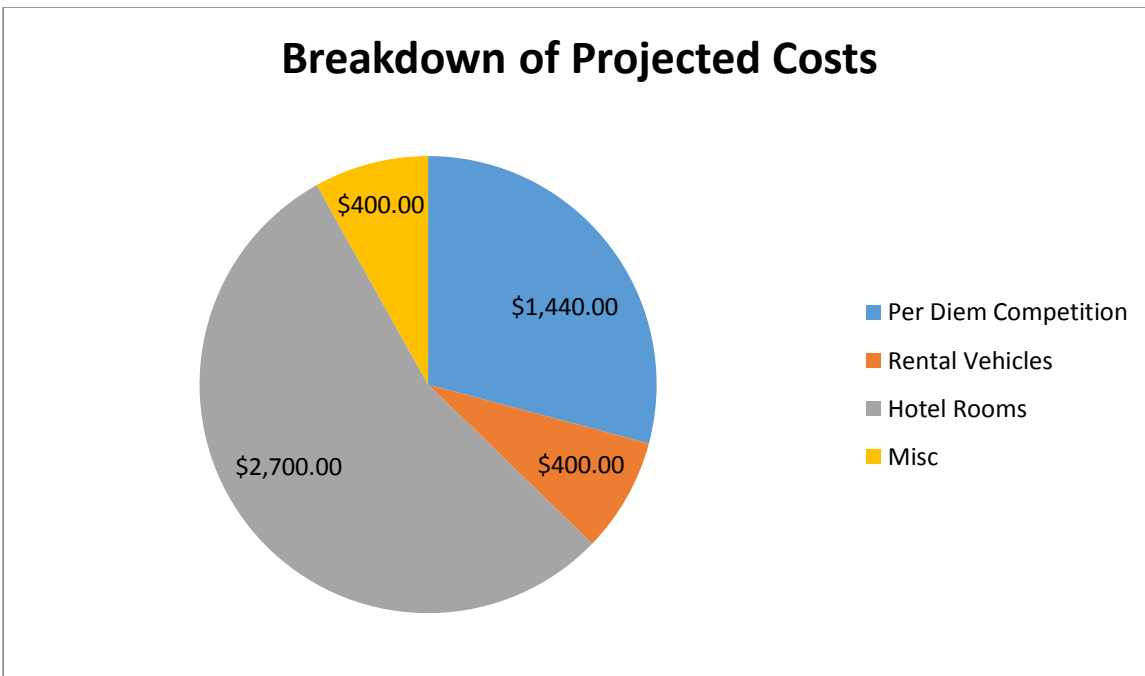


Figure 185: Pie Chart of Projected Costs

Table 34: Itemized Budget and Projected Costs

Vendor	Part Number	Cost	Quantity	Total
Starting Budget				\$15,000.00
	NASA Allowance			\$600.00
	Boeing Contribution			\$2,000.00
Total Budget				\$17,600.00
Full Scale Rocket				\$1,113.25
ApogeeRockets	12 ft 5.5" outer tube	\$56.95	3	\$170.85
already owned	8 ft 5.5" inner tube			
ApogeeRockets	PNC 5.38" Short Nose Cone	\$54.95	2	\$109.90
Giant Leap	Cesaroni L1030	\$176.15	4	\$704.60
ApogeeRockets	54mm motor sleeve	\$23.95	1	\$23.95
Giant Leap	54mm Motor Casing 6 grain	\$103.95	1	\$103.95
Small Scale Rocket				\$531.13
ApogeeRockets	4 ft parachute	\$132.68	1	\$132.68
Giant Leap	38 mm motor reloads	\$65.15	2	\$130.30
ApogeeRockets	38 mm motor sleeve	\$16.49	1	\$16.49
ApogeeRockets	38mm retainer	\$31.03	2	\$62.06
ApogeeRockets	PNC-4.00" x 9.5" Nose Cone	\$19.95	2	\$39.90
ApogeeRockets	12 ft 4" outer tube	\$38.95	3	\$116.85
ApogeeRockets	8 ft 4" coupler	\$10.95	3	\$32.85
General Rocketry				\$881.64
ApogeeRockets	shock cord - 100lb	\$0.31	50	\$15.50
ApogeeRockets	shock cord - 300lb	\$0.49	50	\$24.50
Giant Leap	Small Fireball Anti-Zipper	\$15.97	2	\$31.94
Giant Leap	Large Fireball Anti-Zipper	\$19.83	3	\$59.49
Giant Leap	Small Parachute Protectors	\$11.01	1	\$11.01
Giant Leap	Large Parachute Protectors	\$12.45	2	\$24.90
Dragon Pate	1/8" x 24" x 48" quasi-isotropic	\$564.30	1	\$564.30
Loftis Steel	Fin water jet cutting	\$150.00	1	\$150.00
AGSE/Payload				\$2,166.02
Firgelli	L16-P Linear Actuator - 140mm - 150:1 - 12 volts - Yes, Add LAC (Linear Actuator Control Board)	\$100.00	1	\$100.00
Firgelli	LAC Board Case	\$12.00	1	\$12.00
Firgelli	USB Cable	\$4.00	1	\$4.00
Firgelli	DC Power Supply - 12 volts	\$10.00	1	\$10.00

Amazon	Arduino UNO R3	\$22.00	3	\$66.00
CrustCrawler	MX-28 Turntable with actuator	\$348.00	1	\$348.00
CrustCrawler	SG Gripper Hardware	\$129.00	1	\$129.00
Logitech	HD Pro Webcam	\$99.99	1	\$99.99
McMaster-Carr	6061 3/8" Aluminum Rod	\$11.85	4	\$47.40
McMaster-Carr	Shaft Collar	\$1.77	12	\$21.24
McMaster-Carr	Worm-Drive Hose Clamp	\$11.63	1	\$11.63
McMaster-Carr	6061 Aluminum 1/8" x 1-1/4" x 1-1/4" Legs	\$3.90	4	\$15.60
McMaster-Carr	Swiveling level mount	\$5.20	4	\$20.80
McMaster-Carr	1/4"-20 threaded cap screw, 2-1/4" long	\$3.63	1	\$3.63
McMaster-Carr	threaded steel rod, 1/4"-20 x 1ft	\$0.62	10	\$6.20
McMaster-Carr	Steel Nylon-insert hex locknut 1/4"-20	\$3.18	1	\$3.18
McMaster-Carr	yellow plated steel hex nut 1/4"-20	\$3.31	1	\$3.31
McMaster-Carr	PTFE washer 1/4"	\$3.48	1	\$3.48
McMaster-Carr	SAE 841 flanged sleeve bearing 3/8"	\$1.56	10	\$15.60
McMaster-Carr	Leveling mount, 5/8"-11 x 6"	\$9.39	4	\$37.56
McMaster-Carr	Polyethylene flat washer	\$8.12	1	\$8.12
McMaster-Carr	Plain Grade 5 Steel Hex Nut 5/8"-11	\$6.91	1	\$6.91
McMaster-Carr	Aluminum Sheet .125" Thick	\$56.67	2	\$113.34
McMaster-Carr	Aluminum Sheet 1/4" thick	\$30.39	2	\$60.78
McMaster-Carr	Aluminum 1/2" thick	\$8.76	1	\$8.76
McMaster-Carr	Aluminum rectangular bar, 1/4" x 2" x 1'	\$4.99	1	\$4.99
NVIDIA	Jetson TK1	\$192.00	2	\$384.00
Trossen Robotics	12" Stroke Linear Actuator	\$113.95	2	\$227.90
Trossen Robotics	8" Stroke Linear Actuator	\$109.95	1	\$109.95
Trossen Robotics	Linear Actuator mounting bracket	\$14.25	3	\$42.75
Trossen Robotics	dual linear actuator controller	\$119.95	2	\$239.90
Launch 2				\$776.43
Dragon Plate	1/8" x 24" x 24" quasi-isotropic	\$347.40	1	\$347.40
ApogeeRockets	J330 motor	\$65.15	3	\$195.45
ApogeeRockets	38mm motor retainer	\$31.03	1	\$31.03
ApogeeRockets	38mm motor casing	\$59.15	1	\$59.15
Giant Leap	Shock cord 1/2" Kevlar	\$4.34	20	\$86.80
Giant Leap	Shock cord 1/4" Kevlar	\$2.83	20	\$56.60
Competition Rocket				\$1,295.05
ApogeeRockets	4 feet of 4" body tube	\$38.95	2	\$77.90

ApogeeRockets	54mm 3G motor casing	\$69.39	2	\$138.78
ApogeeRockets	P54-3G J380 motor	\$91.50	4	\$366.00
ApogeeRockets	PerfectFlite StratoLogger Altimeter	\$85.55	2	\$171.10
ApogeeRockets	Nose Cone	\$19.95	4	\$79.80
PerfectFlite	StratologgerCF	\$49.46	2	\$98.92
ApogeeRockets	#500 Ball Bearing Swivel	\$7.00	4	\$28.00
ApogeeRockets	36" Fruity Chutes Classic Elliptical	\$83.46	1	\$83.46
FruityChutes	30" Elliptical Parachute	\$79.00	2	\$158.00
ApogeeRockets	Aero Pack 54mm Retainer - L	\$31.03	3	\$93.09
Competition AGSE/Payload				\$2,775.72
McMaster-Carr	Low-Carbon Steel Rod	\$4.28	4	\$17.12
McMaster-Carr	High-Speed Steel Drill Bit	\$15.78	2	\$31.56
McMaster-Carr	Nylon Flanged Bearing	\$3.94	2	\$7.88
McMaster-Carr	Mini hi Precision SS Ball Bearing	\$5.12	6	\$30.72
McMaster-Carr	Steel Thrust Ball Bearing Steel Washers	\$2.01	9	\$18.09
McMaster-Carr	O-Ring Cord Stock	\$0.21	10	\$2.10
AMTEK	Lead Screw	\$24.24	3	\$72.72
AMTEK	Lead Screw Nut	\$11.56	4	\$46.24
Micromo	Lead Screw Motor	\$135.40	2	\$270.80
McMaster-Carr	General Purpose Tap Starting (Taper), 1/4"-28	\$5.35	1	\$5.35
McMaster-Carr	Black-Oxide Alloy Steel Socket Head Cap Screw 1/4"-28; 1/2"	\$7.29	1	\$7.29
McMaster-Carr	Flat Point Socket Set Screw Type 316 Stainless Steel, 8-32, 3/16"	\$5.07	1	\$5.07
McMaster-Carr	Black-Oxide Socket Head Cap Screw Alloy Steel, M2, 6mm	\$10.60	1	\$10.60
McMaster-Carr	Clamp-on Helical Flexible Shaft Coupling Aluminum, 3mm Dia	\$35.74	1	\$35.74
McMaster-Carr	Corrosion Resistant Dowel Pin , 3/8"; 1"	\$12.60	1	\$12.60
McMaster-Carr	Aluminum U-Bolt 5/16"-18 for 2-1/2" Pipe	\$4.36	2	\$8.72
Loftis Steel	3/4" Aluminum Plate	\$26.90	1	\$26.90
McMaster-Carr	Steel Ball Bearing Dbl Sealed, NO. R2 for 1/8" Shaft Dia, 3/8" OD	\$3.12	6	\$18.72
McMaster-Carr	High-Speed Steel Extended-Reach Drill Bit Uncoated, 3/16"	\$16.01	2	\$32.02
McMaster-Carr	High-Speed Steel Decimal Chucking Reamer .3780" Dia	\$29.08	1	\$29.08
McMaster-Carr	Nylon Ribbed Shank Rivet .187" Hole Dia	\$3.44	1	\$3.44
McMaster-Carr	Low-Carbon Steel Rod 3/8" Diameter	\$4.28	3	\$12.84
Plastic Supply	3/4", 3' x 3' Acrylic	\$166.07	1	\$166.07
SparkFun	LED - RGB Clear Common Cathode	\$1.95	5	\$9.75
SparkFun	LED - Super Bright Red	\$0.95	5	\$4.75

SparkFun	LED - Super Bright Blue	\$0.95	5	\$4.75
SparkFun	LED - Super Bright Yellow	\$0.95	5	\$4.75
Trossen Robotics	Dynamixel AX-12A Robot Actuator	\$44.90	2	\$89.80
Trossen Robotics	Linear Actuator Mounting Bracket	\$14.25	1	\$14.25
Loftis Steel	Aluminum Plates	\$219.00	1	\$219.00
Haydon Kerk	Lead Screw- Vertical (1/2"-10, 36" Length)	\$97.20	1	\$97.20
Haydon Kerk	Lead Screw- Horizontal (1/2"-10, 24" Length)	\$64.80	1	\$64.80
Haydon Kerk	Lead Nut- 1/2"-10	\$17.22	3	\$51.66
McMaster-Carr	Timing Belt Pulley (motor and table shafts)	\$12.53	2	\$25.06
McMaster-Carr	Timing Belt	\$2.75	2	\$5.50
McMaster-Carr	Black Oxide Steel Drive Shafts (3/8" OD, 36" length)	\$21.29	8	\$170.32
McMaster-Carr	3mm to 5mm Helical Shaft Coupling	\$36.82	1	\$36.82
McMaster-Carr	4mm to 6mm Helical Shaft Coupling	\$41.44	1	\$41.44
McMaster-Carr	Lead Screw Radial Bearings (1/4" ID, 1/2" OD)	\$4.98	7	\$34.86
McMaster-Carr	Neodymium Disc Magnet	\$1.04	5	\$5.20
McMaster-Carr	Turntable Thrust Bearing- Cage Assembly	\$4.31	1	\$4.31
McMaster-Carr	Turntable Radial Bearings	\$7.64	2	\$15.28
McMaster-Carr	Ultra-Gold Hex L-Key	\$13.73	1	\$13.73
McMaster-Carr	Ultra-Gold Hex L-Key	\$13.01	1	\$13.01
McMaster-Carr	Lead Screw Thrust Bearings (3/8" ID, 13/16 OD")	\$2.54	6	\$15.24
McMaster-Carr	Multipurpose 6061 Aluminum L-bracket (4ft)	\$13.31	2	\$26.62
McMaster-Carr	Bolt (10-24 1-1/4" Length) (pack of 50)	\$10.94	1	\$10.94
McMaster-Carr	Nut (10-24, Locknut, Low Profile) (pack of 100)	\$3.14	1	\$3.14
McMaster-Carr	Bolt (8-32 1/2" Length) (pack of 25)	\$7.39	1	\$7.39
McMaster-Carr	Bolt (10-24 1/2" Length) - Threadlocking (pack of 25)	\$6.38	1	\$6.38
McMaster-Carr	Bolt (M2-0.4 8mm Length) (pack of 25)	\$8.36	1	\$8.36
McMaster-Carr	Bronze Bushings (3/8" ID, 1/2" OD) w/ Graphite	\$1.44	20	\$28.80
McMaster-Carr	Turntable Thrust Bearing- Washer	\$5.96	2	\$11.92
Micromo	Vertical Motor	\$230.82	1	\$230.82
Micromo	Horizontal Motor	\$189.71	1	\$189.71
DigiKey	Encoder Optical Gap 3CH 500CPR	\$30.60	2	\$61.20
DigiKey	Codewheel 3CH 500CPR 1/4"	\$20.90	2	\$41.80
TheHardWareCity	9oz 5 Minute Fast Drying Epoxy - 6 Pack	\$65.83	3	\$197.49
Mouser Electronics	7" LCD DispCapew/tch	\$89.00	1	\$89.00
Mouser Electronics	Dynamic Speaker	\$2.35	3	\$7.05
Mouser Electronics	Dynamic Speaker	\$3.92	3	\$11.76

McMaster-Carr	Teflon Washers	\$2.89	2	\$5.78
McMaster-Carr	4-40 Bolts (1/2 in length)	\$8.55	1	\$8.55
McMaster-Carr	4-40 Bolts (1-3/4 in length)	\$8.06	1	\$8.06
McMaster-Carr	3/4in Standoff for 4-40 bolt	\$0.45	7	\$3.15
McMaster-Carr	4-40 Nut (low profile)	\$2.36	1	\$2.36
McMaster-Carr	4-40 tooth lock washer	\$2.29	1	\$2.29
Shipping				\$320.73
Launches & Outreach				\$776.33
	Launch 1			\$187.6
	Launch 2			\$288.73
	Full-scale Test Launch			\$300.00
Remaining Budget				\$7,161.19
Projected Expenses				\$4,940.00
	Per Diem Competition			\$1,440.00
	Rental Vehicles			\$400.00
	Hotel Rooms			\$2,700.00
	Misc			\$400.00
Cushion				\$2,221.19

Table 35: Parts List As Flown

Part	Quantity	Price	Total
Competition AGSE			\$2,044.40
Legs (and 8 leg nuts)	4	\$9.39	\$37.56
AGSE Table	1	\$45.00	\$45.00
Rocket stand	2	\$10.00	\$10.00
Rocket stand bracket	2	\$1.66	\$3.33
Rocket stand screws	6	\$0.18	\$0.18
Servo mount	1	\$2.00	\$2.00
AX-12A	3	\$44.90	\$134.70
Servo sled	1	\$16.00	\$16.00
Servo spindle	1	\$8.00	\$8.00
Servo sled bearings	2	\$4.98	\$9.96
Pulleys	2	\$12.53	\$25.06

Timing belt	2	\$2.75	\$5.50
Bearing cup	1	\$20.00	\$20.00
Servo shaft	1	\$10.00	\$10.00
Servo shaft thrust bearing	1	\$4.31	\$4.31
Servo shaft ball bearing	2	\$7.64	\$15.28
Servo shaft spacer	1	\$0.13	\$0.13
Lead screw ball bearing	4	\$4.98	\$19.92
Lead screw thrust bearing	6	\$2.54	\$15.24
Guide rods	8	\$21.29	\$170.32
Lead Screw- Vertical (1/2"-10, 36" Length)	1	\$97.20	\$97.20
Lead Screw- Horizontal (1/2"-10, 24" Length)	1	\$64.80	\$64.80
Lead nuts (1/2"-10)	2	\$17.22	\$34.44
AGSE base	1	\$17.00	\$17.00
AGSE top plate	1	\$6.00	\$6.00
AGSE vertical carriage plates	2	\$6.00	\$12.00
AGSE Side plates	2	\$13.00	\$26.00
Horizontal carriage plates	2	\$6.00	\$12.00
Horizontal end plate	1	\$6.00	\$6.00
Carriage Bronze Bushings (3/8" ID, 1/2" OD) w/ Graphite	16	\$1.44	\$23.04
Horizontal motor	1	\$189.71	\$189.71
Horizontal motor mount	1	\$2.00	\$2.00
Encoders	2	\$30.60	\$61.20
Encoder mount	1	\$4.00	\$4.00
Encoder wheel	2	\$20.90	\$41.80
Shaft couple - horizontal	1	\$36.82	\$36.82

Shaft couple - vertical	1	\$41.44	\$41.44
Vertical motor mount	1		\$4.00
Vertical motor (2237S012CXR+26A 16:1+MG26 from Micromo)	1	\$230.82	\$230.82
Lead screw shaft collar (1/4")	1	\$1.86	\$1.86
3/8" shaft collars	8	\$1.77	\$14.16
gripper arm	1	\$2.50	\$2.50
gripper arm bracket	2	\$2.00	\$2.00
CrustCrawler Gripper Components	1	\$30.00	\$30.00
Gripper phalanges	2	\$6.00	\$6.00
Teflon Washers	2	\$2.89	\$5.78
4-40 Bolts (1/2 in length)	1	\$8.55	\$8.55
4-40 Bolts (1-3/4 in length)	1	\$8.06	\$8.06
3/4in Standoff for 4-40 bolt	7	\$0.45	\$3.15
4-40 Nut (low profile)	1	\$2.36	\$2.36
4-40 tooth lock washer	1	\$2.29	\$2.29
Beagle Bone Black	1	\$55.00	\$55.00
NVidia Jetson TK1	1	\$192.99	\$192.99
Camera	1	\$99.99	\$99.99
PCB	4	\$33.00	\$132.00
1/4 - 20, 3/4 Bolt	2	\$0.14	\$0.29
10 - 24, 1-1/4 Bolt	10	\$0.11	\$1.09
10 - 24, 1/2 Bolt	32	\$0.10	\$3.30
8 - 32, 1/2 Flathead Bolt	6	\$0.30	\$1.77
8 - 32, 3/4 Bolt	8	\$0.10	\$0.83
2 - 56, 5/8 Bolt	2	\$0.25	\$0.50

M2, 8mm Bolt	10	\$0.13	\$1.30
M2.5, 14mm Bolt	8	\$0.11	\$0.88
M3, 8mm Bolt	4	\$0.07	\$0.27
1/4, .750 Washer	2	\$0.35	\$0.70
10, .750 Washer	8	\$0.25	\$2.00
2, .250 Washer	2	\$0.04	\$0.08
10 - 24 Locknut	10	\$0.09	\$0.94
8 - 32 Nut	12	\$0.08	\$0.96
2 - 56 Nut	2	\$0.03	\$0.06
Competition Rocket			\$756.35
4" Blue Tube	2	\$38.95	\$77.90
54mm 3G motor casing	1	\$69.39	\$69.39
P54-3G J380 motor	1	\$91.50	\$91.50
Nose Cone	1	\$19.95	\$19.95
StratologgerCF	2	\$49.46	\$98.92
#500 Ball Bearing Swivel	4	\$7.00	\$28.00
30" Elliptical Parachute	2	\$79.00	\$158.00
Aero Pack 54mm Retainer - L	1	\$31.03	\$31.03
1/8" quasi-isotropic carbon fiber	1	\$115.80	\$115.80
Plywood Centering Rings	4	\$3.00	\$12.00
Epoxy	1	\$10.97	\$10.97
Small Fireball Anti-Zipper	2	\$15.97	\$31.94
4" coupler Blue Tube	1	\$10.95	\$10.95
Competition Payload			\$432.39
Guide Rods	3	\$4.28	\$12.84
Rear Bulkhead	1	\$8.00	\$8.00
Male Bulkhead	1	\$5.50	\$5.50
Female Bulkhead	1	\$5.75	\$5.75

Forward Plate	1	\$7.90	\$7.90
Payload Tray	1	\$2.50	\$2.50
Forward Limit Switch Bracket	1	\$0.28	\$0.28
Rear Limit Switch Bracket	1	\$0.28	\$0.28
Motor Mount	1	\$2.00	\$2.00
Limit Switch Plungers	1	\$2.00	\$2.00
Bearing Retention Collar	1	\$3.00	\$3.00
Electronics Tray	1	\$4.00	\$4.00
Lead Screw	1	\$24.24	\$24.24
Lead Screw Nut	1	\$11.56	\$11.56
Faulhaber Motor and Gearhead	1	\$135.40	\$135.40
Limit Switches	2	\$1.95	\$3.90
10-32 Nuts	1	\$3.14	\$3.14
Shaft Coupler	1	\$35.74	\$35.74
Guide rod Bushings	3	\$1.44	\$4.32
1/4-28 x 1/2" SHCS	3	\$1.09	\$3.28
Thrust Bearings	4	\$2.54	\$10.16
Ball Bearings	2	\$4.98	\$9.96
4-40 x 3/8 SHCS	3	\$0.36	\$1.09
4-40 x 1/2 SHCS	3	\$0.41	\$1.22
4-40 set screw	3	\$0.12	\$0.36
.002 Shims	1	Already Owned	
Arduino	1	\$22.00	\$22.00
Arduino Motorshield	1	\$12.00	\$12.00
Stratologger	1	\$85.55	\$85.55
4-40 x 3/8 Flat Head Screw	4	Already Owned	

4-40 Nylon Screws	4	Already Owned	
Aluminum Standoffs	2	Already Owned	
Hall Effect Sensor	1	\$6.95	\$6.95
1/4 Diameter Neodymium Magnets x2	2	Already Owned	
Breakaway Connector Pins	1	Free Sample from Company	
5/16" x 2 1/2" U-bolts	1	\$4.36	\$4.36
1/4-20 Nuts	4	\$0.07	\$0.28
3 LEDs (2 RGB, 1 Amber)	3	\$0.95	\$2.85

Table 36: Costs as Flown

System	Cost as Flown (Launch 1)	Cost as Flown (Launch 2)	Cost as Flown (Competition)
Launch Vehicle	\$531.13	\$776.43	\$756.35
Payload Bay	\$0.00	\$187.00	\$432.39
AGSE	\$0.00	\$0.00	\$2044.40
Misc. Hardware	\$100.00	\$200.00	\$0.00
Total	\$631.13	\$1,163.43	\$3233.14

8.2 Timeline

The Vanderbilt Aerospace Club has outlined a timeline for the construction and testing of both the launch vehicle and AGSE system. There is some flexibility to the schedule, as there are external factors that may affect our timeline, but we plan to follow the schedule as strictly as possible. A Gantt chart outlining the phases of construction and testing can be found in the appendix in section 10.3: *Project Timeline*.

8.2.1 Major Milestone Schedule

Shown below is a list of the major milestones that have occurred and are planned for the team. Milestones highlighted in blue are NASA-designated ones, whereas ones highlighted in gold are Vanderbilt-designed.

Milestone Date	Milestone Description
09/25/2014	Beginning of subscale rocket work and ordering of materials
10/06/2014	Proposal Due
10/15/2014	Beginning of payload bay and AGSE work and ordering of materials
10/31/2014	Web Presence Established
11/03/2014	Completed construction of first subscale rocket
11/05/2014	PDR & Presentation Posted
11/14/2014	PDR Presentation
11/15/2014	First launch of subscale rocket <ul style="list-style-type: none"> • Testing of basic recovery systems and launch procedures • Jettison of dummy payload bay
11/18/2014	Objection detection algorithms developed
12/06/2014	Completion of second subscale rocket <ul style="list-style-type: none"> • Rebuilt tailcone section • Include dummy payload bay • Modular so that first payload bay prototype can be flown with it
12/11/2014	Completion of payload bay prototype Second launch of subscale rocket <ul style="list-style-type: none"> • 1st flight to confirm rocket design after previous failure • 2nd flight with prototype payload bay
12/12/2014	Beginning of final payload bay fabrication
01/16/2015	Control of AGSE actuators established, completion of first AGSE prototype
01/16/2015	CDR & Presentation Posted
01/27/2015	CDR Presentation
01/28/2015	Completion of final payload bay design and installation into rocket

01/30/2015	Finish modification of launchpad
03/15/2015	First full-scale launch <ul style="list-style-type: none"> Completion of full-scale rocket, final payload bay design, AGSE Integration of the three systems
03/16/2015	FRR & Presentation Posted
03/18/2015 - 03/24/2015	FRR Presentations
04/07/2015	Travel to Huntsville, AL Launch Readiness Review
04/10/2015	Launch Day
04/29/2015	Post-Launch Assessment Review Posted
05/11/2015	Announcement of Winning SL Team

8.2.2 Critical Project Path

Shown below is a flow chart of the critical project path. It outlines main tasks and what tasks can be completed in parallel and what ones are dependent upon the completion of others.

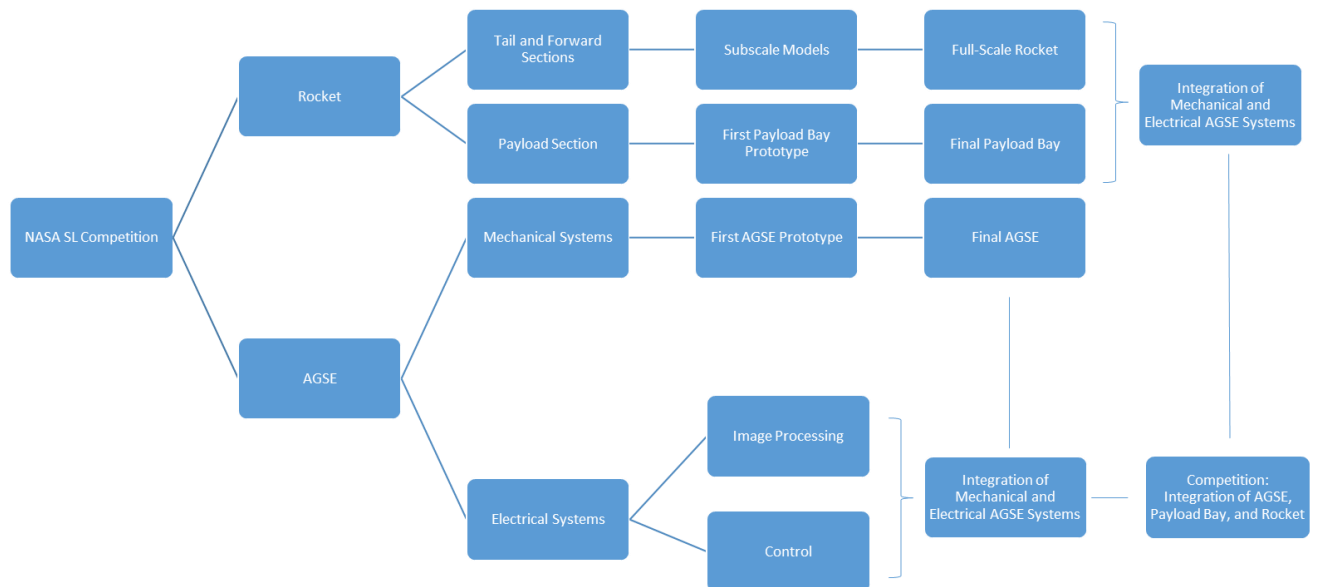


Figure 186: Critical Project Path

The project naturally splits into two main focuses: the rocket and the AGSE. Within the rocket, the propulsion and recovery sections (tail and forward sections) could be developed independently from the payload containment section (payload section). Both of these parts underwent design evolution, with the rocket first being designed as a subscale before upgrading to a full-scale and the payload bay going through two design changes. Meanwhile, the AGSE developed in two sections as well: the electrical and the mechanical sides. The two were able to progress independently as the control and image processing parts of the AGSE were made to be modular in nature. The AGSE went through two design iterations, much like the rocket and payload bay. The electrical and mechanical systems were then integrated, and the payload bay and the rocket were integrated. With the AGSE and rocket now integrated, the system is ready for competition.

8.3 Educational Engagement Plan and Status

8.3.1 Educational Plan

Vanderbilt's Aerospace Club, in partnership with Vanderbilt's Department of Teaching and Learning, visits schools and other places of learning in Tennessee to teach students about physics and rocketry, and to build enthusiasm about careers in STEM. This year, we visited 5 schools and one science museum, each for a full day, frequently teaching in multiple classrooms throughout the school day. In addition to those officially counted outreach event, we visited Cannon County High School on October 10th, reaching all 9th graders in the country as well as many students in higher grades, who share a science class with 9th graders, though this trip was conducted before the announcement of teams for the SL competition. While this trip cannot be directly counted as part of our outreach activities for the year, we have collected validation data on the effects of our efforts there. This has been and will continue to be included with comparable data from other activities to validate and potentially improve the outreach curriculum.

8.3.2 Educational Lesson Plan Summary

Our educational outreach seeks to provide an authentic STEM learning experience for the middle school students. In our outreach efforts, we want middle school students to be actively engaged in the engineering design process while meaningfully acquiring science content and skills. Furthermore, we want the engagement to generate interest not only in rocketry, but in engineering as a whole. When students approach science with the perception that they are going to use what they learn, they are more likely to develop meaningful understandings of scientific content and processes. Therefore, we use a goal-directed, hands-on educational approach in which student activity centers on answering a driving question. When this activity is framed around an engineering design problem, students engage in the construction of scientific knowledge because they are working toward a goal that requires them to apply that knowledge – much like the practice of actual engineers. Our curricular materials include a learning sequence in which students progressively refine their understanding of scientific principles underlying rocket design by iteratively participating in the engineering design process. These learning events focus on the use of simple models to develop students' science proficiency by leveraging best practices in teaching and learning, while working through rigorous science and engineering

knowledge, experiments, and practices. In addition, pre- and post-assessments are administered to assess the effectiveness our curriculum in improving their understanding of the scientific content and the engineering design process.

8.3.3 Educational Lesson Plan Details

Our lesson plan begins with a brief introduction that describes what the Vanderbilt Aerospace Club does and how we became interested in engineering and rocketry. We then simply describe how the students will be working through the design process through three fan cart experiments in order to answer the question “How do we get our rocket to reach 3,000ft?” The students are then broken up into small groups and their first task is to brainstorm experiments that may be useful in helping them answer the question posed to them earlier. This element of the lesson allows students to become invested in the experiments they are about to complete. The students are then guided through three fan cart experiments. The first experiment teaches Newton’s third law by having them measure the time it takes the cart to cross the track with different fan speeds. The second experiment teaches Newton’s second law by having the students add mass to the cart and measure the time it takes to cross the track given a constant fan speed. Lastly, the third experiment teaches Newton’s first law by having the fan set on a 1sec delay. The students will note how the cart acts before the fan is on, while the fan is on, and after the fan has stopped. Throughout each experiment, the worksheet provides an easy place for students to make predictions as well as to record the data they acquire. After the experiments are finished, we guide the class through a discussion session to help apply what they learned about basic physics and Newton’s laws to rocketry. This discussion helps them answer the question posed to them earlier in the class. Team members teach students that an engineer must be conscious of the amount of force the rocket motor creates, the mass of the rocket, and the length of time for which the rocket motor burns. The lesson plan outlined above provides students with a hands-on opportunity to learn about rockets and to apply such knowledge to a real world rocket scenario.

8.3.4 Educational Engagement Status

8.3.4.1 Cannon County High School

On October 10, members of the team traveled to Cannon County High School in rural Tennessee to perform a test of the teams outreach curriculum. Team members presented the material to all science classes containing freshmen, so as to ensure that every freshman in the county got the chance to go through the program. Students worked through the 3 fan cart experiments, discussed what they learned, and the got to see the bottle rocket demonstration. This happened before the official start date of the competition, so the students will not be counted toward the teams outreach activities in any way. The event is still relevant and of use, however. The pre and post assessments described above were issued to these students and the results have been collected. This data will be included with the next school visit, to better characterize the effects of our curriculum. In the meantime, the data will be used to identify the strengths and weaknesses of the current program, so the total package can be optimized for the next event. Furthermore, this event allowed members of the team to become more familiar with process of presenting, and get practice engaging students in the target age range.

8.3.4.2 Adventure Science Center

On October 25, members of the team took part in the Nashville Adventure Science Center’s “Spooky Science Day” event by setting up an activity booth related to rockets and basic physics principals. Children of all ages learned about concepts like pressure, gravity, projectile motion, and Newton’s Laws while playing a fun and exciting game. The system is essentially a rig that allows students to shoot “rockets” made of straws at a target. Participants were given control of the angle of trajectory and amount of compressive force on the air, as ways to aim. This activity is exciting and sparks creative discussions as groups of kids try to decide how to aim and why. The team reached a large number of children, teachers, and parents over the course of the day, increasing excitement about learning physics and applying school concepts to real life.

8.3.4.3 Linden Middle School

On November 21st, the team traveled to Linden Middle School in Perry County, TN. While there, the team was able to bring our standard Newton’s Laws curriculum to students ranging from 5th to 8th grade. As described in the lesson plan overview, students were taught about Newton’s Laws and the engineering design cycle, then took part in the experiments, applied what they had learned in lecture to what they saw in those experiments, and then saw a bottle rocket demonstration to cement interest in engineering. Finally, classes with extra time were able to speak informally with team members about college, engineering, and career opportunities available to them.

The team conducts an evaluation of all of its school visits, by having teachers administer a pretest before the team arrives and then a posttest a few days after the team leaves. The exams are identical, allowing the team to compare knowledge before and after the visit. The subjects covered in the test include basic applications of Newton’s laws and the engineering design cycle. This allows the team to assess both the students’ comprehension of the science and their understanding of the specific application example used in the lesson. In addition to questions about the subject matter, the test asks students to rate their interest in engineering and science careers. Using this data, the team is able to gauge whether students are becoming more interested in STEM careers, which can be just as important as determining how much of the specific information they absorbed.

The lesson plan and testing process used to validate this outreach was also used in a practice run the team took on prior to the team announcements. Because the activity came so early, the students reached by the activity will not be counted, but the data the team received is still important. In order to better understand the effectiveness of the curriculum, data from that trip has been combined with the results from the activity on November 21.

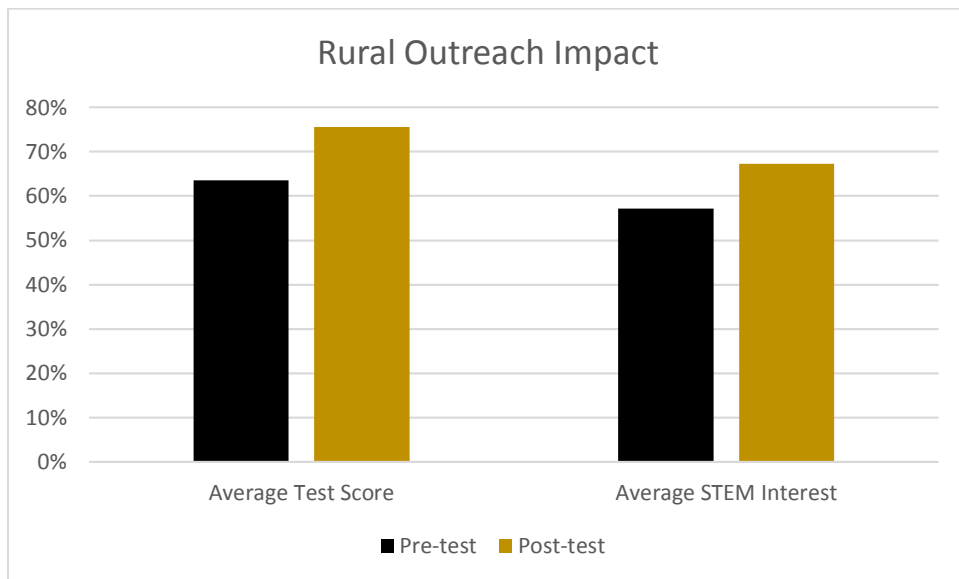


Figure 187: Pre- and Post-Outreach Statistics for Rural Schools

Before our visit, students scored an average of 63.5%. Afterward, that average rose 12 points to 75.5%. That increase alone is a sign of noteworthy improvement, but a look at the breakdown of scores shows that the improvement is even more significant. The pre-test results show the pattern of a normal distribution, with nearly half of the students, 45%, falling between a 6 and an 8 out of 10. The post-test results, on the other hand, continuously increase with score, such that over half of students now fell between 8 and 10.

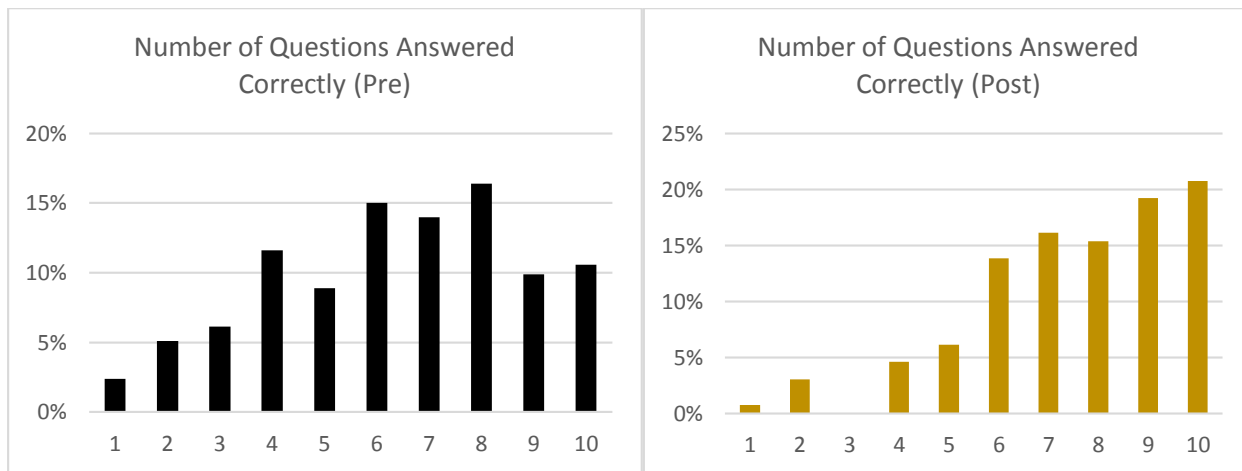


Figure 188: Test Results Before and After Outreach

Interest level also increased, rising from an initial value of 2.9 out of 5 to 3.4 in the post-test. The trend here was slightly different. Students who initially indicated an interest level of 1 or 2 primarily remained there, though a few did move up by a single point. The majority of the movement was in students who indicated a moderate interest. Most students indicating an interest of 3 on the pre-test changed to a 4 or 5 on post-test. As a result of this, the team is

looking at ways to focus more on engaging students appear unenthusiastic, as we have already shown an ability to excite those with a moderate to high initial interest level.

8.3.4.4 Hunters Bend Elementary School

On November 21st, the Vanderbilt Aerospace team visited Hunters Bend Elementary School in nearby Franklin Tennessee. All 5th grade students attending the school took part in the team's standard fan cart based lesson plan, designed to show them the physical implications of Newton's Laws and allow them to better understand how classroom learning is applicable to the real world. As with other such events, the team conducted an evaluation of the outreach efforts by issuing tests to all the students before and after the activity that gauged their knowledge and interest level. Before our visit, students scored an average of 68.2%. Afterward, that average rose over 17 points to 83.3%. In addition to the averages, it is clear from the graph that a relatively normal distribution was replaced by one in which the vast majority of the students scored in the top 3 levels. Interest level increased only slightly, rising from an initial value of 3.2 out of 5 to 3.4 in the post-test. This is a smaller increase than the team aims for, but the final value average is exactly the same as the previous event and in the range of most such events through the years, indicating that the students here most likely started with an above average interest level, making it more difficult to develop sizable gains. This is most likely the result of the more suburban and affluent community with a significantly higher average level of education than the more rural communities we visit.

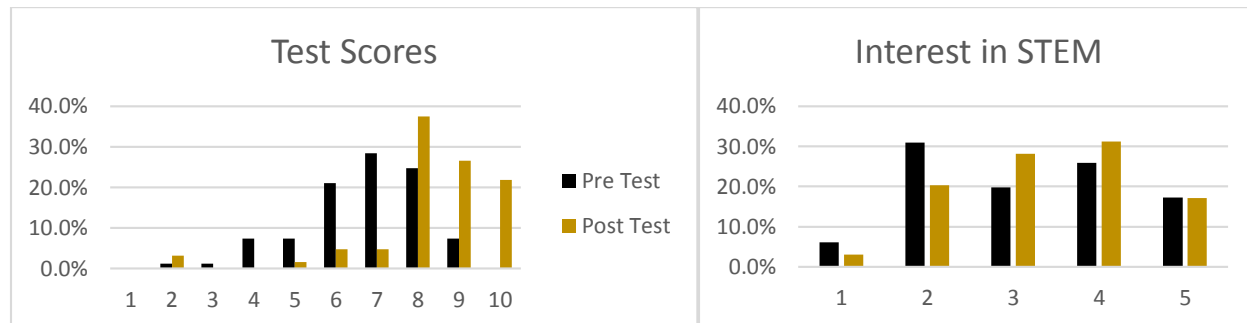


Figure 189: Results of Hunters Bend Outreach Evaluation

8.3.4.5 Winfree Bryant Middle School

On February 6th, the team visited Winfree Bryant Middle School in Lebanon, TN for an outreach event that spanned an entire school day with a ratio of just 12 students per instructor (team member). The team broke up into groups of 2 to teach in many classrooms throughout the school. The same PowerPoint presentation as previous events was used, but with an additional section detailing the major components of a rocket. After the presentation, students were each given 20 oz soda bottles and a collection of construction materials such as cardboard, construction paper, duct tape, and such. With help from team members, the students applied Newton's Laws to the design of a bottle rocket. Great care was taken to lead students through a typical, if abbreviated, engineering design cycle in which they identified the problem, came up with a solution and analyzed their design in terms of Newton's Laws. Once everyone had finished their rockets, all of the classes for that period came together outside to hold a

tournament to see whose rocket would go the highest. Students had a great time and were genuinely interested in using Newton's Laws to help them, rather than simply making something that look like a rocket. As with other outreach events, the team conducted an evaluation of this event. Unfortunately, weather interfered with this. Extreme winter weather canceled schools in the greater Nashville area for 2 full weeks, making it impossible for the team to recover the pre-test, or have teachers administer the post-test.



Figure 190: 7th grade students at Winfree Bryant Middle School learn more about the shape and purpose of fins on a rocket.

8.3.4.6 Montgomery Bell Academy

On March 9th, the team traveled to Montgomery Bell Academy in Nashville to demonstrate the AGSE prototype and payload bay. In a large weekly meeting of the entire student body, the team gave a short presentation about the competition and what the team has done in the past. Then, the teams operated the AGSE in a partially autonomous mode that allowed the presenters to explain each step before initiating it. In addition to showing the physical process of successfully fining, collecting, and depositing the sample, the team also used projectors to show the OpenCV code running and images from the camera in the various stages of processing. The students were excited and interested throughout the process, even applauding in a special organized way that MBA alumni on the team inform us was previously reserved for the team's state championship in football.

In addition to the main presentation, members of the team stayed throughout the day to talk to physics classes. These much smaller groups allowed the team to talk in more detail about the tools and processes used to create the AGSE and payload bay. The team also took the opportunity to talk to students about engineering and college/career opportunities in STEM.

Many students were interested in what kinds of engineering there were, and about the differences between parallel engineering and science fields (Chemical Engineering vs. Chemistry).

8.3.4.7 Page High School

The success of our trip to MBA inspired the team to schedule one final outreach to do the same kind of thing at another school in the area. On March 13th, therefore, the team travelled to Page High School in Franklin, TN. Over the course of the school day, members of the team talked to students from 9th to 12th grade about the rocket and AGSE and about engineering in general. After giving a 20 min presentation and showing a video about the competition, we would open the floor for question and answer sessions that frequently lasted the entire rest of the hour long period. Questions covered the project, engineering, and STEM careers, but also college life, the application process, and a number of other topics that got students more interested in attending college and studying STEM.

9 Conclusion

While the fundamental tasks assigned to the AGSE and launch vehicle are common to all teams, there is room for innovation in the areas of efficiency, repeatability, and execution. Our design is characterized by its optimized design allowing for the fewest possible opportunities for system failure. In real operations, such as the SLS program this challenge parallels, the resulting reliability is of the utmost importance. With massive amounts time and resources being poured into such missions, and no capability for human intervention or repair, it is key that all systems be capable performing their assigned tasks with perfect reliability. This opens up opportunities for innovative improvements in limiting failure modes and state-space preservation for those situations where 100% failure prevention simply isn't possible. As the competition continues, the team hopes that this streamlined design will allow us to perform the task in the most effective and consistent way possible while also opening up the possibility of even further innovation.

10 Appendix

10.1 Safety and Regulations Documents

For ease of access, the appendix with MSDS sheets, safety codes, Federal Aviation Regulations, etc. is posted on the Vanderbilt SL Team website in the Documents section. It can be found at the following web address:

<http://www.vanderbilt.edu/USLI/2015/documents.htm>

10.2 Electrical Drawings

10.2.1 AGSE Statechart

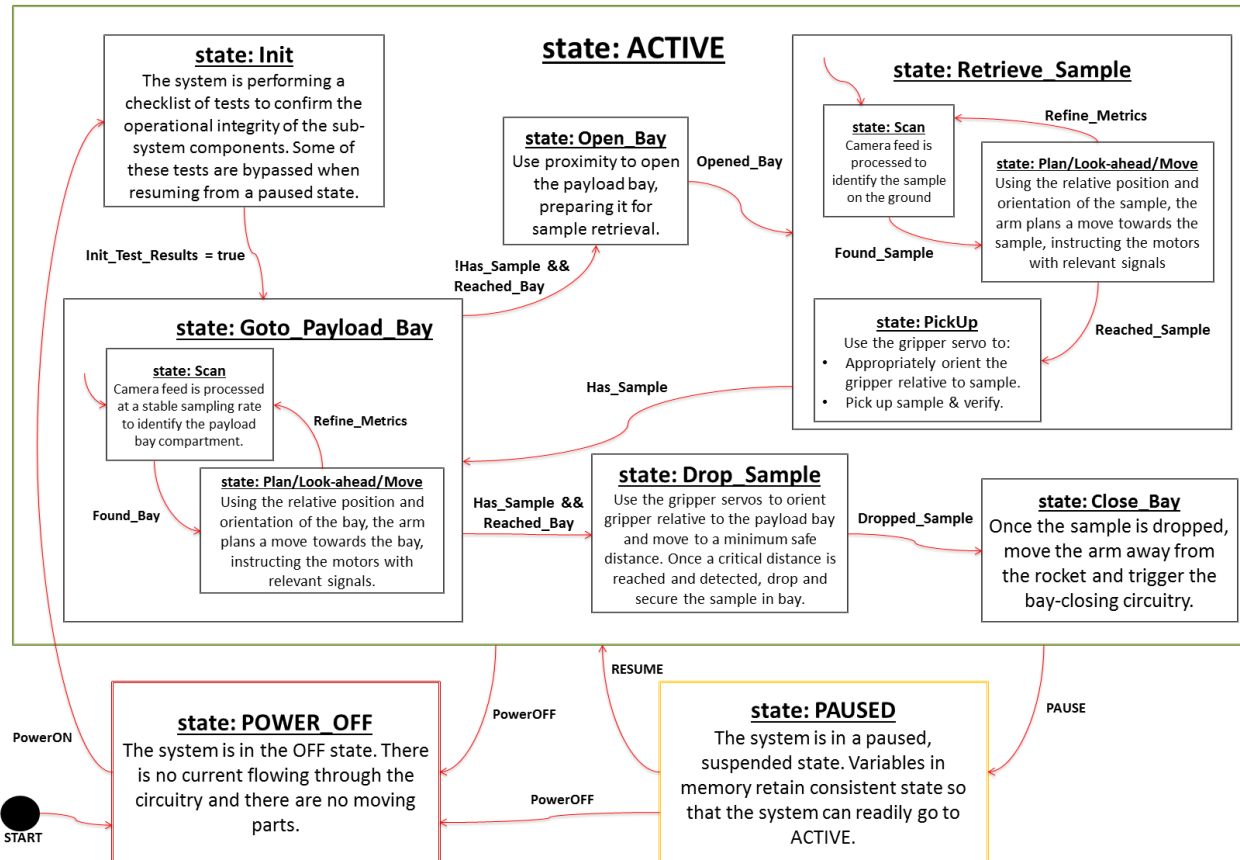


Figure 191: AGSE Statechart

Figure 192: AGSE Statechart with Payload Bay Interaction

10.2.2 Payload Bay Statechart

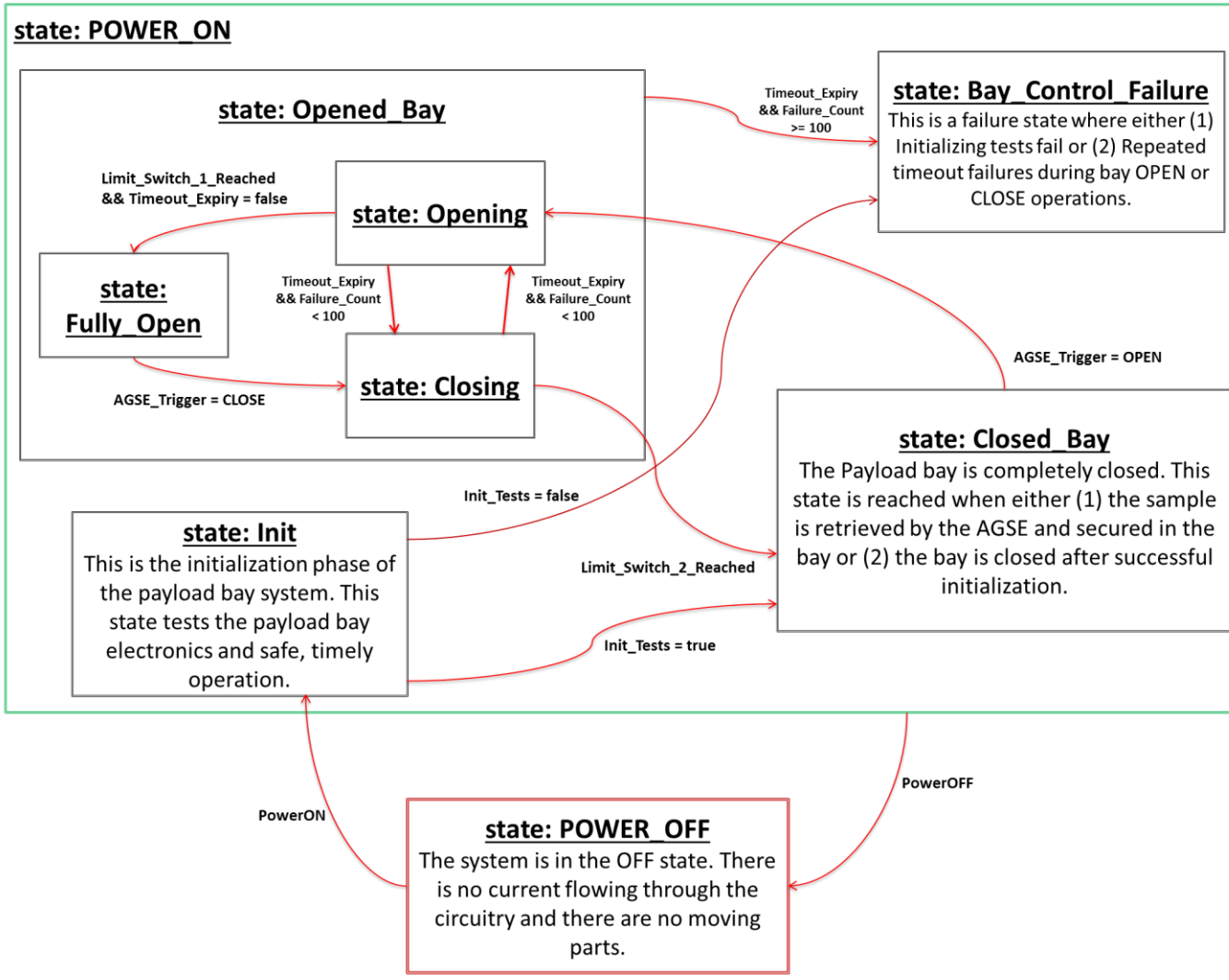


Figure 193: Payload Bay Statechart

10.2.3 Payload Bay Control Electronics

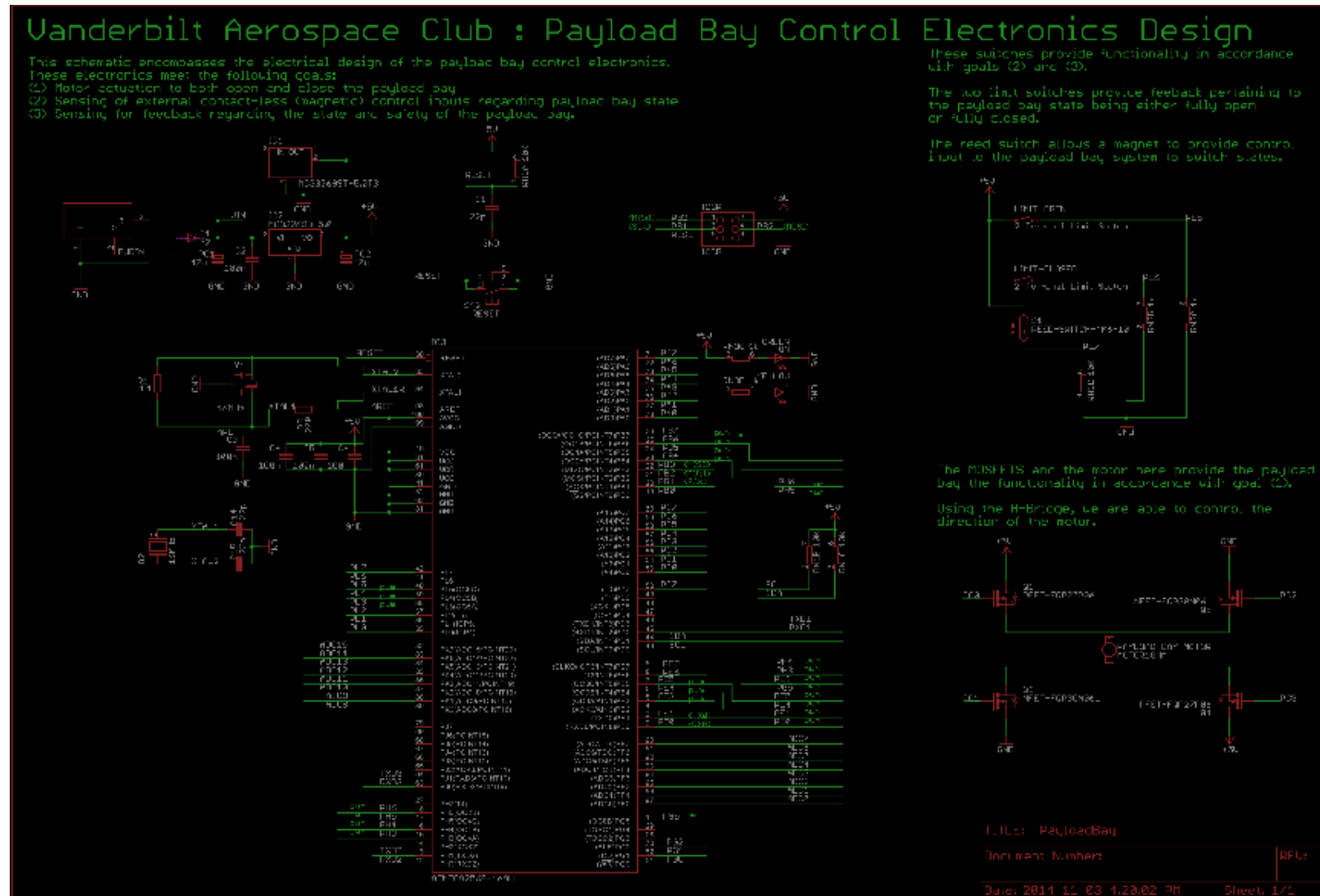


Figure 194: Payload Bay Control Electronics

10.2.4 AGSE Control Electronics

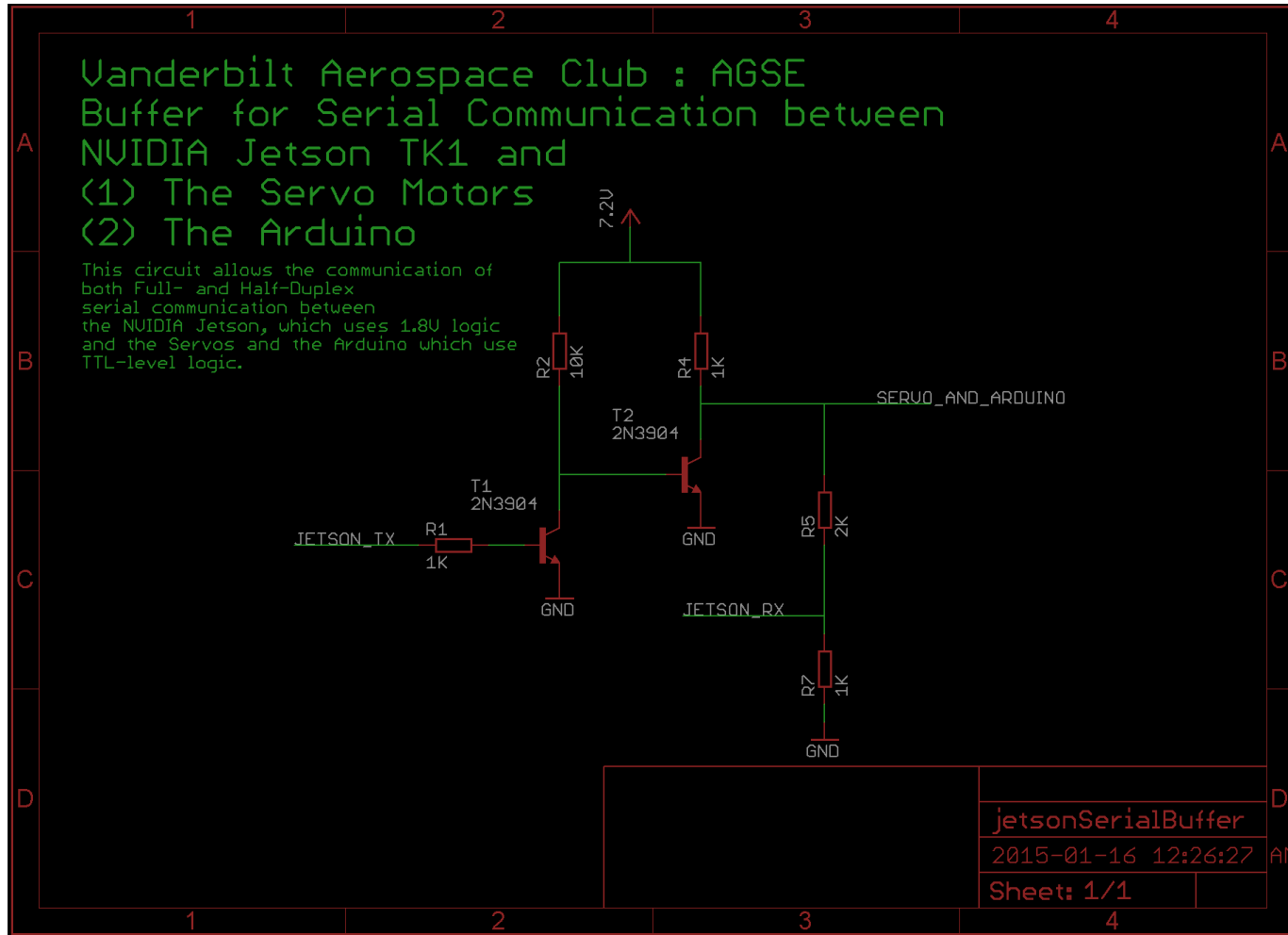


Figure 195: AGSE Buffer Circuit Diagram

Vanderbilt Aerospace Club : AGSE Motor Control Board

This schematic encompasses the electrical design of the AGSE motor control board. These circuits meet the following goals:

1. Vertical DC linear actuator motor control
2. Radial DC linear actuator motor control
3. Encoder Feedback for vertical motor encoder
4. Encoder Feedback for radial motor encoder
5. 12 V to 5 V power regulation for BeagleBone Black
6. Serial Buffer for controlling daisychained servos:
 - * Main gripper servo motor
 - * Gripper wrist rotation servo motor
 - * AGSE arm base rotation servo motor

This board mounts as a cape on the BeagleBone Black, providing it power and handling the associated connections for motor feedback and control.

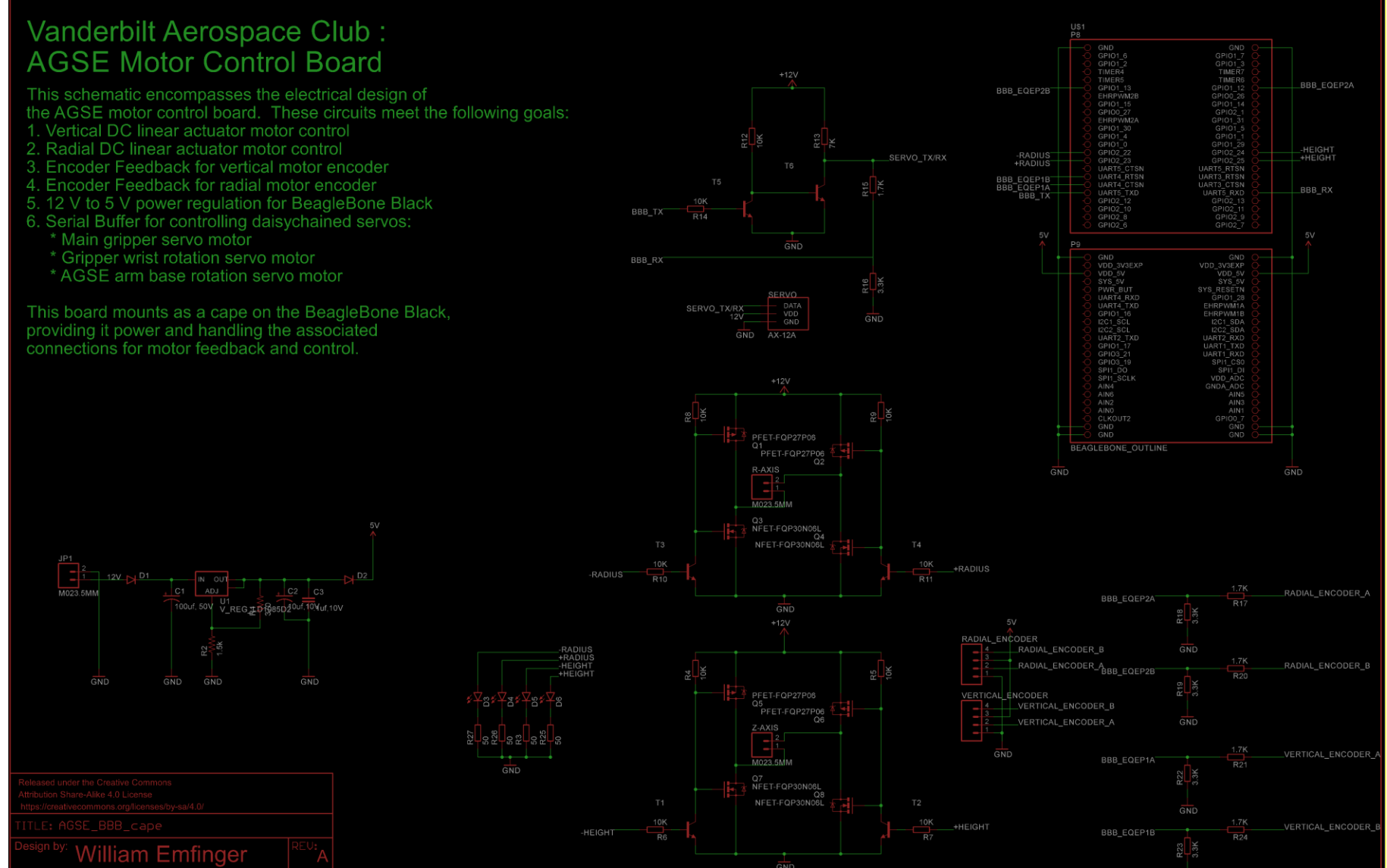


Figure 196: AGSE Motor Control Diagram for Linear Actuators

10.3 Project Timeline

10.3.1 Gantt Chart

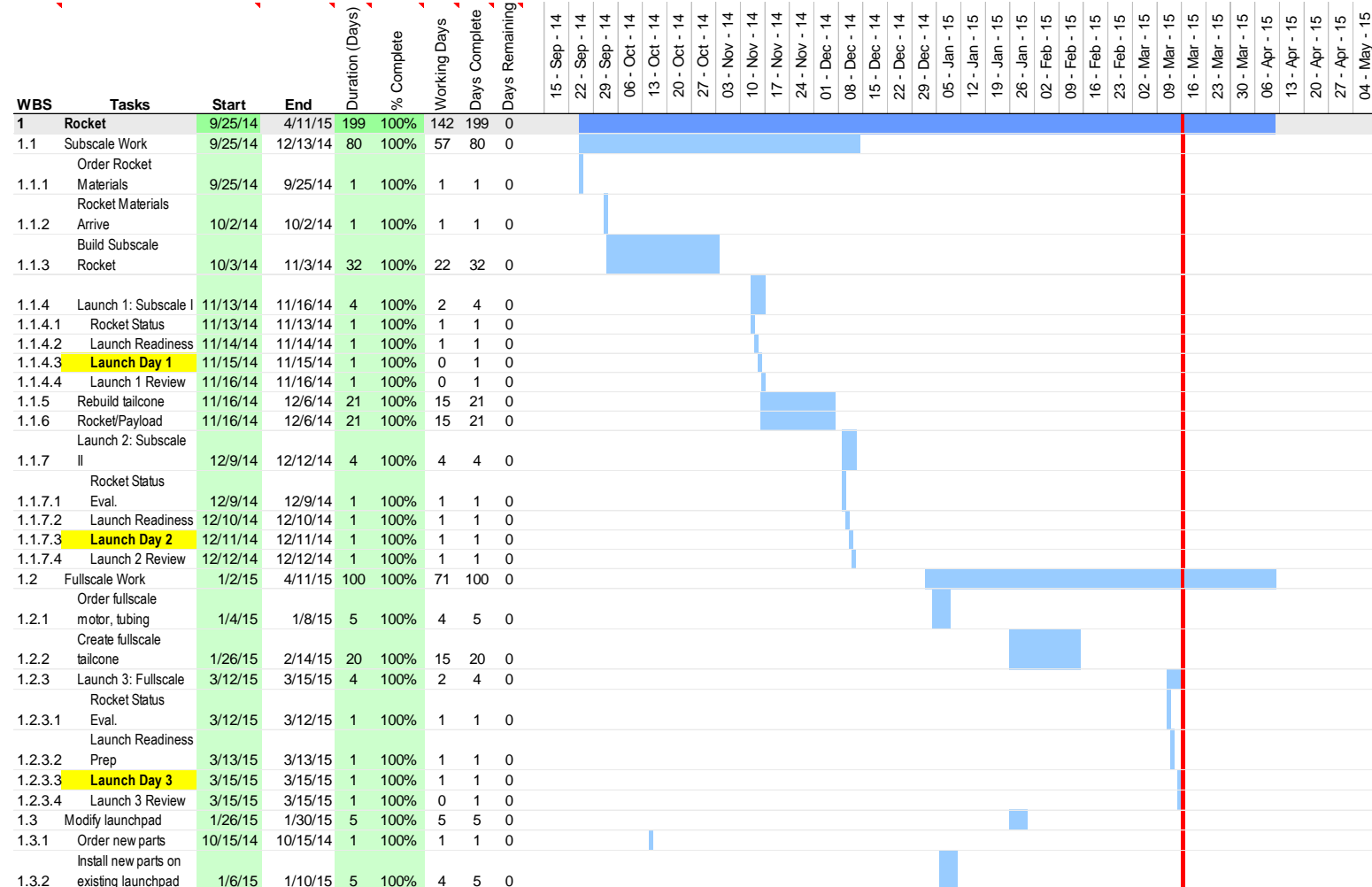


Figure 197: Gantt Chart for Rocket Portion of Project

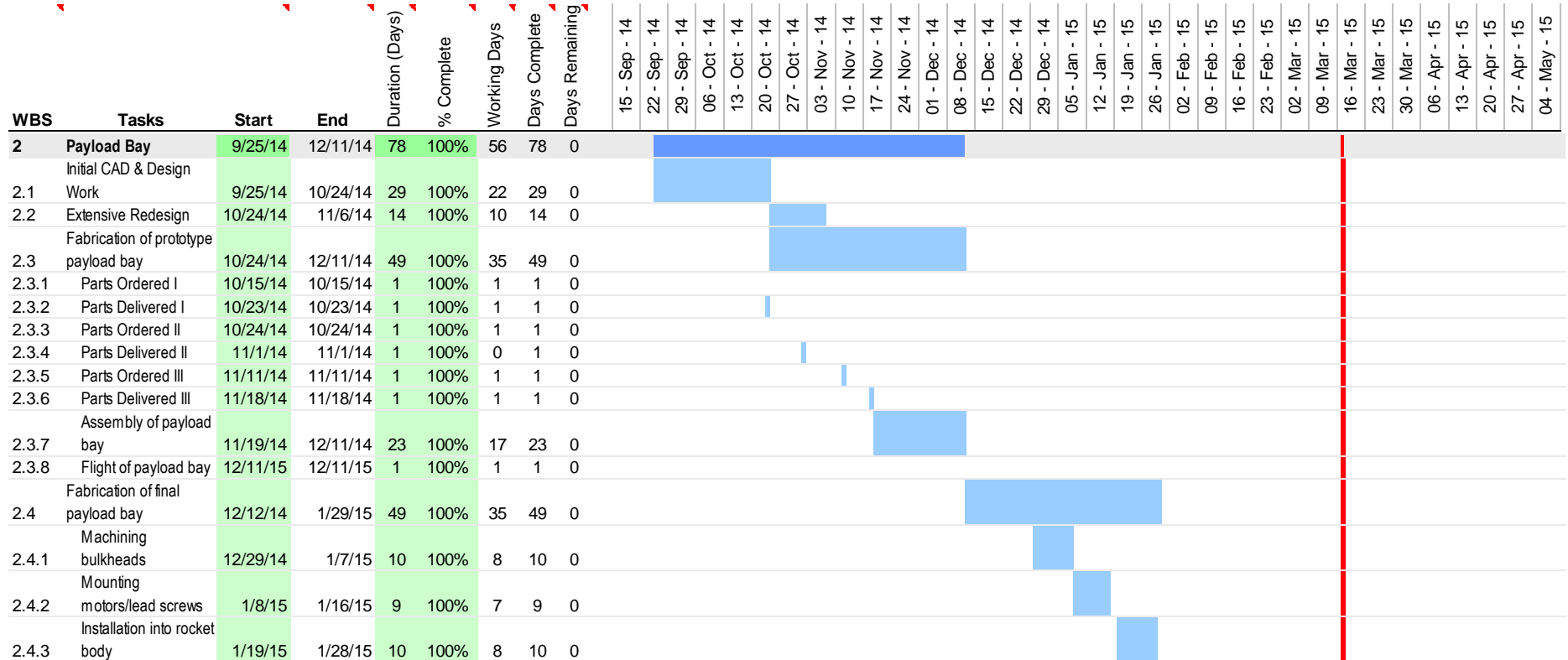


Figure 198: Gantt Chart for Payload Bay Portion of Project

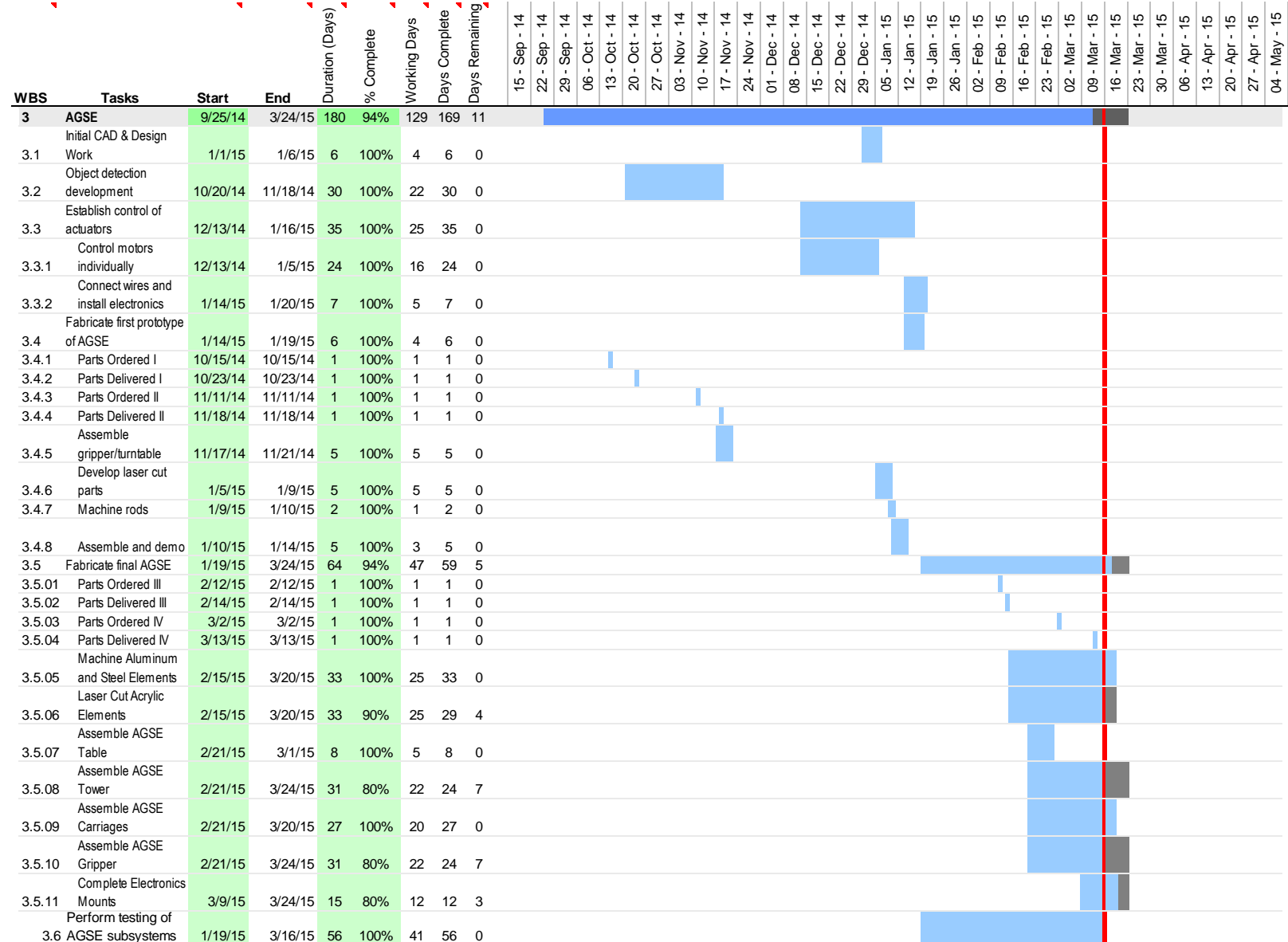


Figure 199: Gantt Chart for AGSE Portion of Project

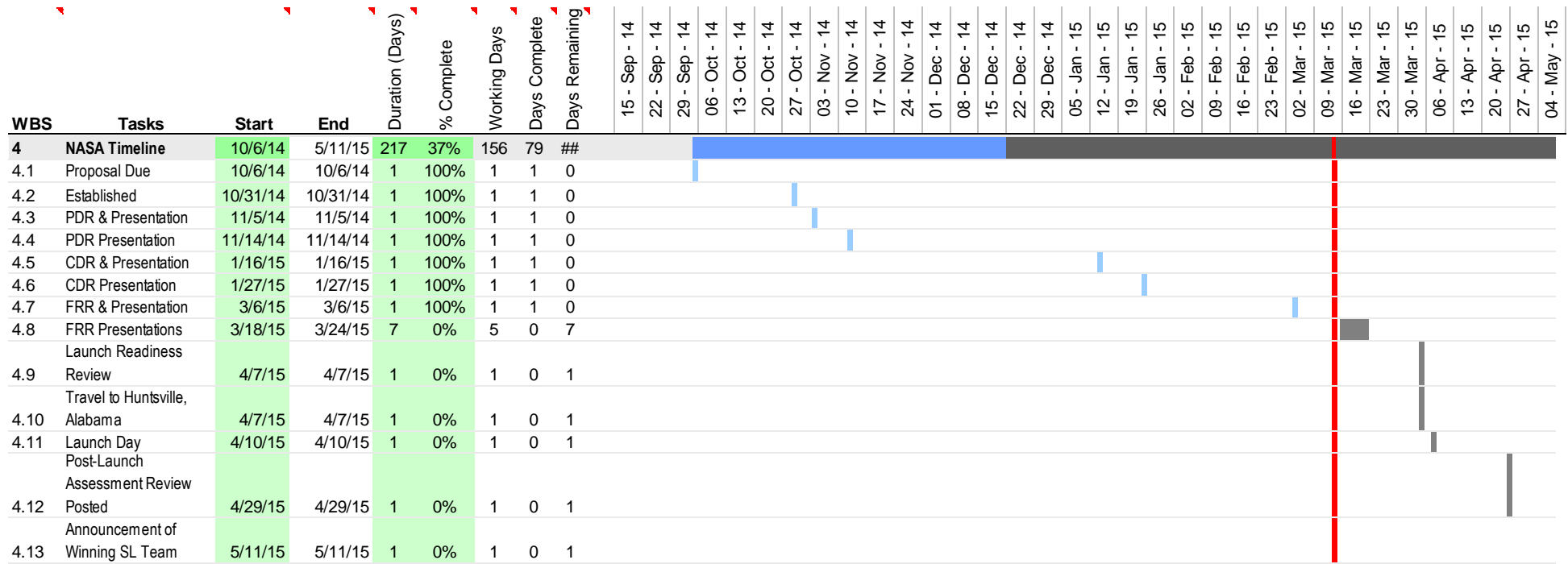


Figure 200: Gantt Chart for NASA Timeline

10.4 Sources

- [1] Matthies, Larry, et al. "Computer vision on Mars." *International Journal of Computer Vision* 75.1 (2007): 67-92.
- [2] Ayache, Nicholas. "Medical Computer Vision, Virtual Reality and Robotics: Promising Research Tracks." *BMVC*. 1995.
- [3] Bonin-Font, Francisco, Alberto Ortiz, and Gabriel Oliver. "Visual navigation for mobile robots: A survey." *Journal of intelligent and robotic systems* 53.3 (2008): 263-296.
- [4] Cheng, Frank, and Xiaoting Chen. "Integration of 3D stereo vision measurements in industrial robot applications." *International Conference on Engineering & Technology*. 2008.
- [5] Widmann, G. "Image-guided surgery and medical robotics in the cranial area." *revolution* 17 (2007): 18.
- [6] Abolmaesumi, Purang, et al. "Image-guided control of a robot for medical ultrasound." *Robotics and Automation, IEEE Transactions on* 18.1 (2002): 11-23.
- [7] Adler Jr, John R., et al. "Image-guided robotic radiosurgery." *Neurosurgery* 44.6 (1999): 1299-1306.
- [8] Howe, Robert D., and Yoky Matsuoka. "Robotics for surgery." *Annual Review of Biomedical Engineering* 1.1 (1999): 211-240.
- [9] Ferguson, Dave, Maxim Likhachev, and Anthony Stentz. "A guide to heuristic-based path planning." *Proceedings of the international workshop on planning under uncertainty for autonomous systems, international conference on automated planning and scheduling (ICAPS)*. 2005.
- [10] Ersson, Torvald, and Xiaoming Hu. "Path planning and navigation of mobile robots in unknown environments." *Intelligent Robots and Systems, 2001. Proceedings. 2001 IEEE/RSJ International Conference on*. Vol. 2. IEEE, 2001.
- [11] Herrington, Daniel. "Easy Image Processing Camera Interfacing for Robotics." *CIRCUIT CELLAR* (2003): 44-53.
- [12] Theis, Christoph, Ioannis Iossifidis, and Axel Steinlage. "Image processing methods for interactive robot control." *Proc. IEEE Roman International Workshop on Robot-Human Interactive Communication*. 2001.
- [13] Saxena, Ashutosh, Sung H. Chung, and Andrew Y. Ng. "3-d depth reconstruction from a single still image." *International Journal of Computer Vision* 76.1 (2008): 53-69.
- [14] Alqasemi, Redwan, Sebastian Mahler, and Rajiv Dubey. "A Double Claw Robotic End-Effector Design." *Florida Conference on Recent Advances in Robotics*. May. 2007.

- [15] Ramaiah, P. S., M. Venkateswara Rao, and G. V. Satyanarayana. "A microcontroller based four fingered robotic hand." International Journal of Artificial Intelligence & Applications (IJAIA) 2.2 (2011): 90-102.
- [16] Bicchi, Antonio, and Alessia Marigo. "Dexterous grippers: Putting nonholonomy to work for fine manipulation." The International Journal of Robotics Research 21.5-6 (2002): 427-442.
- [17] Ohol, S. S., and S. R. Kajale. "Simulation of Multifinger Robotic Gripper for Dynamic Analysis of Dexterous Grasping." Proceedings of the World Congress on Engineering and Computer Science, San Francisco. 2008.
- [18] Volpe, Richard, and Robert Ivlev. "A survey and experimental evaluation of proximity sensors for space robotics." Robotics and Automation, 1994. Proceedings., 1994 IEEE International Conference on. IEEE, 1994.
- [19] <http://en.wikipedia.org/wiki/SCARA>
- [20] Urrea, Claudio, and John Kern. "Modeling, Simulation and Control of a Redundant SCARA-Type Manipulator Robot." Int J Adv Robotic Sy 9.58 (2012).
- [21] Eliot, Elias, Deepak BBVL, and D. R. Parhi. "Design & Kinematic Analysis of an Articulated Robotic Manipulator." (2012).
- [22] Dinger, Steven, John Dickens, and Adam Pantanowitz. "Robotic Arm for Remote Surgery." arXiv preprint arXiv:1307.5641 (2013)
- [23] : R. Haberle, C.P. McKay, O. Gwynne, D. Atkinson, G. Landis, R. Zurek, J. Pollack and J. Appelbaum, “Atmospheric Effects on the Utility of Solar Power on Mars,” Resources of Near Earth Space, 799-818. U. Arizona Press Space Science Series (1993).

10.5 AGSE Machining Plan

As mentioned in section 5.5.4.1: *Prep Work*, a plan for the machining of the raw materials for the AGSE was developed in order to play into the machining strengths of each member of the team. The highlighted portions on the right side of the table link to other spreadsheets with more detail on the machining of the particular part, including ranking of necessary precision, difficulty, relevant dimensions, and tools and machines needed. An example of this detail is shown on the next page.

Groups	People	Description		Priority 1	Priority 2	Priority 3
Fab Group 1	Fred, Connor	Tasked with primarily <u>milling</u> operations: Plates, etc.	Fab Group 1	Lead Carriage (Vertical) Follower Carriage (Vertical) Top End Plate (Vertical) Bottom End Plate (Vertical)	Back Side Plate (Vertical carriage) Front Side Plate (Vertical carriage) Lead Carriage (Horizontal) Follower Carriage (Horizontal) Far End Plate (Horizontal)	Motor Mount (Vertical) Motor Mount (Horizontal)
Fab Group 2	Jacob, Chris	Tasked with primarily <u>lathe</u> operations:				
Fab Group 3	Connor, Alex, Cam?	Responsible for fabricating AGSE accessories, including support for the Rocket/Rail				
Grad Group	Dexter, Ben		Fab Group 2	Guide Rods (Vertical) Turntable Bearing Cup Turntable Shaft	Lead Screw (Vertical) Lead Screw (Horizontal) Guide Rods X4 (Horizontal)	-----Help Fab Group 1----
			Fab Group 3	Table Rail Support L-Bracket for Rail Support x2	Servo Sled -----Help Fab Group 1----	
Outline of Schedule			Grad Group	----- As Needed -----		
2/12/2015	Present on Status of Parts and Detailed Schedule					
2/19/2015	Update of Progress; Timeline to begin testing this week					
2/26/2015	Final AGSE to be Presented					

Figure 201: Machining Plan Developed by Team for AGSE

Part	Machines	Spec. Operations	Difficulty (1-3)	Relevant Dimensions	Required Precision
Back Side Plate	Mill	Tap	1		
Square Sides	Mill				Medium
Guide rod centering holes x4	Mill			Diameter: 0.375", Depth: 1/8", Spacing: 3"	High
Guide rod bolt holes x4	Mill			For 10-24 bolts, Spacing: 3"	High
Drill and Tap top and bottom x4	Mill, Tap by hand	Tap		For 10-24 bolts, Tap 1/2" Deep	Medium

Figure 202: Sample Detail Table of AGSE Machined Part for Back Side Plate within Vertical Carriage

10.6 Machine Drawings

Appended are machine drawings of the full-scale rocket design and AGSE. The following table shows the numbering system for the machine drawings. Only parts that have changed since CDR are shown.

Table 37: Machine Drawings Parts Tree

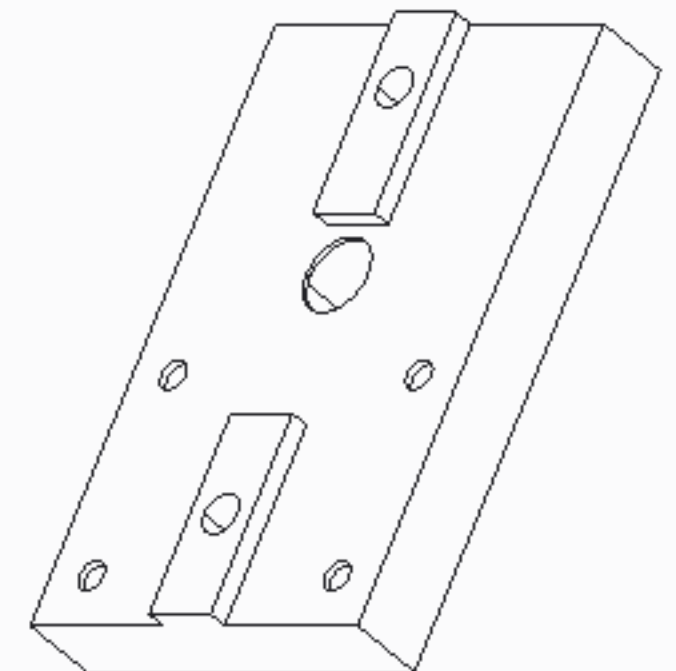
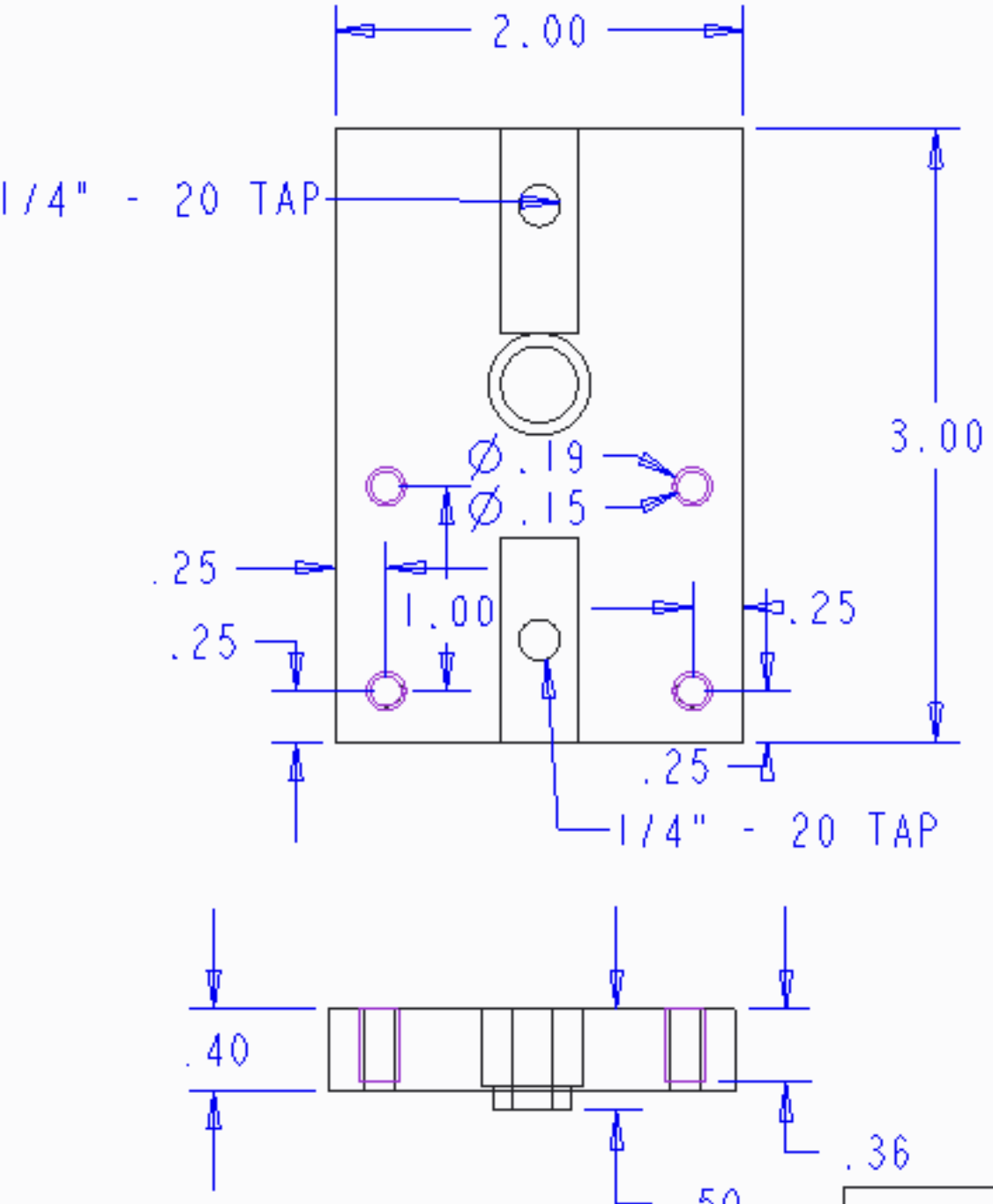
OVERALL AGSE ASSEMBLY		VU-MAIN	COMPLETE
Base Section			
	Servo Sled	VU-B-1000	COMPLETE
	Servo Mount	VU-B-2000	COMPLETE
	Servo Spindle	VU-B-3000	COMPLETE
	Bearing Cup	VU-B-4000	COMPLETE
	Servo Shaft	VU-B-5000	COMPLETE
	Table	VU-B-6000	COMPLETE
	Base	VU-B-7000	COMPLETE
	Rocket/Rail Support	VU-B-8000	COMPLETE
Vertical Section			
	Vertical Guide Rod	VU-V-1000	COMPLETE
	Vertical Lead Screw	VU-V-2000	COMPLETE
	Vertical Carriage Plate	VU-V-3000	COMPLETE
	Vertical Top Plate	VU-V-4000	COMPLETE
	Vertical Motor Mount	VU-V-5000	COMPLETE
	Vertical Encoder Mount	VU-V-6000	COMPLETE
Horizontal Section			
	Horizontal Guide Rod	VU-H-1000	COMPLETE
	Horizontal Lead Screw	VU-H-2000	COMPLETE
	Horizontal Side Plate	VU-H-3000	COMPLETE
	Horizontal Motor Mount	VU-H-4000	COMPLETE
	Horizontal Carriage Plate	VU-H-5000	COMPLETE
	Horizontal End Plate	VU-H-6000	COMPLETE
Gripper Section			
	Gripper Servo Mount	VU-G-1000	COMPLETE
	Gearframe Bottom Plate	VU-G-2000	COMPLETE
	Gearframe Top Plate	VU-G-3000	COMPLETE
	Gearframe Wrist Servoplate	VU-G-4000	COMPLETE
OVERALL ROCKET ASSEMBLY		VU-MAIN	COMPLETE
NOSECONE SECTION		VU-N-0000	COMPLETE
FORWARD SECTION MAIN ASSEMBLY		VU-F-0000	COMPLETE
TAILFIN SECTION MAIN ASSEMBLY		VU-T-0000	COMPLETE

3/16/2015

PART NAME: SERVO SLED

FRR PART NUMBER: VU-B-1000

REV A



ISOMETRIC VIEW

MATL: Aluminum

TOL: $\pm .005$
UNLESS OTHERWISE NOTED

SCALE: 1.000

DESIGN ENG: Ben G

VANDERBILT Aerospace Club

DRAFTING ENG: ALEX G

DFT: FINAL CHECKED BY: DEXTER W B.S.

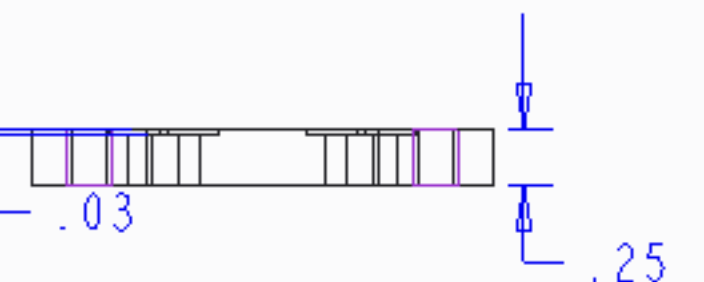
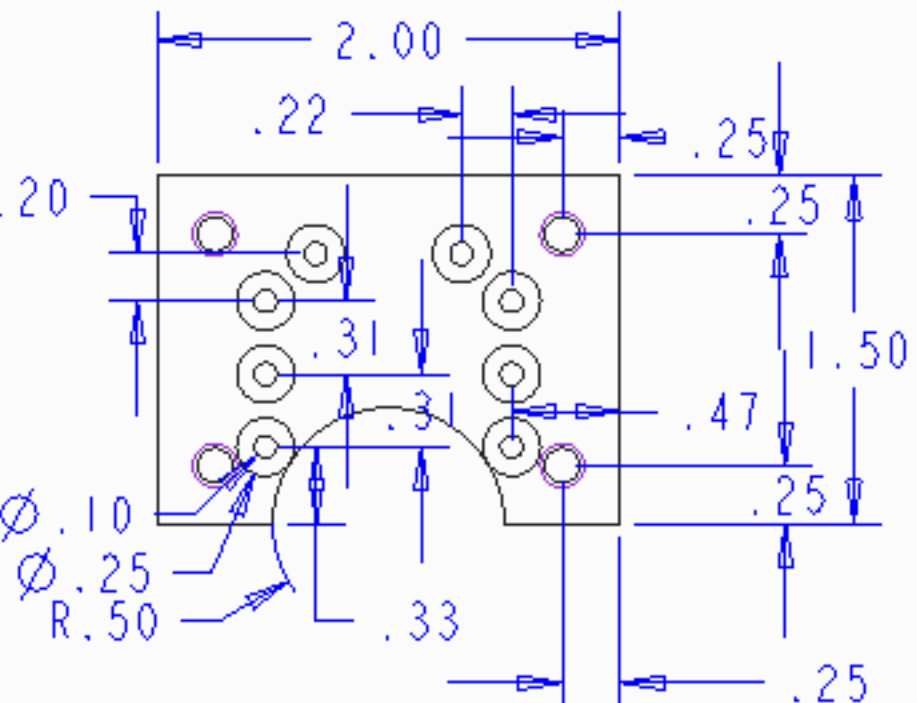
QTY: 1 ALLOCATION: FLIGHT

3/16/2015

PART NAME: Servo Mount

FRR PART NUMBER: VU-B-2000

REV A



ISOMETRIC VIEW

MATL: Acrylic

TOL: ±.005
UNLESS OTHERWISE NOTED

SCALE: 1.000

DESIGN ENG: Ben G.

VANDERBILT Aerospace Club

DRAFTING ENG: ALEX G

DFT: FINAL CHECKED BY: DEXTER W B.S.

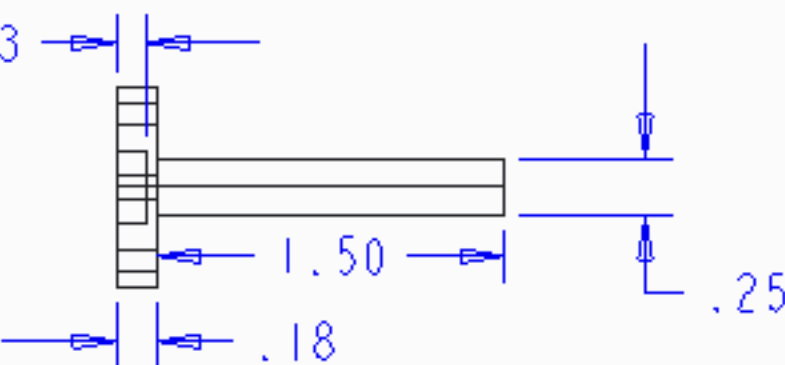
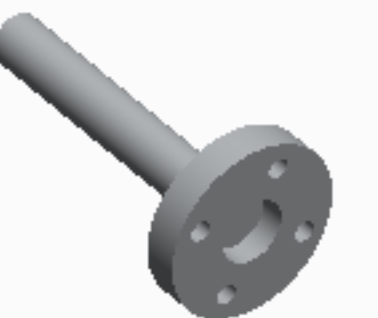
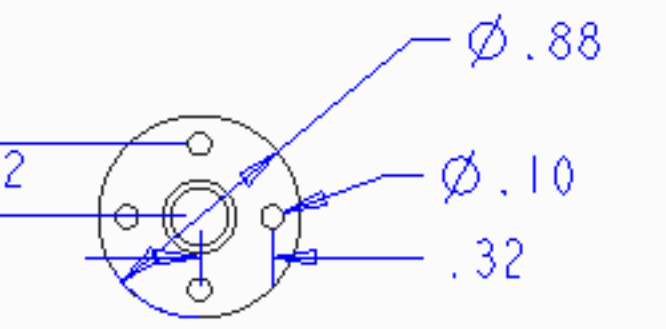
QTY: 1 ALLOCATION: FLIGHT

3/16/2015

PART NAME: Servo Spindle

FRR PART NUMBER: VU-B-3000

REV A



ISOMETRIC VIEW

MATL: BRASS

TOL: ±.005
UNLESS OTHERWISE NOTED

SCALE: 1.000

DESIGN ENG: BEN G.

VANDERBILT Aerospace Club

DRAFTING ENG: ALEX G

DFT: FINAL CHECKED BY: DEXTER W B.S.

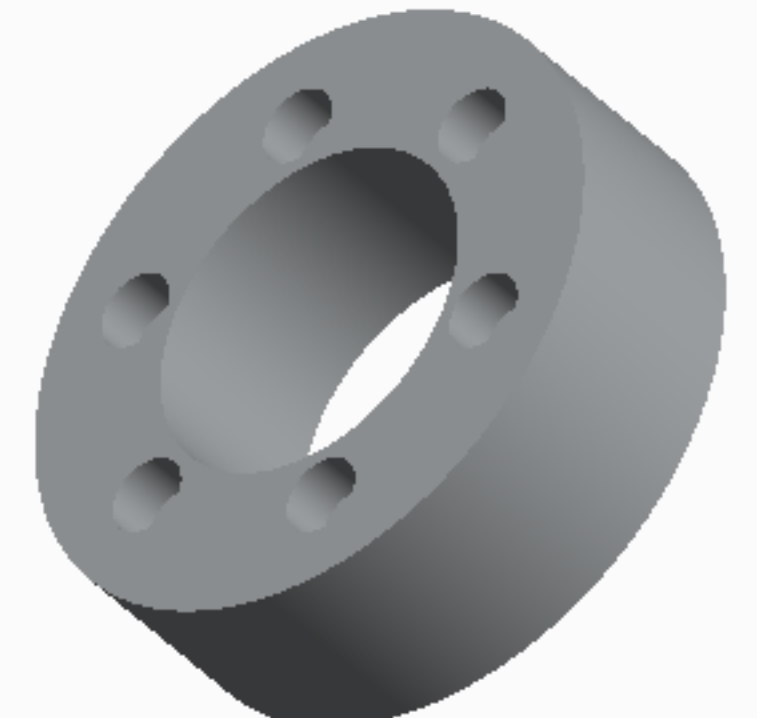
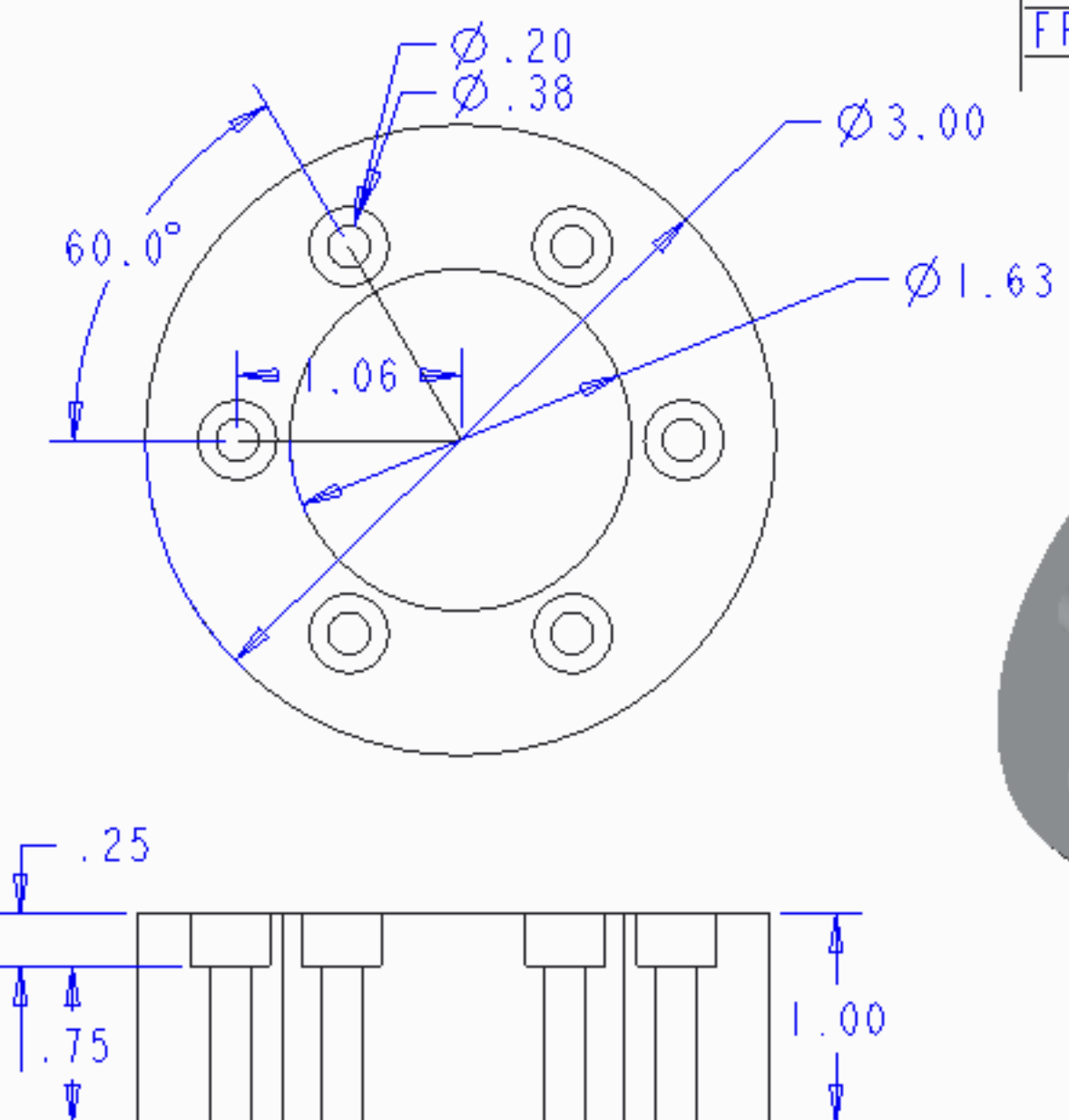
QTY: 1 ALLOCATION: FLIGHT

3/16/2015

PART NAME: BEARING CUP

FRR PART NUMBER: VU-B-4000

REV A



ISOMETRIC VIEW

MATL: ALUMINIUM

TOL: $\pm .005$
UNLESS OTHERWISE NOTED

SCALE: 1.000

DESIGN ENG: BEN G.

VANDERBILT Aerospace Club

DRAFTING ENG: ALEX G

DFT: FINAL CHECKED BY: DEXTER W B.S.

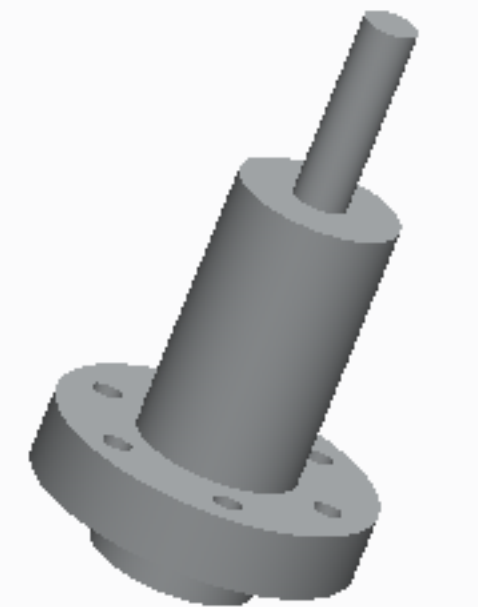
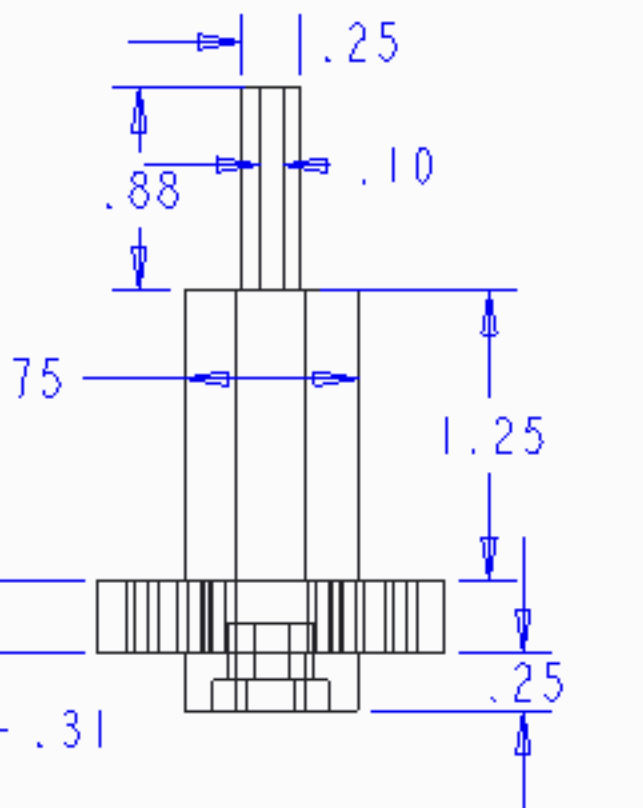
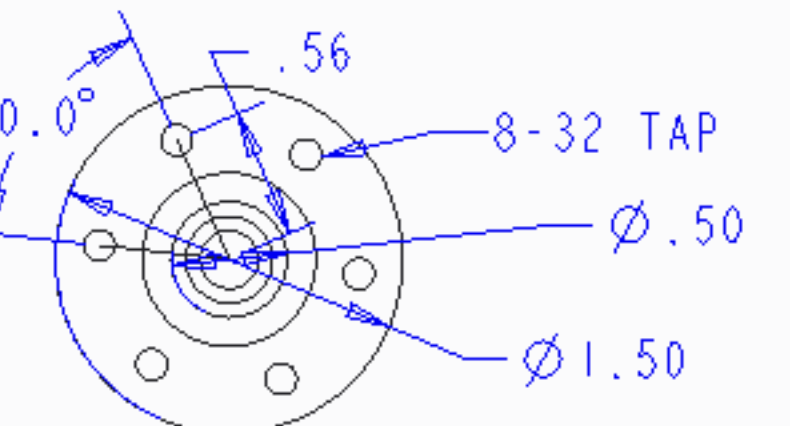
QTY: 1 ALLOCATION: FLIGHT

3/16/2015

PART NAME: SERVO SHAFT

FRR PART NUMBER: VU-B-5000

REV A



ISOMETRIC VIEW

MATL: ALUMINIUM

TOL: ±.005
UNLESS OTHERWISE NOTED

SCALE: 1.000

DESIGN ENG: BEN G.

VANDERBILT Aerospace Club

DRAFTING ENG: ALEX G

DFT: FINAL CHECKED BY: DEXTER W B.S.

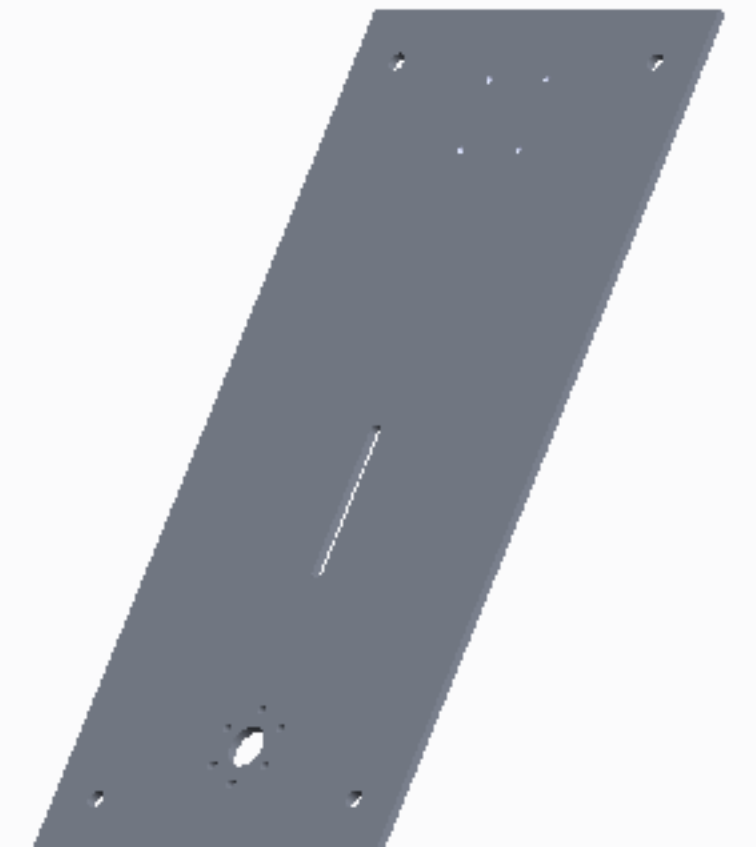
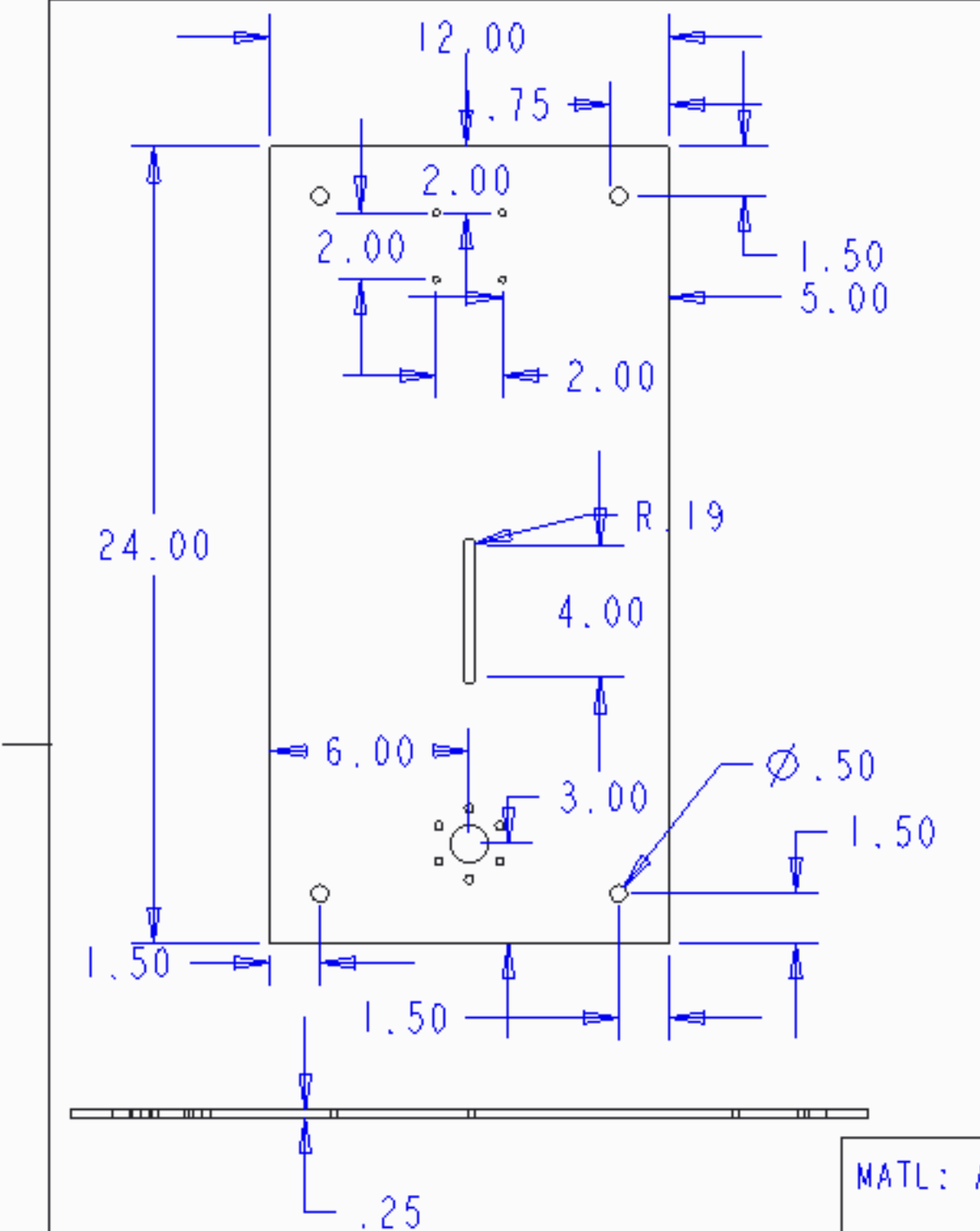
QTY: 1 ALLOCATION: FLIGHT

3/16/2015

PART NAME: AGSE TABLE

FRR PART NUMBER: VU-B-6000

REV A



ISOMETRIC VIEW

MATL: ALUMINIUM

TOL: ±.005
UNLESS OTHERWISE NOTED

SCALE: .175

DESIGN ENG: BEN G.

VANDERBILT Aerospace Club

DRAFTING ENG: ALEX G

DFT: FINAL CHECKED BY: DEXTER W B.S.

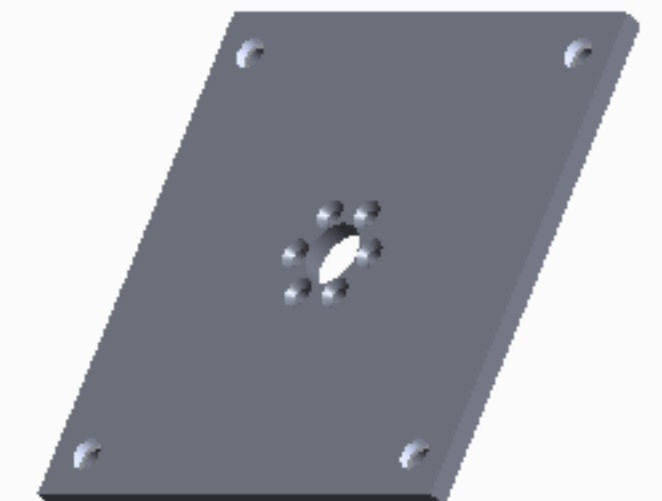
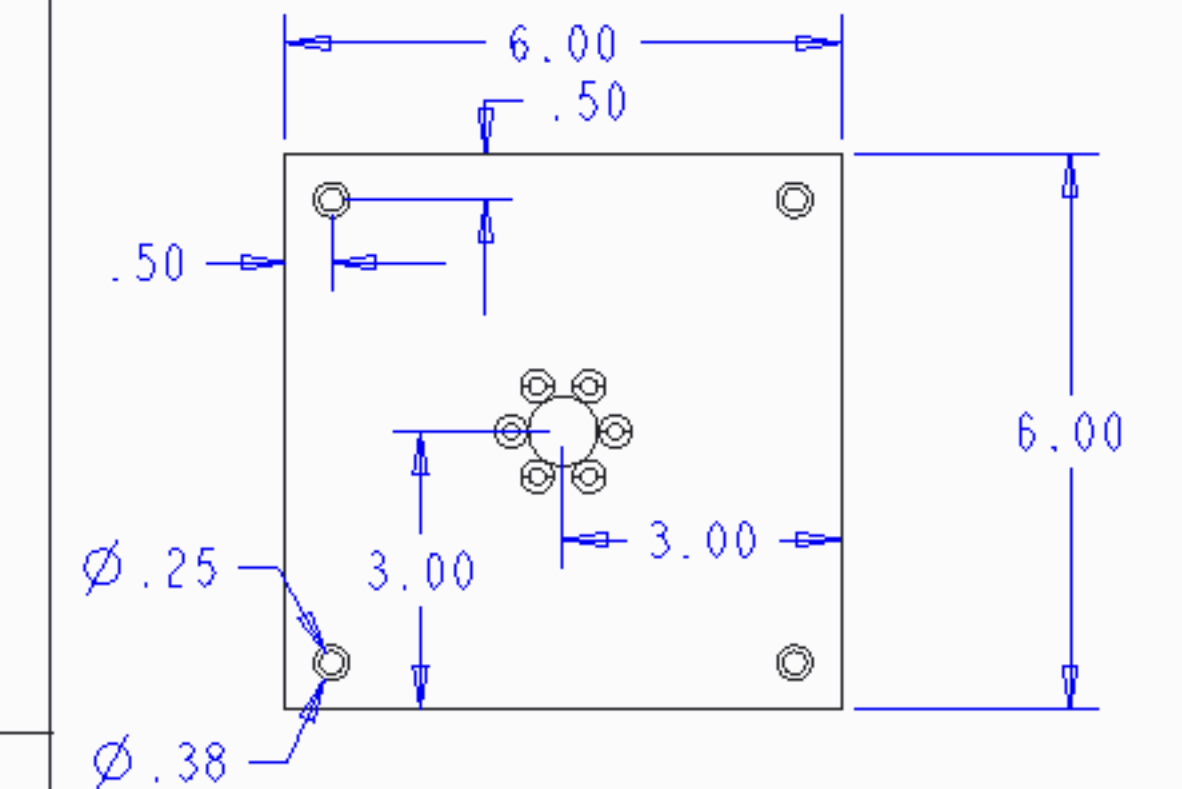
QTY: 1 ALLOCATION: FLIGHT

3/16/2015

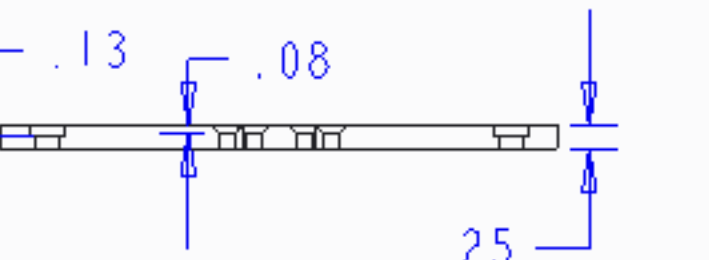
PART NAME: AGSE BASE

CDR PART NUMBER: VU-B-7000

REV A



ISOMETRIC VIEW



MATL: ALUMINIUM

TOL: $\pm .005$
UNLESS OTHERWISE NOTED

SCALE: 0.400

DESIGN ENG: BEN G.

VANDERBILT Aerospace Club

DRAFTING ENG: ALEX G

DFT: FINAL CHECKED BY: DEXTER W B.S.

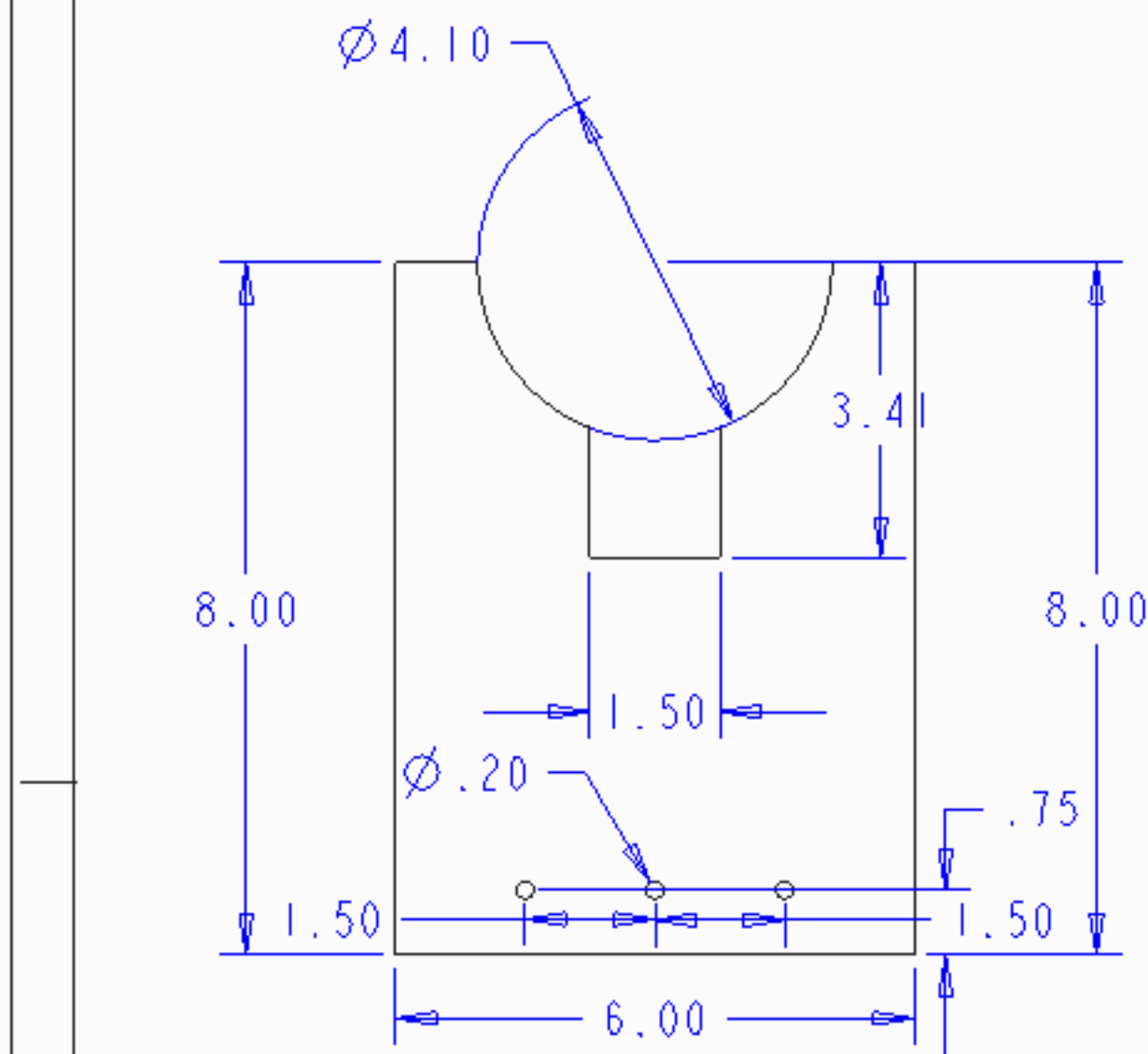
QTY: 1 ALLOCATION: FLIGHT

3/16/2015

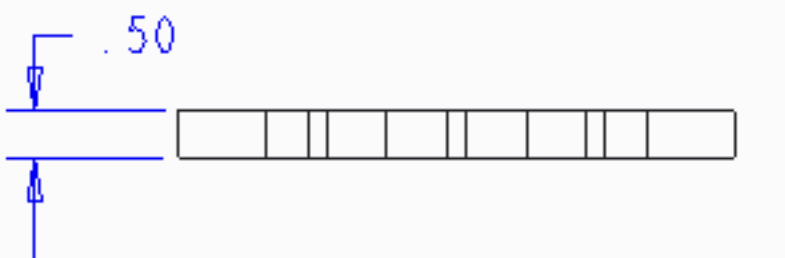
PART NAME: ROCKET & RAIL SUPPORT

FRR PART NUMBER: VU-B-8000

REV A



ISOMETRIC VIEW



MATL: ACRYLLIC

TOL: $\pm .005$
UNLESS OTHERWISE NOTED

SCALE: 0.250

DESIGN ENG: BEN G.

VANDERBILT Aerospace Club

DRAFTING ENG: ALEX G

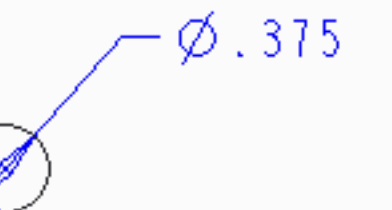
DFT: FINAL CHECKED BY: DEXTER W B.S.

QTY: 1 ALLOCATION: FLIGHT

3/16/2015

PART NAME: VERTICAL GUIDE RODE

FRR PART NUMBER: VU-V-1000 REV A



SCALE 1.000

31.50

ISOMETRIC VIEW

MATL: BLACK OXIDE
COATED STEEL

TOL: $\pm .005$
UNLESS OTHERWISE NOTED

SCALE: 0.100

DESIGN ENG: BEN G.

VANDERBILT Aerospace Club

DRAFTING ENG: ALEX G

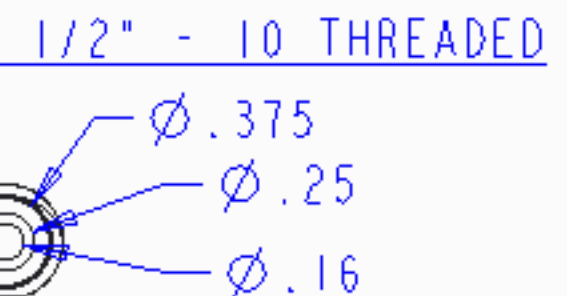
DFT: FINAL CHECKED BY: DEXTER W B.S.

QTY: 4 ALLOCATION: FLIGHT

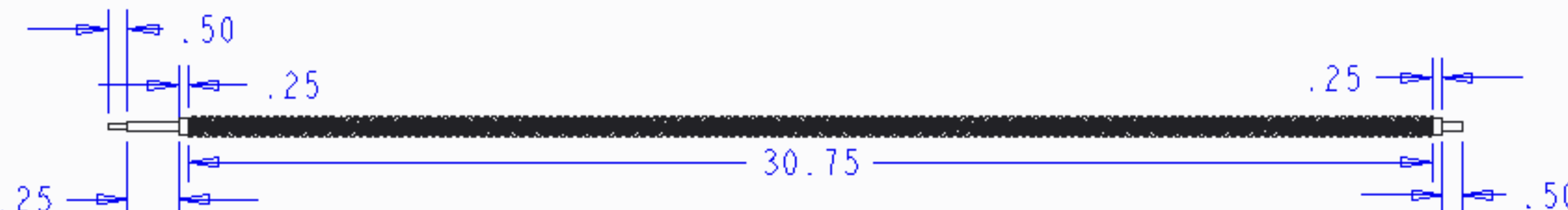
3/16/2015

PART NAME: VERTICAL LEAD SCREW

FRR PART NUMBER: VU-V-2000 REV A



SCALE 1.000



SCALE 0.250

MATL: STEEL

TOL: ±.005
UNLESS OTHERWISE NOTED

SCALE: 0.071

DESIGN ENG: BEN G.

VANDERBILT Aerospace Club

DRAFTING ENG: ALEX G

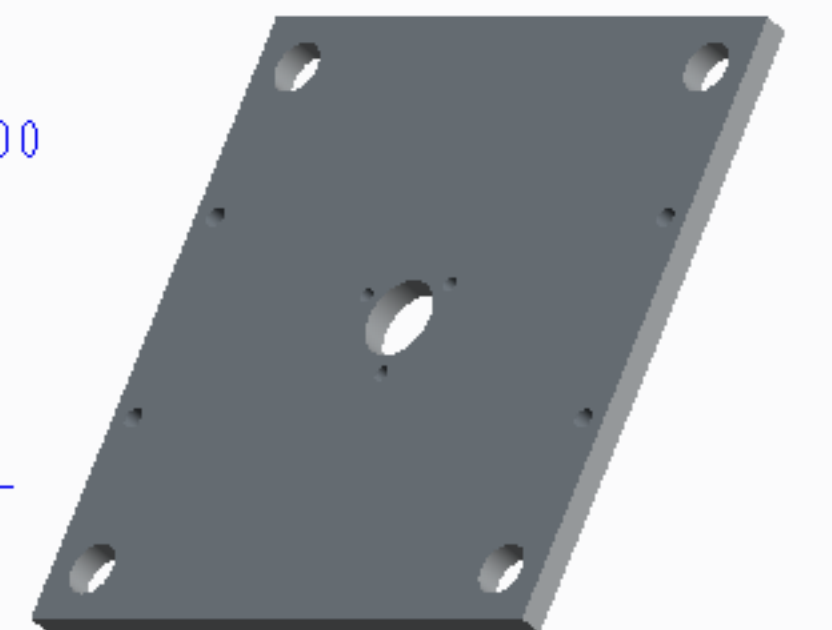
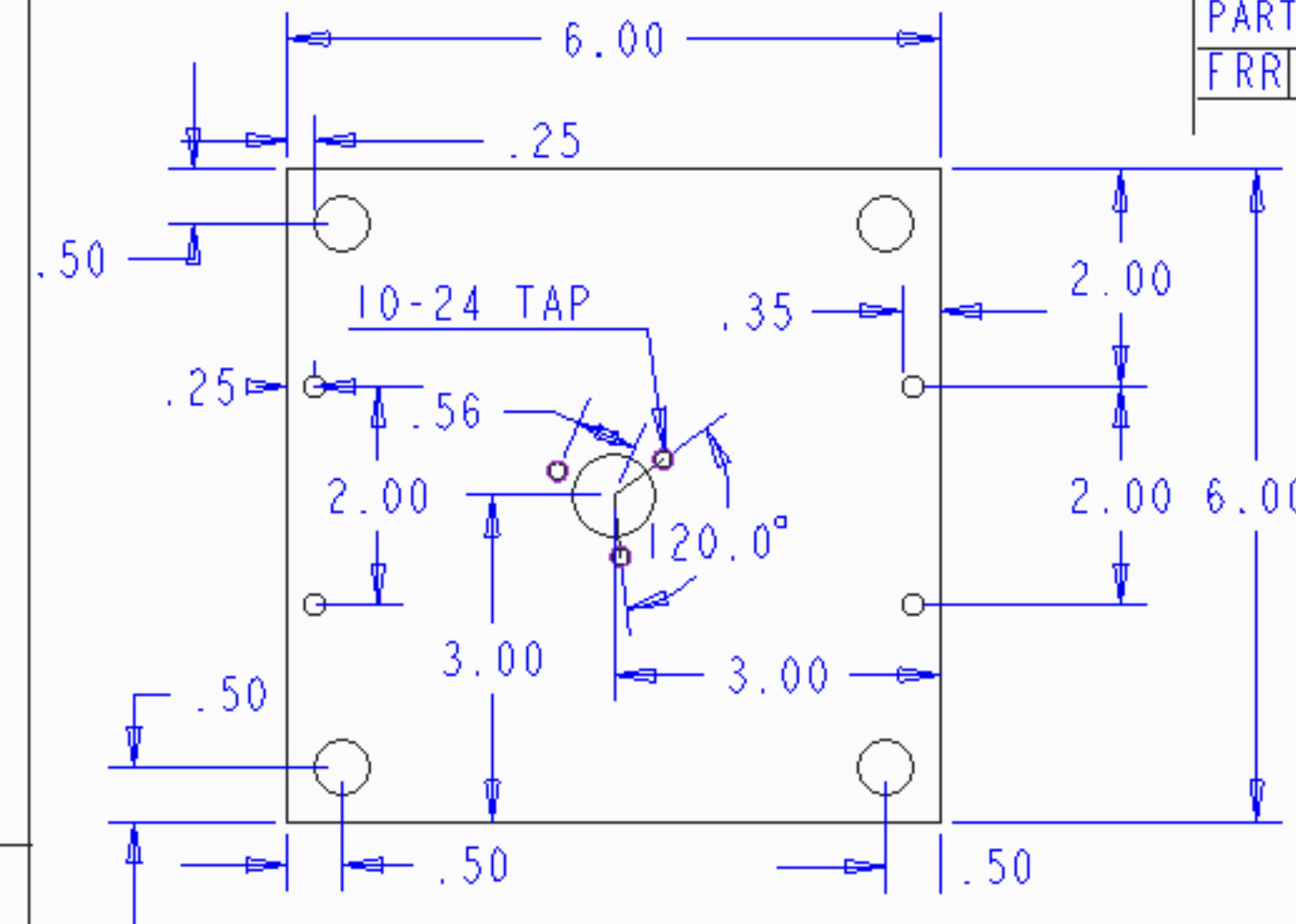
DFT: FINAL CHECKED BY: DEXTER W B.S.

QTY: 1 ALLOCATION: FLIGHT

3/16/2015

PART NAME: VERTICAL CARRIAGE PLATE

FRR PART NUMBER: VU-V-3000 REV A



ISOMETRIC VIEW

MATL: ALUMINIUM

TOL: ±.005
UNLESS OTHERWISE NOTED

SCALE: 0.500

DESIGN ENG: BEN G.

VANDERBILT  Aerospace Club

DRAFTING ENG: ALEX G

DFT: FINAL CHECKED BY: DEXTER W B.S.

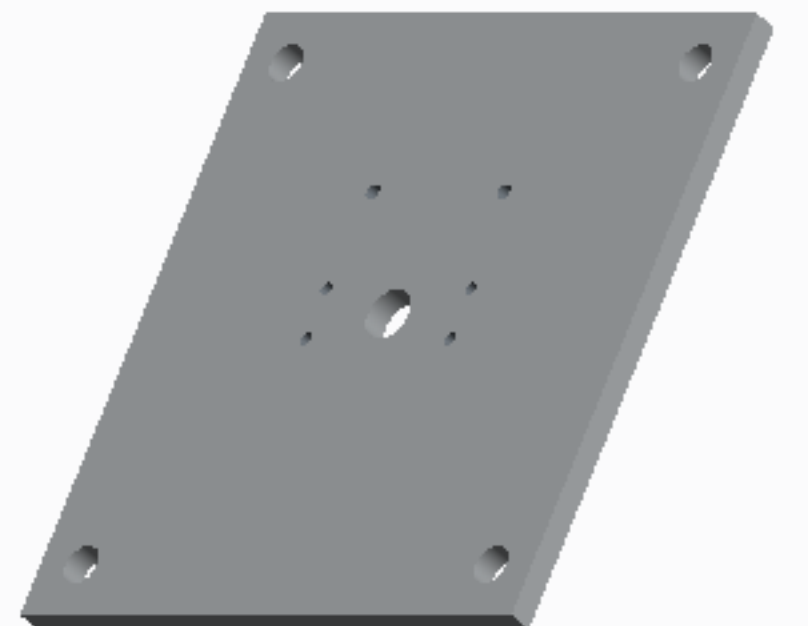
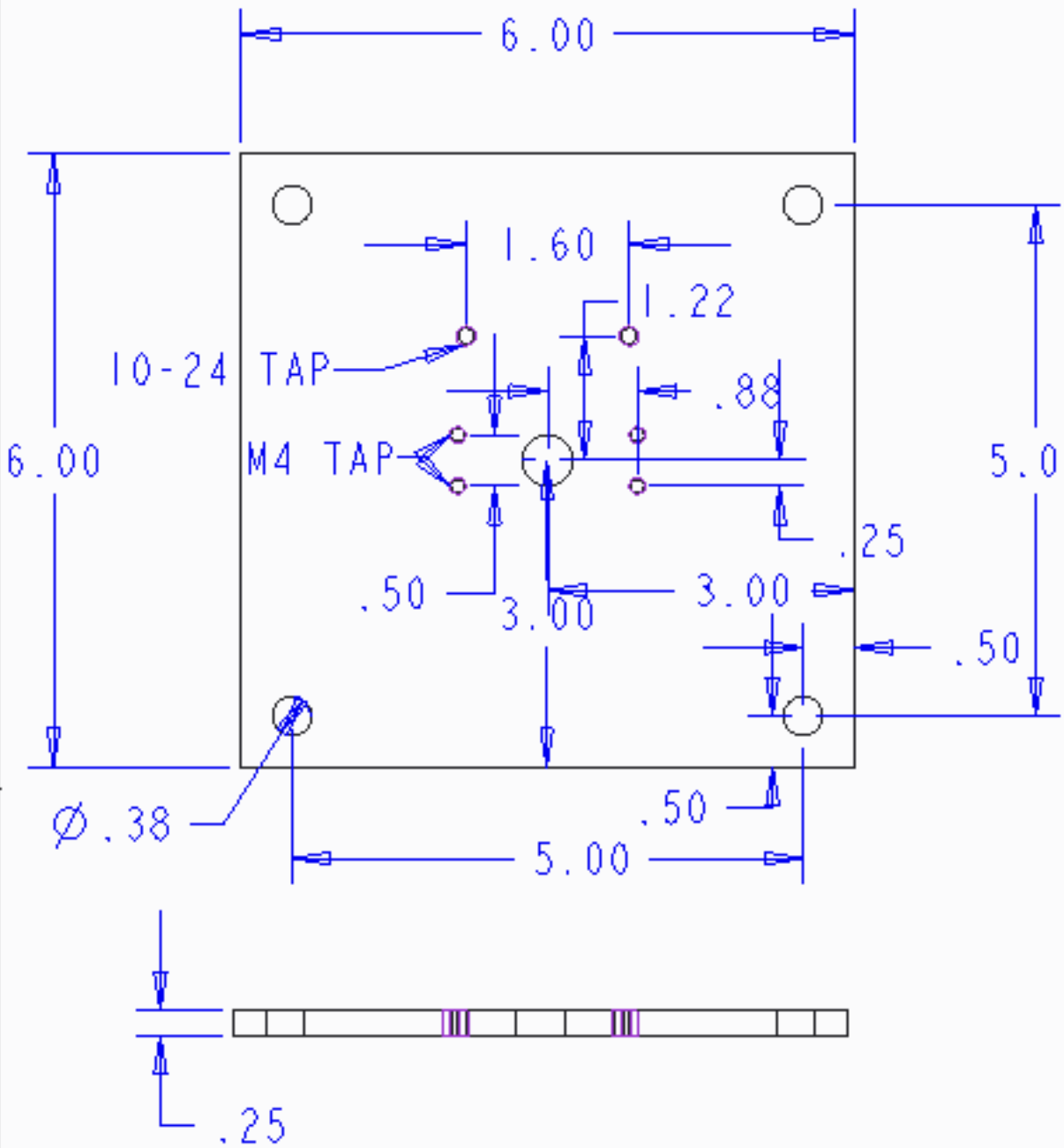
QTY: 2 ALLOCATION: FLIGHT

3/16/2015

PART NAME: VERTICAL TOP PLATE

FRR PART NUMBER: VU-V-4000

REV A



ISOMETRIC VIEW

MATL: ALUMINIUM

TOL: $\pm .005$
UNLESS OTHERWISE NOTED

SCALE: 0.500

DESIGN ENG: FRED F.

VANDERBILT Aerospace Club

DRAFTING ENG: ALEX G

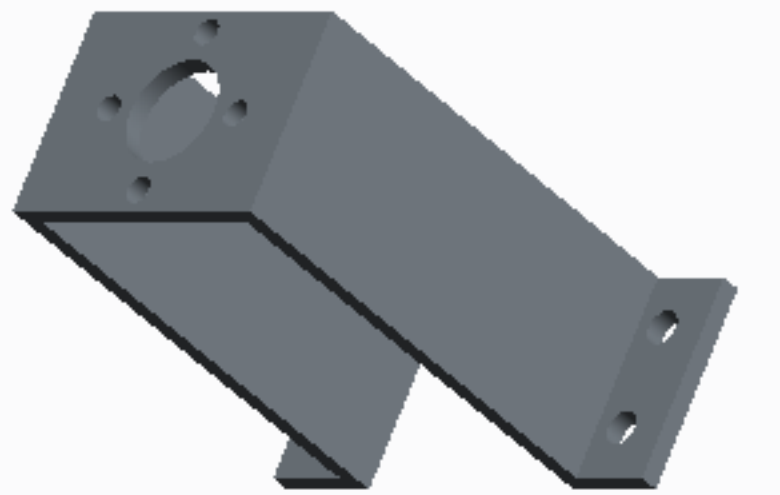
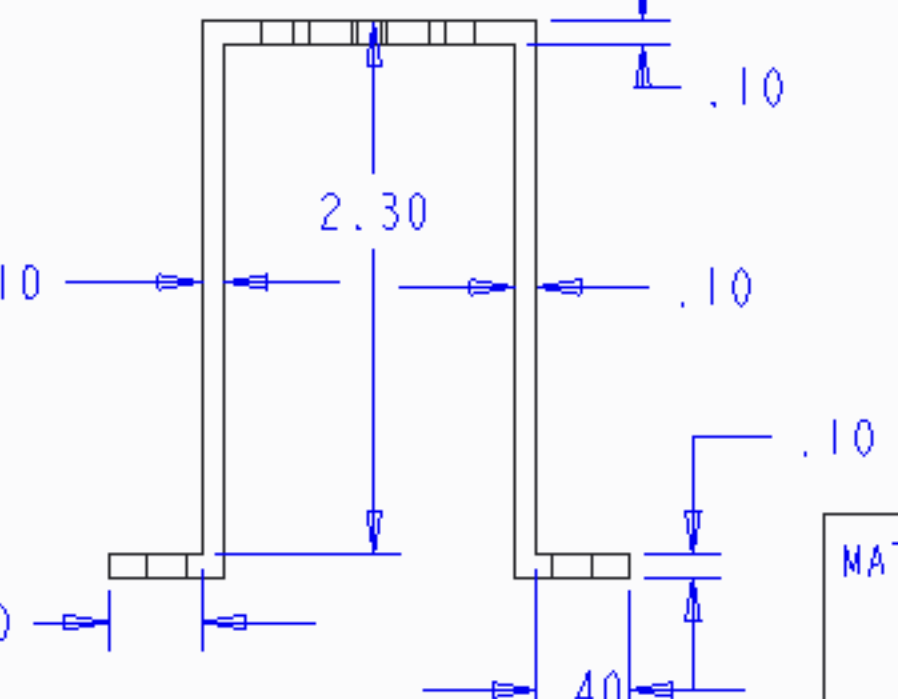
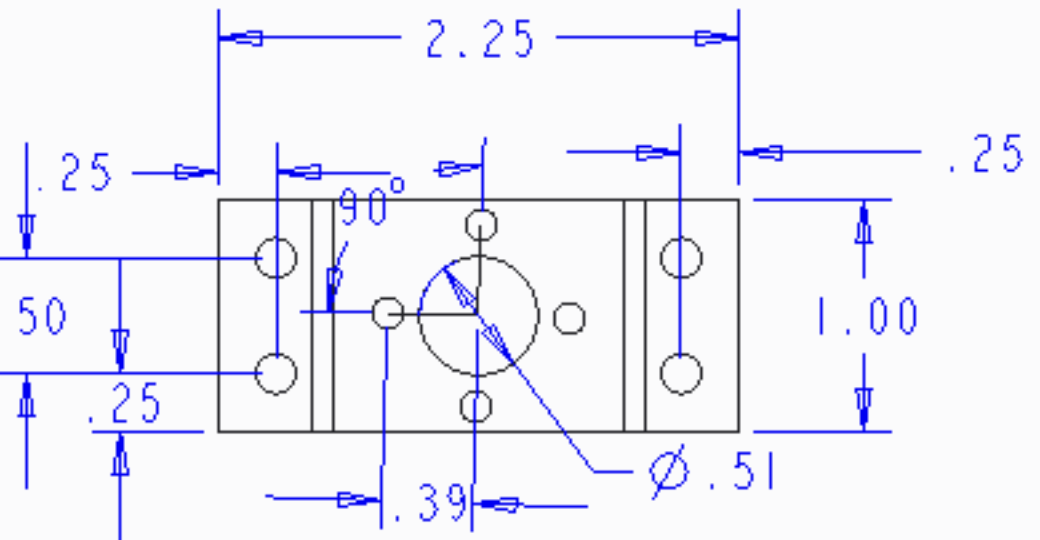
DFT: FINAL CHECKED BY: DEXTER W B.S.

QTY: 1 ALLOCATION: FLIGHT

3/16/2015

PART NAME: VERTICAL MOTOR MOUNT

FRR PART NUMBER: VU-V-5000 REV A



ISOMETRIC VIEW

MATL: ALUMINIUM

TOL: ±.005
UNLESS OTHERWISE NOTED

VANDERBILT Aerospace Club

DRAFTING ENG: ALEX G

SCALE: 1.000

DFT: FINAL

CHECKED BY: DEXTER W B.S.

DESIGN ENG: CAM R.

QTY: 1

ALLOCATION: FLIGHT

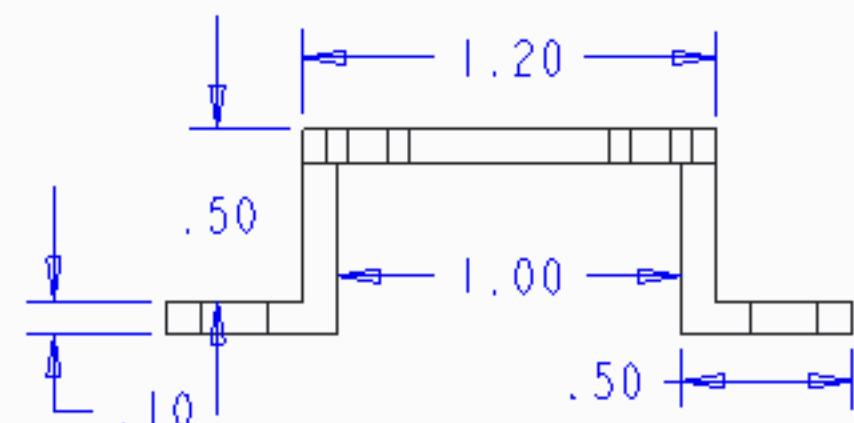
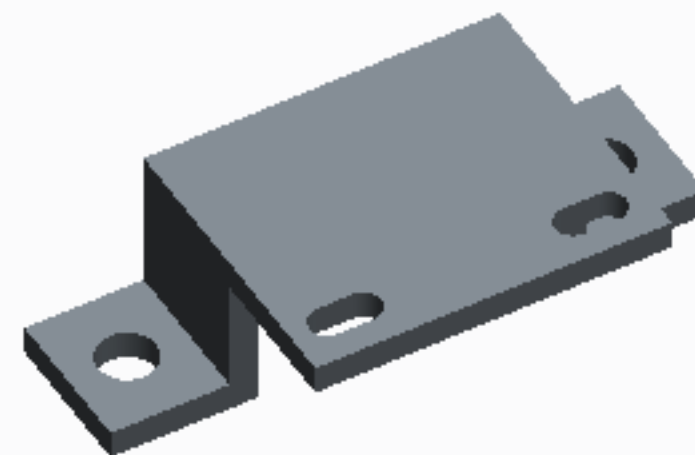
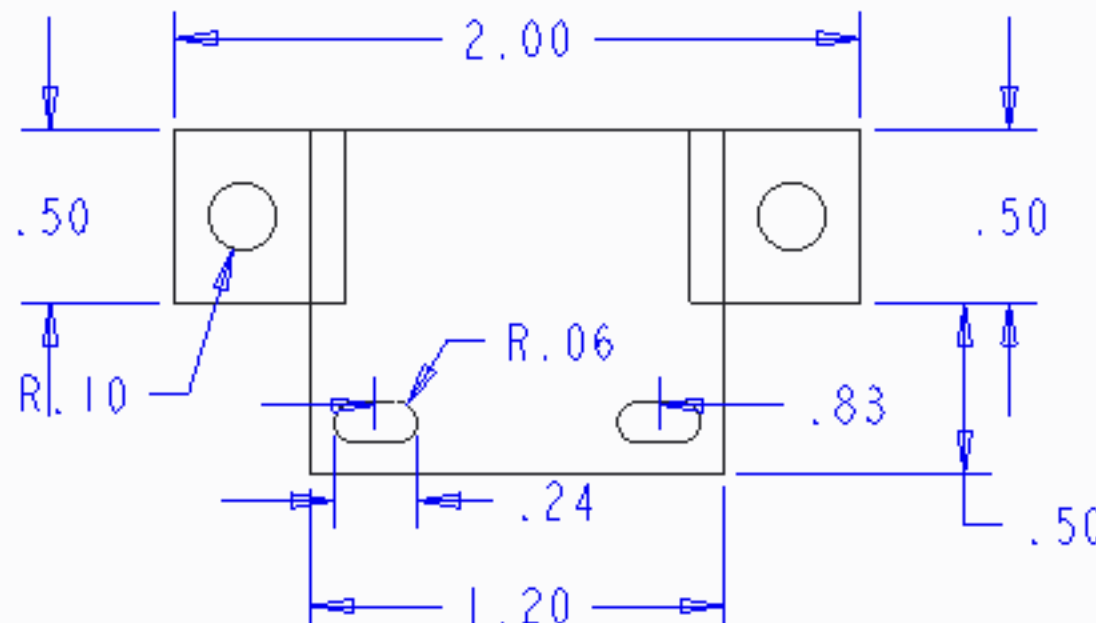
3/16/2015

PART NAME: VERTICAL ENCODER MOUNT

FRR PART NUMBER: VU-V-6000

REV

A



ISOMETRIC VIEW

MATL: ALUMINIUM

TOL: $\pm .005$
UNLESS OTHERWISE NOTED

SCALE: 1.50

DESIGN ENG: JACOB M.

VANDERBILT



Aerospace Club

DRAFTING ENG: ALEX G

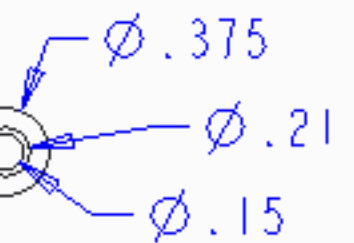
DFT: FINAL CHECKED BY: DEXTER W B.S.

QTY: 1 ALLOCATION: FLIGHT

3/16/2015

PART NAME: HORIZONTAL GUIDE ROD

FRR PART NUMBER: VU-H-1000 REV A



SCALE 1.000

ISOMETRIC VIEW

.03

1.00

SCALE 0.300

24.50

10-24 TAP

MATL: BLACK OXIDE
COATED STEELTOL: ±.005
UNLESS OTHERWISE NOTED

SCALE: 0.100

DESIGN ENG: BEN G.

VANDERBILT Aerospace Club

DRAFTING ENG: ALEX G

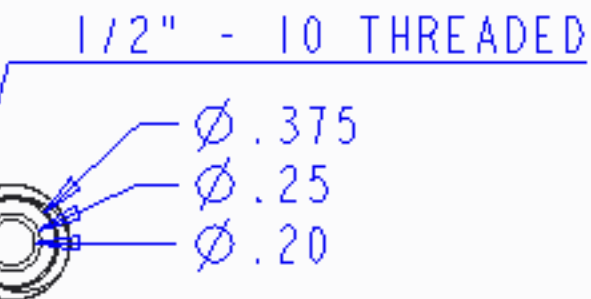
DFT: FINAL CHECKED BY: DEXTER W B.S.

QTY: 4 ALLOCATION: FLIGHT

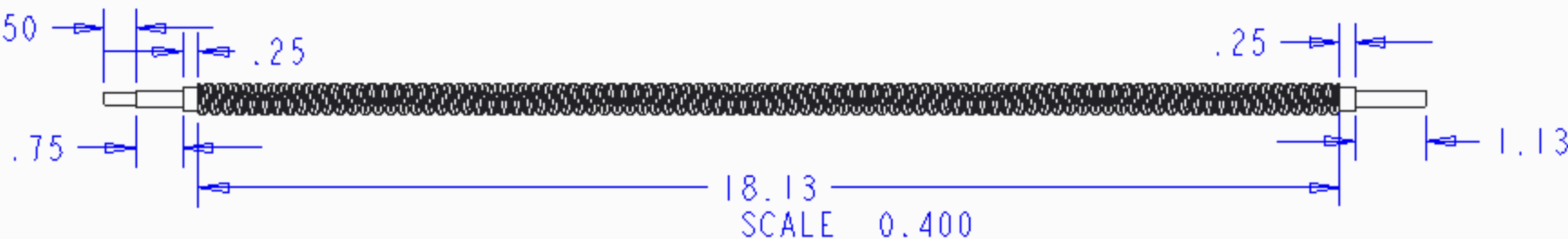
3/16/2015

PART NAME: HORIZONTAL LEAD SCREW

FRR PART NUMBER: VU-H-200 REV A



SCALE 1.000



MATL: STEEL

TOL: $\pm .005$
UNLESS OTHERWISE NOTED

SCALE: 0.111

DESIGN ENG: BEN G.

VANDERBILT Aerospace Club

DRAFTING ENG: ALEX G

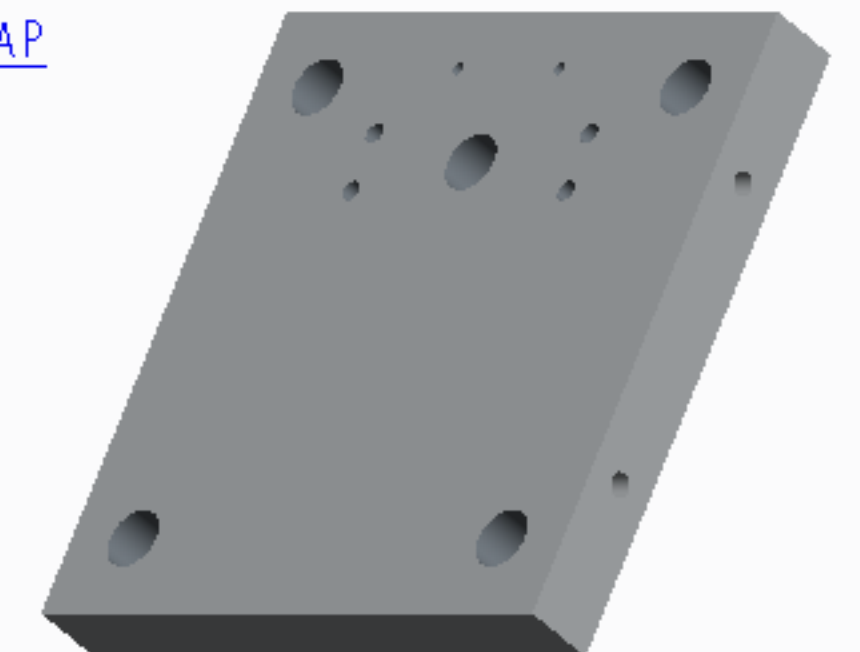
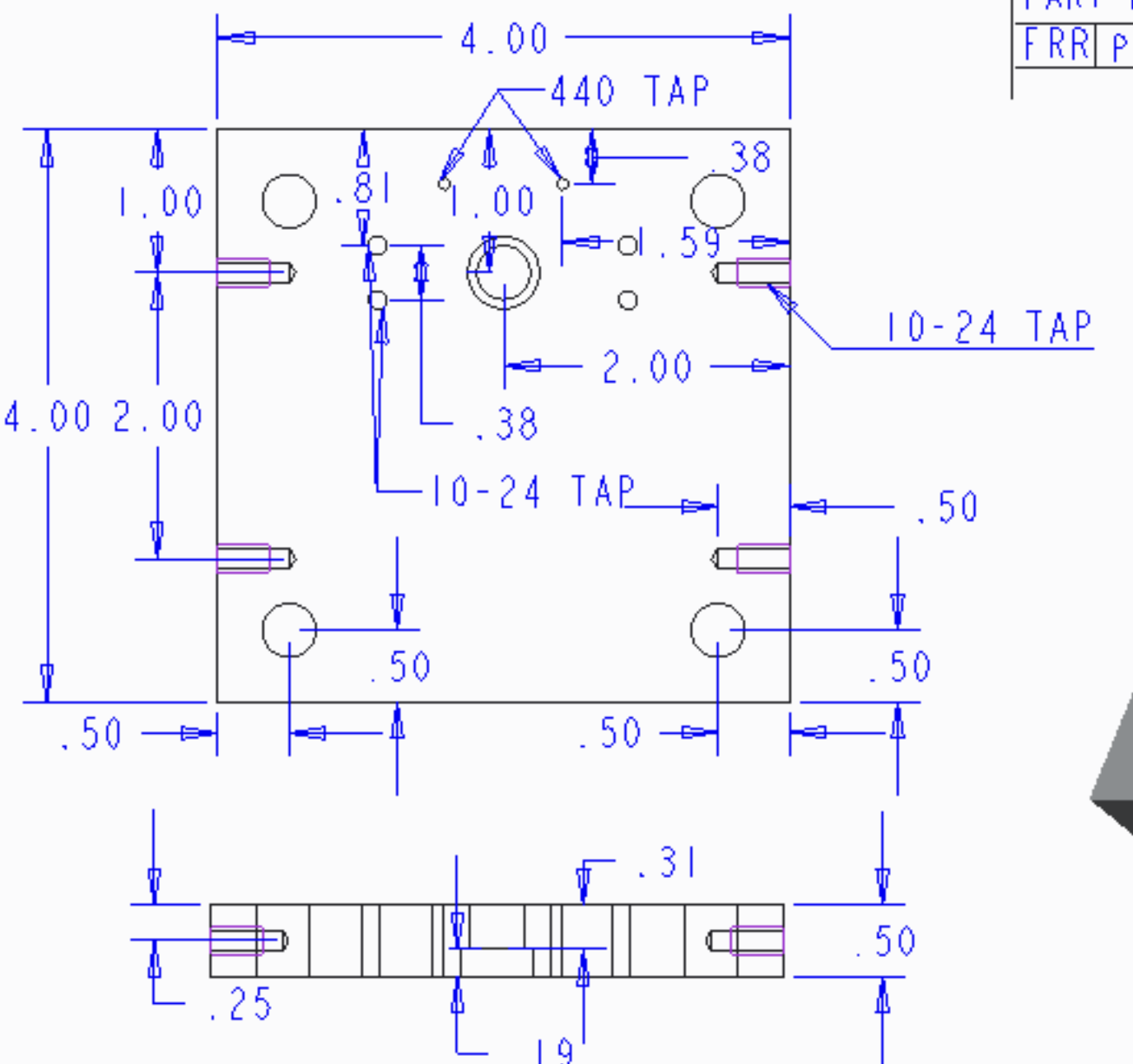
DFT: FINAL CHECKED BY: DEXTER W B.S.

QTY: 1 ALLOCATION: FLIGHT

3/16/2015

PART NAME: HORIZONTAL SIDE PLATE

FRR PART NUMBER: VU-H-3000 REV A



ISOMETRIC VIEW

MATL: ALUMINIUM

TOL: $\pm .005$
UNLESS OTHERWISE NOTED

SCALE: 0.750

DESIGN ENG: BEN G.

VANDERBILT Aerospace Club

DRAFTING ENG: ALEX G

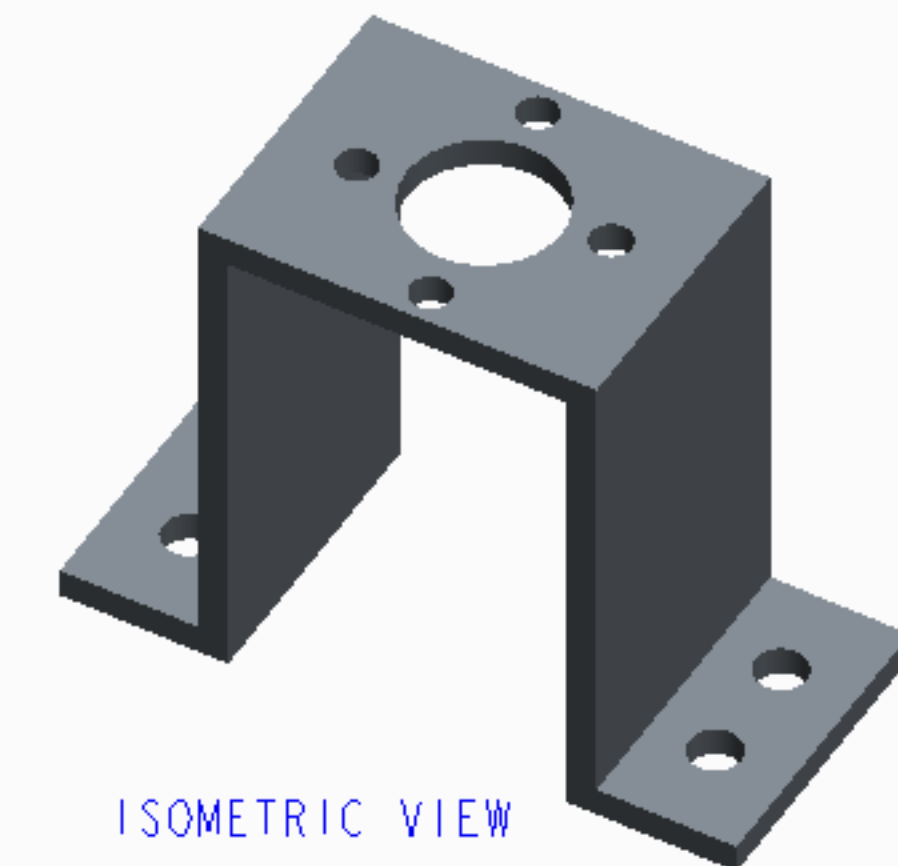
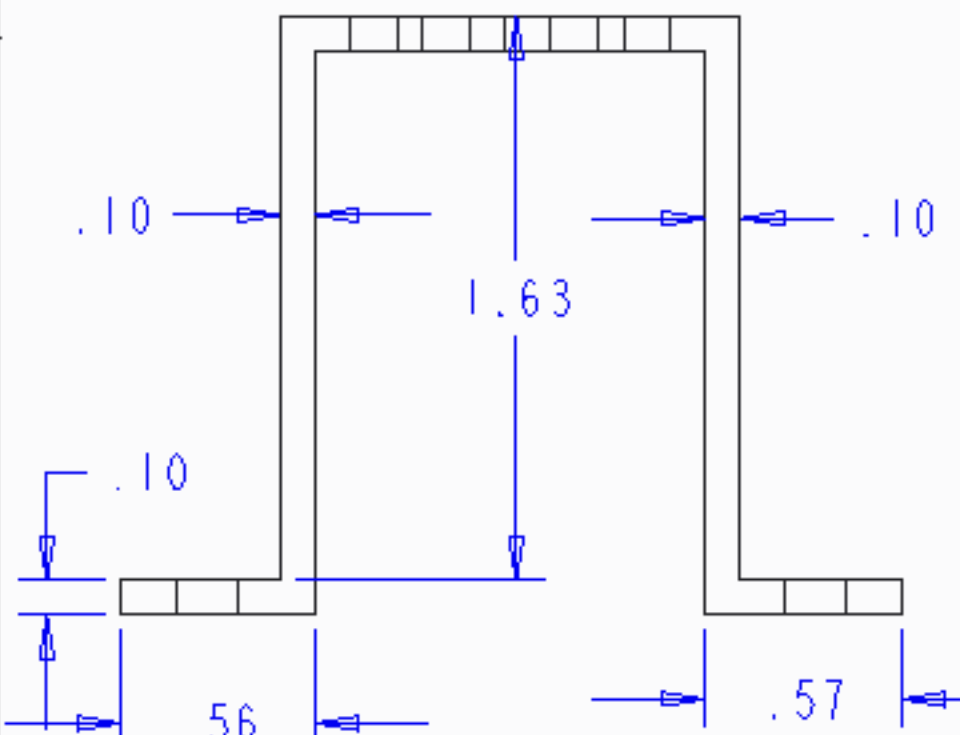
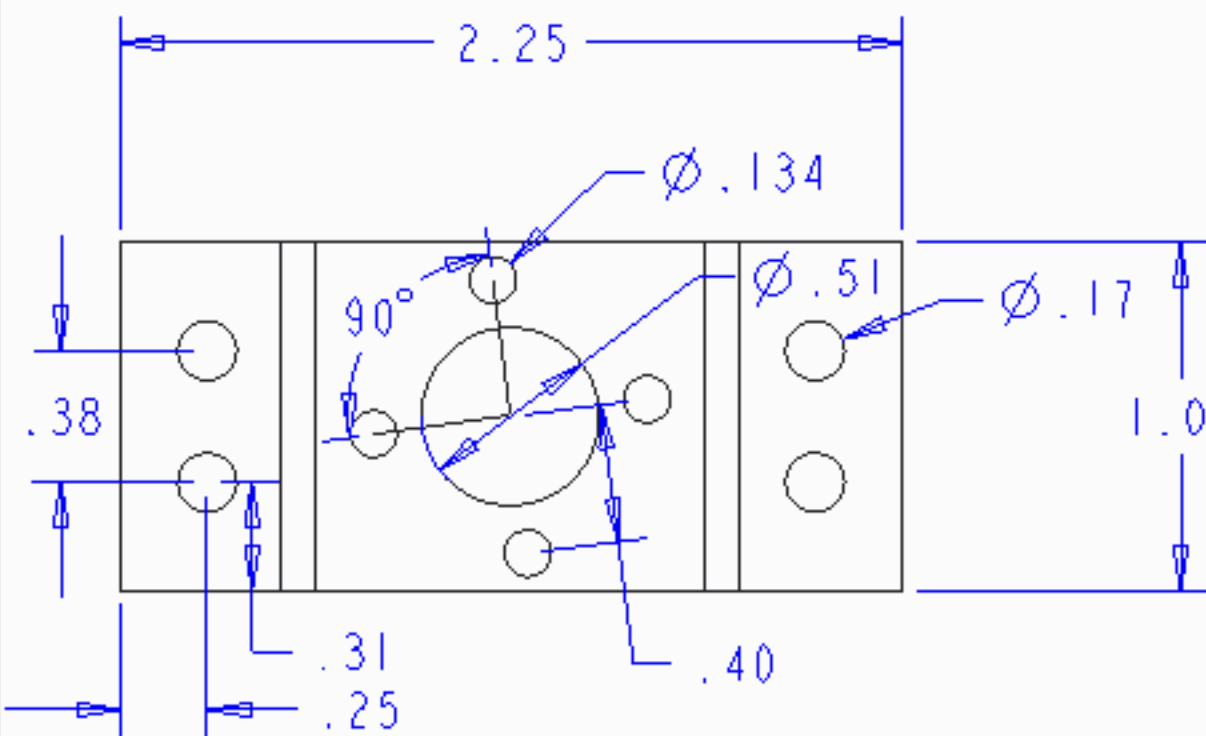
DFT: FINAL CHECKED BY: DEXTER W B.S.

QTY: 2 ALLOCATION: FLIGHT

3/16/2015

PART NAME: HORIZONTAL MOTOR MOUNT

FRR PART NUMBER: VU-H-4000 REV A



ISOMETRIC VIEW

MATL: ALUMINIUM

VANDERBILT Aerospace Club

TOL: ±.005
UNLESS OTHERWISE NOTED

DRAFTING ENG: ALEX G

SCALE: 1.5

DFT: FINAL CHECKED BY: DEXTER W B.S.

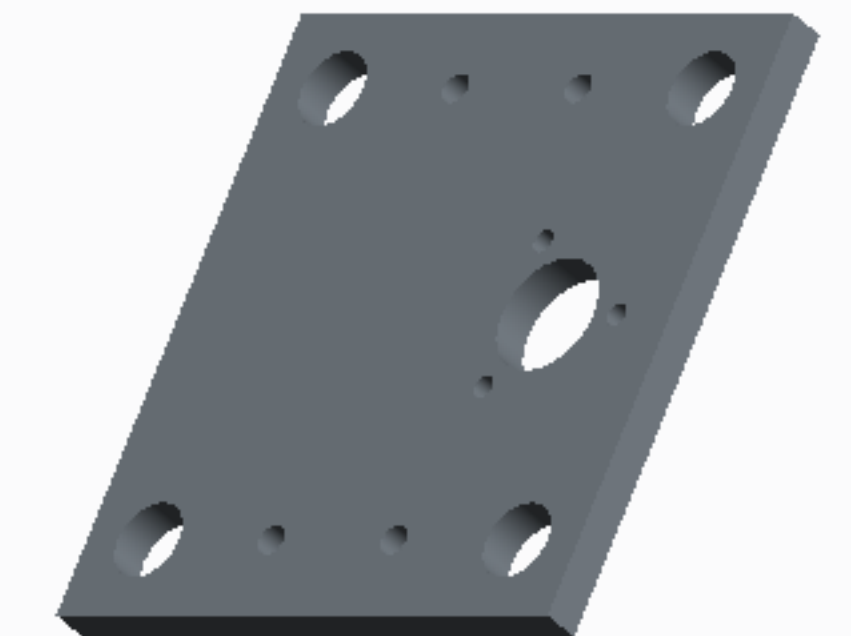
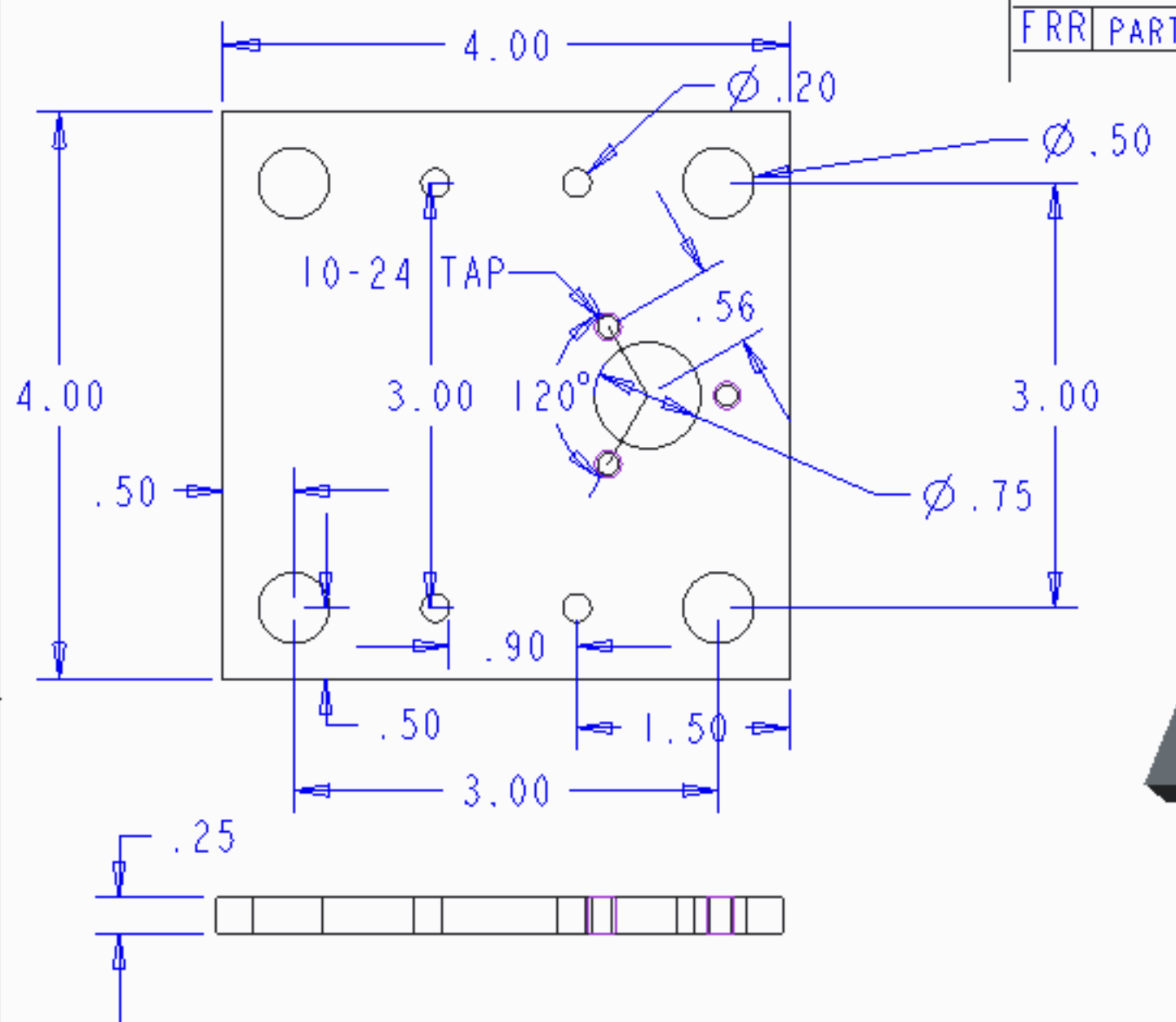
DESIGN ENG: FRED F.

QTY: 1 ALLOCATION: FLIGHT

3/16/2015

PART NAME: HORIZONTAL CARRIAGE PLATE

FRR PART NUMBER: VU-H-5000 REV A



ISOMETRIC VIEW

MATL: ALUMINIUM

TOL: $\pm .005$
UNLESS OTHERWISE NOTED

SCALE: 0.750

DESIGN ENG: FRED F.

VANDERBILT Aerospace Club

DRAFTING ENG: ALEX G

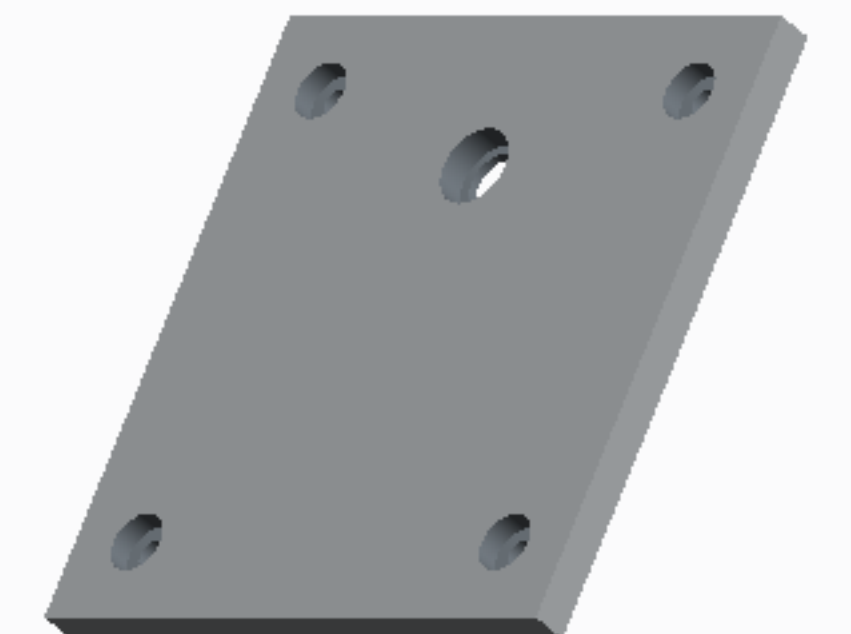
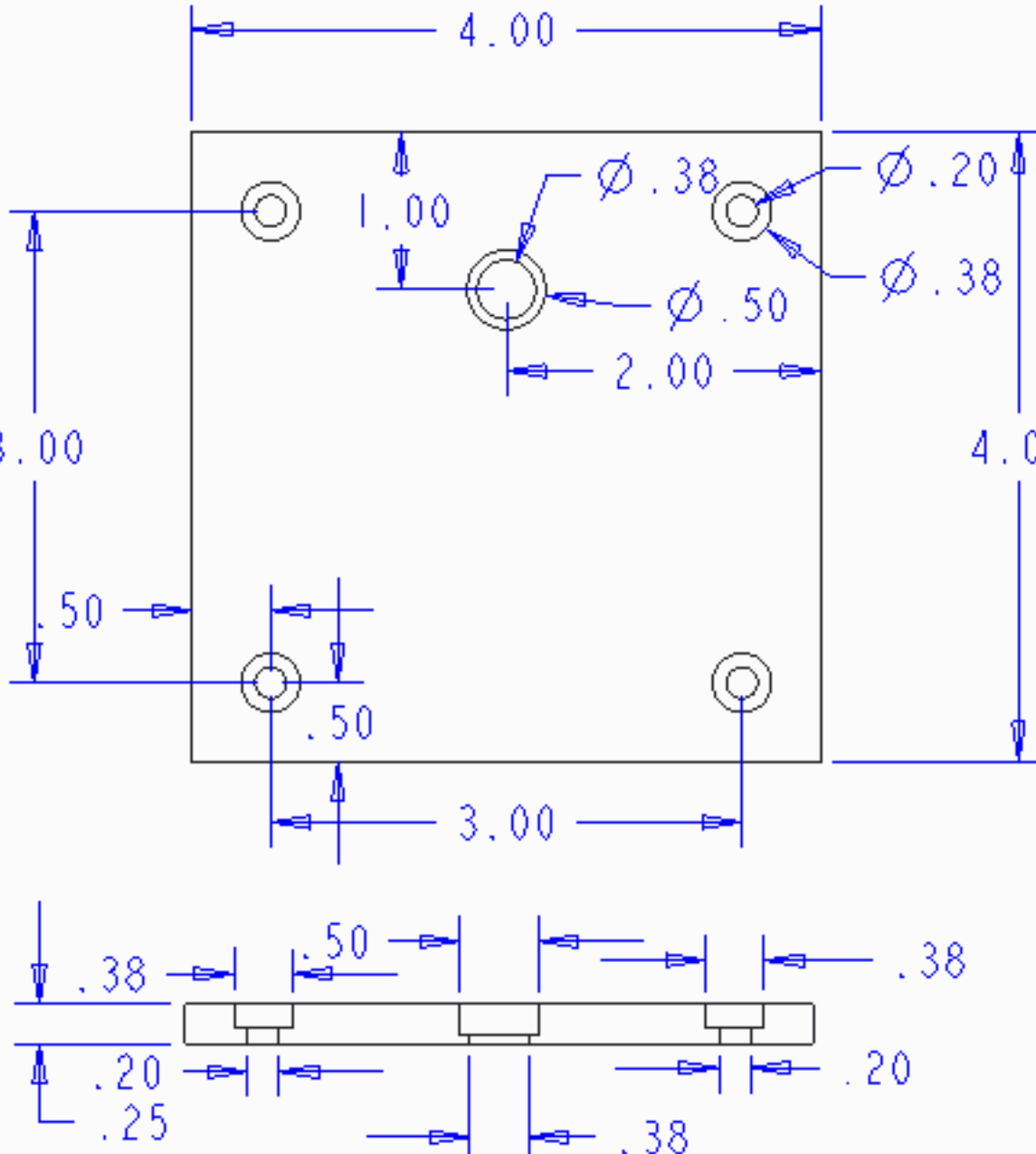
DFT: FINAL CHECKED BY: DEXTER W B.S.

QTY: 2 ALLOCATION: FLIGHT

3/16/2015

PART NAME: HORIZONTAL END PLATE

FRR PART NUMBER: VU-H-6--- REV A



ISOMETRIC VIEW

MATL: ALUMINIUM

TOL: $\pm .005$
UNLESS OTHERWISE NOTED

SCALE: 0.500

DESIGN ENG: CAM R.

VANDERBILT Aerospace Club

DRAFTING ENG: ALEX G

DFT: FINAL CHECKED BY: DEXTER W B.S.

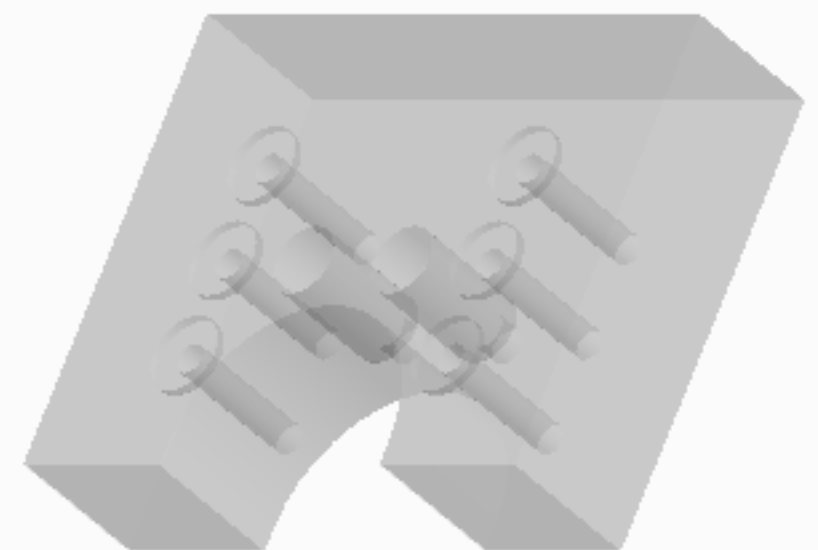
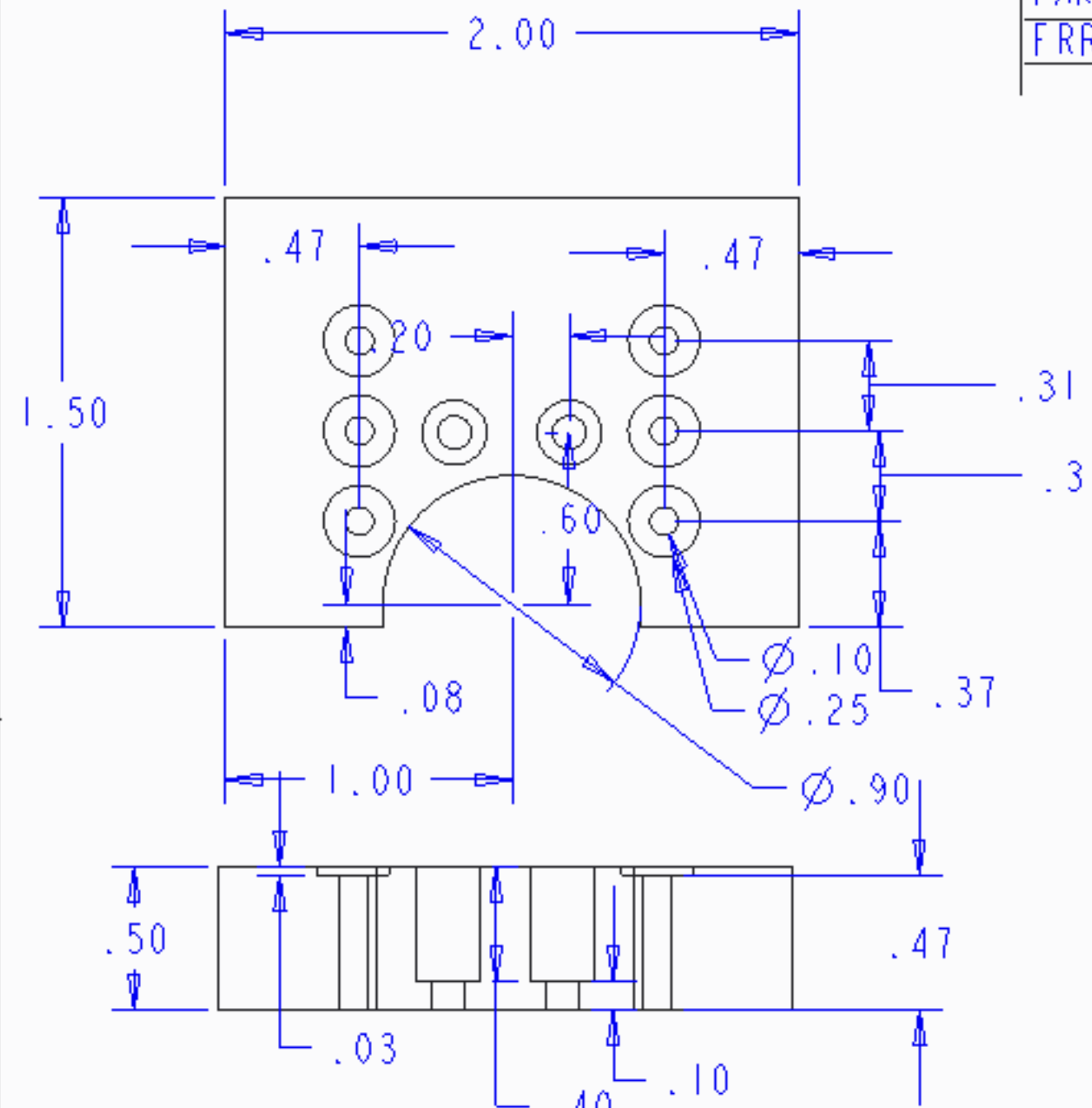
QTY: 1 ALLOCATION: FLIGHT

3/16/2015

PART NAME: GRIPPER SERVO MOUNT

FRR PART NUMBER: VU-G-1000

REV A



ISOMETRIC VIEW

MATL: ACRYLLIC

TOL: $\pm .005$
UNLESS OTHERWISE NOTED

SCALE: 1.000

DESIGN ENG: CHRIS L.

VANDERBILT Aerospace Club

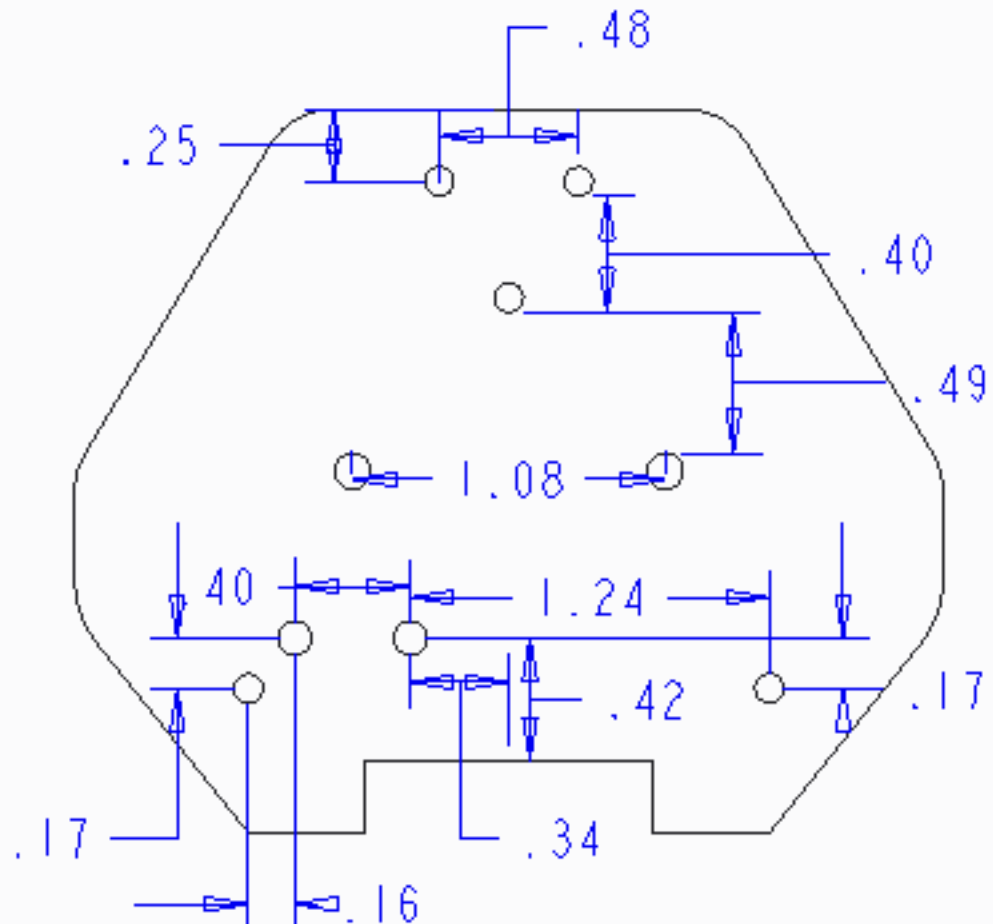
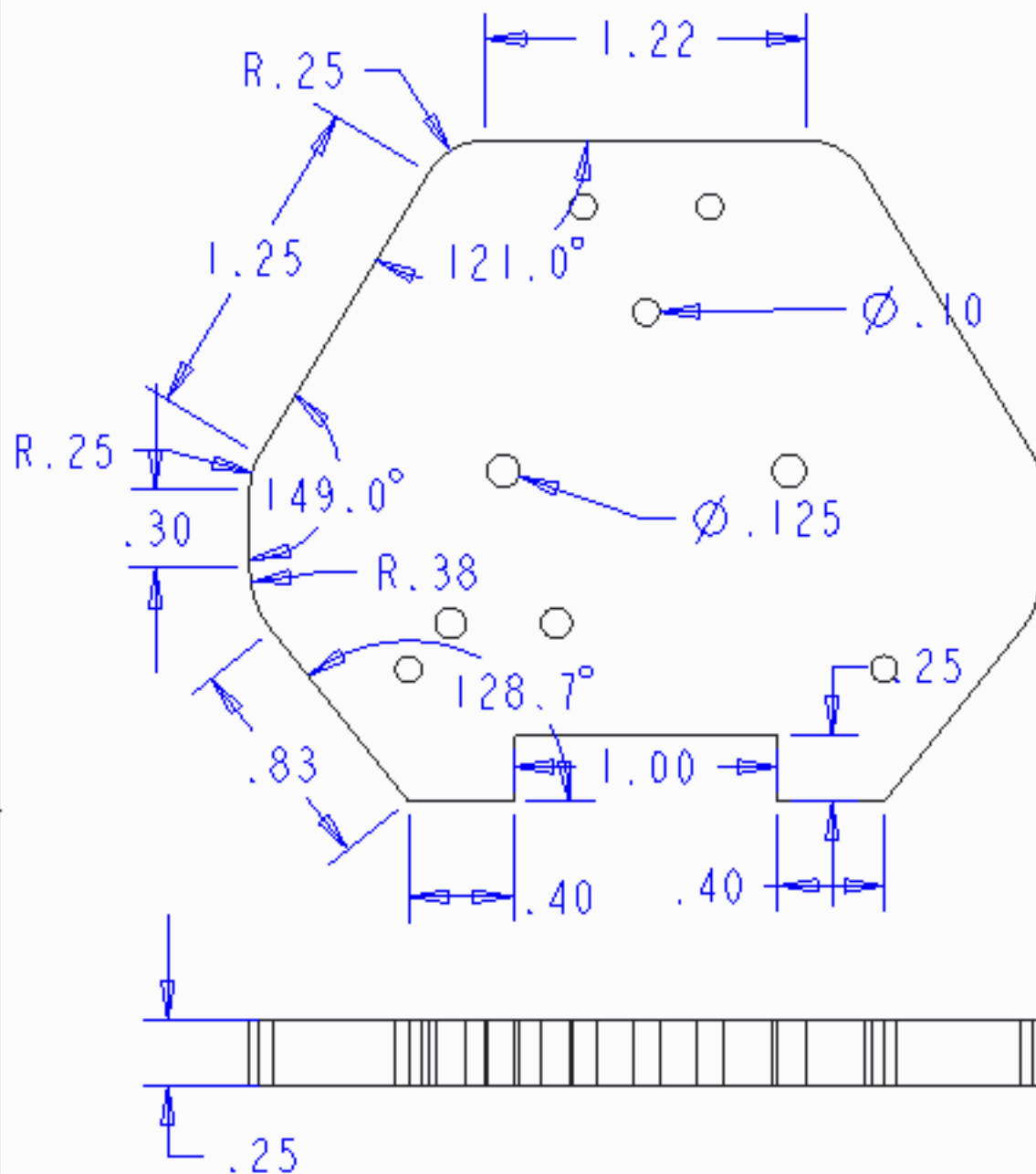
DRAFTING ENG: ALEX G

DFT: FINAL CHECKED BY: DEXTER W B.S.

QTY: 1 ALLOCATION: FLIGHT

3/16/2015

PART NAME:	GRIPPER GEARFRAME BOTTOM PLATE
FRR	PART NUMBER: VU-G-2000
REV	A



MATL: ACRYLLIC

TOL: ±.005
UNLESS OTHERWISE NOTED

SCALE: 1.000

DESIGN ENG: CHRIS L.

VANDERBILT Aerospace Club

DRAFTING ENG: ALEX G

DFT: FINAL CHECKED BY: DEXTER W B.S.

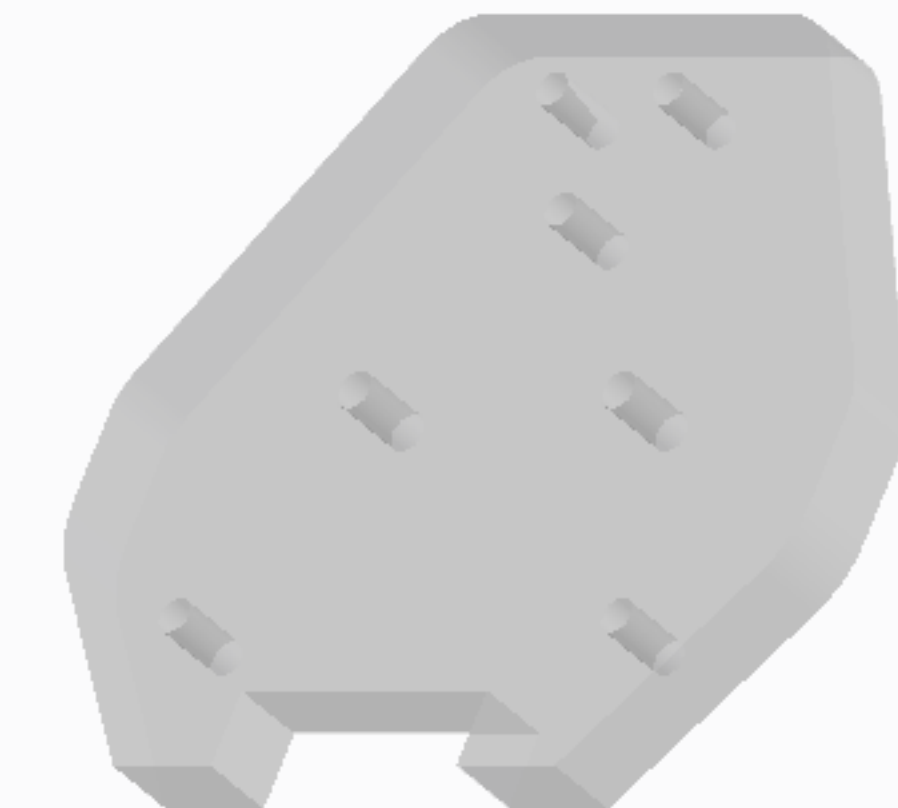
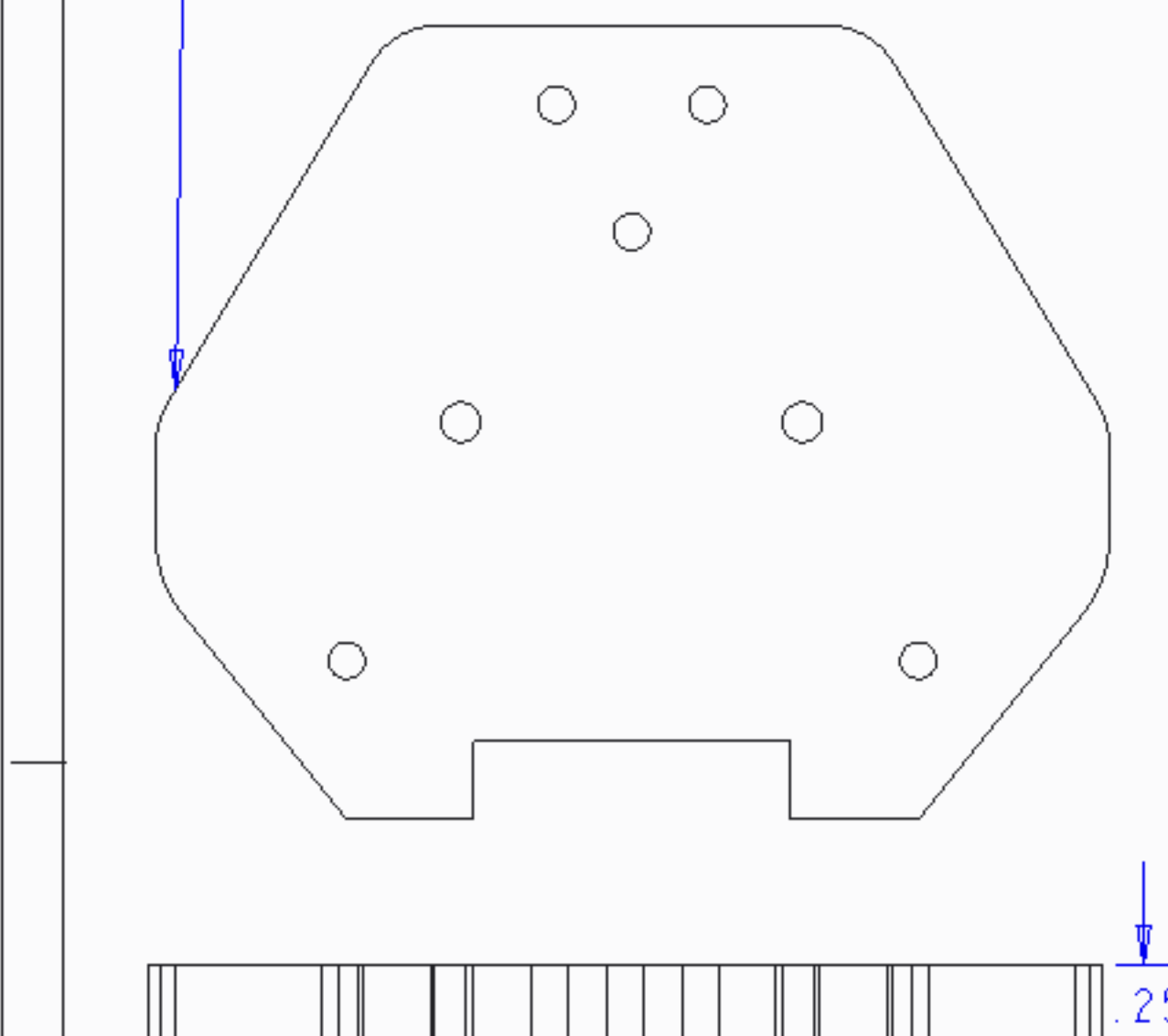
QTY: 1 ALLOCATION: FLIGHT

3/16/2015

PART NAME: GRIPPER GEARFRAME TOP PLATE

FRR PART NUMBER: VU-G-3000 REV A

GEOMETRY SAME AS BOTTOM PLATE



ISOMETRIC VIEW

MATL: ACRYLLIC

TOL: ±.005
UNLESS OTHERWISE NOTED

SCALE: 1.5

DESIGN ENG: CHRIS L.

VANDERBILT  Aerospace Club

DRAFTING ENG: ALEX G

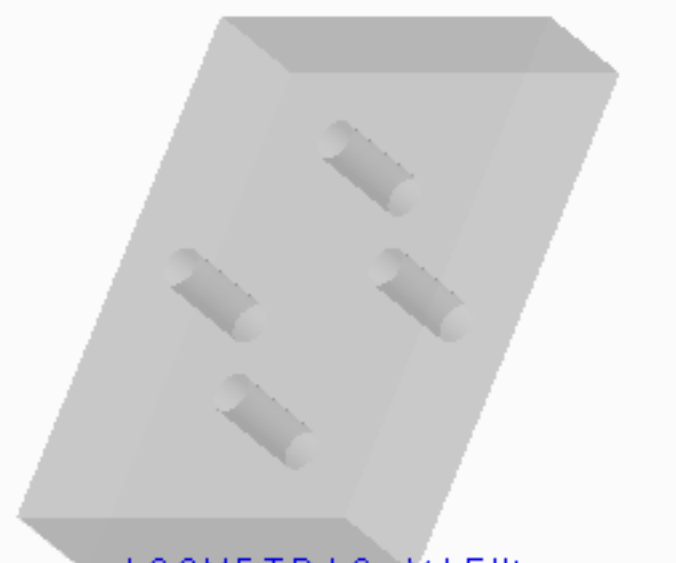
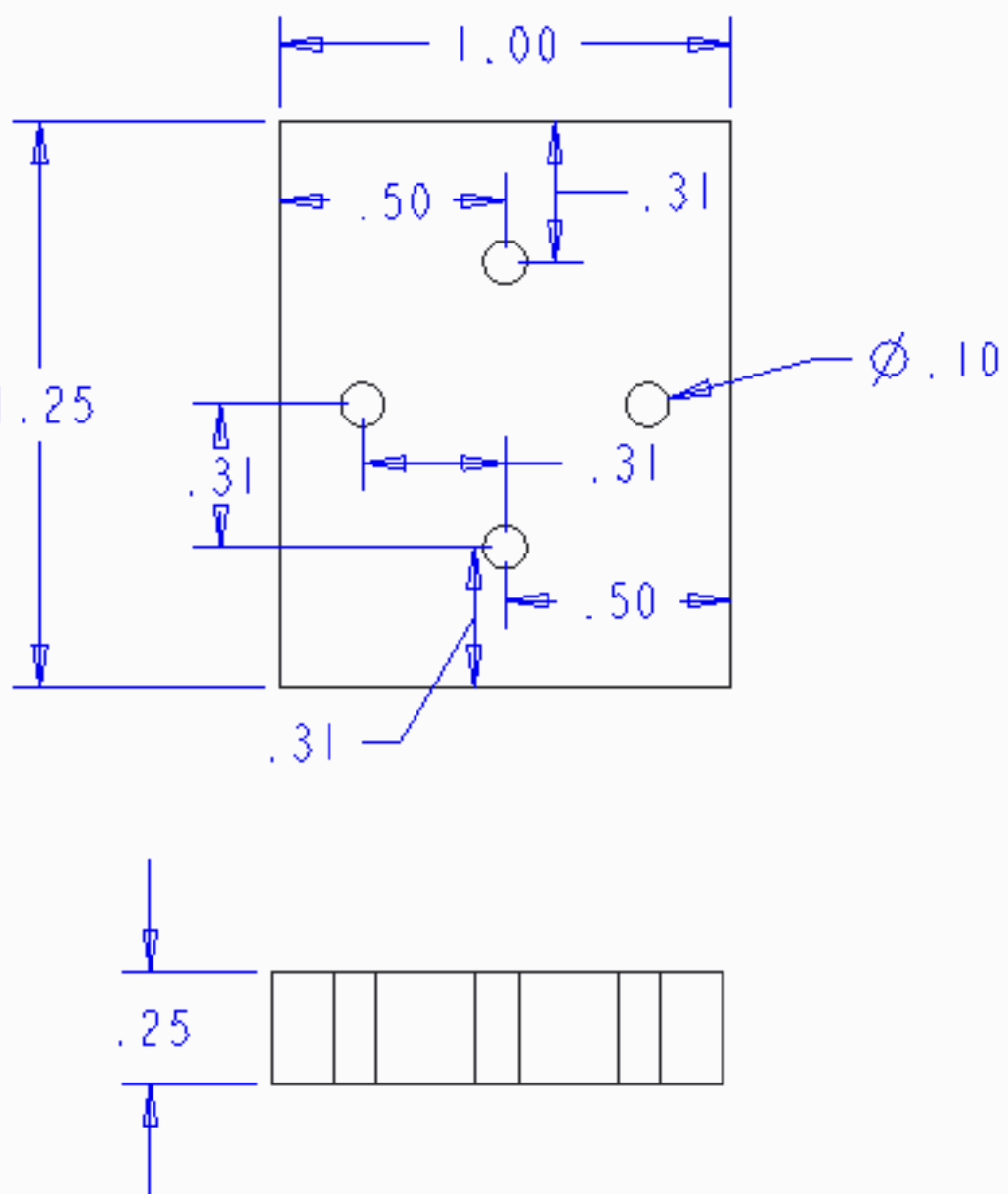
DFT: FINAL CHECKED BY: DEXTER W B.S.

QTY: 1 ALLOCATION: FLIGHT

3/16/2015

PART NAME: GRIPPER WRIST SERVO PLATE

FRR PART NUMBER: VU-G-4000 REV A



ISOMETRIC VIEW

MATL: ACRYLLIC

TOL: $\pm .005$
UNLESS OTHERWISE NOTED

SCALE: 2.000

DESIGN ENG: CHRIS L.

VANDERBILT  Aerospace Club

DRAFTING ENG: ALEX G

DFT:

FINAL

CHECKED BY: DEXTER W B.S.

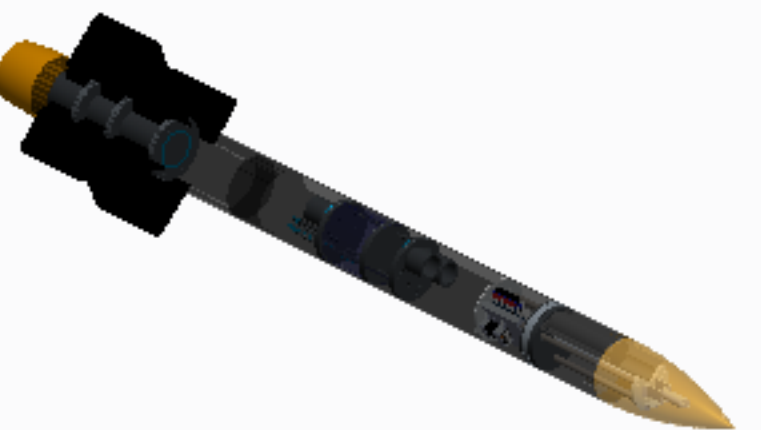
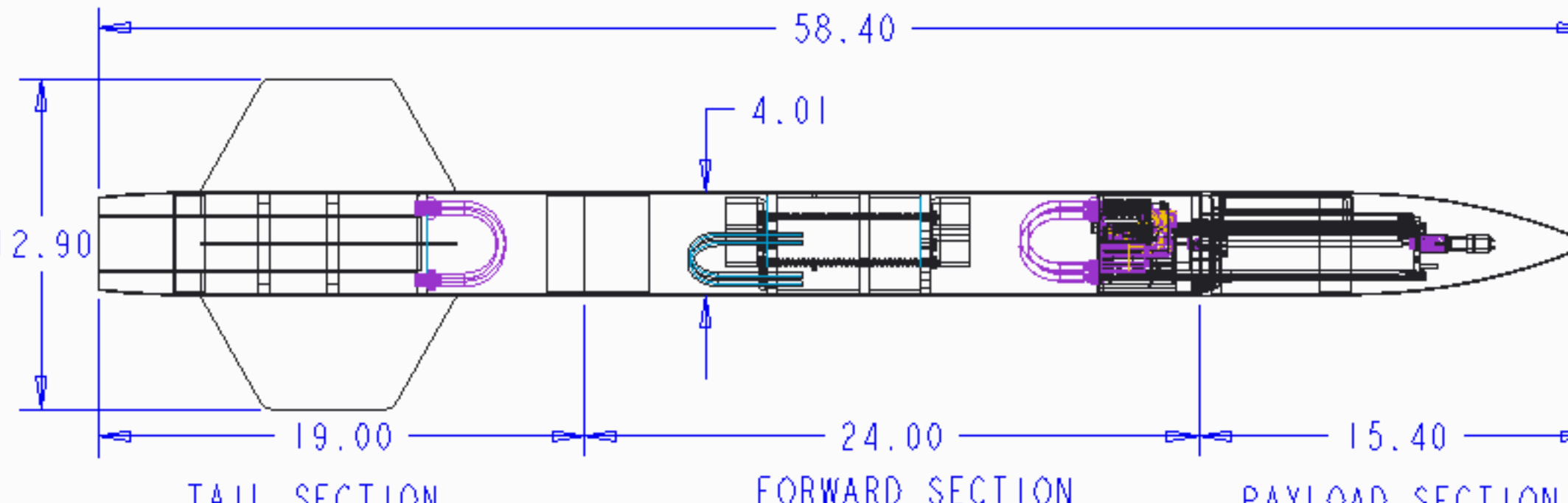
QTY: 1

ALLOCATION: FLIGHT

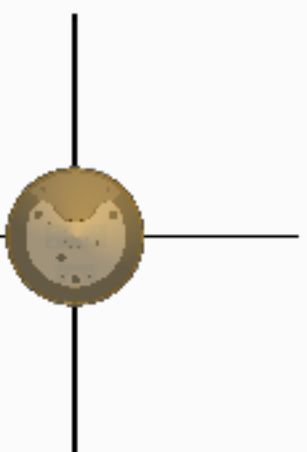
3/16/2015

PART NAME: OVERALL ROCKET ASSEMBLY

FRR PART NUMBER: VU-MAIN REV A



SCALE 0.075



TOP VIEW

VANDERBILT Aerospace Club

TOL: ±.005
UNLESS OTHERWISE NOTED

DRAFTING ENG: ALEX G

SCALE: .150

DFT: FINAL

CHECKED BY: DEXTER W B.S.

DESIGN ENG: TEAM

QTY: 1

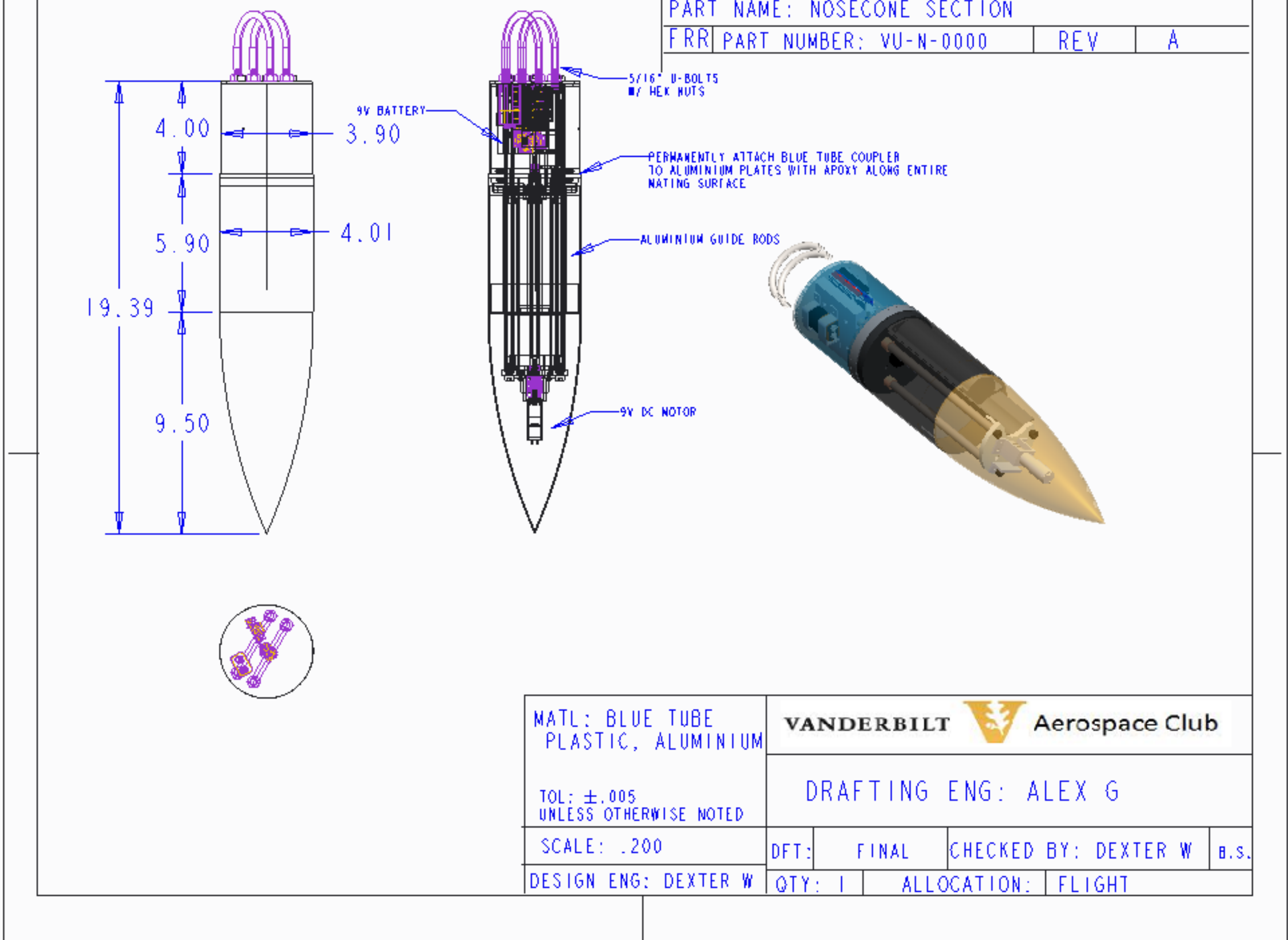
ALLOCATION: FLIGHT

3/16/2015

PART NAME: NOSECONE SECTION

FRR PART NUMBER: VU-N-0000

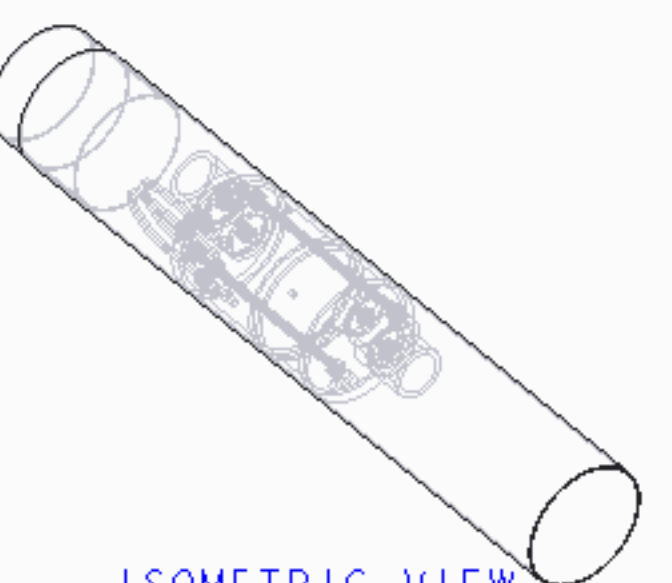
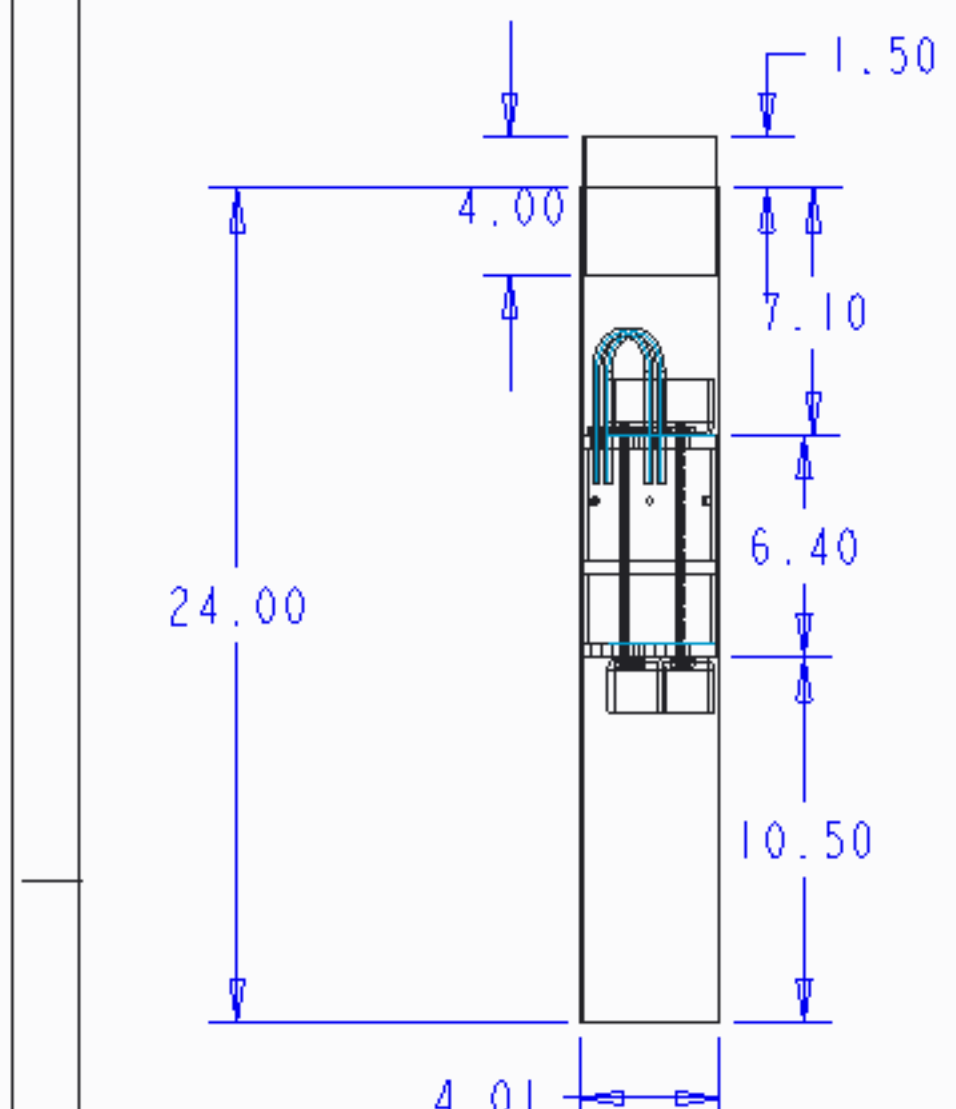
REV A



3/16/2015

PART NAME: FORWARD SECTION ASSEMBLY

FRR PART NUMBER: VU-F-0000 REV A



MATL:

TOL: ±.005
UNLESS OTHERWISE NOTED

SCALE: 0.083

DESIGN ENG: DEXTER W

VANDERBILT Aerospace Club

DRAFTING ENG: ALEX G

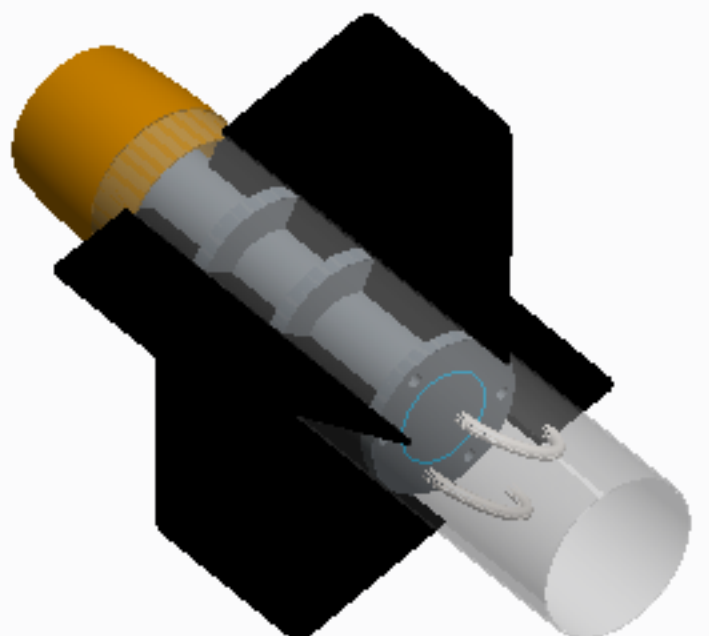
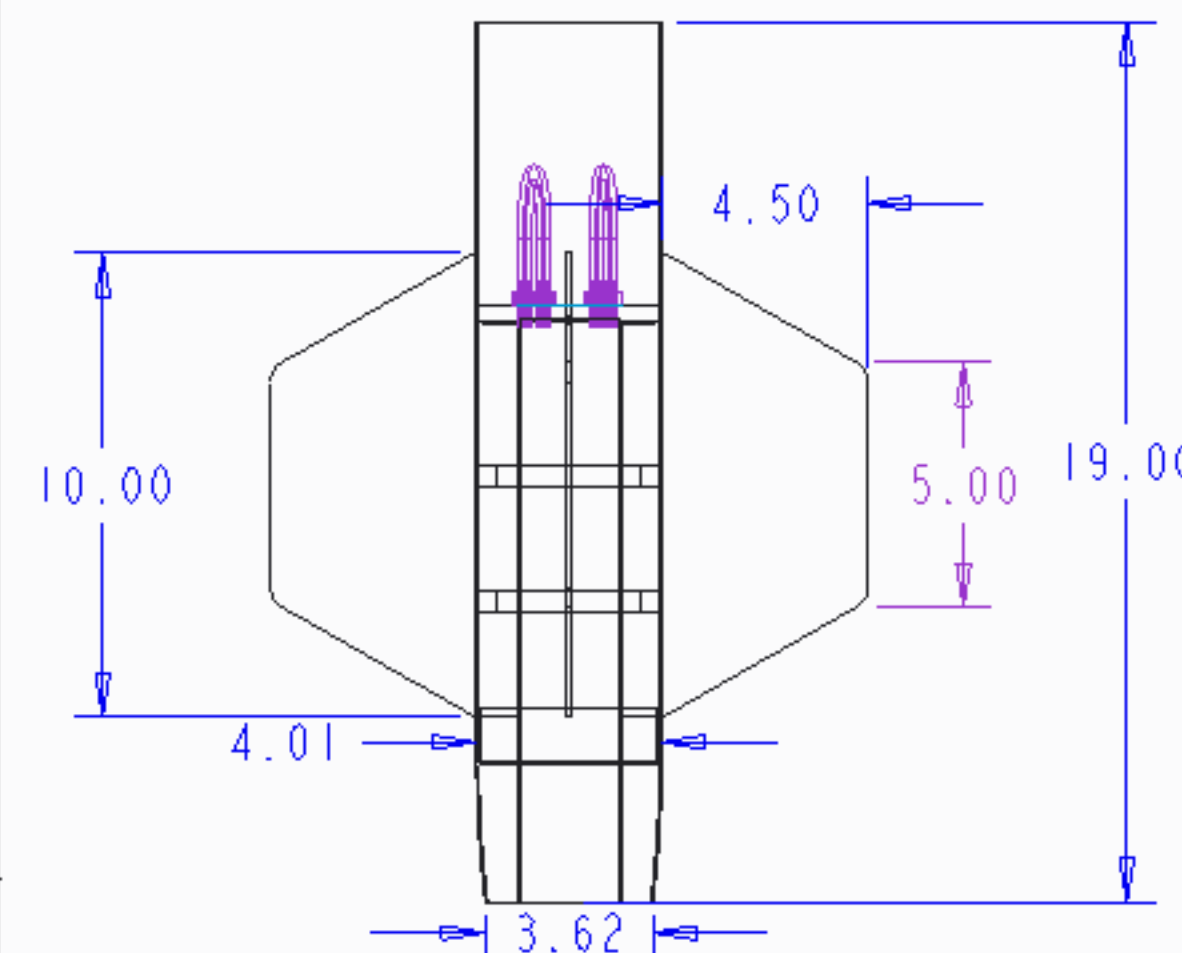
DFT: FINAL CHECKED BY: DEXTER W B.S.

QTY: 1 ALLOCATION: FLIGHT

3/16/2015

PART NAME: TAIL SECTION MAIN ASSEMBLY

FRR PART NUMBER: VU-T-0000 REV A



ISOMETRIC VIEW

MATL:

VANDERBILT  Aerospace ClubTOL: ±.005
UNLESS OTHERWISE NOTED

DRAFTING ENG: ALEX G

SCALE: 0.200

DFT: FINAL CHECKED BY: DEXTER W B.S.

DESIGN ENG: CONNOR C

QTY: 1 ALLOCATION: FLIGHT

Note: remember extra shock chord bag
in the future

Setup and Assembly Checklists

Launch location Setup

Intentionally Skipped →

- Unload equipment and materials from vehicles.
- Setup tent and secure with stakes.
- Assemble portable tables.
- Place stands for each rocket section on tables.
- Place rocket sections on stands.
- Place avionics/electronics box on own table.
- Ensure desired launch pad location will provide a sturdy base for rocket launch.

⚠ WARNING: If no such ground condition exists, abort launch.

- Place launch pad components near desired launch location.

Launch Pad Setup

- Insert the four launch pad legs into the launchpad plate.
- Minimize the height the launchpad is configured from the ground.
- Bolt on the launch rail base to the main launch pad and face it away from any spectators.
- Pivot the launch rail joint into a horizontal configuration.
- Secure the top launch rail section to the base via the joining piece and secure with bolts ensuring a flush fit.
- Reorient the launch rail to the vertical configuration and secure with bolts.
- Use a level placed on the launch pad in a vertical configuration to verify that the launch pad is oriented perpendicular to the launch area. Adjust the leg heights by twisting the launch legs using a wrench to the necessary positions in order to ensure the launch rail is in the correct vertical alignment.

⚠ WARNING: This step is imperative for straight flight.

- Undo the bolts that secure the launch rail in the vertical position and pivot the launch rail to be horizontal in order to integrate with the AGSE table.
- If necessary, use ladder to support launch rail in horizontal position so that tipping does not occur.
- Inspect fully assembled launch pad to ensure it provides a sturdy base for the rocket during launch.

⚠ WARNING: If any damage exists, abort launch.

Note: add
Luging
Hr rail

- Connect an Ethernet cable to the ethernet port of the beaglebone black. Connect the other end of this cable to the network switch at the base of the AGSE.
- Using a multimeter, measure the battery voltage for each of the two 12VDC Lead-Acid batteries. Use caution to not short the terminals of the battery! Ensure that the measured voltage is within the acceptable range of the batteries and the power supply (each battery should be within 11.5VDC-13.5VDC).
- Connect the batteries in series using the supplied battery connectors.
A WARNING: Use caution not to short the terminals of the batteries
- Using a multimeter, measure the voltage over the two terminals coming from the batteries that are now connected in series. Ensure that the measured voltage is within the acceptable range for the input of the power supply (14-36VDC)
A WARNING: Use caution not to short the two terminals
- Connect the negative battery connector to the negative power supply input on the DC/DC converter.
- Connect the positive battery connector to the positive power supply input on the DC/DC converter.
- Using a multimeter, measure the voltage across the output terminals of the DC/DC power supply. Use caution to not short the terminals of the power supply! Ensure that the measured voltage is within the acceptable range for the AGSE power (11.5-12.5VDC).
- Connect the main AGSE power cable to the DC/DC converter output terminals. Use caution to ensure proper polarity and no short circuits!
- Press the power-button on the Nvidia Jetson TK1
- Ensure the User Interface Panel powers on; screen should turn on and lights should turn on.

Tail Section Check and Assembly

- Insert the tail cone around the exposed rocket motor tube.
- Inspect the tail section for any damage from transportation and handling, specifically the structural integrity of the fins, body and motor tubes, and bulkheads.

Avionics Assembly and Integration

- Inventory all avionics equipment.
- Inspect all avionics equipment for safety and security.

A WARNING: If any such components or equipment that cannot be readily repaired or replaced damage exists, abort mission.

- Ensure the StratoLogger altimeters are secure and set for apogee and 1000ft and that the connections are secure.
- Connect all charge ignition wires connecting altimeters to wire terminals outside the avionics bay. Seal interior holes on the bulkhead with putty.
- Connect arming switches to each altimeter.
- Place batteries in clip. Tape and zip tie. Check the 9V battery terminals.
- Check voltage on new 9V batteries.
- Connect 9V batteries to each altimeter and secure to lower avionics bay bulkhead using zip ties/tape.
- Verify correct wiring scheme for both altimeters.

A WARNING: Failure to perform this step may result in incorrect deployment of recovery system in flight.

- Turn on RF transmitter in avionics bay.
- Install top avionics bay bulkhead thus enclosing avionics bay.
- Place parachute charges in blast caps and secure with blue painters tape.
- Inspect all separation ignition wires.
- Seal wire passage holes into avionics bay with removable putty.
- Place putty over all wire terminals in parachute sections to ensure screws do not loosen.

Payload Section

- Attach 9V battery to connectors.
- Test actuation of payload bay using Hall Effect sensor and magnet to trigger activation.
- Turn on RF transmitter in electronics bay.

*Not
fired
seen*

Recovery System Assembly and Integration

- Take inventory of all recovery equipment.
- Inspect all Kevlar fiber shock cords, protective blankets, and anti-zipper devices for safety and security.
- NOTE: Connect shock cords to bulkheads and bays before insertion when possible
- Forward section
 - Mount avionics bay inside forward section, align and secure.
 - Confirm that altimeter switches can be reached after installation inside forward section
 - Seal avionics bulkheads with removable putty.
 - Inspect static pressure ports for obstructions.
 - Inspect rocket parachute for hardware defects and security
 - Ensure all shock cord and parachute connections are in their proper locations.
 - Visually inspect the deployment charges for secure connection.
 - Visually verify that deployment charges are secured in their respective blast caps.
 - Fold and load payload parachute into nose cone followed by shock cord, folded using a z-fold.
 - Join nose cone to forward section of rocket via three 4-40 nylon shear pins.

⚠ WARNING: failure to use three shear pins may result in premature jettison of payload section in flight.

Payload section

- Connect shock cord to top of payload section.
- Connect opposite end of shock cord to parachute.
- Connect bottom of avionics bay to its respective position on the shock cord.
- Place payload parachute charges in blast caps in nose cone and secure with blue painters tape.
- Inspect all separation ignition charges.
- Connect parachute to nose cone bulkhead via a shock cord.
- Inspect payload parachute for hardware defects and security.
- Ensure all shock cord and parachute connections are in their proper locations.
- Visually inspect the deployment charges for secure connection.
- Visually verify that deployment charges are secured in their respective blast caps.
- Load parachute and shock cord, folded using a z-fold, into forward section of rocket below avionics bay.
- Join forward section of rocket to the aft section via three 4-40 nylon shear pins.
- Once rocket is loaded onto launch rail and ready for launch, arm each altimeter and listen for correct sequence of beeps before launching.

Section names need to be updated

Rocket Motor Installation

- Motor should be stored in own container for transport and secured to avoid drops or impacts.
⚠ WARNING: Failure to transport motor safely and securely may result in cracking of propellant grains and inflight motor failure.
- Inspect the motor to ensure that no damage occurred during transportation or handling that could result in such failures.
⚠ WARNING: If such damage has occurred, abort mission and safely dispose of faulty motor under the supervision of the safety officer.
- Insert the Cesaroni P54-3G J380 motor into rocket motor tube and tighten the positive screw cap retention ring. Applying baby powder to the exterior of the motor can help facilitate installation.
- Verify that the positive screw cap retention ring is securely fastened to the rocket.

Launch Vehicle, Launch Rail, and AGSE Integration

- Carefully carry rocket assembly to the launch pad.
- Line up the launch lugs that are attached with the rocket to the launch rail slots. Very slowly slide the launch lugs onto the rail guides making sure not to put a bending moment the rocket.
⚠ WARNING: failure to slide launch lugs onto the rail guides slowly may result in detaching the launch lugs and flight failure
- Rest rail in horizontal position on rocket stand on AGSE table

Launch Checklist

- N/A {
- Start AGSE using User Interface Panel
 - AGSE autonomously collects sample and places it into payload section of rocket
 - ⚠ WARNING: if AGSE is showing any sort of dangerous or otherwise unpredictable behavior, hit pause switch**
 - Payload section closes and AGSE moves out of the way of the rocket
 - AGSE stopped using User Interface Panel
 - Once the launch vehicle is oriented so that the tail cone is placed one foot off the launch pad, slowly raise the launch rail back into a vertical configuration and bolt down the pad so that it will not pivot.
 - Altimeter-beeping sequence is all systems go.
 - Check for loose fittings in the fins, rocket sections, payload, and launch lugs.
 - Insert the Cesaroni Profire igniter into the rocket motor and attach the leads that connect the igniter to the ignition trigger.
 - Ensure the ignition system is wired to the power source.
 - Move to safe distance, at least 100yd from the launch pad.
 - Loudly announce that the "range is hot" and ensure everyone is a safe distance from the launch pad.
 - Insert the key and listen for high-pitch sound of continuity.
 - Ensure skies are clear of aircraft and birds.
 - Begin initial countdown to launch at T-minus 10 seconds.
 - At T-minus 1 second, depress button on ignition system to launch.
 - Immediately after launch, remove key from ignition system.
 - Disconnect ignition system leads from power source.

Post-Launch Checklist

- Visually track the rocket throughout the flight. Once the main parachute has opened, begin to predict the landing position. As soon as the launch vehicle lands during a full scale test flight begin heading towards the launch vehicle. Or on competition day, as soon as NASA gives the OK to go recover the launch vehicle begin to head towards the launch vehicle.
- Record apogee as measured by the altimeters by listening to the audible beeps produced by the StratoLogger altimeters.
- Carry the sections of the rocket back to the staging area.
- Mark and discard the 9V battery.
- Check for structural damage on the airframe.
- Check for rocket and payload parachute damage.
- Discard the spent engine casing.
- Check for fractures in the avionics section.
- Debrief the launch, including: motor used, rocket configuration, altitude achieved, avionics on-board, and rocket recovery.